Second edition

Diagnostic Ultrasound

Physics and Equipment

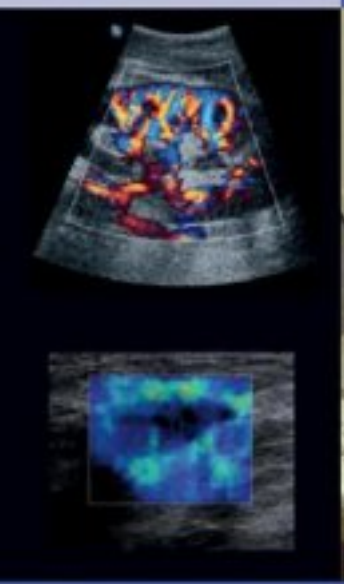

Edited by **Peter Hoskins**, **Kevin Martin** and **Abigail Thrush**

CAMBRIDGE

Medicine

Diagnostic Ultrasound

Physics and Equipment

Second Edition

Diagnostic Ultrasound

Physics and Equipment

Second edition

Edited by

Peter Hoskins BA, MSc, PhD, DSc, FIPEM, FInstP
Reader in Medical Physics
Edinburgh University
Edinburgh, UK

Kevin Martin BSc, PhD, FIPEM
Retired Consultant Medical Physicist
Leicester, UK

Abigail Thrush BSc, MSc, MIPEM
Principal Medical Physicist
Barts and the London NHS Trust
London, UK

CAMBRIDGE
UNIVERSITY PRESS

CAMBRIDGE UNIVERSITY PRESS
Cambridge, New York, Melbourne, Madrid, Cape Town, Singapore,
São Paulo, Delhi, Dubai, Tokyo

Cambridge University Press
The Edinburgh Building, Cambridge CB2 8RU, UK

Published in the United States of America by Cambridge University Press, New York

www.cambridge.org
Information on this title: www.cambridge.org/9780521757102

First edition published by Greenwich Medical Media Limited 2003

This edition published by Cambridge University Press 2010

Printed in the United Kingdom at the University Press, Cambridge

A catalogue record for this publication is available from the British Library

Library of Congress Catalogung in Publication data
Diagnostic ultrasound : physics and equipment / [edited by] Peter Hoskins, Kevin Martin, Abigail Thrush. – 2nd ed.
p. ; cm.
Includes bibliographical references and index.
ISBN 978-0-521-75710-2 (pbk.)
1. Diagnostic ultrasonic imaging. I. Hoskins, Peter. II. Martin, Kevin, 1948– III. Thrush, Abigail. IV. Title.
[DNLM: 1. Ultrasonography–methods. 2. Physical Phenomena. 3. Ultrasonography–instrumentation.
WN 208 D5367 2010]
RC78.7.U4D516 2010
616.07′543–dc22 2010016391

ISBN 978-0-521-75710-2 Paperback

Contents

Contributors

Mairéad Butler MPhys, PhD, MInstP
Research Assistant in Medical Physics
University of Edinburgh, UK

Aline Criton PhD
Ultrasound Director
SuperSonic Imagine, France

Francis Duck PhD, DSc, FIPEM, MBE
Consultant Medical Physicist
Royal United Hospital Bath and
Bath University, UK

Nick Dudley BSc, MSc, PhD, FIPEM
Consultant Medical Physicist
United Lincolnshire Hospitals, UK

Tony Evans BSc, MSc, PhD, CEng
Senior Lecturer in Medical Physics
University of Leeds, UK

Peter Hoskins BA, MSc, PhD, DSc, FIPEM, FInstP
Reader in Medical Physics
University of Edinburgh, UK

Tom MacGillivray BSc, MSc, PhD
Research Fellow in image processing
University of Edinburgh, UK

Kevin Martin BSc, PhD, FIPEM
Retired Consultant Medical Physicist
Leicester, UK

Carmel Moran BSc, MSc, PhD, FIPEM
Reader in Medical Physics
University of Edinburgh, UK

Kumar Ramnarine BSc, MSc, PhD, CSci, MIPEM
Principal Medical Physicist
University Hospitals of Leicester
NHS Trust, UK

Adam Shaw BA, MA(Cantab)
Senior Research Scientist
National Physical Laboratory,
Middlesex, UK

Abigail Thrush BSc, MSc, MIPEM
Principal Medical Physicist
Barts and the London NHS Trust, UK

Tony Whittingham BSc, MSc, PhD, FInstP, CPhys, FIPEM
Retired Consultant Medical Physicist
Newcastle-upon-Tyne, UK

Preface to the second edition

The aims and intended audience of this second edition remain unchanged from the first edition. The aim is to provide the underpinning knowledge of physics and instrumentation needed in order to practise ultrasound in a clinical setting. The book is primarily aimed at sonographers and clinical users in general, and will also serve as a first textbook for physicists and engineers. The text concentrates on explanations of principles which underpin the clinical use of ultrasound systems. The book contains relatively few equations and even fewer derivations. In the last 7 years a number of techniques which existed in embryo form in 2002 have become available on commercial ultrasound systems, and are used in a sufficient number of hospitals to justify inclusion in this book. There are additional chapters dedicated to 3D ultrasound, contrast agents and elastography. The other chapters have been updated to include developments in technology, quality assurance and safety. We hope that this second edition of 'Diagnostic Ultrasound Physics and Equipment' will meet the needs of sonographers, physicists and engineers in their training and practice.

Peter Hoskins
Kevin Martin
Abigail Thrush
Autumn 2009

Preface to the first edition

This book is an introductory text in the physics and instrumentation of medical ultrasound imaging. The level is appropriate for sonographers and clinical users in general. This will also serve as a first textbook for physicists and engineers. The text concentrates on explanations of principles which underpin the clinical use of ultrasound systems, with explanations following a 'need to know' philosophy. Consequently, complex techniques, such as Doppler frequency estimation using FFT and 2D autocorrelation, are described in terms of their function, but not in terms of their detailed signal processing. The book contains relatively few equations and even fewer derivations. The scope of the book reflects ultrasound instrumentation as it is used at the time of submission to the publishers. Techniques which are still emerging, such as tissue Doppler imaging (TDI) and contrast agents, are covered in a single chapter at the end of the book. Techniques which are even further from commercial implementation, such as vector Doppler, are not covered. We hope this book fills the gap in the market that we perceive from discussions with our clinical colleagues, that of a text which is up to date and at an appropriate level.

Peter Hoskins
Abigail Thrush
Kevin Martin
Tony Whittingham
Summer 2002

Chapter 1

Introduction to B-mode imaging

Kevin Martin

The application of ultrasound to medical diagnosis has seen continuous development and growth over several decades. Early, primitive display modes, such as A-mode and static B-mode, borrowed from metallurgical testing and radar technologies of the time, have given way to high-performance, real-time imaging. Moving ultrasound images of babies in the womb are now familiar to most members of the public through personal experience of antenatal scanning or via television. Modern ultrasound systems do much more than produce images of unborn babies, however. Modern ultrasound systems are able to make detailed measurements of blood movements in blood vessels and tissues, visualize moving structures in 3D, and make measurements related to the stiffness of tissues.

Improvements in technology have been followed by widespread acceptance and use of ultrasound in medical diagnosis. Applications have progressed from simple measurements of anatomical dimensions, such as biparietal diameter, to detailed screening for fetal abnormalities, detection of subtle changes in tissue texture and detailed study of blood flow in arteries. In many areas, ultrasound is now chosen as the first line of investigation, before alternative imaging techniques.

This book describes the physics and technology of diagnostic ultrasound systems in use at the time of writing. The book may be divided into four sections; basic physics and B-mode imaging in Chapters 1–6; Doppler ultrasound in Chapters 7–10; quality assurance and safety in Chapters 11–12, and recent technology in Chapters 13–15. This chapter covers the very basic concepts involved in B-mode imaging.

Basic principles of ultrasound image formation

We begin the explanation of ultrasound image formation with a description of a B-mode image and the basic principles of its formation. In essence, these principles are still used in modern B-mode systems, although they may be used within more complex arrangements designed to enhance performance.

A B-mode image is a cross-sectional image representing tissues and organ boundaries within the body (Figure 1.1). It is constructed from echoes, which are generated by reflection of ultrasound waves at tissue boundaries, and scattering from small irregularities within tissues. Each echo is displayed at a point in the image, which corresponds to the relative position of its origin within the body cross section, resulting in a scaled map of echo-producing features. The brightness of the image at each point is related to the strength or amplitude of the echo, giving rise to the term B-mode (brightness mode).

Usually, the B-mode image bears a close resemblance to the anatomy, which might be seen by eye, if the body could be cut through in the same plane. Abnormal

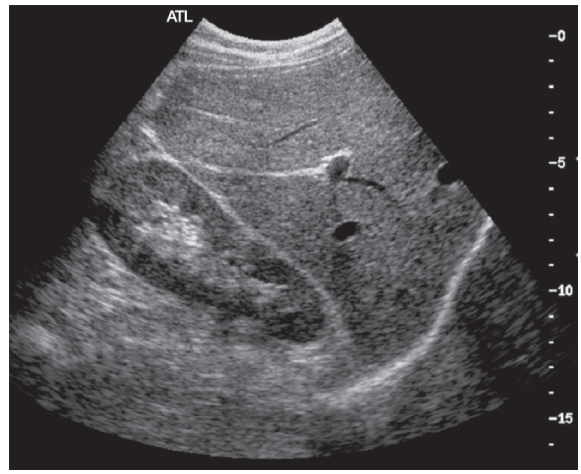

Fig. 1.1 An example of a B-mode image showing reflections from organ and blood vessel boundaries and scattering from tissues.

Diagnostic Ultrasound: Physics and Equipment, ed. Peter Hoskins, Kevin Martin and Abigail Thrush. Published by Cambridge University Press.

anatomical boundaries and alterations in the scattering behaviour of tissues can be used to indicate pathology.

To form a B-mode image, a source of ultrasound, the transducer, is placed in contact with the skin and short bursts or pulses of ultrasound are sent into the patient. These are directed along narrow beam-shaped paths. As the pulses travel into the tissues of the body, they are reflected and scattered, generating echoes, some of which travel back to the transducer, where they are detected. These echoes are used to form the image.

To display each echo in a position corresponding to that of the interface or feature (known as a target) that caused it, the B-mode system needs two pieces of information. These are

(1) the range (distance) of the target from the transducer and
(2) the direction of the target from the active part of the transducer, i.e. the position and orientation of the ultrasound beam.

Echo ranging

The range of the target from the transducer is measured using the pulse–echo principle. The same principle is used in echo-sounding equipment in boats to measure the depth of water. Figure 1.2 illustrates the measurement of water depth using the pulse–echo principle. Here, the transducer transmits a short burst or pulse of ultrasound, which travels through water to the seabed below, where it is reflected, i.e. produces an echo. The echo travels back through the water to the transducer, where it is detected. The distance to the seabed can be worked out, if the speed of sound in water is known and the time between the pulse leaving the transducer and the echo being detected, the 'go and return time', is measured.

To measure the go and return time, the transducer transmits a pulse of ultrasound at the same time as a clock is started ($t = 0$). If the speed of sound in water is c and the depth is d, then the pulse reaches the seabed at time $t = d/c$. The returning echo also travels at speed c and takes a further time d/c to reach the transducer, where it is detected. Hence, the echo arrives back at the transducer after a total go and return time $t = 2d/c$. Rearranging this equation, the depth d can be calculated from $d = ct/2$. Thus, the system calculates the target range d by measuring the arrival time t of an echo, assuming a fixed value for the speed of sound c (usually 1540 m s^{-1} for human tissues).

In the above example, only one reflecting surface was considered, i.e. the interface between the water and the seabed. The water contained no other interfaces or irregularities, which might generate additional echoes. When a pulse travels through the tissues of the body, it encounters many interfaces and scatterers, all of which generate echoes. After transmission of the short pulse, the transducer operates in receive mode, effectively listening for echoes. These begin to return immediately from targets close to the transducer, followed by echoes from greater and greater depths, in a continuous series, to the maximum depth of interest. This is known as the pulse–echo sequence.

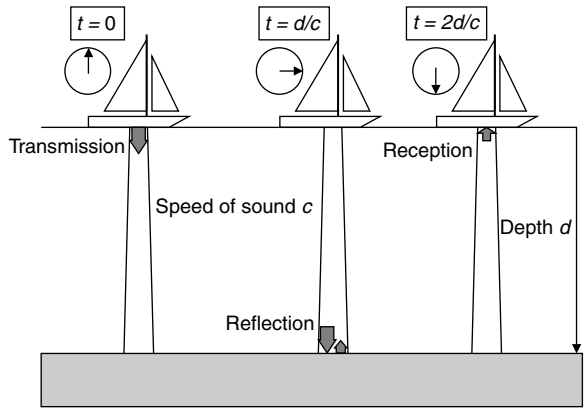

Fig. 1.2 Measurement of water depth using the pulse–echo principle. The depth is worked out by measuring the time from transmission of the pulse to reception of the echo. The speed of sound must be known.

Image formation

The 2D B-mode image is formed from a large number of B-mode lines, where each line in the image is produced by a pulse–echo sequence. In early B-mode systems, the brightness display of these echoes was generated as follows.

As the transducer transmits the pulse, a display spot begins to travel down the screen from a point corresponding to the position of the transducer, in a direction corresponding to the path of the pulse (the ultrasound beam). Echoes from targets near the transducer return first and increase the brightness of the spot. Further echoes, from increasing depths, return at increasing times after transmission as the spot travels down the screen. Hence, the distance down the display at which each echo is displayed is related to its depth below the transducer. The rate at which the display spot travels down the screen determines the scale of the image. A rapidly moving spot produces a magnified image.

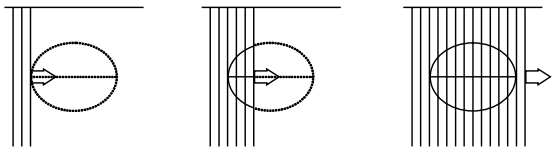

Fig. 1.3 Formation of a 2D B-mode image. The image is built up line by line as the beam is stepped along the transducer array.

The pulse–echo sequence, described above, resulted in the display of one line of information on the B-mode image. A complete B-mode image, such as that in Figure 1.1, is made up typically of 100 or more B-mode lines.

Let us consider a linear array probe, as described in Chapter 3, where the image is formed as illustrated in Figure 1.3. During the first pulse–echo sequence, an image line is formed, say on the left of the display. The active area of the transducer, and hence the beam, is then moved along the array to the adjacent beam position. Here a new pulse–echo sequence produces a new image line of echoes, with a position on the display corresponding to that of the new beam. The beam is progressively stepped along the array with a new pulse–echo sequence generating a new image line at each position.

One complete sweep may take perhaps 1/30th of a second. This would mean that 30 complete images could be formed in 1 s, allowing real-time display of the B-mode image. That is, the image is displayed with negligible delay as the information is acquired, rather than recorded and then viewed, as with a radiograph or CT scan.

B-mode formats

The B-mode image, just described, was produced by a linear transducer array, i.e. a large number of small transducer elements arranged in a straight line (see Chapter 3). The ultrasound beams, and hence the B-mode lines, were all perpendicular to the line of transducer elements, and hence parallel to each other (Figure 1.4a). The resulting rectangular field of view is useful in applications, where there is a need to image superficial areas of the body at the same time as organs at a deeper level.

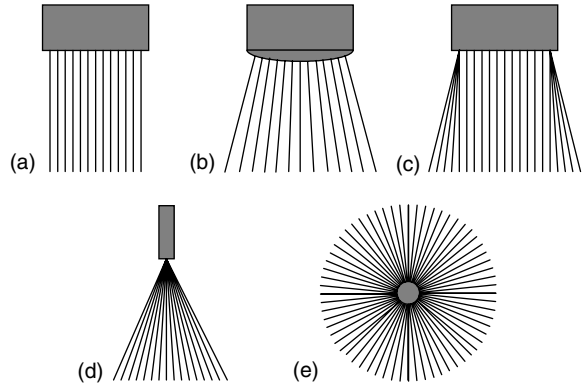

Fig. 1.4 Scan line arrangements for the most common B-mode formats. These are (a) linear, (b) curvilinear, (c) trapezoidal, (d) sector and (e) radial.

Other scan formats are often used for other applications. For instance, a curvilinear transducer (Figure 1.4b) gives a wide field of view near the transducer and an even wider field at deeper levels. This is also achieved by the trapezoidal field of view (Figure 1.4c). Curvilinear and trapezoidal fields of view are widely used in obstetric scanning to allow imaging of more superficial targets, such as the placenta, while giving the greatest coverage at the depth of the baby. The sector field of view (Figure 1.4d) is preferred for imaging of the heart, where access is normally through a narrow acoustic window between the ribs. In the sector format, all the B-mode lines are close together near the transducer and pass through the narrow gap, but diverge after that to give a wide field of view at the depth of the heart.

Transducers designed to be used internally, such as intravascular or rectal probes, may use the radial format (Figure 1.4e) as well as sector and linear fields of view. The radial beam distribution is similar to that of beams of light from a lighthouse. This format may be obtained by rotating a single element transducer on the end of a catheter or rigid tube, which can be inserted into the body. Hence, the B-mode lines all radiate out from the centre of the field of view.

Chapter 2

Physics

Kevin Martin and Kumar Ramnarine

Introduction

Ultrasound is a high-frequency sound wave, which can be used to form images of internal body organs, as described briefly in the previous chapter. Ultrasound travels through the tissues of the body in a way which makes it possible to form useful images using relatively simple techniques, as described in Chapter 1. However, the image-formation process includes some approximations, which give rise to imperfections and limitations in the imaging system. In order to be able to use diagnostic ultrasound systems effectively and to be able to distinguish imperfections in the image from genuine diagnostic information, the user must have an appreciation of the basic principles of ultrasound propagation in tissue.

Waves

Transverse waves

A wave is a disturbance with a regularly repeating pattern, which travels from one point to another. A simple and familiar example is a wave on the surface of a pond caused by a stone being thrown into the water (Figure 2.1a). Here, water displaced by the stone causes a local change in the height of the water, which causes a change in height in the water immediately adjacent to it and so on. Hence a wave travels out from the point of entry of the stone. An important aspect of the nature of this wave is that it is only the disturbance which travels across the pond, and not the water. The surface of the water at each point in the pond, as shown by a floating object (Figure 2.1b), simply goes up and down like a weight on the end of a spring, giving rise to the oscillating nature of the wave. Energy is transported across the pond from the stone to the shore. This type of wave on the surface of water is described as a transverse wave because the local movement of the water surface is at 90° (transverse) to the direction of travel.

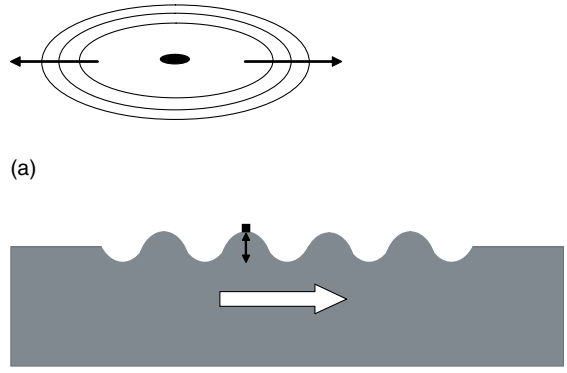

Fig. 2.1 Waves on the surface of a pond: (a) waves on the surface of a pond travel out from the point of entry of a stone; (b) only the disturbance travels across the pond. The water surface simply goes up and down.

Sound waves

The sound waves used to form medical images are longitudinal waves, which propagate (travel) through a physical medium (usually tissue or liquid). Here, the particles of the medium oscillate backwards and forwards along the direction of propagation of the wave (see Figure 2.2). Where particles in adjacent regions have moved towards each other, a region of compression (increased pressure) results, but where particles have moved apart, a region of rarefaction (reduced pressure) results. As in the transverse wave case, there is no net movement of the medium. Only the disturbance and its associated energy are transported.

The most familiar sound waves are those that travel in air from a source of sound, e.g. a musical instrument

Diagnostic Ultrasound: Physics and Equipment, ed. Peter Hoskins, Kevin Martin and Abigail Thrush. Published by Cambridge University Press.

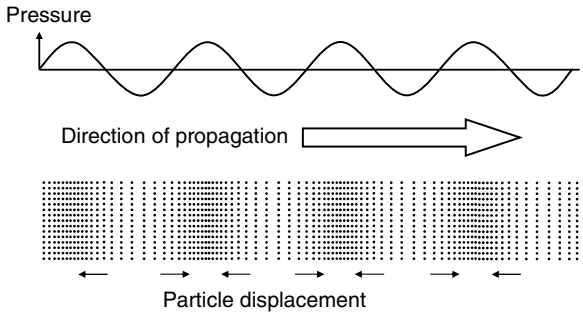

Fig. 2.2 In a longitudinal wave, particle motion is aligned with the direction of travel, resulting in bands of high and low pressure.

or a bell, to the human ear. The surface of a bell vibrates when it is struck. The oscillating motion of the surface pushes and pulls against the air molecules adjacent to it. Neighbouring air molecules are then set in motion, which displace their neighbours and so the disturbance travels through the air as a sound wave. When the sound wave reaches the listener's ear, it causes the eardrum to vibrate, giving the sensation of sound. Energy from the bell is transported by the wave to the eardrum, causing it to move.

Frequency, speed and wavelength

Frequency

When the bell above is struck, its surface vibrates backwards and forwards at a certain frequency (number of times per second). An observer listening to the sound at any point nearby will detect the same number of vibrations per second. The frequency of the wave is the number of oscillations or wave crests passing a stationary observer per second (Figure 2.3) and is determined by the source of the sound wave. Frequency is normally given the symbol f and has units of hertz (1 Hz = 1 cycle per second). Sound waves with frequencies in the approximate range 20 Hz to 20 kHz can be detected by the human ear. Sound waves with frequencies above approximately 20 kHz cannot be heard and are referred to as ultrasound waves.

Speed

As will be shown in more detail later, the speed at which a sound wave travels is determined by the medium in which it is travelling. The speed of sound is normally given the symbol c and has units of $m\,s^{-1}$ (metres per second). Examples are the speed of sound in air ($330\ m\ s^{-1}$) and water ($1480\ m\ s^{-1}$).

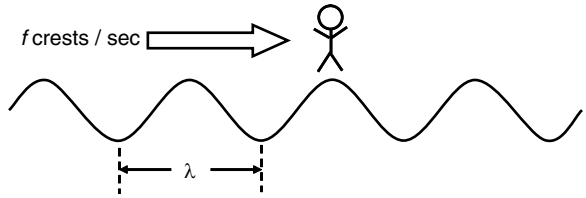

Fig. 2.3 The frequency f of a wave is the number of wave crests passing a given point per second. The wavelength λ is the distance between wave crests.

Wavelength

The wavelength of a wave is the distance between consecutive wave crests or other similar points on the wave, as illustrated in Figure 2.3. Wavelength is normally given the symbol λ (lambda) and has units of metres or millimetres.

A wave whose crests are λ metres apart and pass an observer at a rate of f per second must be travelling at a speed of $f \times \lambda$ metres per second. That is, the speed of sound $c = f\lambda$. However, it is more accurate physically to say that a wave from a source of frequency f, travelling through a medium in which the speed of sound is c, has a wavelength λ, where $\lambda = c/f$.

For example, a sound wave from a 30 kHz source travelling through water ($c \approx 1500\ m\ s^{-1}$) has a wavelength of 50 mm, whereas a wave from the same source travelling through air ($c = 330\ m\ s^{-1}$) has a wavelength of about 10 mm.

Phase

As a sound wave passes through a medium, the particles are displaced backwards and forwards from their rest positions in a repeating cycle. The pattern of displacement of the particles with time can often be described by a sine wave (Figure 2.4a). This pattern of displacement is as would be seen in the height of a rotating bicycle pedal when viewed from behind the bicycle. A complete cycle of the pedal height corresponds to a complete 360° rotation. The height of the pedal at any point in the cycle is related to the angle of the pedal when viewed from the side. The phase of the pedal is its position within such a cycle of rotation and is measured in degrees. For example if a position of horizontal (zero height) and to the rear is defined as a phase of 0°, a phase of 90° will correspond to the pedal being in the vertical position where its height is at a maximum. At 180°, the pedal is horizontal and forwards with a

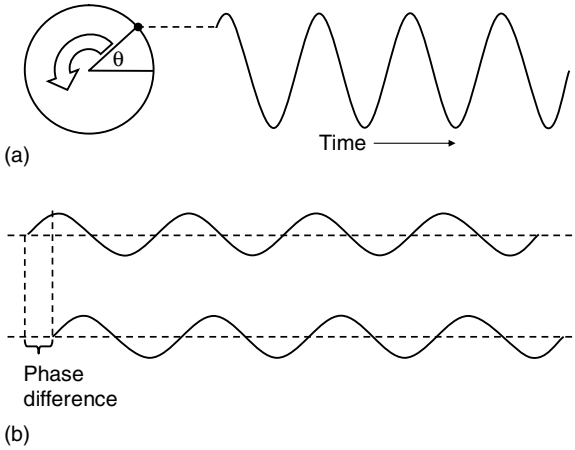

Fig. 2.4 (a) Phase describes the position within a cycle of oscillation and is measured in degrees. (b) Two waves of the same frequency and amplitude can be compared in terms of their phase difference.

height of zero. The height reaches its minimum value at 270° when the pedal is vertically down.

Two waves of the same frequency may differ in terms of their phase and can be compared in terms of their phase difference, measured in degrees (Figure 2.4b). Phase difference is an important concept when waves are added together, as described later in this chapter.

Pressure, intensity and power

As explained earlier, a sound wave passing through a medium causes the particles of the medium to oscillate back and forth along the direction of propagation (i.e. longitudinally). The maximum distance moved by a particle from its normal rest position is a measure of the amplitude (or strength) of the wave. This is referred to as the displacement amplitude. The longitudinal motion of the particles results in regions of compression and rarefaction so that at each point in the medium the pressure oscillates between maximum and minimum values as the wave passes. The difference between this actual pressure and the normal rest pressure in the medium is called the excess pressure, p, which is measured in pascals (Pa), where 1 Pa equals 1 N m^{-2} (the newton N is a measure of force). When the medium is compressed, the excess pressure is positive. When the medium undergoes rarefaction, the pressure is less than the normal rest pressure, and so the excess pressure is negative. The amplitude of the wave may also be described by the peak excess pressure, the maximum value during the passage of a wave. Excess pressure is commonly referred to simply as the pressure in the wave.

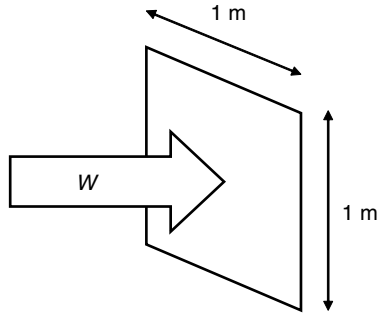

Fig. 2.5 Intensity is the power W flowing through unit area e.g. 1 W m^{-2}.

As the sound wave passes through the medium, it transports energy from the source into the medium. The rate at which this ultrasound energy is produced by the source is given by the ultrasound power. Energy is measured in joules (J) and power is measured in watts (W) where 1 W = 1 J s^{-1}.

The ultrasound produced by the source travels through the tissues of the body along an ultrasound beam, and the associated power is distributed across the beam. As will be seen later in this chapter, the power is not distributed evenly across the beam, but may be more concentrated or intense near the centre. The intensity is a measure of the amount of power flowing through an area of the beam cross section. Intensity is defined as the power flowing through unit area presented at 90° to the direction of propagation (Figure 2.5). Intensity I is measured in W m^{-2} or mW cm^{-2}.

As one might expect intuitively, the intensity associated with a wave increases with the pressure amplitude of the wave. In fact intensity I is proportional to p^2.

Speed of sound

The speed of propagation of a sound wave is determined by the medium it is travelling in. In gases (e.g. air) the speed of sound is relatively low in relation to values in liquids, which in turn tend to be lower than values in solids. The material properties which determine the speed of sound are density and stiffness. Density is a measure of the weight of a material for a given volume. For example, a 5 cm cube of steel weighs much more than a 5 cm cube of wood because steel has a higher density. Density is normally given

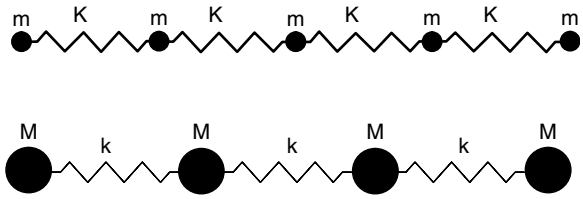

Fig. 2.6 The speed of sound in a medium is determined by its density and stiffness, which can be modelled by a series of masses and springs.

the symbol ρ (rho) and is measured in units of kg m^{-3}. Stiffness is a measure of how well a material resists being deformed when it is squeezed. This is given by the pressure required to change its thickness by a given fraction. Stiffness is usually denoted by the symbol k (units of Pa).

A simple picture of how the density and stiffness of a material determine its speed of sound can be obtained from the model shown in Figure 2.6, which consists of two lines of weights, or more correctly masses, connected by springs. The small masses (m) model a material of low density and the large masses (M) a material of high density. In the two models shown, the small masses are linked by springs of high stiffness K and the large masses by springs of low stiffness k. A longitudinal wave can be propagated along the row of small masses (m) by giving the first mass a momentary push to the right. This movement is coupled to the second small mass by a stiff spring causing it to accelerate quickly to the right and pass on the movement to the third mass, and so on. As the masses are light (low density), they can be accelerated quickly by the stiff springs (high stiffness) and the disturbance travels rapidly.

In the second case, a momentary movement of the first large mass M to the right is coupled to the second mass by a weak spring (low stiffness). The second large mass will accelerate relatively slowly in response to the small force from the weak spring. Its neighbours to the right also respond slowly so that the disturbance travels relatively slowly.

Hence, low density and high stiffness lead to high speed of sound whereas high density and low stiffness lead to low speed of sound. Mathematically this is expressed in the following equation:

$$\text{Speed of sound } c = \sqrt{k/\rho}$$

Table 2.1 Speed of sound in human tissues and liquids (from Duck 1990).

Material	c (m s^{-1})
Liver	1578
Kidney	1560
Amniotic fluid	1534
Fat	1430
Average tissue	1540
Water	1480
Bone	3190–3406
Air	333

Although gases have low density, they have very low stiffness (high compressibility), leading to relatively low speed of sound compared to liquids and solids.

Table 2.1 shows typical values for the speed of sound in various materials, including a number of different kinds of human tissue. The most important point to note from this table is that the values for the speed of sound in human soft tissues are rather similar. In fact they are sufficiently similar that the B-mode image-forming process can assume a single, average value of 1540 m s^{-1} without introducing significant errors or distortions in the image. All the values shown (with the exception of fat) are within 5% of this average value and are not much different from the value in water. The speed of sound in air is much lower because of its low stiffness, and that in bone is much higher because of its high stiffness.

Frequencies and wavelengths used in diagnosis

The ultrasound frequencies used most commonly in medical diagnosis are in the range 2–15 MHz, although frequencies up to 40 MHz may be used in special applications and in research. The wavelengths in tissue which result from these frequencies can be calculated using the equation given earlier, which relates wavelength λ to the frequency f and speed c of a wave:

$$\lambda = \frac{c}{f}$$

Assuming the average speed of sound in soft tissues of 1540 m s^{-1}, values of λ at diagnostic frequencies are as shown in Table 2.2.

Table 2.2 Wavelengths used in diagnosis.

f (MHz)	λ (mm)
2	0.77
5	0.31
10	0.15
15	0.1

The wavelengths in soft tissues which result from these frequencies are within the range 0.1–1 mm. As will be seen later in this chapter and in Chapter 5, the wavelength of the ultrasound wave has an important influence on the ability of the imaging system to resolve fine anatomical detail. Short wavelengths give rise to improved resolution, i.e. the ability to show closely spaced targets separately in the image.

Reflection of ultrasound waves

In Chapter 1, a B-mode image was described as being constructed from echoes, which are generated by reflections of ultrasound waves at tissue boundaries and by scattering from small irregularities within tissue. Reflections occur at tissue boundaries where there is a change in acoustic impedance (see below). When an ultrasound wave travelling through one type of tissue encounters an interface with a tissue with different acoustic impedance, some of its energy is reflected back towards the source of the wave, while the remainder is transmitted into the second tissue.

Acoustic impedance

The acoustic impedance of a medium z is a measure of the response of the particles of the medium in terms of their velocity, to a wave of a given pressure. Acoustic impedance $z = p/v$, where p is the local pressure and v is the local particle velocity. It is analogous to electrical impedance (or resistance R), which is the ratio of the voltage (V) applied to an electrical component (the electrical driving force or pressure) to the resulting electrical current (I) which passes through it (the response), as expressed in Ohm's law: $R = V/I$.

The acoustic impedance of a medium is again determined by its density (ρ) and stiffness (k). It can be explained in more detail, as with the speed of sound, by modelling the medium as a row of small or large masses (m) and (M) linked by weak or stiff springs (k) and (K) as shown in Figure 2.7.

In this case, however, the small masses m are linked by weak springs k, modelling a material with low density and low stiffness. The large masses M are linked by stiff springs K, modelling a material with high density and stiffness.

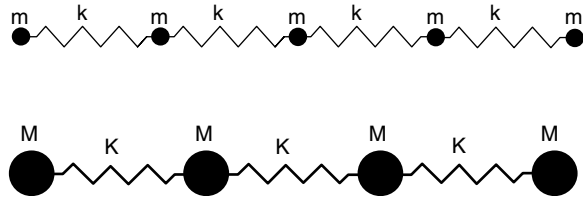

Fig. 2.7 The acoustic impedance of a medium is determined by its density and stiffness, which can be modelled by a series of masses and springs.

If a given pressure (due to a passing wave) is applied momentarily to the first small mass m, the mass is easily accelerated to the right (reaching increased velocity) and its movement encounters little opposing force from the weak spring k. This material has low acoustic impedance, as particle movements within it (in terms of velocity) in response to a given pressure are relatively large. In the second case, the larger masses M accelerate less in response to the applied pressure (reaching lower velocity) and their movements are further resisted by the stiff springs. Particle velocity (the response) in this material is lower for a given applied pressure and it has higher acoustic impedance. The acoustic impedance z of a material is given by:

$$z = \sqrt{\rho k}$$

By combining this equation with that for the speed of sound given earlier, it can be shown also that:

$$z = \rho c$$

Acoustic impedance z has units of kg m^{-2} s^{-1}, but the term rayl (after Lord Rayleigh) is often used to express this unit.

Table 2.3 gives values of z for some common types of human tissue, air and water. Table 2.3 shows that values for z in most human soft tissues are very similar. For air, which has low density and low stiffness, z is very small. For bone, which has high density and high stiffness, z is much higher.

Reflection

When a sound wave travelling through one medium meets an interface with a second medium of different acoustic impedance, some of the wave is transmitted

Table 2.3 Values of acoustic impedance.

Material	z (kg m^{-2} s^{-1})
Liver	1.66×10^6
Kidney	1.64×10^6
Blood	1.67×10^6
Fat	1.33×10^6
Water	1.48×10^6
Air	430
Bone	6.47×10^6

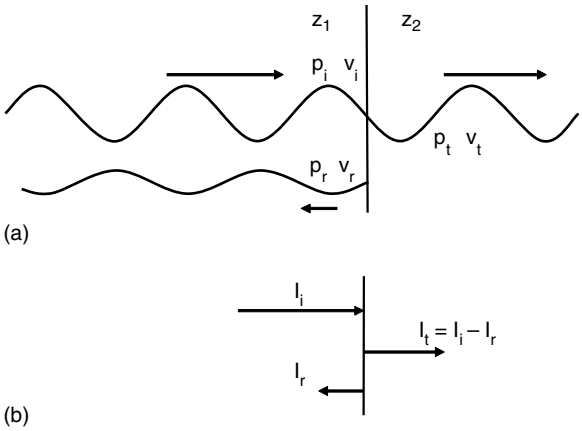

Fig. 2.8 (a) Total particle pressure and velocity cannot change abruptly across an interface. So a reflected wave is formed when there is a change in acoustic impedance. (b) The intensity transmitted across an interface is the incident intensity minus that reflected.

into the second medium and some is reflected back into the first medium. The amplitudes of the transmitted and reflected waves depend on the change in acoustic impedance. Figure 2.8a shows a sound wave travelling through a medium with acoustic impedance z_1, incident on an interface with a second medium with acoustic impedance z_2. The acoustic impedance changes abruptly at the interface. However, the motion of the particles of the medium, and hence their pressure and velocity, must be continuous across the interface to avoid disruption of the medium. To achieve this, the total wave pressure and velocity at the interface in medium 1 must equal those in medium 2 near to the interface. That is $p_i + p_r = p_t$ and $v_i + v_r = v_t$.

From this condition it can be shown that:

$$\frac{p_r}{p_i} = \frac{z_2 - z_1}{z_2 + z_1}$$

Table 2.4 Amplitude reflection coefficients of interfaces.

Interface	R_A
Liver–kidney	0.006
Kidney–spleen	0.003
Blood–kidney	0.009
Liver–fat	0.11
Liver–bone	0.59
Liver–air	0.9995

where p_i and p_r are the pressure amplitudes of the incident and reflected waves respectively near the interface.

This ratio of reflected to incident pressure is commonly referred to as the amplitude reflection coefficient R_A. It is very important to ultrasound image formation as it determines the amplitude of echoes produced at boundaries between different types of tissue.

Table 2.4 shows values of amplitude reflection coefficient for some interfaces that might be encountered in the body. For most soft tissue to soft tissue interfaces, the amplitude reflection coefficient is less than 0.01 (1%). This is another important characteristic for ultrasound imaging as it means that most of the pulse energy at soft tissue interfaces is transmitted on to produce further echoes at deeper interfaces. The amplitude reflection coefficient at a tissue–fat interface is about 10% due to the low speed of sound in fat. At an interface between soft tissue and air, as might be encountered within the lungs or gas pockets in the gut, the reflection coefficient is 0.999 (99.9%), so no further useful echoes can be obtained from beyond such an interface. For this reason, it is important to exclude air from between the ultrasound source (the transducer) and the patient's skin to ensure effective transmission of ultrasound. At an interface between soft tissue and bone, the amplitude reflection coefficient is approximately 0.5 (50%), making it difficult also to obtain echoes from beyond structures such as ribs. Note that the reflection coefficient is not related to the frequency of the wave; it is determined only by the change in z at the interface between the two media.

The intensity reflection coefficient describes the ratio of the intensities of the reflected (I_r) and incident waves (I_i). As intensity is proportional to pressure squared, the intensity reflection coefficient R_i is given by:

$$\frac{I_r}{I_i} = R_i = R_A^2 = \left(\frac{z_2 - z_1}{z_2 - z_1}\right)^2$$

At the interface, the energy flow of the incident wave in terms of its intensity must be conserved and is split between the transmitted wave and the reflected wave.

Hence $I_i = I_t + I_r$. Alternatively, $I_t = I_i - I_r$ (Figure 2.8b).

The intensity transmission coefficient $T_i = I_t / I_i$ and from above it can be shown that $T_i = 1 - R_i$. For example, if 0.01 (1%) of the incident intensity is reflected, then the other 0.99 (99%) must be transmitted across the boundary.

The law of reflection

In this description of reflection, it has been assumed that the interface is large compared to the wavelength of the wave and that the wave approaches the boundary at 90° (normal incidence). Under these circumstances, the reflected and transmitted waves also travel at 90° to the interface. In clinical practice, the wave may approach the interface at any angle. The angle between the direction of propagation and a line at 90° to the interface (the normal) is called the angle of incidence θ_i (which has been 0° so far) as shown in Figure 2.9a. Similarly, the angle between the direction of the reflected wave and the normal is called the angle of reflection θ_r.

For a flat, smooth interface, the angle of reflection $\theta_r = \theta_i$ the angle of incidence. This is referred to as the law of reflection. As will be seen in Chapter 5, reflection at strongly reflecting interfaces can lead to a number of image artefacts.

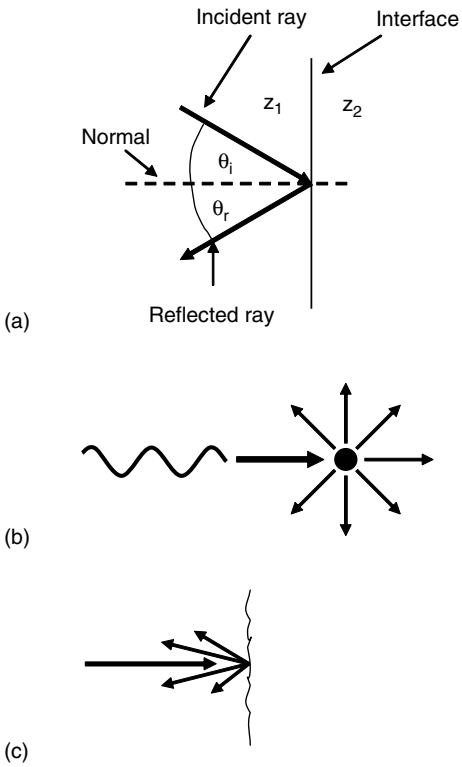

Fig. 2.9 Ultrasound waves are reflected at large interfaces and scattered by small targets: (a) at a large, smooth interface, the angle of reflection is equal to the angle of incidence; (b) small targets scatter the wave over a large angle; (c) a rough surface reflects the wave over a range of angles.

Scattering

Reflection, as just described, occurs at large interfaces such as those between organs, where there is a change in acoustic impedance. Within the parenchyma of most organs (e.g. liver and pancreas), there are many small-scale variations in acoustic properties, which constitute very small-scale reflecting targets (of size comparable to or less than the wavelength). Reflections from such very small targets do not follow the laws of reflection for large interfaces. When an ultrasound wave is incident on such a target, the wave is scattered over a large range of angles (Figure 2.9b). In fact, for a target which is much smaller that the wavelength, the wave may be scattered uniformly in all directions. For targets of the order of a wavelength in size, scattering will not be uniform in all directions but will still be over a wide angle.

The total ultrasound power scattered by a very small target is much less than that for a large interface and is related to the size d of the target and the wavelength λ of the wave. The scattered power is strongly dependent on these dimensions. For targets which are much smaller than a wavelength ($d << \lambda$), scattered power is proportional to the sixth power of the size d and inversely proportional to the fourth power of the wavelength, i.e.:

$$W_s \propto \frac{d^6}{\lambda^4} \propto d^6 f^4$$

This frequency dependence is often referred to as Rayleigh scattering.

Organs such as the liver contain non-uniformities in density and stiffness on scales ranging from the cellular level up to blood vessels, resulting in scattering characteristics which do not obey such simple rules over all frequencies used in diagnosis. The frequency dependence of scattering in real liver changes with frequency over the diagnostic range (3–10 MHz). The scattered power is proportional to f^m, where m increases with

frequency from approximately 1 to 3 over this range (Dickinson 1986).

There are two important aspects of scattering for ultrasound imaging. Firstly, the ultrasonic power scattered back to the transducer by small targets is small compared to that from a large interface, so the echoes from the parenchyma of organs such as the liver are relatively weak. Secondly, as ultrasound is scattered over a wide angle by small targets, their response, and hence their appearance in the image, does not change significantly with the angle of incidence of the wave. Liver parenchyma looks similar ultrasonically regardless of the direction from which it is imaged. In contrast, the appearance of large interfaces is strongly dependent on the angle of incidence of the ultrasound beam, as described in Chapter 5.

Tissues such as muscle have long-range structure in one direction, i.e. along the muscle fibres, and do not scatter ultrasound uniformly in all directions. Consequently, the appearance of muscle in an ultrasound image may change with the relative orientations of the ultrasound beams and the muscle fibres.

Diffuse reflection

The description of reflection given above assumed a perfectly flat, smooth interface. Some surfaces within the body may be slightly rough on the scale of a wavelength and reflect ultrasound waves over a range of angles, an effect similar to scattering from small targets. This type of reflection is known as diffuse reflection (Figure 2.9c).

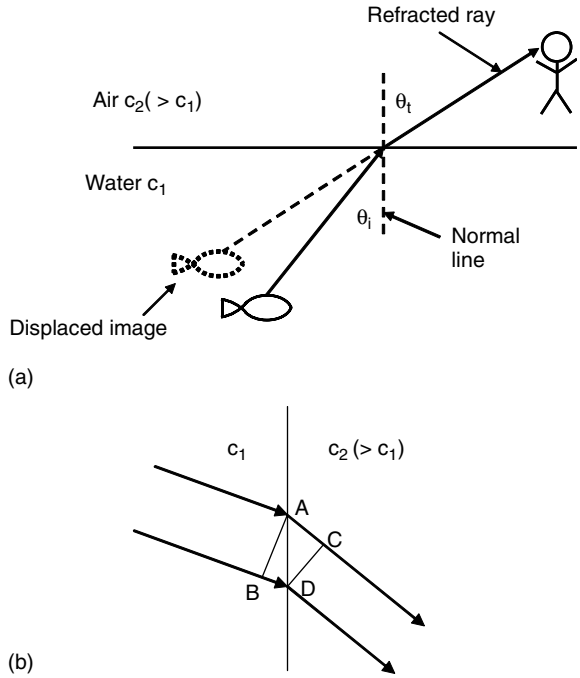

Fig. 2.10 (a) When a wave crosses a boundary at an angle, where there is a change in the speed of propagation, the wave is refracted, i.e. there is a change in the direction of travel causing image displacement. (b) The edge of the incident wave front at A passes into medium 2 first, where it travels more quickly than the edge at B. By the time the wave edge at B has travelled to the interface (at point D), a wave front from point A has travelled a greater distance to point C. The new wave front CD is hence deviated away from the normal.

Refraction

In the description of reflection above, the angle of the reflected wave at a large interface was the same as that of the incident wave and it was assumed that the transmitted wave carried on in the same direction as the incident wave. This is true where the speed of sound is the same in both media. However, where there is a change in the speed of sound from the first medium to the next (and the angle of incidence is not 90°), the direction of the transmitted wave is altered due to refraction.

Refraction is commonly observed with light waves. For example, when an object below the surface of water is looked at from the air above, light from the object is refracted as it emerges into the air, causing the apparent position of the object to be displaced from its real position (Figure 2.10a). As the speed of light in water is lower than that in air, the light emerging from the water is refracted away from the normal. The underwater object appears to an observer as though it is in line with the emerging beam of light, rather than in its true position. Refraction of ultrasound waves at boundaries where the speed of sound changes can also cause displacement of the image of a target from its true relative position in the patient, as described in Chapter 5.

Refraction can be explained as shown in Figure 2.10b. A wave front AB, travelling in medium 1, arrives at an interface with medium 2 where $c_2 > c_1$. The edge of the wave at A then passes into medium 2, where it travels more quickly than the edge at B, which is still in medium 1. By the time the wave edge at B has travelled to the interface (at point D), a wave front from point A will have travelled a greater distance to point C. The new wave front CD is hence deviated away

from the normal at angle θ_t. When the wave crosses an interface where the speed of sound increases, the angle to the normal also increases. Conversely, when the wave experiences a reduction in the speed of sound as it crosses the interface, the angle to the normal also decreases. The relationship between the angles θ_i, θ_t, c_1 and c_2 is described by Snell's law:

$$\frac{\sin\theta_i}{\sin\theta_t} = \frac{c_1}{c_2}$$

Snell's law shows that the angles of the incident and transmitted waves are the same when the speeds of sound in the two media are the same. The change in the direction of propagation of the wave as it crosses the boundary increases with increasing change in the speed of sound, i.e. larger changes in the speed of sound give rise to stronger refraction effects.

Attenuation

When an ultrasound wave propagates through soft tissue, the energy associated with the wave is gradually lost so that its intensity reduces with distance travelled, an effect known as attenuation. The way in which intensity falls with increasing distance is illustrated in Figure 2.11. The pattern is that of an exponential decay curve, where the rate of decrease is rapid at first but becomes more gradual as the intensity reduces. The curve follows the simple rule that the fractional decrease in intensity is the same for every centimetre travelled into the tissue.

For example, if the intensity is reduced by a factor of 0.7 in the first cm, it will be reduced again by 0.7 in the second cm and again by 0.7 in the third cm. In relation to the intensity I_0 at the surface, it will be reduced to 0.7 I_0 after 1 cm, 0.49 I_0 after 2 cm ($0.7 \times 0.7 = 0.49$) and to 0.34 I_0 after 3 cm ($0.7 \times 0.7 \times 0.7 = 0.34$).

The attenuation over a given distance in cm can be calculated more conveniently if the fractional decrease in intensity over each cm is expressed in decibels (dB). The dB is used to express a factor or ratio on a logarithmic scale. As the rate of attenuation per cm in dB is related to the logarithm of the ratio (see Appendix A), the attenuation over each cm travelled can be added rather than multiplied, and we can then measure attenuation in dB per cm. A ratio of 0.7 is equal to 1.5 dB, so for the graph in Figure 2.11 the intensity is reduced by 1.5 dB for each cm of travel. After 1 cm, it is reduced by 1.5 dB, after 2 cm it is reduced by 3 dB (1.5 + 1.5) and after 3 cm it is reduced by 4.5 dB (1.5 + 1.5 + 1.5). The rate at which the intensity of the wave is attenuated, in dB cm^{-1}, is referred to as the attenuation coefficient.

An ultrasound wave can be attenuated by several mechanisms as it travels through tissue. The most important mechanism is absorption, in which ultrasound energy is converted into heat (Parker 1983). In most diagnostic systems, ultrasound propagates in the form of a beam, as described later in this chapter. The attenuation of practical interest is the rate at which ultrasound intensity in the beam decreases with distance. As well as absorption, the intensity in the beam may be reduced due to scattering of ultrasound out of the beam and to divergence or spreading of the beam with distance.

Absorption

Absorption is the process by which ultrasound energy is converted into heat in the medium. When an ultrasound wave passes through a medium, its particles move backwards and forwards in response to the pressure wave, as described earlier. At low frequencies, the particles are able to move in step with the passing pressure wave and energy associated with the motion of the particles is effectively passed back to the wave as it moves on. However, the particles of the medium cannot move instantaneously and at high frequencies may be unable to keep up with the rapid fluctuations in pressure. They are unable to pass back all of the energy associated with their movements to the passing wave as they are out of step and some energy is retained by the medium, where it appears as heat. Absorption is likely to be strongest at frequencies which excite natural modes of vibration of the particular molecules of the

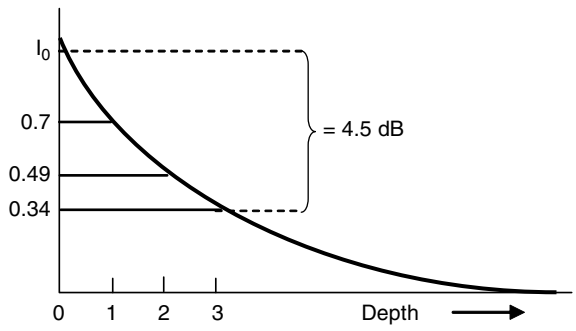

Fig. 2.11 The ultrasound intensity is attenuated (reduced) by the same fraction for each unit of distance travelled into the medium. This equates to attenuation by the same number of dB for each unit of distance.

medium as it is at such frequencies that they are most out of step with the passing wave. Understanding of the mechanisms and vibrational modes which lead to absorption of ultrasound is still imperfect, but absorption has been found to be strongly dependent on tissue composition and structure. For example, tissues with high collagen content such as tendons and cartilage show high absorption, whereas those with high water content show lower absorption. Water and liquids such as urine, amniotic fluid and blood have low absorption and low attenuation. Estimates of the contribution of absorption to attenuation are variable, but for many tissues absorption is the dominant loss mechanism.

Dependence on frequency

Attenuation of ultrasound by biological tissues increases with frequency. The attenuation coefficient of most tissues, when expressed in dB cm^{-1}, increases approximately linearly with frequency, i.e. doubling the frequency will increase the attenuation by approximately a factor of 2. Hence, for most tissues, it is possible to measure ultrasound attenuation in dB cm^{-1} MHz^{-1}. This allows the total attenuation of an ultrasound pulse to be calculated easily from the frequency and the distance travelled. For example, if a tissue attenuates by 0.7 dB cm^{-1} MHz^{-1}, then a 5 MHz ultrasound wave, after travelling a distance of 10 cm, will be attenuated by 5 MHz × 10 cm × 0.7 dB cm^{-1} MHz^{-1} = 35 dB.

Note that this attenuation is experienced by the transmitted pulse as it travels into tissue and by the echoes as they return to the transducer. Hence, for the example just given, echoes from a depth of 10 cm will be smaller than those received from tissues close to the transducer by 70 dB.

Table 2.5 shows measured values of attenuation for some human tissues expressed in units of dB cm^{-1} MHz^{-1}. Values are typically in the range 0.3–0.6 dB cm^{-1} MHz^{-1} for soft tissues but much lower for water (and watery body fluids). Attenuation in bone is very high and does not increase linearly with frequency as in the case of soft tissues.

When attenuation is large, the echoes returned from deeper targets may be too weak to detect. Hence, for imaging large or deep organs, a low frequency (3–5 MHz) must be used. High frequencies (10–15 MHz) can only be used to image relatively small, superficial targets (e.g. thyroid) as they are attenuated more rapidly. The short wavelengths associated with high-frequency ultrasound leads to improved resolution of image detail. The operator must choose the optimum frequency for each particular application. This is a compromise that ensures that the best image resolution is obtained, while allowing echoes to be received from the required depth.

Table 2.5 Values of attenuation for some human tissues.

Tissue	Attenuation (dB cm^{-1} MHz^{-1})
Liver	0.399
Brain	0.435
Muscle	0.57
Blood	0.15
Water	0.02
Bone	22

Ultrasound beams

The description of ultrasound wave propagation so far has concentrated mainly on the properties of the wave and how it is affected by the medium in the direction of propagation. The principles outlined apply regardless of the sideways extent of the wave, i.e. in the transverse direction. It is clear from the outline of B-mode image formation given in Chapter 1 that to be able to define the origin of an echo in the imaged cross section, the extent of the wave in the transverse direction has to be very limited. That is, the wave must propagate along a narrow corridor or beam. This section describes the formation and properties of ultrasound beams.

Interference of waves

So far, we have considered only a single wave propagating through a medium. When two or more waves from different sources propagate through the same medium, they interfere with each other. That is, the effects of each individual wave are added at each point in the medium. This is to be expected, as the pressure at a point in the medium will be the sum of the pressures on it from the different waves. Figure 2.12 shows the simple case of two waves with the same frequency and amplitude propagating in the same direction. In Figure 2.12a, the waves are in phase or in step with each other and the peaks of the two waves coincide, as do the troughs. In this case the resulting wave amplitude is twice that of the individual waves. This case is referred to as constructive interference, as the resulting amplitude is greater than that of both the individual waves. In Figure 2.12b, the waves are in anti-phase, and the peaks of one wave coincide with

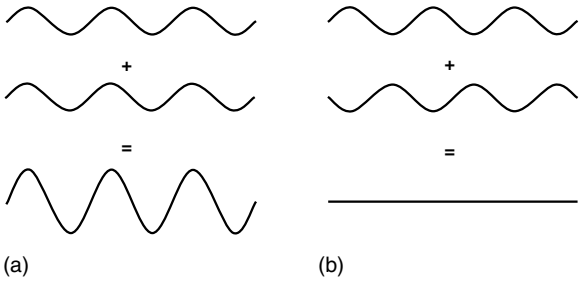

Fig. 2.12 The effects of two waves travelling through the same medium are added, i.e. the waves interfere with each other: (a) waves with the same phase interfere constructively (add); (b) waves with opposite phase interfere destructively (cancel).

the troughs of the other. Hence, at each point in the medium the particles are being pushed in one direction by the first wave and by the same pressure in the opposite direction by the second wave. The resulting pressure on the particles is zero and the effects of the waves cancel out. This case is referred to as destructive interference.

Diffraction

When a source generates a sound wave, the way in which the wave spreads out as it moves away from the source is determined by the relationship between the width of the source (the aperture) and the wavelength of the wave. If the aperture is smaller than the wavelength, the wave spreads out as it travels (diverges), an effect known as diffraction. This is rather like the wave on a pond, spreading out from the point of entry of a small stone. For a sound wave from a small point source inside a medium, the wave spreads out as an expanding sphere (a spherical wave) rather than a circle as on a water surface. The small scattering targets within tissue described earlier effectively act as sources of such spherical waves.

If the width of the source is much greater than the wavelength of the wave, the waves are relatively flat (plane) rather than curved and lie parallel to the surface of the source. Such waves travel in a direction perpendicular to the surface of the source with relatively little sideways spread, i.e. in the form of a parallel-sided beam.

These two different cases of curved waves from a small source and plane waves from a large source can be linked by considering the large source to be made up of a long row of small sources, as shown in Figure 2.13.

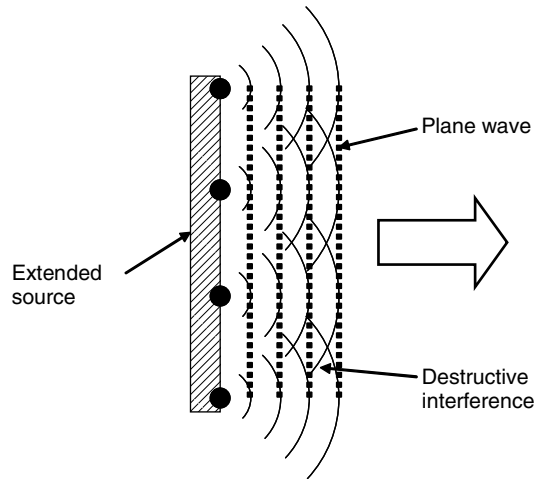

Fig. 2.13 An extended source can be considered as a row of small point sources (only four points shown for clarity). Spherical waves from each interfere to form a series of wave fronts.

Each of the small sources generates a sound wave of the same frequency and amplitude and all are in phase with each other. The curved waves from each propagate outwards and the parts of the curve which are parallel to the surface of the source align to form plane waves. The other, non-parallel parts of the curved waves tend to interfere destructively and cancel out. The diagram shows only four point sources for clarity, but in practice the large source is considered as a continuous series of small sources. This view of the generation of a plane wave from a large plane source is put to practical use in forming ultrasound beams from rows of small sources (array transducers) as described in the next chapter.

Ultrasound beams from practical sources

An ideal ultrasound beam would be one that is very narrow throughout its whole length. This would allow fine detail to be resolved at all imaged depths. However, at the frequencies available for ultrasound diagnosis, a parallel-sided beam would require a source which is too wide to be useful in forming images, as it would need to be many wavelengths across. A very narrow source would give a beam which is narrow near the source but diverges rapidly and again is not useful for forming images. Practical ultrasound sources must compromise between these two extremes to give the optimum combination of narrow beam width and minimal divergence.

The plane disc source

One example of a practical source of ultrasound is a plane disc transducer, also referred to as a plane circular piston source. The surface of this source is a flat disc and it is assumed that all parts of the surface move backwards and forwards exactly in phase and with the same amplitude. The surface of the disc source can be considered to be made up of many small elements, each of which emits a spherical wave. The pressure amplitude at each point in the beam is determined by the sum of the spherical waves from all of the elements (Figure 2.14). The different path lengths, from the various elements to the summing point, mean that each of the spherical waves has a different phase when it arrives. At some points, this results in overall constructive interference, giving rise to an amplitude maximum. At other points, the overall effect is destructive and a minimum is formed. At points close to the source, the path lengths can be different by several wavelengths.

The basic shape of the ultrasound beam produced by a plane disc transducer is illustrated in Figure 2.15a. To a first approximation, it can be divided into two parts. These are:

(1) the near field, which is roughly cylindrical in shape and has approximately the same diameter as the source and
(2) the far field, which diverges gradually.

Figure 2.15b shows the real distribution of pressure amplitude within a beam from a plane disc source. Within the near field, the pressure amplitude of the wave is not constant everywhere, but shows many peaks and troughs. As the source is circular, these pressure variations have circular symmetry. That is, the peaks and troughs are in the form of rings centred on the beam axis. The end of the near field is defined as being the distance from the source at which the maximum path length difference is $\lambda/2$. This distance, the near field length, is given by the expression a^2/λ, where a is the radius of the source. Figure 2.15c shows that the pressure amplitude along the beam axis reaches a final maximum value at this point.

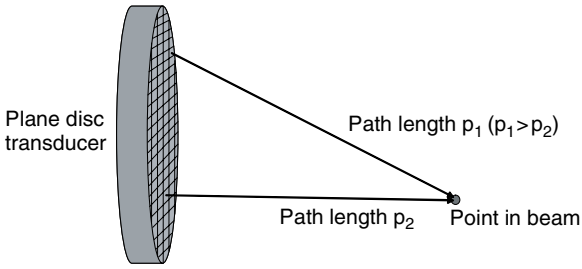

Fig. 2.14 The surface of the disc source can be considered to be made up of many small elements, each of which emits a spherical wave. The pressure amplitude at each point in the beam is determined by the sum of the spherical waves from all of the elements. The different path lengths, from the various elements to the summing point, mean that each of the spherical waves has a different phase when it arrives.

In the far field, destructive interference does not occur in the central lobe of the beam, as the path length differences are all less than $\lambda/2$. The resulting beam structure is relatively simple, showing a maximum value on the beam axis, which falls away uniformly with radial distance from the axis. The intensity along the beam axis in the far field falls approximately as the inverse square law, i.e. proportional to $1/z^2$, where z is the distance from the transducer.

The beam diverges in the far field at an angle given by $\sin \theta = 0.61\ (\lambda/a)$, where θ is the angle between the beam axis and the edges of the central lobe of the beam.

Hence, when the aperture a is similar in size to the wavelength λ, the near field is short and the beam diverges rapidly in the far field, i.e. θ is large. When a is large compared to λ, the near field is long and there is little divergence in the far field, i.e. θ is small. For this type of source, the optimum beam shape is achieved when it is 20 to 30 wavelengths in diameter. For example, a 3 MHz source with a radius of 7.5 mm (diameter = 30 λ) has a near-field length of 112.5 mm and an angle of divergence of 2.3° in the far field. A 10 MHz source with a radius of 2 mm has a near-field length of 27 mm and an angle of divergence in the far field of 2.6°. Hence, increased frequency allows the source diameter and the beam width to be scaled down while maintaining the beam shape in terms of low divergence in the far field.

This description of a beam from a disc source relates to what is called the 'main lobe' of the beam. The angle of divergence θ defines the edge of the main lobe in the far field because destructive interference causes a minimum to be formed in the pattern of interference at that angle. At increasing angles to the main lobe greater than θ, alternate maxima and minima are formed, as can be seen in Figure 2.15b. The regions containing these maxima are referred to as side lobes. Side lobes are weaker than the main lobe but can give rise to significant echoes if they are incident on a strongly reflecting

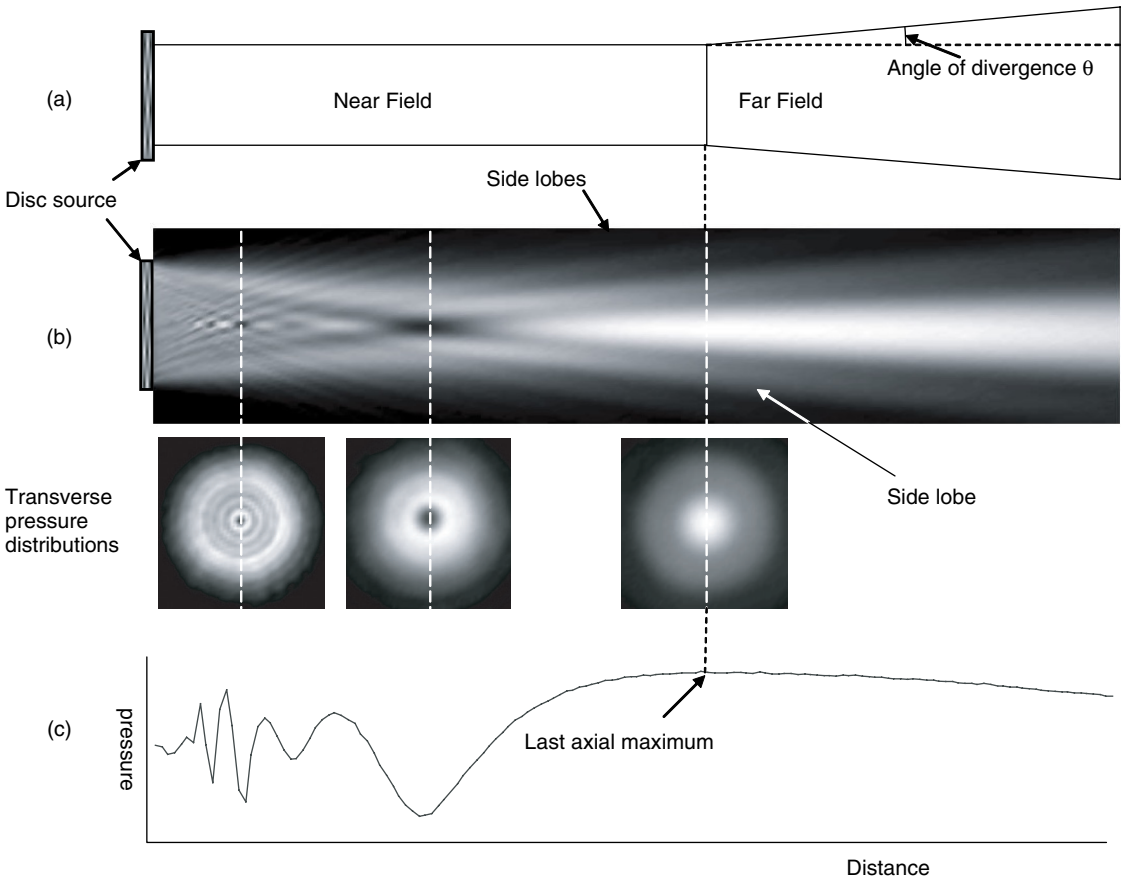

Fig. 2.15 The ultrasound beam from a plane disc source consists of a near field, in which the pressure distribution is complex, and a far field, in which it is more uniform.

target adjacent to the main lobe, resulting in acoustic noise in the image. Manufacturers normally design their transducers to minimize side lobes. This can be done by applying stronger excitation to the centre of the transducer than at the edges, a technique known as apodization. Apodization reduces the amplitude of side lobes but leads to an increase in the width of the main lobe.

This description of the beam from a plane disc-shaped source assumes that the transmitted wave is continuous and hence contains only a single frequency. For imaging purposes, the source must produce a short burst or pulse of ultrasound, which gives distinct echoes from interfaces. As described later, a short pulse contains energy at a range of frequencies rather than just one, each of which produces a slightly different beam. These are effectively added together in the pulsed beam, resulting in smearing out of the pressure variations compared to those in the continuous-wave beam shown in Figure 2.15.

Focusing

For imaging purposes, a narrow ultrasound beam is desirable as it allows closely spaced targets to be shown separately in the image. For a practical plane disc source of a given frequency, the aperture is chosen to give the best compromise between beam width and beam divergence.

A worthwhile improvement to the overall beam width can be obtained by focusing. Here, the source is designed to produce wave fronts which are concave rather than flat, as shown in Figure 2.16a. Each part of the concave wave travels at right angles to its surface, so that the waves converge towards a point in the beam, the focus, where the beam achieves its minimum width. Beyond the focus, the waves become convex and the beam diverges again, but more rapidly than for an unfocused beam with the same aperture and frequency. The distance from the source to the focus is the focal length *F*.

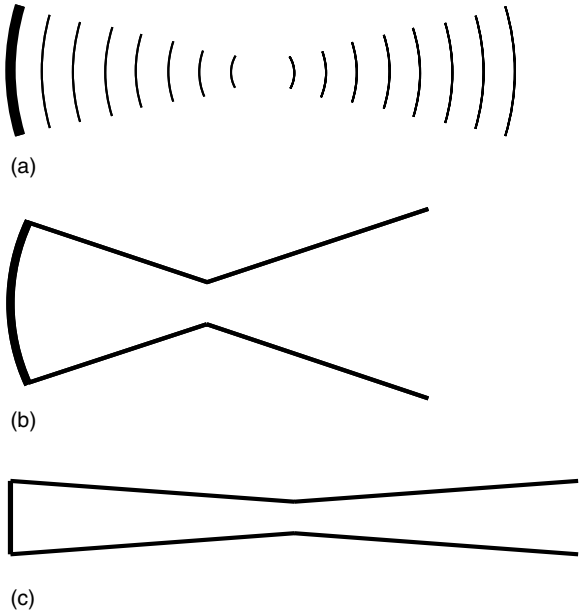

Fig. 2.16 Focusing of ultrasound beams: (a) the wave fronts from a curved source converge towards a focus; (b) the effect is strong if the focus is in the first part of the near field; (c) focusing is weak beyond half the near-field length.

The focusing effect on a beam is strongest when the focal length F is short in relation to the near-field length of a similar unfocused transducer (Figure 2.16b). Here, the waves converge rapidly to a very narrow beam width at the focus then diverge rapidly again beyond that point.

The beam width W at the focus for strong focusing is given approximately by the equation $W = F\lambda/a$. Focusing is weak (Figure 2.16c) when the focal length F is more than half of the near-field length (Kossoff 1979).

For a single-element source, focusing is usually achieved in one of two ways. These are by use of:

(1) a curved source and

(2) an acoustic lens.

The curved source (Figure 2.17a) is manufactured with a radius of curvature of F and hence produces curved wave fronts which converge at a focus F cm from the source. An acoustic lens is attached to the face of a flat source and produces curved wave fronts by refraction at its outer surface as in the case of an optical lens (Figure 2.17b). A convex lens is made from material which has a lower speed of sound than tissue. Wave fronts from the source pass into the lens at

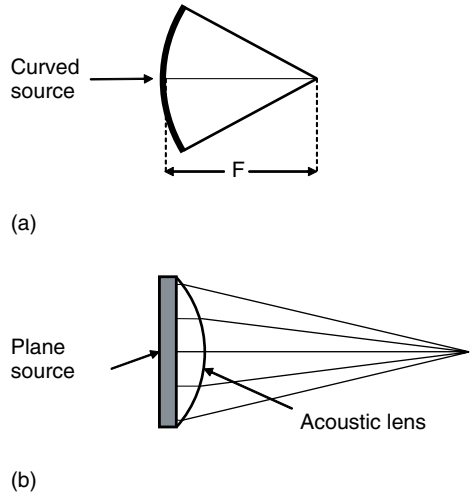

Fig. 2.17 Focusing methods: (a) focusing can be achieved by using a curved source; (b) focusing can also be achieved by adding an acoustic lens to a plane source.

normal incidence and are undeviated. On arrival at the interface between the lens and tissues, the increase in the speed of sound causes the direction of propagation to be deviated away from the normal and a converging wave front is formed.

The ultrasound pulse

As described earlier, a B-mode image is formed from echoes produced by reflection from interfaces and scattering from smaller targets. To produce a distinct echo which corresponds to a particular interface, ultrasound must be transmitted in the form of a short burst or pulse. To allow echoes from closely spaced interfaces to be resolved separately, the pulse must be short. A typical ultrasound pulse consists of a few cycles of oscillation at the nominal frequency of the wave, as illustrated in Figure 2.18a. The wave amplitude increases rapidly at the leading edge, reaches a peak and then decreases more slowly in the trailing edge.

The pulse spectrum

When a source is excited continuously to produce a continuous wave whose pressure varies as a pure sine wave, the wave has a specific frequency. A graph of wave amplitude against frequency would show a single value at that frequency and zero at other frequencies. A pulsed wave can be described as being constructed from a range of frequencies centred on the nominal frequency. Interference between the components at the

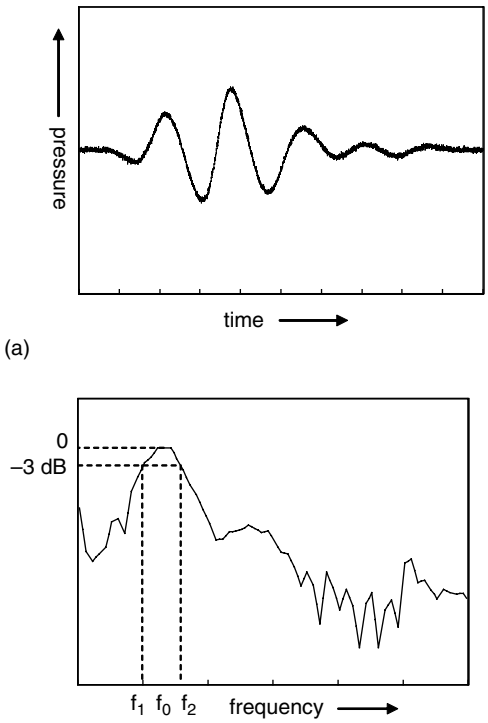

Fig. 2.18 The pressure waveform and spectrum of a typical ultrasound pulse: (a) a typical ultrasound pulse consists of a few cycles of oscillation; (b) the pulse contains a range of frequencies (a spectrum) dominated by a centre frequency f_0.

different frequencies effectively results in the formation of a pulse. The graph of amplitude versus frequency for a pulse shows a distribution of frequency components centred on the nominal frequency or centre frequency (Figure 2.18b). A short pulse contains a wide range of frequencies.

A short pulse gives precise time resolution and hence distance resolution and its echoes contain information at a wide range of frequencies. The information contained in an echo from a long pulse is concentrated near the nominal frequency and gives a stronger signal at that frequency. However, a long pulse results in poor distance resolution.

The graph of amplitude versus frequency for a pulse is termed the pulse spectrum and the range of frequencies it contains is the bandwidth. The width of the spectrum is commonly measured in terms of the −3 dB bandwidth (Figure 2.18b), which is the difference between frequency values above (f_2) and below (f_1) the peak frequency (f_0) at which the amplitude of the spectrum has fallen by 3 dB from its maximum value.

Non-linear propagation

In the description of propagation of sound waves given earlier in this chapter, the wave propagated with a fixed speed determined by the properties of the medium. It was also assumed that there was a linear relationship between the amplitude of the wave at the source and the amplitude elsewhere in the beam. Adding two waves with the same amplitude and phase resulted in a wave with twice the amplitude. This description of linear propagation is a good approximation to reality when the amplitude of the wave is small.

At high pressure amplitudes (>1 MPa), this simple picture breaks down and non-linear propagation effects become noticeable (Duck 2002, Humphrey 2000). The speed at which each part of the wave travels is related to the properties of the medium and to the local particle velocity, which enhances or reduces the local speed. At high pressure amplitudes, the medium becomes compressed, resulting in an increase in its stiffness and hence an increase in the speed of sound. In addition, the effect of particle velocity becomes significant. In the high-pressure (compression) parts of the wave, particle motion is in the direction of propagation, resulting in a slight increase in phase speed, whereas in the low-pressure (rarefaction) parts of the wave motion is in the opposite direction and the phase speed is slightly reduced. As the wave propagates into the medium, the compression parts of the wave gradually catch up with the rarefaction parts. In a plane wave, the leading edges of the compression parts of the wave become steeper and may form a 'shock' front, an instantaneous decrease in pressure. In diagnostic beams (Figure 2.19a shows a diagnostic pulse propagating in water), the compression parts become taller and narrower, while the rarefaction parts become lower in amplitude and longer (Duck 2002).

The rapid changes in pressure in the compression part of the wave appear in the pulse spectrum as high-frequency components. As shown in Figure 2.19b, these are multiples of the original or fundamental frequency f_0 known as harmonics. A frequency of $2f_0$ is known as the second harmonic, $3f_0$ as the third harmonic and so on. The figure shows that the original pulse spectrum is effectively repeated at these harmonic frequencies. Non-linear propagation results in some of the energy in the pulse being transferred from the fundamental frequency f_0 to its harmonics. As the pulse travels further into the medium, the high-frequency components are

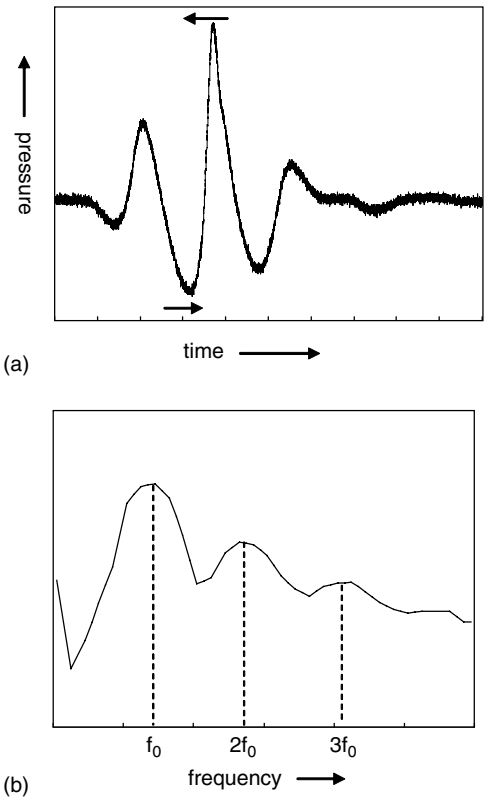

Fig. 2.19 The pulse waveform and spectrum for a high-amplitude pulse: (a) at high pressure amplitudes, the pulse waveform becomes distorted due to non-linear propagation; (b) the spectrum of the distorted pulse contains significant components at multiples of the centre frequency (harmonics).

attenuated more rapidly than the low-frequency components and the pulse shape becomes more rounded again as the overall amplitude is reduced.

Harmonic imaging

The changes in the pulse spectrum are put to good use in harmonic imaging, as described in Chapter 4. In harmonic imaging, a pulse is transmitted with fundamental frequency f_0, but due to non-linear propagation the echoes returned from within the tissues contain energy at harmonic frequencies $2f_0$, $3f_0$, etc. The imaging system ignores the frequencies in the fundamental part of the spectrum and forms an image using only the second harmonic ($2f_0$) part of the pulse (Desser *et al.* 2000, Tranquart *et al.* 1999). The effective ultrasound beam which this produces, the harmonic beam, is narrower than the conventional beam

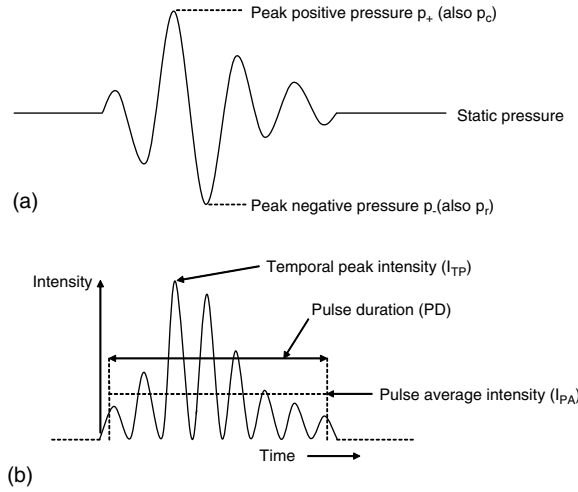

Fig 2.20. (a) The peak positive and peak negative pressures are the maximum and minimum values of pressure in the medium during the passage of an ultrasound pulse. (b) The intensity is related to the pressure squared and is always positive. The temporal peak intensity is the maximum value during the pulse. The pulse average intensity is the average value over the duration of the pulse.

and suppresses artefacts such as side lobes. This is due to the fact that non-linear propagation and hence the formation of harmonics occurs most strongly in the highest-amplitude parts of the transmitted beam, i.e. near the beam axis. Weaker parts of the beam such as the side lobes and edges of the main lobe produce little harmonic energy and are suppressed in relation to the central part of the beam. Harmonic imaging can also reduce other forms of acoustic noise such as the weak echoes due to reverberations and multiple path artefacts, as described in Chapter 5.

Acoustic pressure and intensities within the ultrasound beam

As described earlier in this chapter, when an ultrasound wave passes a point in a medium, the particles of the medium are alternately compressed together and pulled apart, leading to oscillations in the local pressure. The local pressure variation due to the passage of a typical ultrasound pulse is illustrated in Figure 2.20a. The maximum value of pressure during the passage of the pulse is the peak positive pressure or peak compression. The minimum value of pressure is the peak negative pressure or peak rarefaction. Before and after the passage of the pulse, the pressure in the medium

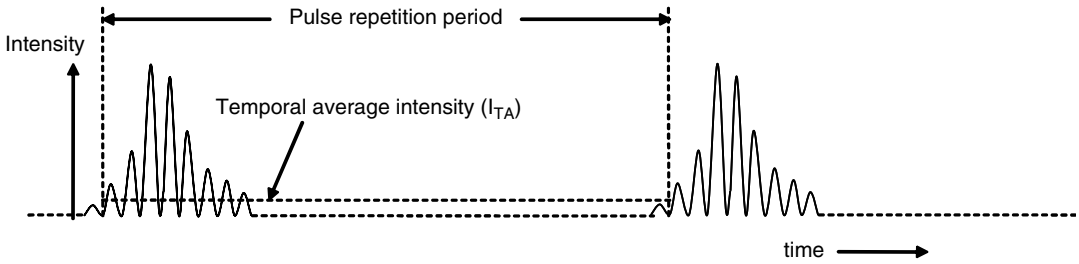

Fig. 2.21. The intensity waveform is repeated with every pulse–echo cycle. The temporal average intensity is the average value over a complete pulse–echo cycle and is much lower than the pulse average intensity.

is the local static pressure. The local acoustic pressure variations due to the passage of a pulse along the beam may be measured using a hydrophone, as described in Appendix E.

The local intensity variations associated with the pulse and the beam may be derived from the pressure variations using the following equation:

$$I = \frac{p^2}{z}$$

Where I and p are the instantaneous values of intensity and pressure respectively and z is the acoustic impedance of the medium. Figure 2.20b shows the intensity waveform corresponding to the pressure waveform above. Note that because the values of pressure at each point in the waveform are squared, all values of intensity are positive. Each positive and negative peak in the pressure waveform results in a peak in the intensity waveform. The maximum value of intensity during the passage of the pulse is the temporal peak intensity.

The time taken for the pulse to pass a point in the medium is the pulse duration (PD). As the start and finish of the intensity waveform can be difficult to define, the accepted method for calculating the pulse duration involves integrating the waveform to give the pulse intensity integral (AIUM/NEMA 2004). This takes the form of a rising staircase from zero to the final value of the integral (PII) as the pulse passes. The time interval between the points at which the staircase reaches the 10% and 90% values (T_{10} and T_{90}) of the final value is measured. The pulse duration is given by:

$$\mathrm{PD} = 1.25 \times \left(T_{90} - T_{10}\right)$$

The pulse average intensity I_{PA} is the average value of intensity during the pulse. This is calculated from:

$$I_{PA} = \mathrm{PII} / \mathrm{PD}$$

Assuming a stationary beam, the intensity waveform is repeated at the point in the medium with each pulse–echo cycle (see Chapter 3). The rate at which the waveform is repeated is the pulse repetition frequency. The intensity waveform may be averaged over the duration of one complete pulse–echo cycle to give the temporal average intensity I_{TA} (Figure 2.21). I_{TA} is much smaller than I_{PA} because the average includes the relatively long time between pulses, which is approximately 1000-times longer than the duration of the pulse itself. I_{TA} is a useful measure of the rate at which energy deposition may accumulate in the tissue, resulting in heating effects.

It is clear from Figure 2.15 that the values of pressure, and consequently the various intensity parameters, change with position in the beam. The highest value in the beam of any given intensity parameter is the spatial peak intensity (Figure 2.22). The intensity may also be averaged over the cross-sectional area of the beam to give the spatial average intensity.

To give complete specifications of intensity parameters within an ultrasound beam, the temporal and spatial intensity definitions are combined. These give intensity parameters, which are useful in characterizing the acoustic output of ultrasound systems. The most commonly used combinations are as follows:

I_{sptp} – the spatial peak temporal peak intensity is the maximum value in the pulse at the point in the beam where it is highest.

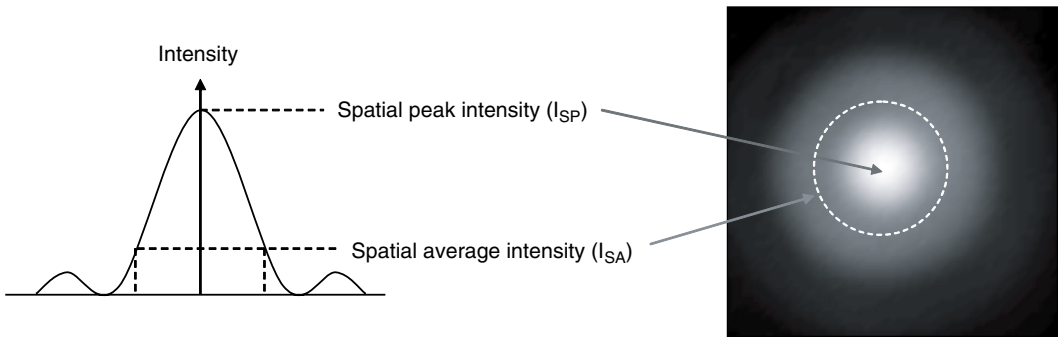

Fig. 2.22. The values of the various intensity parameters change with position in the beam also. The highest value in the beam is the spatial peak intensity. The average value over the area of the beam is the spatial average intensity.

I_{sppa} – the spatial peak pulse average intensity is the average value over the pulse duration at the point in the beam where it is highest.

I_{spta} – the spatial peak temporal average intensity is temporal average intensity at the point in the beam where it is highest.

I_{sata} – the spatial average temporal average intensity is the temporal average intensity averaged over the beam area (usually –6 dB area).

For further reading on characterization of ultrasound beams, see Preston (1991).

Questions

1. Explain the term acoustic impedance and state the tissue properties which determine its value.
2. What is the difference between acoustic impedance and acoustic absorption?
3. A medium attenuates ultrasound at a rate of 0.7 dB cm^{-1} MHz^{-1}. A target at a depth of 5 cm below the transducer is imaged with a 3 MHz ultrasound pulse. By how many dB will the echo from the target be attenuated compared to a similar target at a depth of 1 cm?
4. Explain why bone and gas limit the areas of clinical application of ultrasound.
5. Two tissue types have speed of sound and density of (a) 1580 m s^{-1} and 1.1×10^3 kg m^{-3} and (b) 1460 m s^{-1} and 0.9×10^3 kg m^{-3}. Calculate the intensity reflection coefficient for a large interface between them.
6. Explain the term refraction and how it might affect ultrasound images.
7. A plane disc transducer, with a diameter of 1.5 cm, is driven at 3 MHz to produce a continuous-wave beam in tissue with a speed of sound of 1500 m s^{-1}. (a) Calculate the near-field length of the beam and its angle of divergence in the far field. (b) Estimate the beam width at the focus if a lens is added with a focal length of 6 cm.
8. Explain how focusing of an ultrasound beam can be achieved and how its effects depend on the dimensions of the transducer and the ultrasound wavelength.
9. Explain the origin of acoustic noise in B-mode images and how it can be reduced by the use of harmonic imaging.
10. The peak value of acoustic pressure measured in an ultrasound beam in water is 1 MPa. What is the corresponding instantaneous intensity in W m^{-2}? Assume the speed of sound in water is 1500 m s^{-1} and its density is 1000 kg m^{-3}.

References

AIUM/NEMA UD3 rev. 2 (2004). *Standard for Real-Time Display of Thermal and Mechanical Acoustic Output Indices on Diagnostic Ultrasound Equipment*. UD 3–2004. American Institute for Ultrasound in Medicine / National Electrical Manufacturers Association, USA.

Desser TS, Jedrzejewicz T, Bradley C (2000) Native tissue harmonic imaging: basic principles and clinical applications. *Ultrasound Quarterly,* **16**, 40–8.

Dickinson RJ (1986). Reflection and scattering. In CR Hill, ed., *Physical Principles of Medical Ultrasonics*. Chichester: Ellis Horwood.

Duck FA (1990). *Physical Properties Of Tissue – A Comprehensive Reference Book*. London: Academic Press.

Duck FA (2002). Nonlinear acoustics in diagnostic ultrasound. *Ultrasound in Medicine and Biology*, **28**, 1–18.

Humphrey VF (2000). Nonlinear propagation in ultrasonic fields: measurements, modeling and harmonic imaging. *Ultrasonics,* **38**, 267–72.

Kossoff G (1979). Analysis of focusing action of spherically curved transducers. *Ultrasound in Medicine and Biology,* **5**, 359–65.

Parker KJ (1983). Ultrasonic attenuation and absorption in liver tissue. *Ultrasound in Medicine and Biology,* **9**, 363–9.

Preston RC , ed. (1991). *Output Measurements for Medical Ultrasound*. Berlin: Springer.

Tranquart F, Grenier N, Eder V, Pourcelot L (1999). Clinical use of ultrasound tissue harmonic imaging. *Ultrasound in Medicine and Biology,* **25**, 889–94.

Chapter 3

Transducers and beam-forming

Tony Whittingham and Kevin Martin

Introduction

The basic principles of B-mode scanning were introduced in Chapter 1. The way the beam is formed and swept through the patient (scanned) in different types of scanner will now be described in more detail.

The *transducer* is the device that actually converts electrical transmission pulses into ultrasonic pulses and, conversely, ultrasonic echo pulses into electrical echo signals. The simplest way to interrogate all the scan lines that make up a B-mode image is to physically move the transducer so that the beam is swept through the tissues as the pulse–echo cycle is repeated. This was the original method used but it has been superseded by electronic scanning methods which use multi-element array transducers with no moving parts. Array transducers allow the beam to be moved instantly between positions, and give the additional benefit of allowing the shape and size of the beam to be changed to suit the needs of each examination. The *beam-former* is the part of the scanner that determines the shape, size and position of the interrogating beams by controlling electrical signals to and from the transducer array elements. In transmission, it generates the electrical signals that drive each individual transducer element, and in reception it combines the individual echo sequences received by all the transducer elements into a single echo sequence.

The echo sequence produced by the beam-former for each scan line is then amplified and processed in various ways before being used in the formation of the B-mode image. These processes are the subject of Chapter 4.

Which beam do you mean?

Before discussing transducers and beam-forming further, it will be helpful to consider the idea of beams a little more. In Chapter 2, the shape and size of the beam transmitted by a simple disc transducer were discussed. In most imaging techniques, ultrasound is transmitted in short pulses. The 'transmission beam' then represents the 'corridor' along which the pulses travel. The lateral extent of the pulse is determined by the width of the beam at each depth.

It is also possible to talk of a 'receive beam', which describes the region in which a point source of ultrasound must lie if it is to produce a detectable electrical signal at the receiving transducer. In the case of a simple disc transducer, since the same transducer is used for both transmission and reception (at different times, of course), the transmission beam has an identical shape and size to the receive beam. In other words, the points in the transmission beam that have the greatest intensity will also be the points in the receive beam where a point source would produce the greatest electrical signal at the transducer. However, in the case of array transducers, the combination of transducer elements used for transmission is usually different from that used for reception, and so the two beams are different in shape and size.

Figure 3.1 shows a beam from an array transducer. This is moved electronically along the length of the transducer face, sweeping out a flat scan plane, which defines the image cross section obtained from the patient. The plane illustrated, which passes through the beam at right angles to the scan plane, is the elevation plane. The shape and size of the beam in the scan plane are different from those in the elevation plane, and it is necessary to be clear which plane is being considered. The beam width in the scan plane determines what is referred to as the lateral resolution of the scanner, whereas that in the elevation plane defines the 'slice thickness', and hence the acoustic noise of the image and, to some extent, the sensitivity of the scanner. The transmitting and receiving apertures of array transducers are generally rectangular rather

Diagnostic Ultrasound: Physics and Equipment, ed. Peter Hoskins, Kevin Martin and Abigail Thrush. Published by Cambridge University Press.

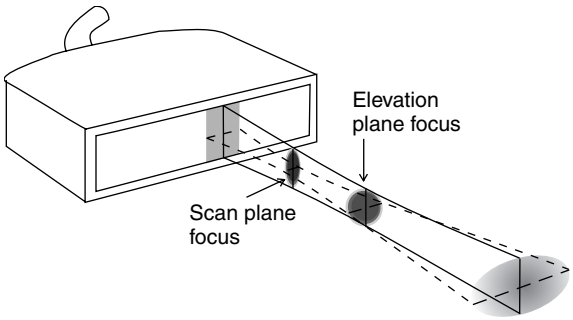

Fig. 3.1 The rectangular beam aperture of an array transducer produces a beam with non-circular cross-sections. In this example, the focal beam width in the vertical (elevation) direction is wider and at a greater range than that in the horizontal (scan) plane.

than circular. This results in the beams having rectangular cross sections close to the transducer, becoming roughly elliptical towards the focal region and beyond. These topics are discussed under the headings of the different types of transducer below. Lateral resolution and slice thickness are also discussed more fully in Chapter 5.

Common features of all transducers and transducer elements

All transducers or transducer elements have the same basic components: a piezoelectric plate, a matching layer and a backing layer, as shown in Figure 3.2. Usually, there is also a lens, but in array transducers it is usual for one large lens to extend across all the transducer elements. The number, size, shape and arrangement of transducer elements vary according to the transducer type and application, but these will be addressed in detail later, as each transducer type is discussed.

Piezoelectric plate

The actual sound-generating and detecting component is a thin piezoelectric plate. Piezoelectric materials expand or contract when a positive or negative electrical voltage is applied across them and, conversely, generate positive or negative voltages when compressed or stretched by an external force (Figure 3.3). Some piezoelectric materials, such as quartz, occur naturally but the piezoelectric material normally used for transducers in medical imaging is a synthetic ceramic material: lead zirconate titanate (PZT). Various types of PZT are available and are chosen according to the

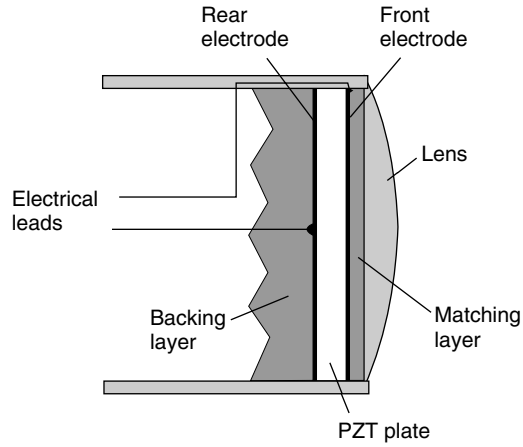

Fig. 3.2 The basic component elements in an imaging ultrasound transducer.

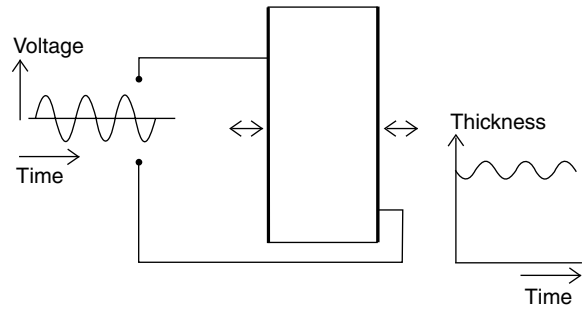

Fig. 3.3 Changes in voltage across a PZT plate produce corresponding changes in thickness.

properties required, such as high sensitivity, or the ability to cope with large acoustic powers.

The thin plate of PZT is coated on both sides with conductive paint, forming electrodes, to which electrical connections are bonded. In order to transmit an ultrasonic pulse, a corresponding oscillating voltage is applied to the electrodes, making the PZT element expand and contract at the required frequency (Figure 3.3). The back and forth movements of the front face send an ultrasonic wave into the patient's tissues. In reception, the pressure variations of returning echoes cause the PZT plate to contract and expand. The voltage generated at the electrodes is directly proportional to the pressure variations, giving an electrical version (the echo signal) of the ultrasonic echo.

The PZT slab vibrates most strongly at the frequency for which its thickness is half a wavelength, giving rise to the term 'half-wave resonance'. Resonance occurs because an ultrasound wave propagating across the thickness of the PZT plate is partially reflected at the front and back faces, and thus continues to travel

back and forth (reverberate) within the PZT plate. As the plate thickness is equal to half the wavelength, the wave travels a full wavelength in the PZT on each round trip. This means that the reflected wave arrives back in phase with the original wave, and adds constructively to it to produce a greater output. A PZT plate with a thickness equal to half a wavelength[1] at the required centre frequency is therefore used, as this will resonate and produce a large output at this frequency.

Backing layer

PZT has advantages as a transducer material in that it is efficient at converting electrical energy to mechanical energy, and vice versa, and is relatively easy to machine or mould to any required shape or size. However, it has one significant disadvantage in that it has a characteristic acoustic impedance that is about 20-times higher than that of the soft tissue. If the front face of the PZT plate were to be in direct contact with the patient, a large fraction (approximately 80%) of the ultrasound wave's power would be reflected at the PZT–tissue interface (see 'Reflection' in Chapter 2). If nothing were to be done about this, the internal reverberations within the PZT, referred to above, would be very strong and would continue long after the applied driving voltage had finished.

This unwanted ringing can be much reduced by having a backing (damping) layer behind the PZT, made of a material with both a high characteristic acoustic impedance and the ability to absorb ultrasound. If the impedance of the backing layer were identical to that of PZT, all the sound energy would cross the boundary between the PZT and the backing layer, and none would be reflected back into the PZT. Once in the backing layer the sound would be completely absorbed and converted into heat. This would eliminate ringing, but would be at the expense of sensitivity, as some of the energy of the electrical driving pulse and also of the returning echo sound pulses would be wasted as heat in the backing layer. In modern practice, a backing layer with an impedance somewhat lower than that of the PZT is used. This compromise impedance is chosen to give a useful reduction in reflection without lowering sensitivity too much. The remaining ringing is removed by using matching layers, as discussed next.

[1] The wavelength here is calculated using the speed with which sound propagates between the two flat faces of the PZT plate. In array probes, discussed later, the plate is made up of PZT elements separated by narrow barriers (kerfs), having a lower speed of sound, so the average speed across the plate is lower than that in pure PZT.

Matching layer(s)

Apart from the ringing problem, the fact that only about 20% of the wave's power would be transmitted through the front PZT–patient interface means there is also a potential problem of poor sensitivity. In order to overcome this, at least one 'impedance matching layer' is bonded to the front face of the PZT. A single matching layer can increase the transmission across the front face to 100%, provided that two important conditions are met. First, the matching layer should have a thickness equal to a quarter of a wavelength. Second, it should have an impedance equal to $\sqrt{(z_{PZT} \bullet z_T)}$, where z_{PZT} is the impedance of PZT and z_T is the impedance of tissue. The explanation behind this remarkable achievement is that the sound reverberates back and forth repeatedly within the matching layer, producing a series of overlapping waves, at the interface to the patient, that are in phase with each other and hence combine to give a large resultant wave. At the same time, another series of waves is sent back into the PZT, which together exactly cancel out the wave originally reflected at the PZT–matching layer interface (Figure 3.4).

One hundred per cent transmission through the matching layer only occurs at one frequency for which its thickness is exactly one-quarter of a wavelength. It is normal to choose the matching layer thickness to be correct for the centre frequency of the pulse, as there is more energy at this frequency than at any other. Smaller, but nevertheless worthwhile, improvements in transmission will occur at frequencies close to the centre frequency. However, at frequencies well removed from the centre frequency the matching layer

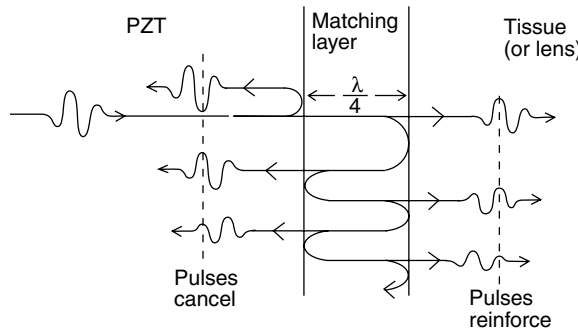

Fig. 3.4 Quarter-wave matching layer. Reverberations within the plate produce multiple transmissions into the patient that reinforce each other to give a large-amplitude resultant pulse. The resultant of the multiple reflections back into the PZT cancel out the original (top) reflection back into the backing layer.

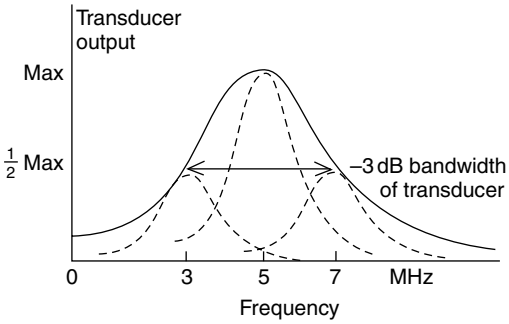

Fig. 3.5 The −3 dB bandwidth of a transducer is the range of frequencies over which the output power for a given applied peak-to-peak voltage is within a factor of 2 of the maximum. A multi-frequency probe must have a large bandwidth, so that it can transmit and receive pulses with several different centre frequencies (pulse spectra shown dashed).

will not be very effective. A −3 dB transducer bandwidth (Figure 3.5) can be defined, in a similar way to the pulse bandwidth, described in Chapter 2. For a transducer, it is the range of frequencies over which its efficiency, as a converter of electrical energy to sound energy or vice versa, is more than half its maximum. It is evident that, although the matching layer improves sensitivity at the centre frequency, it also acts as a frequency filter, reducing the bandwidth. For a transducer with a matching layer, a −3 dB bandwidth of about 60% of the centre frequency can be achieved. Thus, a 3 MHz transducer with a matching layer could have a −3 dB bandwidth of up to 1.8 MHz.

A large transducer bandwidth is crucial to good axial resolution, since the latter depends on a large pulse bandwidth (consistent with a short pulse, for example) and the pulse bandwidth cannot be more than that of the transducer producing it. The transducer bandwidth can be increased by using two, or more, matching layers, progressively reducing in characteristic impedance from the PZT to the patient's skin. The reason why this leads to a greater bandwidth is that the impedance change, and hence the reflection coefficient, at the PZT front face is less than that for the case of a single matching layer. This applies at all frequencies, so there is less difference in the performance at the centre frequency relative to that at other frequencies. Improvements in backing layer and multiple-matching-layer technologies have meant that −3 dB bandwidths greater than 100% of centre frequency are now available.

A large transducer bandwidth is also needed for harmonic imaging (Chapter 4) and other modern developments. It is also a prerequisite of a 'multi-frequency transducer'. This type of transducer allows the operator to select one of a choice of operating frequencies according to the penetration required. Whatever centre frequency is selected, short bursts of oscillating voltage at that frequency are applied across the PZT plate to produce the ultrasound transmission pulses. At the same time, the receiving amplifiers (Chapter 4) are tuned to that frequency. In order for a single transducer to be able to operate at three frequencies, say 3, 5 and 7 MHz, it would need to have a centre frequency of 5 MHz and a bandwidth of 4 MHz, which is 80% of the centre frequency (Figure 3.5). Note that the bandwidths of the pulses generated at the upper and lower frequencies must be less than that of the transducer itself – this means the axial resolution to be expected from a probe in multi-frequency mode will be less than that which would be possible if the whole transducer bandwidth were used to generate a full 5 MHz bandwidth pulse.

Lens

A lens is usually incorporated after the matching layer. Near the focus of the lens, the width of the beam is least and the transmitted amplitude, or receive sensitivity, is greatest. In linear-array transducers, focusing in the scan plane is achieved entirely by electronic means, and so a cylindrical lens, producing focusing only in the plane perpendicular to the scan plane (elevation plane), is used. In phased-array transducers (see later) the lens may have some curvature (focusing action) in the scan plane as well as in the elevation plane, in order to augment the electronic focusing in the scan plane.

For further reading on transducer design and construction, see McKeighen (1998).

Developments in transducer technology

The performance of the transducer in terms of its efficiency and bandwidth is critical to the overall performance of the ultrasound system. Transducer performance has been improved through the development of new materials and fabrication techniques and through the introduction of new transducer technologies. An important stage in the development of a transducer is the creation of a computer model of its acoustical and electrical behaviour. The model contains values for the acoustical and electrical properties of the materials and the dimensions of the elements. The model can be improved by comparing the predicted transducer performance with physical measurements. The effects of design modifications,

such as cutting individual array elements into two or three narrower sub-elements to reduce lateral modes of vibration, can then be tested and optimized before manufacture (Powell *et al.* 1997).

Traditional PZT materials are piezoceramics formed from small polycrystalline grains of the base materials, moulded to shape and fired at high temperatures. During transducer manufacture, the PZT must be polarized to activate its piezoelectric properties, by heating while a high voltage is applied to the electrodes. The granular structure limits the alignment of piezoelectric domains during this process and hence the piezoelectric efficiency of the device. Transducers are now commercially available which use alternative piezoelectric materials grown as single crystals. These include lead titanate (PT) doped with various other elements, such as lead, magnesium and niobium (PMN–PT) or lead, zinc and niobium (PZN–PT). When cut into wafers for transducer manufacture, the single-crystal structure allows complete polarization of the material and hence a stronger response in transmission and reception (greater sensitivity and penetration). The improved performance of these materials allows manufacturers to design transducers with increased bandwidth without loss of sensitivity, which is used to advantage in multi-frequency operation and harmonic imaging. However, the increased electrical and mechanical fragility of these materials at present limits their application to lower frequencies, which make use of greater element width and thickness (Chen and Panda 2005, Ming Lu and Proulx 2005).

Prototype transducers have been demonstrated using capacitive micro-machined silicon transducers. These are small hollow drums between a pair of electrodes manufactured using silicon technology developed for electronic components. When an electrical voltage is applied to the electrodes, the electrostatic attraction between them reduces the thickness of the drum. The effect can be used to generate ultrasound waves in a similar way to an electrostatic loudspeaker. The individual drums are only a few microns across and must be aggregated to form a transducer element for use at MHz frequencies. The use of silicon technology gives the possibility of fabricating the transducer and its associated electronics on the same piece of silicon (Daft *et al.* 2005).

Linear- and curvilinear-array transducers (beam-stepping arrays)

A common type of transducer is the linear array, or its curved version – the curvilinear array. Linear arrays offer a rectangular field of view (Figure 3.6) that maintains its width close up to the transducer face and are therefore particularly suitable when the region of interest extends right up to the surface (e.g. neck or limbs). Curvilinear arrays work in the same way as linear arrays, but differ in that the array of elements along the front face forms a curve, rather than a straight line. They share the same benefit of a wide field of view at the surface, but have the additional advantage that the field of view becomes wider with depth. They are therefore popular for abdominal applications, including obstetrics. However, in order to maintain full contact, it is necessary to press the convex front face slightly into the patient. This makes the linear array more suitable than the curvilinear array for applications where superficial structures, such as arteries or veins, should not be deformed, or where the skin is sensitive. An answer to this problem is offered by trapezoidal (virtual curvilinear) arrays, discussed later.

From the outside, a linear-array transducer appears as a moulded block designed to fit comfortably into the operator's hand with a rubber lens along the face that makes contact with the patient (Figure 3.7). Behind the lens is a matching layer, and behind this is a linear array of typically 128 regularly spaced, narrow, rectangular transducer elements, separated by narrow barriers

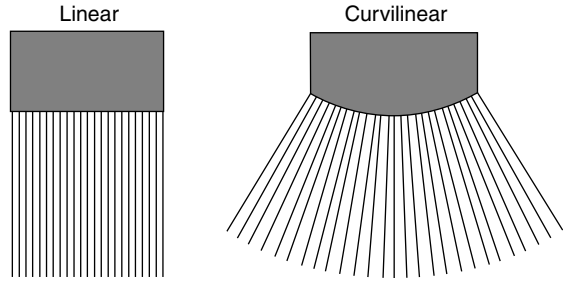

Fig. 3.6 Linear and curvilinear scan formats.

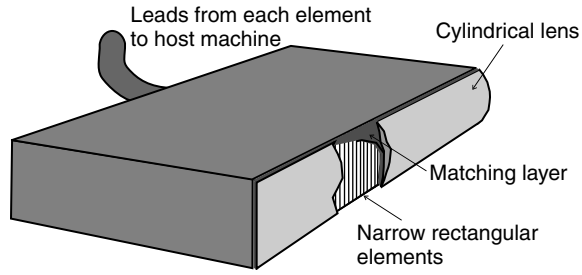

Fig. 3.7 Cut-away view of a linear-array transducer, showing the elements, matching layer and lens.

(kerfs), made of an inert material, usually a polymer or epoxy. Some linear-array transducers have as many as 256 elements, but cost considerations and fabrication difficulties mean that 128 is a more common number. Note that these numbers are chosen, rather than say 200 or 100, since they are 'round' numbers in binary terms, and hence more convenient for digital control and processing.

The width of each array element is typically about 1.3 wavelengths (λ), being a compromise that gives a reasonably wide array ($128 \times 1.3\,\lambda = 83$ mm at 3 MHz), and hence a wide field of view, while still allowing the elements to be narrow enough to radiate over a wide range of angles in the scan plane (Chapter 2). The longer side of each element determines the width of the beam in the elevation direction, and a typical value of about 30 λ means a weakly focused beam is possible. Weak focusing gives a reasonably narrow width at all depths. Since all transducer dimensions are proportional to wavelength, high-frequency transducers are smaller than low-frequency ones. Thus, assuming 128 elements, a 3 MHz (λ = 0.5 mm) transducer might typically have a lens face measuring about 85 mm by 15 mm, with each element being about 0.65 mm wide, whereas a 7.5 MHz (λ = 0.2 mm) transducer will have a lens face measuring about 35 mm by 6 mm, with each element being about 0.25 mm wide.

The front electrodes of all the elements are usually connected together, so they share a common electrical lead. However, the rear electrode of each element is provided with a separate electrical lead (Figure 3.8), allowing the signals to and from each element to be individually processed by the beam-former. In practice, each element is usually further 'sub-diced' into two or three even narrower elements. This is done because otherwise each element would be approximately as wide as it is thick[2] and an undesirable resonant vibration across the element width would accompany, and take energy from, the desired thickness vibration. This mechanical sub-dicing does not affect the number of electrically addressable elements, since the rear electrodes of the two or three sub-diced elements making up the original element are connected together and share a single lead.

[2] Although the typical element width of 1.3 λ might seem very different to the element thickness of 0.5 λ, the former is for a wave in tissue, while the latter is for a wave in PZT. Since the speed of sound, and hence the wavelength, in PZT is 2–3-times higher than it is in the tissue, the two dimensions are, in fact, similar.

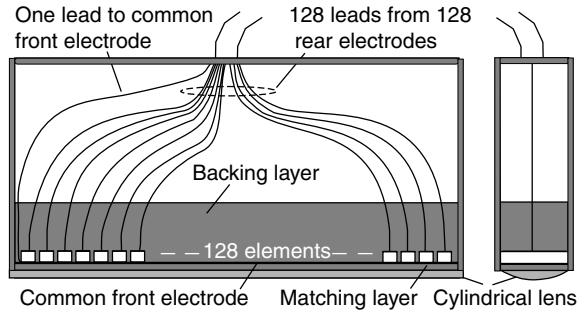

Fig. 3.8 Section through a linear-array transducer. For clarity, the sub-dicing of each element is not shown.

Active group of elements

In order to interrogate a particular scan line, an 'active group' of adjacent transducer elements, centred on the required scan line, is used. While that scan line is being interrogated, all the other elements in the probe are disconnected and idle. First, a pulse is transmitted, say using the central 20 elements of the group. This pulse travels along the transmit beam, centred on the scan line. As soon as the pulse has been transmitted, a different combination of elements, still centred on the scan line, act together as a receiving transducer, defining the receive beam. The number of elements used for reception is initially less than that used for transmission, but this number is progressively increased as echoes return from deeper and deeper targets until it eventually exceeds that used for transmission (see 'Scan plane dynamic focusing and aperture in reception' below). Both the transmit and receive beams can be focused, or otherwise altered, by controlling the signals to or from each of the elements in the active group, as described below.

Once all echoes have been received from one scan line, a new active group of elements, centred on the next scan line, is activated. This is achieved by dropping an element from one end of the old group and adding a new one at the other end (Figure 3.9). This advances the centre of the active group, and hence the scan line, by the width of one element. The new scan line is then interrogated by a new transmit and receive beam, centred on that line. The process is repeated until all the scan lines across the field of view have been interrogated, when a new sweep across the whole array is commenced.

Beam shape control in the scan plane

Scan plane focusing in transmission

Since the cylindrical lens does nothing to reduce the beam width in the scan plane, an electronic method

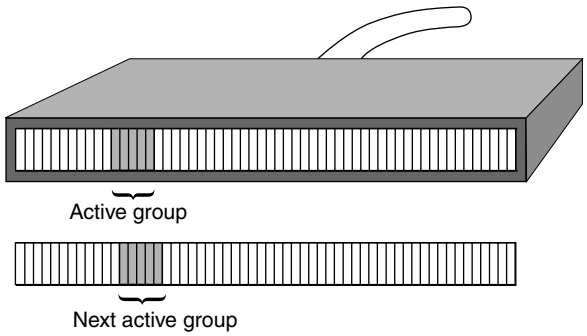

Fig. 3.9 The active group is stepped along the array by dropping an element from one end and adding a new on to the other. In reality, the active group would contain at least 20 elements rather than the five shown here.

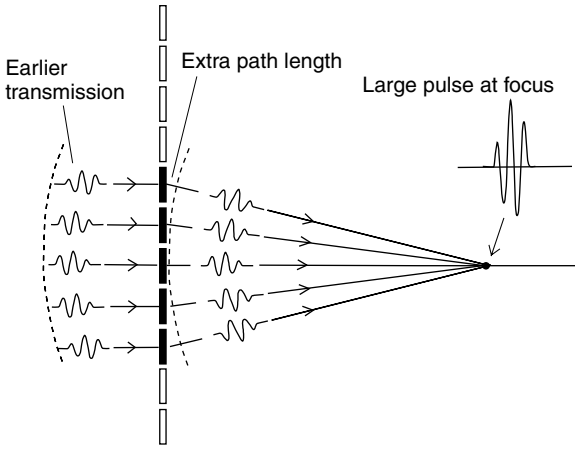

Fig. 3.10 Creating a transmission focus for a linear-array transducer. In order to form a large-amplitude pulse at the focus, pulses from all elements must arrive there at the same time. This is achieved by transmitting slightly earlier from elements that are further from the centre of the group.

of focusing must be provided, if good lateral resolution is to be achieved. This is controlled by the operator, who sets the transmission focus at the depth for which optimum lateral resolution is desired. This ensures that the transmission beam is as narrow as possible there (the receive beam must also be narrow there, but this is considered next). Usually an arrowhead or other indicator alongside the image indicates the depth at which the transmission focus has been set. Pulses from all the elements in the active group must arrive at the transmission focus simultaneously in order to concentrate the power into a narrow 'focal zone'. However, the distance between an element and the focus, which lies on the beam axis passing through the centre of the group, is slightly, but crucially, greater for the outer elements of the group than for more central elements. Pulses from elements further from the centre of the active group must, therefore, be transmitted slightly earlier than those nearer the centre (Figure 3.10). The manufacturer builds a look-up table into the machine for each possible choice of transmission focus depth available to the operator. These tell the controlling computer the appropriate 'early start' for each element. At points outside the required focal zone, the individual pulses from different elements arrive at different times, producing no more than weak acoustic noise.

Scan plane dynamic focusing and aperture in reception

Focusing in reception means that, for each scan line, the scanner is made particularly sensitive to echoes originating at a specified depth (the receive focus) on the scan line. This also results in the receive beam being narrowed near this focus, further improving lateral resolution. In order for the sensitivity to be high for an echo coming from, or near, the receive focus, the echo signals produced by all transducer elements in the active group must contribute simultaneously to the resultant electronic echo signal. As in the case of transmission focusing, allowance must be made for the fact that the distance between the required focus and a receiving element is greater for elements situated towards the outside of the group than for those near the centre. This is done by electronically delaying the electrical echo signals produced by all transducer elements except the outermost, before summing them together (Figure 3.11). The delays are chosen such that the sum of the travel time as a sound wave (from the focus to a particular element) plus the delay imposed on the electrical echo signal is the same for all elements. This means that the imposed electronic delays are greater for elements closer to the centre of the active group, for which the sound wave travel times are least. In this way, the echo signals are all aligned in phase at the summing point and a large-summed signal is obtained for echoes from the desired receive focal zone, but only a weak-summed signal (acoustic noise) results from echoes from elsewhere.

In practice, focusing in reception is controlled automatically by the machine, with no receive focus control available for the operator. This is because the ideal depth for the reception focus at any time is the depth of origin of the echoes arriving at the transducer at that time.

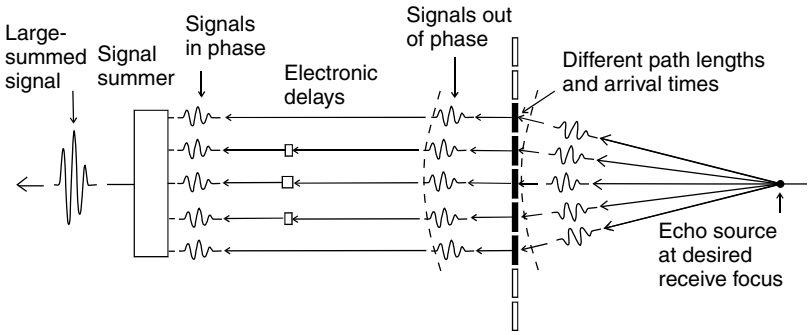

Fig. 3.11 Creating a receive focus for a linear-array transducer. In order to obtain a large echo signal from a target at a desired receive focus, contributions from all elements must arrive at the signal summer at the same time. This is achieved by electronic delays that are greater for elements closer to the centre of the group.

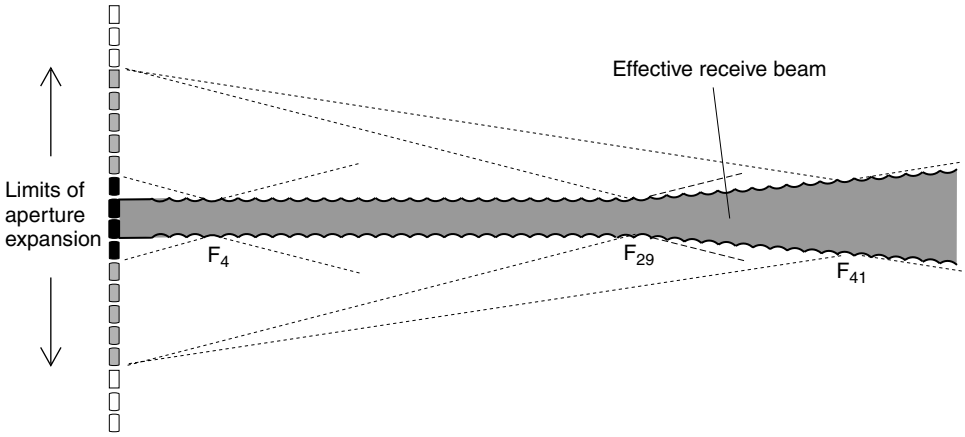

Fig. 3.12 Dynamic focusing and aperture in reception. The machine automatically changes the delays so that the receive focus advances at the rate of 1 cm every 13 μs. At the same time the aperture is expanded, so that the width of the beam at all the foci remains constant (up to the 29th focus in this example). If the aperture stops expanding, the beam widths at deeper foci become progressively greater. The scalloped lines enclosing all the focal zones indicate the 'effective receive beam'.

This is zero immediately after transmission, becoming progressively greater as echoes return from deeper and deeper targets. Since the time needed for a two-way trip increases by 13 μs for every additional 1 cm of target depth, the machine automatically advances the receive focus at the rate of 1 cm every 13 μs. The continual advancement of the receive focus to greater and greater depths gives rise to the name 'dynamic focusing in reception'. In fact, high-performance machines advance the reception focus in several hundred tiny steps (as many as one for each image pixel down a scan line), during the echo-receiving interval after each transmission. The 'effective reception beam' (Figure 3.12) consists of a sequence of closely spaced focal zones, and is therefore narrow over a wide range of depths, not just at a single focal zone.

At the same time as the receive focus is advanced, the number of elements in the active receive group is increased. The reason for this comes from the fact (Chapter 2) that the beam width at the focus is inversely proportional to the transducer aperture. It is, therefore, desirable that the active receiving group has as many elements (as large an aperture) as possible. However, there is no benefit in using a large group when receiving echoes from superficial targets, since elements far from the centre of the group would not be able to receive echoes from them – these targets would be outside the individual receive beams of the outer elements (Figure 3.13). Such elements would be able to receive echoes from deeper targets, but they would contribute nothing but noise for echoes from close targets. Thus the maximum number of elements it is worth including in the beam increases with time after transmission, in proportion to the depth of the reception focus. This means the beam width in the successive focal zones remains fairly constant, keeping lateral resolution as uniformly good as possible at all depths.

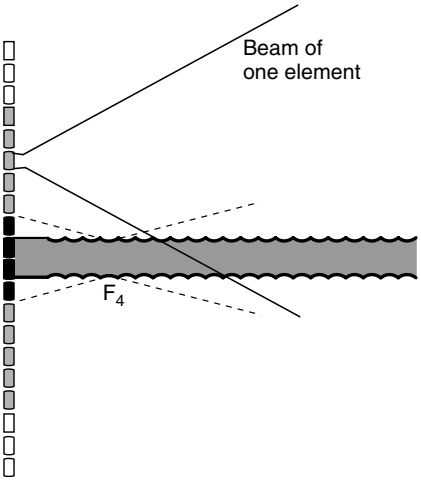

Fig. 3.13 An element can only contribute usefully to the receive active group if the target lies in the individual beam of that element. Here, elements outside the four elements nearest the scan line cannot receive echoes from focal zone F_4 or nearer. The maximum useful aperture for the active group increases as the depth of the receive focus increases.

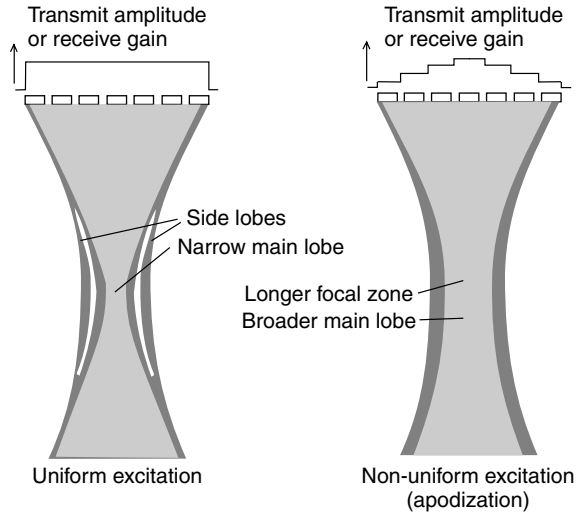

Fig. 3.14 Apodization. By exciting outer elements less than those in the centre, side lobes can be suppressed and the focal zone extended. However, the width of the main lobe is increased. Non-uniform amplification of echoes from different elements can achieve similar changes in the receive beam.

Many machines limit the number of elements in the receiving group, on cost grounds, to a maximum of about 30. This means a constant receive beam width is only maintained up to the depth at which the aperture expansion is stopped (Figure 3.12). At greater depths, the beam becomes wider, and lateral resolution becomes noticeably worse. In some more sophisticated (expensive) machines, however, the receiving group continues to expand until all the elements in the array are included. Such machines can maintain good lateral resolution to much greater depths.

Scan plane apodization

Another beam-forming process, known as 'apodization', can also be employed. In transmission, this involves exciting the elements non-uniformly in order to control the intensity profile across the beam. For example, if the inner elements are excited more than the outer elements, side lobes can be reduced in amplitude and the focal zone can be extended. However, as these benefits are at the expense of a broadening of the main lobe (Figure 3.14), a compromise is necessary and this is one judgement in which there is no common view among manufacturers. Apodization of the receive beam can be achieved by giving different amplifications to the signals from each element. The receive beam apodization can be changed dynamically to control side lobe characteristics as the receive focus is advanced.

Scan plane multiple-zone focusing

Further improvement in lateral resolution, albeit at the expense of frame rate, is possible by sub-dividing each scan line into two or more depth zones and interrogating each zone with a separate transmission pulse, focused at its centre (Figure 3.15). For example, the operator might select transmission foci at two different depths – F_1 and F_2. These would be indicated by two arrowheads or other focus indicators down the side of the image. One pulse would be transmitted with a focus at F_1 and echoes from depths up to about half-way between F_1 and F_2 would be captured. Then a second pulse would be transmitted with a focus at F_2 and echoes from all greater depths would be captured. The greater the number of transmission focal zones, the greater the depth range over which the 'effective transmission beam' is narrow. Unfortunately, the greater the number of focal zones, the longer is spent on each scan line, and so the lower the frame rate.

When using multiple-transmission focal zones, other transmission parameters such as centre frequency, pulse length and shape, aperture, and apodization may

all be optimized independently for each of the focal zones. These changes can take account of the fact that pulses sent out to interrogate deeper regions will experience greater attenuation of the high frequencies in their spectra.

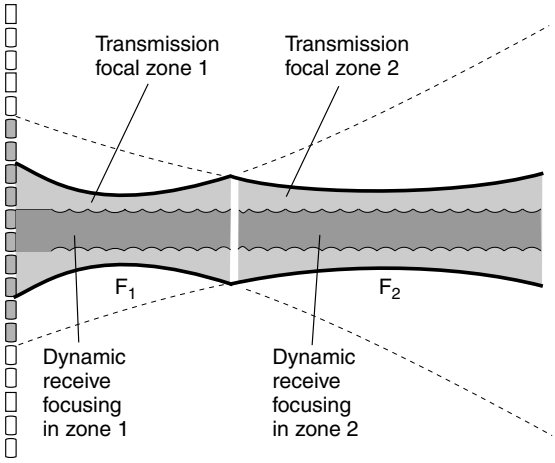

Fig. 3.15 Multiple-zone focusing. The operator has selected two focal zones (F_1 and F_2). Targets lying between the transducer and a point about half-way between the two foci are interrogated with a transmission pulse focused at F_1. Targets beyond the half-way point are interrogated by transmitting another pulse along the same scan line, but focused at F_2. The heavy and light scalloped lines indicate the 'effective transmission beam', and the 'effective receive beam', respectively.

Grating lobes

Grating lobes can occur with any transducer having regularly spaced elements, such as a linear or curvilinear array or a phased array (discussed later). They are weak replicas of the main beam, at substantial angles (up to 90°) on each side of it (Figure 3.16a). They are named 'grating lobes' after the analogous phenomenon that occurs when a light beam passes through a grating of closely and regularly spaced narrow slits (a diffraction grating) to form a series of new deflected beams on each side of the original beam. Grating lobes contribute spurious echoes (acoustic noise) and effectively widen the beam in the scan plane, degrading both lateral resolution and contrast resolution.

Consider the arrival of an echo from a distant target or receive focus at an angle to the main beam. The pulse will reach the various transducer elements at slightly different times. As the angle considered increases, the difference in arrival times at a pair of adjacent elements will increase. If the distance between adjacent elements is large enough, an angle will exist for which this time difference is a full wave period (Figure 3.16b). Thus when, say, the first peak in the pulse is arriving at the more distant element of the pair, the second peak in the pulse will be arriving at the nearer element. When summed in the beam-former, the coincidence of these two peaks (and of other peaks and troughs in the pulse) will lead to the electrical pulses from the two transducer elements reinforcing each other. The regular element spacing means the same thing happens for every pair of adjacent elements in the receive aperture,

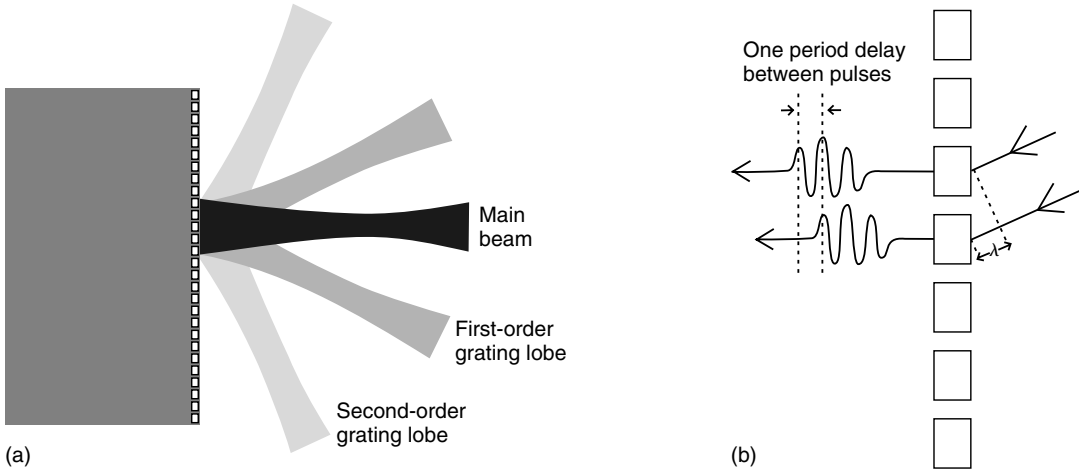

Fig. 3.16 (a) Grating lobes are weak replicas of the main beam, at angles of up to 90°. The greater the angle from the straight ahead direction, the weaker the grating lobe. (b) The first grating lobe occurs at that angle for which the arrival times of an echo at adjacent elements differ by one period.

so that a large-amplitude electronic echo pulse (grating lobe signal) is produced when electrical pulses from all the elements in the active group are combined.

Depending on the spacing of the elements and the number of cycles in the pulse, second- or even third-order grating lobe pairs may exist outside the first grating lobes. For these, the pulse arrives at one element two or three periods, respectively, ahead of that at its neighbouring element. However, for an Nth-order grating lobe to exist, there must be at least N cycles in the pulse; otherwise, there could be no constructive overlap between the signals from two elements. Clearly, the longer pulses and continuous waves used for Doppler techniques are more likely than the 2–3 cycle pulses used for imaging to produce such high-order grating lobes. In all cases, the greater the angle at which a grating lobe occurs, the weaker it will be, since each element is less efficient at transmitting or receiving sound waves in directions at large angles to the straight ahead direction.

The explanation given above has been for reception, but similar arguments apply in transmission by considering the arrival of pulses from pairs of adjacent elements at a distant point in the scan plane.

The smaller the centre-to-centre distance between elements, the larger is the angle needed to produce the difference of one period needed for the first grating lobe. If this distance is less than half a wavelength, even a pulse arriving at an angle of 90° would produce a time difference less than half a period. This would mean there could be no overlap at all between the first peak in the electrical pulse from one element and the second peak in the electrical pulse from the nearer adjacent element. Consequently, *there can be no grating lobes, if the centre-to-centre distance between elements is half a wavelength or less.*

Applying this rule to clinical linear-array probes with 128 or so elements, grating lobes are always to be expected, since the centre-to-centre distance between elements is then typically about 1.3 λ. For the relatively few probes with 256 elements, and thus a centre-to-centre distance of about 0.65 λ, grating lobes will still occur but will lie at much greater angles to the intended beam. This results in much weaker grating lobes, due to the fall-off in transmission and reception efficiency with angle, as explained above.

Slice thickness

Since the transmit and receive beams have a certain width in the elevation direction, echoes may be received from targets situated close to, but not actually in, the intended scan plane. Such echoes will contribute acoustical noise and will, therefore, tend to limit penetration and contrast resolution. In effect the image is the result of interrogating a slice of tissue, rather than a two-dimensional plane. At any particular depth, the thickness of the slice is equal to the width of the beam in the elevation direction. The slice thickness is least at the depth at which the cylindrical lens is focused, and hence this is the depth where least acoustic noise can be expected (Figure 3.1). It is also the depth at which the greatest sensitivity can be achieved. The variation of sensitivity with depth depends on the depth at which the operator sets the scan plane transmission focus, but if this coincides with the elevation focus, the beam will be at its narrowest in both dimensions and the sensitivity at that depth will be particularly high.

Slice thickness may be improved at other depths by the use of so-called multi-row arrays. Multiple rows are created by dividing each of the 200 or so strip elements of a one-dimensional array into three or five separate contiguous sections. In the simplest implementation, the 1.25D array, the multiple rows are used simply to expand the aperture from one row to say five as target depth increases. In the 1.5D array (Figure 3.17), electronic delays may be applied with delay symmetry to the signals to and from each row, in order to reduce beam width in the elevation direction, using the electronic focusing techniques (such as transmission focusing and dynamic focusing in reception) described above for the scan plane. The focal length in the elevation plane can thus be changed automatically to match the scan plane focal length. The names used (1.25D and 1.5D) are

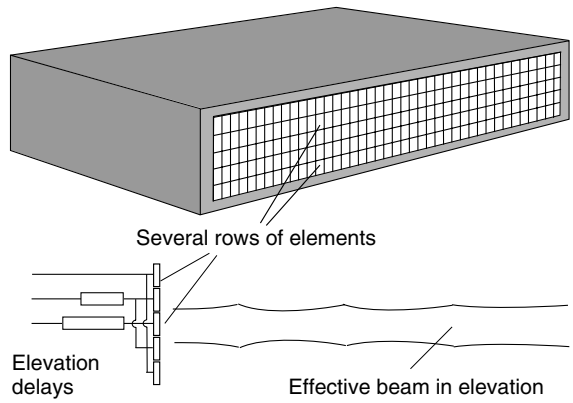

Fig. 3.17 Multiple-row (1.5D) linear-array probe. Transmission and receive focusing techniques normally used for beam-forming in the scan plane can be used to control focusing in the elevation plane. This means a narrower slice thickness and hence less acoustic noise.

intended to distinguish transducers with slice thickness control from full two-dimensional (2D) arrays, with equal numbers of elements in both directions, which are discussed later under 3D imaging (Thomenius 1996).

Strongly convex curvilinear-array transducers

Curvilinear arrays can be made with such tight curvature that their field of view becomes sector-shaped (Figure 3.18). The advantages of a sector format include a small 'acoustic window' at the body surface, and an increasingly wide field of view at depth. Phased-array scanning systems (discussed next) are particularly well suited to sector scanning, but strongly convex curvilinear arrays allow manufacturers of linear-array systems to offer sector scanning transducers, without having to build in the specialized electronics that phased-array transducers require. However, the convexity of the curvilinear transducer face means that it is less suitable in situations where the flat face of a phased-array transducer is needed.

The maximum useful size of the active element group of a curvilinear array is more limited than in a linear array employing the same-sized elements. Consequently, beam width in the focal zone is greater, and lateral resolution is poorer, than in a comparable linear array. This is primarily due to the fact that, as the number of active elements is increased, the outermost elements point more and more away from the centre line of the group (scan line), until eventually they cannot transmit or receive in that direction at all. Also, the longer paths between the outer elements and a receive focus mean that the problems of providing compensating delays are more challenging.

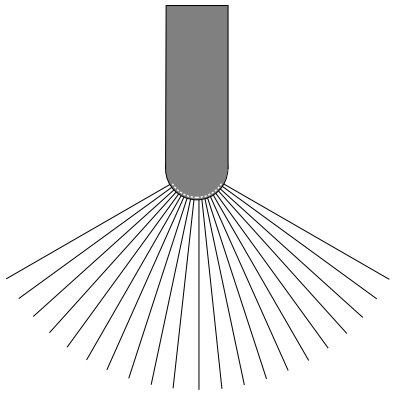

Fig. 3.18 A strongly convex curvilinear array offers many of the advantages of a sector scan format for linear-array systems.

Phased-array transducers (beam-steering arrays)

The phased-array transducer produces a 'sector' scan format in which the scan lines emanate in a fan-like formation from a point in the centre of the transducer face (Figure 3.19). As with all types of scanner, each scan line represents the axis of a transmit–receive beam.

The phased-array transducer is constructed in a similar way to the linear-array transducer. There are typically 128 rectangular transducer elements sharing a common lead to all front electrodes, and an individual lead to each rear electrode, as well as matching and backing layers (Figure 3.20). A lens provides fixed weak focusing in the elevation direction, and in some cases a modest degree of focusing in the scan plane to augment the electronic focusing in that plane. However, the transducer array is much shorter in the scan plane direction, with an overall aperture of typically 30 λ square. The individual elements are much narrower ($\lambda/2$) and one advantage of this is that they do not need to be sub-diced, as is the case for the wider elements in a linear array. Unlike the linear

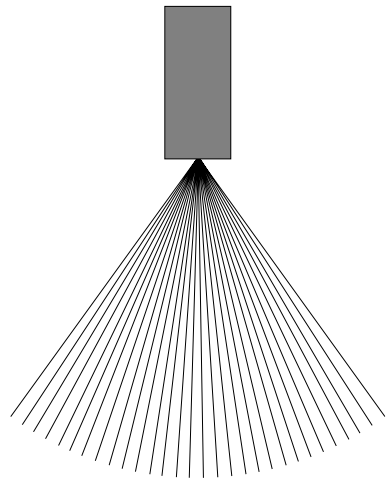

Fig.3.19 Sector scan format of a phased-array transducer.

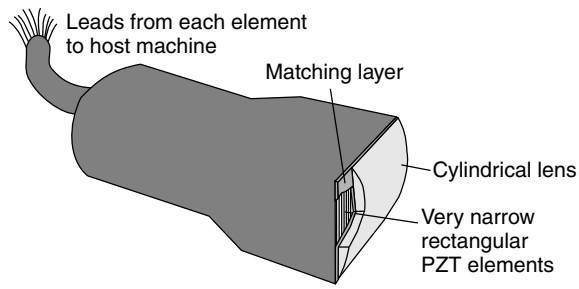

Fig. 3.20 Cut-away view of the elements, matching layer and lens of a phased-array transducer.

array, which uses a different 'active group' of elements to interrogate each scan line, all the elements in the phased array are used to form the transmit and receive beams for every scan line. Since the array dimension and method of focusing in the elevation direction (cylindrical lens) is the same as for a linear array, the two types of transducer give similar slice thickness.

Electronic beam-steering and focusing in the scan plane

Similar signal-delaying techniques to those previously described for linear-array transducers are used to achieve focusing of the transmit and receive beams in the scan plane. However, as well as being focused in the scan plane, the beams must also be steered by up to ±45°. The principle behind beam-steering is really just an extension of that used for focusing. In fact, it follows automatically from arranging for the transmission focus and the multiple-receive foci to all lie on an oblique scan line.

Scan plane focusing (and steering) in transmission

As described previously for linear-array transducers, focusing in transmission requires that pulses from all the elements arrive simultaneously at the transmission focus. The early starts needed by each element can be pre-calculated by the manufacturer for each possible position of the transmission focus along the various scan lines (Figure 3.21). The fact that the transmission focus on a particular scan line is not directly in front of the transmitting elements is of little consequence, provided the transmission beams of the individual elements diverge sufficiently to allow the sound from every element to reach it. The use of very narrow elements ensures this, since, as described in Chapter 2, a very narrow element will have an extremely short near field and a far field with a very large angle of divergence.

Scan plane focusing (and steering) in reception

Similarly, in reception, carefully pre-selected electronic delays are used to ensure that an echo from a desired receive focus takes the same time to reach the signal summer, irrespective of which element is considered (Figure 3.22). As for a linear-array, dynamic focusing is used in reception, so again there is no receive focus control available to the operator. The fact that all the receive foci lie along a scan line at some angle to the probe's axis does not matter, provided that each element can receive from ('see') any receive focus. This is ensured by the very narrow width of the elements.

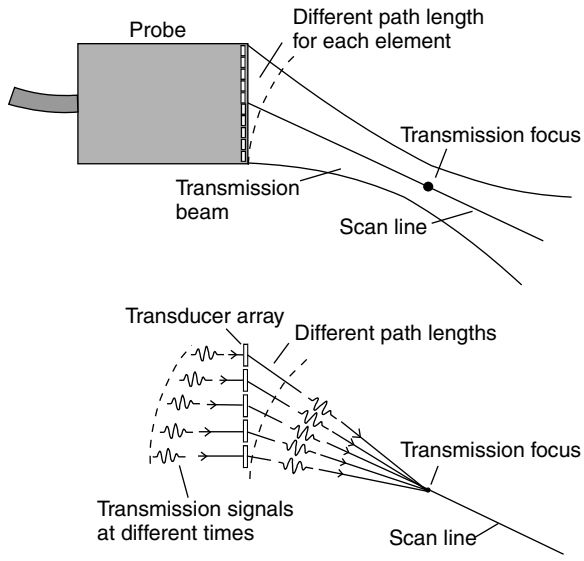

Fig. 3.21 Creating a transmission focus for a phased-array transducer. The principle is the same as for a linear-array transducer, except that the focus lies on a scan line that is generally oblique.

Other techniques for improving lateral resolution, such as apodization and multiple-zone focusing in transmission, are also used in phased-array systems. These techniques are identical to those already described for linear-array systems.

Image quality variation across the field of view

When using a phased-array transducer, the operator should always angle the probe so that any region of particular interest is in the centre of the field of view. This is where beam deflections are least and, as discussed below, where beam widths are least and signal-to-noise ratio is highest. It will, therefore, be where the best lateral resolution, the highest sensitivity and the best contrast resolution are obtained.

Dependence of beam width and sensitivity on angle

A particular artefact of phased arrays is that the width of the beam, measured at its focus, increases with increasing steering angle (Figure 3.23). Hence lateral resolution becomes poorer towards the sides of the sector-shaped field of view. The width of a strongly focused beam at its focus is inversely proportional to the ratio of transducer

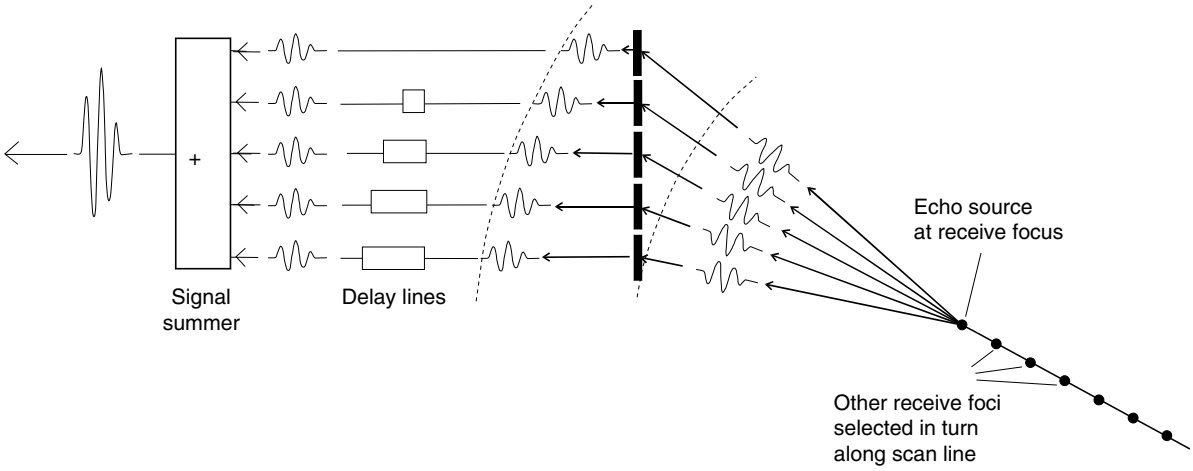

Fig. 3.22 Creating a receive focus for a phased-array transducer. The principle is the same as for a linear-array transducer, except that the receive foci lie along a scan line that is generally oblique.

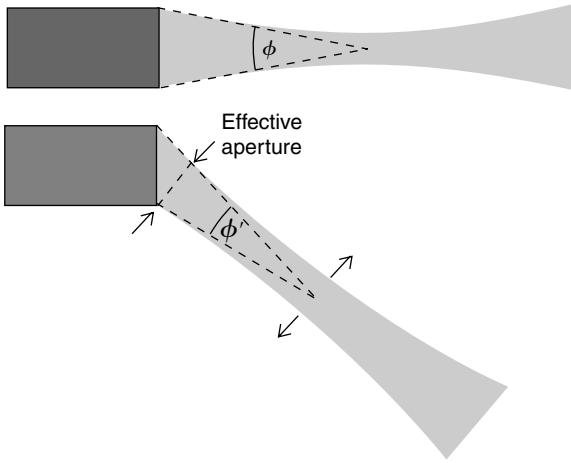

Fig. 3.23 The beam from a phased array transducer becomes wider as the angle of deflection increases. This is because the angular width of the transducer, as seen from the focus, becomes less ($\varphi' < \varphi$).

aperture to focal length (Chapter 2). Another way of expressing this would be to say the beam width becomes smaller, if the angular width of the transducer, as 'seen' from the focus, is large. Just as a door or window looks wider when viewed from directly in front than from somewhat to the side, so the angular width of the transducer aperture is greatest when seen from a point on a scan line at right angles to the probe face, and is less when seen from a scan line steered to a large angle.

Another problem is that, because the individual elements are most efficient when transmitting in, or receiving from, directions close to the 'straight ahead' direction, sensitivity decreases with steering angle.

Grating lobes

In general, the close spacing of the elements in phased arrays tends to reduce the seriousness of grating lobes compared to those in linear arrays. In view of the 'half-wavelength' criterion given earlier when discussing grating lobes for linear arrays, it might be thought that grating lobes should be impossible for phased arrays, since their element widths are less than half a wavelength ($\lambda/2$). However, wavelength (λ) here refers to that of the centre frequency of the pulse, and it should be remembered that a typical wide-bandwidth pulse will have significant energy at frequencies much higher than this. Such higher frequencies have shorter wavelengths and so may not satisfy the $\lambda/2$ condition. Thus weak side lobes at these higher frequencies will in fact occur.

Furthermore, such grating lobes will grow stronger at large steering angles (Figure 3.24). As mentioned previously, the individual transducer elements are most efficient when transmitting in, or receiving from, directions close to the 'straight ahead' direction. Since beam-steering deflects the grating lobes as well as the intended beam, steering the main lobe to one side will also steer the grating lobe that is following behind it more towards the straight ahead direction. This grating lobe will therefore strengthen and generate more acoustic noise, at the same time as the deflected main lobe is weakening.

Hybrid beam-stepping/beam-steering transducers

Some scanning techniques involve steering the beams from a linear- or curvilinear-array transducer away

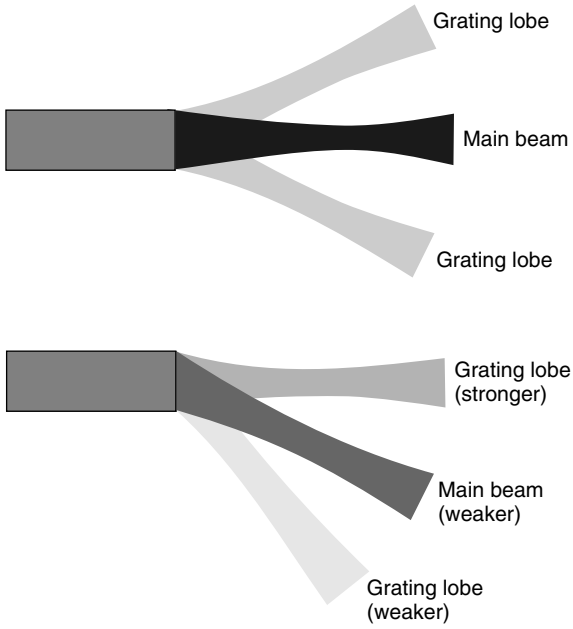

Fig. 3.24 Grating lobes from a phased-array transducer are generally weak. As the deflection of the main beam increases, some grating lobes point more ahead and so become stronger. At the same time the main beam becomes weaker.

from the normal straight ahead direction. One example is in a duplex linear-array system (see 'Mixed mode scanning', later) where the Doppler beam is deflected to reduce the angle it makes with the direction of blood flow in a vessel lying parallel to the skin surface.

Beam-steering in linear arrays is achieved using the combined focusing and steering technique that was described earlier for phased-array scanners. However, the relatively large width of transducer elements in linear-array transducers compared to those in phased arrays leads to greater problems. As the beam is progressively deflected there is greater reduction in sensitivity and greater acoustic noise from grating lobes. Despite these problems, a number of hybrid scan formats have been developed for linear arrays, in which both beam-stepping and beam-steering are used.

Trapezoidal (virtual curvilinear) scanning

Some linear-array systems achieve a trapezoidal field of view by steering the scan lines situated towards the ends of the transducer progressively outwards (Figure 3.25). Such transducers provide the large field of view advantage of a curvilinear array, without the tissue compression problem that a convex front face generates.

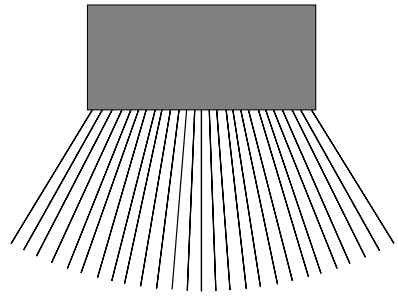

Fig. 3.25 A trapezoidal scanning format is similar to that of a curvilinear transducer, but with the practical advantage of a flat transducer face.

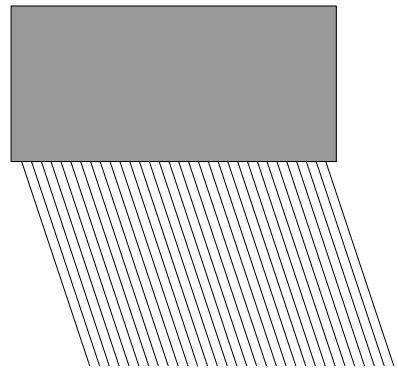

Fig. 3.26 A linear-array transducer with beam-steering.

Steered linear-array transducers

It is sometimes advantageous to be able to steer the whole field of view of a linear-array transducer to one side – to view blood vessels under the angle of the jaw, for example. A number of manufacturers, therefore, provide the option of steering all transmit and receive beams (i.e. all the scan lines) to the left or right, producing a parallelogram-shaped field of view (Figure 3.26).

Compound scanning

An extension of the steered linear-array technique is to superimpose several such angled views in a single 'compound' scan (Figure 3.27). This technique, which is possible for both linear and curvilinear transducers, gives more complete delineation of the curved boundaries of anatomical features, since many such boundaries only give a strong reflection where the scan lines meet them at perpendicular incidence. Compounding

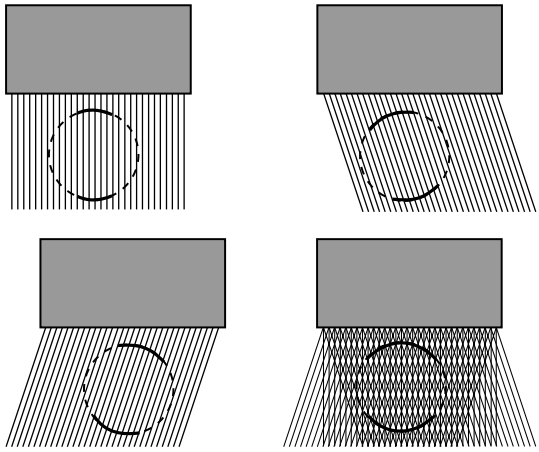

Fig. 3.27 Compound scanning. Several scans from different directions are averaged. This gives more complete delineation of organ boundaries as well as reduced noise and speckle.

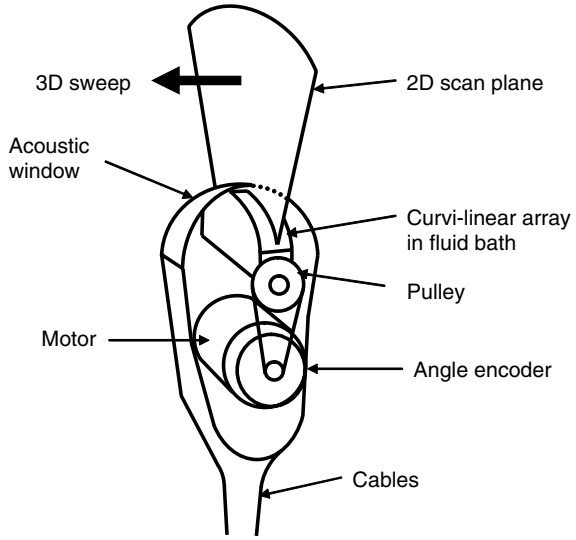

Fig. 3.28 The mechanical 3D transducer contains a stepped array mounted on a swivel in an enclosed fluid bath beneath a thin acoustic window. The image plane is swept from side to side by a motor coupled via pulleys and drive belt. 3D volumes can be acquired at up to 5 Hz.

also produces much finer 'speckle patterns' (Chapter 5) and reduced acoustic noise. Whereas a genuine tissue target, detected in several different views, will always be shown at the same point in the final image, speckle and noise patterns will be different for each view and will tend to be cancelled out.

Compounding involves a loss of temporal resolution, since each displayed frame is the average of several sweeps. In common with the 'frame-averaging' noise-reduction technique described in Chapter 4, this introduces a degree of 'persistence' to the image. Thus, if each displayed image was the average of the previous nine different sweeps (views), and an organ cross section were to change instantly from A to B, nine frames would need to pass before all trace of the image of A was lost from the displayed image. Where necessary, a reasonably high-speed compromise is possible by displaying the average of just the last three or so sweeps.

3D/4D transducers

The beam formation and scanning techniques described so far have all been designed to acquire echo information from a single cross section through the target tissues. The echo information would then be processed and displayed as a real-time 2D, B-mode image (see Chapter 4). The same beam formation and scanning techniques can be extended to acquire echo information from a 3D volume of tissue. The resulting 3D volume data set can then be processed to create a number of alternative modes of display, as described in Chapter 13. Repetition of the 3D acquisition and display at a few hertz (refresh rates up to 20 Hz are possible) results in a moving 3D display, referred to as 4D.

There are two commonly used approaches to the design of 3D / 4D transducers. The design illustrated in Figure 3.28 incorporates an array transducer, in this case a curvilinear array, mounted on a swivel inside an enclosed bath of acoustic coupling fluid (linear-array transducers are also used). The transmit pulse and returning echoes pass through a thin acoustic window to acquire a 2D section from the adjacent tissues. A motor, coupled to the swivel by pulleys and a drive belt, rotates the transducer array so that the 2D scan plane is swept at 90° to the imaged plane, to interrogate and acquire echoes from a pyramidal volume of tissue. The orientation of each scan plane is measured by an angle encoder attached to the motor. A sequence of closely spaced, adjacent 2D sections is acquired, which constitutes a 3D volume data set. By repeating the sweeping motion of the array from side to side, a 4D image can be created. Due to the mechanical nature of the transducer movement, 4D acquisition rates are limited to a few volumes per second.

The spatial resolution of the acquired data is subject to the same limitations as described earlier for

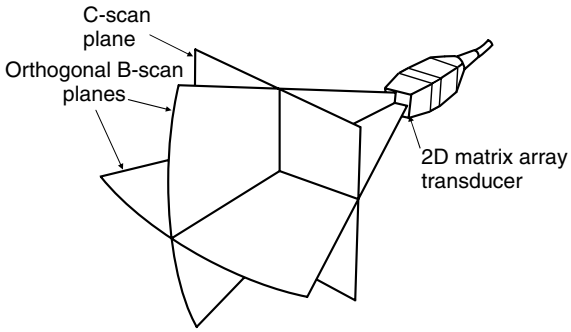

Fig. 3.29 The 2D matrix-array transducer has a square array of elements, e.g. 50 × 50. It uses beam-steering techniques to sweep a 2D sector scan through a 3D volume or interrogate orthogonal B-scan planes. Volume data can be displayed as a series of B-scan planes or as a C-scan. 3D display modes are also widely used.

linear-array transducers. That is, the lateral resolution in the original scan plane is much better than that in the elevation plane, due to the lack of electronic focusing in the elevation direction. Hence the units of volume, the voxels, are not square and B-scan images, created in the elevation plane from the 3D data, will have reduced lateral resolution.

The alternative, commonly used 3D transducer is the 2D matrix array (Figure 3.29). This transducer contains several thousand square elements arranged in a two-dimensional matrix. Using beam-steering techniques as described earlier, the matrix array can be used to create a 2D sector scan in a single plane. By applying beam-steering techniques also in the orthogonal direction (elevation), the 2D sector can be swept sideways to describe a pyramidal volume. As the matrix of elements is square, it is possible to achieve equivalent resolution in the lateral (scan plane) and elevation directions by applying the same degree of electronic focusing and aperture control to both planes. However, the spatial resolution is subject to the limitations of phased array transducers described above and the relatively small number of elements (approximately 50) along each side of the array. As the matrix array has no moving parts, the 3D acquisition rate is limited only by speed-of-sound considerations (see next section). If the imaged depth and angle of sweep are restricted, volume rates of up to about 20 Hz are possible. The stored volume data can be interrogated and displayed as a sequence of adjacent 2D sector scans in any B-mode plane or as a C-scan, where the imaged section is parallel to the transducer face. Alternative modes of 3D display, including surface rendering, are described in detail in Chapter 13.

Time-saving techniques for array transducers

Real-time operation requires compromises between three competing qualities:

(1) temporal resolution;
(2) size of the field of view;
(3) image quality (e.g. lateral resolution, contrast resolution, dynamic range).

Improvements in any one of these must be at the expense of one or both of the other two (see Chapter 5). For example, a reduction in frame rate occurs if the maximum depth is increased (more time per scan line) or the width of the field of view is increased (more scan lines). Multiple-zone transmit focusing improves lateral resolution, but this is at the expense of temporal resolution because of the need to remain longer on each scan line while interrogating several zones instead of just one. Compound scanning improves image quality through reduced speckle and acoustic noise and by better boundary delineation, but reduces temporal resolution. Some of the techniques described in Chapter 4, such as frame averaging and tissue harmonic imaging by pulse inversion, improve image quality, but are at the expense of temporal resolution.

If time can be used more efficiently, the time savings can be used to increase one or more of the above three qualities. The following techniques are examples of this.

Write zoom

This technique presents a full-screen real-time image of a restricted area of the normal field of view, selected by the operator (Figure 3.30). Once selected, write zoom restricts the interrogation process to this operator-defined region of interest. One obvious way of using the consequent time savings would be to increase the frame rate. Alternatively, some or all of the time savings could be used to improve lateral resolution, both by narrowing the beam using multiple-zone focusing and by increasing the line density.

Line multiplexing

The frame-rate penalty associated with using multiple-zone transmission focusing can be reduced by breaking the usual 'rule' that all echoes should have returned from one scan line before transmitting along the next

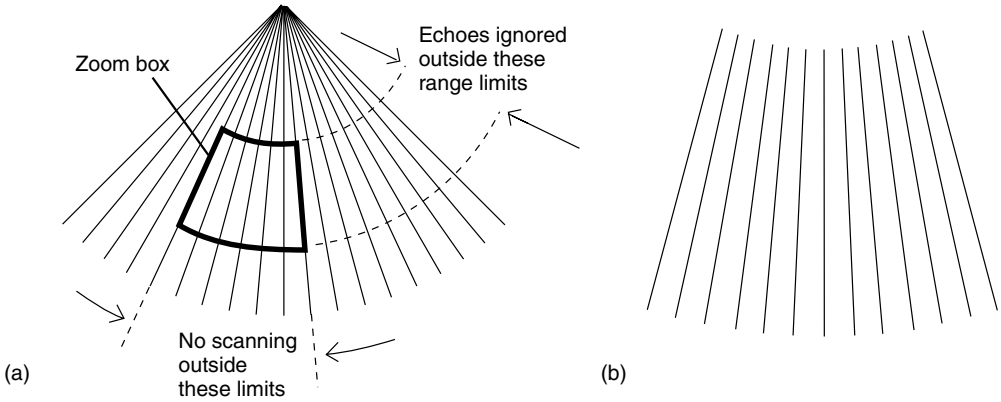

Fig. 3.30 Write zoom. A 'zoom box' is defined by the operator (a). Scanning is then restricted to this area (b), allowing either a higher frame rate or improved lateral resolution by scanning with narrower, more closely spaced beams, or both.

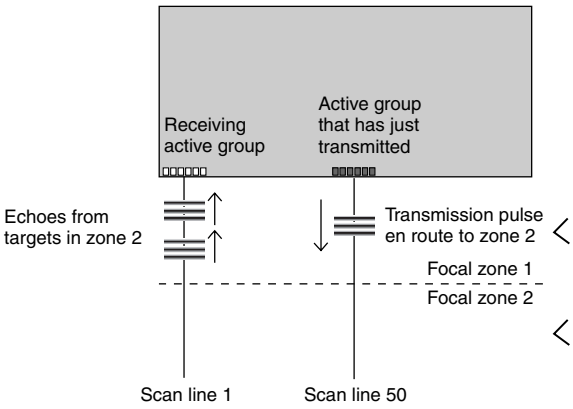

Fig. 3.31 Line multiplexing saves time. A pulse is already on its way to a particular zone on a new line (e.g. line 50), as echoes are being received from that zone on the old line (e.g. line 1).

line. Instead, interrogation of each line may be divided over several periods, interspersed with periods spent interrogating other lines. For example (Figure 3.31), when echoes have been received from the first (most superficial) focal zone on scan line 1, rather than wait for the unwanted echoes from deeper structures to return before transmitting to the second focal zone on line 1, a transmission is sent from another active group centred on a well-removed scan line (e.g. scan line 50) to interrogate the first focal zone of that line. The choice of a distant scan line, in this case about half-way along the transducer, ensures that the unwanted echoes from one line do not reach the receiving element group on the other line. As soon as the echoes have arrived from the first zone on line 50, a transmission might then be sent to the first focal zone on scan line 2, etc. Only when the first focal zone on all the scan lines has been interrogated are the second focal zones on all lines interrogated. These, too, are interrogated in the scan line sequence 1, 50, 2, 51, etc., to save time in the same way. Note that, although more than one transmission pulse is in flight at a time, echo reception does not take place on more than one line at a time.

Parallel beam-forming in reception

Since dynamic focusing is used in reception, the effective receive beam is narrower than the weakly focused transmit beam. In fact, it can be arranged for the transmit beam to accommodate two receive beams side by side (Figure 3.32). By sharing the same transmitted pulse, the echoes from targets located on two adjacent scan lines can be processed simultaneously ('in parallel') in two separate receive beam-formers (Thomenius 1996). The different focusing delays for each receive beam may be in the form of hardware or software. In the former case, each element is connected to two physically separate beam-forming circuits. In the latter case, the two sets of delays are applied on a time-shared basis to digital samples of the echo signal from each element. In some cardiac applications, where high frame rates can be important, as many as four scan lines are interrogated in parallel ('quad processing'). However, this requires an even broader transmission beam and hence some further compromise in lateral resolution. This last technique was introduced commercially in the 1980s, when it was known as 'exploso-scanning' (Shattuck *et al.* 1984).

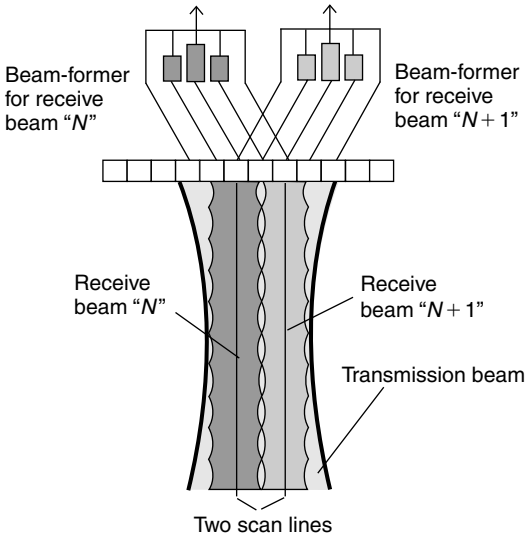

Fig. 3.32 Parallel beam-forming in reception saves time. One pulse is transmitted down a weakly focused transmission beam. Two receive beam-formers act in parallel to simultaneously interrogate two scan lines lying within the transmission beam, using just that one transmission pulse.

High-frame-rate imaging

In traditional B-mode imaging, frame rates of up to 30–60 Hz may be easily achieved using sweeping of a single beam through the tissue, building up the image one line at a time. For some of the more advanced techniques described later in this book, such as 3D ultrasound, strain imaging and shear-wave imaging, traditional beam-forming techniques are unable to provide the frame rate required. Use of the time-saving techniques above may be sufficient in some cases to increase frame rate. Frame rates of up to 200 Hz have been achieved in 2D cardiac imaging by restricting the field of view in depth and breadth, and by reducing the line density (D'Hooge *et al.* 2002).

Some applications, such as shear-wave imaging (Chapter 15), require very high frame rates which cannot be achieved by tinkering with the conventional beam-former. This section describes two methods for producing very high frame rates. These techniques have become possible in recent years due to the availability of digital beam-forming and high-speed processing. These methods are able to produce a complete 2D image from a single transmission pulse, at the expense of reduced spatial resolution. For imaging to 50 mm depth, the time for transmission and reception of the ultrasound pulse at a speed of 1540 m s^{-1} is 64 ms, so that the equivalent frame rate is 15 kHz. For imaging at 25 mm depth, the maximum frame rate becomes 30 kHz.

Synthetic-aperture imaging

In this technique, instead of a focused beam, a single element or a group of two or three elements is used to transmit spherical waves which insonate the entire field of view (Figure 3.33a). Conventional receive focusing is used as shown in Figure 3.33b. In this way it is possible to obtain an image with just one pulse, with consequent increase in frame rate, albeit at lower spatial resolution than for conventional imaging. In practice a series of low-resolution images is acquired, each for different positions of the transmit element(s) (Figure 3.34). The images may be summed to produce a final high-resolution image. In recursive imaging, for an array of M elements the acquisition sequence is repeated. The first high-resolution frame is made from emissions 1 to M, the second from emissions 2 to M+1, the third from emissions 3 to M+2 and so on. In this way a new high-resolution image is produced after every emission, but there is temporal overlap between the images. Alternatively, fewer emissions may be used to form an image, which results in improved temporal resolution, but at the expense of reduced spatial resolution. This approach has been used to produce both B-mode and colour flow images.

The term 'synthetic-aperture imaging' originates in radar imaging from a moving object such as an aeroplane or satellite, where several spherical-wave transmissions are made with time as the object moves over the terrain of interest. The size of the aperture formed by the moving object is much bigger (potentially many hundred times) than the size of the aeroplane or satellite, and the (transmit) aperture so formed is described as 'synthetic'. In the case of synthetic-aperture ultrasound, the sequence of transmissions is similar to radar; spherical waves generated from a small source whose position moves along the face of the array.

A limitation of the synthetic-aperture method in ultrasound imaging is that only a single element, or a very small number of elements, is used in transmission. This limits the amplitude of the transmitted ultrasound pulse, which may lead to signal-to-noise problems in the reconstructed images.

Further reading may be found in Misaridis and Jensen (2005) and Jensen *et al.* (2006), including the use

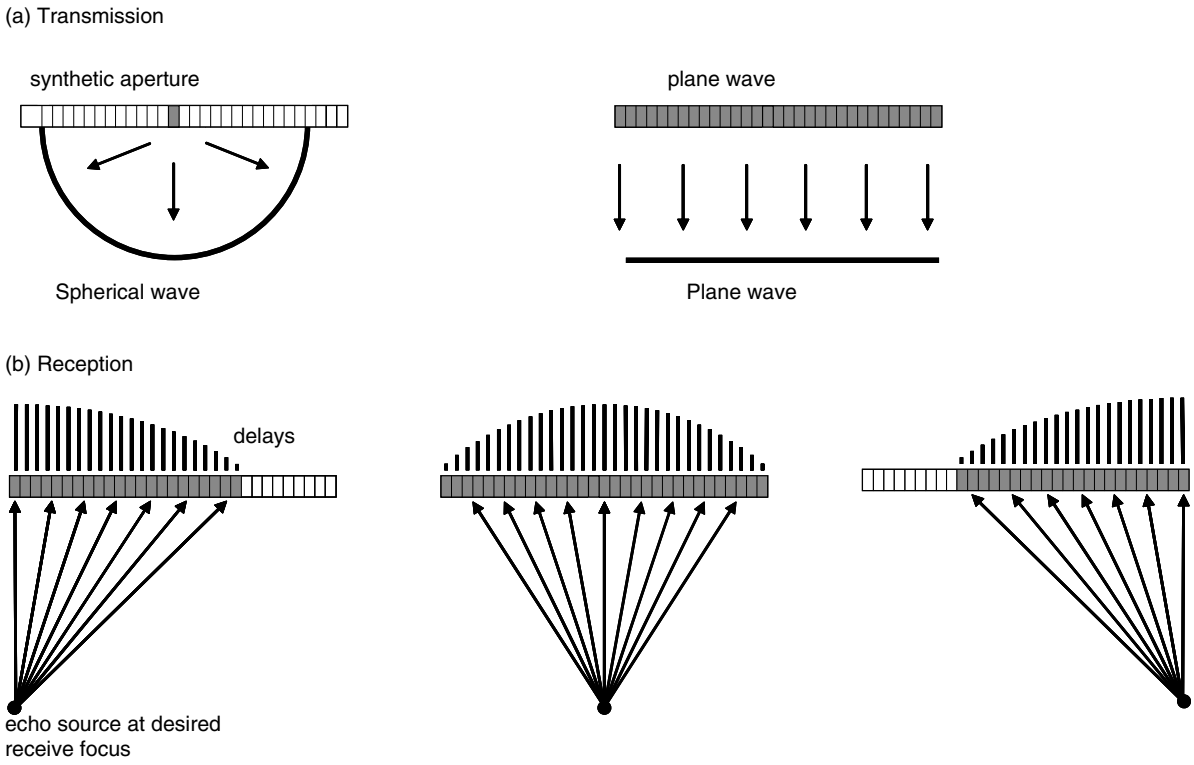

Fig 3.33 Very high-frame-rate imaging. (a) Transmission; a single pulse is used to fill the whole field of view, synthetic-aperture imaging produces a spherical wave from a single element or a very small group of elements; in plane-wave imaging all elements are stimulated at the same time. (b) Reception; for both synthetic-aperture and plane-wave imaging conventional beam-forming techniques are used to achieve focusing of the received echoes. The echoes produced from three locations are shown along with the delays for each element of the array.

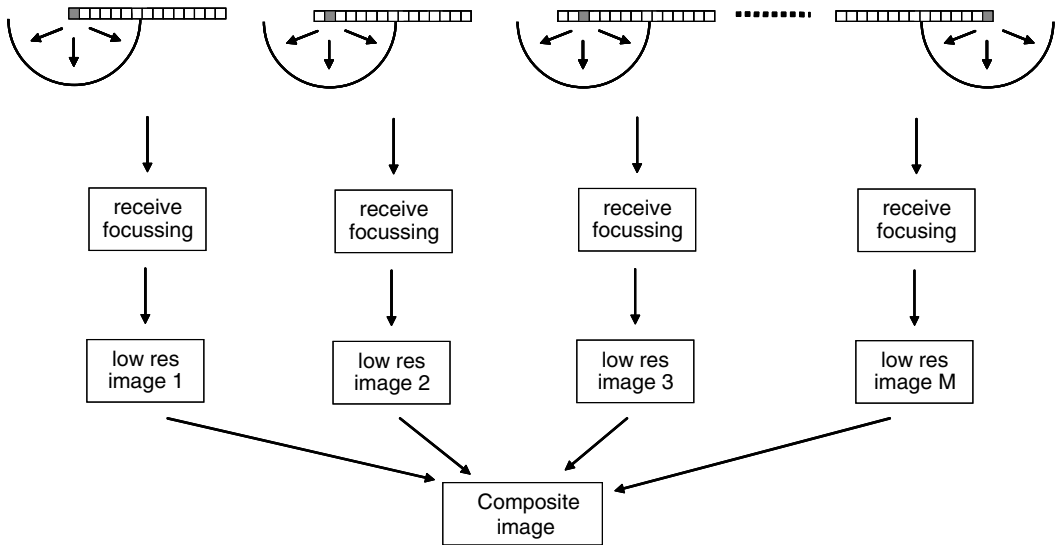

Fig 3.34 Synthetic-aperture imaging. For each low-resolution image that is formed, the element is stepped along the array. For an array of *M* elements, a series of *M* low-resolution images is formed. A high-resolution image may be formed by compounding the *M* low-resolution images.

of multiple transmit beams with different codes to further increase frame rate.

Plane wave techniques

This method was developed in the context of shear-wave imaging (see Chapter 15), where a method was needed to track shear waves as they propagated through tissue at speeds of 1–10 m s^{-1}. The propagation of shear waves is important in elastography, as described in Chapter 15. Elastographic techniques attempt to provide information on the stiffness of tissues. Shear waves, produced by mechanical or acoustic shaking of the tissue, propagate through the tissue from the source of disturbance. The speed at which shear waves propagate is related to the stiffness of the tissues, hence the need to develop an imaging method which is able to measure the speed of propagation. The shearwave velocity in soft tissues is in the range 1–10 m s^{-1}, so that the shear waves will take 1–10 ms to traverse a region 1 cm in width. In order to acquire several snapshots of the wave as it traverses this region, frame rates of several thousand Hz are required. This is impossible to achieve using conventional ultrasound imaging, which as noted above is able to produce frame rates typically up to about 60 Hz.

Instead of spherical waves produced from a single element as noted above for synthetic-aperture imaging, all elements are used to produce a plane wave (Figure 3.33a). An image is produced by beam-forming in reception (Figure 3.33b). This is a low-resolution image due to the lack of beam-forming in transmission. Image quality may be increased by forming a series of images from steered plane waves of different directions and compounding these (Montaldo *et al.* 2009); however, with reduced frame rate.

Mixed-mode scanning

Array scanners make it possible for the operator to highlight a specific scan line on a B-mode image and simultaneously generate a real-time M-mode scan, A-mode scan or a Doppler spectrum for that line on the same display screen.

This is particularly useful in cardiological applications, where a phased-array transducer is commonly used because of its ability to fit between ribs. Here, the simultaneous display of an M-mode line and a real-time B-mode (2D) scan allows the operator to check that the M-mode line is placed, and remains, in the correct anatomical position (Figure 3.35). Although the two scans appear to be formed simultaneously, in fact the beam-former rapidly switches back and forth between B-mode and M-mode interrogations. After every few lines of B-mode interrogation, the beam is made to jump to the selected M-mode scan line for one transmission and echo acquisition sequence. It then jumps back to continue the B-mode scan for another few lines; then jumps back to the M-mode line, etc.

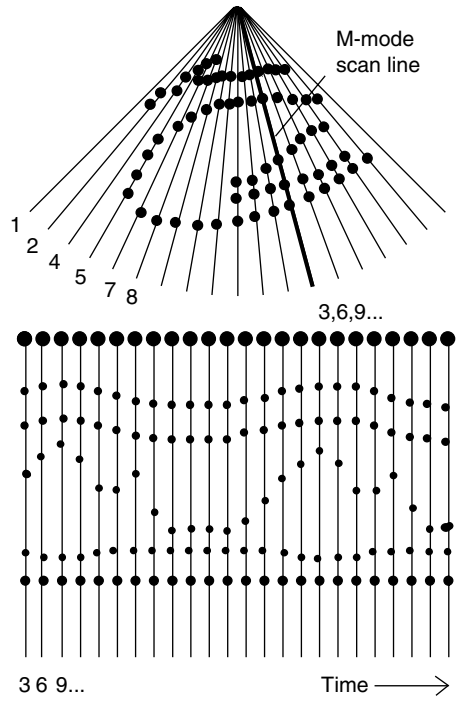

Fig. 3.35 Mixed M-mode and B-mode scanning. The first two transmissions are directed along two lines of the B-mode. The third is transmitted along the M-mode scan line. The fourth and fifth pulses interrogate the next two B-mode scan lines; then the sixth interrogates the M-mode scan line again; etc. Thus the two scans proceed in parallel.

'Duplex' Doppler scanning is another example of mixed-mode scanning. Here, Doppler measurements are made of blood flow or tissue movements in a 'sample volume', whose position is indicated on a 'Doppler line' on the B-mode image (Chapter 9). This line can be set by the operator to be either parallel to or at an angle to the image scan lines. When set at an angle to the scan lines, the beam-steering and focusing techniques described earlier (see 'Phased array transducers') are used to interrogate that line.

As explained in Chapter 9, the Doppler line must be interrogated at a high repetition frequency, much higher than would be possible even by jumping to the Doppler line after every B-mode line. The Doppler line is therefore interrogated without interruption, except for very brief periods (about 20 ms) every second or so, as determined by the operator, in which the machine

performs one complete 'update' frame of the B-mode. Each of these B-mode update images is held frozen on the screen next to the on-going Doppler display until it is automatically replaced by the next one. Note that the pulses transmitted along the Doppler line usually have a lower frequency and greater length than those transmitted along the imaging lines.

Mechanically scanned transducers

Mechanical scanning may be used for special applications at frequencies above around 15–20 MHz. This is due to the difficulties of fabricating high-frequency linear- or phased-array transducers, although array transducers operating at up to 50 MHz have been produced for small animal scanning (Foster *et al.* 2009). Mechanical scanners producing rectangular, or trapezoidal, fields of view may be used for high-frequency scanning of superficial sites, such as the eye and skin. Here, the transducer is driven back and forth inside an enclosed water-bath at the end of a hand-held probe. The transducer must move in a water-filled bath, rather than in air, since the latter would result in virtually zero transmission across both the transducer–air and the air– skin interfaces (Chapter 2). Part of the wall of this water-bath is made from a thin plastic membrane, allowing transmission into the patient. Reverberations (Chapter 5) between the transducer and this wall (effectively the patient) can cause a noticeable artefact. Linear mechanical scanning is only practical for transducers operating at frequencies above 10 MHz or so, because of the vibration that heavier, lower-frequency transducers would produce when constantly reversing direction. Despite the general disadvantages that are commonly associated with the moving components and water-baths of mechanical scanners – bulk, vibration, leakage, wear and tear, etc. – a general advantage of all mechanical scanners over linear- or phased-array transducers is that they do not suffer from grating lobes, and thus generate less acoustic noise.

Endo-cavity transducers

Endo-cavity transducers are intended for insertion into a natural body cavity or through a surgical opening. A number of different types are represented in Figure 3.36. The ability to place the transducer close to a target organ or mass means that there is less attenuation from intervening tissue, which in turn means a higher frequency may be used and superior lateral and axial resolution obtained. The image distortions and artefacts due to any tissue heterogeneity or strongly

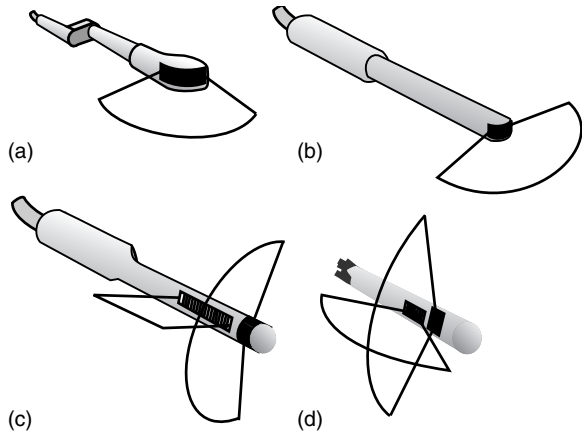

Fig 3.36 Examples of endo-transducers. (a) Curvilinear transducer for trans-vaginal scanning. (b) 'End-fire' curvilinear-array transducer for trans-rectal or trans-vaginal scanning. (c) 'Bi-plane' trans-rectal transducer with both a linear array and a curvilinear array – allowing both transverse and longitudinal scans of the prostate. (d) Trans-oesophageal transducer with two phased arrays set at right angles, giving two orthogonal cross sections of the heart.

reflecting or refracting interfaces between the transducer and the target are also reduced.

All the beam-forming techniques previously mentioned are employed in endo-cavity transducers, the choice being determined primarily by the anatomical features and constraints of the particular application. Thus, a curvilinear array offers a field of view of an appropriate shape for trans-vaginal scanning. The wide field of view close to a linear array is suitable for imaging the prostate from the rectum. Phased arrays give a wide field of view for visualizing the left side of the heart from a transoesophageal probe.

360° mechanically scanned endo-probes

These rotate a transducer about the axis of a probe so that the beam sweeps through a 360° circle, in a similar way to a light beam sweeping around a lighthouse. Such probes consist of an outer tube within which is a rotating inner rod, bearing the outwardly pointing transducer. In order for the signals to and from the transducer to cross between the stationary and rotating parts, either slip-rings or a transformer arrangement are used.

The technique can be used with low-frequency transducers, but because of the size and mass of the transducers such scanners are likely to be limited to

low frame rates or involve manual rotation of the transducer. A disposable rubber sheath may be clamped to the outer tube which, when inflated with water, provides an offset between the rotating transducer and the patient. Applications of this type of probe include scanning the prostate from within the rectum, and imaging the bladder wall with a probe introduced into the bladder via the urethra.

High-frequency versions (e.g. 30 MHz) can be inserted via a catheter into a blood vessel in order to visualize the vessel wall. The transducer is attached to a rotating wire within a non-rotating outer cable. One difficulty with this method is that friction between the rotating wire and the outer cable causes the cable, and hence the transducer, to weave around within the blood vessel. The continual movement of the viewing point with respect to the target leads to difficulties in interpreting the images. The cylindrical-array probes discussed next do not have this problem and offer an alternative method for intra-luminal scanning.

Intra-luminal and intra-cardiac catheter probes using transducer arrays

Strongly convex transducers were discussed earlier as an exaggerated form of curvilinear array. The ultimate development of this idea is to curve a linear array so tightly that a complete cylindrical array is formed. Such transducer arrays offer an alternative to the mechanical 360° scanners mentioned above (Figure 3.37a).

Tiny, high-frequency (e.g. 2 mm diameter, 30 MHz), cylindrical arrays, mounted on catheters, can be inserted into a blood vessel. This gives a direct high-resolution image of the internal wall of the blood vessel. One construction method is to mount the transducer elements, their connecting leads and other electronic hardware on a flexible printed circuit and then roll this into the required final cylindrical form. Probes made this way have been designed as single-use, disposable devices.

Another type of probe designed for intra-cardiac imaging has a 64-element phased array (5–9 MHz) mounted on the side of a 3-mm-diameter catheter (Figure 3.37b). The catheter can be introduced into the heart via the femoral or jugular vein (Proulx *et al.* 2005).

A problem facing the designers of catheter-mounted arrays is that it is not possible to accommodate 128 or so leads within the narrow catheter. Consequently, the arrays have fewer elements, and in some cases the 'synthetic-aperture' technique is employed. This allows

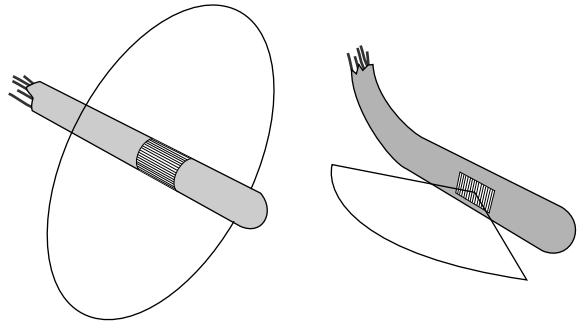

Fig 3.37 (a) Intra-luminal transducer with a cylindrical high-frequency (typically 30 MHz) array, providing 360° transverse images of blood-vessel walls. (b) Intra-cardiac phased-array transducer mounted on the end of a steerable catheter.

the number of leads to be a fraction of the number of array elements. Electronic switches are mounted next to the transducer array so that a given lead can be connected to one of several different elements as required. After each transmission, the echo sequence from the selected elements is digitized and stored. Several transmission–reception sequences are carried out along the same scan line, with the leads being connected to different elements for each one. When all the elements have been selected, all the stored echo sequences are summed together, with each sequence being delayed relative to the others by the appropriate amount. These delay-time intervals are just those that would have been used if the echo sequences from all the elements had been available at the same time – as in the electronic focusing techniques described earlier in this chapter.

Questions

1. Explain the functions of the various layers of a typical ultrasound transducer. Why are thicknesses of $\lambda/2$ and $\lambda/4$ used for the piezoelectric layer and the matching layer?
2. Explain the process used with a linear-array transducer to generate a set of adjacent B-mode lines.
3. Explain the process used with a phased-array transducer to move the beam through the target tissues.
4. Explain how electronic focusing is achieved with a linear-array transducer. How is the focusing

affected by the wavelength, aperture size and focal length?

5. Explain how the receive beam from a linear array can be made narrower than a transmit beam.
6. Describe the advantages and disadvantages of multiple-transmit-zone focusing.
7. Explain the origin of grating lobes in a beam from an array transducer. How can they be reduced or avoided?
8. Why is the image quality from a phased-array transducer better in the centre of the sector than it is near the edges?
9. Explain the interaction between temporal resolution, imaged depth and image quality in a real-time imaging system. What methods might be used to overcome such limitations?
10. Describe the construction of an endo-cavity transducer and explain its advantages and limitations compared to transcutaneous scanning.

References

Chen J, Panda R (2005). Commercialization of piezoelectric single crystals for medical imaging applications. *IEEE Ultrasonic Symposium Proceedings*, 235–40.

Daft C, Wagner P, Bymaster B, *et al.* (2005). cMUTs and electronics for 2D and 3D imaging: monolithic integration, in-handle chip sets and system implications. *IEEE Ultrasonic Symposium Proceedings*, 467–78.

D' Hooge J, Konofagou E, Jamal F, *et al.* (2002). Two-dimensional ultrasonic strain rate measurement of the human heart in vivo. *IEEE Transactions on Ultrasonics, Ferroelectrics and Frequency Control*, **49**, 281–6.

Foster FS, Mehi J, Lukacs M, *et al.* (2009). A new 15–50 MHz array-based micro-ultrasound scanner for preclinical imaging. *Ultrasound in Medicine and Biology*, **35**, 1700–8.

Jensen JA, Nikolov SI, Gammelmark KL, Pedersen MH (2006). Synthetic aperture ultrasound imaging. *Ultrasonics*, **44**, E5–E15.

McKeighen RE (1998). Design guidelines for medical ultrasonic arrays. *Proceedings of the SPIE,* **3341**,2–18,

Ming Lu X, Proulx TL (2005). Single crystals vs. PZT ceramics for medical ultrasound applications. *IEEE Ultrasonic Symposium Proceedings*, 227–30.

Misaridis T, Jensen JA (2005). Use of modulated excitation signals in medical ultrasound. Part III: high frame rate imaging. *IEEE Transactions on Ultrasonics, Ferroelectrics and Frequency Control*, **52**, 208–19.

Montaldo G, Tanter M, Bercoff J, Benech N, Fink M (2009). Coherent plane-wave compounding for very high frame rate ultrasonography and transient elastography. *IEEE Transactions on Ultrasonics, Ferroelectrics and Frequency Control*, **56**, 489–506.

Powell DJ, Wojcik GL, Desilets CS, *et al.* (1997). Incremental 'model-build-test' validation exercise for a 1-D biomedical ultrasonic imaging array. *IEEE Ultrasonics Symposium Proceedings*, 1669–74.

Proulx TL, Tasker D, Bartlett-Roberto J (2005). Advances in catheter-based ultrasound imaging intracardiac echocardiography and the ACUSON AcuNavTM ultrasound catheter. *IEEE Ultrasonic Symposium Proceedings*, 669–78.

Shattuck DP, Weinshenker MD, Smith SW, von Ramm OT (1984). Explososcan: a parallel processing technique for high speed ultrasound imaging with linear phased arrays. *Journal of the Acoustical Society of America*, **75**, 1273–82.

Thomenius KE (1996). Evolution of ultrasound beam-formers. *IEEE Ultrasonic Symposium Proceedings*, 1615–22.

Chapter 4

B-mode instrumentation

Kevin Martin

Signal amplitude processing

The beam-forming techniques described in the previous chapter are used to acquire echo information from different parts of the imaged cross section by selection of the transducer array elements and manipulation of the relative timings of their transmit and receive signals. These yield echo sequences, which represent the B-mode image lines and define the spatial properties of the image. The brightness of the image at each point along the B-mode line is determined by the amplitude of the echo signals received at the transducer. The echo signals must be processed to produce the final image brightness. The processing methods used are described in this chapter.

Figure 4.1 illustrates, in block-diagram form, the essential elements of the complete B-mode system, and shows that the B-mode amplitude information is processed in various ways before storage in the image memory, from where the image is displayed. Although it is probably easiest to imagine that, as illustrated, amplitude processing is applied to the B-mode image lines only after the beam-former, in practice some must be applied at an earlier stage to allow the beam-forming processes to be carried out. Also, some processing may be carried out after the image memory to improve the displayed image or optimize its characteristics for a particular clinical application.

Amplification

The echo signals generated at the transducer elements are generally too small in amplitude to be manipulated and displayed directly and need to be amplified (made bigger). Figure 4.2(a) shows the conventional symbol

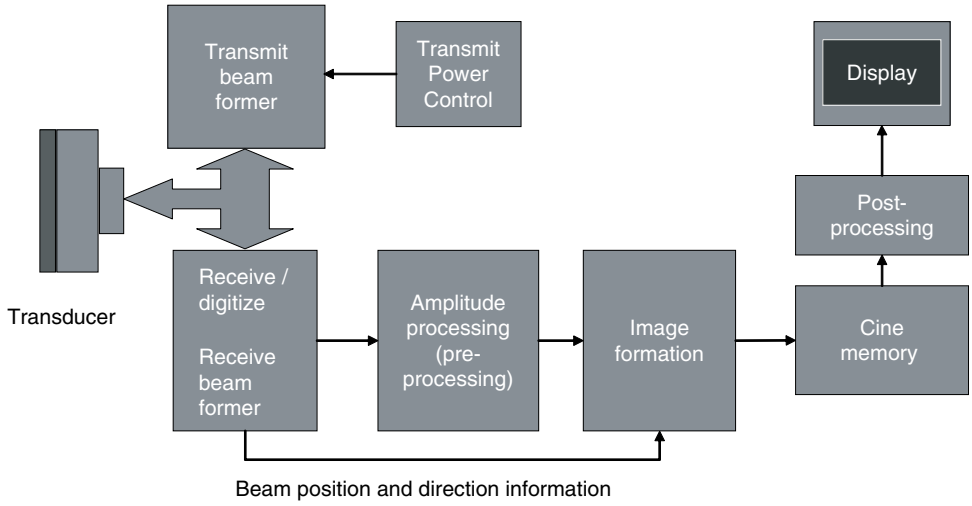

Fig. 4.1 The amplitude of the echo signals must be processed before storage in the image memory. Some amplitude processing also takes place before beam-forming.

Diagnostic Ultrasound: Physics and Equipment, ed. Peter Hoskins, Kevin Martin and Abigail Thrush. Published by Cambridge University Press.

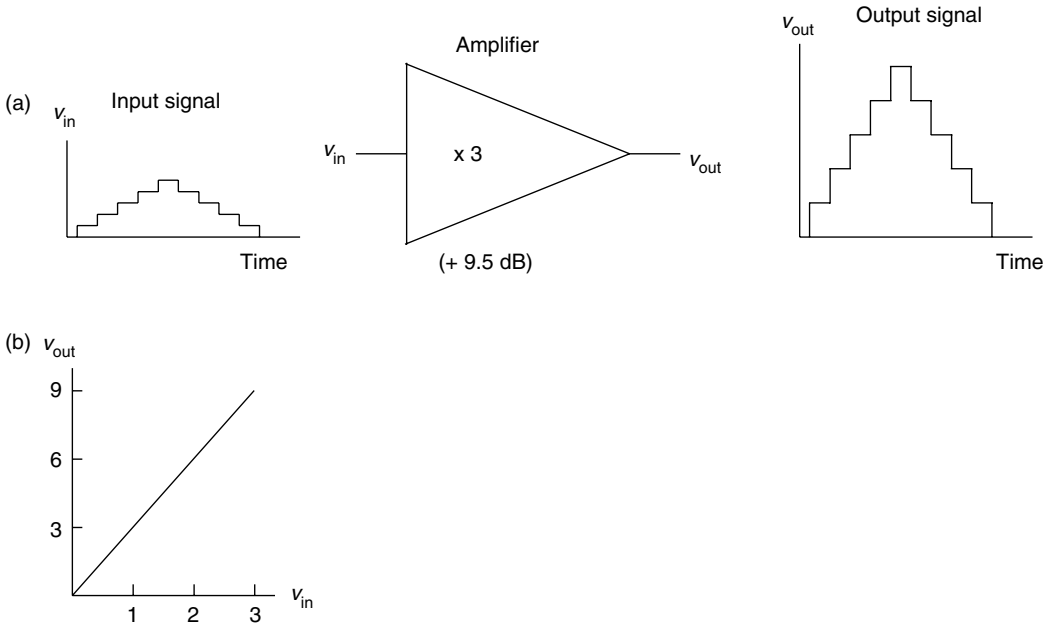

Fig. 4.2 Linear amplification. (a) The amplifier gain (×3) is the same for all signal levels. The gain is also constant with time. (b) A graph of output voltage against input voltage is a straight line.

for an electronic amplifier. This device in reality consists of numerous transistors and other electronic components, but can be treated as a single entity with an input terminal and an output terminal. The voltage signal to be amplified (V_{in}) is applied to the input terminal, and the amplified voltage signal (V_{out}) is available at the output terminal. The voltage gain of the amplifier is defined by the ratio V_{out}/V_{in}. Figure 4.2(a) illustrates the effect that a simple amplifier would have on a stepped voltage input signal. There are two points to note. First, in the output signal, each step is larger than the corresponding step in the input signal by the same ratio. That is, the voltage gain (in this case ×3) is the same for all voltage levels in the input signal. This is referred to as linear amplification, because a graph of V_{out} against V_{in}, as illustrated in Figure 4.2(b), is a straight line. Second, the voltage gain is constant with time. Each of the downward steps in the second half of the signal is amplified to the same extent as the corresponding upward steps in the first half. An amplifier of this type is used to amplify all echo signals equally, irrespective of when they return to the transducer. The overall gain control, available to the user on most B-mode systems, applies this type of gain to the echo signals. The effect on the image is to make all echoes brighter or darker, whatever their depth in the image.

Transmit power control

Most B-mode imaging systems allow user control of the amplitude of the pulse transmitted by the transducer. This control is often labelled as 'transmit power' and allows the user to reduce the transducer output from its maximum level in steps of several decibels (e.g. 0, −3, −6, −9 dB). The effect is to change the amplitude of the voltage used to drive the transducer, and hence the amplitude of the transmitted pulses. Reducing the amplitude of the transmitted pulses reduces the amplitudes of all resulting echoes by the same number of decibels. The effect is similar to reducing the overall gain applied to the received echoes. Reducing the transmit power reduces the exposure of the patient to ultrasound and the risks of any adverse effects (see Chapter 12). In many circumstances, the reduction in echo amplitudes can be compensated for by increasing the overall gain. However, where echoes of interest are weak due to a weakly scattering target or attenuated due to overlying tissue, their amplitudes may be reduced to below the system noise level. Increasing the overall gain cannot lift the signal above the noise level as the noise will be amplified with the signal. The operator should set the transmit power level to the minimum level which allows all

relevant echoes to be displayed clearly after adjustment of the overall gain.

Time–gain compensation

Attenuation

As described in Chapter 2, when a transmitted ultrasound pulse propagates through tissue, it is attenuated (made smaller). Echoes returning through tissue to the transducer are also attenuated. Hence, an echo from an interface at a large depth in tissue is much smaller than that from a similar interface close to the transducer (Figure 4.3). The attenuation coefficient of tissues is measured in dB cm^{-1} (see Appendix A). For example, if a particular tissue attenuates an ultrasound pulse by 1.5 dB cm^{-1}, the amplitude of the pulse will be reduced by 15 dB when it reaches an interface 10 cm from the transducer. The echo from this interface will be attenuated by 15 dB also on its journey back to the transducer, so that compared to an echo from a similar interface close to the transducer, the echo will be smaller by 30 dB. In this tissue, echoes received from similar interfaces will be smaller by 3 dB for each centimetre of depth.

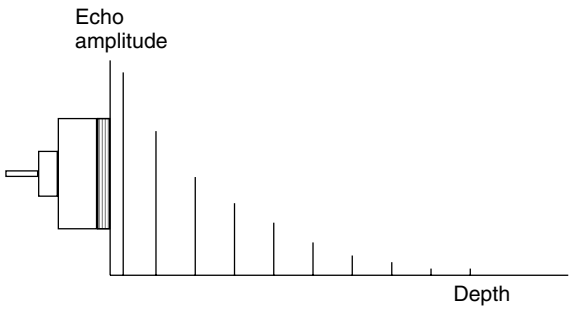

Fig. 4.3 Attenuation results in echoes from interfaces at large depths being smaller than those from similar interfaces near the transducer.

Time–gain control

In a B-mode image, the aim is to relate the display brightness to the strength of the reflection at each interface regardless of its depth. However, as we have just noted, echoes from more distant targets are much weaker than those from closer ones. Hence, it is necessary to compensate for this attenuation by amplifying echoes from deep tissues more than those from superficial tissues. As echoes from deep interfaces take longer to arrive after pulse transmission than those from superficial interfaces, this effect can be achieved by increasing the amplification of echo signals with time. The technique is most commonly called time–gain compensation (TGC), but is sometimes referred to as swept gain. It makes use of an amplifier whose gain may be controlled electronically, so that it can be changed with time. At the start of the pulse–echo sequence, as echoes are being received from the most superficial interfaces, the gain is set to a low value (Figure 4.4a). It is then increased with time to apply a higher gain to echoes arriving from greater depths. For the example above, when the pulse and the echo are each attenuated by 1.5 dB cm^{-1}, the gain must be increased by 3 dB cm^{-1}. This equates to an increase in gain of 3 dB for every 13 µs after transmission of the ultrasound pulse (assuming a speed of sound in tissue of 1540 m s^{-1}). After TGC, echoes from similar interfaces should have the same amplitude, regardless of their depth (Figure 4.4b).

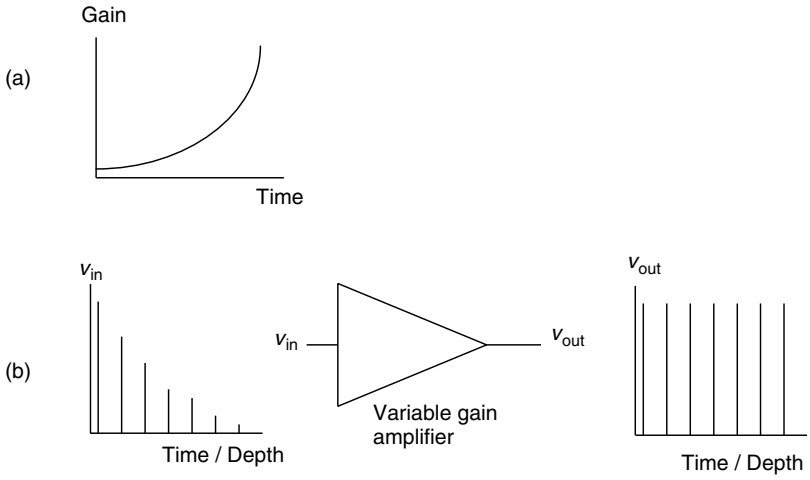

Fig. 4.4 Time–gain compensation (TGC). (a) The gain applied by the TGC amplifier increases with time after transmission to compensate for the greater attenuation of echoes from larger depths. (b) After TGC, echoes from similar interfaces should be equal in amplitude regardless of depth.

The actual rate of attenuation of ultrasound with depth is determined by the ultrasound frequency and the type of tissue. The ultrasound system applies TGC to the received signals at a rate (in dB per cm) designed to compensate for attenuation in average tissue at the current transducer frequency. Adjustments to this base level, to compensate for changes in tissue type within the imaged cross section, can then be applied manually by the operator. The most common arrangement for manual TGC adjustment is a set of slide controls as illustrated in Figure 4.5. Each slide alters the gain of the TGC amplifier at specific times after transmission, i.e. for echoes returning from a specific range of depths within the tissue. When all slides are in the central position, the average rate of TGC is applied, related to the frequency of the transducer. Moving the top slide to the right increases the gain applied to echoes from superficial tissues. The bottom slide adjusts the gain applied to the deepest echoes. In adjusting the TGC, the operator seeks to eliminate any trend for the average image brightness to change with depth. There can be no question of making all echoes equal in brightness, of course, nor would this be desirable, since the differences in scattered echo strength between different tissues is crucial to the interpretation of the image.

Some manufacturers now incorporate fully automatic TGC systems, which analyse the overall image brightness to identify and correct for any trends in image brightness down or across the image.

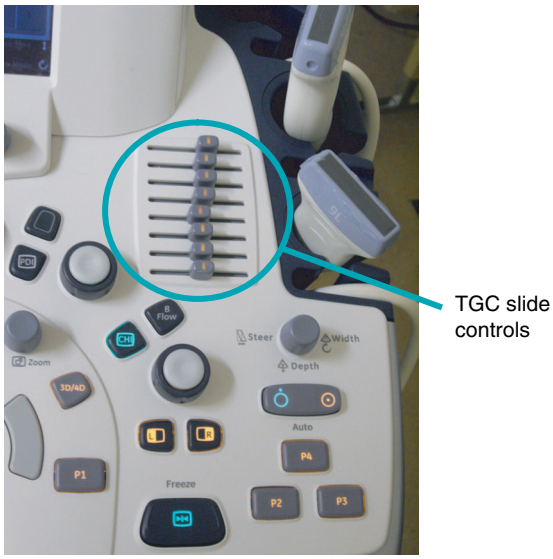

Fig. 4.5 TGC is most commonly adjusted using a set of slide controls, each of which affects the gain at a different depth.

Dynamic range of echoes

As discussed in Chapter 2, when an ultrasound pulse is incident on an interface or a scatterer, some of the incident intensity is usually reflected or scattered back to the transducer. For reflection at a large interface, as might be encountered at an organ boundary, the reflected intensity ranges from less than 1% of the incident intensity for a tissue–tissue interface to almost 100% for a tissue–air interface. The intensities of echoes received from small scatterers depend strongly on the size of the scatterer and the ultrasound wavelength, but are usually much smaller than echoes from large interfaces. Hence, the range of echo amplitudes detected from different targets is very large.

Figure 4.6 shows the relative voltages at the transducer produced by typical echoes from different targets. In this figure, the reference level used for expressing echo amplitudes in decibels is that from a tissue–air interface. Note that because the echoes are all weaker than that from the tissue–air interface, their decibel levels are negative. Also a voltage ratio of 10 between any two amplitudes corresponds to a difference of 20 dB. The figure shows that if the echo from a tissue–air interface gives a transducer voltage of 1 V, that due to echoes from blood will be of the order of 10 μV. Even smaller signals will be produced by the transducer, but these are likely to be lost in background electrical noise and cannot be detected. The dynamic range of signals at the transducer is defined as the ratio of the largest echo amplitude which does not cause distortion of the signal, to the smallest that can be distinguished from noise. The dynamic range is expressed in decibels.

Weak echoes produced by scattering within tissue give information about organ parenchyma, while

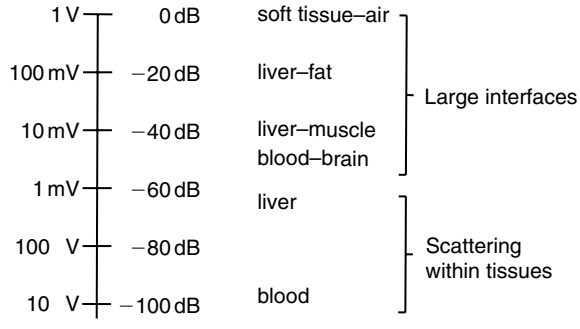

Fig. 4.6 Echoes due to reflections at interfaces are much larger than those due to scattering from within tissues, leading to a large range of possible amplitudes of diagnostically relevant echoes .

strong echoes from large interfaces give information about the size and shape of organs and other tissue features. To be useful diagnostically, a B-mode image should contain both types of echo. Figure 4.6 shows that the range of echo amplitudes displayed needs to be about 60 dB (−20 to −80 dB compared to a soft tissue–air interface) to include echoes from a typical tissue to tissue interface (e.g. liver–fat) as well as echoes due to scattering within tissue.

However, this range of echo amplitudes cannot be displayed without further processing. The ratio of the brightest level that the viewing screen can display to the darkest is typically about 20 dB. Therefore, if the gain of the B-mode system was adjusted to display an echo signal from a liver–fat interface at peak white level on the display, an echo from a liver–muscle interface would be displayed as the darkest available grey. All weaker echoes from tissue scattering would be displayed at black level and not visible. Alternatively, if the gain was increased to display weak echoes scattered from tissue (say at the −80 dB level in Figure 4.6) as dark grey, the echoes from within the liver would be displayed at peak white. Echoes with greater amplitudes (e.g. from blood–brain, liver–fat interfaces) would also be displayed at peak white and could not be distinguished.

Compression

To allow echoes from organ interfaces and organ parenchyma to be displayed simultaneously in a B-mode image, it is necessary to compress the 60 dB range of the echoes of interest into the 20 dB range of brightness levels available at the display. Compression is achieved using a non-linear amplifier as illustrated in Figure 4.7.

Unlike the linear amplifier described earlier for overall gain, this non-linear amplifier provides more gain for small signals than for large signals. Hence, weak echoes are boosted in relation to large echoes. A graph of the output voltage against input voltage for this amplifier is a curve (Figure 4.7a) rather than the straight line of the linear amplifier. In this example, an input voltage of 2 units gives an output voltage of 4 units (gain of 2) while an input voltage of 6 units gives an output voltage of 6 units (gain of 1). Normally, the amplifier used to compress the signal range has a logarithmic characteristic, so that the output voltage is related to the logarithm of the input voltage. Using this type of amplifier, weak echoes from scattering within the tissue can be boosted more than the large echoes from interfaces, so that both types of echo can be displayed at the same time.

In practice, the range of echo amplitudes which need to be compressed into the display range depends on the application. For example, when trying to identify local tissue changes in the liver, a wide dynamic range of echoes needs to be displayed, so that these weak echoes are made to appear relatively bright in the image. For obstetric work, interpretation of the shapes in the image may be aided by reducing the displayed dynamic range, so that weak echoes are suppressed and areas of amniotic fluid are clearly identified.

Some commercial B-mode systems provide a dynamic range control (sometimes labelled compression). This control essentially allows adjustment of the curve in Figure 4.7a to alter the dynamic range of echo

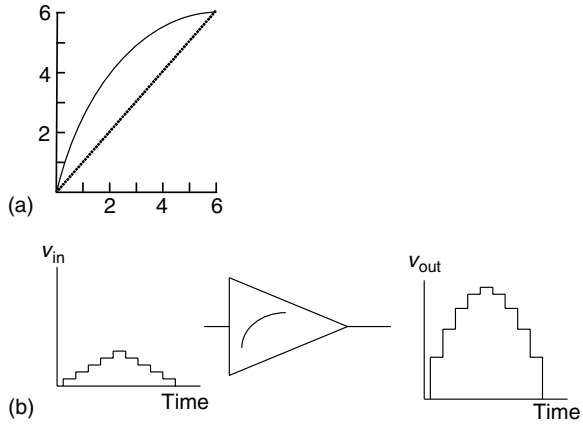

Fig. 4.7 (a) To compress the dynamic range of echoes, an amplifier with a non-linear gain characteristic is used. (b) The amplifier applies more gain to small echoes than to large echoes so that both can be displayed at the same time.

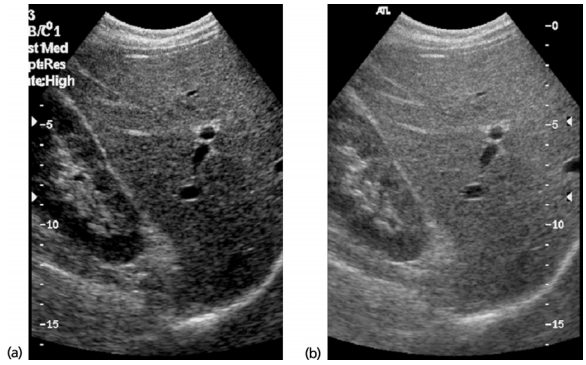

Fig. 4.8 Increasing the dynamic range setting from (a) 40 dB to (b) 80 dB increases the gain for small echoes, making it easier to detect irregularities in the texture of the liver.

amplitudes displayed. Figure 4.8 shows the effects of altering the dynamic range control on an image of a liver and right kidney. In Figure 4.8a, the dynamic range is set to 40 dB while in Figure 4.8b it is set to 80 dB. In both images, the brightness of the echo from the diaphragm (the curved bright echo in the lower right corner) is similar. In relation to this echo, the echoes from within the liver are brighter when the dynamic range is set to 80 dB than when it is set to 40 dB. Irregularities in the liver texture would be easier to detect with a dynamic range setting of 80 dB.

Analogue-to-digital conversion

The echo signals received by the transducer elements are analogue signals. That is, their amplitudes can vary continuously from the smallest to the largest value. The beam-forming techniques described in Chapter 3 are implemented using digital techniques. The beam-formed signal continues in digital form as it is further processed and the B-mode image is assembled and stored in the image memory. Hence, at an early stage in the signal-processing chain, the echo signal must be converted from analogue to digital form. The conversion process is illustrated in Figure 4.9.

At regular, frequent intervals in time, the amplitude of the analogue echo signal is measured, or sampled, producing a sequence of numbers corresponding to the amplitude values of the samples. If the numbers and the time interval between them are recorded, it is possible to regenerate the signal at a later time by reading the numbers out again at the same rate through a device which produces a voltage proportional to the stored number (a digital-to-analogue converter).

In digital form, the signal is quantized. That is, it can have only a limited number of values, unlike the analogue signal, which was continuously variable. In Figure 4.9, the signal can be quantized into 1 of only 10 different values and the recovered waveform will be a relatively crude representation of the original. Apart from zero, the smallest value that can be recorded is 1 and the largest 10, so the maximum dynamic range of echoes that can be recorded is 20 dB (see Appendix A). The analogue-to-digital converters (ADCs) used in modern B-mode systems convert the signal into a much larger number of more closely spaced values, so that the regenerated signal is a much more faithful recording of the original. Also, since the smallest value that can be digitized is smaller, the dynamic range (the ratio of the largest to smallest value) is greater. In Figure 4.9, the signal levels are shown as decimal numbers. In practice, the binary system of counting is used instead (see Appendix B).

Therefore, the input to the ADC is an analogue signal whose amplitude varies continuously with time, and the output is a corresponding stream of binary numbers as illustrated in Figure 4.10. Each column of

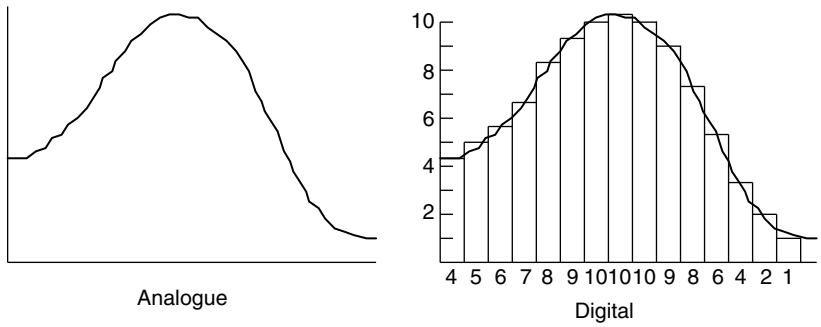

Fig. 4.9 Analogue-to-digital conversion involves measuring the amplitude of the signal at regular intervals in time. The signal can then be stored as a set of numbers.

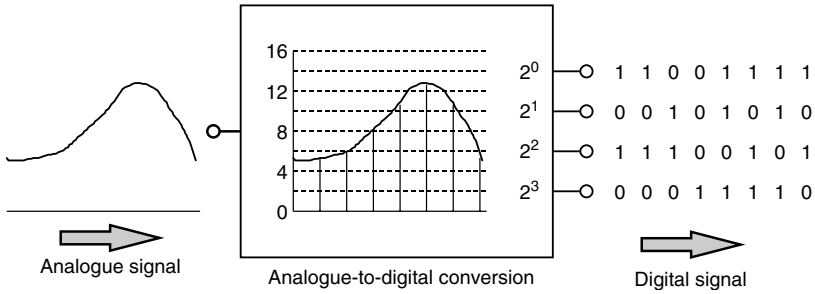

Fig. 4.10 In real ADCs, the continuous analogue signal is converted to a stream of binary numbers.

Table 4.1 Dynamic ranges for binary systems.

Bits	Max count	DR (dB)
4	15	24
8	255	48
10	1023	60
12	4095	72

binary numbers represents the amplitude of one sample of the signal, the column on the extreme right corresponding to the leading edge of the analogue signal and those progressively to the left, the following parts of the signal. The sequence of binary numbers may undergo various digital processing stages before storage in the image memory.

The precision to which the ADC can measure the amplitude of the signal is normally described by the number of bits (binary digits) available at the output. The 4-bit system illustrated in Figure 4.10 can digitize the signal to 16 different values (including 0). Table 4.1 shows the number of different signal values available with various numbers of bits. The number of bits also determines the dynamic range of signals that can be digitized, since this is equal to the ratio of the largest binary value to the smallest. In the case of a 4-bit number, the ratio is 15:1, giving a dynamic range of approximately 24 dB. Some modern B-mode systems can digitize the echo signal to 12 bits, so that 4096 levels are available, and a dynamic range of approximately 72 dB can be processed and stored. Note that each extra bit of the ADC increases the maximum number of levels by a factor of 2, and hence the dynamic range by an additional 6 dB.

At diagnostic frequencies, the amplitude of the echo signal changes rapidly with time. To preserve detail in the stored image, the ADC must sample the echo signal at a high enough rate to capture these changes. In modern B-mode systems, it is not uncommon to sample at 40 MHz, i.e. 40 million samples per second. To be able to regenerate the signal faithfully after storage, the sample rate must be at least twice the highest frequency present in the analogue signal. A sample rate of 40 MHz fulfils this requirement for most frequencies used for B-mode imaging.

Advantages of digitization

The echo signal at the transducer is an analogue signal and, for echoes generated by scattering within tissue, is relatively weak. When such signals are processed electronically as analogue signals, they are vulnerable to being degraded by electrical noise and by interference from nearby electrical equipment and from neighbouring parts of the B-mode system. The signal-processing techniques available in analogue electronics are relatively limited in their performance. Analogue processing circuits may introduce distortions to the signal, if they are not well designed, and storage of such signals is difficult and can add further noise and distortions. Stored analogue images, e.g. on magnetic tape or discs, may degrade or drift with time due to changes in the storage medium.

Once a signal has been converted into digital form, it consists simply of a set of numbers, which are essentially immune to noise, interference and distortion. Digital information can be stored conveniently in electronic memory or on a magnetic or optical medium without degrading with time. The retrieved image information is identical to the original. The power and flexibility of digital storage methods are familiar to most people through their widespread use in audio and video recording devices.

Perhaps, the most important advantage of digitization for B-mode imaging is that it makes digital processing of echo information possible. Using built-in, dedicated computing devices, digital echo information can be processed by powerful mathematical techniques to improve the image quality. While some of these processes may be carried out in real time, others make use of information that has been stored temporarily in a digital memory. For example, information relating to an adjacent part of the image or a previous pulse–echo cycle might be used in conjunction with the current B-mode line to enhance image quality.

Harmonic imaging

As described in Chapter 2, harmonic imaging of tissue is useful in suppressing weak echoes caused by artefacts (see Chapter 5), which cloud the image and can make it difficult for the operator to identify anatomical features with confidence. Such echoes, often referred to as clutter, are particularly noticeable in liquid-filled areas, such as the heart or within a cyst, and are a common problem when imaging large patients, due to the effects of fatty tissue on the ultrasound beam.

As a high-amplitude ultrasound pulse propagates through the tissue, non-linear effects cause energy at the transmitted frequency f_0 to be transferred into the harmonic frequencies $2f_0$, $3f_0$, etc. This effect is

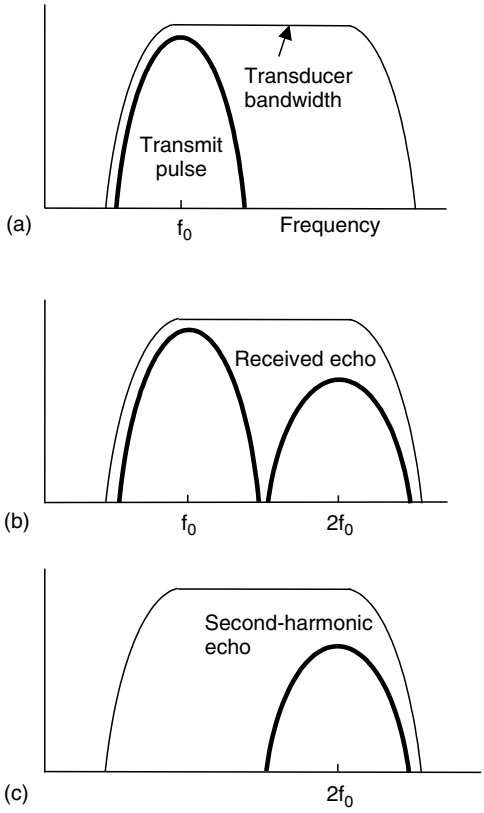

Fig. 4.11 Harmonic imaging. (a) In harmonic imaging, the pulse is transmitted at frequency f_0 using the lower half of the transducer bandwidth. (b) Echoes are received containing information at f_0 and $2f_0$. (c) The frequencies in the echoes around f_0 are filtered out and the image is formed from the $2f_0$ part of the echo.

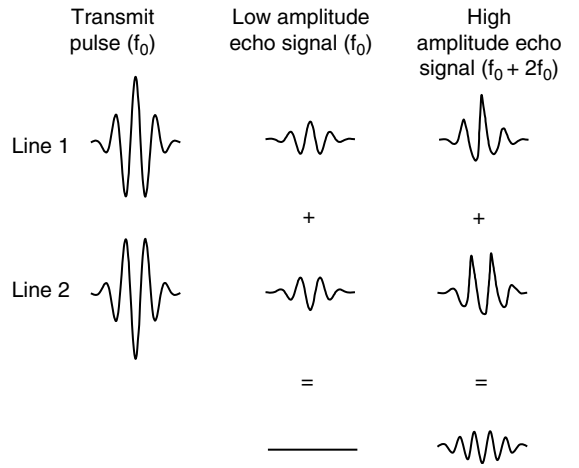

Fig. 4.12 Pulse-inversion imaging. On Line 1, a pulse is transmitted at f_0 and the line of echoes stored. A second pulse is transmitted along the same beam with its phase inverted. The resulting line of echoes (Line 2) is added to Line 1. Low-amplitude echo signals cancel out while distorted, high-amplitude signals do not. The component of the high-amplitude signal at f_0 cancels, leaving the component at $2f_0$.

strongest for the high-amplitude parts of the beam, i.e. on the beam axis, but weak for small echoes, such as those arising from reverberations and other multiple-path artefacts. In harmonic imaging, the image is formed by using only the second-harmonic energy in the returned echoes, suppressing the weak artefactual echoes and enhancing those from the beam axis. This can result in a clearer image, improving the accuracy of diagnosis.

Harmonic imaging can be achieved using a transducer with a wide bandwidth, which can respond to both the fundamental frequency f_0 and its second harmonic $2f_0$, as illustrated in Figure 4.11. In transmission (Figure 4.11a), the transmit frequency f_0 is chosen to ensure that the pulse spectrum sits in the lower half of the transducer's frequency response curve. In reception (Figure 4.11b), the received echoes contain information around the transmit frequency f_0 and its second harmonic $2f_0$. To achieve harmonic imaging, the received echoes are passed through a band-pass filter, which allows through only frequencies around $2f_0$ and rejects frequencies around f_0 (Figure 4.11c). As the clutter echoes are low amplitude and their energy is mainly at the fundamental frequency, they are suppressed, giving a clearer image (Desser *et al.* 2000, Tranquart *et al.* 1999).

To allow the filter to achieve good suppression of the clutter signal, the spectra of the transmit pulse and its second harmonic need to be well separated, with no overlap. To achieve this, the frequency spectrum of the pulse must be made narrower than for normal imaging. Reduction of the width of the spectrum results in an increase in the length of the pulse in time, reducing the axial resolution of the system as described in Chapter 5.

A harmonic image can be produced also by a technique known as pulse-inversion imaging (see Figure 4.12). This technique requires two consecutive pulse–echo cycles for each beam position. In the first pulse–echo cycle, a pulse at the chosen fundamental frequency f_0 is transmitted and the line of echoes is received and stored digitally. A second pulse, which is an inverted version of the first, is then transmitted down the same

B-mode line. The line of echoes generated by the second pulse is added to the stored first line (Simpson *et al.* 1999). Low-amplitude echoes, from the edges of the beam or from reverberations, are generated by linear propagation and are undistorted replicas of the transmission pulse, containing only the fundamental frequency f_0. Corresponding low-amplitude echoes in the first and second lines cancel out as each is an inverted version of the other. In the higher-amplitude parts of the beam, the transmitted pulse is distorted due to non-linear propagation and harmonic generation. Echoes from these regions have a high harmonic content at $2f_0$ and do not cancel out, creating a harmonic image.

The advantage of the pulse-inversion method is that the pulse spectrum does not need to be reduced in width and hence axial resolution can be maintained. The disadvantage is that the need for two pulse–echo cycles per line can reduce the frame rate and cause artefacts if the imaged target moves between the two pulse–echo cycles (Ma *et al.* 2005).

Coded excitation

One of the fundamental challenges for manufacturers and users of ultrasound is to optimize the choice of transmit frequency for different clinical applications. A high frequency allows the formation of a narrow beam and a short transmit pulse, leading to good spatial resolution (see Chapter 5). However, high frequencies are attenuated more rapidly, giving reduced penetration into tissue. Conventionally, high frequencies, e.g. 10 MHz, would be used only to image superficial structures, such as the thyroid or arteries of the neck. A low frequency, e.g. 2.5 MHz, gives good penetration but relatively poor resolution and might be used to image the heart or the liver of a large patient.

Attenuation of the transmitted pulse and returned echoes increases with depth, and the limit of penetration for a conventional pulse corresponds to the depth from which echoes are no longer larger in amplitude than the background system noise. Greater penetration can be achieved by increasing the amplitude of the transmit pulse. However, maximum pressure amplitudes generated in tissue by the transmit pulse are limited by regulation and other safety issues (see Chapter 12).

Coded excitation of the transmit pulse can be used to increase the signal-to-noise ratio for a given frequency and hence help to improve penetration, without increasing the pulse amplitude. Pulse coding methods employ transmit pulses which are much longer than a conventional 3–4-cycle imaging transmit pulse. The use of a long transmit pulse leads to an improvement in signal-to-noise ratio, but without further processing would result in very poor axial resolution. By embedding a digital code into the long transmit pulse, good axial resolution can be recovered and signal-to-noise ratio improved by identifying the transmitted code within the received echoes (Chiao and Hao 2005, Nowicki *et al.* 2006).

Figure 4.13a shows an example of a digital code (1,1,0,1) that might be used. To embed the code within the transmit pulse, the pulse is divided into four time intervals, in this case, each two wave periods long. The value of the digital code in each segment (1 or 0) is represented

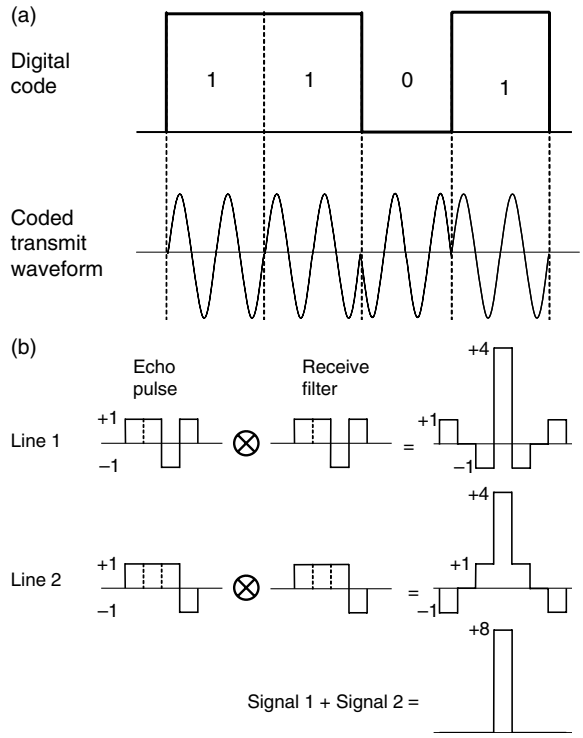

Fig. 4.13 Coded excitation. (a) A digital code can be embedded into the transmit pulse by changing the phase of the waveform. The time elements corresponding to a digital '1' can be represented by a positive phase and those corresponding to a digital '0' by a negative phase. (b). The digital code can be extracted from the returned echoes using a matched filter, which contains the original code. A large signal is received when the code and filter match, but with range lobes before and after. Range lobes can be cancelled out using a second complementary code.

by the phase of the excitation waveform used. The starting phase in the '0' segment is opposite to that in the '1' segments. In Figure 4.13b, the envelope of the detected echo is given a value of +1 where the '1' phase is detected and −1 for the '0' phase. As the echoes of the coded pulse are received, they are stepped through a matched filter, which contains a copy of the transmitted code. This is a correlation filter, in which the received signal is convolved (as indicated by the circled cross symbol) with a time-reversed version of the transmitted pulse. At each time step (equal to the time segments in the transmit pulse), the code values of each segment are multiplied by the values they overlap in the filter and added together. The resulting signal has amplitude of +4 at the time step where the echo exactly overlies the code in the matched filter. However, positions before and after this also result in non-zero values, which give rise to range lobes on the signal. Longer codes and more complex sequences (e.g. Barker codes) may be used to achieve greater increases in signal-to-noise ratio and reduced range lobe level (Chiao and Hao 2005).

The range lobes can be cancelled out by transmitting a second pulse along the same B-mode line with a complementary code as shown in Figure 4.13b; the first pulse and the complementary pulse are described as a 'Golay pair' (Eckersley *et al.* 2007). When the output signals from the two lines are added together, the range lobes cancel and the resulting signal has an amplitude of +8 and a duration of one time segment. However, the use of multiple pulse–echo cycles on each line results in a reduction in frame rate and may lead to artefacts if the target tissue is not stationary.

An alternative approach to embedding a digital code in the transmit pulse is to transmit a chirp (Pedersen *et al.* 2003). This is a long pulse, in which the transmit frequency is swept from a low to a high value (within the bandwidth of the transducer). The received echoes are again stepped through a matched filter, which gives a large output value for the brief time interval when the received echo matches the receive filter. Chirp excitation requires only a single pulse per line but requires a more complex and costly transmission pulse generator.

Amplitude demodulation

The ultrasonic pulse transmitted by the B-mode system consists of several cycles of oscillation at a frequency of a few megahertz. Echoes from reflecting interfaces are of the same form. A typical echo signal due to a reflection at a single interface is illustrated in Figure 4.14a. It consists of oscillations above and below the zero baseline.

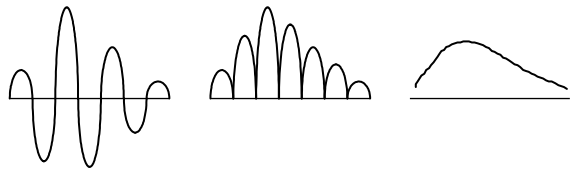

Fig. 4.14 The echo signal is demodulated to remove the variations at the transmit frequency (the radio frequency) and leave just the echo amplitude information. (a) Radio frequency pulse, (b) rectification and (c) low-pass filter.

The envelope of the signal is described by a pair of curves passing through the peaks above and below the baseline. The strength of the reflection at the interface determines the height or amplitude of the envelope of the pulse (after TGC), and it is this information which determines the brightness of each point in the B-mode display. One half of this envelope or amplitude signal is extracted from the high-frequency signal by a process called amplitude demodulation, as illustrated in Figure 4.14.

The signal is first rectified (Figure 4.14b), i.e. one half of the waveform is inverted, so that all half cycles are aligned on the same side of the baseline. The rectified signal is then smoothed by passing it through a low-pass filter, which removes the high-frequency oscillations and retains the slowly varying envelope (Figure 4.14c). Most modern B-mode systems demodulate the echo signal after the ADC. That is, the process is carried out on the stored digital information using fast computing techniques.

Image formation and storage

The image memory

The B-mode image is assembled in the image memory using the processed amplitude signal and information from the beam-former on the time since transmission (range), and the position and direction of the ultrasound beam, i.e. the scan line. This process is called writing to the image memory. From the image memory, this echo information is read out to the display monitor. Both writing and reading processes are described in detail later.

The image memory is a digital memory similar to that used in a personal computer. Just as the brightness information of the echo sequence has to be quantized to convert it into digital form before storage in the image memory, the information describing the position of echoes in the image must also be broken into

discrete locations to allow storage. The image memory divides the image into a 2D array of picture elements or pixels. These are rather like the 2D grid system of a map (Figure 4.15).

Each pixel has an address, which is analogous to the grid reference or coordinate system used in maps. Any pixel can be addressed uniquely using its column number, i.e. its position on the horizontal axis, and its row number, i.e. its position on the vertical axis. To allow storage of fine detail, the image is broken into a large number of small pixels, just as in the digitization of the brightness signal. In a modern B-mode system, the image memory might consist of an array of about 1000 × 1000 elements. The area of the image within the boundary of one pixel is represented by a single value of brightness. Each memory location corresponding to a pixel stores a binary number corresponding to the representative echo amplitude or brightness for that pixel. This number is typically 8–12 bits long (see Appendix B).

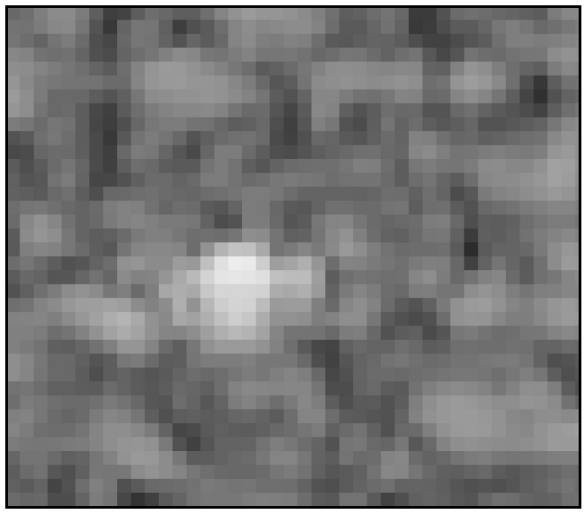

Fig. 4.15 The image consists of a 2D array of picture elements (pixels). The grey level of each pixel is recorded as a number in the corresponding location within the image memory.

Writing to the image memory

The process of storing B-mode information in the image memory is referred to as writing to the memory. The writing process for each image line begins at a point in the image corresponding to the active part of the transducer face and progresses across the 2D memory array in a direction corresponding to the axis of the ultrasound beam. The process is illustrated in Figure 4.16 for the case of a linear-array transducer, producing vertical B-mode lines, with the transducer face near the top of the image.

Immediately after transmission of the ultrasound pulse, the system addresses the image pixel corresponding to a position immediately below the centre of the active part of the transducer face. The binary number representing the amplitude of the echo from this point is written to this memory location. The system then addresses the next pixel along the projected track of the image line, writes the representative value of amplitude into that memory location and moves on to address the next pixel. The rate at which this write sequence progresses down the line of image pixels is determined by the field of view selected by the operator.

As described in Chapter 1, the go and return time t for a pulse to reach an interface (at range d) and the echo to return to the transducer is given by the equation

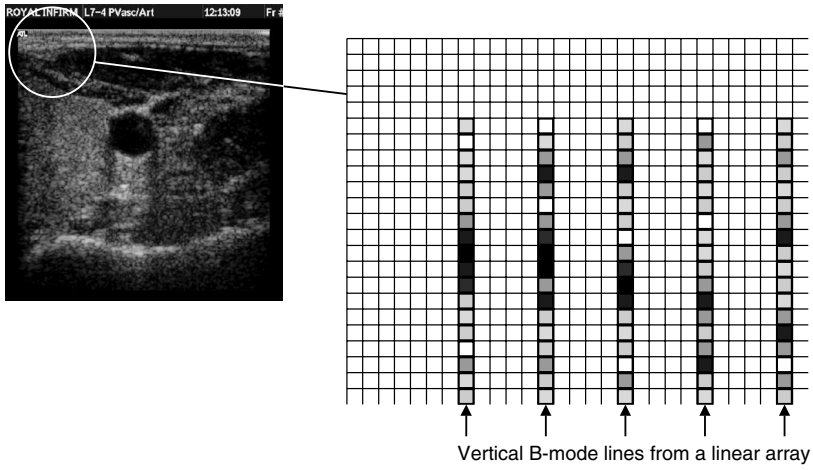

Fig. 4.16 Image lines are formed by writing to each pixel in turn as echoes arrive from increasing depths.

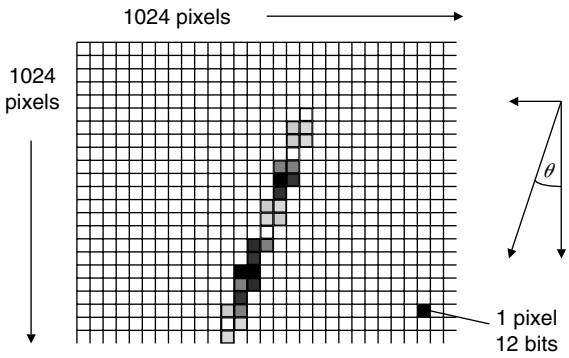

Fig. 4.17 For sector transducers, image lines are written at angle θ by changing row and column addresses.

$t = 2d/c$, where c is the speed of sound. At the average speed of sound for soft tissues (1540 m s^{-1}), this equates to approximately 13 µs for each centimetre of range from the transducer. Hence, if a maximum imaged depth of 10 cm is chosen, then each line of pixels corresponding to an image line must be addressed and written in a total time of 130 µs. The spacing of adjacent image lines across the memory is chosen to maintain the scale factor in the horizontal direction.

In the linear array case, the stored ultrasonic line was aligned with a column of pixels, and the system needed only to change the address of the row to write the line into memory. In the case of sector and curvilinear fields, most of the ultrasonic lines cross the memory array at an angle θ to the columns of pixels (Figure 4.17), and the row and column addresses must be changed simultaneously to progress along the correct track.

Interpolation

In linear-array systems, the image lines may not always be stored in adjacent columns in the image memory (Figure 4.16). The pixels between are filled by the system's computer using interpolation between values in adjacent filled pixels. The case of linear interpolation in one dimension is illustrated in Figure 4.18. If two adjacent lines are 5 pixels apart and have amplitude values of 5 and 10 at a particular depth, the intervening 4 pixels would be given intermediate values on a linear scale, i.e. 6, 7, 8, 9. In real systems, interpolation is more sophisticated and takes into account the values of neighbouring pixels in 2D and is not necessarily linear.

Interpolation is used extensively in writing sector and curvilinear scanning formats to the image memory. For these formats, the spacing between the lines increases with depth and interpolation is more important.

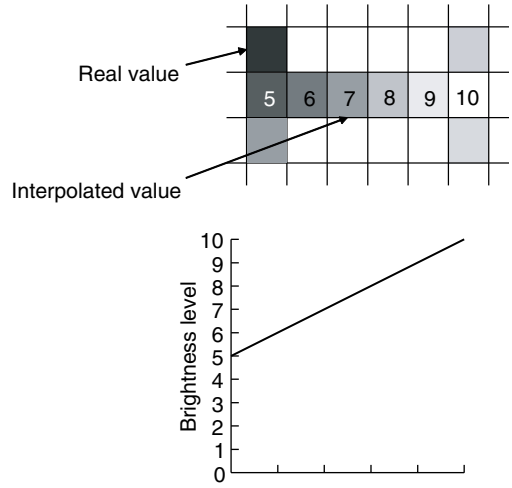

Fig. 4.18 Pixels which are not crossed by image lines are filled in by interpolation between adjacent values. This can be a linear process.

Write zoom

There are two ways to increase the magnification of part of an image. One is to use the conventional depth control, but this involves losing the deeper parts of the image from the display. Hence, features which are deep within the tissue cannot be magnified by this means. The second method, known as write zoom, was introduced in Chapter 3 and allows the display of a selected region of interest (ROI) remote from the transducer. The user outlines the ROI by adjusting the position and dimensions of an on-screen display box, with the image set to a relatively large depth. When ROI display mode is activated, the B-mode system interrogates only those lines which pass through the ROI. For each of these lines, echoes originating from between the transducer and the near side of the ROI box are ignored. In each pulse–echo sequence, the system waits until echoes arrive from the depth marked by the near side of the box, and writes the subsequent echo amplitude information into the memory on a large scale. Information from within the ROI then fills the image memory.

Reading from the image memory

When brightness information is written to the image memory, the pixel address sequence follows the course of the ultrasonic line in the imaged tissue. To view the image, it must be read out to a display device in a sequence which is compatible with the display format. The display monitor screen is also composed of a 2D array of elements, each of which emits light when activated. These are addressed one at a time by the monitor

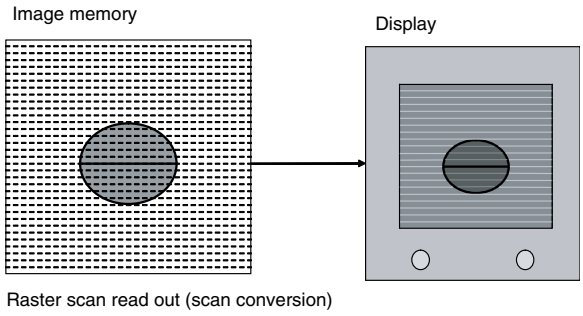

Fig. 4.19 Grey-level values are read out from the memory in a raster scan synchronized to the display monitor.

in a sequence of horizontal lines or raster scan, starting at the top left of the screen and finishing at the bottom right (see Figure 4.19). The stored image is read out from the image memory by interrogating each pixel in turn in synchronism with the display raster. The stored binary values are converted to an analogue level to control the brightness of the display. The process does not degrade the information stored in the memory and can be repeated indefinitely, if required. Hence, the image memory performs the function of scan conversion from ultrasonic line format to monitor display format.

Read zoom

Read zoom is another way of magnifying part of the image. During normal read-out, the display raster interrogates the whole area of the image memory. Where the imaged depth is larger than the imaged width, this can result in inefficient use of the screen area, and imaged features appear small on the display, as described above under the heading 'Write zoom'. The read zoom function addresses and reads out a selected part of the stored image defined by the user with an on-screen ROI box similar to that used with the write zoom function. The area of the image memory interrogated by the display raster is then just that required to show the selected area.

An advantage of read zoom over write zoom is that read zoom can be applied to a previously stored image of the total area of interest and the zoomed area moved around to examine different parts of the image on an expanded scale. The disadvantage over write zoom is that when a large image magnification is used, the number of image memory pixels being displayed may become so small that individual pixels become obvious. A higher-quality image can be obtained by using write zoom, but the echo information for this needs to be acquired after the ROI box is set. Read zoom is rather like taking a wide-angle photograph of a scene and then examining parts of it with a magnifying glass. The details are enlarged, but the imperfections of the photographic process may be apparent. Write zoom is the equivalent of using the optical zoom or a telephoto lens on a camera to image a small part of the scene. The image quality and definition are maximized, but there are no information available from other parts of the scene.

Image update modes

Real-time display

In most medical imaging processes (e.g. X-ray, CT and MRI), there is a significant time delay between image acquisition and image display, so that diagnosis is made on information which may be many minutes old. Formation of a single ultrasound B-mode image in the image memory takes typically of the order of 1/30 s, so that, if repeated continuously, 30 images can be formed each second. This rate is referred to as the frame rate and is measured in hertz. Also, the time delay between image acquisition and display is relatively short (a few tens of milliseconds). This leads to the description 'real-time' imaging, i.e. images of events within the patient are displayed virtually as they happen. The real-time nature of the process is an important aspect of ultrasound imaging and, coupled with the use of a hand-held probe in contact with the patient, gives a highly interactive form of investigation. Real-time imaging allows the study of the dynamic behaviour of internal anatomy, such as the heart, and can aid identification of normal anatomy (e.g. gut from peristalsis) and pathology (e.g. movement of a gallstone).

The display monitor typically displays a complete image in 1/25 s, giving 25 images per second. To avoid conflicts between the reading and writing processes, buffer memories are used to store echo data on a temporary basis, so that the two processes can proceed independently of each other.

Freeze mode

If the image acquisition process (writing) is stopped, so that data in the image memory remain unchanged, but are still read out repeatedly to the display, the image is said to be frozen. All commercial systems have a freeze button, which activates this mode. Freeze mode is used while measurements are made on features in the image and hard-copy records made. Normally, the transducer stops transmitting ultrasound pulses in this mode.

Cine loop

The image formation process described so far has implied the existence of a single image memory in which the image is formed. In fact, most current B-mode systems have multiple image memories (up to 2000) and continue to store each frame as it is formed in the next available image memory, eventually cycling around to overwrite memory number 1 when number 2000 is filled. The image is frozen at the end of the dynamic event of interest or examination and the multiple image memories allow the last 2000 frames to be reviewed in real time or individual frames to be selected and printed as hard copies. Sections of the stored data can be stored as movie clips as part of a patient report. For the heart, which has a regular, repetitive movement, the recorded frames can be displayed as a cine loop, repeating the cardiac cycle and allowing diagnosis after the examination has been completed.

Post-processing

Frame averaging

When consecutive B-mode images are formed and stored in the image memories, they contain small frame-to-frame variations due to random imposed electrical noise. If the stored frames are then read out directly to the display in the same sequence, the constantly changing random noise patterns in the image can be very distracting and mask weak displayed echoes. This random noise effect can be reduced by frame-to-frame averaging of images. Random noise events then tend to be averaged out, while constant ultrasonic image features are reinforced, improving the signal-to-noise ratio of the image.

In the process described earlier for reading out the image from the image memory to the display, the most recent B-mode frame was read out from the image memory, pixel by pixel in a raster format. This real-time image would contain obvious flickering noise patterns. To achieve frame averaging, the value of each pixel that makes up the raster pattern of the display is calculated as the average value of the corresponding pixels (e.g. row 10, pixel number 35) in each of the most recent few frames. The number of averaged frames is typically in the range 1–5, selected by the user.

Frame averaging is effective in suppressing random image noise, making it easier to study areas of anatomy that generate weak echoes, e.g. weakly scattering or deep tissues. However, the averaging effect slows the time response to changes in the image, resulting in smearing of the image of moving targets (e.g. heart valves). Long persistence (five frames) is useful for optimizing the image signal-to-noise ratio for relatively stationary images such as liver, whereas short persistence (zero persistence being one frame) must be used to image rapidly moving targets, such as heart valves.

Grey-level transfer curves

In addition to controlling the dynamic range, as described earlier, most modern B-mode systems allow further modification of the gain curve that relates echo amplitude to displayed brightness level. Such processing would normally be applied to the stored image as it is read out from the image memory to the display and hence comes under the heading of post-processing. Figure 4.20 shows a set of commonly used

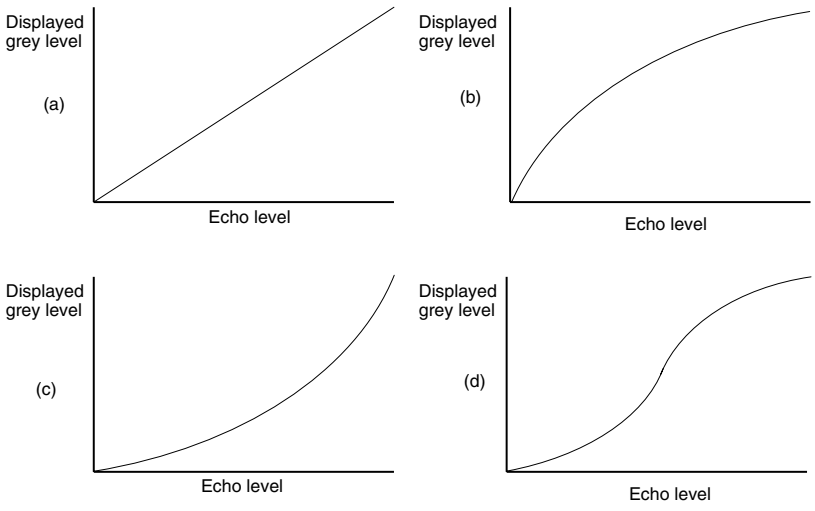

Fig. 4.20 Grey-scale post-processing curves. (a) Linear, (b) small echo contrast enhancement, (c) high echo contrast enhancement, (d) mid echo contrast enhancement.

grey-level curves (also referred to as the gamma curve). In Figure 4.20a, there is a linear relationship between the stored image brightness level and the displayed image brightness, with contrast assigned equally to all levels. In Figure 4.20b, more contrast is assigned to low-level echoes such as those from within the liver to aid differentiation of normal from abnormal tissue regions. In Figure 4.20c, more grey levels are assigned to higher echo levels to aid diagnosis for organs whose tissues scatter more strongly and give a brighter image. Figure 4.20d shows a grey-level curve that may be used to enhance contrast for mid-level echoes. A selection of grey-level curves such as these is available to the user via the set-up menu of most commercial B-mode systems. Such grey-level processing curves may also be selected automatically by the system as part of the optimization of system parameters for particular clinical applications. For example, if the user selects a vascular application setting on the system, the grey-level curve chosen is likely to be different from that chosen to optimize for general abdominal or musculo-skeletal applications.

Edge enhancement

The B-mode images formed and stored in the image memories may contain a number of imperfections, such as indistinct or incomplete organ boundaries, due to variable orientations of the target interfaces to the direction of the ultrasound beam, or prominent speckle (see Chapter 5). Further image-processing methods would normally be applied to reduce such imperfections and improve the diagnostic quality of the images.

Where the targets of interest include blood vessels or anatomical interfaces, the boundary echoes can often be made clearer or more complete by applying edge enhancement. The echo patterns across features such as vessel walls contain abrupt changes in image brightness. These abrupt changes give rise to higher spatial frequencies in the image. To enhance the appearance of the walls of vessels and other anatomical features, a spatial high-pass filter can be applied to the two-dimensional image. This has the effect of making the boundary echoes more prominent. Normally, different levels of edge enhancement can be selected by the user to suit the particular clinical investigation.

While edge enhancement may help to clarify the boundaries of vessels and organs in the image, the application of a spatial filter which emphasizes changes in brightness across the image also has the effect of emphasizing noise patterns and speckle which also contain high spatial frequencies. The user must use such processing facilities intelligently to optimize the image for the particular investigation.

Adaptive image processing

The edge enhancement technique referred to above is useful where boundaries need to be emphasized. The B-mode image normally contains various forms of image noise or clutter such as pixel sampling noise and speckle (see Chapter 5). These would normally be suppressed by applying a spatial filter to the image with the opposite characteristic to the edge enhancement filter (a spatial low-pass filter), i.e. one which suppresses changes in brightness across the image and has a smoothing effect.

The limitation of both types of spatial filter is that they are applied uniformly to the whole image and so cannot be applied at the same time. Adaptive image processing is used by some manufacturers to avoid this limitation. The two-dimensional B-mode image is analysed on a number of scales to identify and map the spatial frequency content and identify structural features. Structural features, e.g. vessel or lesion boundaries, can then be emphasized by applying a smoothing filter along the line of the boundary, while applying an edge enhancement filter across the boundary. Areas containing no identifiable boundaries are smoothed to reduce noise and speckle.

Display, output, storage and networking

A modern ultrasound system has a flat-screen display, has some capacity locally for storing video clips and images, and is connected to an imaging network, so that any hardcopy is performed using a high-quality communal printer, and all data are archived in a large central datastore. The era of the stand-alone ultrasound system which is connected to its own printer and own video recorder is rapidly becoming a thing of the past. Many older ultrasound systems still in use will have older technology; video recorders, thermal printers, cathode ray tube displays etc. This section concentrates on flat-screen network-based ultrasound systems. Details of older technology can be found in the first edition of this book (Hoskins *et al*. 2003).

Display

Recent years have seen a move away from traditional cathode ray tube displays, to flat-screen displays. Generally liquid crystal displays (LCD) are used. These are widely used as computer and TV displays and are able to produce high-quality images suitable for real-time video data from ultrasound systems.

Local storage

A modern ultrasound imaging system usually contains an on-board computer. Individual images and image sequences may be stored on the local hard disc, and retrieved and displayed as necessary. Older ultrasound systems tended to store image and video data in proprietary formats, which made it difficult to transfer images to an imaging network (see below) or for the operator to incorporate digital images into reports and slide-shows. Modern systems allow storage of images in several widely used formats, such as avi and mpeg for video, tiff and jpeg for individual images, and DICOM format for networking. They also have computer-compatible recording facilities such as a USB port and a DVD writer.

Integration with an imaging network

The modern radiology department is based on imaging systems, including ultrasound scanners, which are connected to an imaging network. This system is generally referred to as a picture archiving and communication system (PACS). A PACS system typically has workstations for review and reporting of image data, printers for producing hard copy of images and reports, and a large memory store for archiving patient data. Most reporting for ultrasound is performed in real time, with the operator saving images or video clips which illustrate the lesion (if present) or the measurement. Hard copy of images for inclusion in patient notes is usually done using a high-quality laser printer, though there may be no hard copy of images, with inclusion of only the report in the notes. Instead, if the referring clinician wants to inspect the images he or she can do so at a local terminal, connected to the hospital network, on the ward or in the clinic.

Compared to film-based radiology, PACS has considerable advantages including: rapid access of images throughout the hospital, reduced requirement for hard copy and hard copy storage, reduction in lost images, and hence reduction in repeat examinations due to lost images.

As PACS involves technologies which evolve relatively rapidly, further up-to-date information is best found at relevant websites such as wikipedia.

Questions

1. Compare the effects on a B-mode image of adjusting the overall gain and the transmit power. How should the operator optimize the settings of each and what risks should be taken onto account?
2. A 5 MHz transducer is used to image a region of tissue which attenuates at a rate of 0.7 dB $cm^{-1} MHz^{-1}$. Explain how the scanning system compensates for the attenuation and how the operator sets the TGC. At what rate in dB μs^{-1} will the system increase the gain when the TGC is correctly applied?
3. Explain what is meant by the dynamic range of echoes received at the transducer. Why is it necessary to be able to display a wide dynamic range of echoes?
4. Why is it necessary to compress the dynamic range of echoes and how is this achieved by the scanning system? How does the dynamic range setting affect the B-mode image and how should the operator choose the optimum value of compression?
5. A diagnostic ultrasound beam is incident on two isolated targets with diameters of 10 μm and 20 μm respectively. Calculate the ratio of the ultrasonic powers scattered by the two targets. How will the echoes from targets such as these differ from that from a large plane interface in terms of amplitude and dependence on angles of incidence?
6. Explain what is meant by interpolation and why it is used in the formation of ultrasound images.
7. Describe the principle of operation of tissue harmonic imaging and its advantages and limitations for B-mode imaging. Under what circumstances would harmonic imaging be most useful clinically?
8. Describe the trade-off that the operator must make in choosing the ultrasound transmit frequency. How can coded excitation help?
9. Explain the meanings of the terms read zoom and write zoom. Compare their benefits and limitations in B-mode imaging. How might each be affected by the size of the image memory?

10. Explain what is meant by the term post-processing. Describe 2 examples of post-processing and how they improve image quality as well as any limitations.

References

Chiao RY, Hao X (2005). Coded excitation for diagnostic ultrasound: a system developer's perspective. *IEEE Transactions on Ultrasonics, Ferroelectrics and Frequency Control*, **52**, 160–70.

Desser TS, Jedrzejewicz T, Bradley C (2000). Native tissue harmonic imaging: basic principles and clinical applications. *Ultrasound Quarterly*, **16**, 40–8.

Eckersley RJ, Tang MX, Chetty K, Hajnal J (2007). Microbubble contrast agent detection using binary coded sequences. *Ultrasound in Medicine and Biology*, **33**, 1787–95.

Hoskins PR, Thrush A, Martin K, Whittingham TA. (2003). *Diagnostic ultrasound physics and equipment*. London: Greenwich Medical Media.

Ma Q, Ma Y, Gong X, Zhang D (2005). Improvement of tissue harmonic imaging using the pulse-inversion technique. *Ultrasound in Medicine and Biology*, **31**, 889–94.

Nowicki A, Klimonda Z, Lewandowski M, et al . (2006). Comparison of sound fields generated by different coded excitations – experimental results. *Ultrasonics*, **44**, 121–9.

Pedersen MH, Misarids TX, Jensen JA (2003). Clinical evaluation of chirp-coded excitation in medical US. *Ultrasound in Medicine and Biology*, **29**, 895–905.

Simpson DH, Chin CT, Burns PN (1999). Pulse inversion Doppler: a new method for detecting nonlinear echoes from microbubble contrast agents. *IEEE Transactions on Ultrasonics, Ferroelectrics and Frequency Control*, **46**, 372–82.

Tranquart F, Grenier N, Eder V, Pourcelot L (1999). Clinical use of ultrasound tissue harmonic imaging. *Ultrasound in Medicine and Biology*, **25**, 889–94.

Chapter 5

Properties, limitations and artefacts of B-mode images

Kevin Martin

Introduction

The B-mode image-forming processes described so far have assumed an ideal imaging system operating in an ideal medium. As described in Chapter 2, real ultrasound beams have significant width and structure, which change with distance from the transducer, and ultrasound pulses have finite length. The speed of sound and the attenuation coefficient are not the same in all tissues. These real properties give rise to imperfections in the image, which are essentially all artefacts of the imaging process. However, those that are related primarily to the imaging system (beam width, pulse length, etc.) are usually considered as system performance limitations, as they are affected by the design of the system. Those that arise due to properties of the target medium (e.g. changes in attenuation and speed of sound) are considered as artefacts of propagation.

Imaging system performance

The performance of a particular B-mode system can be characterized in terms of image properties which fall into three groups, i.e. spatial, amplitude and temporal. At the simplest level, spatial properties determine the smallest separation of targets which can be resolved. The amplitude properties determine the smallest and largest changes in scattered or reflected echo amplitude which can be detected. The temporal properties determine the most rapid movement that can be displayed. However, the ability to differentiate between neighbouring targets, or to display targets clearly, may depend on more than one of these property types.

Spatial properties

Lateral resolution

An ideal imaging system would display a point target as a point in the image. The image of a point target produced by a real imaging system is spread out due to the finite beam width and pulse length, so that it appears as a blurred dot or streak. Figure 5.1 illustrates the effect of beam width on the image of a point target. Here, a point target is imaged with a linear-array system, which has a practical lateral beam width (Figure 5.1a). Echoes from the point target are returned at each beam position where the beam overlaps the target. However, the imaging system assumes that the beam has zero width, and so displays each echo on the image line corresponding to the current beam axis.

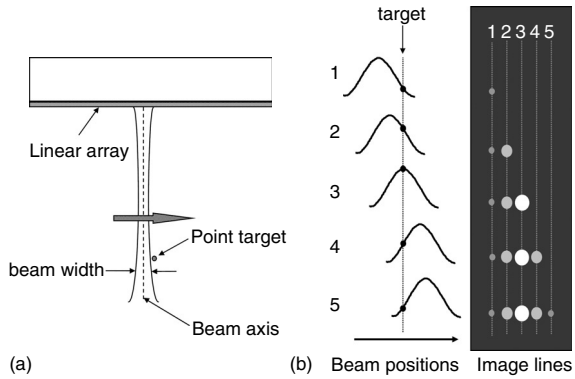

Fig. 5.1 Echoes are registered in the image at each beam position where the beam overlaps the target. The resulting lateral spread of the image depends on the beam width at the target depth.

At beam position 1 (Figure 5.1b), the right-hand edge of the beam just intercepts the target and a weak echo is produced, but is displayed on image line 1 corresponding to the current position of the beam axis. At beam position 2, the target is still off axis, but in a more intense part of the beam. A larger echo is produced, which is displayed on image line 2. At beam position 3, the target is on axis and the largest echo is produced and displayed on image line 3. At beam positions 4 and 5, the target is in progressively less intense parts of the beam, giving weaker echoes, which are

Diagnostic Ultrasound: Physics and Equipment, ed. Peter Hoskins, Kevin Martin and Abigail Thrush. Published by Cambridge University Press.

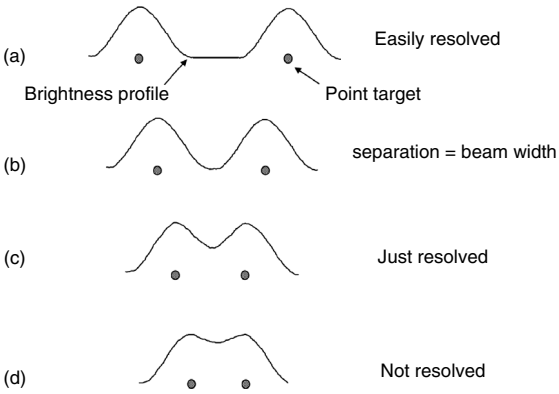

Fig. 5.2 The brightness profiles from laterally spaced targets begin to merge when their spacing is less than the beam width. The targets are just resolved in the image when the spacing is about half the beam width.

displayed on image lines 4 and 5. The resulting brightness profile across the image due to the point target is similar in width and shape to the beam profile at that depth.

As described in Chapter 2, the beam width varies with distance from the transducer. It is narrow in the focal region, but wider at other depths. Small lateral beam width and hence minimal image spread is achieved by using multiple transmit focal zones and swept focus during reception (Chapter 3).

The lateral resolution of an imaging system is usually defined as the smallest separation of a pair of identical point targets at the same range in the image plane which can be displayed as two separable images. Figure 5.2a shows the brightness profiles along a horizontal line on the image passing through two such point targets. Here, the targets are separated by a distance which is greater than the beam width, and two distinct images are displayed. As the targets are moved closer together, their brightness profiles meet when their separation equals the beam width (Figure 5.2b). They then effectively overlap until there is no discernible reduction in brightness between the two and their images are not separable (Figure 5.2d). At a critical separation, the images are just separable (Figure 5.2c). The separation at this point, which is about half the beam width, is a measure of the lateral resolution at that range. Thus, at best, lateral resolution is half the beam width, but can be made worse by other factors.

Slice thickness

The lateral resolution, just described, refers to pairs of targets within the scan plane. The ultrasound beam has

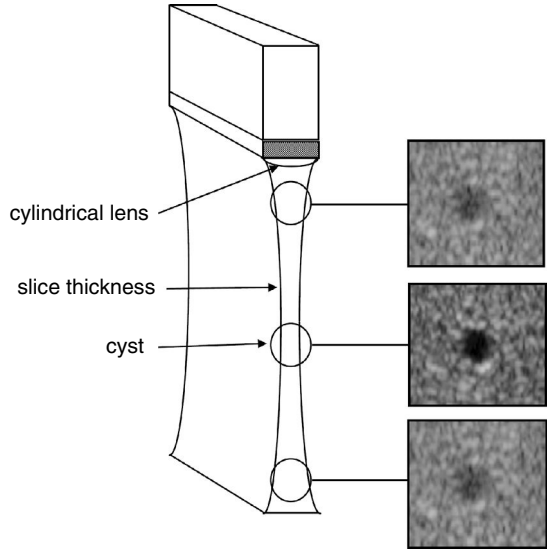

Fig. 5.3 The slice thickness is usually greater than the beam width in the scan plane and can lead to infilling of small cystic structures in the image, especially outside the focal region.

significant width also at right angles to the scan plane, giving rise to the term 'slice thickness'. Slice thickness is determined by the width of the ultrasound beam at right angles to the scan plane (the elevation plane) and varies with range. Conventional array transducers have fixed focusing in this direction due to a cylindrical acoustic lens attached to the transducer face (Figure 5.3). As the transducer aperture is limited in the elevation plane, focusing is relatively weak and so slice thickness is generally greater than the beam width that can be achieved in the scan plane, where wide apertures and electronic focusing are available.

The effect of slice thickness is most noticeable when imaging small liquid areas, such as cysts and longitudinal sections of blood vessels (Figure 5.3). The fluid within a simple cyst is homogeneous and has no features which can scatter or reflect ultrasound. Hence, it should appear as a black, echo-free area on the image. The surrounding tissues, however, contain numerous small features and boundaries, which generate a continuum of echoes. A small cyst, imaged by an ideal imaging system with zero slice thickness, would appear as a clear black disc within the echoes from the surrounding tissues. However, when a small cyst is imaged by a real imaging system whose slice thickness is comparable to or larger than the diameter of the cyst, the slice may overlap adjacent tissues, generating echoes at the same range as the

cyst. Such echoes are displayed within the cystic area in the image as if they were from targets, such as debris, within the cyst. The same artefact, often referred to as 'slice thickness artefact', is observed in a longitudinal image of a blood vessel whose diameter is comparable to, or smaller than, the slice thickness.

For a conventional array transducer with a single row of elements and a fixed cylindrical lens, the beam width is fixed in the elevation direction, and there is little the operator can do to reduce this artefact, other than always selecting a transducer with an elevation focus that matches the target depth. Slice thickness artefact can be reduced by the use of a multi-row transducer (see Chapter 3). Multi-row transducers are now available commercially and achieve reduced slice thickness by using electronic focusing and/or variable aperture in the elevation direction.

Axial resolution

When a point target is imaged by a real imaging system, the spread of the image in the axial direction is determined by the length of the ultrasound pulse. Figure 5.4a illustrates the shape of a typical pulse envelope. It has a short and steep rising edge and a longer falling edge. When an interface is imaged using such a pulse, the echo is much smaller in amplitude, but has a similar shape. Hence, the displayed brightness profile in the axial direction is similar to the shape of the pulse envelope as illustrated.

Axial resolution is defined usually as the smallest separation of a pair of targets on the beam axis which can be displayed as two separable images. Figure 5.4a shows the brightness profiles from two interfaces on the beam axis separated by more than the length L of the pulse along the beam axis. The profiles do not overlap and the images are separate.

When a pair of interfaces are separated by $L/2$, as in Figure 5.4b, the two-way trip from interface 1 to 2 involves a total distance L, and the leading edge of the echo from interface 2 meets the trailing edge of the transmit pulse as it arrives at interface 1. Hence, the axial brightness profiles from reflections at the two interfaces just begin to overlap. As the interfaces are brought closer together (Figure 5.4c), the brightness profiles of the echoes cannot be distinguished in the image. At a critical separation, which is less than $L/2$, the images are just separable. Thus, the axial resolution of a B-mode system is approximately half the pulse length.

Image contrast

The brightness of an echo from a large interface between tissues is determined by the reflection coefficient of the

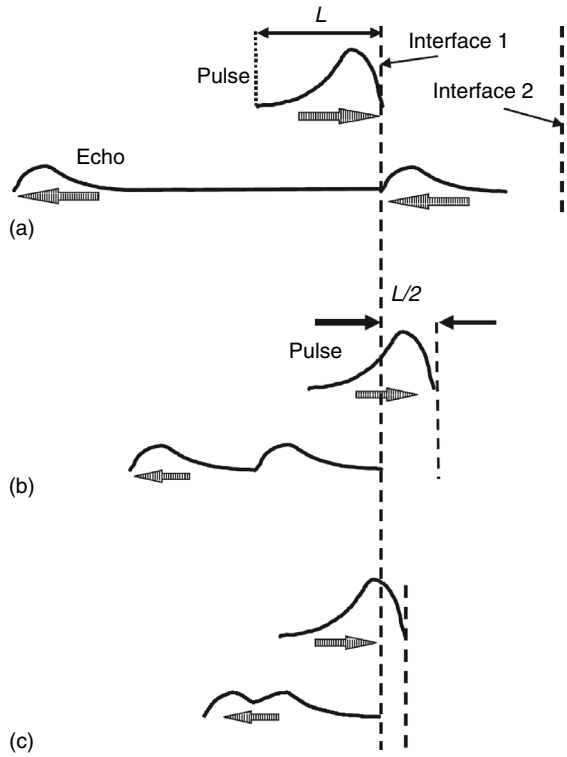

Fig. 5.4 The pulse has to 'go and return' from one interface to the next. Hence, the brightness profiles from targets along the beam axis begin to merge when their spacing is less than half the pulse length.

interface as described in Chapter 2. The brightness of echoes representing scatter from within tissues varies according to the tissue type and its state. The absolute value of brightness of such echoes in the display is affected by gain settings, frequency, etc. and is not normally of direct value in diagnosis. However, the use of relative brightness to differentiate tissues within the image is an important aspect of ultrasound diagnosis. The overall relative brightness of echoes within different organs (liver, spleen and kidney) is an aid to identification and can reflect pathological change. Of more importance to diagnosis, small local changes in echo brightness are often related to pathological change in that part of the tissue.

Recognition by the operator of changes in echo brightness is a relatively complex process, which depends on the characteristics of the imaging system and the human visual system and on the viewing conditions. The smallest change which can be displayed clearly by the imaging system is limited by image noise,

i.e. random fluctuations in brightness in different parts of the image. For all imaging systems, some noise arises from electronic processes in the image detection and processing circuits. In ultrasound images, there is also acoustic noise, the most prominent type of which is speckle.

Speckle

We have already seen that targets which are closer together than approximately half a beam width (lateral and elevation) and half a pulse length cannot be resolved as separate features in the image. Another way of stating this is to say that targets which lie within a volume, called the sample volume, defined by these three dimensions cannot be resolved separately. We also know that in the axial direction, the pulse, and hence the sample volume, contains several cycles of the transmitted wave.

Within most tissues, there are numerous features and irregularities within the sample volume at any instant, which scatter ultrasound from the pulse back to the transducer. The scattering strength and distribution of these scatterers within the sample volume are random, so that the echoes they generate vary randomly in amplitude and position (phase), as seen in Figure 5.5. As the voltage generated by the transducer at each point in time can have only a single value, the value registered is the sum of contributions from many scatterers. Echoes which are in phase add constructively, while those that are in anti-phase add destructively, leading to random fluctuations in brightness in the displayed image called speckle. The form of the speckle pattern is related to the dimensions of the sample volume. For example, since the beam width is generally greater than the pulse length, the pattern includes prominent streaks in the lateral direction whose lengths are similar to the beam width. In the focal region of the beam, where the beam width is small, such streaks are much shorter.

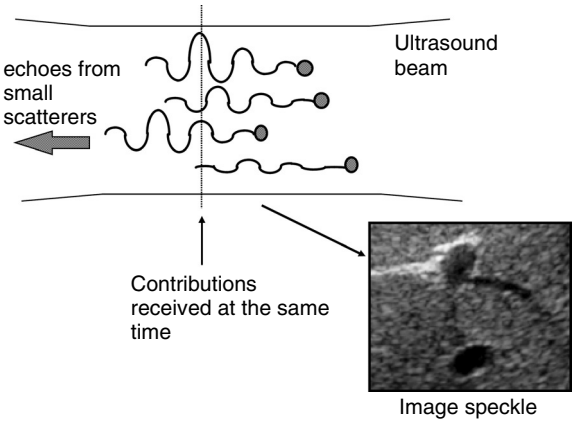

Fig. 5.5 Echoes from small scatterers within the sample volume have random amplitude and relative phase. These add together at the transducer to produce random fluctuations in the image brightness called speckle.

Some recent developments in ultrasound technology have the effect of reducing image speckle. For example, in real-time compound imaging, the beams from a linear array are deflected to extra positions on each side of the straight-ahead position using phased array techniques. The images obtained from the different beam directions are summed (compounded). The random fluctuations in image brightness due to speckle tend to be averaged out, so that they are less apparent in the image.

Perception of changes in brightness

Perception of changes in image brightness is affected by a number of factors. Clearly, if the difference in average brightness level of two areas in the image is small compared to average fluctuations in brightness due to speckle, the tissues will not appear to be different. If the change in average level is similar to, or greater than, the speckle variations, the difference should be observable.

The perception of differences in image brightness is affected also by the characteristics of the human visual system (Hill 2004). The visual system is adapted to detect sharp boundaries in an image and is less sensitive to changes in brightness if the change is gradual. Hence, a small change in overall brightness of the liver compared to that of a neighbouring organ is more difficult to identify than a 1 cm region of reduced echo brightness within the liver. Such small percentage changes in brightness are perceived more easily if the overall brightness level is high. Hence, if the operator is interested in detecting local changes in echo brightness in the liver, it is beneficial to adjust the gain settings of the system to display these echoes at an above-average level of brightness. This can be achieved through adjustment of grey-level processing curves, overall gain and output power.

Movement

Imaging of rapidly moving structures, such as valve leaflets in the heart, requires that the image repetition rate (the frame rate) is high. To show the movement of a valve leaflet smoothly, the system needs to display it in several positions (say five) between the closed and open positions. As the leaflet takes only about 0.1 s to open, five images are needed in every 0.1 s, a frame rate of 50 Hz.

Tissues such as the liver and other abdominal organs can be imaged successfully with much lower frame rates. Here, relative movement between the tissues and the ultrasound transducer is caused mainly by the patient's respiration and by slow operator-guided movement of the probe across the patient's skin, both of which can be suspended temporarily. Frame rates of less than 10 Hz can be tolerated, therefore, in the abdomen. Ultrasound image formation in modern equipment involves many complex processing steps. However, these are performed in a short time by high-speed digital electronics and do not reduce the image repetition rate. However, the travel time of ultrasound to the target and back is a fundamental part of the imaging process and limits the rate at which images can be acquired.

Consider an image from a stepped linear array consisting of N ultrasonic lines interrogating the tissue to a maximum depth D (Figure 5.6a). To form each ultrasound line, the pulse must travel to depth D and echoes return from that depth before the pulse for the next line is transmitted.

If the speed of sound in the tissue is c, the time per line is $2D/c$, i.e. the go and return time to depth D. The total time to form N lines is then $2DN/c$. This is the frame time or time to form one complete B-mode image. The frame rate = 1/frame time. That is, the frame rate = $(c/2DN)$ Hz.

This equation shows that increasing the depth D or the number of lines N reduces the frame rate, whereas decreasing D or N increases it. Hence, reducing the imaged depth to the minimum required to see the tissues of interest will help to avoid low frame rates. Some ultrasound imaging systems allow the operator also to reduce the width of the imaged area (Figure 5.6b). If the spacing between the ultrasound lines is constant, then this reduces the number of lines in the image and increases the frame rate.

The frame rate may be increased also by spacing the image lines further apart, so that the total number in the imaged area is reduced. Some systems have a frame rate control that provides a trade-off with line spacing, and thus image quality.

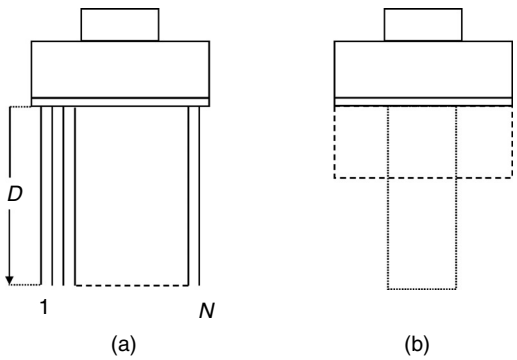

Fig. 5.6 (a) The frame time, and hence the frame rate, is determined by the imaged depth D and the number of lines N. (b) The frame rate can be maximized by reducing the imaged depth or width to the minimum required.

Artefacts

When forming a B-mode image, the imaging system makes a number of assumptions about ultrasound propagation in tissue. These include:

(1) the speed of sound is constant,
(2) the beam axis is straight,
(3) the attenuation in tissue is constant, and
(4) the pulse travels only to targets that are on the beam axis and back to the transducer.

Significant variations from these conditions in the target tissues are likely to give rise to visible image artefacts. Most artefacts may be grouped into speed-of-sound artefacts, attenuation artefacts or reflection artefacts according to which of the above conditions is violated.

Speed-of-sound artefacts

Range errors

As described earlier, a B-mode image is a scaled map of echo-producing interfaces and scatterers within a slice through the patient, in which each echo signal is displayed at a location related to the position of its origin within the slice. The location of each echo is determined from the position and orientation of the beam and the range of the target from the transducer.

The distance d to the target is derived from its go and return time t, i.e. the time elapsed between transmission of the pulse and receipt of the echo from the target. In making this calculation, the system assumes that $t = 2d/c$, where the speed of sound c is constant at 1540 m s^{-1}, so that t changes only as a result of changes in d. However, if the speed of sound c in the medium between the transducer and the target is greater than 1540 m s^{-1}, the echo will arrive back at the transducer earlier than expected for a target of that range (i.e. t is reduced). The system assumes that c is still 1540 m s^{-1} and so displays the echo as if from a target nearer to the transducer. Conversely, where c is less than 1540 m s^{-1}, the echo arrives relatively

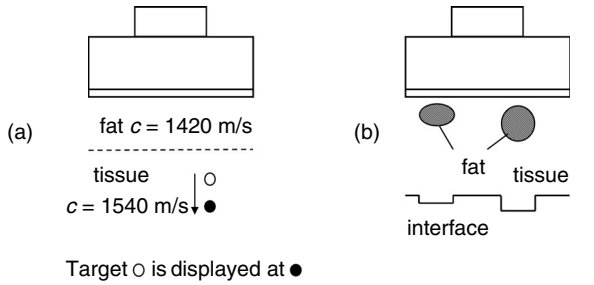

Fig. 5.7 (a) The low speed of sound in a superficial fat layer results in the images of all targets beyond it being displaced away from the transducer. (b) Superficial regions of fat can result in visible distortion of smooth interfaces.

late and is displayed as if it originated from a more distant target. Such range errors may result in several variations of image artefacts depending on the pattern of changes in the speed of sound in the tissues between the transducer and the target. These include:

(1) misregistration of targets,
(2) distortion of interfaces,
(3) errors in size and
(4) defocusing of the ultrasound beam.

Misregistration of targets occurs as illustrated in Figure 5.7a, where the average speed of sound between the transducer and target is greater or less than 1540 m s^{-1}. A discrete target will be displayed too near or too far away from the location of the transducer face due to early or late arrival of the echo. In practice, this might be due to a thick layer of fat under the skin surface. The speed of sound in fat could be as low as 1420 m s^{-1}, approximately 8% less than the assumed speed of sound of 1540 m s^{-1}. For a uniform layer of fat, all targets beyond the fat would be displaced away from the transducer, but this error would not be noticeable, as it would be applied to all targets equally.

Boundary distortion

Range errors due to speed-of-sound variations may be more obvious in the presence of non-uniform regions of fat superficial to a smooth interface (Figure 5.7b). Here the parts of the interface which are imaged through a region of fat will be displaced to greater depths with respect to other parts and the resulting irregularities in the interface can be detected readily by eye.

Size errors

Errors in displayed or measured size of a tissue mass may occur if the speed of sound in the region deviates significantly from 1540 m s^{-1}. For example, if the speed of sound in the mass is 5% less than 1540 m s^{-1}, the axial dimension of the displayed mass will be 5% too large. For most purposes, an error of 5% in displayed size is not noticeable. However, for measurement purposes, an error of 5% may need to be corrected.

Phase aberration

As described in Chapter 3, electronic focusing in transmit and receive is achieved by calculating the time of flight of the pulses and echoes from each element in the active aperture to the focal point. Electronic delays are then applied to ensure that the transmit pulses from each element arrive at the focus at the same time and the echoes received from the focus by each element are aligned in phase before they are added together. In transmit, the element delays are designed to produce a circular wavefront which converges to a focus (Figure 5.8a). The time-of-flight calculations are based on the assumption that the speed of sound in the intervening tissues is uniform at a value of 1540 m s^{-1}. Test object studies have shown that where the speed of sound in the medium is not 1540 m s^{-1}, the ultrasound beam becomes defocused (Dudley *et al.* 2002, Goldstein 2004).

In real tissues, the speed of sound does vary by a few percent from the assumed mean value of 1540 m s^{-1} (see Chapter 2), resulting in discrepancies between the calculated time of flight for each element and the real value. If there are variations in the speed of sound within the volume of tissue through which the beam passes, this gives rise to distortion of the wavefront and defocusing (Figure 5.8b). This effect is a significant problem as the beam passes through subcutaneous fat, resulting in significant loss of resolution for deeper tissues. The effect is often referred to as phase aberration and is a major limitation on the ultimate performance of ultrasound imaging systems, especially at higher frequencies where the effects of time errors on signal phase are greater (Flax and O'Donnell 1988, Trahey *et al.* 1991). A complete solution to phase aberration would effectively require the speed of sound in all regions of the image plane to be mapped so that corrections could be applied for every individual path between the transducer elements and all points in the image. Numerous solutions have been proposed for reducing the effects of phase aberration, but implementation has proved to be difficult.

Partial solutions to this problem are now available commercially based on the use of alternative values for the assumed average speed of sound. For example, by forming several versions of the image with different

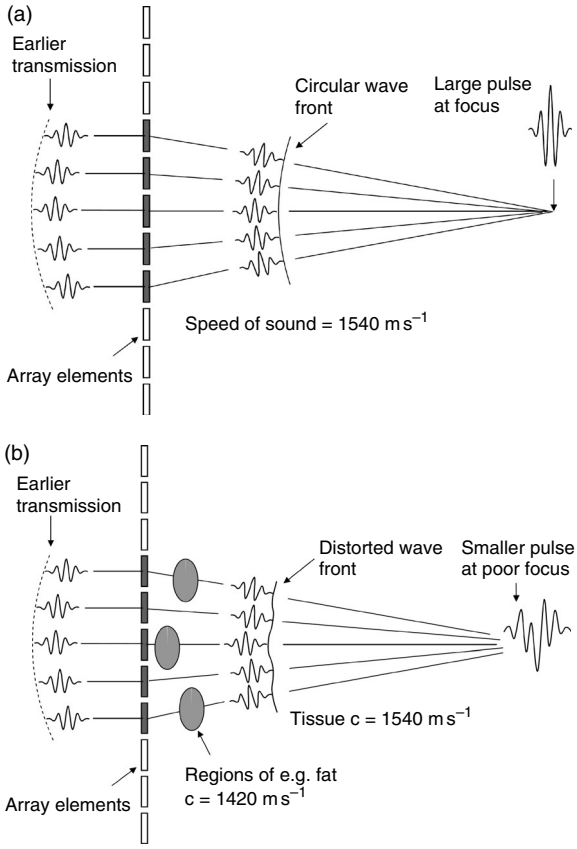

Fig. 5.8 (a). A transmit focus is produced with an array transducer by delaying the transmit pulses from the central elements of the aperture. The delays are designed to produce a circular wavefront in a medium with speed of sound of 1540 m s^{-1}, which converges to a focal point. (b). Where the pulses from the elements pass through different regions of tissue in which the speed of sound is not 1540 m s^{-1}, e.g. fat, the resulting wavefront is distorted, resulting in a longer, lower-amplitude pulse at a less well-defined focus. The effect is referred to as phase aberration.

speeds of sound, the value which gives the most effective focus can be identified as that which gives the highest spatial frequencies in the image (McGlaughlin 2007).

Refraction

As described in Chapter 2, an ultrasound wave will be deflected by refraction when it is obliquely incident on an interface, where there is a change in the speed of sound. When an ultrasound wave propagates in the form of a beam, the direction of propagation is the beam axis, which may be deviated by a change in

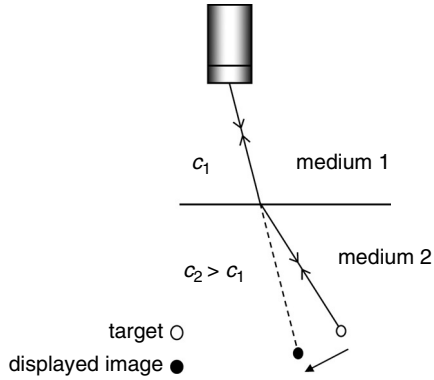

Fig. 5.9 An echo received via a refracted beam is displayed in the image as if originating from a straight beam, and hence is displaced from its correct position.

the speed of sound. In writing an ultrasonic line of echoes into the image memory, the B-mode system addresses a line of pixels across the memory assuming that the beam axis is straight, and displays all echoes at points along the assumed scan line at a range corresponding to their time of arrival. Hence, echoes received via a refracted beam will be displayed as if they originated on an undeviated axis (Figure 5.9) and will be displaced from their correct location in the image.

A refraction artefact is seen in some subjects when imaging the aorta in cross section through the superficial abdominal muscles. Here, the ultrasound beams may be refracted towards the centre of the abdomen by the oblique interface at the medial edges of the abdominal muscles. As the muscle structure is symmetrical, two side-by-side images of the aorta may be formed.

Edge shadowing artefact

Refraction effects have been proposed as an explanation for the formation of an artefact referred to as edge shadowing (Steel *et al.* 2004, Ziskin *et al.* 1990). This artefact is commonly seen beneath the lateral edges of cystic regions such as the gall bladder and is demonstrated in Figure 5.10c, where a pair of vertical dark streaks can be seen beneath the edges of the image of a cystic cylinder within a tissue-mimicking phantom. Edge shadowing is most likely to be observed where the speed of sound inside the cystic structure is different from that in the surrounding tissues, particularly where its value is less. A beam incident on the upper surface of the cyst to the right of the centre will be refracted to the left as it enters the cyst. As the beam is stepped to consecutive positions from the centre of

the cystic structure towards the lateral edge, its angle of incidence at the upper surface of the cyst increases with respect to the normal (90° to the surface). The angle through which the beam is refracted increases with increasing angle of incidence and increases most rapidly towards the edge of the cyst, resulting in divergence of the beams beneath the cyst edges. The reduced line density and greater beam divergence result in a reduction of the image brightness in these regions. Where the speed of sound in the cystic region is greater than that in the surrounding medium, it is also possible that the beam can be reflected into the cystic region where the echo levels produced are small.

Attenuation artefacts

During each pulse–echo cycle of the B-mode imaging sequence, the outgoing pulse and returning echoes are attenuated as they propagate through tissue, so that echoes from deep targets are weaker than those from similar superficial targets. As described in Chapter 4, time–gain compensation (TGC) is applied to correct for such changes in echo amplitude with target depth. Most systems apply a constant rate of compensation (expressed in dB cm^{-1}), designed to correct for attenuation in a typical uniform tissue at the current transmit frequency. Also, the operator can usually make additional adjustments

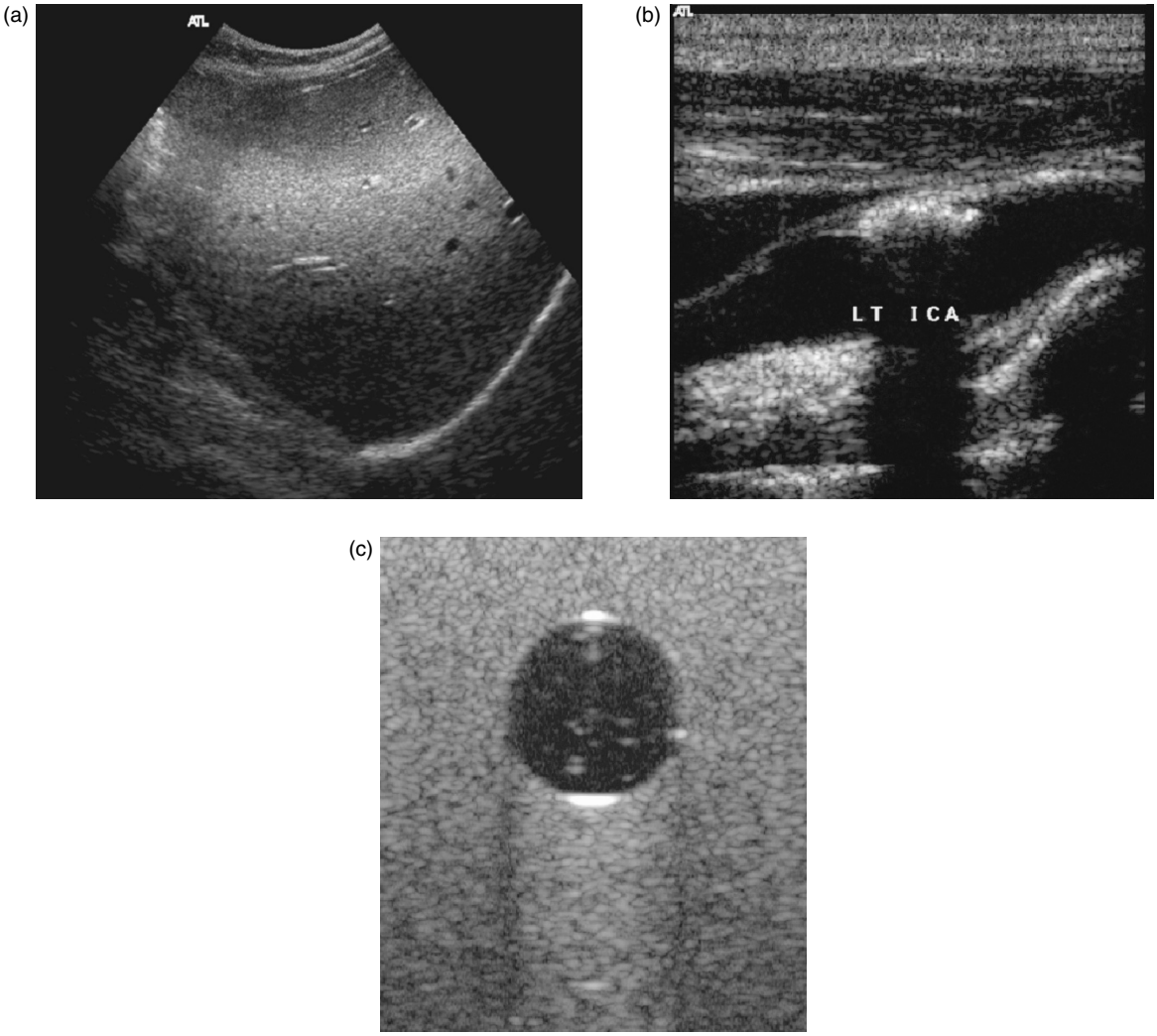

Fig. 5.10 (a) Incorrect setting of the TGC controls can result in non-uniform image brightness. (b) Under compensation of echoes from beyond highly reflecting or attenuating objects such as plaque in the carotid artery results in acoustic shadowing. (c) Overcompensation of echoes from beyond low-attenuation liquid-filled structures results in post-cystic enhancement.

to the compensation via slide controls, which adjust the gain applied to specific depths in the image.

TGC artefacts may appear in the image when the applied compensation does not match the actual attenuation rate in the target tissues. A mismatch may occur due to inappropriate adjustment by the operator or to large deviations in actual attenuation from the constant values assumed. As the same TGC function is normally applied to each line in the B-mode image, inappropriate adjustment of TGC controls would result in bright or dark bands of echoes across the image of a uniform tissue (Figure 5.10a). Under some circumstances, these might be interpreted as abnormalities.

TGC artefacts due to substantial local deviations in tissue attenuation are of more interest as they usually have diagnostic value. Acoustic shadowing occurs distal to a region of increased attenuation, where all echoes in the shadow are reduced compared to those arising lateral to the shadow. This is because the TGC is set to compensate for the lower attenuation in the adjacent tissues, and so does not adequately boost echoes returning from beyond the region of higher attenuation. These undercompensated echoes are displayed at a reduced brightness. The most striking examples of acoustic shadowing are those due to highly reflecting and attenuating calcified lesions, such as gallstones or blood vessel plaque (Figure 5.10b). Shadowing may also occur posterior to some more strongly attenuating tissue lesions, e.g. breast masses.

Post-cystic enhancement, which is the opposite of acoustic shadowing, occurs posterior to regions of low attenuation. Here, compensation is applied to echoes arising from behind the cyst assuming that these echoes have been attenuated by the same depth of tissue as those from regions lateral to the cyst. As the attenuation in the liquid of the cyst is very low compared to that in tissue, the echoes from tissues distal to the cyst are still relatively large and are displayed at a higher brightness level. Post-cystic enhancement (Figure 5.10c) can be a useful diagnostic indication of a liquid-filled lesion.

Reflection artefacts

Specular reflection

In Chapter 2, it was shown that when an ultrasound wave meets a large plane interface between two different media, the percentage of ultrasound intensity reflected is determined by the acoustic impedance values of the two media. A large change in acoustic impedance gives a strong reflection at the interface. The amplitude of the echo from an interface received back at the transducer is determined not only by the reflection coefficient at the interface and attenuation in the intervening medium, but also by the angle of incidence of the beam at the interface and the smoothness of the surface.

When reflection is from a large, smooth interface, i.e. an interface which is larger than the beam width, specular reflection occurs. That is, the reflected ultrasound propagates in one direction. When the angle of incidence is zero (normal incidence), the reflected echo from a large, smooth interface travels back along the same line as the incident beam to the transducer, where it is detected (Figure 5.11a). When the angle of incidence is not zero, the beam is reflected to the opposite side of the normal at the angle of reflection. The angle of reflection is equal to the angle of incidence. Hence, when a beam is incident on a large, smooth interface at an angle of incidence of 10° or more, the reflected beam misses the transducer and no echo is received.

This specular reflection artefact is seen commonly when imaging through the liver to the diaphragm, a large smooth curved interface. Those parts of the diaphragm which reflect the beam at near normal incidence give rise to strong echoes in the image. Other parts of the diaphragm where the angle of incidence is greater than 10° are not shown in the image, because the reflected beam misses the transducer.

When the interface is rough or irregular on the scale of the ultrasound wavelength or smaller,

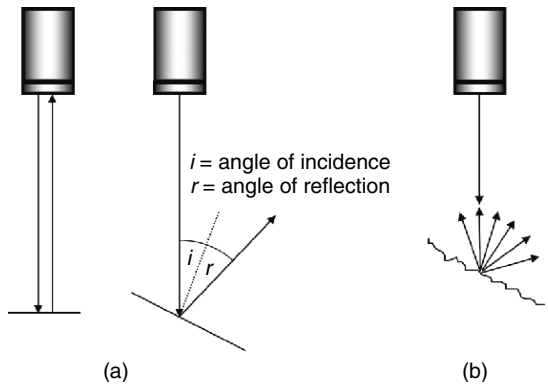

Fig. 5.11 (a) Specular reflection occurs at a large, smooth interface. A strong echo can only be received at near normal incidence. (b) A large, rough interface gives a diffuse reflection, which may be received over a wider range of angles.

diffuse reflection occurs. Here, the incident pulse is reflected over a wide range of angles (scattered), so that echoes may be received back at the transducer even when the angle of incidence is quite large (Figure 5.11b).

Mirror-image artefact

Mirror-image artefact arises also due to specular reflection of the beam at a large smooth interface. It is most obvious when the reflection coefficient is large (e.g. at a tissue–air interface). If the reflected beam then encounters a scattering target, echoes from that target can be returned along a reciprocal path (i.e. via the reflecting interface) back to the transducer, where they are received (Figure 5.12). As in the case of refraction artefact, the B-mode system assumes that all echoes arise from points along a straight beam. Hence, the reflected echoes are displayed in line with the original beam at a point beyond the strongly reflecting interface. The displayed effect is that of a mirror image of the scattering target displayed behind the reflecting surface, as is observed when viewing a conventional optical mirror. Mirror-image artefact can often be observed posterior to the diaphragm. Figure 5.12 shows an example of echoes from the liver displayed in this position.

Reverberations

Reverberations arise also due to reflections of pulses and echoes by strongly reflecting interfaces. However, they occur only for normal incidence of the beam at the interface and can involve multiple reflections. Reverberations occur most commonly where there is a strongly reflecting interface parallel to the transducer face at a relatively small depth. As illustrated in Figure 5.13a, the echo from the interface arrives at the transducer and is displayed in the B-mode image. Some of the energy in the returned echo is then reflected at the transducer face, however, and returns to the reflecting interface as if it was a weak transmitted pulse, returning as a second echo (reverberation). As the time taken for the second echo to arrive is twice that taken by the first echo, the B-mode system displays it at twice the depth of the first echo. This process can continue to give further weak echoes at multiples of the depth of the reflecting interface. The weakness of these echoes is compensated partly by the TGC, which applies increased gain to echoes with longer go and return times.

Reverberations can often be distinguished from genuine echoes by the way that they move in the image in response to gentle pressure on the skin surface exerted via the transducer. As the operator presses the transducer slowly down into the tissue surface, genuine echoes in the image come up to meet the transducer at the same rate. However, as the path length for the first reverberation is twice that of the echo, a 1 cm movement of the transducer results in a 2 cm movement of the reverberation in the image. Hence the reverberation will travel towards the transducer at twice the rate of the genuine echo.

Reverberations commonly appear in images of liquid-filled areas, such as the bladder, due to multiple reflections between the transducer and the anterior bladder wall (Figure 5.13b). They are more obvious in such liquid-filled regions, which do not normally generate other echoes.

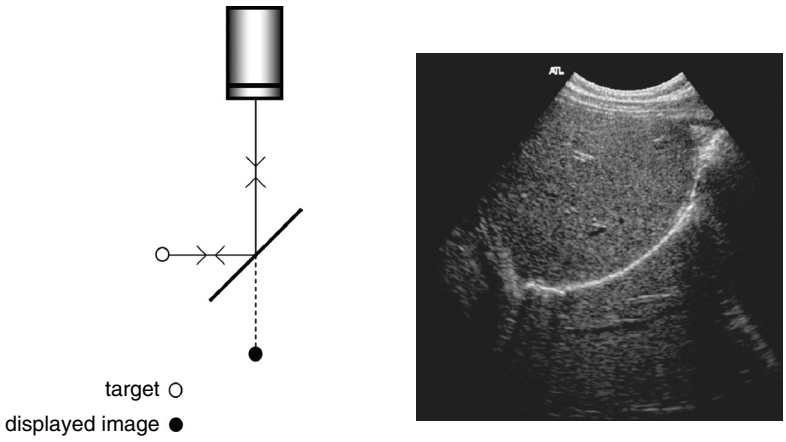

Fig. 5.12 Mirror-image artefact can occur beyond a strongly reflecting interface. Scattered echoes from targets in front of the interface are received via reflection at the interface. These are displayed in the straight-ahead position behind the interface. The image shows liver echoes displayed behind the diaphragm.

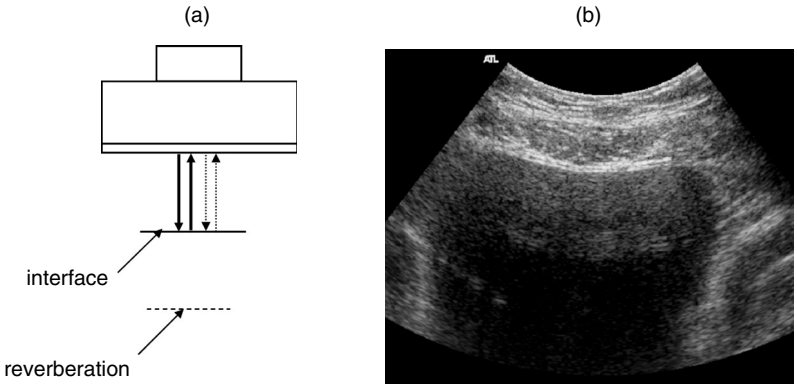

Fig. 5.13 (a) Reverberations are generated when the echo from a strongly reflecting interface parallel to the transducer is partially reflected from the transducer face back to the interface. This generates a second echo, which is displayed at twice the depth of the interface. (b) Reverberations are seen most commonly within liquid-filled areas such as the bladder, as shown here.

Questions

1. Define the term lateral resolution and explain how its value is determined by the beam width. What steps can the operator take to optimize lateral resolution?
2. Explain why the slice thickness of an array transducer is normally greater than the beam width in the scan plane. What limits does large slice thickness impose on the imaging performance of the array and what steps can the operator take to minimize them?
3. Explain why the axial resolution of a B-mode image is approximately half the pulse length rather than the whole pulse length.
4. Describe the origin of speckle in ultrasound images and its dependence on beam characteristics. How does speckle affect image interpretation and what techniques may be used to reduce it?
5. Discuss the compromise between resolution and frame rate which applies to linear-array scanners. Explain the advantage of using a small region of interest.
6. A fetal femur is aligned parallel to the skin surface in the image plane of a sector scanner with the centre of the femur in the centre of the field of view. There is a layer of fat with speed of sound 1420 m s^{-1} between the transducer and the uterus, in which the speed of sound is 1540 m s^{-1}. Discuss the effects of the fat on the measured length of the femur.
7. For the previous example, discuss the effect that the fat layer may have on the lateral resolution of the B-mode image. How might this affect the measurement accuracy?
8. Explain the process that leads to the formation of an acoustic shadow behind a gall stone. Give another example of an attenuation artefact and explain how such artefacts can provide diagnostic information.
9. Describe the appearance in an ultrasound image of a large smooth plane interface lying parallel to the skin surface, when imaged with a curvilinear array. How might a reverberation appear in the image if there is a large liquid region beneath the interface? How can the operator distinguish the reverberation from a genuine echo?
10. Describe the formation of a mirror-image artefact. What anatomical features are likely to produce this effect?

References

Dudley NJ, Gibson NM, Fleckney MJ, Clark PD (2002). The effect of speed of sound in ultrasound test objects on lateral resolution. *Ultrasound in Medicine and Biology,* **28**, 1561–4.

Flax SW, O'Donnell M (1988). Phase-aberration correction using signals from point reflectors and diffuse scatterers: basic principles. *IEEE Transactions on Ultrasonics, Ferroelectrics and Frequency Control,* **35**, 758–67.

Goldstein A (2004). Beam width measurements in low acoustic velocity phantoms. *Ultrasound in Medicine and Biology*, **30**, 413–16.

Hill CR (2004). In CR Hill, J Bamber, GR ter Haar, eds., *Physical Principles of Medical Ultrasonics*. Chichester: Wiley.

McGlaughlin GW (2007). Practical aberration correction methods. *Ultrasound*, **15**, 99–104.

Steel R, Poepping TL, Thompson RS, Macaskill C (2004). Origins of the edge shadowing artifact in medical ultrasound imaging. *Ultrasound in Medicine and Biology,* **30**, 1153–62.

Trahey GE, Freiburger PD, Nock LF, Sullivan DC (1991). In vivo measurements of ultrasonic beam distortion in the breast. *Ultrasonic Imaging*, **13**, 71–90.

Ziskin MC, Follette PS, Blathras K, Abraham V (1990). Effect of scan format on refraction artifacts. *Ultrasound in Medicine and Biology,* **16**, 183–91.

Chapter 6

B-mode measurements

Nick Dudley

Introduction

Measurements have a significant role in many areas of ultrasound practice. Some of the earliest ultrasound measurements were made in the field of obstetrics, originally in A-mode. A small range of measurements was quickly established in regular practice and this range has been considerably developed over the years. The most frequently performed measurements range from nuchal translucency in detecting abnormalities, through crown–rump length, biparietal diameter and femur length for dating, to abdominal circumference (AC) and head circumference (HC) for growth assessment. All of these may affect the management of pregnancy and therefore accuracy and reproducibility of measurements are important.

There is also a long history of measurement in echocardiography. Early measurements were made using the M-mode image and this is still used in modern clinical practice. Echocardiography images a dynamic process; the advantage of M-mode is that it contains information on both distance and time in a single image, so that changes in dimensions during the cardiac cycle may be measured. Cine-loop displays and imaging workstations now provide this temporal information in B-mode in a highly accessible form, facilitating measurement of changes in areas and volumes, e.g. for estimating left ventricular ejection fraction.

Most abdominal and small parts examinations are qualitative. Measurements are sometimes used, ranging from the gall bladder wall and common bile duct (a few millimetres) to the kidneys and liver (centimetres).

In vascular ultrasound, vessel diameters have been measured for many years in the diagnosis of, for example, aneurysms. In modern practice, vascular dimensions are often used in conjunction with Doppler ultrasound in assessing blood flow; accuracy is then more important since small errors in vessel diameter may result in large errors in blood flow estimation, particularly in small vessels. The high spatial resolution of modern systems allows measurement of small distances, e.g. intimal thickness.

In the following sections the implementation and application of measurement systems will be described. Measurement uncertainty is often overlooked in the development and use of clinical measurements; possible sources of error and practical means for improving accuracy and reproducibility will be discussed.

Measurement systems

Modern measurement systems have the sophistication and flexibility provided by digital electronics and software control. In the early days of ultrasound, particularly before the advent of digital scan converters, only simple axial measurements were possible on scanners. These were made on the A-mode display by aligning the ultrasound beam with the targets to be measured, and identifying and placing markers on the appropriate signals on the display. The scanner took the time interval between these positions on the A-mode display and converted it to distance using the assumed speed of sound. Other measurements, e.g. in the horizontal plane, could be made only on hard copy of the B-mode image using a ruler and scale factors derived from axial distance measurements, or in the case of non-linear measurements using a planimeter or even a piece of string.

These early measurements were difficult and required great care. It is remarkable that early ultrasound practitioners were able to demonstrate the value of measurements. The fact that some of the normal data produced are close to modern values and are still referred to is a testament to the care and dedication of these pioneers.

Diagnostic Ultrasound: Physics and Equipment, ed. Peter Hoskins, Kevin Martin and Abigail Thrush. Published by Cambridge University Press.

Modern calliper systems

Measurements made using ultrasound callipers range from simple linear distance measurements to more complex volume measurements. Scanners will often be able to perform calculations using measurements.

Measurements are made on the image stored in the scan converter and therefore depend on the accurate placement of image data in the memory, as described in Chapter 4. Each ultrasound scanner will use an assumed ultrasound velocity, usually 1540 m s^{-1}, to calculate distance along the beam axis, and a variety of algorithms, depending on the probe geometry, to calculate the final location of each echo in the image memory.

Distances within the scan converter image memory are then measured from pixel centre to pixel centre using an electronic calliper system. The measurement will generate a distance in pixels, from the centre of one calliper to the centre of the other calliper, which is then converted to millimetres or centimetres using a conversion factor. This conversion factor is necessary since the pixel size will depend on selected depth, scale and magnification settings; the conversion factors will be related to these settings.

The most common type of calliper control on modern scanners is a track-ball, although some smaller or older scanners may have less sophisticated devices. The track-ball is the most user-friendly option, as it allows callipers to be placed quickly. Some track-ball systems, however, are very sensitive and difficult to accurately control; for linear measurements, this is irritating but should not compromise accuracy, but for non-linear measurements significant errors may be introduced. Many track-ball systems are adjustable in software, so that their sensitivity can be altered to suit the user.

Linear distance, i.e. a measurement in a straight line between two points, was the first type of measurement made and is still the most commonly used.

Non-linear distance, circumference and area

Non-linear distances, including irregular circumferences, are often calculated from a tracing. The calliper is fixed at one end or point on the structure and the outline is traced using the track-ball. During the tracing the system will either plot a line guided by the track-ball movement, or place dots or crosses at intervals of, for example, 10 mm. The system then calculates the length of the trace, usually by calculating and summing the linear distances between points at intervals along the tracing.

The circumference of a structure is the distance around the perimeter and is widely used in obstetrics, e.g. fetal AC. There are several possible measurement methods, the choice depending on the regularity of the structure. Circumferences may be traced in the same way as other non-linear distances, fitted or plotted using a number of methods.

Whichever method is used to generate the perimeter of a structure, the area is simply calculated by multiplying the number of pixels enclosed by the area of each pixel. This is not often used, although it has been suggested that it may be more accurate and reproducible than circumference (Rossavik and Deter 1984). Area measurements are more commonly used in combination to calculate a volume.

Many systems now include ellipse fitting as an option for circumference and area measurement. This is a quick and useful method for structures that are truly elliptical. Callipers are initially placed on the extremes of the long or short axis of the ellipse (any diameter for a circle). The length of the other axis is then adjusted using the track-ball, making the ellipse larger or smaller to fit the measured structure. Most scanners allow both size and position of the ellipse to be adjusted, so that it may be moved around the screen to match the structure.

Once the size of the ellipse has been fixed, the system calculates the circumference by using a formula. Generally, systems approximate the ellipse to a circle, averaging the long and short axes (d_1 and d_2) and using the equation for the circumference of a circle:

$$\text{circumference} = \pi \times (d_1 + d_2)/2 = 1.57 \times (d_1 + d_2)$$

This is a good approximation unless the long and short axes are very different, in which case some systems apply a correction factor depending on the difference between the two axes in order to improve the accuracy of the approximation.

Some manufacturers are offering a further alternative, where a series of points is plotted around a structure by successively moving and fixing the calliper (point-to-point method). The system then joins the points with straight lines or curves, depending on the manufacturer, and calculates the circumference. This is less time-consuming than tracing but more so than ellipse-fitting, and is useful for measuring non-elliptical structures.

Volume

There are two useful methods for estimating volume from two-dimensional images. Most commonly, a calculation from three linear measurements is used, as shown in Figure 6.1. This method requires two images to be acquired at 90° to each other, e.g. sagittal and transverse images, and three orthogonal diameters to be measured. The volume is calculated by multiplying the diameters together and then multiplying by a constant value, *k*, appropriate for the shape. The shape is often assumed to be approximate to a sphere, for which the required '*k*' value is 0.52. Where a sphere is not a good approximation, it may be possible to derive a more appropriate constant from measurements on a number of patients. This requires comparison with an accurate measurement of volume by another means, e.g. in measuring bladder volume the ultrasound measurements can be compared with the volume of urine collected when the bladder is completely emptied. Other structures measured in this way include the gestation sac and cardiac ventricles.

Some manufacturers offer a single image method, e.g. for bladder volume estimation, where only height and breadth of the structure are measured in a single plane. This method relies heavily on an assumption of the shape of the structure at 90° to the scan plane and should be used with extreme caution.

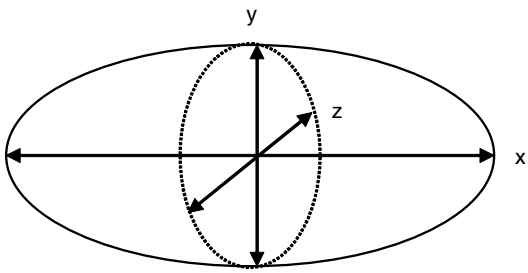

Volume = k . x . y . z
(k often chosen as 0.52)

Fig. 6.1 Volume estimation from three orthogonal measurements.

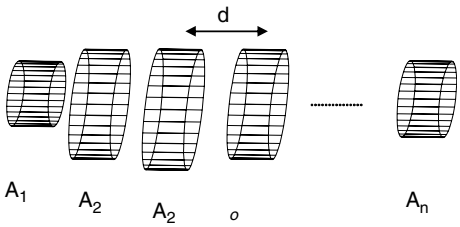

Volume = $A_1 . d_1 + A_2 . d_2 + ... + A_n . d_n$

Fig. 6.2 Volume estimation by summing slices.

An alternative method is to make area measurements on a series of adjacent slices. The volume of each slice is calculated by multiplying its area by the distance between slices, as shown in Figure 6.2. The slice volumes are added together to obtain the result. This is likely to be a more accurate method but is more time-consuming and is not widely used.

It is now possible to make volume measurements using three-dimensional ultrasound. Early examples include the prediction of birthweight (Lee *et al.* 1997), assessment of cardiac left ventricular volume and function (Kuhl *et al.* 1998) and measurement of neonatal cerebral ventricles (Kampmann *et al.* 1998).

Automatic measurement

Modern image-processing computers provide the opportunity for automating measurements. Although this is not a straightforward process, as the computer must perform some of the operations of the human eye–brain system in determining edges and boundaries, successful systems have been developed for cardiology and for obstetrics, which are both measurement-intensive, and significant time savings may be made.

Calculations

Modern ultrasound scanners have the facility to perform and store measurements. It is, therefore, possible to programme the system to calculate other parameters from measurements made by the operator. Examples include bladder volume, as described earlier, fetal weight and cardiac volumes.

When a measurement function is selected, the operator must then make the measurements and store them under the appropriate name. The scanner may allow for several measurements of each parameter to be made and automatically averaged. Once the measurements have been stored, the result will be calculated using the programmed formula.

Measurement errors

Ultrasound measurements may be different from the true value for a number of reasons. The difference between the observed and true values is called the 'error of observation'. It is important in any measurement to consider two types of error, viz. random and systematic. Many errors are a combination of these two types, although in different circumstances one or the other may be dominant. Both systematic and random errors affect accuracy. Reproducibility depends largely on random errors.

Table 6.1 Ten measurements of the circumference of a test object, made by two observers.

	Observer 1	Observer 2
	317	330
	317	325
	318	323
	321	315
	325	316
	321	318
	323	318
	319	322
	318	321
	322	314
Mean	320	320
CoV	0.9%	1.6%

Random errors

Random errors are accidental in nature and are often due to the observer, either directly or in the use of a system that lacks precision. For example, if the true diameter of a structure is 9.5 mm, and the calliper increment is 1 mm, the observer will never obtain a single true measurement. These errors are often revealed by repeated measurements, where several values above and below the true value are likely to be obtained. Averaging these measurements will reduce the error and produce a result closer to the true value.

A widely used measure of random error is the coefficient of variation (CoV). This is the ratio of the standard deviation to the mean of a series of measurements, expressed as a percentage.

Table 6.1 shows two series of traced measurements made on a test object. Note that although the mean values are the same, the two observers have generated different random errors. The CoV reflects the fact that the second observer has made a wider range of measurements. It is also interesting to consider the potential consequences of making only a single measurement in a clinical situation, as there is a 13 mm difference between the first values obtained by the two observers. This shows the importance of making multiple measurements and averaging.

Systematic errors

Systematic errors are generally consistent in direction and relative size. Both observer- and instrument-related systematic errors are possible in ultrasound as illustrated by the following examples.

(1) A sonographer consistently placing callipers just inside the edges of a structure will generate a systematically smaller result than colleagues placing callipers exactly on the edges.
(2) If an ultrasound scanner is incorrectly calibrated to 1600 m s^{-1}, all axial measurements made in a medium with velocity 1540 m s^{-1} will be systematically larger by approximately 4%.

Systematic errors are not revealed by repeated measurements, but may be found by comparison between observers or by measurement of appropriate test objects, depending on the source of error. This is illustrated by Table 6.1, where the true circumference of the test object was 314 mm; there was a systematic error of 6 mm in both series of measurements.

Some degree of systematic error related to the imaging process is inevitable in ultrasound, but it is possible to reduce it to low levels by careful choice of scanner and methods.

Compound errors

Where measurements are combined in some way, e.g. as a ratio or in a volume estimation, the potential errors in the individual measurements are compounded, leading to a larger potential error in the result. The error in a product or ratio is approximately equal to the sum of the fractional errors in each variable. For example, if the potential error in fetal AC and HC measurements is 3%, the potential error in the AC/HC ratio is approximately 6%.

Sources of errors in ultrasound systems

Human error

There are many possible causes of human error, including inadequate or inappropriate training, inexperience, lack of locally agreed standards or failure to follow local procedures. These will result in either measurement of inappropriate images or incorrect calliper placement. A common source of error is in the measurement of oblique, rather than longitudinal or transverse, sections, leading to overestimation. The frequency, magnitude and effect of human error in fetal measurement have been widely explored (Chang *et al.* 1993, Dudley and Chapman 2002, Sarmandal *et al.* 1989).

Failure to confirm or average measurements by repetition, and errors related to the measurement facilities, such as an over-sensitive track-ball, may also be considered as human error. A measurement system

that is difficult to use will deter sonographers from making repeat measurements. This will increase the likelihood, and probably the size, of errors.

The use of evidence-based standards and protocols, training, audit and careful selection of equipment can reduce human errors.

Image pixel size and calliper precision

The ultrasound image is made up of pixels, as described in Chapter 4. The smallest distance that can be represented in the image is one pixel and so all distance measurements have an inherent uncertainty of ±1 pixel. For example, if an image is 512 pixels square and the image depth is set to 20 cm, each pixel represents one 512th of 20 cm, i.e. 0.39 mm.

A further limitation may be the calliper increment. All calliper systems have a limited calliper increment which may be larger than the pixel size, e.g. 1 mm. The true calliper increment is never smaller than the pixel size, as the calliper must move a minimum of 1 pixel at a time.

When measuring small structures, it is therefore important to magnify the real-time image using either depth/scale or write zoom controls. The pixel size in the magnified image will be smaller, reducing this uncertainty. These errors are random in nature.

Image resolution

Ultrasound images have a finite spatial resolution, as discussed in Chapter 5. The edges of structures may, therefore, appear blurred or enlarged, and callipers may be placed beyond the true dimensions. Errors due to lateral beam width may be minimized by optimizing focal settings, so that the resolution is best at the region of measurement.

Resolution may not always present a problem, as measurements are usually compared with a normal range or with previous measurements. If, however, measurements are made on a scanner with performance significantly different to that used to develop reference values, then they may be misleading. An area where this has been evaluated and documented is in the measurement of fetal femur length. Jago *et al.* (1994) demonstrated systematic differences between femur length measurements made with older and more modern scanners. Differences in beam width of about 2 mm generated femur length differences of about 1 mm; it is worth noting that differences of this magnitude can be generated on any scanner by an inappropriate focal depth setting.

Since lateral resolution is generally inferior to axial resolution, errors are more likely in non-axial measurements. However, the distal margins of structures can be blurred as a result of poor axial resolution or due to reverberation in highly echogenic structures. It is, therefore, important to make axial measurements between the proximal edges of structures (leading edge to leading edge), e.g. when measuring the fetal biparietal diameter.

Gain settings can have a significant effect on resolution, but as the technology develops this has become less of a problem, as gain is more easily managed on modern equipment. Resolution may be generally improved by the use of higher ultrasound frequencies where possible.

Velocity/distance calibration

Since measurements are made on the digitized image in the scan converter memory, it is important that echoes are accurately placed in the image. This depends on the velocity assumed for calculation of the axial origin of echoes and on the algorithms used to calculate the position of scan lines in the image. Any error in echo placement can lead to a measurement error.

If echoes have been correctly placed, accuracy of any measurement then depends largely on the accuracy of in-built conversion factors to translate the number of pixels between calliper positions into a real distance. A set of factors is required for each probe geometry and for scale or depth settings. With the increasing range of probes and the availability of continuously variable scale settings, it is important that the electronics or software used to make these conversions is carefully designed and tested.

The consequence of incorrect calibration is a systematic error in all measurements or, more subtly, differences between measurements made on different scale settings. Velocity errors inherent in the equipment can be avoided by rigorously testing calliper accuracy prior to purchase and at commissioning.

Ultrasound propagation

Ultrasound scanners are generally designed to assume an ultrasound velocity of 1540 m s^{-1}. This represents a mean velocity in human soft tissue. True soft tissue velocities vary about this mean by approximately 5% and this may lead to slight distortions in the image (as described in Chapter 5) and, therefore, to measurement errors.

The clinical impact of these distortions will depend on the anatomy under investigation. Measurements of

a single organ may be incorrect if the velocity within the organ is not 1540 m s^{-1}, but so long as the velocity is the same in other patients there will be no error between patients. Measurements that cross structural boundaries may be adversely affected when compared with normal ranges or between patients, where the contribution of each structure to total distance varies. In most clinical situations, however, a single structure is measured. Where other structures are included, their size and velocity differences are often small, e.g. blood vessels included in an organ diameter measurement.

Advances in beam-forming techniques have enabled speed-of-sound corrections to be applied to real-time images. The average speed of sound in the imaged tissues is calculated from echo return times and the image is constructed using this estimate rather than the usual 1540 m s^{-1}. A more accurate image is displayed and the absolute accuracy of measurements will be improved. However, if these measurements are then compared with those made without speed-of-sound correction, there will be a systematic difference proportional to the ratio of the uncorrected and corrected speeds. It is important either that measurement comparisons are made using the same calibration speed or that measurements are adjusted to account for the speed correction before comparison with normal values or ranges.

A further source of distortion is refraction, where the ultrasound beam changes direction as it crosses boundaries between tissues with different velocities. This has a greater potential clinical impact as distortions may be introduced into a structure by proximal tissues or by the structure itself. Refraction is described in more detail in Chapter 5.

An area where the possibility of measurement errors due to refraction should always be considered is obstetrics. Refraction around the maternal mid-line can lead to apparently stretched objects (Figure 6.3a) and refraction in the fetal skull may shorten biparietal diameter measurements if the measured surfaces are not at 90° to the beam axis (Figure 6.3b). The biparietal diameter should be measured along the beam axis.

Errors in circumference and area

Circumference and area measurements are subject to all of the above errors. Traced measurements are particularly sensitive to human error, where calliper controls may be difficult to manipulate in generating an accurate outline. This leads to systematic and random errors, as every deviation is added to the circumference. In clinical practice, structural outlines are not always completely and reliably visualized and this may also lead to errors.

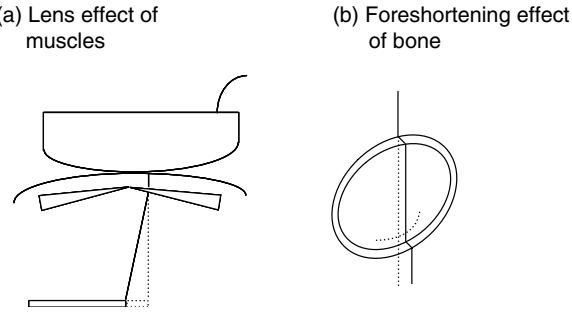

Fig. 6.3 The effect of refraction. Solid lines show the true ultrasound path and the true position of the structure, dotted lines show the assumed ultrasound path and the refracted position of the structures in the image. (a) Effect of refraction by muscles close to the transducer face; (b) effect of refraction by bone.

The magnitude of the systematic error in tracing depends on several factors. Difficulty in manipulating the track-ball accurately will increase the error, as will any lack of care on the part of the operator. The separation of points on the tracing used by the system to calculate the distance is also important. If the points are far apart, this will result in a shortening of the distance and if the points are too close together every small deviation will be included, increasing the measurement. Errors as high as 15% have been documented (Dudley and Griffith 1996). The optimum number of points depends on the sensitivity of the track-ball and the distance measured; this will be determined in the design of the equipment. For a fetal AC in the third trimester, one point per centimetre might be appropriate.

In the clinical situation, errors will usually be larger than those shown in Table 6.1, as measurements are rarely repeated 10 times and it is more difficult to obtain a good image from a patient than from a test object. Examples of clinical inter-observer CoVs for circumferences and areas of 3% and 5%, respectively, have been reported (Owen *et al.* 1996, Sarmandal *et al.* 1989).

Alternative methods are less prone to errors of operator dexterity. Ellipse fitting provides an accurate and reproducible measurement, provided that the outline of the structure is clearly visualized and is elliptical in shape. The point-to-point methods described earlier can provide accurate and reproducible results,

with the advantage that the points may be fitted to any shape. This method is likely to give the most accurate and reproducible results in clinical practice, provided sufficient points are used.

Area measurements are somewhat more reliable where outline tracing is erratic, as small areas are both added to and subtracted from the true area by deviations outside and inside the outline. Mean errors are typically less than 1.5% with CoV of less than 0.5%.

Errors in volume

Since volume estimation methods always use a combination of measurements, they are subject to compound errors as described above. If the volume is the product of three diameters, each with a potential error of 5%, the potential error in the volume is approximately 15% (neglecting any assumptions about shape).

The human error may be large, as the method may rely on finding maximum diameters of an irregular structure or measuring multiple areas. In many cases, however, the largest errors may be introduced by assumptions used in calculations, especially when measurements used are from a single scan plane only. The shape of a structure will vary from patient to patient, reducing the validity of 'constants' used in the calculation.

One solution to the problem of variable shape is to develop different constants for the shapes encountered. This has been proposed for the measurement of bladder volume, where Bih *et al.* (1998) have derived constants for a number of shapes.

Summary of errors

In a controlled situation, e.g. test object, with careful measurement, errors can be summarized as shown in Table 6.2. In clinical practice, errors depend on additional factors such as the quality of image acquired, the shape of structures measured and any assumptions used when combining quantities in calculations. With careful imaging, measurement and choice of methods, it is possible to achieve errors similar to those shown in Table 6.2, although some clinical measurements may have errors of two or three times this size. Calculated parameters, such as volume, may have errors of up to 100%.

Interpretation of measurements

Once measurements have been made, they must be interpreted. This requires an understanding of the source and magnitude of any possible errors, an aspect that is often ignored. Measurements that do not rely on operator dexterity or assumptions about shape tend to have the smallest errors. In the clinical situation, errors are influenced by other factors including the ease of obtaining and recognizing the correct section for measurement. Where landmarks are well recognized and reproduced in clinical practice, measurements are widely used and are interpreted with confidence. The size of errors must be considered in the context of the normal biological variation of the measurement. A 5 mm measurement uncertainty is insignificant in a 50 mm normal range, but highly significant in a 5 mm normal range. Absolute accuracy is generally more important for small structures than for large structures, e.g. an error of 0.1 mm in a nuchal translucency measurement can make a significant difference to the estimated risk of Down's syndrome.

The variation in size of errors between equipment, together with inter-operator and inter-centre variation, may limit the value of clinical ultrasound. Understanding and reducing this variation may allow ultrasound measurement to be used to its full potential. It is important to evaluate and minimize human error in order to achieve the best value from the precision and accuracy of modern equipment.

Use of normal reference data

Interpretation often involves a reference normal range or chart. This introduces a further potential source of human error in the reading of values or transcription of measurements. It is also important to consider how these data were derived. What technique was used? What was the uncertainty in the results? There may have been systematic errors and there are always random errors. Were these addressed?

Systematic errors in the derivation of normal data may be significant compared to the normal ranges, particularly when the equipment used was inferior to that available today. If these errors were not evaluated in the originating centre, this limits the value of the data. The uncertainty this generates is illustrated by the following example.

In measuring the fetal AC, some centres trace directly around the perimeter while others fit an ellipse. In generating normal ranges, Chitty *et al.* (1994) found the average tracing to be 3.5% greater than the ellipse measurement. This is consistent with the findings of Tamura *et al.* (1986), who found an average difference of 3.1% between the methods. These measurements were made in the late 1980s and early 1990s. Dudley and Chapman

Table 6.2 Dependency and errors in each type of measurement.

Type of measurement	Error depends on	Approximate size of error
Linear	Pixel size	0.1–0.5 mm
	Calliper increment	0.1–1 mm
	Resolution	0.1–5 mm
Ellipse (circumference and area)	Ellipse calculation	1%
Point to point (circumference and area)	Point-to-point calculation	1%
	Number of points	1–5%
Tracing (circumference)	Track-ball sensitivity	2%
Tracing (area)	Operator dexterity	1%

(2002) found a difference of 1.5% between the two methods in a clinical setting, but even in a single centre this varied between sonographers, ranging from 0.5% to 2.1%. This difference has been reproduced in test-object measurements (Dudley and Griffith 1996) and represents the systematic error associated with operator dexterity and the sensitivity of the calliper control.

Normal ranges and charts may be evaluated against local practice and equipment by comparison with results from patient measurements. This is straightforward where large numbers of normal measurements are made, e.g. antenatal screening. A dating chart can be evaluated by plotting a number of measurements, say 20 at each gestational age, and assessing their distribution within the normal range; they should be centred on the mean and the majority should be within the normal range. Where a large amount of normal data is not available the evaluation requires more careful judgement, considering where the measurements should fall with respect to the normal range based on knowledge of the likely composition of the patient population.

Measurement packages

Most ultrasound scanners now arrive equipped with 'measurement packages'. As well as providing a variety of measurement methods, these packages include programmed charts and automatic calculations to aid interpretation. Examples include fetal growth charts, fetal weight estimation and bladder volume calculation. Although charts and calculations will be based on published data the source may well be the choice of the manufacturer. Many manufacturers offer a selection of pre-installed charts and also provide the facility for users to enter their own preferred data.

Use of such packages removes a potential source of human error, as the sonographer is no longer required to make manual calculations or read from graphs. It is essential, however, that the equipment purchaser makes active decisions in the choice of charts and calculation algorithms, and ensures that these are thoroughly tested before being put into clinical use.

Summary

Measurements are performed in many clinical ultrasound specialities. Modern calliper systems are generally flexible, offering a range of measurements and calculations.

Errors are present, to varying degrees, in most measurements and can arise from the instrumentation, the ultrasound propagation properties of tissue and the equipment operator. These errors can be minimized by adopting good practice at all stages of equipment selection and use.

The choice of equipment is important. Systematic and random errors can be minimized by thorough evaluation of measurement controls and packages prior to purchase, although reliable measurements and the highest-quality images may not always be available in the same instrument. At acceptance testing, systematic and random errors should be quantified, so that they may be reflected in the choice of normal reference data and reporting policies. Any programmed charts and calculations should be consistent with locally accepted practice.

Measurement technique is important. All users should understand locally accepted practice, which should be clearly defined in written procedures. Good practice should include the appropriate selection of probe type and frequency, the optimum use of image

magnification, setting focal zones at the region of measurement, avoiding image distortion due to refraction whenever possible and the correct and careful placement of callipers. Methods should be appropriate for the selected normal reference data. Random errors can be greatly reduced by performing repeated measurements and using average results.

In interpretation of measurements, clinicians should always be aware of the size of any uncertainty in the result and the size of the normal biological variation. Where these are both small, results may be interpreted with confidence, otherwise a degree of caution is required.

In order to minimize errors, the following steps must be taken:

(1) Buy a scanner with correct calibration and good reproducibility.
(2) Train and assess staff to national standards where available. As a minimum, ensure local consistency by training and audit.
(3) Use an appropriate method of measurement.
(4) Overcome the limitations of pixel size and resolution by making the best use of scale/depth, magnification and focusing controls, so that the measured structure is large and optimally resolved within the field of view.
(5) Repeat measurements to increase certainty. This either gives confidence where the same value is obtained or allows reduction of the random error by averaging.

Questions

1. What is the conventionally assumed average speed of sound?
2. If an image is displayed in a 512-pixel-square matrix, with a scale setting of 5 cm in order to make a small measurement (e.g. nuchal translucency, common bile duct, intimal thickness, valve leaflet thickness), what is the pixel size?
3. How does an ultrasound scanner work out pixel size for a linear array image: (a) axially; (b) laterally?
4. What are the methods available for measuring a circumference?
5. How may volume be estimated from a combination of sagittal and transverse images?
6. What is a random error and what are the sources?
7. What is a systematic error and what are the sources?
8. List the measurements made in a clinical field you are familiar with, and for each measurement note the typical distances measured and the optimum image scale/depth/zoom setting.

References

Bih LI, Ho CC, Tsai SJ, Lai YC, Chow W (1998). Bladder shape impact on the accuracy of ultrasonic estimation of bladder volume. *Archives of Physical Medicine and Rehabilitation,* **79**, 1553–6.

Chang TC, Robson SC, Spencer JAD, Gallivan S (1993). Ultrasonic fetal weight estimation: analysis of inter- and intra-observer variability. *Journal of Clinical Ultrasound,* **21**, 515–19.

Chitty LS, Altman DG, Henderson A, Campbell S (1994). Charts of fetal size: 3. Abdominal measurements. *British Journal of Obstetrics and Gynaecology,* **101**, 125–31.

Dudley NJ, Chapman E (2002). The importance of quality management in fetal measurement. *Ultrasound in Medicine and Biology,* **19**, 190–6.

Dudley NJ, Griffith K (1996). The importance of rigorous testing of circumference measuring calipers. *Ultrasound in Medicine and Biology,* **22**, 1117–19.

Jago JR, Whittingham TA, Heslop R (1994). The influence of scanner beam width on femur length measurements. *Ultrasound in Medicine and Biology,* **20**, 699–703.

Kampmann W, Walka MM, Vogel M, Obladen M (1998). 3-D sonographic volume measurement of the cerebral ventricular system: in vitro validation. *Ultrasound in Medicine and Biology,* **24**, 1169–74.

Kuhl HP, Franke A, Janssens U, et al. (1998). Three-dimensional echocardiographic determination of left ventricular volumes and function by multiplane transesophageal transducer: dynamic in vitro validation and in vivo comparison with angiography and thermodilution. *Journal of the American Society of Echocardiography,***11**, 1113–24.

Lee W, Comstock CH, Kirk JS, et al. (1997). Birthweight prediction by three-dimensional ultrasonographic volumes of fetal thigh and abdomen. *Journal of Ultrasound in Medicine,* **16**, 799–805.

Owen P, Donnet ML, Ogston SA, et al. (1996). Standards for ultrasound fetal growth velocity. *British Journal of Obstetrics and Gynaecology,* **103**, 60–9.

Rossavik IK, Deter RL (1984). The effect of abdominal profile shape changes on the estimation of fetal weight. *Journal of Clinical Ultrasound*, **12**, 57–9.

Sarmandal P, Bailey SM, Grant JM (1989). A comparison of three methods of assessing inter-observer variation applied to ultrasonic fetal measurement in the third trimester. *British Journal of Obstetrics and Gynaecology,* **96**, 1261–5.

Tamura RK, Sabbagha RE, Wen-Harn P, Vaisrub N (1986). Ultrasonic fetal abdominal circumference: comparison of direct versus calculated measurement. *American Journal of Obstetrics and Gynecology*, **67**, 833–5.

Chapter 7

Principles of Doppler ultrasound

Peter Hoskins

The Doppler effect enables ultrasound to be used to detect the motion of blood and tissue. Most Doppler ultrasound systems provide both spectral Doppler displays and colour Doppler images. Many of the features of these two modalities are common, and are described in this chapter. Specific details of spectral Doppler and colour Doppler systems are given in the chapters following this.

The descriptions that follow in this chapter refer to the detection and display of blood flow, as this is the most common application of Doppler techniques. Chapter 8 describes the use of Doppler in detection of tissue motion.

Doppler ultrasound systems

The Doppler effect

The Doppler effect is observed regularly in our daily lives. For example, it can be heard as the changing pitch of an ambulance siren as it passes by. The Doppler effect is the change in the observed frequency of the sound wave (f_r) compared to the emitted frequency (f_t) which occurs due to the relative motion between the observer and the source, as shown in Figure 7.1. In Figure 7.1a, both the source and the observer are stationary so the observed sound has the same frequency as the emitted sound. In Figure 7.1b, the source is moving towards the observer as it transmits the sound wave. This causes the wavefronts travelling towards the observer to be more closely packed, so that the observer witnesses a higher frequency wave than that emitted. If, however, the source is moving away from the observer the wavefronts will be more spread out, and the frequency observed will be lower than that emitted (Figure 7.1c). The resulting change in the observed frequency from that transmitted is known as the Doppler shift, and the magnitude of the

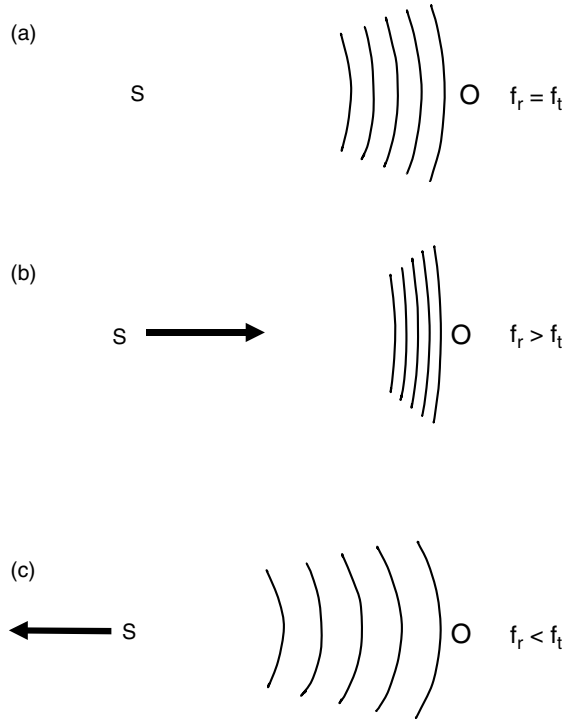

Fig. 7.1 Doppler effect as a result of motion of the source (S) relative to a stationary observer (O). (a) There is no motion and the observer detects sound at a frequency equal to the transmitted frequency. (b) The source moves towards the observer and the observer detects sound at a higher frequency than that transmitted. (c) The source moves away from the observer and the observer detects a lower frequency than that transmitted.

Doppler shift frequency is proportional to the relative velocity between the source and the observer.

It does not matter whether the source or the observer is moving. If either one is moving away from the other, the observer will witness a lower frequency than that emitted.

Diagnostic Ultrasound: Physics and Equipment, ed. Peter Hoskins, Kevin Martin and Abigail Thrush. Published by Cambridge University Press.

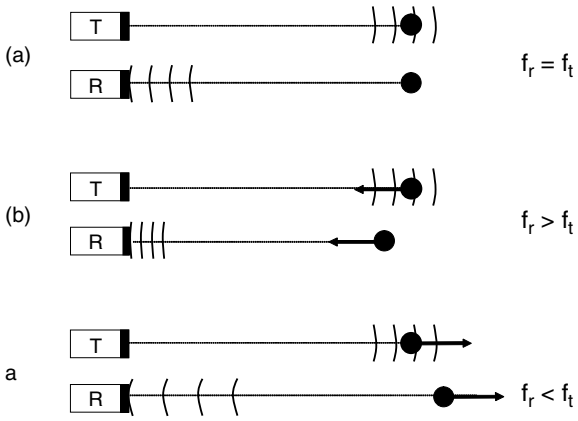

Fig. 7.2 The Doppler effect occurring due to motion of blood. In each case the probe transmits ultrasound which strikes the blood. Separate elements are shown for transmission (T) and reception (R). Ultrasound is scattered by the region of blood, some of which returns to the transducer. (a) The probe and blood are not moving; the frequency of the ultrasound received by the transducer is equal to the transmitted frequency. (b) The blood is moving towards the probe; the blood encounters more wavefronts and the frequency of the ultrasound received by the transducer is greater than the transmitted frequency. (c) The blood is moving away from the probe; the blood encounters fewer wavefronts and the frequency of the ultrasound received by the transducer is less than the transmitted frequency.

Conversely, if either the source or observer move towards the other, the observer will witness a higher frequency than that emitted.

Ultrasound can be used to assess blood flow by measuring the change in frequency of the ultrasound scattered from the moving blood. Usually the transducer is held stationary and the blood moves with respect to the transducer, as shown in Figure 7.2. The ultrasound waves transmitted by the transducer strike the moving blood, so the frequency of ultrasound as experienced by the blood is dependent on whether the blood is stationary, moving towards the transducer or moving away from the transducer. The blood then scatters the ultrasound, some of which travels in the direction of the transducer and is detected. The scattered ultrasound is Doppler frequency shifted again as a result of the motion of the blood, which now acts as a moving source. Therefore, a Doppler shift has occurred twice between the ultrasound being transmitted and received back at the transducer (hence the presence of the '2' in Equation (7.1)).

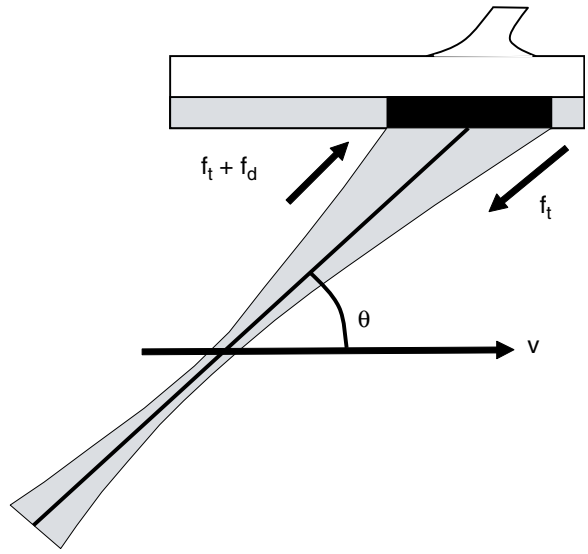

Fig. 7.3 A beam of ultrasound is produced by a linear array in which the active elements are shown in black. Ultrasound is transmitted whose centre frequency is f_t. This strikes blood moving at velocity v. The angle between the beam and the direction of motion is θ. The received ultrasound frequency has been Doppler-shifted by an amount f_d, so that the detected frequency is $f_t + f_d$.

The detected Doppler shift frequency (f_d) is the difference between the transmitted frequency (f_t) and the received frequency (f_r). The Doppler shift frequency f_d depends on the frequency of the transmitted ultrasound, the speed of the ultrasound as it passes through the tissue (c) and the velocity of the blood (v) (Figure 7.3). This relationship can be expressed by the Doppler equation:

$$f_d = f_r - f_t = \frac{2 f_t v \cos\theta}{c} \qquad (7.1)$$

The detected Doppler shift also depends on the cosine of the angle θ between the path of the ultrasound beam and the direction of the blood flow. This angle is known as the angle of insonation. The angle of insonation can change as a result of variations in the orientation of the vessel or the probe. Many vessels in the upper and lower limbs run roughly parallel to the skin, although if the vessel is tortuous the angle of insonation will alter. In the abdomen there is considerable variation in the orientation of vessels which will result in many different angles of insonation. The operator is also able to alter the angle of insonation by adjustment

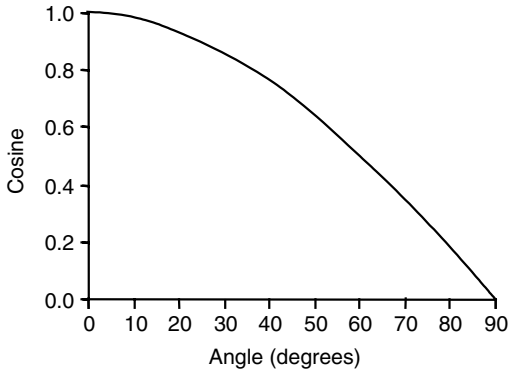

Fig. 7.4 The cosine function. This has a maximum value of 1.0 when the angle is 0°, and a value of 0 when the angle is 90°.

of the orientation of the probe on the surface of the skin. The relationship between an angle and the value of its cosine is shown in Figure 7.4. It is often desirable that the operator can adjust the angle of insonation to obtain the highest Doppler frequency shift possible. The highest Doppler frequency shift from any specific vessel occurs when the vessel and the beam are aligned; that is, when the angle of insonation is zero and the cosine function has the value of 1.0. The least desirable situation occurs when the angle approaches 90° as then the Doppler frequency shift will be minimum. In clinical practice it is often not possible to align the beam and the vessel. As a rule, provided the angle is less than about 60°, good-quality spectral waveforms can be obtained.

If the angle of insonation of the ultrasound beam is known it is possible to use the Doppler shift frequency to estimate the velocity of the blood using the Doppler equation. This requires rearrangement of Equation (7.1) to give

$$v = \frac{c f_d}{2 f_t \cos\theta} \qquad (7.2)$$

In diseased arteries the lumen will narrow and the blood velocity will increase. This provides the means by which the lumen diameter may be estimated using Doppler ultrasound. The blood velocity is estimated within the narrowed region, and converted into a percentage stenosis using standard tables.

Doppler displays

The main display modes used in a modern Doppler system are described below.

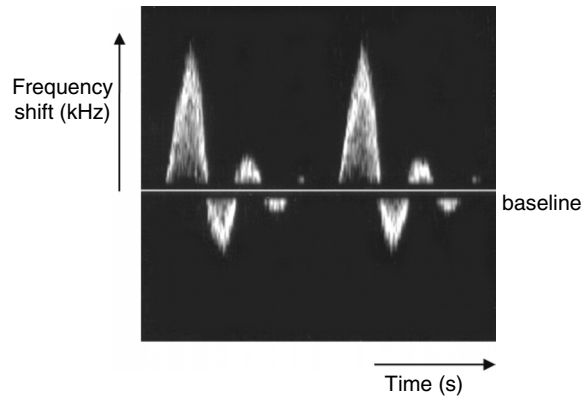

Fig. 7.5 Spectral display. This is a display of the Doppler frequency shift versus time. The Doppler waveform from the femoral artery is shown. Vertical distance from the baseline corresponds to Doppler shift, while the greyscale indicates the amplitude of the detected ultrasound with that particular frequency.

- *Spectral Doppler:* all the velocity information detected from a single location within the blood vessel is displayed in the form of a frequency shift–time plot (Figure 7.5). Vertical distance from the baseline corresponds to Doppler shift, while the greyscale indicates the amplitude of the detected ultrasound with that particular frequency.
- *2D colour flow imaging:* the Doppler signal is displayed in the form of a 2D colour image superimposed on the B-scan image (Figure 7.6). Colour represents the Doppler shift for each pixel, averaged over the area of the pixel.

The advantage of the 2D colour display is that it allows the user to observe the presence of blood flow within a large area of the tissue. The spectral Doppler display allows closer inspection of the changes in velocity over time within a single small area. Both colour flow and spectral Doppler systems use the Doppler effect to obtain blood-flow information. In this respect they are both Doppler systems. The two modalities complement each other, providing the user with a wide range of useful information.

Continuous-wave and pulsed-wave Doppler

There is not the restriction in Doppler systems as there is for B-mode devices that the ultrasound must be transmitted in the form of pulses. Some Doppler ultrasound systems, known as continuous-wave (CW) systems,

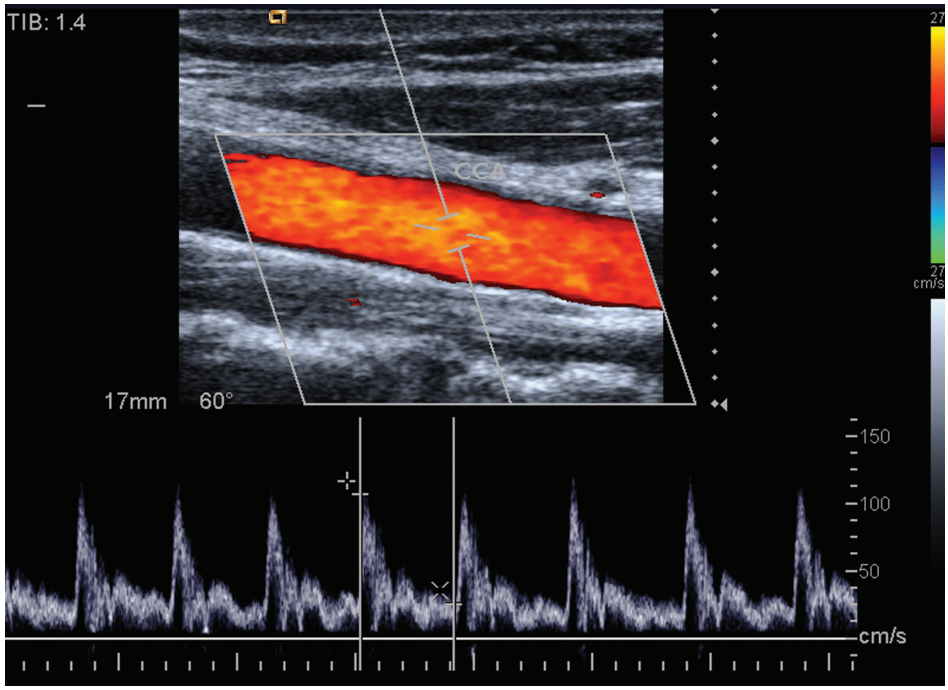

Fig. 7.6 Colour Doppler display. This is a display of the mean (or average) Doppler frequency, at each point in a 2D slice of the tissue from blood, superimposed on the B-mode display. The example also shows simultaneous display of spectral Doppler.

transmit ultrasound continuously. Other Doppler systems, known as pulsed-wave (PW) systems, transmit short pulses of ultrasound. The main advantage of PW Doppler is that Doppler signals can be acquired from a known depth. The main disadvantage is that there is an upper limit to the Doppler frequency shift which can be detected, making the estimation of high velocities more challenging.

In a CW Doppler system there must be separate transmission and reception of ultrasound (Figure 7.7a). In the pencil probe this is achieved using two elements, one which transmits continuously and one which receives continuously. The region from which Doppler signals are obtained is determined by the overlap of the transmit and receive ultrasound beams. In a PW system it is possible to use the same elements for both the transmit and receive (Figure 7.7b). In the pencil probe only one element is needed, serving both the transmit and receive functions. The region from which Doppler signals are obtained is determined by the depth of the gate and the length of the gate, which can both be controlled by the operator.

The received ultrasound signal is processed by the Doppler signal processor to extract the Doppler frequency shifts, which are then displayed in the form of spectral Doppler or colour Doppler.

The ultrasound signal received by the transducer

Before considering in detail the Doppler signal processor, the nature of the ultrasound signal received at the transducer must be considered, as this will determine the subsequent signal processing that is performed.

When ultrasound is emitted from the transducer it will pass through regions of tissue and regions of blood contained in veins and arteries. The blood will almost certainly be moving, but some of the tissue may also be moving. For example, the arteries move during the cardiac cycle, the heart moves as a result of contraction, and tissues in contact with the arteries and with the heart will also move. The received ultrasound signal consists of the following four types of signal:

- echoes from stationary tissue
- echoes from moving tissue
- echoes from stationary blood
- echoes from moving blood.

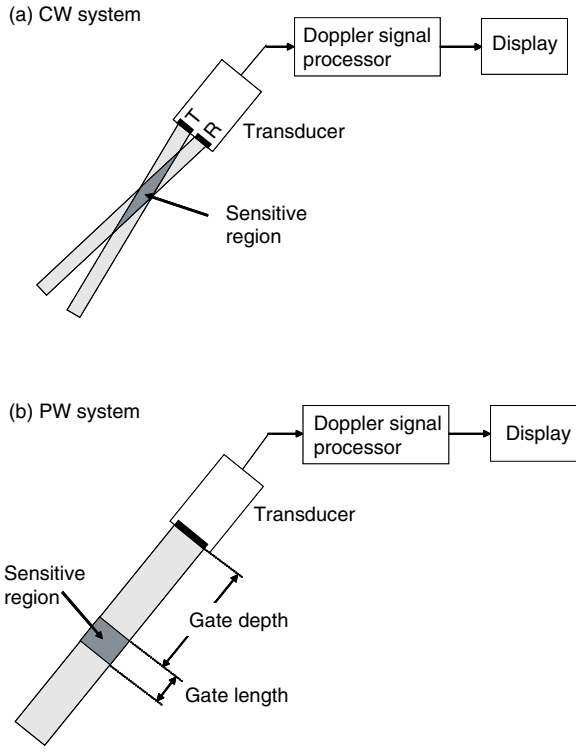

Fig. 7.7 Schematic of CW and PW Doppler system consisting of the transducer, the Doppler signal processor and the display. (a) In a CW Doppler system there must be separate transmission and reception of ultrasound. In the pencil probe this is achieved using two elements, one which transmits continuously and one which receives continuously. The region from which Doppler signals are obtained is determined by the overlap of the transmit and receive ultrasound beams. (b) In a PW system it is possible to use the same element or elements for both transmit and receive. In the pencil probe only one element is needed, serving both the transmit and receive functions. The region from which Doppler signals are obtained is determined by the depth and length of the gate, which are both controlled by the operator.

The task for a Doppler system is to isolate and display the Doppler signals from blood, and remove those from stationary tissue and from moving tissue. Table 7.1 shows the amplitude of signals from blood and tissue, and it is clear that the signal from blood is extremely small compared to tissue; typically 40 dB smaller (Table 7.1). The maximum blood velocity occurs when disease is present, and is about 6 m s^{-1}.

Table 7.1 Typical velocities and signal intensities.

	Velocity ranges	Signal intensity
Blood	0–600 cm s^{-1}	Low
Tissue	0–10 cm s^{-1}	40 dB higher than blood

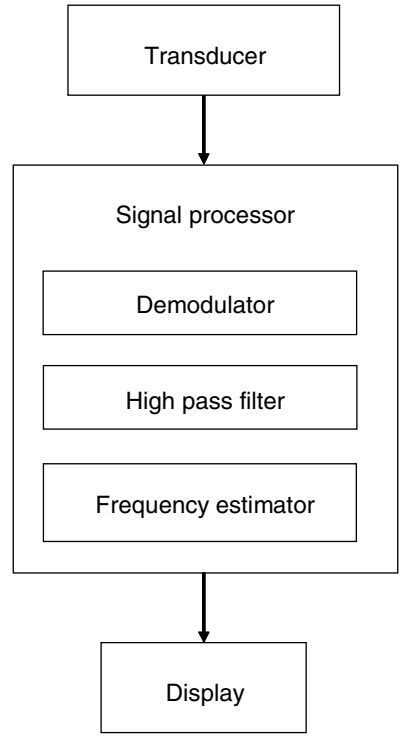

Fig. 7.8 The Doppler signal processor can be considered to be made of three parts; the demodulator, the high-pass filter and the frequency estimator.

The maximum tissue velocity occurs during the systolic phase of the heart where the myocardium attains a velocity of up to 10 cm s^{-1}. In general, Doppler signals from blood are of low amplitude and high-frequency shift, whereas those from tissue are of high amplitude and low-frequency shift. These differences provide the means by which true blood flow signals may be separated from those produced by the surrounding tissue.

The CW Doppler signal processor

Dedicated signal-processing algorithms are used to produce the Doppler signals from the received ultrasound signal. There are three steps in the process (Figure 7.8): 'demodulation' is the separation of the Doppler frequencies from the underlying transmitted

signal; 'high-pass filtering' is the removal of the tissue signal; 'frequency estimation' is where the Doppler frequencies and amplitudes are calculated. There are important differences between the CW and the PW Doppler signal processor which are described in the next section.

Demodulation

The Doppler frequencies produced by moving blood are a tiny fraction of the transmitted ultrasound frequency. Equation (7.1) shows that, if the transmitted frequency is 4 MHz, a motion of 1 m s^{-1} will produce a Doppler shift of 5.2 kHz, which is less than 0.1% of the transmitted frequency. Extraction of the Doppler frequency shift information from the ultrasound signal received from tissue and blood is called 'demodulation'. This process is generally invisible to the user as there are no controls which the user can adjust to alter this process. The process of demodulation consists of comparison of the received ultrasound signal with a 'reference' signal which has the same frequency as the transmit echo. This process is illustrated in Figure 7.9, which shows the ultrasound signal obtained from a CW Doppler system being used with a small moving target. The received ultrasound signal has a slightly different frequency compared to the reference signal. The first step of the demodulation process consists of multiplying together the reference signal with the received signal. This process is called 'mixing'. This produces the signal shown in Figure 7.9c, which consists of a low-frequency component (the Doppler frequency) arising from the moving target, and a high-frequency component arising from the transmit frequency. The high-frequency component can be removed by simple filtering, revealing the Doppler frequency (Figure 7.9d). The end result of demodulation for the example of Figure 7.9 is the removal of the underlying high-frequency transmit signal, revealing the blood flow Doppler signal.

The example above described demodulation when there was a single moving target present. In reality the sensitive region of the ultrasound system is unlikely to be placed within a region in which all the blood is moving at the same velocity. It is more likely that there will be a range of blood velocities present within the sensitive region, with low velocities present near the vessel wall and higher velocities present near the vessel centre. In addition the sensitive region for a CW system will usually encompass moving tissue. When there are

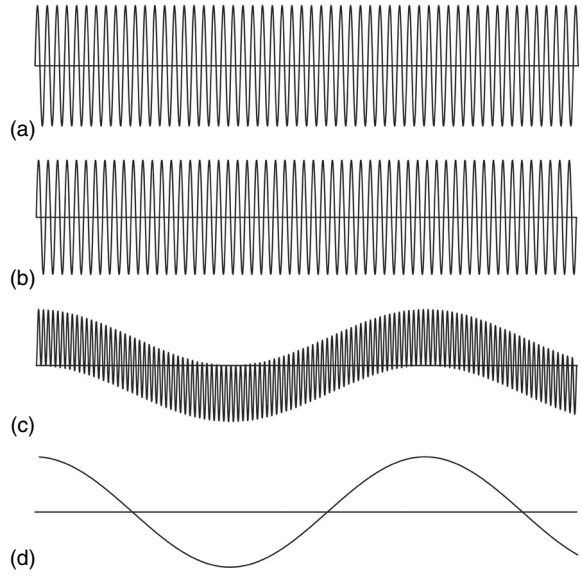

Fig. 7.9 Doppler demodulation for CW Doppler. (a) Reference signal of frequency f_t. (b) Detected signal which has been Doppler-shifted and whose frequency is $f_r = f_t + f_d$. (c) The reference signal is multiplied by the detected signal. (d) The high-frequency oscillations are removed by low-pass filtering. The end result is the Doppler frequency shift signal f_d (the example shown contains no clutter).

signals from both blood and tissue present, and multiple velocities, the process of demodulation is best understood with reference to the detected ultrasound frequency (Figure 7.10). The received signal from a region in which blood is flowing consists of a high-amplitude clutter signal from stationary and slowly moving tissue, and Doppler-shifted components from the moving blood. Blood moving towards the transducer gives rise to a positive shift, while blood moving away from the transducer gives rise to a negative Doppler shift. Demodulation removes the high frequencies arising from the transmit frequency, leaving both the Doppler shift signal from blood flow and the clutter signal from tissue motion. At this stage in the process it is not possible to differentiate the tissue signal from the blood flow signal. This requires another step (high-pass filtering) as described below.

Another way of viewing the process of demodulation is that it converts a high-frequency signal (MHz, or millions of cycles per second) into a low-frequency signal (kHz, or thousands of cycles per second). It

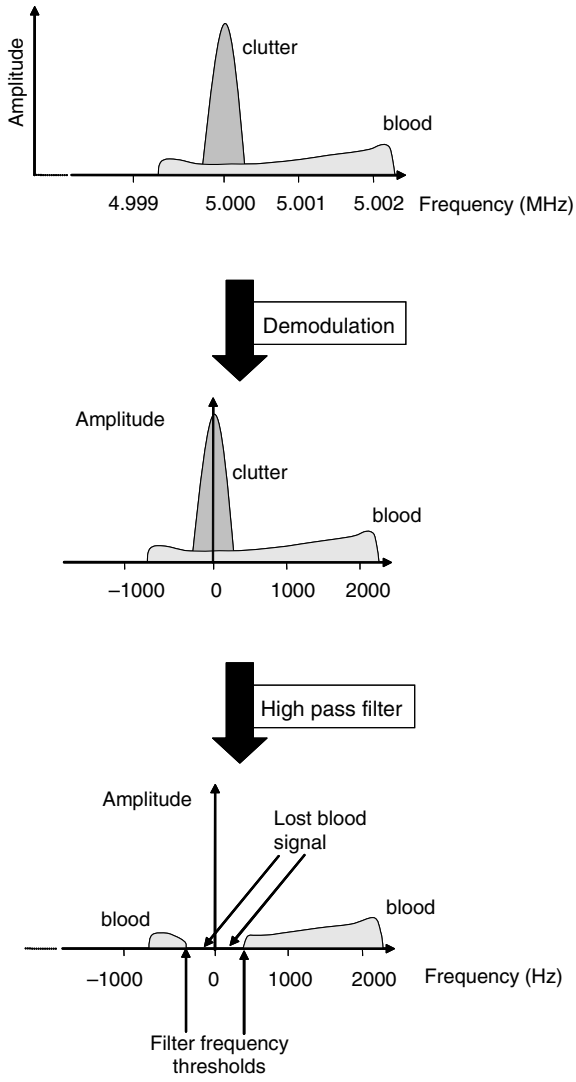

Fig. 7.10 Demodulation and high-pass filtering. Top: the received signal, from a region in which blood is flowing, consists of a high-amplitude clutter signal from stationary and slowly moving tissue, and Doppler-shifted components from the moving blood. Blood moving towards the transducer gives rise to a positive shift, while blood moving away from the transducer gives rise to a negative Doppler shift. Middle: demodulation removes the high-frequency signals arising from the transmit frequency, leaving the Doppler shift signal from both blood flow and the clutter signal from tissue motion. Bottom: the high-pass filter acts to remove the clutter signal. A consequence of this is that the very lowest blood velocities are also removed.

is easier for the ultrasound system to digitize and process signals which are of lower frequency. This is important as computational efficiency is crucial to ultrasound system design. High-speed processing is expensive, and increases the cost of the system to the user.

High-pass filtering

We saw above that the signal arising from demodulation can contain Doppler frequency shifts arising from both blood flow and tissue motion. If no further processing were performed then the estimated Doppler signals from blood would be overwhelmed by the large-amplitude signal from tissue. In order to correctly estimate the Doppler shift frequencies from blood, the Doppler signals from tissue must be removed. This step is referred to as the 'wall-thump filter' or 'cut-off filter' in spectral Doppler.

The tissue signals are called 'clutter'. This term originates from radar and refers to stationary objects such as trees and buildings which interfere with the detection of moving targets such as aeroplanes. Removal of clutter can be performed using a number of methods. The basis for discrimination between the blood signal and the tissue signal is that signals from tissue tend to be low frequency and high amplitude, and those from blood are high frequency and low amplitude. The simplest approach, and that adopted by many Doppler systems, relies on a frequency filter (Figure 7.10). Removal of components below a certain threshold frequency will remove the Doppler shift components arising from the tissue. An unfortunate consequence of this process is that the Doppler frequency shifts from slowly moving blood will also be lost. In general the filter frequency is set by the user to just suppress tissue signals. In cardiology applications a high-filter setting of 300 Hz or more is necessary since myocardium and valves are travelling at high speeds (up to 10 cm s^{-1}), and the detection of high blood velocities is of interest. In obstetrics, low settings of 50–80 Hz are more typical as it is important to be able to detect the low velocities at end-diastole. After filtering, the Doppler frequency shift data are in a form suitable for the third step in the process, the frequency estimator.

Frequency estimation

When information concerning blood velocity is required then some form of frequency estimator must be used. As CW systems provide no information on the depth from which the blood flow signal

has returned, it is not possible to use a colour flow display. CW systems display the time–velocity waveform, either in the form of spectral Doppler, or in the form of a single trace.

A spectrum analyser calculates the amplitude of all of the frequencies present within the Doppler signal, typically using a method called the 'fast Fourier transform' (FFT), in which a complete spectrum is produced every 5–40 ms. In the spectral display (Figure 7.5) the brightness is related to the power or amplitude of the Doppler signal component at that particular Doppler frequency. The high speed with which spectra are produced means that detailed and rapidly updated information about the whole range of velocities present within the sample volume can be obtained.

Before the advent of real-time spectrum analysis, it was common to display only a single quantity related in some way to the blood velocity. A relatively simple electronics device known as the 'zero-crossing detector' produces an output proportional to the root mean square of the mean Doppler frequency. However, the zero-crossing detector is sensitive to noise, and the output depends strongly on the velocity profile within the vessel. Its use in a modern Doppler system is no longer justified.

Origin and processing of the Doppler signal for PW systems

The Doppler signal

There is a crucial difference between CW and PW systems in that for PW systems a received ultrasound signal is not available continuously, as it is for CW systems. This is illustrated in Figure 7.11, which shows a point target moving away from the transducer, and the received ultrasound signal for consecutive ultrasound pulses. For each consecutive pulse the target moves further away from the transducer, and consequently the echo is received at a later time from the start of the transmit pulse. As the echo pattern moves further away from the transducer with each consecutive pulse, so the amplitude of the signal at a specific depth changes, as shown in Figure 7.11. In PW Doppler systems the location of the Doppler gate defines the range of depths from which the Doppler signal arises. The Doppler signal is contained within the series of consecutive received echoes from the gate. The Doppler signal is then revealed by the subsequent signal processing.

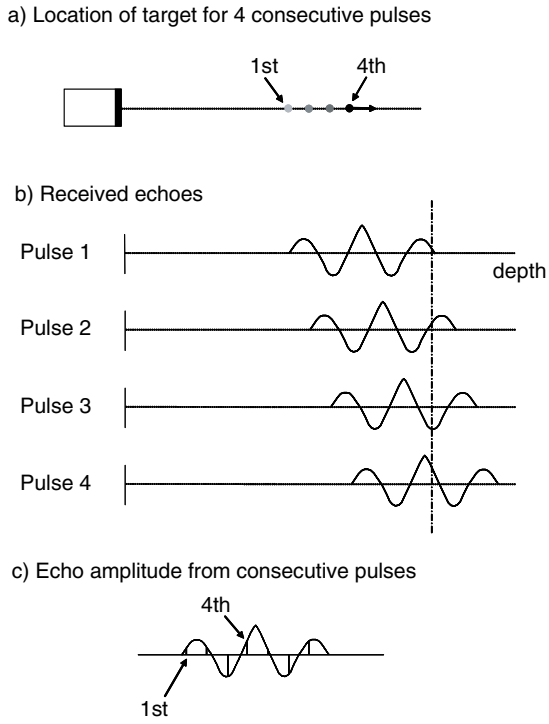

Fig. 7.11 Received echoes in PW Doppler. (a) A single target moves away from the transducer. Consecutive ultrasound pulses are emitted which strike the target at increasing depth. (b) The received echoes are displayed at increasing depth. A vertical dashed line is shown corresponding to a fixed depth. The amplitude of the echo changes as it crosses the dashed line for each consecutive pulse. The change in amplitude of the received echoes with depth contains the Doppler shift, which is extracted by demodulation. (c) Amplitude of consecutive echoes from the depth indicated by the dashed line in (b) shown as a function of time.

PW Doppler signal processor

In PW Doppler systems the basic steps of demodulation, high-pass filtering and frequency estimation are essentially the same as for CW Doppler. Figure 7.9 has shown how demodulation works for CW systems. Figure 7.12 shows the demodulator in action for PW Doppler. Although the reference signal (Figure 7.12a) is produced continuously, the received ultrasound signal (Figure 7.12b) from the Doppler gate is only produced once for every ultrasound pulse. The process of 'mixing' (Figure 7.12c) and low-pass filtering (Figure 7.12d) produces the Doppler signal. This signal has the same overall shape as the demodulator output from the CW Doppler system. This is the

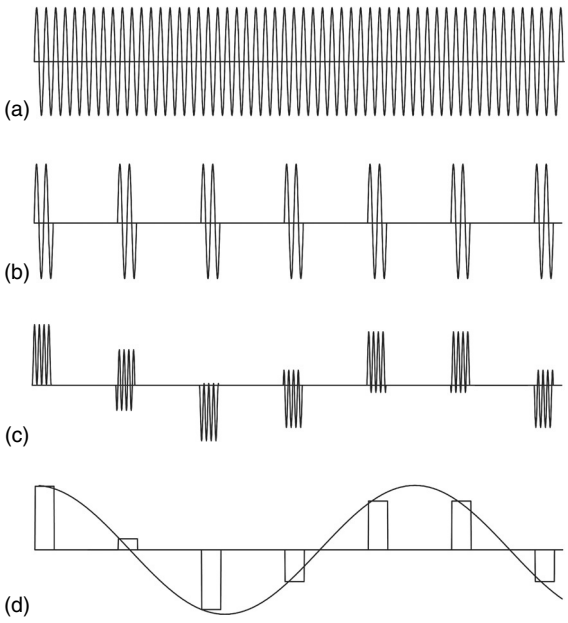

Fig. 7.12 Doppler demodulation for PW Doppler. (a) Reference signal of frequency f_t. (b) The received ultrasound signal consists of consecutive echoes which have passed through the electronic gate. (c) The reference signal is multiplied by the detected signal. (d) The high-frequency oscillations are removed by low-pass filtering. The end result is the Doppler frequency shift signal f_d (the example shown contains no clutter).

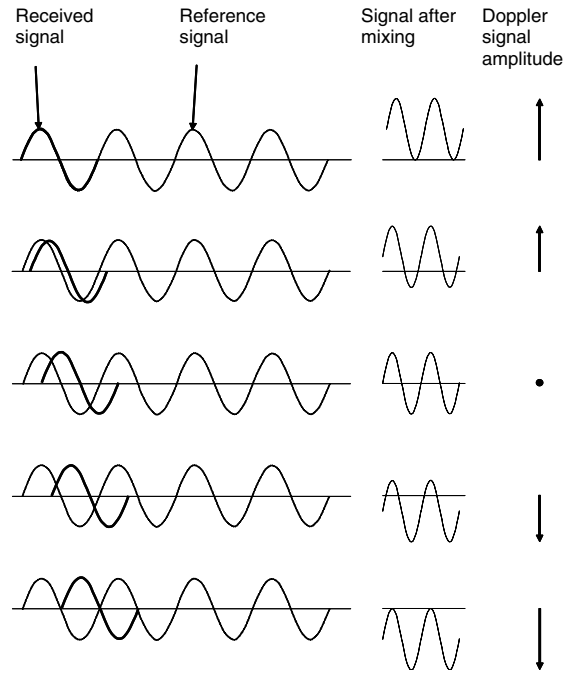

Fig. 7.13 PW Doppler is a 'phase-domain process'. The received ultrasound signal is shown in comparison to the reference signal for five consecutive ultrasound pulses. Also shown are the signal after the reference and received signal have been multiplied, and the final detected Doppler signal after low-pass filtering. The first ultrasound signal is in phase with the reference signal and the detected Doppler amplitude achieves its peak positive value. For consecutive echoes the received and reference signals become misaligned until, in the 5th pulse of this example, they are 'out of phase' and the detected Doppler amplitude reaches its peak negative value.

reason that the displayed Doppler signals from CW and PW Doppler appear to be very similar, often indistinguishable.

This process of Doppler frequency detection is usually referred to by physicists as the 'phase-domain' method; PW Doppler systems which use it are referred to as 'phase-domain systems'. The term 'phase' refers to the degree of correspondence between the received echo and the reference echo in the demodulation process. This can be explained by further consideration of the demodulation process. Figure 7.13 shows the received echoes from consecutive pulses with respect to the reference frequency. Figure 7.13 also shows the amplitude of the signal after the reference and received signals have been multiplied, and the amplitude of the detected Doppler signal. The peak positive amplitude of the detected Doppler signal arises when the reference and received signals are aligned or 'in phase'. As the reference and received frequencies gradually become misaligned the detected Doppler signal amplitude gradually decreases. When the reference and received signals are completely misaligned or 'out of phase' the demodulated amplitude reaches its peak negative value.

For spectral Doppler, estimation of the Doppler shift frequencies for the purpose of display is performed using the same FFT method as used for CW Doppler.

In colour flow imaging, the Doppler frequency estimator must calculate the mean (or average) Doppler shift frequency for each pixel of the 2D image. In order for colour images to be displayed at a suitable frame rate for real-time viewing, typically above 10 frames per second, the estimator must calculate this frequency value very quickly, usually in 1–2 ms. One possibility is to perform FFT, then calculate the mean frequency and colour code this value. This is not used in practice. The preferred

option is to use a device called an 'autocorrelator'. This calculates the mean frequency directly, and is computationally more efficient (and hence faster) than the FFT approach.

Aliasing

The main difference between CW and PW Doppler, in terms of the display of blood velocities, is in the estimation of high velocity. Provided that there are a sufficient number of ultrasound pulses per wavelength it is possible to estimate the Doppler frequency shift accurately from the demodulated PW signal. If the pulse repetition frequency (PRF) is too low, the Doppler frequency shift cannot be estimated properly. This phenomenon is called 'aliasing', and is a feature of pulsed Doppler systems, but not CW Doppler systems. This phenomenon can be explained with reference to Figure 7.14. The true Doppler signal is shown in Figure 7.14a. If the PRF is high (Figure 7.14b) then there are a sufficient number of samples to enable the Doppler system to detect the frequency correctly. As the PRF drops there comes a point at which the Doppler signal is only just sampled sufficiently. This is the case in Figure 7.14c where there are two samples per cycle. This is called the 'Nyquist limit'. This is equivalent to saying that the maximum Doppler frequency shift which can be detected is half of the PRF, i.e. PRF = $2f_{d(max)}$. If the PRF drops further (Figure 7.14d) the Doppler system can no longer calculate the correct frequency.

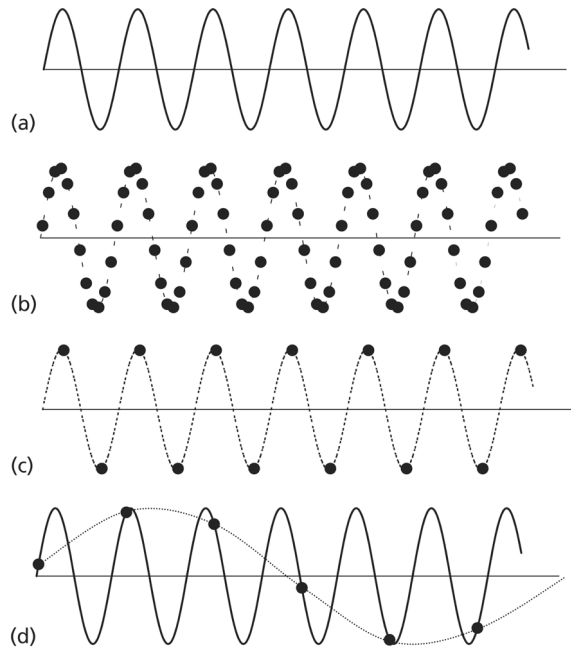

Fig. 7.14 Aliasing. (a) Doppler signal from CW system with a single-frequency f_d. (b) PW Doppler, PRF > $f_d/2$: there are many samples for each cycle of the Doppler signal, and as a consequence the Doppler frequency is correctly detected. (c) PW Doppler; PRF = $f_d/2$: there are two samples per cycle and the Doppler frequency is estimated correctly. (d) PW Doppler, PRF < $f_d/2$: there are fewer than two samples per cycle, and the detected frequency (dashed line) is less than the true Doppler frequency (solid line).

Do PW Doppler systems measure the Doppler effect?

There has been some debate in the literature about whether PW Doppler systems actually use the Doppler effect in their operation, and about whether PW Doppler systems have the right to be called 'Doppler' systems. This is not an issue which impacts upon the clinical use of Doppler systems and these readers may wish to skip the remainder of this section.

The Doppler effect can be considered to be a dilatation or expansion of the ultrasound wave. CW Doppler operates by directly measuring this dilatation or expansion. For a PW Doppler system there will also be dilatation or expansion of each individual echo arising as a result of the Doppler shift. However, PW Doppler systems do not measure this dilatation or expansion, hence strictly speaking are not true Doppler shift detectors. However, the similarity in overall shape of the demodulator output for CW and PW systems is the reason that the equation describing the Doppler shift (Equation (7.1)) may be used for PW Doppler. In quantitative terms, these considerations are unimportant for the clinical use of CW or PW Doppler. The interested reader is referred to Section 4.2.2.5 in the textbook by Evans and McDicken (2000) and Example 4.2 in the textbook by Jensen (1996) for further explanations of this interesting phenomenon.

Time-domain systems

Another method for calculation of the velocity of a moving object such as blood is to divide the distance the object travels by the time taken. This is the

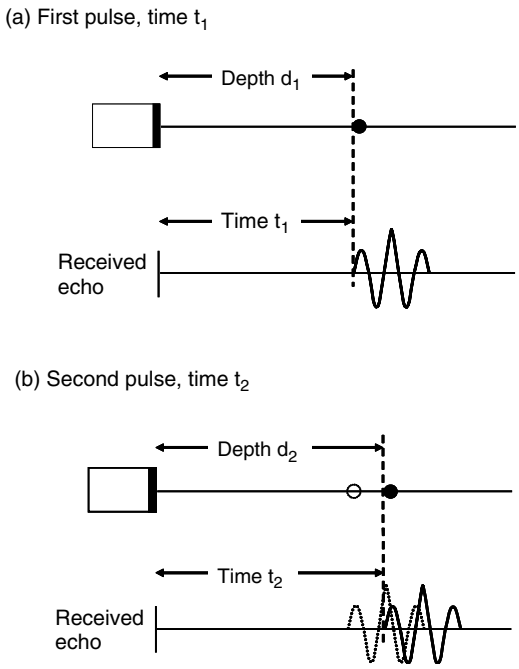

Fig. 7.15 Velocity estimated from time-domain method. A single target moves away from the transducer. The target position and echo are shown for two consecutive pulses: (a) first pulse (time t_1) and (b) second pulse (time t_2). The change in depth is calculated by estimating the depth the target has moved, and dividing this by the time interval between consecutive pulses.

principle used in the time-domain Doppler system, which uses the PW approach. Figure 7.15 shows the position of a moving target and the corresponding echo for two consecutive ultrasound pulses. For the second ultrasound pulse the target and hence the echo are located further from the transducer. The estimation of the target velocity is performed by the following steps.

Estimate distance travelled by target

As described in Chapter 1, estimation of the depth from which echoes are received is performed automatically by the machine from the time between transmission and reception of the echo, assuming that the speed of sound c is 1540 m s^{-1}. For the first and second pulses the depth of the moving target is estimated as

$$d_1 = c\,t_1/2, \qquad d_2 = c\,t_2/2$$

The factor of 2 above is to allow for the total distance travelled by the ultrasound, which is two times the depth of the target. The distance d_m moved between the two consecutive pulses is then estimated from the difference in estimated depths:

$$d_m = d_2 - d_1$$

$$d_m = c(t_2 - t_1)/2 \qquad (7.3)$$

The time-domain system estimates the difference in the time the echo is received between consecutive echoes using a process called 'cross-correlation', which is described in more advanced text books.

Calculate time taken for target to move

The time taken for the target to move is simply the time between consecutive echoes, which is called the 'pulse repetition interval' or PRI. For Figure 7.15 the PRI is the time between transmission of the first and second pulses, which is

$$\text{PRI} = t_2 - t_1 \qquad (7.4)$$

The PRI is equal to the inverse of the PRF:

$$\text{PRI} = 1/\text{PRF}$$

For example, if the PRF is 1000 Hz, the PRI is 1/1000 s, which is 0.001 s or 1 ms.

Calculate velocity of target

The velocity of the target is calculated from the distance travelled and the time taken:

$$v = d_m / \text{PRI} \qquad (7.5)$$

Using Equations (7.3) and (7.4) in combination with (7.5) gives Equation (7.6), in which the blood velocity is expressed in terms of the measured time difference between consecutive echoes:

$$v = (t_2 - t_1)\, c\, \text{PRF}/2 \qquad (7.6)$$

Commercial time-domain Doppler systems

Phase-domain systems use demodulated data, whereas time-domain systems require calculations to be performed on the RF data. The increase in computational power with the use of RF rather than demodulated data makes time-domain systems more

Table 7.2 Common features of Doppler systems

Feature	Description
Aliasing	The highest Doppler frequency shift that can be measured is equal to PRF/2
Angle dependence	Estimated Doppler frequency is dependent on the cosine of the angle between the beam and the direction of motion
Doppler speckle	Variations in the received Doppler signal give rise to a 'speckle' pattern seen in spectral and colour systems
Clutter breakthrough	Tissue motion giving rise to Doppler frequencies above the wall thump or clutter filter may be displayed on spectral Doppler or colour flow systems
Loss of low Doppler	Blood velocities which give rise to low Doppler frequencies (as a result of low frequencies velocity or angle near to 90°) will not be displayed if the value of the Doppler frequency is below the level of the wall thump or clutter filter

expensive than phase-domain systems. This increase in cost has been the main reason for the predominance of phase-domain Doppler systems, though a commercial time-domain system was produced for imaging of blood flow, and some tissue-Doppler systems are based on time-domain processing.

Other features

The basic steps of both spectral Doppler and colour flow systems are similar, as illustrated in Figure 7.8, so there will be a number of similar features. Table 7.2 lists common features which are described in detail in the chapters on spectral and colour systems.

Questions

1. Explain the Doppler effect as used in ultrasound assessment of blood velocities.
2. What are the two main types of display for Doppler ultrasound data?
3. What is the purpose of the high-pass filter in the Doppler signal-processor?
4. Which of these methods for measuring Doppler frequency shift suffers from aliasing: (i) continuous-wave Doppler; (ii) pulsed-wave Doppler?
5. Which of these methods for measuring Doppler frequency shift suffers from angle dependence (i.e. dependence on the direction of the blood velocities): (i) continuous-wave Doppler; (ii) pulsed-wave Doppler?
6. If the sample volume depth is increased, what is the effect on PRF and on the maximum detectable Doppler frequency shift?
7. In a patient examination of, say, the femoral artery, what is the effect of an increase in transducer central frequency from 5 to 10 MHz on the maximum detectable Doppler frequency shift?
8. To estimate blood velocity what two pieces of information must be measured from the patient?

References

Evans DH, McDicken WN (2000). *Doppler Ultrasound: Physics, Instrumentation, and Signal Processing*. Chichester: Wiley.

Jensen JA (1996). *Estimation of Blood Velocities Using Ultrasound*. Cambridge: Cambridge University Press.

Chapter 8

Blood flow

Abigail Thrush

Introduction

The development of colour flow imaging has led to an increase in the investigation of blood flow to aid diagnosis of both vascular and non-vascular disorders. An understanding of the physical properties of blood flow is essential when interpreting colour flow images and Doppler spectra. For example, the presence of reverse flow within a vessel as seen on a colour image may be due to the presence of disease or may be normal flow within the vessel. Changes in the velocity of the blood or the shape of the Doppler spectrum can help in locating and quantifying disease. A poor understanding of how blood flows in normal and diseased vessels may lead to misdiagnosis or to loss of useful clinical information. Blood flow is a complex pulsatile flow of a non-homogeneous fluid in elastic tubes; however, some understanding can be obtained by considering the simple model of steady flow in a rigid tube (Caro *et al.* 1978; Nichols and O'Rourke 1999).

Structure of the vessel walls

The structure of the arterial wall can change due to disease and these changes may be observed using ultrasound. Artery walls consist of a three-layer structure. The inner layer, the intima, is a thin layer of endothelium overlying an elastic membrane. The middle layer, the media, consists of smooth muscle and elastic tissue. The outer layer, the adventitia, is predominantly composed of connective tissue with collagen and elastic tissue. The intima–media layer can be visualized with ultrasound in the carotid arteries and is normally of the order of 0.5–0.9 mm thick, when measured using ultrasound. Arterial disease will lead to changes in the vessel wall thickness that may eventually lead to a reduction of flow or act as a source of emboli. Vein walls have a similar structure to arteries but with a thinner media layer. Blood vessels not only act as a conduit to transport the blood around the body but are complex structures that respond to nervous and chemical stimulation to regulate the flow of blood.

Laminar, disturbed and turbulent flow

The flow in normal arteries at rest is laminar. This means that the blood moves in layers, with one layer sliding over the other. These layers are able to move at different velocities, with the blood cells remaining within their layers. However, if there is a significant increase in velocity, such as in the presence of a stenosis, laminar flow may break down and turbulent flow occurs. In turbulent flow, the blood moves randomly in all directions at variable speeds, but with an overall forward flow velocity. In the presence of turbulence, more energy is needed, i.e. a greater pressure drop is required if the flow rate is to be maintained. Turbulent flow may be seen distal to severe stenosis, as shown in the spectral Doppler waveform in Figure 8.1. This demonstrates an increase in spectral broadening due to the range of velocities present within the turbulent flow and this may be used to indicate the presence of disease. The transition from laminar flow to turbulent flow is displayed diagrammatically in Figure 8.2. The appearance of disturbed flow, such as the presence of vortices (spiral flow or eddies) or areas of flow reversal, do not in themselves indicate the presence of disease

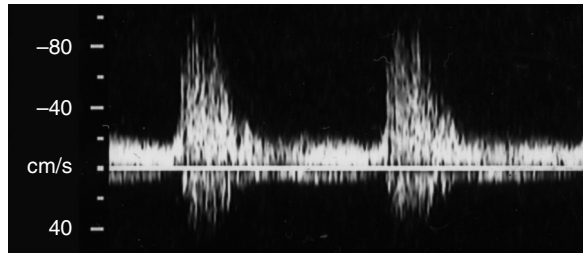

Fig. 8.1 Spectral Doppler display demonstrating turbulent flow.

Diagnostic Ultrasound: Physics and Equipment, ed. Peter Hoskins, Kevin Martin and Abigail Thrush. Published by Cambridge University Press.

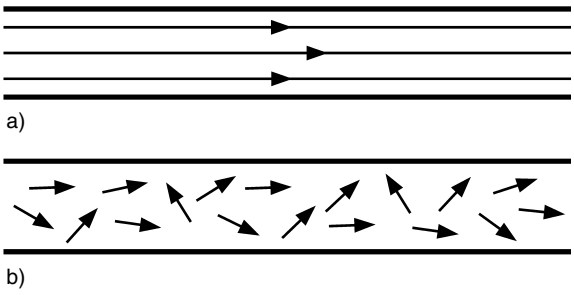

Fig. 8.2 Schematic diagram showing (a) laminar flow and (b) turbulent flow.

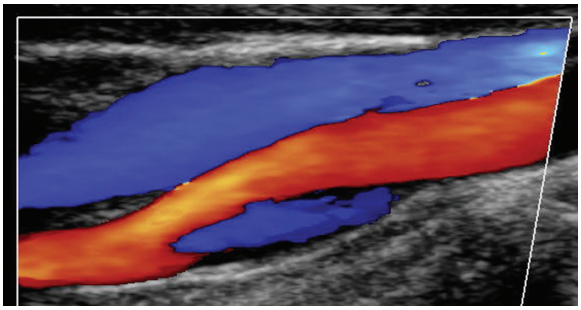

Fig. 8.3 Colour image showing flow reversal (blue in centre of image) in the carotid bulb of a normal internal carotid artery. The vein (blue at top of image) can be seen overlying the carotid artery.

and may be seen in a normal bifurcation as well as beyond a stenosis. For example, flow reversal in the carotid bifurcation (as seen in Figure 8.3 and Figure 8.8) is considered to be a normal finding.

Velocity profiles

The blood within a vessel may not all be moving with the same velocity at any particular point in time. In fact, there is usually a variation in the blood velocity across the vessel, typically with faster flow seen in the centre of the vessel and slowly moving blood near the vessel wall. This variation of blood velocity across the vessel is called the velocity profile. The shape of the velocity profile will affect the appearance of both the colour flow image and the Doppler spectrum.

Considering a simple system of steady (i.e. non-pulsatile) flow of a homogeneous fluid entering a long rigid tube from a reservoir, the flow will develop from a blunt flow profile, with all the fluid moving at the same velocity, to parabolic flow (Caro *et al.* 1978), as shown in Figure 8.4. This change of flow profile occurs due to the viscous drag exerted by the walls, causing the fluid at the wall to remain stationary. This generates a velocity gradient across the diameter of the vessel. The distance over which the flow profile develops from blunt to parabolic flow depends on the diameter of the tube and velocity of the fluid but is usually several times the tube diameter. Similar differences in velocity profile can be seen in different vessels within the body. For example, the flow profile in the ascending aorta is typically blunt but the flow seen in the normal mid-superficial femoral artery tends towards being parabolic. However, the shape of the velocity profile is further complicated by the fact that blood flow is pulsatile. The flow profile across a vessel may be visible on a colour flow image, as shown in Figure 8.5, with the slower moving blood seen near the vessel walls.

Velocity profiles in normal vessels

As the flow in arteries is in fact pulsatile, the velocity profile across an artery varies over time. The direction and velocity of the flow are dependent on the pressure drop along the length of the vessel. The pressure pulse, produced by the heart, travels down the arterial tree and is modified by the pressure wave that has been reflected back from the distal vessels. In the presence of high distal resistance to the flow, such as seen in the normal resting leg, this will lead to a reversal of flow during part of the diastolic phase of the cardiac cycle. This can be seen on the Doppler spectrum shown in Figure 8.6. This reversal of flow will affect the velocity profile seen in the vessel. Figure 8.7a and b shows the predicted velocity profile at different points in the cardiac cycle for a normal common femoral artery and a common carotid artery, respectively (Evans and McDicken 2000). This shows that reverse flow is not seen in a normal common carotid artery but flow reversal, during diastole, is demonstrated in the superficial femoral artery. Figure 8.7a also shows that it is possible for flow in the centre of the vessel to be travelling in a different direction from flow nearer the vessel wall. These changes in flow direction during the cardiac cycle can be observed, using colour flow imaging, as a change from red to blue or blue to red depending on the direction of flow relative to the transducer.

The shape of the velocity profile will also affect the degree of spectral broadening seen on the Doppler spectrum. If a parabolic profile is visualized with a large sample volume, both the low velocities near the vessel wall and the higher velocities in the centre of the vessel will be detected. This leads to a higher degree of spectral broadening in the Doppler spectrum than would be seen for

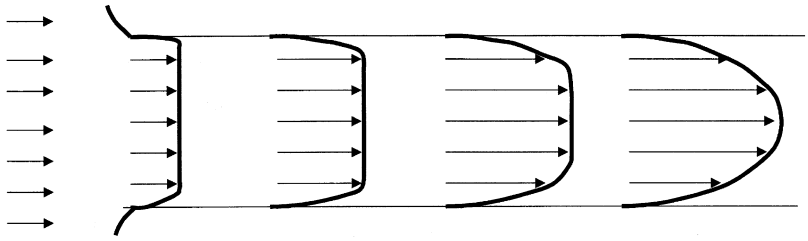

Fig. 8.4 The change in velocity profile, with distance along a rigid tube, from a blunt to a parabolic profile (after Caro *et al.*, 1978, by permission of Oxford University Press).

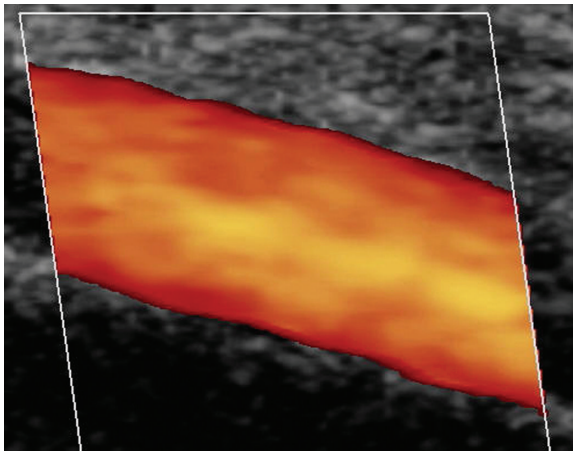

Fig. 8.5 Colour flow image showing high velocities (yellow) in the centre of a normal superficial femoral artery with lower velocities (blue) near the vessel wall.

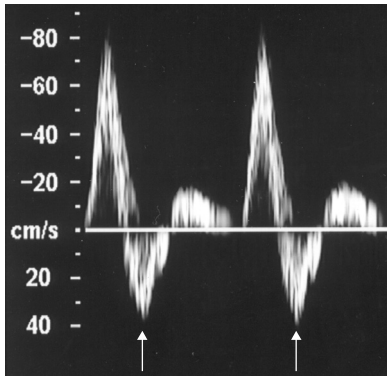

Fig. 8.6 Velocity waveform from a normal superficial femoral artery (arrows indicate reverse flow).

a small sample volume placed in the centre of the vessel (see Chapter 9).

Velocity profiles at branches and curves

The arterial tree branches many times along its length and this branching has an influence on the velocity profile. The velocity profiles found in the normal carotid bifurcation have been extensively studied (Reneman *et al.* 1985) and an example of a velocity profile in a carotid bifurcation is given in the schematic diagram in Figure 8.8. This shows an asymmetric flow profile in the proximal internal carotid artery with the high-velocity flow occurring towards the flow divider and the reverse flow occurring near the wall away from the origin of the external carotid artery. This profile results from pulsatile flow through a vessel of varying dimensions and will depend on the geometry of the bifurcation. An area of flow reversal is commonly seen on colour flow images of the normal carotid bifurcation (Figure 8.3).

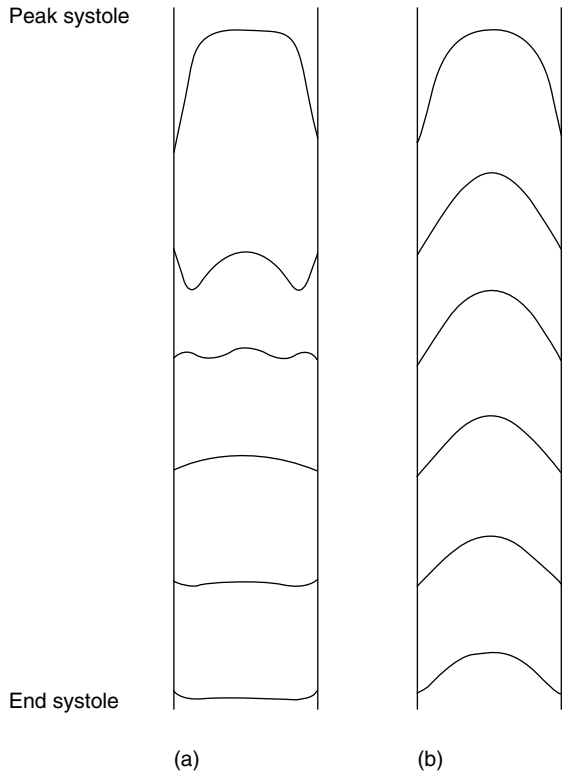

Fig. 8.7 Velocity profiles from (a) a common femoral artery and (b) a common carotid artery, calculated from the mean velocity waveforms (after Evans and McDicken, 2000, with permission of Wiley-Blackwell).

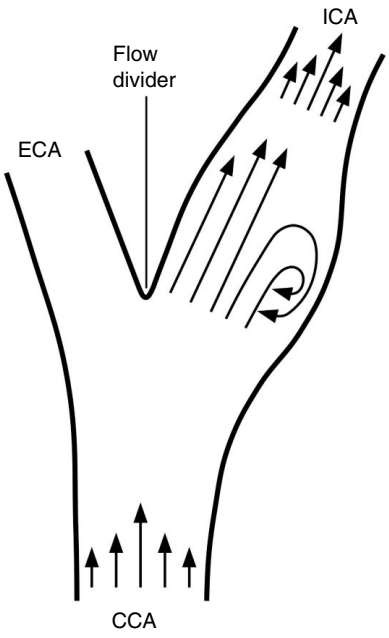

Fig. 8.8 Diagram of an example of velocity patterns observed in the normal carotid bifurcation.

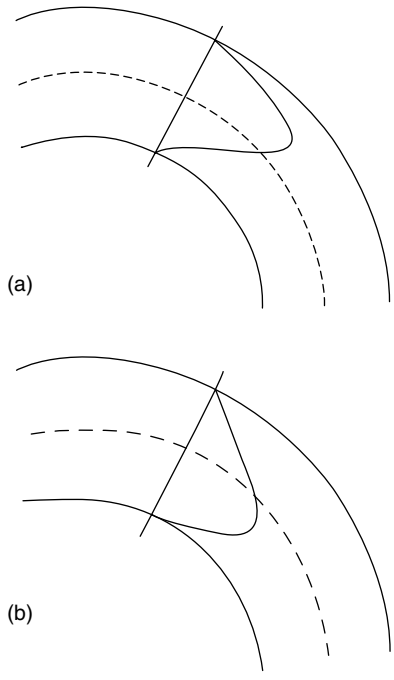

Fig. 8.9 Distortion of (a) parabolic flow and (b) blunt flow due to curvature of the tube (after Caro *et al.*, 1978, by permission of Oxford University Press).

Curvature of a tube will also influence the shape of the velocity profile. The peak velocity within the tube will be skewed off-centre but whether this is to the inner or outer wall of the curve will depend on whether the underlying profile is blunt or parabolic. Figure 8.9 shows the effects of tube curvature on flat and parabolic velocity profiles.

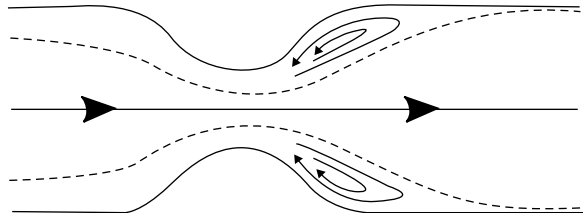

Fig. 8.10 Flow through a constriction followed by a rapid expansion downstream showing the region of flow reversal (from Caro *et al.*, 1978, by permission of Oxford University Press).

Velocity profiles at stenoses

The velocity profile in the vessel can also be altered by the presence of arterial disease. If a vessel becomes narrowed, the velocity of the blood will increase as the blood passes through the stenosed section of the vessel. Beyond the narrowing, the vessel lumen will expand again and this may lead to flow reversal (Caro *et al.* 1978) as shown in Figure 8.10. The combination of the velocity increase within the narrowing and an area of flow reversal beyond is often observed, with colour flow ultrasound, at the site of a significant stenosis (Figure 8.11). It is important to remember that the complex nature of both normal and abnormal blood flow is such that the flow is not necessarily parallel to the vessel walls.

Velocity changes within stenoses

The changes in the velocity of the blood that occur across a narrowing are used in spectral Doppler investigations both to identify the presence of a stenosis and to quantify the degree of narrowing. The relationship between the steady flow, Q, in a rigid tube of cross-sectional area A and the velocity of the fluid, V, is described by

$$Q = V \times A$$

If the tube has no outlets or branches through which fluid can be lost, then the flow along the tube will remain constant. Therefore, the mean velocity at any point along the tube depends on the cross-sectional area of the tube. Figure 8.12 shows a tube of changing

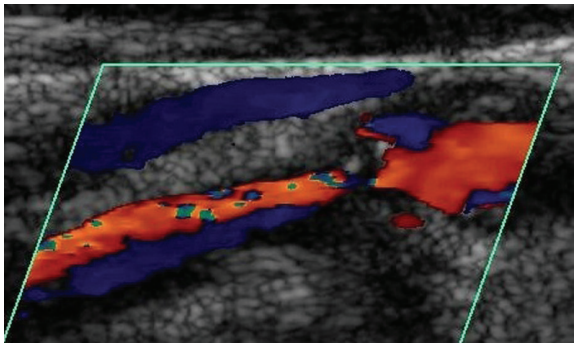

Fig. 8.11 Colour flow image showing the velocity increase as the blood flows through a stenosis, from right to left, with an area of flow reversal (shown as blue) beyond the narrowing. The vein lying over the artery is also seen (blue).

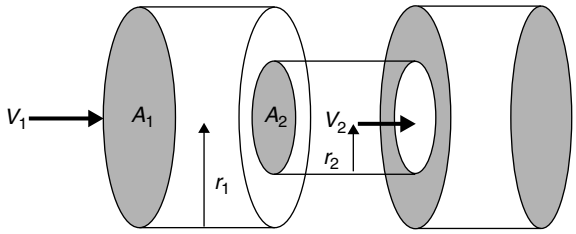

Fig. 8.12 For constant flow, Q, through a tube, the velocity of the fluid increases from V_1 to V_2 as the cross-sectional area decreases from A_1 to A_2 (r is radius).

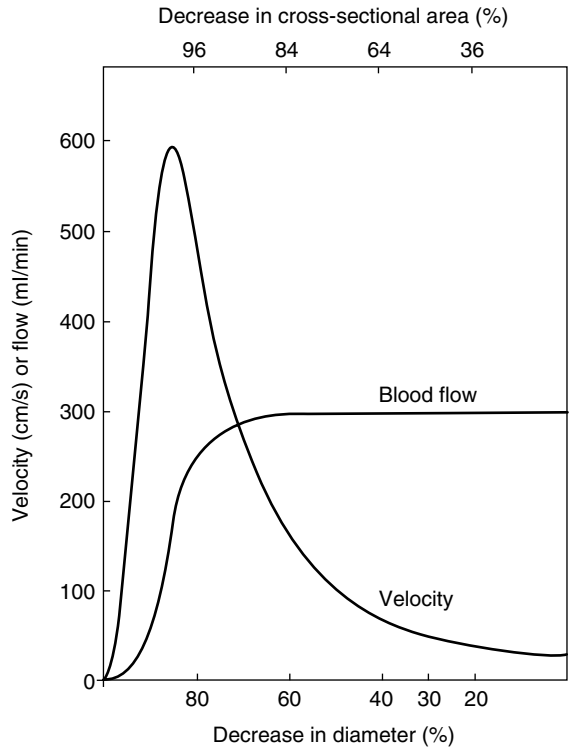

Fig. 8.13 Changes in flow and velocity as the degree of stenosis alters, predicted by a simple theoretical model of a smooth, symmetrical stenosis (after Spencer and Reid, 1979, with permission of LWW Publications).

cross-sectional area (A_1, A_2) and, as the flow (Q) is constant, then:

$$Q = V_1 \times A_1 = V_2 \times A_2$$

This can be rearranged to show that the change in the velocities is related to the change in the cross-sectional area as follows:

$$\frac{V_2}{V_1} = \frac{A_1}{A_2}$$

This relationship actually describes steady flow in a rigid tube and so cannot be directly applied to pulsatile blood flow in elastic arteries. However, it does give an indication as to how the velocity may change across a stenosis.

The graph in Figure 8.13 shows how the flow and velocity within an idealized stenosis varies with the degree of diameter reduction caused by the stenosis, based on the predictions from a simplified theoretical model (Spencer and Reid 1979). This suggests that where the diameter reduction is less than 70–80%, the flow remains relatively unchanged; however, as the diameter reduces further, the stenosis begins to limit the flow (known as a haemodynamically significant stenosis). The graph also shows that the velocity within the stenosis increases with diameter reduction and that these changes in velocity occur at much smaller diameter reductions than required to produce a flow reduction. For this reason, velocity changes are considered to be a more sensitive method of detecting vessel lumen reductions than measurements of flow. Eventually, there comes a point at which the flow drops to such an extent that the velocity begins to decrease and 'trickle flow' is seen within the vessel. The relationships between vessel diameter reductions and velocity described above relate to simple steady-flow models, and the velocity criteria used clinically to quantify the degree of narrowing are produced by comparing Doppler velocity measurements with arteriogram results. Figure 8.14 shows the velocity increase detected at the site of a superficial femoral artery stenosis.

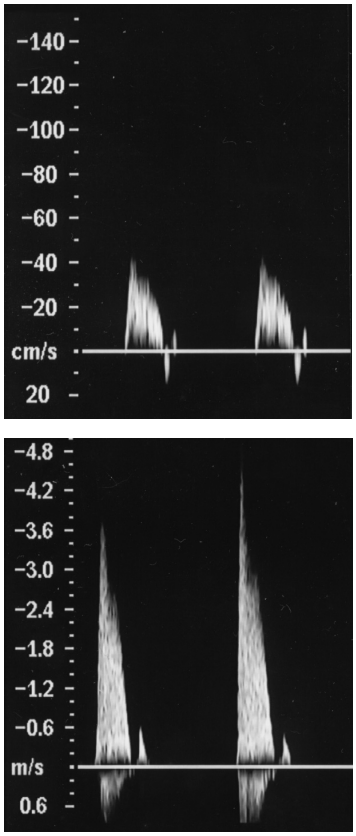

Fig 8.14 Doppler signal obtained (a) proximal to and (b) within a significant stenosis demonstrating a velocity increase from 40 cm s^{-1} to 2.2 m s^{-1}.

Resistance to flow

The concept of resistance is used to describe how much force is needed to drive the blood through a particular vascular bed. Blood flow is due to the pressure drop between different points along the vessel and also depends on the resistance to the flow. This relationship was described by Poiseuille as

$$\text{pressure drop} = \text{flow} \times \text{resistance},$$

where the resistance to flow is given by

$$\text{resistance} = \frac{\text{velocity} \times \text{length} \times 8}{\pi \times \text{radius}^4}$$

Therefore, in the presence of a given pressure drop, increased resistance would result in a reduction in flow. Again this equation describes non-pulsatile flow in a rigid tube and so cannot be directly related to arterial blood flow but indicates that flow not only depends on the pressure drop but is affected by the resistance to flow. It also shows how the resistance is highly dependent on the vessel diameter (r^4 term), with the resistance rapidly increasing as the diameter reduces. In the normal circulation, the greatest proportion of the resistance to flow is thought to occur at the level of the arterioles. The resistance to flow varies from one organ to another. For example, the normal brain, kidney and placenta are low-resistance, compared to muscle at rest. Changes in the resistance to flow may occur during disease, either of the arteries or of the arterioles. For example, abnormal development of the placenta may lead to the placenta being a high-resistance structure, making it difficult for blood to pass through the placenta, with the consequence that the fetus may obtain insufficient nutrition and oxygen and be small for its gestational age. Disease causing narrowing of the arteries, such as the superficial femoral artery, may lead to an increase in resistance to flow through the artery resulting in a reduction in blood flow, causing the patient to experience pain either when walking or at rest.

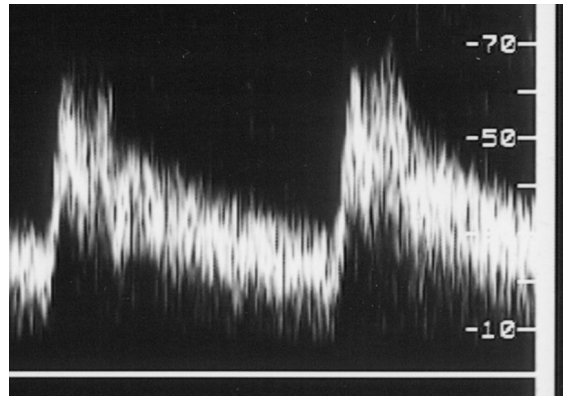

Fig. 8.15 Spectral Doppler obtained from a normal internal carotid artery.

The waveform shape observed at different points in the body is dependent on the outflow resistance of the vessel, i.e. the vascular bed being supplied by the observed vessel. For example, the internal carotid artery supplies the brain, which offers little resistance to flow, and the Doppler waveform has continuous forward flow during diastole, as shown in Figure 8.15. The renal arteries also supply a low-resistance vascular bed and, therefore, a similar waveform shape is observed. However, the peripheral circulation in the normal resting leg offers a higher resistance to flow

and the typical waveform seen in the superficial femoral artery, supplying the leg, demonstrates a high-resistance waveform, with reverse flow seen during diastole (Figure 8.6).

Physiological and pathological changes that affect the arterial flow

Tissue perfusion is regulated by changes in the diameter of arterioles, thus altering peripheral resistance. For example, the increased demand by the leg muscles during exercise will produce a reduction in the peripheral resistance, by dilatation of the arterioles, leading to an increase in blood flow. This also leads to a change in the shape of the waveform, as seen in Figure 8.16a, whereby the flow in diastole is now entirely in the forward direction (compared to Figure 8.6).

The presence of arterial disease can significantly alter the resistance to flow, with the reduction in vessel diameter having a major effect on the change in resistance. The Doppler waveform shape will be affected by an increase in the resistance distal to the site from which the waveform was obtained. This observed change in waveform shape may help indicate the presence of an occlusion distal to the vessel being observed. For example, the waveform in Figure 8.17 shows a Doppler spectrum obtained from a common carotid artery proximal to an internal carotid artery occlusion. This waveform demonstrates a short acceleration time (from the beginning of systole to peak systole) but with an absence of any diastolic flow which is normally seen in the cerebral circulation (Figure 8.15).

Beyond an occlusion the spectrum may also appear abnormal. In the presence of severe disease in the superficial femoral artery, the arterioles may become maximally dilated to reduce the peripheral resistance to maximize the limited blood flow in an attempt to maintain tissue perfusion. A typical spectrum obtained distal to a superficial femoral artery occlusion is shown in Figure 8.16b with the characteristic damped waveform shape with longer systolic acceleration time and increased diastolic flow. The velocity of the flow seen in Figure 8.16b, obtained from a vessel distal to an occlusion, is lower than that seen in Figure 8.16a, which was obtained from a normal vessel with hyperaemic flow due to exercise. The presence of collateral flow, i.e. the blood finding an alternative route to bypass a stenosis

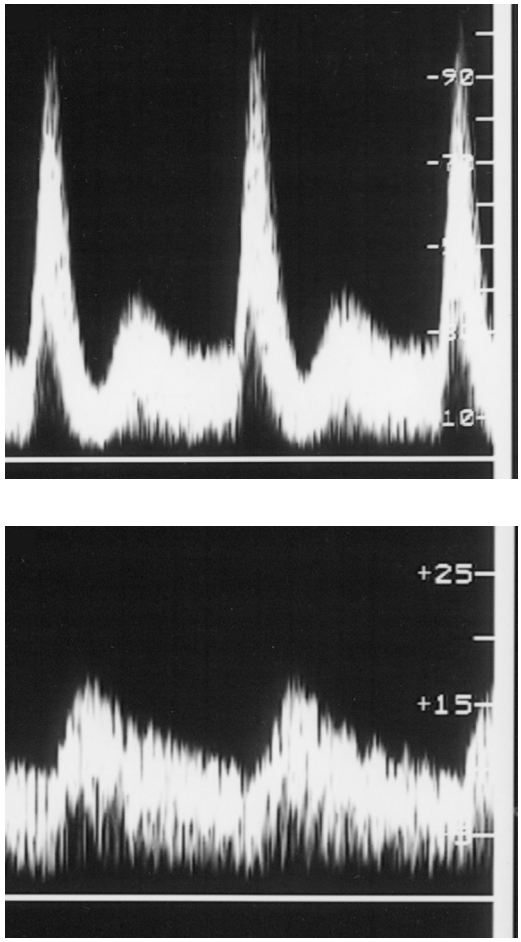

(a)

(b)

Fig. 8.16 (a) Doppler waveform obtained from an artery in the foot, in a normal leg following exercise, demonstrating monophasic hyperaemic flow. (b) Waveform demonstrating low-volume monophasic flow seen in the foot distal to an occlusion of the artery. Higher-velocity flow is seen in the hyperaemic flow in (a) with a peak systolic velocity of 95 cm s^{-1} compared to the low peak systolic velocity of 15 cm s^{-1} seen distal to disease in (b).

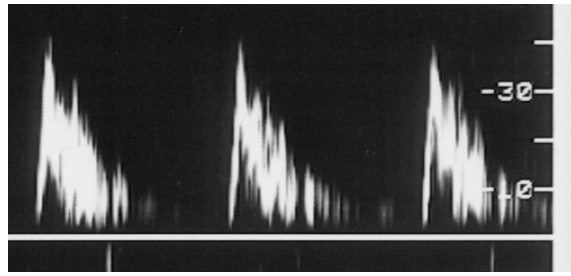

Fig. 8.17 Doppler waveform obtained from a common carotid artery proximal to an occluded internal carotid artery demonstrating a high-resistance waveform.

or occlusion, will also influence the waveform shape both proximal and distal to the disease. Good collateral flow may alter the effect on the waveform shape expected for a given severity of disease, as the collateral pathway may affect the resistance to flow.

Venous flow

Veins transport blood back to the heart. To enable them to perform this function they have thin but strong bicuspid valves to prevent retrograde flow. There are typically a larger number of valves in the more distal veins. Venous flow back to the heart is enhanced by the influence of pressure changes generated by the cardiac cycle, respiration (Figure 8.18) and changes in posture as well as the action of the calf muscle pump. The flow and pressure in the central venous system are affected by changes in the volume of the right atrium which occur during the cardiac cycle. This pulsatile effect can be seen on Doppler spectra obtained from the proximal veins of the arm and neck due to their proximity to the chest. However, flow patterns in the lower limb veins and peripheral arm veins are not significantly affected by the cardiac cycle due to the compliance of the veins, leading to a damping of the pressure changes. The presence of valves and changes in intra-abdominal pressure during respiration also mask the effect of the cardiac cycle on venous flow in the distal veins.

Changes in the volume of the thorax, due to movement of the diaphragm and ribs, also assist venous return. During inspiration, the thorax expands, leading to an increase in the volume of the veins within the chest, resulting in an increase in flow into the chest. During expiration, a decrease in flow is seen. The reverse situation is seen in the abdomen because the diaphragm descends during inspiration, causing the abdominal pressure to increase, encouraging flow into the thorax. When the diaphragm rises, the pressure drops, encouraging flow from the upper leg veins into the abdomen. Respiration effects can be observed on the spectral Doppler display as phasic changes in flow in proximal deep peripheral veins, such as the common femoral vein. Augmentation of flow using breathing manoeuvres is often used in the investigation of venous disorders.

Changes in posture can lead to large changes in hydrostatic pressure in the venous system. When a person is lying supine, there is a relatively small pressure difference between the venous pressure at the ankle and at the right atrium. However, when standing there is a column of blood between the right atrium and veins at the ankle and this produces a significant pressure gradient which has to be overcome in order for blood to be returned to the heart. This can be achieved by the calf muscle pump mechanism assisted by the presence of the venous valves. The muscle compartments in the calf contain the deep veins and venous sinuses that act as blood reservoirs. When the deep muscles of the calf contract, thus causing compression of the veins, blood flow is forced out of the leg and prevented from returning by the venous valves. This also creates a pressure gradient between the superficial and deep veins in the calf causing blood to drain from the superficial to the deep venous system. If there is significant failure of the venous valves in either the superficial or deep venous system, reflux will occur, leading to a less-effective muscle pump and a higher pressure than normal in the veins following calf muscle contraction and relaxation. This may eventually lead to the development of venous ulcers.

Colour flow imaging and spectral Doppler can be used to identify venous incompetence seen as periods of retrograde flow, away from the heart, following compression of the calf (Figure 8.19). Venous outflow

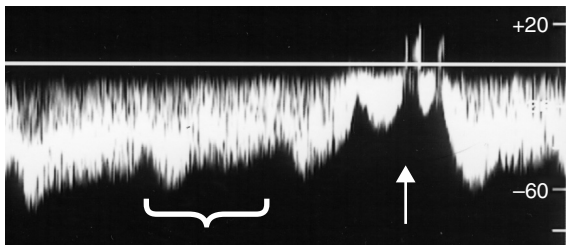

Fig. 8.18 Doppler waveform demonstrating the effect of respiration (indicated by the arrow) and the cardiac cycle (indicated by the bracket) on the blood flow in a subclavian vein.

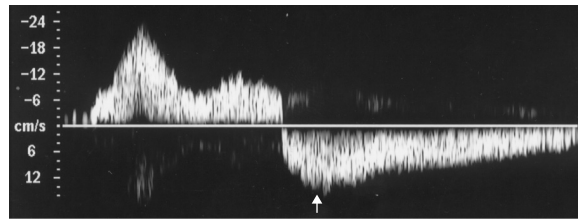

Fig. 8.19 Sonogram demonstrating reversal of flow in the vein, reflux (shown by arrow), due to incompetent valves in the vein.

obstruction leads to a loss of the normal spontaneous phasic flow generated by respiration detected by Doppler ultrasound.

Further reading

Oates C (2001). *Cardiovascular Haemodynamics and Doppler Waveforms Explained*. Cambridge: Greenwich Medical Media.

Questions

1. What is turbulent flow and when does it occur?
2. Describe three situations when reversal of flow may be seen in an artery.
3. If a vessel diameter is reduced, for example at the site of a narrowing, how will this affect the velocity of the blood? Explain why. How can this be used to quantify disease?
4. Describe the factors that affect venous blood flow return to the heart.

References

Caro CG, Pedley TJ, Schroter RC, Seed WA (1978). *The Mechanics of the Circulation*. Oxford: Oxford University Press.

Evans DH, McDicken WN (2000). *Doppler Ultrasound: Physics, Instrumentation, and Signal Processing*. Chichester: Wiley.

Nichols WN, O'Rourke MF (1999). *McDonald's Blood Flow in Arteries*, 2nd edn. London: Edward Arnold.

Reneman RS, van Merode T, Hick P, Hoeks APG (1985). Flow velocity patterns in and distensibility of the carotid artery bulb in subjects of various ages. *Circulation*, **71**, 500–9.

Spencer MP, Reid JM (1979). Quantification of carotid stenosis with continuous-wave (C-W) Doppler ultrasound. *Stroke*, **10**, 326–30.

Taylor KJW, Burns PN, Wells PNT (1995). *Clinical Applications of Doppler Ultrasound*. New York: Raven.

Chapter 9

Spectral Doppler ultrasound

Abigail Thrush

Spectral display

A real-time spectral Doppler display is shown in Figure 9.1 displaying both arterial and venous flow. This displays time along the horizontal axis and the Doppler frequency shift or calculated velocity along the vertical axis. The brightness (or colour) of the display relates to the amplitude of each of the Doppler frequency components present, i.e. the relative proportion of the blood travelling with a particular velocity. The baseline indicated in the centre of the spectral display in Figure 9.1 corresponds to zero Doppler shift or zero velocity. The spectrum contains information about the speed and direction of the blood flow as well as the degree of pulsatility of the flow. Conventionally, it is arranged so that positive Doppler frequency shifts (blood flowing towards the transducer) are plotted above the baseline and negative Doppler shifts (blood flowing away from the probe) are plotted below the baseline, but the operator can invert this display as required. Both arterial and venous flow may be present within the path of the beam and when, as is usually the case, the flow in these vessels is in opposite directions, the Doppler waveforms from the arterial and venous flow appear on opposite sides of the baseline as seen in Figure 9.1. The Doppler ultrasound signal from a blood vessel will contain a range of Doppler frequency shifts. These arise in part from the range of blood velocities present within the region of the vessel being investigated but also arise from a phenomenon called 'intrinsic spectral broadening', which is described later in this chapter.

Doppler ultrasound systems

A spectral Doppler display is produced by performing spectral analysis of the Doppler signal. The Doppler signal can be obtained either from a stand-alone continuous-wave (CW) or pulsed-wave (PW) system or from systems combining Doppler ultrasound with imaging, known as duplex systems. Some of the advantages and disadvantages of these systems are discussed below.

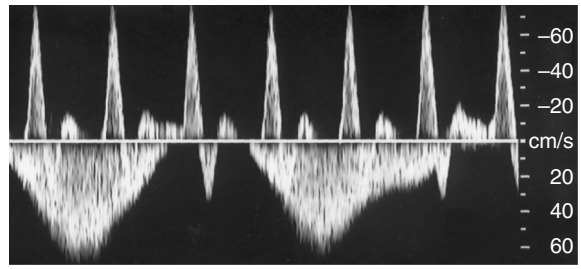

Fig. 9.1 Spectral Doppler display showing arterial flow towards the transducer displayed above the baseline and venous flow away from the transducer displayed below the baseline.

CW Doppler

The CW transducer consists of at least two elements: one to continually transmit and the other to continually receive ultrasound. The frequencies of Doppler signals generated by moving blood are conveniently in the audible range and so can be output to a loudspeaker after amplification and filtering to remove the signal generated by the slow-moving vessel wall. Early Doppler systems had only audio outputs, and this approach is still taken in the simple pocket Doppler devices used in peripheral vascular applications. However, useful information can be provided if spectral analysis of the Doppler signal is performed. The fact that the CW system is continually detecting the blood flow means that CW systems do not suffer from the artefact of aliasing (Figures 7.14 and 9.2). However, the large sensitive region (Figure 7.7) means it is difficult to identify the source of the Doppler signal.

Pulsed-wave Doppler

Pulsed Doppler instrumentation has similarities to CW instrumentation. However, the transducer

Diagnostic Ultrasound: Physics and Equipment, ed. Peter Hoskins, Kevin Martin and Abigail Thrush. Published by Cambridge University Press.

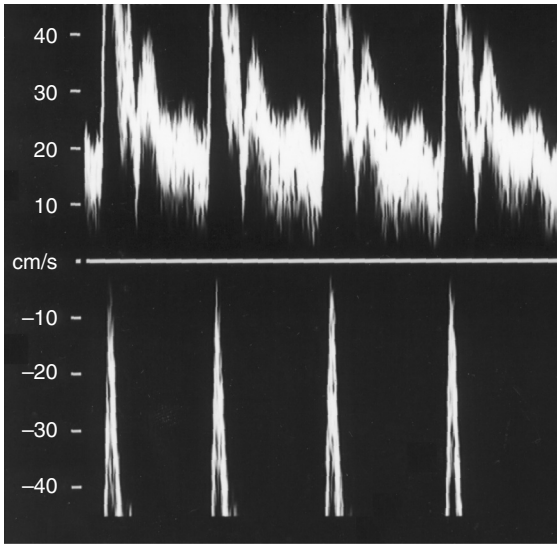

Fig. 9.2 Spectral Doppler display showing aliasing of the signal (seen as wrapping around of the high velocities resulting in their being incorrectly displayed) due to undersampling.

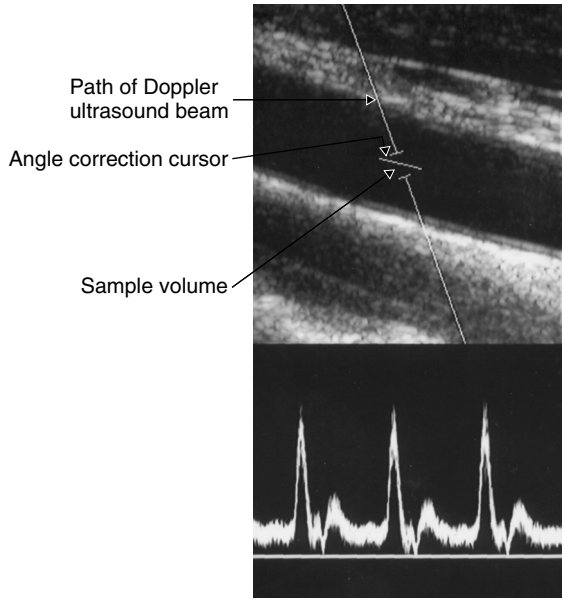

Fig. 9.3 Ultrasound image of a vessel with the path of the spectral Doppler ultrasound beam, sample volume size and angle correction cursor displayed.

is excited with regular short pulses rather than continuously. In order to detect the signal from a specific depth in the tissue, a 'range gate' is used. This enables the system to only receive the returning signal at a given time after the pulse has been transmitted, and then for a limited time. The Doppler signal is, therefore, detected from a specific volume within the body, known as the sample volume, at an identified range (Figure 9.3). The length of time over which the range gate is open is known as the gate length or sample volume length. The operator can control the depth and length of the sample volume, by varying the gate range and length. Thus, PW Doppler has the enormous advantage of allowing the operator to select the origin of the Doppler signal. However, PW Doppler does as a consequence suffer from the artefact of aliasing if the blood flow is undersampled. This can be seen in Figure 9.2 as the high velocities wrapping around the top of the display and shown as flow in the opposite direction (see Chapter 7).

Duplex systems

Initially, both the CW and PW Doppler were used without the aid of imaging and the vessels were located blindly, using only the detected Doppler signal to indicate the presence of the vessel. As imaging ultrasound developed, it become apparent that using Doppler ultrasound in conjunction with imaging, a combination known as duplex ultrasound, would enable better location of the relevant vessel. Duplex Doppler ultrasound enables precise location of the Doppler sample volume, e.g. at the centre of a vessel, as shown in Figure 9.3. It is also possible to estimate the angle of insonation, between the beam and the vessel, using the angle correction cursor, enabling the velocity of the blood to be calculated, using the Doppler equation.

Duplex scanners use arrays of piezoelectric elements to produce, independently, the B-mode imaging, colour flow and spectral Doppler beam, as described in Chapter 3. These multi-element transducers, capable of colour flow imaging and spectral Doppler measurements, include curvilinear-, linear- and phased-array transducers. When combining B-mode imaging with Doppler ultrasound, there is a conflict in the optimal angle of insonation. Ideally, the vessel walls should be imaged with a beam that is at right angles to the vessel whereas the optimal Doppler measurements are made when the beam is parallel to the vessel. Therefore, a compromise has to be reached. Linear-array transducers are able to steer the beam, using beam-forming techniques (described later), by approximately 20° to 30° to the left or right of the path perpendicular to the transducer face. This allows the Doppler beam to be set at an angle to the imaging beam enabling both the imaging and the

Doppler recordings to be made in a vessel that runs parallel to the skin, such as vessels in the limbs and neck. Curvilinear- and phased-array transducers do not usually have the facility to steer the Doppler beam relative to the imaging beam so a suitable compromise for B-mode imaging and Doppler recordings has to be obtained by angling the transducer. Tilting the transducer enables a suitable angle of insonation to be obtained.

Spectral analysis

The Doppler signal obtained from the blood flow can be analysed to find the frequency components in the Doppler signal using a mathematical process known as the Fourier transform. The range of frequency components relates to the range of velocities present within the blood flow. Figure 9.4 shows how the sonogram is produced by displaying consecutive spectra, with frequency displayed along the vertical axis and time along the horizontal axis. A complete spectrum is produced every 5–40 ms and each of these spectra is used to produce the next line in the sonogram. The brightness of the display at each point relates to the relative amplitude of each of the component frequencies, which in turn is an indication of the backscattered power for each value of Doppler frequency shift. If the angle of insonation is measured, using the angle-correction cursor, the vertical frequency scale can be converted to a velocity scale.

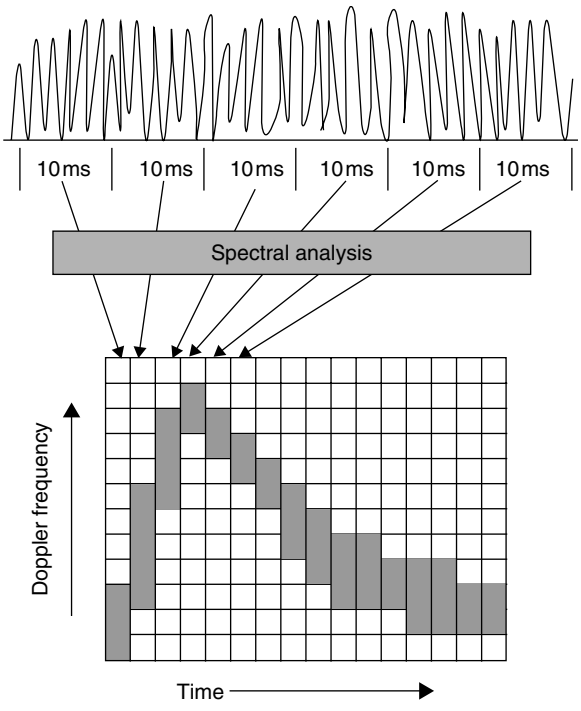

Fig. 9.4 Schematic diagram showing how consecutive spectra produced by the spectrum analysis of the Doppler signal are used to construct the spectral Doppler display.

Spectral Doppler controls and how they should be optimized

Gain

The ultrasound backscattered from blood is of much lower amplitude than the signals returning from the surrounding tissue. As the received backscattered signal from blood is small it will need to be amplified before it can be analysed. Increasing the spectral Doppler gain increases the brightness of the spectrum on the screen. However, the gain control increases the amplitude of not only the Doppler signal but also the background electronic noise. If the Doppler signal is of similar amplitude to the background noise, then no matter how much the gain is increased, only a poor Doppler sonogram will be obtained, as shown in Figure 9.5a. In these situations, it may be necessary to use a lower transmit frequency (resulting in less attenuation of the ultrasound pulse) or a higher transmit power. If the gain is set too high, the Doppler system may become overloaded and may no longer be able to separate the forward and reverse flow accurately. This gives rise to an artefact whereby a mirror image of the true Doppler spectra appears in the reverse channel of the sonogram, as shown in Figure 9.5b. This is not true reverse flow but an artefact that can be eliminated by turning down the Doppler gain. Altering the Doppler gain may also affect the peak velocity detected. Figure 9.5c shows the Doppler sonogram obtained from a flow rig where the gain has been increased over the time of the recording. On the left side where low gain has been used, the measured peak velocity is 128 cm s^{-1}, in the centre it measures 140 cm s^{-1} and on the right, where the gain has been set too high, the peak velocity measures 147 cm s^{-1}. On the far right of the image, where the gain is set too high the Doppler signal appears as saturated white and noise can be seen. Figure 9.5d shows the same effect on a Doppler recoding from a carotid artery with the gain increasing from left to right and the subsequent increase in measured velocity can be seen. The correct gain setting has been achieved in the centre of the displayed signal.

Transmit power

Increasing the output power will increase the amplitude of the transmitted ultrasound, resulting in a higher-

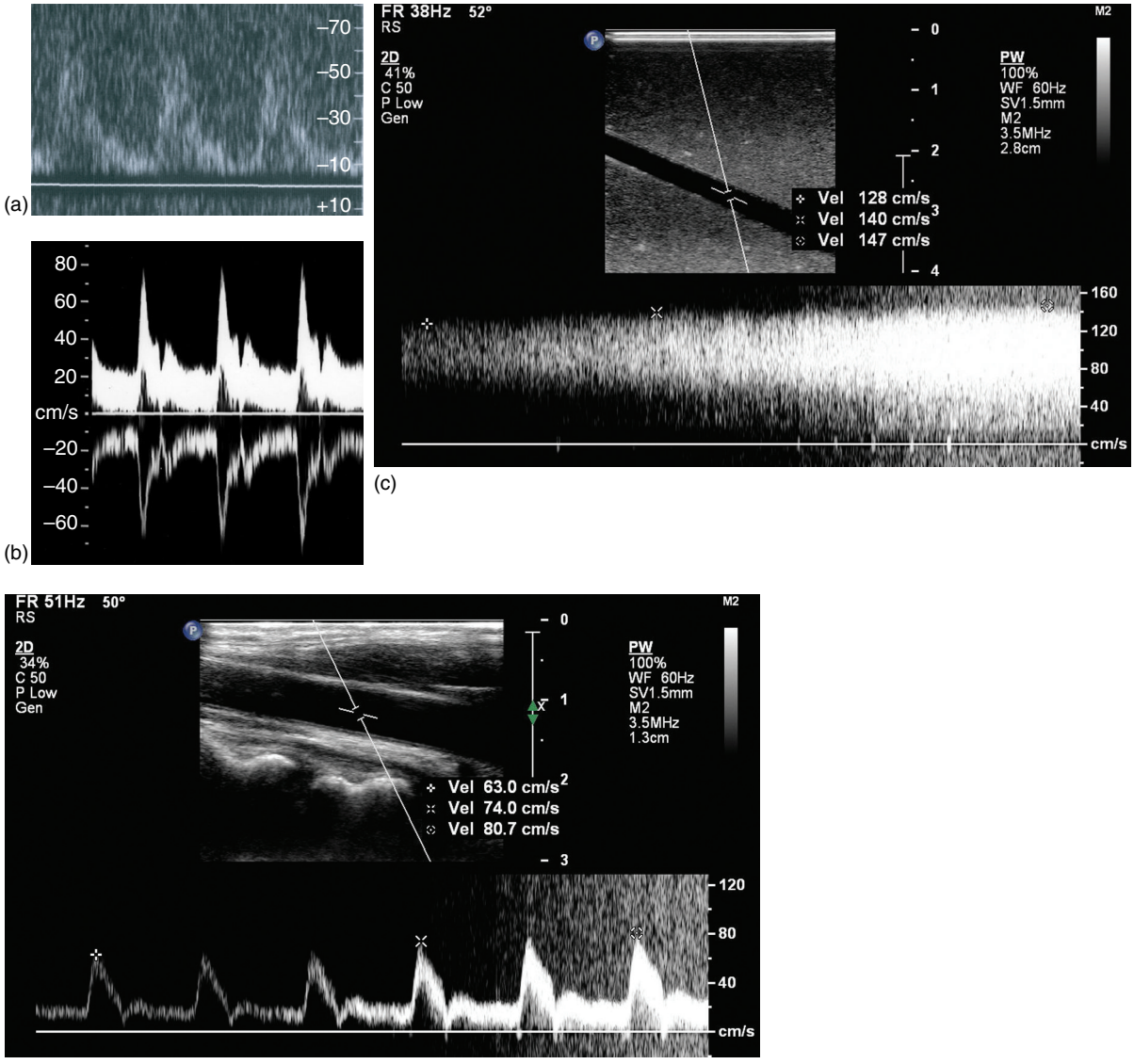

Fig. 9.5 (a) Doppler spectral displayed showing that when the amplitude of the Doppler signal and the background noise are similar, increasing the gain does not help to improve the display. (b) Spectral Doppler display where the gain has been set to high, causing signal to breakthrough on the reverse channel. (c) Spectral Doppler display obtained from a flow rig where the gain has been increased over the time of the recording and the effect this has on the measured peak velocity; (d) shows the same effect on a Doppler recording from a carotid artery with the gain increasing from left to right and the subsequent increase in measured velocity can be seen. The correct gain setting has been achieved in the centre of the displayed signal.

amplitude signal returning to the transducer. The output power of the transducer is altered by the scanner's transmit power control. On some ultrasound systems, the same control may be used to change the output power of all the three modalities: B-mode imaging, spectral Doppler and colour flow imaging. However, increasing the output power will also increase the patient's exposure to ultrasound. Therefore, the transmit power should only be increased after other controls, such as the gain, have been optimized to obtain the best Doppler spectrum. Changes in the output power should be reflected by changes in the displayed mechanical index (MI) and thermal index (TI) (see Chapter 13) displayed on the ultrasound image.

Transmit frequency

As high-frequency ultrasound is attenuated more than low-frequency ultrasound (see Chapter 2), the appropriate Doppler transmit frequency needs to be selected to ensure adequate penetration of the ultrasound. The frequency required will, therefore, depend on the depth of the vessel to be investigated. The Doppler transmit frequency is governed by the transducer that has been selected. Typically ultrasound systems use broadband transducer technology, which means it is possible to operate the transducer over a range of different frequencies without too much loss in efficiency. Therefore, for example, a transducer may use a centre frequency of 5 MHz for B-mode imaging but use a lower frequency of 4 MHz for the Doppler measurements to ensure adequate returning backscattered signal from the blood. If the backscattered ultrasound signal from the blood is weak, it may be possible to improve the penetration of the beam by lowering the transmit frequency by 1 or 2 MHz. If this still does not provide sufficient penetration, it may be necessary to select a transducer that operates at a lower frequency range to enable adequate penetration.

Pulse repetition frequency (scale)

With pulsed Doppler ultrasound, the rate at which the pulses of ultrasound are transmitted is known as the pulse repetition frequency (PRF) and this can be controlled by the operator. On some scanners the PRF control is called the scale and not all scanners display the actual values of the PRF used to produce the Doppler spectrum. The PRF can typically be set between 1.5 and 18 kHz, depending on the velocity of the blood that is to be detected. Most ultrasound scanners have application-specific pre-sets that, if selected, will set the controls, such as the PRF, to a suitable starting value. However, these values may need to be altered during the scan to obtain an optimal spectral display. If the PRF is set too low, aliasing will occur. This gives the appearance shown in Figure 9.2, where the high frequencies present are incorrectly displayed in the reverse channel. The PRF needs to be at least twice the maximum Doppler frequency required to be detected to prevent aliasing, i.e. $\text{PRF} = 2f_{\text{d(max)}}$ (see Chapter 7). This can be overcome by increasing the PRF. However, there will be an upper limit to the PRF that can be used, as the scanner will usually only allow one pulse to be 'in-flight' at a time in order to prevent confusion as to where a returning signal has originated from. If PRF_{max} is the upper limit of the PRF, the maximum velocity, v_{max}, which can be measured will be given by the equation below (also see the Doppler Equation (7.1))

$$\frac{\text{PRF}_{\text{max}}}{2} = \frac{2v_{\text{max}} f_t \cos\theta}{c}$$

This can be re-written as

$$v_{\text{max}} = \frac{\text{PRF}_{\text{max}} c}{4 f_t \cos\theta}$$

For a depth of interest, d, and speed of sound, c,

$$\text{PRF}_{\text{max}} = \frac{c}{2d}$$

The 2, in the equation above, arises from the fact that the pulse has to go to and return from the target. This gives the maximum detectable velocity, v_{max},

$$v_{\text{max}} = \frac{c^2}{8df_t \cos\theta}$$

This shows that the maximum detectable velocity, without aliasing occurring, will be lower when making measurements at depth, or when the angle of insonation is small, giving a $\cos\theta$ term approaching 1. It may be possible to overcome aliasing, once this maximum PRF is reached, by lowering the transmit frequency used or using a larger angle of insonation, giving a smaller $\cos\theta$ term.

When measuring very high blood flow velocities, especially at depth, e.g. in an iliac stenosis in a large abdomen, some scanners will allow a 'high PRF' mode to be selected. This allows more than one pulse to be 'in-flight' at a given time. The higher PRF allows higher velocities to be measured, but also introduces range ambiguity, i.e. a loss of certainty as to the origin of the Doppler signal.

If too high a PRF is used to detect slower-moving blood, the scale of the spectral display will not be fully utilized and the ability to identify changes in the Doppler frequency will be reduced. It is, therefore, important to set the PRF such that the Doppler waveform almost fills the display, without any wrap-around due to aliasing occurring.

Baseline

The baseline represents zero Doppler shift, i.e. zero velocity and, therefore, demarcates the part of the

display used for displaying forward flow (towards the transducer) from that used for reverse flow (away from the transducer). The position of the baseline can be changed by the operator to allow optimum use of all the spectral display, depending on the relative size of the forward and reverse flow velocities present. For example, the position of the baseline may be lowered to prevent aliasing of a positive Doppler shift signal.

Invert

The invert control enables the operator to turn the Doppler display upside down, so that flow away from the transducer is displayed above the baseline and flow towards the transducer is displayed below. This can be indicated by showing negative velocity values above the baseline. Typically, operators prefer to display arterial flow above the baseline.

Filter

The Doppler signal will contain not only the low-amplitude higher Doppler frequencies backscattered from the blood but also high-amplitude lower Doppler frequencies from the slow-moving tissue such as the vessel walls. These unwanted frequencies can be removed by a high-pass filter. As the name suggests, a high-pass filter removes the low-frequency signals while maintaining the high frequencies. There is, however, a compromise in the selection of the cut-off frequency to be used, as it is important not to remove the frequencies detected from the lower-velocity arterial or venous blood flow. Figure 9.6 shows the high-pass filter set at three different levels. The first (a) shows that the filter is set too low and the wall thump, generated by the slow-moving vessel wall, has not been removed. In the second situation (b), the filter has been correctly set to remove the wall thump and in the third situation (c) the filter has been set too high and the diastolic flow has been removed, giving a false impression of the waveform shape, which could lead to a misdiagnosis.

Gate size and position

The size and position of the 'range gate' or 'sample volume' are selected by the operator and can typically be varied between 0.5 and 20 mm in length. The 'gate size' or 'sample volume length' may affect the appearance of the Doppler spectrum, as described below. It is important that care is taken to select the appropriate sample volume length, depending on whether the operator wishes to detect the velocities in the centre of the vessel only or velocities present across the whole vessel.

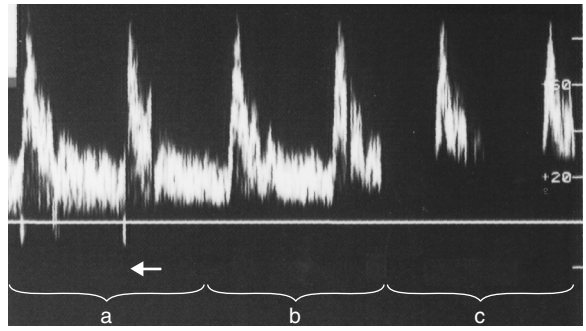

Fig. 9.6 Doppler spectral display showing how the appearance changes with different high-pass filters. (a) The filter is set too low, allowing wall thump (shown by arrow) to be displayed. (b) The filter is set correctly and the wall thump has been removed. (c) The filter is set too high, removing the low velocities including diastolic flow component.

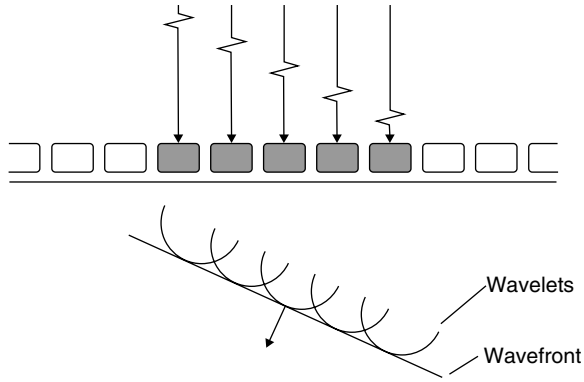

Fig. 9.7 The Doppler beam produced by linear array transducers may be steered by introducing delays between the pulses used to excite consecutive active elements in the array.

Beam-steering angle

The angle of insonation can be altered by changing the orientation of the transducer in relation to the vessel, e.g. by tilting the transducer. Linear-array transducers also have the facility to steer the Doppler beam 20° to the left or right of the centre. The ultrasound beam is electronically steered by introducing delays between the pulses used to excite consecutive active elements. This is similar to the method used to focus the beam, described in Chapter 3, but uses a different sequence of delays. Figure 9.7 shows how the delay

between excitation pulses results in the wavelets produced by each element interfering in such a way that a wave front is no longer parallel to the front of the transducer. The path of the beam can be steered left or right of the centre depending on the delays introduced. Steering the beam in this way is necessary when using a linear-array transducer to detect flow in a vessel that is parallel to the front face of the transducer. This enables a Doppler angle of insonation of 60° or less to be used while the imaging beam remains nearly perpendicular to the vessel wall, optimal for B-mode imaging. However, a steered Doppler beam has a lower sensitivity than a beam that is perpendicular to the transducer face, which may result in a noisy or undetectable Doppler signal and therefore require increased gain. The angle of insonation of the Doppler beam should be optimized to 60° or less to enable a good Doppler signal to be acquired and to minimize errors in velocity measurements (discussed later in the chapter).

Doppler angle cursor

In order to calculate the velocity of blood from the measured Doppler shift frequencies, the angle of insonation between the Doppler beam and the direction of flow must be known. Duplex scanners have the facility to allow the operator to line up an angle cursor with either the vessel wall, as seen on the B-mode image, or the direction of flow, as seen on the colour flow image. Knowing the angle of insonation, the scanner can then convert the Doppler shift frequencies to velocities and a velocity scale will be seen alongside the spectral display. Errors in the alignment of the angle-correction cursor can lead to significant errors in velocity measurement (discussed later in the chapter).

Focal depth

In many systems the Doppler beam is focused and, depending on the ultrasound system, this focus may be fixed or adjustable. In some systems the Doppler beam focal depth automatically follows the sample volume, when the operator moves it.

Greyscale curve

The greyscale curve governs the relative display brightness assigned to the different amplitude signals detected. The relative amplitude signal detected at each frequency relates to the relative proportion of red blood cells moving at each given velocity. The Doppler spectra may be displayed using different greyscale curves or even colour scales.

Factors that affect the spectral Doppler display

Both the shape of the Doppler waveform and the velocity measurements made from it are used to diagnose the disease. However, the spectra may also be affected by factors other than disease (Thrush and Hartshorne 2010). It is important for the operator to understand these effects in order to be able to correctly interpret the Spectral Doppler display, and these factors are discussed below.

Blood flow profile

The velocity profile across a vessel, at a given point of time, may be either blunt, parabolic or part way in between (see Chapter 8). If the width of the Doppler beam and sample volume length are such that it covers the entire vessel, i.e. completely insonates the vessel cross section, then signals from flow across the full width of the vessel will be detected. With a blunt flow profile, all the blood is travelling at a similar velocity, therefore the velocity spectrum would display a narrow spread of velocities as shown in Figure 9.8a. However, the spectral Doppler display for complete insonation of parabolic flow would demonstrate the wider range of velocities present in the vessel as seen in Figure 9.8b.

Non-uniform insonation

Multi-element array transducers typically produce very narrow beams. When an array probe is aligned along the length of a section of vessel, it is the beam width in the elevation plane that is important. If a beam is narrow in this dimension, then the beam will not insonate the entire vessel and so the slower-moving blood on the lateral walls of the vessel will not be detected (as shown in Figure 9.9a). Therefore, the spectrum will no longer represent the true relative proportions of blood moving at the slower velocity in the presence of parabolic or near-parabolic flow.

Sample volume size

The sample volume size and position will also affect the proportion of the blood velocities within the vessel that will be detected. A large sample volume will enable the flow near the anterior and posterior walls to be detected, but, as discussed above, the narrow beam width in elevation may mean that the flow

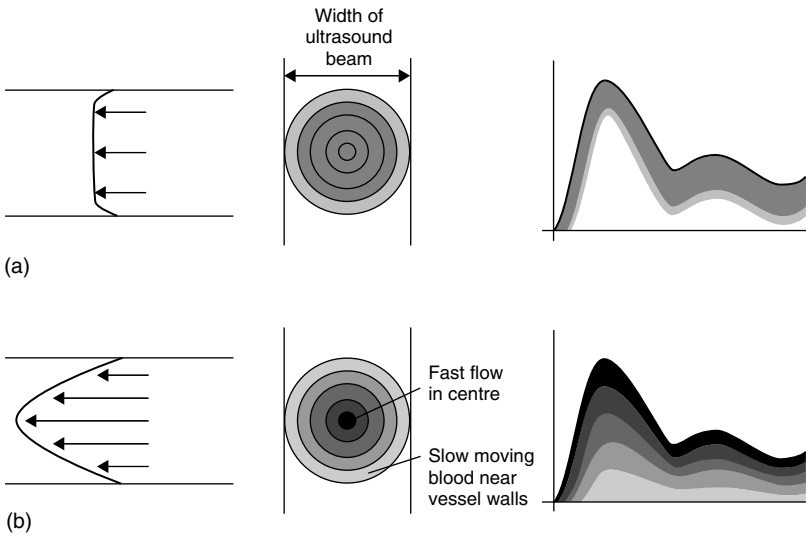

Fig. 9.8 A schematic diagram showing how the velocities displayed in the Doppler spectrum will depend on the velocity profile within the vessel shown for idealized (a) blunt flow and (b) parabolic flow

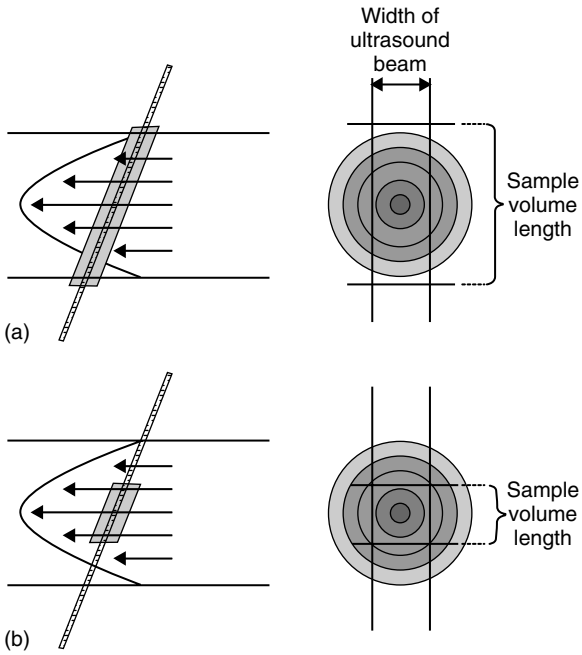

Fig. 9.9 Effect of (a) incomplete insonation and (b) sample volume size on the detected Doppler signal.

near the lateral walls will remain undetected. If only the fast flow in the centre of the vessel is to be measured, then a small sample volume should be selected (Figure 9.9b). It is also important to use a small sample volume when assessing the degree of spectral broadening, i.e. the width of the Doppler spectrum, as an indication of the presence of disturbed flow within a diseased vessel.

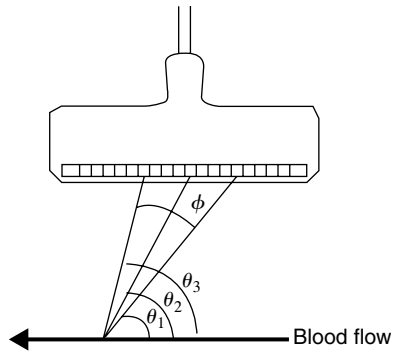

Fig. 9.10 A number of elements of a linear-array transducer are used to produce the Doppler beam, leading to a range of angles of insonation (θ).

Intrinsic spectral broadening

The Doppler beam is produced by a sub-group of elements within the array (as shown in Figure 9.10), producing a Doppler aperture. This means that, in reality, the Doppler beam insonates the blood at a range of different angles due to the shape of the beam. Array transducers use a number of elements to form the Doppler beam and different elements will produce different angles of insonation. For example, in the diagram shown in Figure 9.10, the element on the far right of the sub-group will produce a smaller angle of insonation (θ_1) and will, therefore, detect a larger Doppler shift frequency than the element on the far left of the sub-group. This will lead to a spreading of the range of Doppler shift frequencies detected that is due to the beam shape rather than

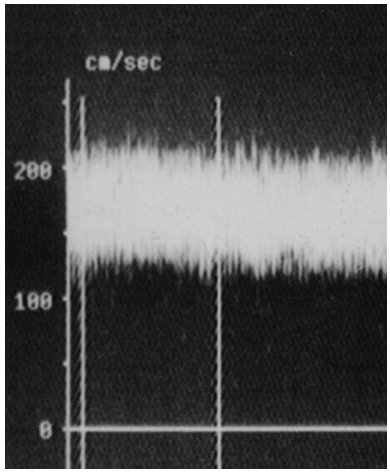

Fig. 9.11 Doppler spectrum obtained from a moving string test object showing a range of velocities despite the fact that the string can only move with a single velocity.

the blood flow. This effect is known as intrinsic spectral broadening (Hoskins 1996, Hoskins *et al.* 1999, Thrush and Evans 1995). It can be demonstrated by making ultrasound velocity measurements from a single moving target, such as a string driven by a motor at constant speed. The Doppler spectra produced using a 5 MHz linear-array transducer insonating moving string is shown in Figure 9.11. This demonstrates that, instead of the Doppler spectra displaying a single velocity for the moving string, a spread of velocities is displayed. As the string (unlike blood) is moving at a single velocity, the spreading of the detected velocities seen in the spectra is due to intrinsic spectral broadening, i.e. due to the ultrasound system rather than the motion being detected. The degree of spectral broadening will depend on the angle of insonation used, with larger angles of insonation generating a larger degree of intrinsic spectral broadening, Figure 9.12 shows the spread of Doppler frequencies obtained, using an Acuson scanner with a 7 MHz transducer and the sample volume set at 2–3 cm depth, from a moving string test object over a range of beam-to-string angles of insonation. It can be seen that the degree of spectral broadening increases as the angle of insonation increases toward 90°. This spectral broadening effect can lead to errors when making velocity measurements, or estimating the range of velocities present due to disturbed or turbulent flow in the presence of arterial disease.

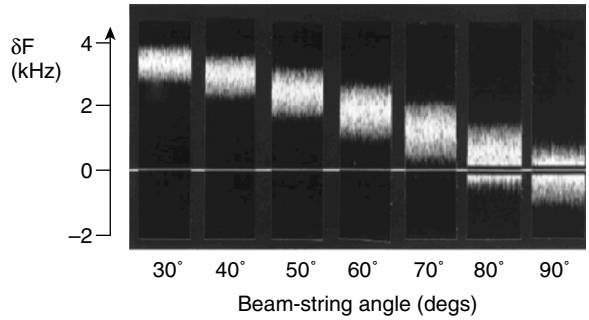

Fig. 9.12 The Doppler shift frequency δF (kHz) detected from a moving string test object with constant velocity using an Acuson system over a range of angles of insonation. (Reprinted from Hoskins *et al.*, 1999, with permission.)

Equipment set-up

If an inappropriately low PRF is used, this will result in aliasing of the signal. This will alter the appearance of the waveform shape (Figure 9.2) and lead to an underestimate of the peak velocity.

The high-pass filter is used to remove unwanted low-frequency signals arising from the slow-moving vessel walls. However, if the filter is set too high the waveform shape may be significantly altered (see Figure 9.6), e.g. the filter may remove the low frequencies detected during diastole. If the gain is set too high, a mirror image of the spectrum will be seen (see Figure 9.5b). If the gain is set too low, all the detected velocities may not be adequately displayed.

Effect of pathology on the spectral Doppler display

Changes in detected Doppler frequency shift

The velocity of blood increases as blood passes through a narrowing (as described in Chapter 8) and velocity measurements or velocity ratios are often used to quantify the degree of narrowing of a vessel. Velocity ratios compare the velocity in the normal vessel proximal to a stenosis with the highest velocity at or just beyond the stenosis. A significant stenosis or occlusion may lead to a reduction in flow and this will be indicated by the presence of untypically low velocities proximal or distal to the site of disease.

Changes in spectral broadening

The presence of disturbed or turbulent flow can lead to an increase in spectral broadening which may be used as an indicator of disease. However, spectral broadening should be interpreted cautiously as intrinsic spectral broadening can be introduced due to properties of the ultrasound scanner.

Changes in waveform shape

The shape of the Doppler spectrum will depend on which vessel is investigated. For example, the waveform shape detected in the internal carotid artery (Figure 8.15), which supplies blood flow to the brain, is very different from the waveform shape detected from the femoral arteries (Figure 8.6), which supply the leg. Significant disease either proximal or distal to the measurement site will also affect the waveform shape and can, therefore, provide a useful indication of the presence and possible site of disease (Chapter 8).

Artefacts

Some of the artefacts that spectral Doppler suffers from are of the same origin as imaging ultrasound artefacts in that the ultrasound beam does not follow the expected path, or that the ultrasound has been attenuated. This leads to the following artefacts:

- *Shadowing:* this is due to highly reflecting or attenuating structures, such as bowel gas or calcified vessel wall, overlying the blood flow, leading to a loss of Doppler signal.
- *Multiple reflections:* in the presence of a strongly reflecting surface, e.g. a bone–tissue or air–tissue interface, multiple reflections may occur, leading to the appearance that Doppler signals have been detected outside the vessel. This will affect both the spectral Doppler and the colour flow. An example of where this is often seen is when imaging the subclavian artery as it passes over the lung, leading to the appearance of a second vessel lying within the lung. This is known as a mirror image.
- *Refraction:* this occurs if an ultrasound beam passes a boundary between two media with different propagation speeds, at an angle of less than 90°. This can lead to misregistration of both the image and the Doppler sample volume.

Other artefacts seen in spectral Doppler relate to production of the Doppler spectrum. These artefacts include the following:

- *Aliasing:* this occurs due to undersampling of the blood flow (see Figure 9.2) and can be corrected by increasing the Doppler PRF.
- *Angle dependence:* the Doppler shift frequencies detected are dependent on the angle of insonation by the cosθ term. The larger the angle of insonation the smaller the Doppler shift frequencies detected, possibly leading to a poorer-quality Doppler spectrum. As the angle of insonation approaches 90°, the Doppler signal may be very small and, therefore, may be removed by the high-pass filter.
- *Intrinsic spectral broadening:* this occurs due to the geometry of the ultrasound beam and the vessel (see Figures 9.10 and 9.11).
- *Range ambiguity:* this occurs when more than one pulse is in-flight at a time, such as when a high PRF is used to investigate high-velocity flow at depth, as the origin of the Doppler signal is no longer certain.
- *Inverted mirror image of the Doppler spectrum:* this can occur if the gain is set too high (see Figure 9.5b).

Measurements and their potential sources of errors

Velocity

Measurements of blood velocities are often used to quantify disease. Duplex imaging allows an estimate of the angle of insonation (θ) between the Doppler ultrasound beam and the blood flow. The velocity of the blood (v) can then be estimated from the measured Doppler shift frequency (f_d), using the Doppler equation, as the transmitted frequency of the Doppler beam (f_t) is known and the speed of sound in tissue (c) is assumed to be constant (1540 m s^{-1}):

$$v = \frac{f_d c}{2 f_t \cos\theta}$$

There is often a spread of velocities present within the Doppler sample volume due to the groups of blood cells moving at different velocities. The effect of intrinsic spectral broadening will lead to a further spreading of the measured velocities. Therefore, when measuring velocity, a choice has to be made whether to use the maximum or the mean Doppler frequency. Peak systolic velocity, the maximum velocity at peak systole,

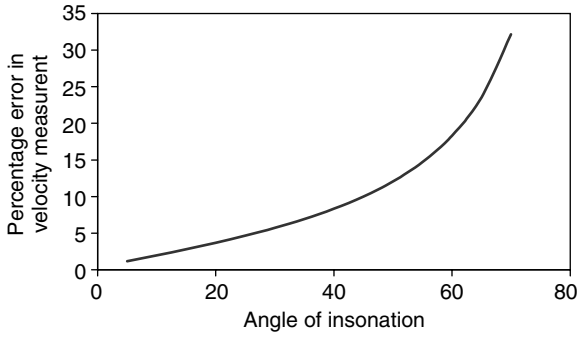

Fig. 9.13 Graph showing the relationship between the percentage error in the velocity measurement as the angle of insonation increases, for a 5° error in the placement of the angle-correction cursor.

and velocity ratios are used to quantify vascular disease (Thrush and Hartshorne 2010). The velocity ratio is given by the maximum peak systolic velocity within a stenosis, v_{sten}, and in the normal vessel proximal to the stenosis, v_{prox}, as follows:

$$\text{Velocity ratio} = v_{sten} / v_{prox}$$

The ultrasound scanner can also calculate the mean velocity by finding the average of all the velocities detected at a given instant in time. As well as spot measurements of velocity at given points in time, many ultrasound systems are also capable of providing velocity measurements averaged over time. One such measurement is the mean velocity averaged over a number of complete cardiac cycles, usually known as time-average velocity, TAV. This can be used to estimate blood flow as described later in the chapter.

Errors in velocity measurements due to the angle of insonation

An estimate of the angle of insonation is required to convert the detected Doppler shift frequency into a velocity measurement. Any inaccuracy in placing the angle-correction cursor parallel to the direction of flow will lead to an error in the estimated angle of insonation. This, in turn, will lead to an error in the velocity measurement. As the velocity calculation depends on the $\cos\theta$ term, the error created due to cursor misplacement will be greater for larger angles of insonation. Figure 9.13 shows the relationship between the percentage error in the velocity measurement as the angle of insonation increases, where there is a 5° error in placement of the angle-correction cursor. Ideally, the angle of insonation should be kept at or below 60° in order to minimize the effect of errors due to imperfectly positioning the angle-correction cursor on an image. However, estimating the angle of insonation is not always straightforward, especially in the presence of disease. Some of the limitations are listed below.

Direction of flow relative to the vessel walls

The direction of the blood flow may not be parallel to the vessel wall, especially in the presence of a stenosis. Therefore, lining the angle-correction cursor to be parallel to the walls may lead to large errors in estimating the true angle of insonation, which, in turn, will lead to errors in the velocity estimation. If there is a clear image of the flow channel through a narrowing, it may be possible to line the angle cursor up with the flow channel. However, the maximum velocity caused by a stenosis may be situated just beyond the stenosis, and the direction of flow may be less obvious there.

Location of site of maximum velocity and direction of flow from colour image

The advent of colour flow imaging has enabled better assessment of the direction of the blood flow, especially if the vessel lumen is unclear on the B-mode image. The colour image may also be used to identify the site of maximum velocity, although this can be misleading since the colour image displays the mean velocity of the blood relative to the direction of the Doppler beam, rather than the actual blood velocity. As the velocity estimated is angle-dependent, the point at which the highest velocity is displayed on the colour flow image may not be the site of the true highest velocity. Instead the highest velocity displayed may be the site at which the angle of insonation is smallest. If the direction of blood flow has changed relative to the Doppler beam, within the imaged area, there will be different angles of insonation at different sites in the colour flow image. Ideally, both the colour and the spectral Doppler assessment of velocity changes across a stenosis should be used to locate the site of the maximum velocity.

Out-of-plane angle of insonation

It is important to remember that the interception of the ultrasound beam with the blood flow occurs in a three-dimensional space and not just in the two-dimensional plane shown on the image. Therefore, the transducer should be aligned with a reasonable length of the vessel, seen in longitudinal section on the image (see Figure 9.3). This ensures that the angle between

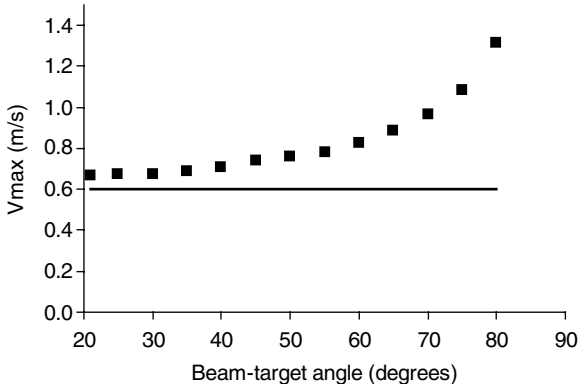

Fig. 9.14 Errors in velocity measurements due to intrinsic spectral broadening: an example plot showing the maximum velocity, measured using an ultrasound scanner, of a moving string test object over a range of angles of insonation. The solid line shows the true velocity of the string. (Graph courtesy of P. R. Hoskins.)

the beam and the flow is approaching zero in the non-imaging plane, and this results in the minimum to enable minimal error.

Doppler ultrasound beam aperture creates a range of angles

The wide aperture used by multi-element transducers used to produce the Doppler beam means that the beam produces a range of angles of insonation (Figure 9.10). Ideally, if the maximum velocity is to be measured, then the angle produced by the edge of the beam that gives the smallest angle (θ_1) should be used to estimate the velocity. However, the majority of modern scanners use the angle produced by the centre of the beam (θ_2), to calculate the velocity. This can lead to an overestimate in the velocity. Because the velocity measurement is dependent on the cosθ term, the size of this error is also angle-dependent, becoming greater the larger the angle of insonation. Figure 9.14 (Hoskins *et al.* 1999) shows an example plot of the maximum velocity measured, using an ultrasound scanner, from a moving string test object over a range of angles of insonation. The solid line on the graph shows the true velocity of the moving string. It can be seen that the velocity of the string has been overestimated by the scanner, with the size of this systematic overestimation becoming greater as the angle of insonation increases.

The errors in velocity measurements obtained may also depend on the position of the beam on the screen. When the beam is positioned near the edge of the transducer, the number of elements used to form the beam may be smaller than when the beam is positioned in the centre of the image. This may result in different-size errors caused by intrinsic spectral broadening. Figure 9.15a,b shows two measurements made at the same point in a flow rig with constant flow. It can be seen that the measurement made with the beam positioned close to the edge of the transducer gives a lower velocity measurement (111 cm s^{-1}) than the measurement made with the beam placed in the centre of the field of view (140 cm s^{-1}). It can be seen that the sensitivity of the Doppler beam produced at the edge of the transducer is also lower, compared to that produced in the centre, and more gain is required, resulting in noise seen on the spectral Doppler display. The same effect can be seen in Figure 9.15c,d, where the peak systolic velocity has been measured at the same point in a carotid artery with the Doppler beam at the edge (c) and the Doppler beam in the centre (d) of the transducer, resulting in velocity measurements of 68 and 90 cm s^{-1} respectively. In order to minimize these differences in measurement, ideally measurements should be made with the Doppler beam in the centre of the field of view. The error produced due to spectral broadening can also vary with changes in the sample volume depth as this may result in changes in the active aperture.

The size of errors due to intrinsic spectral broadening is potentially large and may vary between models of scanner and between manufactures (Alexandrov *et al.* 1997, Fillinger and Baker 1996, Kuntz *et al* .1997). Unfortunately, manufacturers of ultrasound scanners provide little data on possible errors in velocity measurements.

Optimizing the angle of insonation

The B-mode and the colour flow images are used to estimate the direction of flow in the area to be investigated so that the spectral Doppler beam can be steered appropriately. The angle of insonation is measured by lining up the angle-correction cursor with the estimated direction of flow. There are many possible pitfalls when making velocity measurements and no single method of estimating the angle of insonation is completely reliable. The various possibilities and their advantages and disadvantages are discussed below.

Velocity ratio measurements

Ideally, the angle of insonation used to make the velocity measurement proximal to and at the stenosis should be similar. This will result in the two velocities having

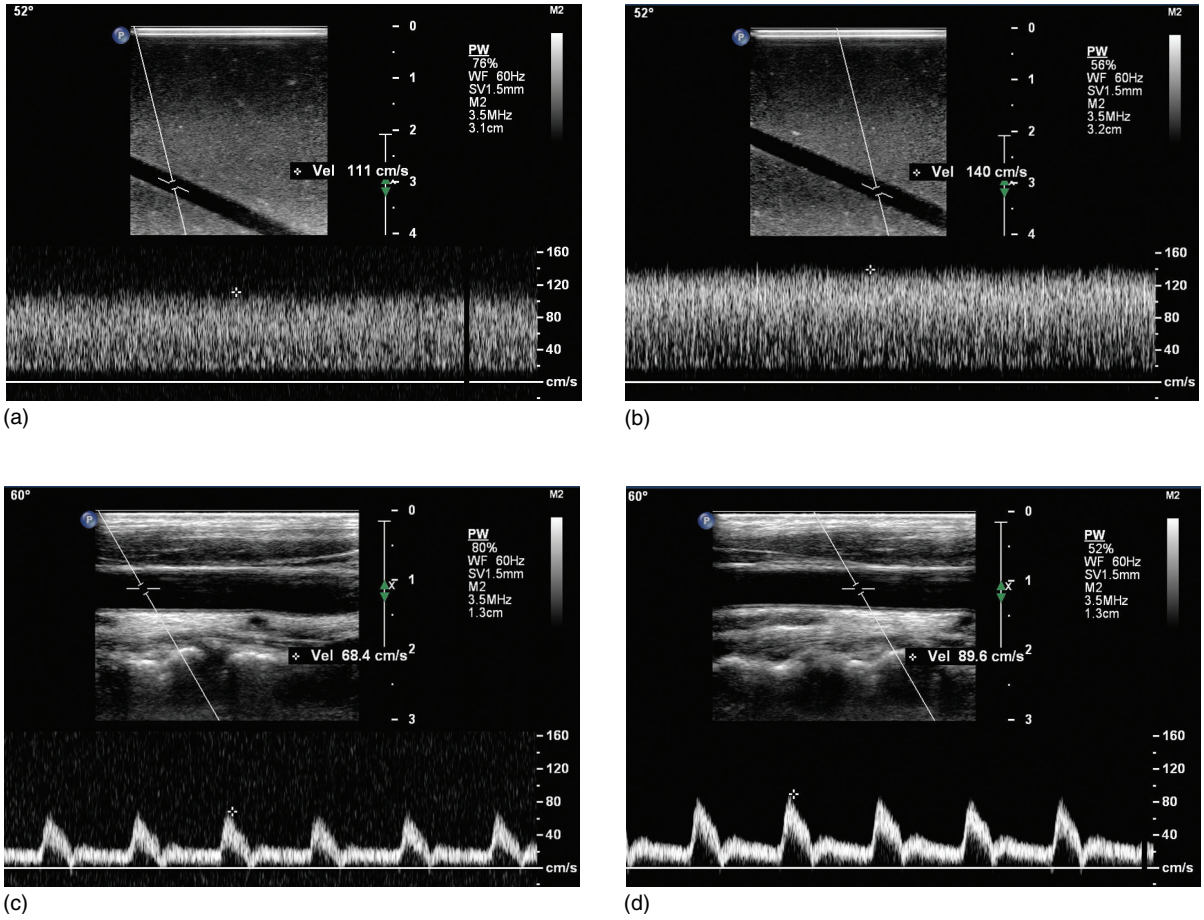

Fig. 9.15 Spectral Doppler displays showing two measurements made at the same point in a flow rig with constant flow. The measurement made with the beam positioned close to the edge of the transducer (a) gives a lower velocity (111 cm s^{-1}) than the measurement made with the beam place in the centre (b) of the field of view (140 cm s^{-1}). Panels (c) and (d) show the same effect where the peak systolic velocity has been measured at the same point in a carotid artery with the Doppler beam at the edge (c) and the Doppler beam in the centre (d) of the transducer, resulting in velocity measurements of 68 and 90 cm s^{-1} respectively.

similar systematic errors that will cancel out when finding the ratio.

Absolute velocity measurements

There are two schools of thought about selecting the angle of insonation at which to make absolute velocity measurements:

(1) *Always set the angle of insonation to 60°:* this ensures that any error in alignment of the angle-correction cursor only leads to a moderate error in the velocity estimate (Figure 9.13) and that the errors caused by intrinsic spectral broadening are kept reasonably constant between measurements.

(2) *Always select as small an angle of insonation as possible:* this ensures that any error in the alignment of the angle-correction cursor produces as small an error in velocity estimation as possible. The error due to intrinsic spectral broadening will also be minimized. However, this error will be different for measurements made at different angles of insonation. This makes comparison between measurements made at different angles less reliable.

In the Joint Recommendations for Reporting Carotid Ultrasound Investigations in the United Kingdom, Oates *et al.* (2009) recommend that the Doppler angle be in the range 45–60° to minimize the effects on

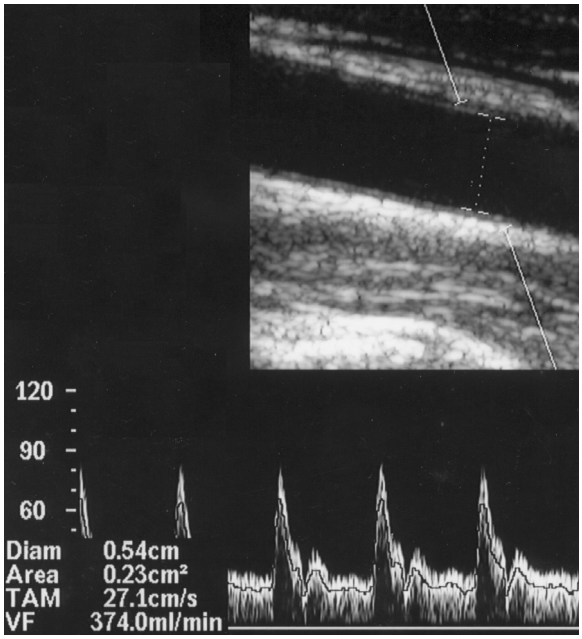

Fig. 9.16 Image and spectral Doppler display showing the technique used to measure time-averaged mean velocity (TAM) and volume flow (VF).

velocity measurement relating to the angle of insonation. The blood velocity may need to be measured at a few points through and beyond the stenosis to ensure the highest velocity has been obtained. Doppler criteria developed over the years may not have been produced with a full understanding of all these possible sources of error. Different models of ultrasound systems may produce different results for the same blood flow. However, despite these sources of error, velocity measurements have been successfully used to quantify vascular disease for the past two decades. A greater understanding of the sources of error in velocity measurement may lead to improvements in accuracy.

Measurement of volume flow

Volume flow is a potentially useful physiological parameter that can be measured using duplex ultrasound. Flow can be calculated by multiplying the time-average velocity, TAV, obtained from the Doppler spectrum, by the cross-sectional area of the vessel, obtained from the B-mode image:

Flow = TAV × cross-sectional area of the vessel.

One method of estimating the cross-sectional area is to measure the diameter of the vessel, d, and calculate the area, A, assuming the vessel is cylindrical as follows:

$$A = \frac{\pi d^2}{4}$$

Some scanners allow the operator to trace around the vessel perimeter to calculate the area but this method relies on a good image of the lateral walls and a steady hand and is therefore prone to error (see Chapter 6). Figure 9.16 shows how the vessel diameter has been obtained from the image and the velocity of the blood has been measured by placing the sample volume across the width of the vessel and estimating the angle of insonation from the image. Although the measurement of flow is relatively simple to perform there are many errors relating to both the measurement of the TAV and to the cross-sectional area (Evans and McDicken 2000). These errors limit the value of one-off absolute flow measurements but serial measurements of flow may provide useful information on flow changes. Volume flow measurements may be useful where large changes in volume flow are diagnostically significant such as in the assessment of arterio-venous fistulas created for haemodialysis access.

Errors in diameter measurement

As the measurement of flow is dependent on the diameter squared, any error in the diameter will produce a fractional error in the flow measurement that is double the fractional error in the diameter measurement. The accuracy of the diameter measurement depends on the resolution of the image and the accuracy of the callipers. Calculation of the cross-sectional area from a diameter measurement assumes that the vessel lumen is circular, which may not be the case in the presence of disease. Also the arterial diameter varies by approximately 10% during the cardiac cycle so, ideally, several diameter measurements should be made and the average found.

Errors in TAV measurement

Incomplete insonation of the vessel will lead to errors in the mean velocity measurements due to an underestimation of the proportion of slower-moving blood near the vessel wall (Figure 9.9). This is the case even if the sample volume is set to cover the near and far wall of the vessel, as the out-of-imaging-plane flow will not be sampled. Incomplete insonation of the vessel can

lead to an overestimate in the measured value of TAV or flow of up to approximately 30%. The use of high-pass filters, if set too high (Figure 9.6), can also lead to an overestimate in the mean velocity since the low-velocity blood flow would be excluded. Aliasing would lead to underestimation of the mean velocity due to the incorrect estimation of the high velocities present within the signal.

Waveform indices

The presence of significant disease can lead to alterations in the spectral Doppler waveform shape and may indicate whether the disease is proximal or distal to the site from which the Doppler waveform is obtained (Chapter 8). Over the years different methods of quantifying the waveform shape have been developed (Evans and McDicken 2000) and modern scanners incorporate the facilities to calculate various indices to help identify changes in the waveform shape.

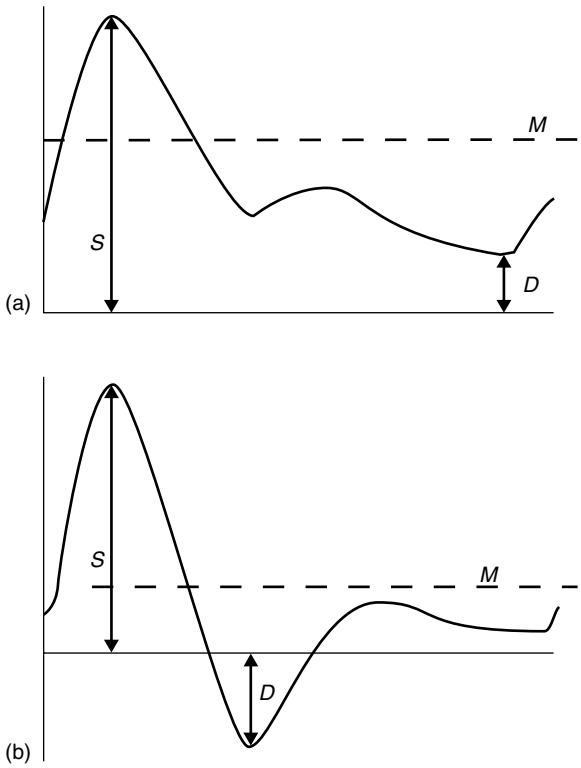

Fig. 9.17 Schematic diagram showing the quantities used in estimation of RI and PI, for (a) a waveform with forward flow only, (b) a waveform with a period of reverse flow.

Pulsatility index

The pulsatility index, PI, can be used to quantify the degree of pulse wave damping at different measurement sites. It is defined as the maximum, either frequency or velocity, of the waveform, *S*, minus the minimum, *D* (which may be negative), divided by the mean, *M*, as shown in Figure 9.17:

$$PI = \frac{(S - D)}{M}$$

Damped flow, beyond significant disease, will have a lower PI value than a normal pulsatile waveform.

Pourcelot's resistance index

The resistance index, RI, is defined as (Figure 9.17)

$$RI = \frac{(S - D)}{S}$$

Spectral broadening

Over the years, there have been several definitions of spectral broadening to quantify the range of frequencies present within a spectrum (Evans and McDicken 2000) and one such definition is

$$SB = \frac{(f_{max} - f_{min})}{f_{mean}}$$

When using these indices, it is important for the operator to understand how their ultrasound system calculates theses values. Increased spectral broadening indicates the presence of arterial disease but some broadening can also be introduced by the scanner itself, as discussed above.

Manual versus automated measurement

Duplex systems may enable the user to choose either to manually trace the maximum velocity over a cardiac cycle or to allow the system to automatically trace the maximum velocity. Manual tracing of the velocity can be both awkward and time-consuming. Automatic measurements are usually quicker to implement but may be inaccurate in the presence of noise. Noise can include random background noise, electrical spikes or signals from other vessels, all of which may result in an incorrect estimation of the velocity. Therefore the automated maximum trace should be displayed alongside the Doppler spectrum so that any large discrepancies can be seen and a judgement made on the accuracy of the measurement.

Automatic tracing of the maximum velocity also allows automated measurement of peak systolic velocity and calculation of various indices which are displayed on the screen, sometimes in real time.

Questions

1. What are the advantages and disadvantages of PW over CW Doppler systems?
2. What is aliasing and how may it be overcome? Are there situations were aliasing cannot be prevented?
3. What is the sample volume length? How might the size of the same volume affect the appearance of the Doppler spectral display?
4. What is intrinsic spectral broadening and what measurement may it affect?
5. When making velocity measurements, how is the angle of insonation measured? Discuss what size of angle of insonation should be used when making velocity measurements. Why is this important?

References

Alexandrov AV, Vital D, Brodie DS, Hamilton P, Grotta JC (1997). Grading carotid stenosis with ultrasound. An interlaboratory comparison. *Stroke*, **28**, 1208–10.

Evans DH, McDicken WN (2000). *Doppler Ultrasound: Physics, Instrumentation, and Signal Processing*. Chichester: Wiley.

Fillinger MF, Baker RJ (1996). Carotid duplex criteria for a 60% or greater angiographic stenosis: variation according to equipment. *Journal of Vascular Surgery*, **24**, 856–84.

Hoskins PR (1996). Measurement of maximum velocity using duplex ultrasound systems. *British Journal of Radiology*, **69**, 172–7.

Hoskins PR, Fish PJ, Pye SD, Anderson T (1999). Finite beam-width ray model for geometric spectral broadening. *Ultrasound in Medicine and Biology,* **25**, 391–404.

Kuntz KM (1997). Duplex ultrasound criteria for identification of carotid stenosis should be laboratory specific. *Stroke*, **28**, 597–602.

Oates CP, Naylor AR, Hartshorne T, *et al.* (2009). Joint Recommendations for Reporting Carotid Ultrasound Investigations in the United Kingdom. *European Journal of Vascular Surgery*, **37**, 251–61.

Thrush AJ, Evans DH (1995). Intrinsic spectral broadening: a potential cause of misdiagnosis of carotid artery disease. *Journal of Vascular Investigation*, **1**, 187–92.

Thrush AJ, Hartshorne TC (2010). *Vascular Ultrasound: How, Why and When*. London: Churchill Livingstone.

Chapter 10

Colour flow and tissue imaging

Peter Hoskins and Aline Criton

Introduction

Doppler ultrasound remained a minority imaging methodology until the introduction of colour Doppler in 1982. In this technique, the motion of the blood is colour-coded and superimposed on the B-mode image. This allows rapid visualization of the flow patterns in vessels, allowing high-velocity jets in arteries and in cardiac chambers to be seen. It quickly became apparent that the ability to visualize flow patterns, such as the presence of intracardiac jets, was of great value. In addition, it considerably speeded up the placement of the Doppler sample volume in spectral Doppler investigation, hence reducing scanning time.

Prior to the introduction of commercial colour flow systems, several approaches were described to provide an image showing the pattern of blood flow. These often relied on manual scanning of the probe over the skin to build up a two-dimensional (2D) image. These systems, which used electronic or mechanical sweeping of the beam, were not real-time, having only a maximum of a few frames per second. These are reviewed in Evans and McDicken (2000),Wells (1994) and Cobbold (2007).

This chapter also includes a description of 'B-flow' imaging in which the B-mode image is modified to enhance the visibility of blood, and Doppler tissue imaging in which colour-coding of motion is applied to tissues such as the myocardium.

Terminology

In the development of any imaging modality, new terminology is introduced, usually by manufacturers. Unfortunately, this leads to a plethora of terms whose meaning may change with time. The term 'colour flow' originally referred only to an ultrasound system in which a 2D image of mean Doppler frequency from blood was displayed using colour coding. For many years now other quantities have been displayed in colour, such as the power of the Doppler signal. In order to provide a consistent terminology, the descriptions below will be used in this chapter:

- *Colour flow:* imaging of blood flow. This is the generic term, which will be used in this chapter, and it encompasses the three modalities below.
- *Colour Doppler*: image of the mean Doppler frequency from blood, displayed in colour superimposed on a B-mode image.
- *Power Doppler*: image in which the power of the Doppler signal backscattered from blood is displayed in colour.
- *Directional power Doppler*: image in which the power of the Doppler signal is displayed, including separate colour coding of blood velocities towards and away from the probe.

2D image production

Production of a 2D colour flow image includes elements of B-mode image formation and pulsed Doppler techniques. As in B-mode image formation, the image is built one line at a time, by transmitting ultrasonic pulses and processing the sequence of returned echoes. However, unlike B-mode image formation in which echo amplitude information is processed to form the image, the echoes are demodulated to produce a Doppler shift signal. In the pulsed-wave spectral Doppler systems described in Chapter 9, Doppler information was obtained from only a single sample volume. In a colour flow system, each line of the image is made up of multiple adjacent sample volumes.

As colour flow is a pulsed-wave Doppler technique, the Doppler shift information for each line is obtained from several transmission pulses. Unlike spectral Doppler, which relies on the fast Fourier transform (FFT) to extract the whole spectrum of frequencies that are present, colour flow imaging uses a technique known as 'autocorrelation', which was introduced in

Diagnostic Ultrasound: Physics and Equipment, ed. Peter Hoskins, Kevin Martin and Abigail Thrush. Published by Cambridge University Press.

Chapter 7. This calculates the mean frequency detected within each sample volume, which is then colour-coded on the display. For the mean Doppler frequency to be detected, at least two pulses are required to be transmitted along each line. However, as a more accurate estimate of the detected mean frequency is obtained when more pulses are used, a typical colour scanner may use about 10 pulses. The requirement of several pulses per line to produce the colour image, compared with a minimum of one in the B-mode image, means that the frame rate for a comparable number of scan lines is much less in the colour image than it is in the B-mode image. For example, if 10 pulses were to be used for each colour line, and one pulse for each B-mode line, then the maximum frame rate for the colour image would be one-tenth that of the B-mode image. There is, therefore, a compromise between the size of the colour image (number of scan lines), accuracy of the frequency estimate (number of pulses per line) and the rate at which the image is updated (frame rate). In order for a sonographer to appreciate the pulsatile nature of blood flow, it is preferable for the machine to maintain a frame rate above 10 frames per second. If the whole field of view were to be used, then the maximum achievable colour frame rate would be only a few frames per second. In order to improve the colour frame rate, the colour-coded flow is only displayed in a limited region of interest called the 'colour box' within the displayed B-mode image. The reduced depth and number of scan lines that this provides enables fewer ultrasound pulses to be sent per colour frame, and hence allows the use of higher colour frame rates. The width and depth of the colour box are under operator control, and the frame rate may be increased by narrowing the box, or by decreasing the box depth. In order to further increase frame rate, the line density may also be reduced on some systems. Typically, frame rates of 10–15 frames per second can be achieved in peripheral arterial applications, though this may fall to five frames per second or less in venous applications, where a large number of pulses are needed for each colour line in order to measure relatively low Doppler shifts. Low frame rates may also result for abdominal and obstetric applications, where the vessel depth is large. Typical colour box shapes and relative sizes are shown in Figure 10.1.

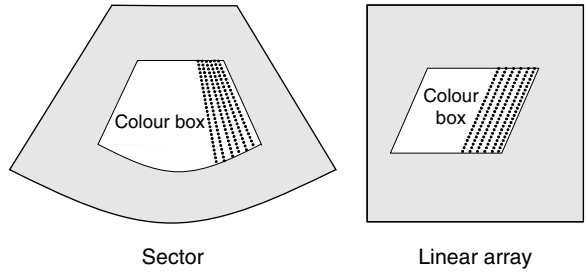

Fig. 10.1 Colour box shapes for (a) sector and (b) linear-array transducers. Within the colour box, the image is built up as a series of colour lines. Each line consists of a series of adjacent sample volumes.

Phase- and time-domain techniques

The common theme of colour flow techniques is that the colour image is derived by consideration of the motion of the blood. There are two basic classes of instrument, dependent on whether they determine the presence of motion by analysis of the phase shift or the time shift, as described in Chapter 7. Few commercial machines use the time-domain approach, probably as this is computationally more demanding, and hence more expensive to implement. Virtually all modern commercial colour flow systems employ the phase-shift approach using autocorrelation detection, and the sections immediately following will refer to this approach.

Colour flow system components

A colour flow system will independently process the received B-mode and colour flow echoes (Figure 10.2). In addition, a spectral Doppler display can be obtained from a single sample volume as selected by the operator. A small number of pulses, typically 2–20, are transmitted and received for each colour line that is produced. Each line is divided into a large number of sections each of which represents a different sample volume. The Doppler signal from all of the gates is processed simultaneously. This situation is different to pulsed-wave spectral Doppler, where only one gate is considered. Figure 10.3 shows the essential components of the colour flow processor. The functions of the components are described below.

Doppler transmitter

Colour flow imaging uses the pulse–echo technique. Modern colour flow systems do not use the same pulses that are used for the B-mode image, but instead use separate lower-frequency pulses, as shown in Table 10.1.

Transducer

Any transducer used for B-mode imaging can, in principle, be used for colour flow. Commercial colour flow scanners typically use linear-, curvilinear- or

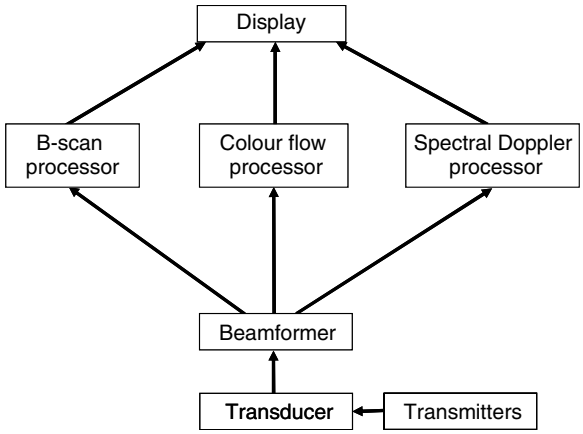

Fig. 10.2 Components of a colour system. For a colour flow system, three types of information are processed: B-mode, colour flow and spectral Doppler.

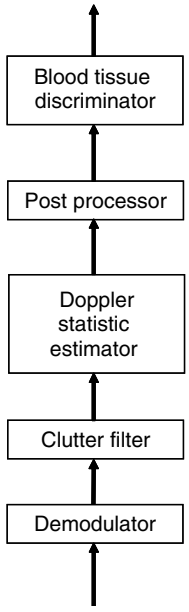

Fig. 10.3 Components of the colour flow processor.

phased-array transducers. The use of mechanically swept systems is possible, but is more problematic as the vibration that is produced can be picked up by the colour flow system, so that careful attention to design is needed in order to reduce false colour display.

Beam-former

This component of the system is the same as the B-mode beam-former discussed in detail in Chapter 3. The beam-former controls all aspects concerned with focusing and sweeping the beam through the tissue to produce a 2D colour image.

Table 10.1 Typical B-mode and colour flow transmit frequencies.

Application	B-mode frequency (MHz)	Colour frequency (MHz)
Peripheral vascular	7–12	4–6
Abdominal/ obstetrics	2–5	2–4
Transcranial	1.5–2.5	1–2

Demodulator

The demodulator extracts the Doppler shift frequencies as discussed in Chapter 7. This process is invisible to the user, with no relevant user controls.

Clutter filter

Clutter refers to signals from stationary and slowly moving tissue. It was noted in Chapter 7 that the signal from tissue is some 40 dB higher than the signal from blood. If it is moving blood that is of interest, then it is necessary to remove, as far as possible, the clutter signal, and so a clutter filter is present in colour flow systems. The clutter filter is analogous to the wall thump filter of spectral Doppler. Early colour flow systems used relatively unsophisticated clutter filters and were unable to detect low-velocity flow (Figure 10.4). The detection of low velocities by modern colour flow systems is linked to the use of a sophisticated clutter filter (Figure 10.5).

Mean-frequency estimator

The requirement for real-time scanning means that Doppler frequencies must be estimated in a much shorter time than is available for spectral Doppler; usually 0.2–2 ms for colour flow, as opposed to 5–40 ms for spectral Doppler. When colour flow systems were introduced in 1982, the processing capabilities available at that time meant that it was not possible to use an FFT approach. This would have meant calculating the full Doppler spectrum followed by extracting the mean frequency. The realization by Namekawa *et al.* (1982) and Kasai *et al.* (1985) that a computationally simple algorithm termed 'autocorrelation' could be used to calculate mean frequency directly was the breakthrough that led to the introduction of real-time colour flow systems into commercial use. In addition to the short time that is available for calculation in colour flow, the number of pulses used for generation of each line is much less than in spectral Doppler; 2–20 in

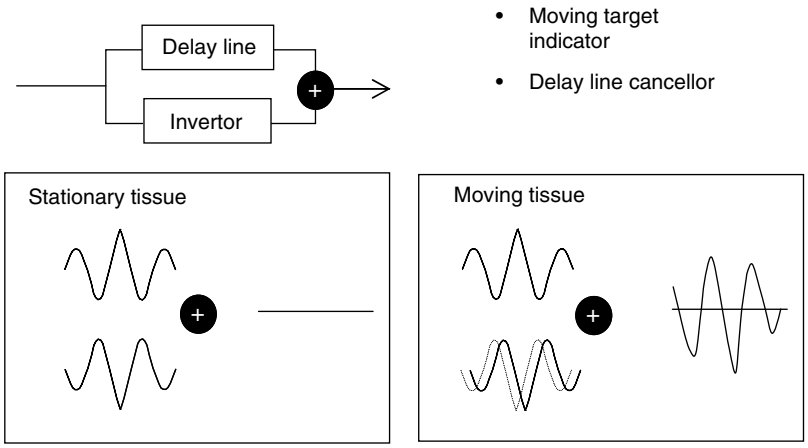

Fig. 10.4 Simple clutter filter. The previous received echo is delayed and added to the current received echo. If the tissue is stationary, consecutive echoes will cancel out, whereas if there is blood or tissue motion, consecutive echoes will not cancel out. This simple method is also called a 'delay line cancellor' or a 'moving target indicator'.

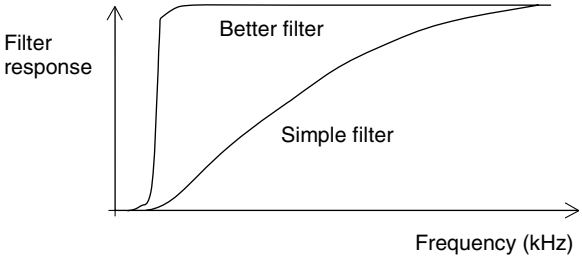

Fig. 10.5 Clutter filter response as a function of Doppler frequency. The ideal filter completely suppresses the clutter, and allows through the Doppler frequencies. The simple delay line cancellor of Figure 10.4 causes suppression of high Doppler frequencies, which will prevent the display of low velocities; however, there is suppression of higher blood velocity signals also. The more complex clutter filter has better low-frequency behaviour.

colour flow as opposed to 80–100 in spectral Doppler. The number of pulses used for generation of each colour line is called the 'ensemble length'.

The autocorrelator provides simultaneous estimates of three quantities:

- *Power:* proportional to the square of the amplitude of the Doppler signal.
- *Mean Doppler frequency:* the mean or average Doppler frequency.
- *Variance:* this is a quantity related to the variability of the Doppler signal. It is defined by the square of the standard deviation of the Doppler signal amplitude, estimated over the ensemble length.

Since the introduction of the autocorrelation technique, there have been many different techniques used to estimate the single quantity that can be displayed on a colour flow image. Some of these techniques have been alternative ways of estimating mean frequency. Other techniques have been for estimation of different quantities, such as maximum Doppler frequency. The descriptions of these techniques are beyond the scope of this book, and are reviewed in Evans and McDicken (2000). Most modern colour flow scanners use a technique called '2D autocorrelation' or variants of this. The 2D autocorrelation technique is described by Loupas *et al.* (1995a, b), and is an extension of the basic autocorrelation technique.

Post-processor

Even under conditions where the blood or tissue velocity is unchanging, the estimated mean Doppler frequency will change to some extent in a random manner. On the colour flow image, this variation manifests itself as a speckle pattern called 'colour speckle'. The cause of this speckle is associated with the variation in echo amplitude received at the transducer arising from the variation in the detailed position of each of the red cells within the sample volume from one pulse to the next. This is the same reason that there is a speckle pattern on B-mode images and on spectral Doppler waveforms. This speckle pattern can mask changes in the displayed colour. However, it is possible to reduce the degree of noise by averaging over several frames. This is the same

frame-averaging technique as used in B-mode imaging, and it gives rise to a persistence effect.

Blood–tissue discriminator

For each pixel of the image, it is possible to estimate the echo brightness level for the B-mode image and also the mean Doppler frequency for the colour flow image. However, it is only possible to display one of these in the final composite image. The function of the blood–tissue discriminator is to ensure that colour is displayed only in regions of true blood flow and not in the presence of moving tissue. There are several methods by which discrimination between the signals from blood and moving tissue can be achieved. These include:

- *Doppler signal amplitude threshold:* in regions of tissue that are moving slowly with respect to the transducer, the Doppler frequency shifts from the tissue will be of high amplitude, but of low Doppler frequency. The clutter filter acts to eliminate these signals. After the clutter filter, the signal from blood is much stronger than the signal from tissue. The use of a simple threshold on the Doppler amplitude is used to determine whether blood or tissue signals are displayed for a given pixel (Figures 10.6 and 10.7) . See the description of the 'colour gain' control below.
- *B-mode amplitude threshold:* if the amplitude of the B-mode image is large, it is likely that the signal

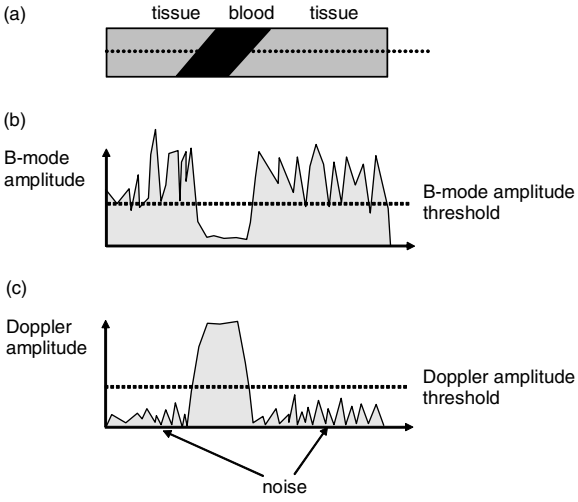

Fig. 10.6 Operation of the blood tissue discriminator. (a) A single image scan line through a region of tissue and flowing blood is shown. (b) Amplitude of B-mode echoes with depth. For values of the amplitude above the threshold, colour is not displayed, and for values below the threshold colour data are displayed. (c) Amplitude of the Doppler signal with depth; for values of the amplitude above the threshold, colour is displayed, and for values below the threshold colour data are not displayed,

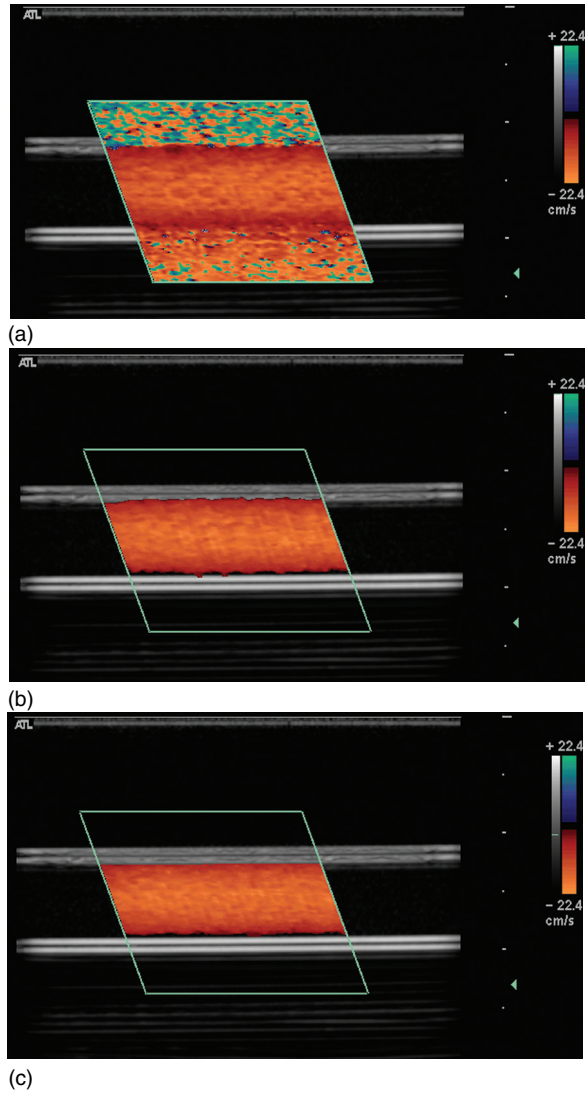

Fig. 10.7 Operation of the blood–tissue discriminator. Colour Doppler images are acquired from a flow phantom with a blood mimic flowing through a tube. (a) No blood–tissue discriminator present – there is colour throughout the colour box consisting of a uniform colour in the region of flow, surrounded by random noise in the surrounding regions. (b) Application of the Doppler amplitude threshold using the colour gain removes most of the colour from the region of no flow; however, there is some 'bleeding' of the colour into the tube. (c) Application of the B-mode amplitude threshold using colour write priority removes the bleeding.

arises from a region of tissue. A threshold based on the amplitude of the B-mode data is used to suppress the display of colour in regions of the image where the B-mode amplitude exceeds the threshold (Figures 10.6 and 10.7). See the description of the 'colour write priority' control below.

- *Flash filter:* rapid motion of either the tissue or of the transducer produces a Doppler shift, which may be displayed as region of colour; these are called 'flash artefacts'. The threshold method described above is often insufficient to remove such flashes. Manufacturers have developed more sophisticated removal methods, based on the detection of very rapid changes in the Doppler signal level, such as are produced by motion of the transducer with respect to the patent, breathing motions, cardiac motion and bowel motion.

Colour flow modes

The three outputs from the autocorrelator (mean frequency, variance and power) can be colour-coded and displayed, either alone or in combination with each other. This produces a number of possible colour modes, which can be selected. In practice, only a few are sensible (Figure 10.8). These are considered below.

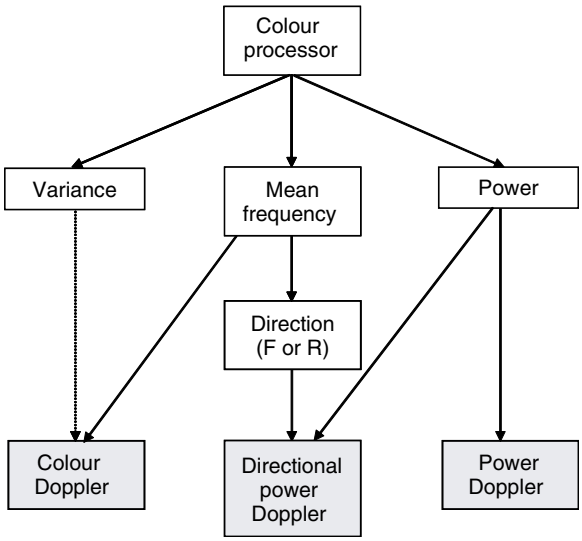

Fig. 10.8 Relationship between calculated quantities and colour flow display modes. The three quantities estimated by the colour flow system are the mean Doppler frequency, the Doppler power and the variance. The colour Doppler image is a display of the mean frequency in which the variance may be added, if required. The power Doppler image is a display of the Doppler power. For directional power Doppler, flow direction is obtained from mean frequency, and used to colour code the power Doppler image.

Colour Doppler

The earliest commercial colour flow systems concentrated on this mode, in which the mean frequency in each pixel is colour-coded. Although in principle any colour scale could be used for the display, most manufacturers adopt a red-based scale for blood flowing in one direction, and a blue-based scale for blood flowing in the opposite direction (Figure 10.9).

Where variance is displayed alone, it is shown as a green colour, together with the red or blue representing the mean frequency, to produce a composite display. This option was widely available on early colour flow machines, where it was thought that variance was related to turbulence produced by narrowed arteries or cardiac valves. Figure 10.10 shows a cardiac jet, where the green colouration in the jet is seen. This mode is not used much outside cardiac applications.

Power Doppler

Display of the power of the Doppler signal had been a feature of early colour flow systems; however, the same instrument settings were used as for colour Doppler and there was not much improvement over the colour Doppler image. It was only when the processing was optimized for power Doppler (Rubin *et al.* 1994) that it became popular, largely due to improved sensitivity over colour Doppler. The first step in this optimization is concerned with the display of noise. In colour Doppler, the noise is present on the image if the colour gain is set too high, and its appearance

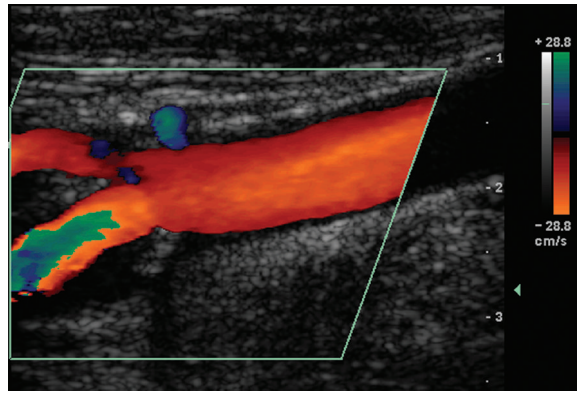

Fig. 10.9 Colour Doppler image of common carotid flow with a blue–red scale.

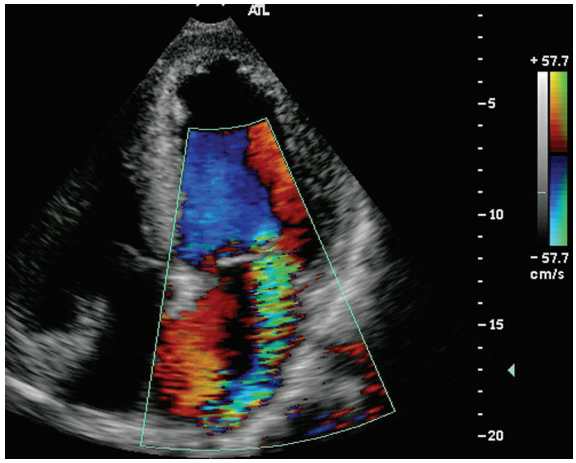

Fig. 10.10 Colour Doppler image of tricuspid regurgitation with variance admixed. Regions of green colouration associated with high variance are seen.

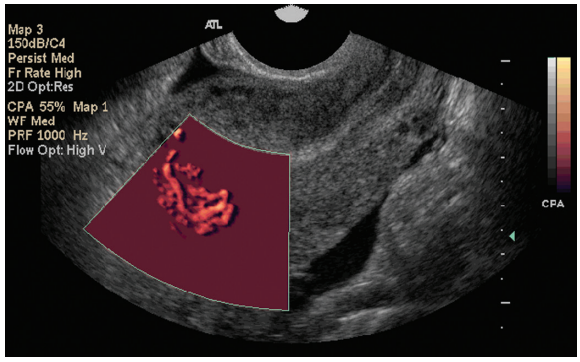

Fig. 10.11 Power Doppler image of arterio-venous fistulae, in which there is colour throughout the colour box.

is a multicoloured mosaic in which the true image from the vessel of interest may be difficult to observe. However, for power Doppler, the noise appears as a low-level uniform hue in which it is easily possible to observe the vessel of interest. Consequently, the first step in optimization is to reduce the level of the threshold used to differentiate between the signal from blood and the signal from noise. The second step recognizes that it is not possible to follow the changes in blood flow with time using power Doppler, so it is not necessary to have good time resolution. Consequently, for power Doppler, the degree of averaging over successive acquired frames (persistence) is much higher than for colour Doppler. This averaging process acts to reduce the colour noise level, and hence make it easier to distinguish small vessels

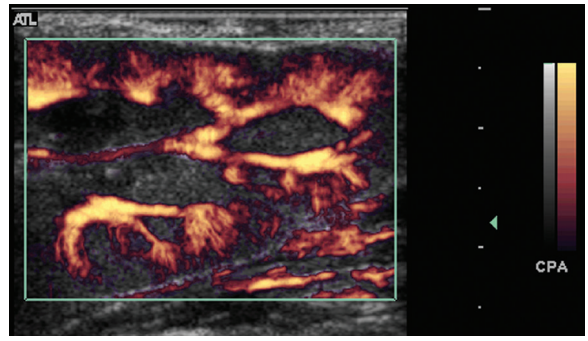

Fig. 10.12 Power Doppler image of the kidney taken intraoperatively consisting of colour superimposed on the B-mode image.

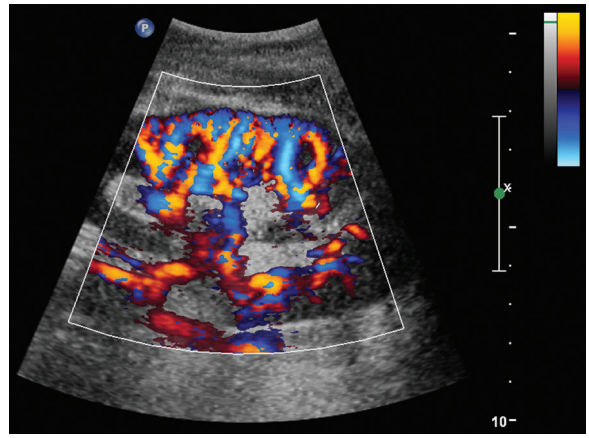

Fig. 10.13 Directional power Doppler from a transplanted kidney.

with low-signal levels. In order to make the best use of the increase in sensitivity, the first manufacturers to use power Doppler displayed colour throughout the colour box. This is shown in Figure 10.11, where small vessels can be seen in yellow above the noise, which is shown in red. The disadvantage of this mode is that the underlying tissue anatomy cannot be seen. Most manufacturers now prefer to display the power Doppler image superimposed on the B-mode image (Figure 10.12). A commonly used colour scale is a 'heated body scale', in which the displayed colour changes through black, red, orange and yellow as the Doppler power increases.

Directional power Doppler

In this mode, the directional information on blood flow is obtained from the mean-frequency data, and used to colour code the power Doppler data (Figure 10.13). This mode is supposed to combine the enhanced

sensitivity of power Doppler with the directional capability of colour Doppler.

Colour controls

There are a large number of instrument settings, which affect the displayed colour image. Thankfully in most modern colour flow systems, the default values of the settings are pre-programmed by the manufacturer for particular clinical applications, which the operator can recall from the applications list. The operator must then adjust a small number of controls for individual patients. In the list below, the controls are classified according to three categories: controls which affect colour image acquisition, controls which affect Doppler signal extraction and frequency estimation, and controls which affect the display of the colour flow signals. The section finishes with a description of the use of controls in clinical practice.

Controls affecting the acquisition of colour flow images

Power or acoustic output

The amplitude of the ultrasound pulses used for generation of the colour flow images may usually be adjusted over a wide range of values. The sensitivity of the instrument will improve as the power increases; however, in order to maintain patient exposure within safe limits, it is best if other controls, such as colour gain, are also used to obtain the desired image quality.

Pulse repetition frequency

The pulse repetition frequency (PRF) is the total number of pulses which the transducer transmits per second. It is limited largely by the maximum depth of the field of view; the transmit–receive time is less for smaller depths and a higher PRF is then possible. The value of the PRF selected in the various system presets, such as arterial or venous, will depend on the expected velocities present in the region of interest, but PRF may need to be altered by the operator, e.g. to prevent aliasing or to enable the detection of low flow. On modern systems, there is not a single control labelled 'PRF'. Instead, PRF is usually determined automatically from various controls, including the colour box size and the velocity scale.

The total number of pulses transmitted is divided between the B-mode image, the colour flow image and spectral Doppler. Maximum PRF for the colour image is achieved when the spectral display is switched off, and the colour box depth and width are reduced as much as possible. This will result in a colour image with a high frame rate.

Steering angle

This control is applicable to linear-array systems, where it is possible to steer the colour beam in a variety of directions with respect to the B-mode scan lines. Most systems provide three angles (e.g. −20°, 0°, +20°), though some provide a choice of five or more directions between this range. Steering the colour beams is desirable in colour flow imaging as many peripheral vessels run parallel to the skin surface, and an ultrasound beam perpendicular to the skin would provide zero Doppler signal. However, optimum B-mode imaging of the vessel is provided in this situation. By a combination of beam steering and probe angulation, it is usually possible to obtain a beam–vessel angle in the range 40–70°, which is sufficient for adequate colour flow image production, as well as good B-mode visualization of vessel walls. The power Doppler image is much less dependent on the beam–vessel angle, as explained below, and it is generally not necessary to steer the beam away from the 0° direction.

Focal depth

Due to frame-rate considerations, it is usual to only have one transmit focal depth for colour flow images. In some systems, the default is set automatically at the centre of the displayed field of view; in others, it is necessary to set this manually at the depth of interest.

Box size

The depth and width of the colour box are set by the user. The box depth directly influences the PRF, with higher PRF, and hence higher frame rates, being possible for box depths that are nearer to the surface. Higher frame rates may also be achieved by restriction of the width of the colour box as this reduces the number of Doppler lines required.

Line density

It is not necessary for the line density (number of Doppler lines per centimetre across the image) of the colour image to be the same as the B-mode image. Reduction in line density increases frame rate; however, this is done at the expense of reduced lateral spatial resolution of the colour image.

Gate length

The gate length will determine the number of cycles in the transmitted pulse, and so alters the sample volume size. This improves sensitivity, but decreases axial resolution.

Depth of field

Reducing the image depth enables higher PRF to be used, and therefore higher frame rates to be achieved.

Controls affecting the extraction and estimation of Doppler frequencies

Filter cut-off

It is common practice to set the filter cut-off frequency as a certain fraction of the total displayed frequency scale, rather than as an absolute value of, say, 200 Hz. This means that as the frequency scale increases, so does the level of the clutter filter. Observation of low blood velocities requires that the frequency scale is set to low values.

There are usually three or four clutter filter options to choose from. Selection of too low a filter level results in breakthrough of the clutter signal from slowly moving tissue.

Ensemble length

The term 'ensemble length' is used to refer to the number of pulses used to generate each colour line. Provided that flow is steady during the time spent measuring the Doppler shifts along one scan line, the variability of estimated mean frequency decreases as the ensemble length (number of pulses per estimate) increases. Low variability is required for accurate estimation of low velocities. In cardiology, it is higher blood velocities that are mainly of interest, whereas in radiology low venous blood velocity may be of more interest. Consequently, the ensemble length is partly determined by the selected application, with longer ensemble lengths used in radiology applications than in cardiology applications. Visualization of low velocities is best achieved by adjustment of the velocity scale, so in many systems the ensemble length is directly linked with the velocity scale. For example, a 10-pulse ensemble will take longer to complete when a low PRF is used than when a high PRF is selected. As the velocity scale is reduced to enable better visualization of low velocities, the increased ensemble length will result in a reduction in frame rate.

Baseline

If aliasing is a problem, then one method of dealing with this is to shift the baseline to enable higher positive velocities to be presented. This is identical to the technique used in spectral Doppler.

Persistence or frame averaging

Persistence refers to the averaging of Doppler shift estimates from current and previous frames. If flow is stable over the averaging period, then strong frame averaging will result in reduced colour noise, enabling better visualization of the true flow pattern. If the degree of frame averaging is kept fixed through the cardiac cycle, then rapidly changing flow patterns will not be properly visualized. Some commercial systems attempt to overcome this by automatic adjustment of the level of frame averaging. For example, if the measured velocity is high, the persistence will be low, enabling visualization of the high-velocity pulsatile flow patterns in arteries; when the velocity is low the persistence will be high, allowing the (usually) less pulsatile flow in veins to be observed.

Controls affecting the display of the colour flow signals

Colour gain

Colour is displayed if the amplitude of the Doppler signal amplitude is above a threshold value (Figure 10.6). The level of the threshold can be adjusted by use of the colour gain control. If the gain is too low then no colour is displayed, whereas if the gain is set too high, then noise may be displayed as a mosaic pattern throughout the image. This control is adjusted for each patient in a similar manner to spectral Doppler gain. Figure 10.14 shows flow in the common carotid artery where the gain is too low, correct, and too high.

Colour write priority

This control ensures that pixels with high B-mode echo values, likely to arise from tissue, are not displayed in colour. The colour write priority enables the operator to adjust the B-mode echo amplitude threshold, above which colour is not displayed and below which colour data are displayed.

Power threshold

This is a threshold on the calculated power value, with no display of colour if the power is below the threshold.

Flash filter

This is the process whereby the colour flashes from transducer or tissue motion are removed. Few details of these are available from manufacturers; however, one possibility is that flash filters are based on the detection of very rapid changes in the Doppler signal level. These could be produced by motion of the transducer with respect to the patient, breathing, cardiac motion and

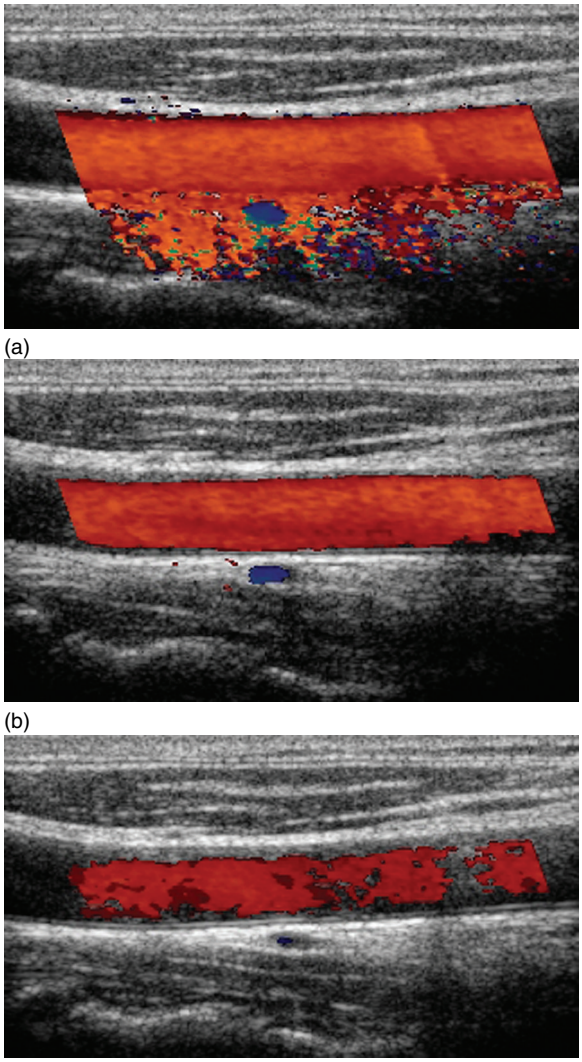

(a)

(b)

(c)

Fig. 10.14 Flow in the common carotid artery at different gain settings. (a) Gain too high with noise in the tissue; (b) gain correct with colour contained within the artery; (c) gain too low with inadequate colour coverage in the artery.

bowel movements. The operator usually has the choice of turning the flash filter on or off.

Use of controls

The operator chooses the probe and the application from the pre-set menu. This provides default values relevant to the typical patient for the application selected. It is usual to start the examination using B-mode in order for the operator to familiarize themselves with the anatomy, then progress to colour flow. The operator adjusts the size of the colour box to cover the desired region. With a linear-array transducer, it is also possible for the operator to steer the colour box in order to optimize the colour Doppler angle of insonation. The mode is selected (Doppler or power), and the scale and baseline are adjusted to enable display of the blood velocity range. The colour gain is adjusted so that as much of the vessel as possible is filled with colour, but at the same time avoiding excess noise in the tissue. A further refinement for colour Doppler is to adjust the probe angulation and steering angle to ensure that a Doppler angle away from 90° is obtained. This avoids colour drop-out due to the action of the clutter filter on the low Doppler shifts obtained near to 90°. This limited sequence of control adjustments is often all that is needed in a colour flow or Doppler tissue examination, although the user can alter other controls, if necessary.

Features of colour flow

Penetration

The penetration depth is the maximum depth at which Doppler signals can be distinguished from noise. Improved penetration can simply be achieved by turning up the output power. High-output power is recognized as being hazardous to the patient, as described in Chapter 12. For targets at the deepest depths, the returning ultrasonic signal and hence detected Doppler signal is of small amplitude due to the effect of attenuation within the tissue. The task of the Doppler system in this situation is to distinguish the true Doppler signal from noise, and good machine design uses low-noise components. A standard signal-processing method to improve the detection of the signal is to combine a large number of measurements by some form of averaging. In this process, the signal size increases in comparison with the random noise that tends to cancel out, hence the signal can be more easily detected from the noise. For Doppler systems, the averaging can involve the use of a larger ensemble length or frame averaging; however, both of these are done at the expense of a lower frame rate.

Display of low velocities

The most important components determining the visualization of low velocities are the clutter filter and the PRF, as noted above. Optimization of machine settings in order to detect low velocities is achieved by increase in the ensemble length, by the use of persistence and

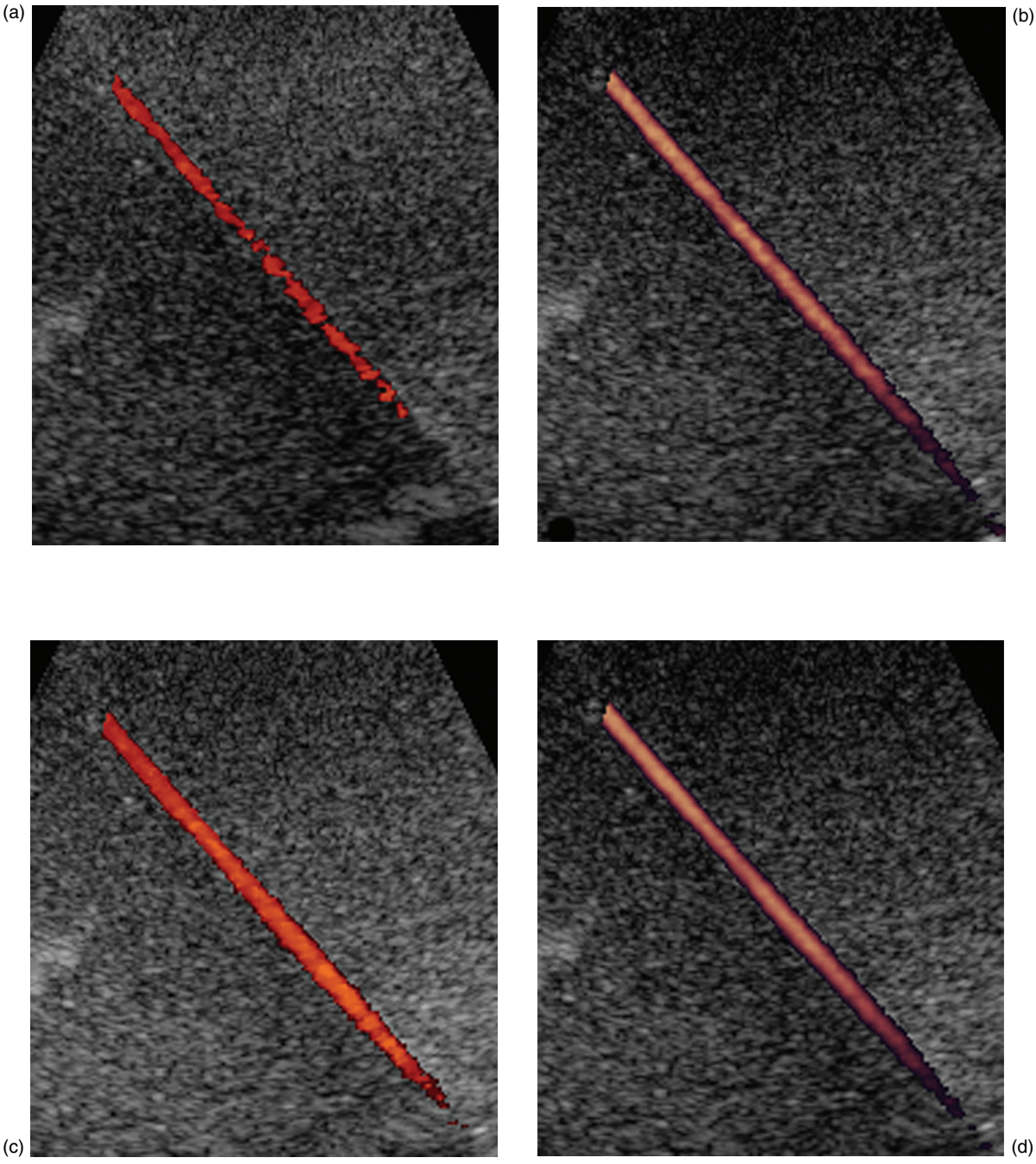

Fig. 10.15 Effect of colour imaging mode and persistence. Images are shown in a 1-mm-diameter vessel taken using a C5–2 curvilinear probe. With persistence turned off, (a) Colour Doppler shows drop-out, (b) power Doppler shows a continuous line of colour with no drop-out. With persistence at maximum a continuous line of colour with no drop-out is shown for (c) colour Doppler and (d) power Doppler.

by the decrease of the PRF and clutter filter. This is performed automatically by selection of the clinical protocol and adjustment of the 'velocity scale', but some systems may allow access to these controls directly by the operator in a hidden menu.

Display of flow in small vessels

The first requirement to display flow in small vessels is that the spatial resolution of the B-mode and colour flow images is adequate. It is the display of flow in small vessels where the superior characteristics of power Doppler over colour Doppler are demonstrated. Figure 10.15 compares colour Doppler and power Doppler images in a simple flow test device consisting of a 1-mm-diameter vessel embedded in tissue-mimicking material. The image of flow in the vessel should ideally be a continuous line of colour.

In Figure 10.15a, b the persistence is set to zero. The colour Doppler image is not continuous, instead showing drop-out at several locations. This is associated with variations in the calculated mean frequency produced by the autocorrelator. Values of mean frequency that are low will trigger the blood–tissue discriminator, and colour will not be displayed. The calculated Doppler power is less variable than the calculated mean frequency, so the power Doppler image of the vessel demonstrates less drop-out.

In Figure 10.15c, d the persistence is increased to maximum for both colour and power Doppler. With this increased persistence both mean frequency and power demonstrate less variability, resulting in fewer values falling below the blood–tissue discriminator threshold.

From this simple example it can be seen that when the same machine settings are used for power and colour Doppler, the penetration depth is similar for the two modalities. The improved detection of small vessels using power Doppler in clinical practice is due to the use of higher frame averaging, and also to the inherently less confusing nature of the power Doppler image, as there is no aliasing effect and only a limited angle dependence (Figure 10.16).

Display of complex flow patterns

The ideal colour Doppler display would provide images in which the displayed colour was related to the velocity of the blood in the scan plane. Similarly, the ideal power Doppler image would provide a display in which the colour was related to the presence or absence of moving blood. There are two phenomena that limit the

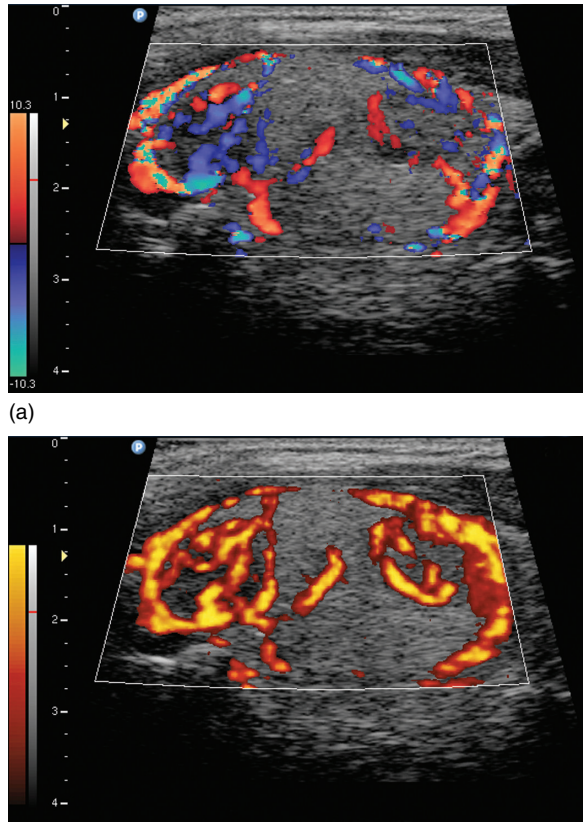

Fig. 10.16 Colour (a) and power (b) Doppler images demonstrating thyroid nodules. The power Doppler image shows the anatomy more clearly than the colour Doppler image.

ability of the technology to provide these ideal displays; angle dependence and aliasing.

The Doppler shift arises primarily from blood motion in the direction of the ultrasound beam; this leads to the cosine dependence on the angle between the beam and the direction of motion, when Doppler frequency is calculated (see Chapter 7). Consequently, colour Doppler demonstrates an angle dependence. In Figure 10.17b, the flow on the left side of the image is displayed as towards the transducer, in red, and the flow on the right is displayed as away from the transducer, in blue. At first glance, the image gives the appearance that the flow is changing direction mid-way across the image; however, careful consideration of the changing angle of insonation allows the observer to establish that the flow is all in one direction. The flow in the centre of the image is not detected due to the poor Doppler angle resulting in small Doppler shift frequencies that are removed by the clutter filter. The power Doppler image maintains a uniform colour over a wide range

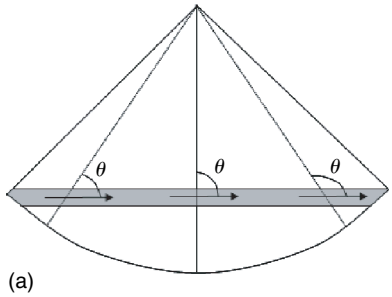

(a)

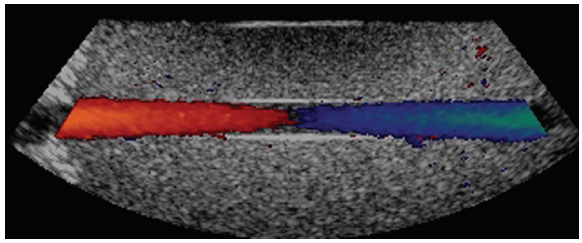

(b)

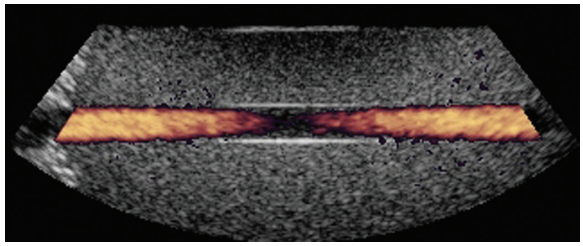

(c)

Fig. 10.17 Angle dependence of colour and power Doppler images. (a) A straight tube is shown in which the flow is identical at all points along the tube. For the sector scanner, the angle θ between the beam and direction of motion varies from the left to the right side of the image. (b) The colour Doppler image shows variation in the displayed colour throughout the length of the tube, with no colour shown at 90°. (c) The power Doppler image shows little variation of displayed colour, except for 90°, when no colour is displayed.

of angles (Figure 10.17c); however, when the angle approaches 90°, the power signal may be lost. This may be understood with reference to Figure 10.18, which shows the received Doppler signal at different angles. As the angle increases the Doppler frequencies fall, but the total Doppler power, indicated by the area under the curve, remains constant. Near 90°, there is some loss of signal due to the clutter filter, and the power reduces. The angle dependence of directional power Doppler is similar to that for power Doppler, with the difference that flows towards and away from the transducer are coded with different colours. Display of tortuous

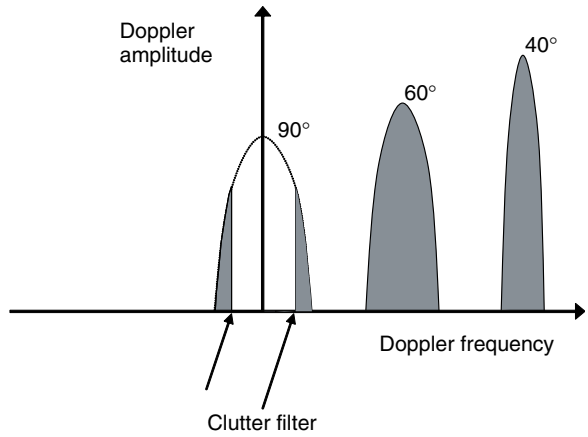

Fig. 10.18 Effect of a change in angle on the Doppler spectrum, at constant blood velocity. As the angle decreases from 40° to 60°, the Doppler frequency shift decreases, but the power of the Doppler signal, represented by the area under the curve, remains approximately constant. However, at angles close to 90°, the Doppler frequencies are low and may be removed by the clutter filter, which causes a reduction in the Doppler power. In the figure, there is only partial removal of the Doppler signal at 90°.

vessels is often confusing using colour Doppler due to the angle dependence (Figure 10.19), whereas the corresponding power Doppler image has a uniform hue and is less confusing.

Increase in blood velocity results in increase in Doppler frequency shift up to a maximum value set by the Nyquist limit (PRF/2). For frequency shifts above the Nyquist limit, there are two consequences of aliasing; the Doppler frequencies are inaccurately calculated, and the direction of flow is inaccurately predicted.

As the Doppler frequency is not estimated in power Doppler, aliasing will not affect the displayed image. An alternative way of understanding this is illustrated in Figure 10.20, which shows that the Doppler shift increases up to a critical velocity. Above this critical velocity aliasing occurs. However, in all cases the area under the curve, which represents the Doppler power, is the same. However, directional power Doppler does suffer from aliasing as directional information is calculated.

Both angle dependence and aliasing can occur in the same image. A flow model of a diseased artery may be used to illustrate these effects. In Figure 10.21b, the increase in mean Doppler frequency within the region of the stenosis is seen as an orange-coloured area, and there is jet formation and recirculation in the post-stenotic region. Increase in flow rate (Figure 10.21c) leads to

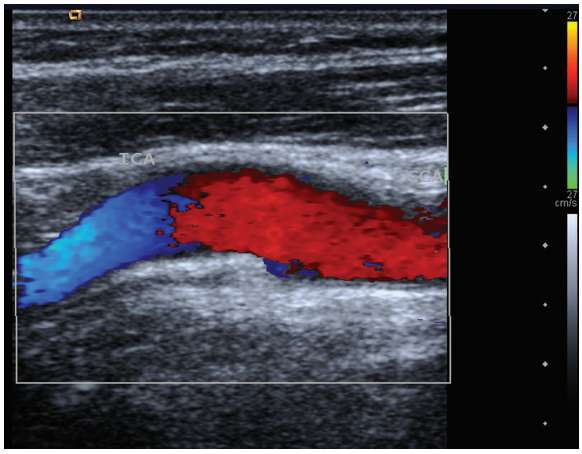

(a)

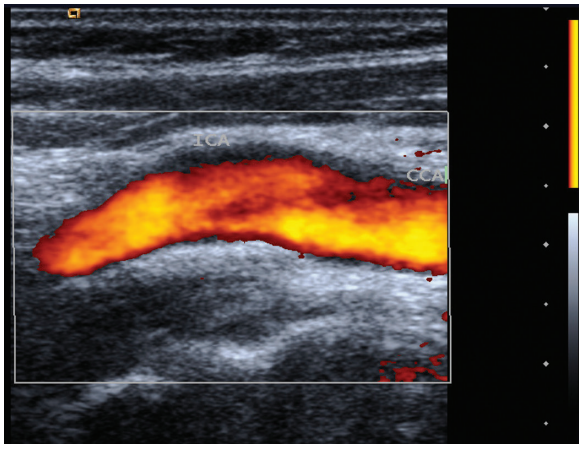

(b)

Fig. 10.19 Display of a tortuous carotid artery using colour Doppler and power Doppler. There are large changes in blood flow direction along the course of the carotid artery. This results in large changes in the displayed colour for the colour Doppler display (a), but only minor changes in colour for the power Doppler display (b).

aliasing, where the previous orange-coloured region is now coloured green. The corresponding power Doppler images are uniformly coloured. At the low flow rate (Figure 10.21b), there is a gap in the region of recirculation, where the velocity is low. The gap is filled when the higher flow rate is used (Figure 10.21c). The practical consequence of this last observation is that considerable care must be taken when using poor filling of the vessel in the power Doppler image as evidence of thrombus.

Display of rapidly changing flow patterns

The ability of the colour Doppler image to follow faithfully the changing flow pattern is determined by frame

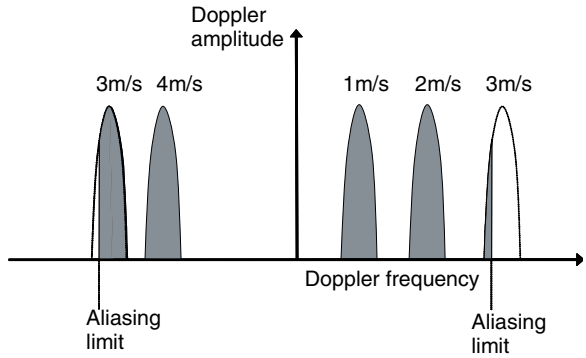

Fig. 10.20 Colour aliasing explanation. As velocity increases from 1 to 2 m s^{-1} the Doppler shift increases. However, when the aliasing limit (or Nyquist limit) is reached, at approximately 3 m s^{-1}, in the figure, the Doppler frequency is not estimated correctly. The Doppler signal for the velocity of 3 m s^{-1} consists of two components, one with a positive Doppler frequency and one with a negative Doppler frequency. The combined Doppler power, represented by the area under the curve of the combined signals, remains unchanged. Consequently, the power Doppler image is insensitive to aliasing.

rate and persistence. As noted above, the frame rate is maximized by the use of a small ensemble length, restriction of the colour box size and (in some systems) by the simultaneous acquisition of multiple beams. For display of lower velocities, a larger ensemble length is required, and the frame rate reduces accordingly. A degree of persistence is acceptable and also desirable as the effect of noise is reduced, and the visualization of small vessels is improved. Although it is possible to observe changes in blood flow during the cardiac cycle using the colour flow image, this task is best performed using spectral Doppler.

In power Doppler, there is no information on the dynamic nature of blood flow, and persistence is set high to obtain maximum noise reduction.

Artefacts

Many of the features of B-mode images are applicable to colour flow images, as the propagation of the ultrasound pulse through the tissue will obey the same physics, whether it is used to produce a B-mode image or a colour flow image. Some of these artefacts have been described earlier in this chapter. The purpose of this section is to list all the major artefacts in one location. Papers which provide further useful reading on colour flow artefacts are those by Hoskins and McDicken

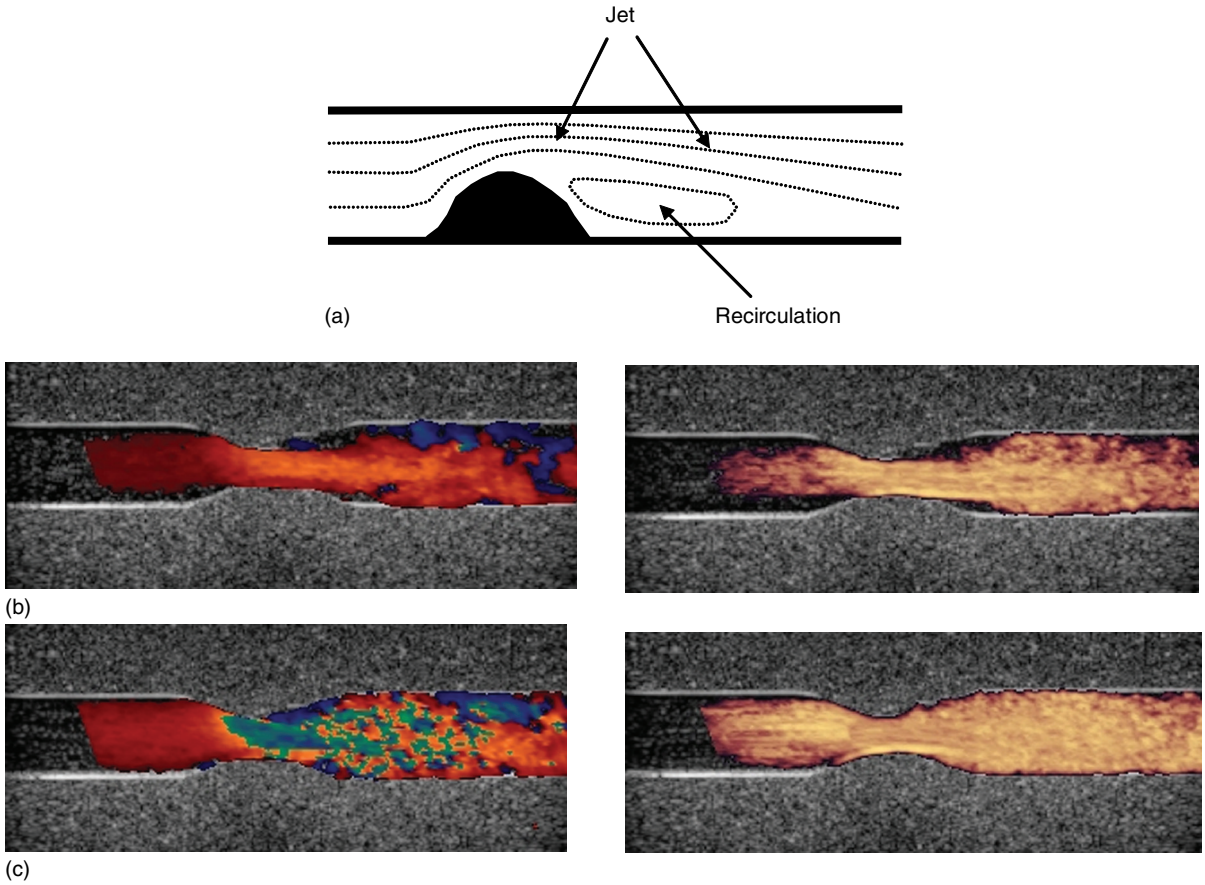

Fig. 10.21 Angle dependence and aliasing demonstrated in a stenosis flow model. (a) In the flow model, there is a localized narrowed region that mimics a stenosis. A blood-mimicking fluid is pumped from left to right through the tube. As the fluid passes through the stenosis, there is increase in velocity with the formation of a jet. In the post-stenosis region there are regions of recirculation, vortex shedding and turbulence. (b) Low flow rate. For the colour Doppler image (left), there is alteration of colour throughout the image; however, the power Doppler image (right) is of a uniform colouration. The jet is clearly seen; however, the fluid in the region of recirculation has low velocity, and the Doppler shift frequencies are suppressed by the clutter filter, resulting in an absence of colour in this region. (c) The flow rate is doubled, resulting in a doubling of velocities. There is aliasing at the narrowest point within the stenosis and in the post-stenotic region for colour Doppler (left). The power Doppler image (right) is unaffected by aliasing and remains of a uniform colouration. The Doppler frequencies from the region of recirculation are now high enough to be not suppressed by the clutter filter, and both colour and power Doppler images no longer demonstrate a flow void.

(1997), Nilsoon (2001), Kamaya *et al.* (2003), Arning *et al.* (2004), Campbell *et al.* (2004) and Rubens *et al.* (2006).

Shadowing

There is reduction in the amplitude of the Doppler signal whenever there is attenuation of the ultrasonic pulse. Hence, colour signal is lost when there is an intervening high-attenuation region or a region of high reflectivity, such as a calcified area or bowel gas. This is similar to the production of shadows on a B-mode image.

Ghost mirror images

Ghost mirror images may be produced by partial reflection of the beam from a highly reflecting surface.

Angle dependence

The displayed colour is dependent on the angle between the beam and the direction of motion as illustrated in Figures 10.17 and 10.19:

- *Colour Doppler:* displayed colour depends on the cosine of the angle.
- *Power Doppler:* little angle dependence on angle except near 90°, where the Doppler frequencies fall below the clutter filter if the velocity is too low.
- *Directional power Doppler:* similar to power Doppler, except it is noted that flow towards and away from the transducer is coded in different colours.

Aliasing

As explained in Chapter 7, the maximum Doppler frequency shift that can be estimated is equal to PRF/2. Higher blood or tissue velocities will be displayed colour-coded with opposite direction:

- *Colour Doppler and directional power Doppler:* both suffer from aliasing.
- *Power Doppler:* does not suffer from aliasing.

Drop-out

This is loss of colour due to the variable nature of the calculated mean frequency or power. If this is high, it is possible that the estimated mean frequency or power will fall below the threshold value used in the blood–tissue discriminator. When this happens, the system does not display colour. For colour flow, the effect is most marked at low velocities and in small vessels.

Noise

There are several types of noise present on the colour image:

- *Electronic noise:* this is produced within the colour flow system electronics. If the colour gain is set too high, the noise will be displayed as colour in regions of tissue in which there is no flow.
- *Clutter breakthrough:* highly echoic regions will produce a large clutter signal which may not be suppressed by the clutter filter. This produces a region of random colour noise in tissue. This artefact has been used clinically, in the detection of calcified regions such as kidney stones, where it is known as the 'twinkling artefact' (Kamaya *et al*. 2003, Rahmouni *et al*. 1996). The artefact may be removed by suitable adjustment of the colour-write priority.
- *Tissue vibration:* a second source of clutter breakthrough arises from moving tissues (cardiac motion, vessel wall motion, bowel movement). These produce Doppler shifts which may be above the level of clutter filter, hence producing patterns of colour not associated with blood flow within regions of tissue.
- *Audio sound:* sound that is produced within the body is indistinguishable from the Doppler shifts produced from blood and tissue. The sound is detected and displayed as regions of colour within tissues. This most obviously occurs during scanning of the neck when the patient speaks; the audio waves pass through the adjacent tissues and are detected by the colour flow system. Sound in the form of 'bruits' arising from turbulent flow in diseased arteries also gives rise to colour noise within tissues.
- *Flash artefacts:* these are false areas of colour on the colour flow image, which are produced when there is movement of the transducer with respect to the tissue. Some systems are able to remove these artefacts by use of a 'flash filter'.
- *Speckle:* the variation in the autocorrelator estimate of mean frequency and power gives rise to a noise superimposed on the underlying colour and power Doppler images; this noise is called 'colour speckle'. This speckle pattern may be reduced by the use of persistence.

Colour display at vessel–tissue boundaries

Ideally the power Doppler image would show a uniform colour up to the edge of the vessel. For colour Doppler, it is known that the blood velocities are low at the edge of the vessel, so that the displayed colour should show this. In practice, there are a number of effects that will lead to incorrect display of colour:

- *Partial volume effect:* at the edge of vessels, the colour sample volume is located partially within the vessel and partially in the tissue. This effect will lead to reduction in Doppler signal amplitude which will cause a change in displayed colour seen on power Doppler images. For colour Doppler, it is the mean frequency in that part of the sample volume that is located within the vessel which is displayed, so the displayed colour is not affected (Figure 10.22).

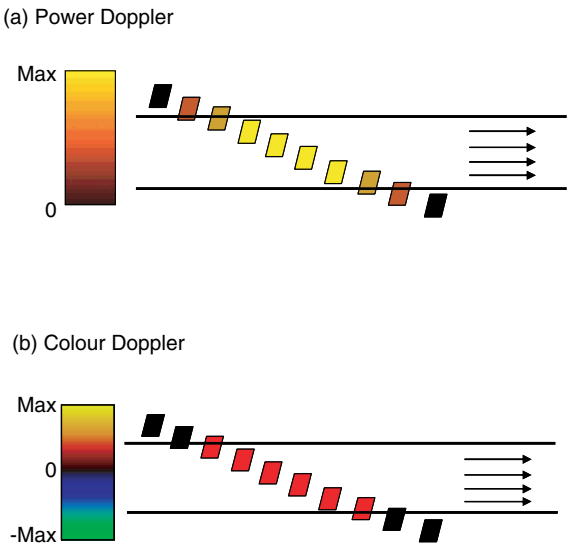

Fig. 10.22 Partial volume effect. In the vessel, it is assumed that all of the blood is moving at the same velocity. (a) Power Doppler – change in colour at the edge of a vessel. (b) Colour Doppler – no effect on the displayed colour.

- *Image smoothing:* if there is any smoothing in the colour image, by averaging of adjacent pixels or by interpolation, this leads to false colours at the edge of vessels for both colour Doppler and power Doppler.
- *Clutter filter and blood–tissue discrimination:* both of these will act to prevent the display of colour at the edge of vessels as the velocities (and hence Doppler frequency shifts) are low, and the tissue signal strength is high.

Measurements

This short section covers measurements, which are occasionally made from the colour flow image by clinical users, though it is noted that the vast majority of quantitative measurements are made using spectral Doppler. In research studies, quantitative analysis of the colour flow image using off-line computer analysis is widely performed; however, these techniques have yet to impact on clinical practice.

Single-site velocity measurement

Some colour flow systems have the capability of showing the mean-frequency value at a specific location chosen by the operator. This can be converted to a velocity using the same angle-correction techniques that are used in spectral Doppler. This information is occasionally useful in clinical research studies, e.g. estimation of the degree of arterial stenosis from peak velocity obtained from the colour Doppler image rather than the spectral Doppler waveform.

Quantitative analysis of flow patterns

Blood flow patterns are known to alter considerably in disease, as described in Chapter 8. However, there is little attempt to use the colour Doppler images to provide quantitative information on the colour flow patterns in disease, as there are not yet methods of quantification which have been shown to be clinically useful.

Volume flow

Calculation of volumetric flow requires estimation of the vessel cross-sectional area and the mean velocity. Ideally, the mean velocity and cross-sectional area should be estimated throughout the cardiac cycle to account for the expansion of the arteries which occurs during the cardiac cycle. If colour flow images are obtained with the vessel imaged in the longitudinal plane, the velocity profile of the vessel can be obtained from the colour flow image, and the diameter obtained from the B-mode image. Estimation of the mean velocity requires an assumption that flow is symmetric within the vessel (i.e. all points at the same radius have the same velocity). Cross-sectional area is obtained from measured diameter assuming that the vessel has a circular cross section. Multiplication of the measured area and mean velocity give the volume flow.

This technique makes a number of assumptions, such as circular vessel, symmetric flow patterns, which limit its use to normal or relatively undiseased vessels. In practice, there is little call for volumetric flow measurement, and this method is not widely used.

Time-domain systems

The essential features of this technique are described in Chapter 7, where it is noted that the change in target depth between consecutive echoes is estimated. Target velocity is then calculated by dividing the change in depth by the pulse repetition interval. The time-domain approach was initially described by Bonnefous and Pesque (1986). It has been used in commercial colour flow systems, and is used for tissue Doppler on some systems.

The time delay is calculated by comparing the echo pattern of consecutive transmission pulses by a

mathematical technique called 'cross-correlation'. This process is carried out by sliding one line of echoes past the other in a series of steps or time shifts, comparing the lines at each step. The time shift which gives the closest correlation for each part of the line gives a measure of how the corresponding target has moved between pulses. This method relies on the detailed echo pattern shifting as a whole, but not changing in its overall shape. However, as a region of tissue or blood moves, the echo pattern will change in overall shape as it moves further away from its original site. This is associated with changes in the relative position of the scatterers as the blood or tissue moves, and also changes in the location of the red cells with respect to the transducer. The change in echo shape is called 'decorrelation', and after a certain distance the echo pattern has changed so much from the original echo pattern that the ultrasound machine cannot measure the time difference between the current and previous echo.

The time-domain method has a number of features which lead to differences in performance compared to the phase-domain method:

- *Aliasing:* as the time delay between pulses is measured, the technique does not suffer from aliasing. The upper limit of velocity detection is associated with the decorrelation described above.
- *Accuracy:* the time-domain method calculates velocity more accurately than the autocorrelator, for the same ensemble length. Consequently, for the same accuracy, the time-domain approach requires a smaller ensemble size, with gains to be made in either frame rate or line density. However, modern colour flow systems use '2D autocorrelation', and the accuracy for this technique is comparable with the time-domain approach, so that this advantage is no longer present.

The time-domain technique calculates the movement along the beam. In other words, only the component of velocity in the direction of the beam is calculated. The time-domain technique is, therefore, dependent on the angle between the beam and the direction of motion.

B-flow

As discussed in Chapter 7, the backscatter signal from blood is at a very low level, hence appears dark on B-mode imaging. However, there are echoes present within blood vessels, and the echo pattern moves as a result of blood flow. If the B-mode gain is increased then these patterns can sometimes be seen. Analysis of the moving echoes has been used to obtain information on blood velocities in research studies (Bohs and Trahey 1991, Trahey *et al.* 1987).

In B-flow imaging the echoes from moving tissues are enhanced. Non-moving regions of blood or tissue are displayed as dark, and regions where the velocity is high are displayed bright (Figure 10.23a). When viewed in real time, or in video format, an impression of flow is obtained. The B-flow method is based on a pair of coded pulses, one pulse the complement of the other. Addition of the echoes from stationary tissues results in cancellation. However, any slight difference in the signal arising from movement will result in a signal which can be displayed. The technique is dependent on the velocity, where higher velocities are displayed brighter, since higher velocities will be associated with greater difference between the echo pair. The B-flow image may be displayed alone (Figure 10.23a), or if desired the B-mode image can be mixed in to produce a more uniform display in which tissue and blood have similar brightness levels (Figure 10.23b). Greyscale B-flow imaging is not quantitative in that it does not measure blood velocity. From a static B-flow image the blood may be hard to distinguish from the tissue, and this is best done by video playback, where movement allows a much clearer distinction of the vessel. B-flow is claimed to have a number of advantages over colour flow, especially that the display is not angle-dependent, it does not suffer from aliasing and the frame rate is higher. Several studies have compared B-flow with existing ultrasound modalities in the assessment of degree of stenosis (Bucek *et al.* 2002, Clevert *et al.* 2007).

It is also possible to modify the B-flow technique slightly to obtain colour B-flow images. Typically two pairs of pulses are used to generate two B-flow signals which are then processed using the colour flow processor to provide a rough indication of velocity and direction. The estimated velocity is not as accurate as would be obtained using 10–12 pulses typical of true colour flow. The velocity and direction information is then used to colour code the B-flow data (Figure 10.23c). This method is designed to retain the high-resolution, high-frame-rate capability of B-flow, while also allowing easier distinction of the vessels from the tissues by the use of colour.

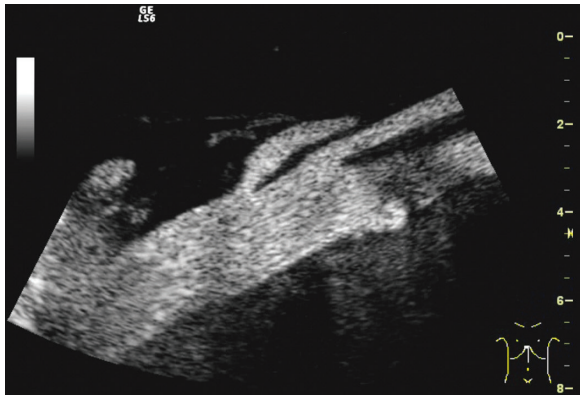

(a)

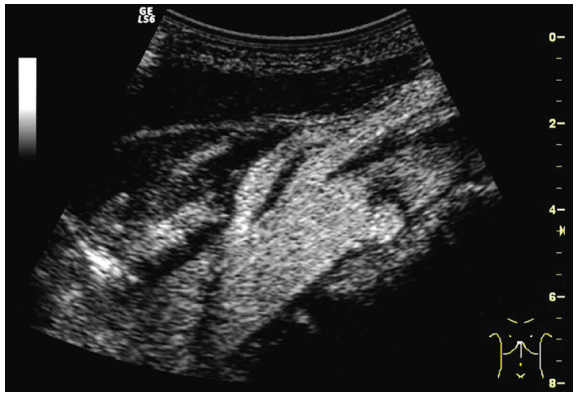

(b)

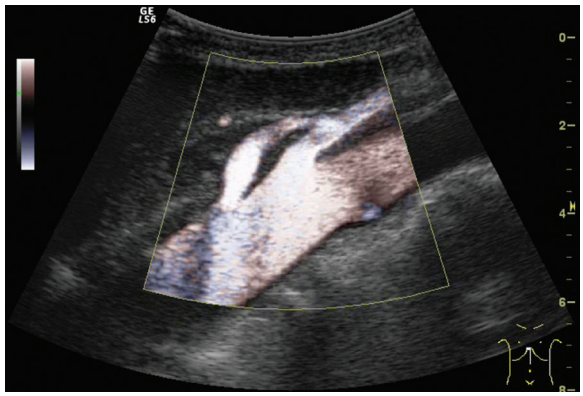

(c)

Fig. 10.23 B-flow image of the celiac trunk: (a) background off, (b) background on, (c) colour B-flow with background on. Images provided by courtesy of Dr. Seeger, University Hospital Kiel, Germany.

Doppler tissue imaging (DTI)

The motion of tissues is traditionally observed using B-mode and M-mode imaging. These methods have been most commonly used to assess the motion of heart valves and the heart wall. It is also possible to obtain information on motion by using the Doppler effect, where it is known as Doppler tissue imaging or DTI (McDicken *et al.* 1992). The DTI mode is a modification of the colour Doppler mode described above for blood flow. Lowering the sensitivity results in recording of signals from the moving tissues rather than from blood, which appears as black on the DTI image. The velocity scale is also lowered in order to account for the much lower velocities present within the tissues compared to the blood. An example of a DTI image from the heart is seen in Figure 10.24. On modern ultrasound machines it is not necessary to adjust the colour flow controls in order to activate DTI. Instead the operator activates DTI directly, and sensitivity, velocity scale and other machine settings are automatically updated.

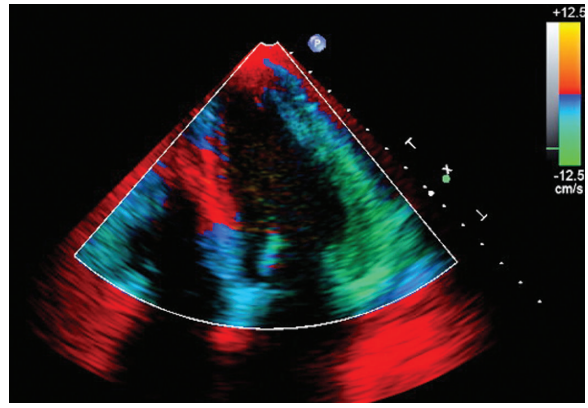

Fig. 10.24 DTI of the heart.

In addition to real-time 2D imaging, it is also possible to acquire DTI M-mode data. This is analogous to the greyscale M-mode trace. In DTI M-mode, the ultrasound beam is fixed in a direction of interest through the tissues and the velocities at different depths are presented on the screen on a vertical line, which is swept across the screen (Figure 10.25) (Fleming *et al.* 1996). Having obtained the velocity information at each pixel in the image, it is possible to estimate how much the tissue has been stretched or compressed (strain) and how fast the tissue is stretched or compressed (strain rate) (Abraham *et al.* 2007, Fleming *et al.* 1996). In clinical use the DTI technique is mostly used in cardiac applications (Abraham *et al.* 2007), though it is possible to use DTI for the study of arterial motion.

Although DTI has been available on commercial ultrasound systems for about two decades it is not

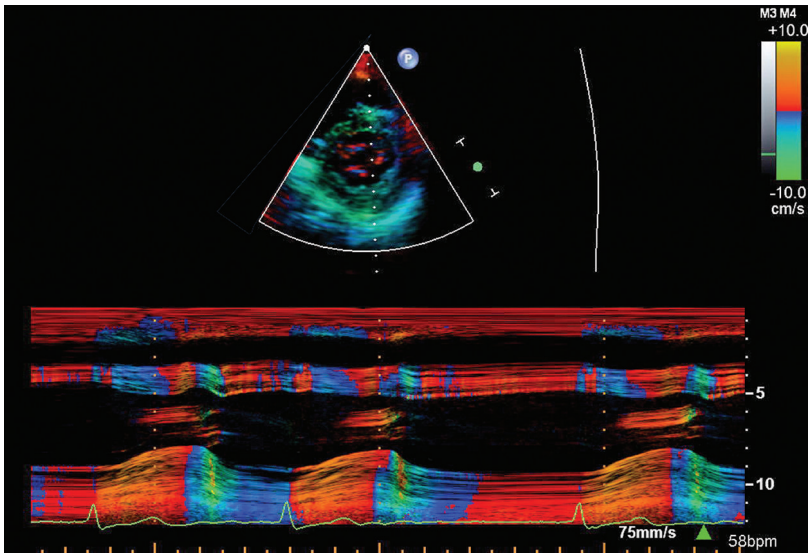

Fig. 10.25 DTI M-mode scan of the heart.

widely used in clinical practice. A large amount of velocity information is presented when real-time DTI is acquired, and it is often necessary to replay this slowly to appreciate the wall motion. The DTI mode also suffers from some of the same limitations as pulsed-wave Doppler for blood flow, in that it is possible to generate aliasing, and there is an angle dependence of the displayed data.

Questions

1. What quantities are displayed in colour Doppler and power Doppler?
2. What three quantities does the colour flow processor calculate for each pixel of the colour flow image?
3. What is the purpose of the blood–tissue discriminator?
4. What is the effect of increase in colour-box depth and width on colour frame rate, and why?
5. What is the effect of increase in persistence on colour Doppler images of pulsatile flow?
6. What is the effect of turning on the flash filter in a colour flow system?
7. Which of these shows strong dependence on the direction (angle) of the blood velocities: (a) colour Doppler, (b) power Doppler, (c) directional power Doppler?
8. Which of these suffer from aliasing: (a) colour Doppler, (b) power Doppler, (c) directional power Doppler?
9. Name three types of noise which might be seen on colour flow images.
10. What adjustments are made to colour signal processing to display tissues for the DTI mode?

References

Abraham TP, Dimaano VL, Liang HY (2007). Role of tissue Doppler and strain echocardiography in current clinical practice. *Circulation*, **116**, 2597–609.

Arning C, Eckert B (2004). The diagnostic relevance of colour Doppler artefacts in carotid artery examinations. *European Journal of Radiology,* **51**, 246–51.

Bohs LN, Trahey GE (1991). A novel method for angle independent ultrasonic-imaging of blood-flow and tissue motion. *IEEE Transactions on Biomedical Engineering,* **38**, 280–6.

Bonnefous O, Pesque P (1986). Time domain formulation of pulse-Doppler ultrasound and blood velocity estimation by cross-correlation. *Ultrasonic Imaging,* **8**, 73–85.

Bucek RA, Reiter M, Koppensteiner I, *et al.* (2002). B-flow evaluation of carotid arterial stenosis: initial experience. *Radiology,* **225,** 295–9.

Campbell SC, Cullinan JA, Rubens DJ (2004). Slow flow or no flow? Color and power Doppler US pitfalls in the abdomen and pelvis. *RadioGraphics,* **24**, 497–506.

Clevert DA, Johnson T, Jung EM, *et al.* (2007). Color Doppler, power Doppler and B-flow ultrasound in the assessment of ICA stenosis: comparison with 64-MD-CT angiography. *European Radiology,* **17**, 2149–59.

Cobbold RSC (2007). *Foundations of Biomedical Ultrasound*. Oxford: Oxford University Press.

Evans DH, McDicken WN (2000). *Doppler Ultrasound: Physics, Instrumentation and Signal Processing*. Chichester: Wiley.

Fleming AD, Palka P, McDicken WN, Fenn LN, Sutherland GR (1996). Verification of cardiac Doppler tissue images

using grey-scale M-mode images. *Ultrasound in Medicine and Biology,* **22**, 573–81.

Hoskins PR, McDicken WN (1997). Colour ultrasound imaging of blood flow and tissue motion. *British Journal of Radiology*, **70**, 878–90.

Kamaya A, Tuthill T, Rubin JM (2003). Twinkling artefact on color Doppler sonography: dependence on machine parameters and underlying cause. *American Journal of Radiology*, **180**, 215–22.

Kasai C, Namekawa K, Koyano A, Omoto R (1985). Real time two-dimensional blood flow imaging using an autocorrelation technique. *IEEE Transactions on Sonics and Ultrasonics,* **32**, 458–64.

Loupas T, Peterson RB, Gill RW (1995a). Experimental evaluation of velocity and power estimation for ultrasound blood flow imaging by means of a two-dimensional autocorrelation approach. *IEEE Transactions on Ultrasonics, Ferroelectrics and Frequency Control,* **42**, 689–99.

Loupas T, Power JT, Gill RW (1995b). An axial velocity estimator for ultrasound blood flow imaging, based on a full evaluation of the Doppler equation, by means of a two-dimensional autocorrelation approach. *IEEE Transactions on Ultrasonics, Ferroelectrics and Frequency Control,* **42**, 672–88.

McDicken WN, Sutherland GR, Moran CM, Gordon LN (1992). Colour Doppler velocity imaging of the myocardium. *Ultrasound in Medicine and Biology,* **18**, 651–4.

Namekawa K, Kasai C, Tsukamoto M, Koyano A (1982). Realtime bloodflow imaging system utilizing autocorrelation techniques. In RA Lerski and P Morley, eds., *Ultrasound' 82*. New York: Pergamon Press, pp. 203–8.

Nilsoon A (2001). Artefacts in sonography and Doppler. *European Radiology,* **11**, 1308–15.

Rahmouni A, Bargoin R, Herment A, Bargoin N, Vasile N (1996). Color Doppler twinkling artefact in hyperechoic regions. *Radiology*, **199**, 269–71.

Rubens DJ, Bhatt S, Nedelka S, Cullinan J (2006). Doppler artefacts and pitfalls (reprinted from Ultrasound Clinics, vol 1, 2006). *Radiologic Clinics of North America*, **44**, 805–35.

Rubin JM, Bude RO, Carson PL, *et al.* (1994). Power Doppler US: a potentially useful alternative to mean frequency based color Doppler US. *Radiology*, **190**, 853–6.

Trahey GE, Allison JW, von-Ramm OT (1987). Angle independent ultrasonic-detection of blood-flow. *IEEE Transactions on Biomedical Engineering,* **34**, 965–7.

Wells PNT (1994). Ultrasonic colour flow imaging. *Physics in Medicine and Biology*, **39**, 2113–45.

Chapter 11

Quality assurance

Tony Evans and Peter Hoskins

Introduction

The term 'quality assurance', or QA, has many definitions and is used in a variety of contexts. Most often it refers to schemes for maintaining the outcomes of some process or activity as measured against a required standard or yardstick. In ultrasound, the outcome is normally the creation of a series of images which have a clinical utility. The concept of QA normally would include a description of the remedial action which needs to be taken when performance falls short of the required standard. Many factors influence the extent to which this is achieved, including: the nature of the clinical problem; the patient; the equipment quality; and the operator's skill level. In this Chapter only the equipment quality aspects are considered and there is no discussion about remedial action which might be taken if a fault is identified. The emphasis is on the detection of a fault or a change in performance at as early a stage as possible in order that technical help can be summoned as appropriate. This approach underpins recent guidance produced within the UK (IPEM in press), and this chapter has been written to be consistent with that guidance.

Standards and guidance

Standards aimed primarily at manufacturers are produced by the International Electrotechnical Commission (IEC) based in Geneva. IEC ultrasound standards are mostly concerned with measurements related to safety (see Chapter 12). There is little IEC guidance relevant to modern systems on image quality or clinically relevant measurements. Standards and guidance relevant to the testing of ultrasound machines in a hospital setting are mostly produced by national bodies; in the UK this is the IPEM, and in the USA this is the AIUM. As noted above, the IPEM has produced recent guidance on the testing of B-mode and Doppler systems (IPEM in press).

Clinical and technical assessment

Since the outcome of any scan is clinical, it is often argued that the assessment of machine performance should also be based on users' judgement of the quality of the images they obtain. Although there is an obvious attraction to this approach, there are also several limitations:

(1) There is likely to be a learning curve; i.e. the user's perception may change as they become more familiar with the machine's controls.
(2) Since the judgement is subjective, it may not be shared by other users.
(3) Subtle changes in performance with time may be missed.
(4) The quality of the clinical image depends on the patient. Since there cannot be a standard patient, there cannot be a standard image quality.
(5) The quality of the image may be influenced by the skill of the operator.

In response to these issues, techniques have been devised to allow QA to be carried out on the machine in the absence of a patient. These techniques often utilize test objects designed to measure specific aspects of machine performance although, for some tests, no equipment is required at all. Any such techniques should satisfy a number of criteria:

(1) They should provide an objective (quantifiable) measure of performance.
(2) The quantity measured should be relevant to the clinical application.
(3) The measurement should be reproducible over a time scale of years.

Diagnostic Ultrasound: Physics and Equipment, ed. Peter Hoskins, Kevin Martin and Abigail Thrush. Published by Cambridge University Press.

(4) The measurement should be sensitive enough to detect a change in performance before it becomes clinically significant.

An extra consideration is whether the aim of the test is to provide some form of absolute performance measure or merely a relative one. An absolute measure is one which allows the performance of a machine to be compared with another one or against a purchase specification. A relative measure is one which is restricted to measuring the machine's performance against that of the same machine at another time. This latter type might be used for asking the question 'Has it gone off?', for example. In general methods and equipment for relative measures are simpler, cheaper and require less expertise than absolute measures. In fact, there is considerable controversy surrounding the reliability and value of the various techniques for achieving absolute performance measurement.

Relative performance measures

A very useful family of scanner tests, often known as air tests, can be carried out with no equipment, as described by Dudley and Chapman (2002) and now incorporated into the latest guidelines from IPEM (in press). The transducer under test is connected to the machine, which has been allowed to warm up and is pre-set to one of its routine clinical settings. Care is taken to ensure that the transducer surface is clean, dry and clear of gel. If the transducer is capable of being operated over an extended frequency range (broadband or multi-frequency) then the frequency should be set to its lowest value. The Overall Gain and TGC are then set to maximum levels and an image such as that shown in Figure 11.1 is obtained. A pattern of reverberation is seen extending well beyond the depth(s) of the focal zone(s). This pattern arises from the large acoustic impedance mismatch between the transducer and the surrounding air giving rise to large multiple and regular reflections such as described in Chapter 5. It is expected that the reverberation pattern will be uniform across the image for any selected depth. Four aspects of performance can be tested with this arrangement.

- Crystal drop out
- Uniformity
- Sensitivity
- Noise.

Crystal drop-out occurs when one or a small number of elements in a linear or curvilinear array are faulty. The result is a vertical line in the image along which

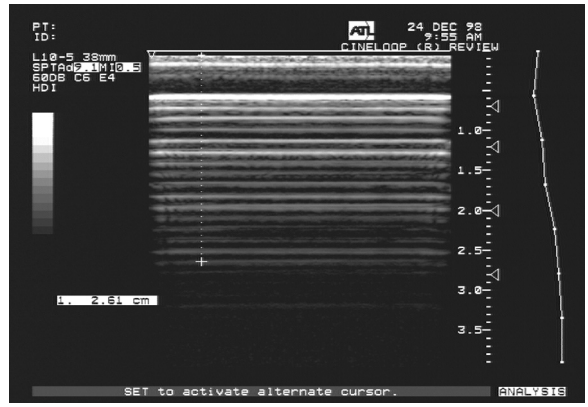

Fig. 11.1 Reverberation pattern seen when a transducer is working into air.

the echo signal is reduced. It can be difficult to spot this because of the use of synthetic-aperture groups but a good way is to take a thin object such as a paper clip and gently run it along the surface of the transducer, to which a small amount of gel has been applied. The clip creates a vertical column of echoes which moves along the array as the paper clip moves (Figure 11.2). If the clip encounters a faulty element section, the brightness of the column displayed will be reduced. It is not necessarily the case that such defects have a significant clinical impact but if drop-out is found in this test, the next step would be to use either a test object (see later) or a clinical image for further evaluation.

It is possible that other small defects in the transducer or scanner itself might be seen by further inspection of this reverberant pattern. In particular the pattern should be uniform across the transducer. Localized bright or dark regions may indicate defects in the transducer lens, for example. In any event, taking hard or soft copy of the pattern at the time of delivery or acceptance will provide a useful reference record against which to measure future performance.

An assessment of sensitivity can be made by examining the depth to which the reverberation pattern extends. Each successive reverberation will be smaller than its predecessor and appear to come from a greater depth. It follows that a change in sensitivity of the transducer is likely to result in a change in the maximum depth. In practical terms, the operator simply has to place a cursor at the depth at which it is perceived that the reverberation pattern ceases and record the depth in question. If the machine develops a fault over time which alters its sensitivity, then it is likely that this depth

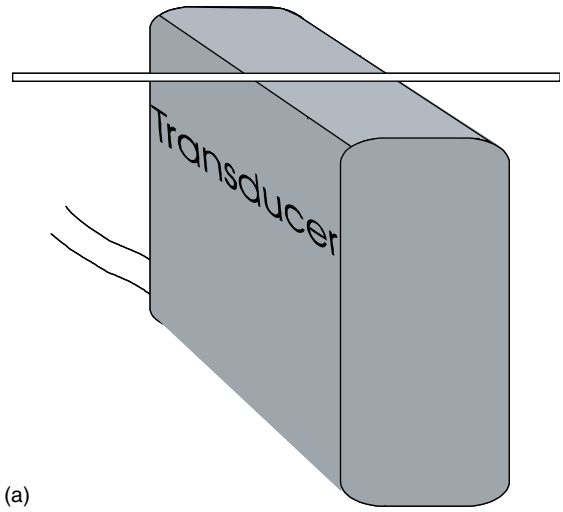

(a)

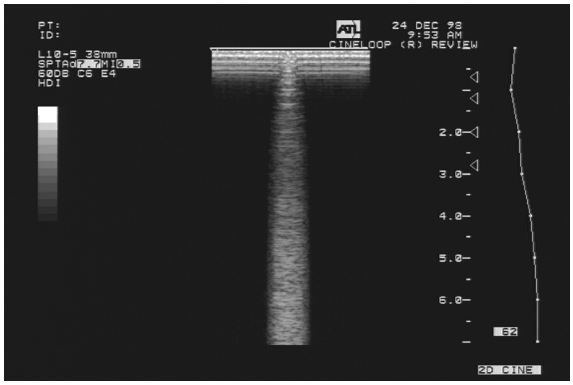

(b)

Fig. 11.2 Use of an unfolded paperclip to search for crystal drop-out. (a) Placement of paper-clip; (b) B-mode image.

value will change. There are several points of caution to be noted, however. First, the Gain and TGC settings must be the same for each occasion when the test is carried out. Second, it is necessary to repeat the test for each transducer on the scanner. Third, it must not be assumed that the test is in any sense absolute. On a different machine a smaller value cannot be interpreted as a poorer performance. Finally, it should be noted that the depth recorded for the limit of reverberation will not necessarily appear the same on hard copy.

The assessment of noise from an air test is a little more complicated. Noise typically appears at depth in the image in the form of fluctuating low-level 'echoes' which do not persist between frames. This distinguishes noise from speckle. If the transducer is stationary, any unchanging pattern is likely to be speckle, whereas signals which come and go in successive frames can be regarded as noise. Noise can obscure real small signals, particularly at depth, and it merits assessment. To do this, the TGC should be adjusted on a real-time image so that noise can be clearly seen at a depth greater than that of the last reverberation. The Overall Gain should then be reduced until the noise vanishes. The challenge now is to devise a means of recording the value of the Overall Gain where this occurs. In some cases the knob may be graduated, or the alphanumeric display on the screen may be used. In many others, it is a challenge to the ingenuity of the operator!

All of the above tests are subject to variations if any of the variety of the extra functions available on modern machines are switched on. These include harmonic imaging, compounding, frame averaging and speckle reduction. It would fair to say that the QA of machines using these functions is not yet well developed.

Absolute performance measures

Parameters

A wide range of devices and techniques for measuring performance have been put forward since ultrasound first became established as clinical tool. These are generally aimed at measuring one or more of a set of performance parameters which are considered to be of clinical importance and they form a sort of 'shopping list' and include the following:

- Axial resolution
- Lateral resolution
- Slice thickness resolution
- Penetration
- Noise
- Contrast resolution
- Geometric accuracy
- Measurement accuracy.

The debate about the clinical relevance of these parameters and the tolerance of their measurement continues. However, a common feature is the use of test objects. The key features of a successful ultrasound test object are:

- The speed of sound in the material matches that assumed by the scanner i.e. 1540 m s^{-1}.
- The attenuation of the material matches that of soft tissue over a wide frequency range.
- The test object material is stable over a long period (years).

- The properties do not depend significantly on room temperature.
- The values obtained are reproducible between operators and between occasions.
- The material contains objects or features which, when imaged, create an echo pattern similar to that of soft tissue.
- The test objects can physically accommodate a wide range of transducer shapes and sizes. The test object needs to be as deep as the anticipated maximum penetration which for low-frequency (3–5 MHz) testing is roughly 15 cm. If only higher-frequency transducers are to be tested, then smaller, and lighter, test objects can be used.

Test object materials and targets

Test objects are typically boxes filled with a tissue-mimicking material (TMM) and this is normally either an aqueous gel or a polyurethane rubber. The gel test objects tend to have a speed of sound closer to 1540 m s^{-1} but they can lose water over time and this limits their shelf life. Polyurethane materials are more stable over time but are less well matched to the desired speed of sound and may exhibit poor temperature stability. In order to create a speckle pattern similar to that of soft tissues, a suitable small-diameter scattering material is added, e.g. graphite powder. The attenuation in the TMM can be controlled by making small changes to the mixture but it is normal for it to be in the range 0.5–0.7 dB cm^{-1} MHz^{-1}. This of course implies that the attenuation increases linearly with frequency. In practice soft tissue does not exhibit exact linearity and neither do TMMs. This limits the useful frequency range of the materials. It should also be noted that simply matching the attenuation of the TMM to tissue does not strictly match the scattering or speckle pattern.

Positioned inside the TMM are targets of some sort. These may be small-diameter nylon filaments, cylinders containing some other material, spheres or other shapes. The filaments are designed to test the resolution of the system. Since this differs in three orthogonal planes (axial, lateral and slice thickness), and also alters with depth, the filament positioning needs to allow for this.

Cylinders are often filled with a material having a scattering characteristic which differs from the surrounding TMM. The purpose is to simulate some clinical feature such as a cyst or a region of pathology. For cyst simulation it is normal to use the same base TMM but to omit the scattering component, thereby creating an echo-free region. Similarly the addition of more scatterers can create a region which is more echogenic that the surroundings and mimic some pathologies. The cylinders are scanned transversely, i.e. across their cross section, and hence the image created is circular. In some cases, a row of cylinders of different diameters is provided and this can be used to identify the smallest simulated cyst which is detectable at that depth. Of course, these 'cysts' also create artefacts such as post-cystic enhancement (see Chapter 5) and this can be used to demonstrate these artefacts and examine the way in which individual machines make them manifest. Cylindrical targets such as these can also be used to assess the contrast resolution of the system.

However, one drawback of using cylindrical targets is that the clarity of their display depends on the axial and lateral resolution of the machine but is largely independent of the slice thickness. The length of the cylinders is normally much greater than the slice thickness resolution. In clinical practice the orientation of a lesion is unlikely to be exactly transverse to the beam and hence test object targets of this type may flatter the machine's capability. One way of addressing this is to use targets which are spherical rather than cylindrical since this achieves symmetry in all planes.

Machine set-up for QA

Whatever test object is being used, it is important to have a clear and reproducible protocol for setting up the machine. The test object should be placed on a firm, flat surface in the scanning room with the lighting dimmed. If the test object has not been stored in the scanning room, it may be wise to leave it for 30–60 minutes to temperature-equilibrate before use. In any case, the machines themselves, including their displays, have a range of warm-up times and consideration should be given as to when to commence the test. A pre-set on the machine is selected which is compatible with the transducer under test and additional functions such as harmonics, compounding etc. should be turned off. The depth display is adjusted so that the useful range of the image fills the screen. At low frequencies this may mean that the bottom of the test object is displayed at the bottom of the screen. In other cases, attenuation will prevent this and the selected depth should be enough to display some noise at the bottom of the machine but only sufficient to demonstrate that this is the true penetration limit. Focusing should be left at the pre-set position unless a local protocol overrides this.

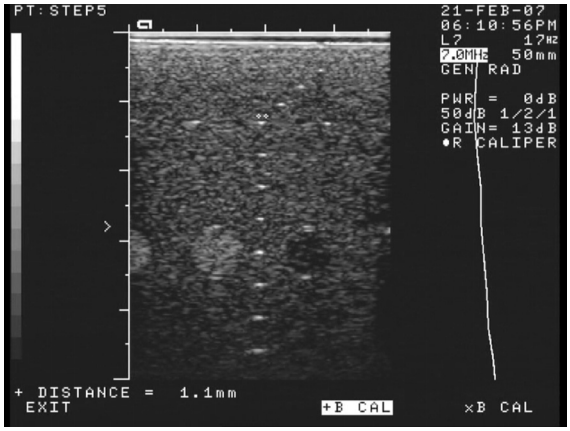

Fig. 11.3 Typical image from a test object.

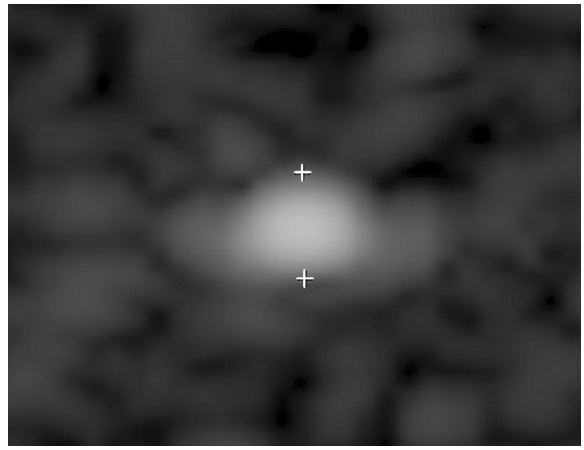

Fig. 11.4 Measurement of axial resolution. A single filament is imaged using a large-scale setting to minimize errors, when its axial extent is measured. Note image has been magnified for the sake of clarity.

If the test object has a well, this is filled with tap water. Scanning gel can be used if this is not practical. The transducer under test is then applied to the scanning surface and the initial image obtained should be examined carefully. The TGC is adjusted to give a uniform speckle brightness over as wide a depth range as possible and the Overall Gain adjusted to achieve a speckle brightness which is typical of the tissue parenchyma for which the transducer is normally used. At this stage it is best to select a section of the test object which has no or few targets. A typical image is shown in Figure 11.3. It should be noted that curvilinear arrays need to be in good acoustic contact over their whole length for these tests and this can be difficult if the well is shallow or insufficient gel is used.

Some practical points are worth mentioning here. If water is used in a test object well, it is common for a type of reverberation artefact to appear associated with echoes from the sides of the well. These are more irritating than misleading, but can often be suppressed by using some damp paper or other absorber at the ends of the well. Secondly, unlike the clinical situation in which pressing harder may help by causing local distortion of the skin surface, it is important not to press too hard on the top surface of the test object. These are typically made of low-density polythene and can be bent and distorted easily. Moreover, any targets inside the object can be pushed out of position if excess surface force is applied.

Spatial resolution measurement

The axial and lateral resolution can be measured from the same frozen image. If the cross section of one of the filaments is scanned and the image frozen and zoomed, an appearance is obtained similar to that in Figure 11.4. Typically a central bright region is seen which has a cigar shape and this may be surrounded by zones which are less bright than the centre but still brighter than the surroundings. The task is to measure the size of the central region. Bearing in mind that the real filament diameter is roughly 0.1 mm or less, the actual displayed size of the central bright region is a measure of the distortion introduced by the system because its resolution is not good enough to display the real filament size. Since the axial resolution is normally better than the lateral resolution, the distortion in the axial plane is less than that in the lateral plane and hence the cigar shape of the image. The axial resolution can be measured using the machine's callipers by measuring the height of the central bright region. It is rarely convenient or practical to use the centre of the calliper cross to mark either the top or the bottom of the region so the recommended approach is to position the first calliper cross such that its vertical arm lies alongside the bright region and its horizontal arm 'rests' on the top of the region and the second cross with its horizontal arm 'rests' on the bottom surface of the bright region.

The lateral resolution measurement is similar except that in this case one side of the vertical arm of the first calliper should be aligned with one side of the bright region and the same side of the vertical arm of the second calliper should be aligned with the opposite side of the region as shown in Figure 11.5. This process should be repeated for all of the filament images in the frozen section to establish the depth dependency of the resolution. The image should then be unfrozen and the procedure repeated until at least three readings are

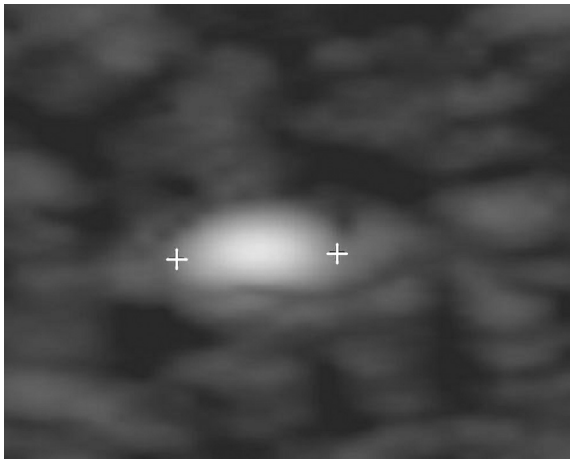

Fig. 11.5 Measurement of lateral resolution using a single wire filament. Note image has been magnified for the sake of clarity.

obtained within ±0.2 mm or 10% of each other, whichever is the greater.

Typically the axial resolution will lie between 0.5 and 1.0 mm and the lateral resolution between 1 mm and 5 mm. Both resolutions will be better at higher frequencies of course, but the lateral resolution in particular will vary with depth. It is expected that the lateral resolution will be best close to a focal zone and hence it is important to record exactly how the focal zones are set up if good reproducibility is to be achieved.

There are two problems with using test objects to assess spatial resolution in this way. First, the decision as to precisely where the central bright zone stops can be difficult and this leads to subjectivity and the consequent inter-operator variability. Second, individual speckle spots can arise in the region of the filament image, merging with the central bright region and influencing the measurement. The former problem can be addressed by good communication and training or alternatively by using computer-aided decision-making (Gibson *et al*. 2001). The latter problem can be minimized by making small (≈0.5 mm) sideways movements of the transducer before freezing the image. The speckle appearance will change on this scale but the filament image should not.

The assessment of slice thickness resolution is more challenging because test objects rarely include filament targets which are positioned in a suitable plane. An ingenious method was devised by Skolnick (1991) which involves scanning a filament column at 45°, as shown in Figure 11.6. It can be shown that the measurements obtained from the wires in this situation are normally a reliable assessment of the slice thickness resolution.

Penetration

The images and sections which are established initially as part of the set-up are suitable for measurement of system penetration. However, it may be more useful to increase the output to a maximum if a true penetration limit is to be established. In either case, the objective is to measure the maximum depth at which echoes arising from scattering structures are detectable. As discussed above for resolution, this measurement has a subjective component. The operator has to determine the depth at which the fine-scale speckle pattern runs out, as is shown in Figure 11.7. Often the speckle pattern is gradually replaced by random noise as the depth increases, and it may be difficult to decide the exact transition point. One useful hint is always to make this measurement in real time without freezing the image. This is because noise changes from one frame to the next, whereas speckle is constant in the absence of transducer or test object movement. If the operator is trying to determine whether a particular pattern is speckle or noise, the 'dancing' of noise signals in real time can be very useful. However, as for the resolution measurement, it has been suggested that penetration measurement values from specific images should be determined by computer rather than humans to improve reproducibility.

Contrast resolution measurement

It is well recognized that the dynamic range and grey-scale transfer curve of ultrasound machines can influence their clinical effectiveness, although there is no clear guidance about how to optimize these for a specific clinical examination. The aim of contrast resolution measurements is to establish the capability of the machine to detect subtle differences in the echogenicity of two targets or regions. To do this, a test object is needed which includes targets of known echogenicity relative to the background TMM. This may take the form of a series of inclusions with scattering coefficients which are in 3-dB steps. Of course, these can be positive or negative steps, i.e. the targets may be either more or less echogenic than their surroundings.

To carry out this test it is necessary to scan a series of suitable objects such as shown in Figure 11.8. A judgement is then required to determine the limits of detectability. Similar issues about subjectivity and the need for computer intervention apply as above.

Geometric accuracy

This is a test to check whether the overall outline shape of an object is preserved when scanned by ultrasound;

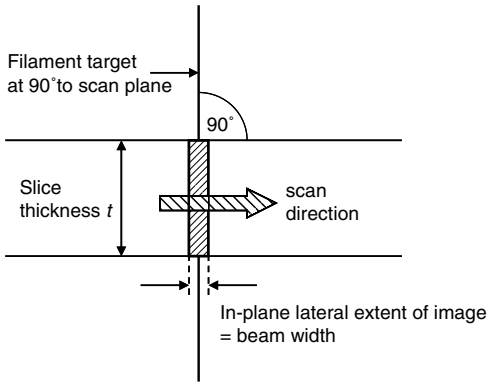

(a)

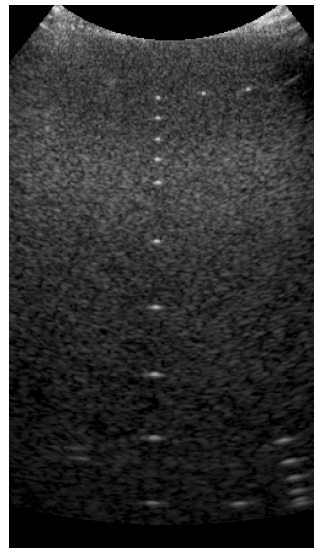

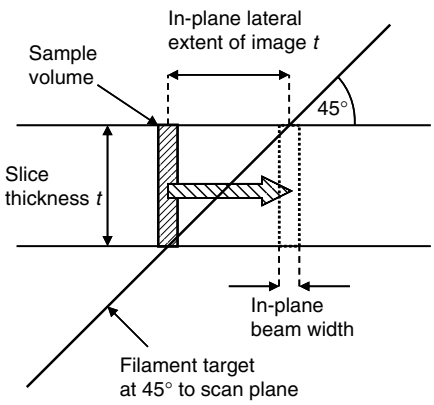

(b)

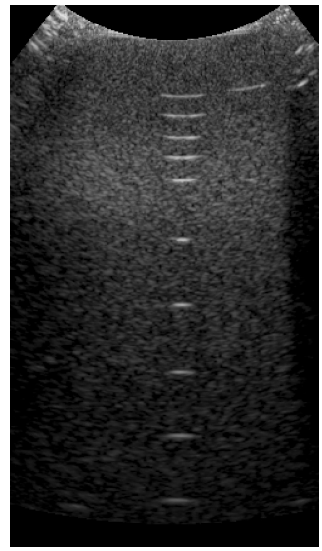

Fig. 11.6 Slice thickness by the Skolnick method. (a) The lateral extent of the filament targets indicates the in-plane beam width, when the scan plane is at 90° to the filament targets. (b) The lateral extent of the filament targets indicates the slice thickness, when the scan plane is rotated to 45° to the filaments. The slice thickness is small only in the out-of-plane focal region.

e.g. is a spherical cyst imaged as having a circular cross section? A grid of filament targets with known separation is needed to do this, such as that shown in Figure 11.9. If the grid is imaged, then the relative lengths of the horizontal and vertical sides should be preserved. Using the machine callipers to check these dimensions is not recommended since a geometric display issue may correspond to a problem in the image memory and hence it is possible for the callipers to record the dimensions correctly while the display is in error. Some external calliper such as a calibrated rule is needed.

Measurement accuracy

The numerous ultrasound clinical examinations which include one or more measurements all rely to some extent on the accuracy of the scanner's measurement system. The accuracy which is needed for clinical safety varies considerably between contexts. For example, the measurement of the length of a kidney need only be accurate to 1 or 2 mm to achieve its clinical purpose, whereas a nuchal translucency measurement in error by 0.2 mm may have significant consequences.

Of course not all measurements are point-to-point linear dimensions. There are examples of perimeters, curve lengths, areas and volumes being measured in different clinical environments. Any QA which is undertaken of measurement accuracy should reflect the demands of the purpose for which the machine is used.

Fig. 11.7 Measurement of penetration. The lower calliper marks the limit of penetration as assessed by the observer.

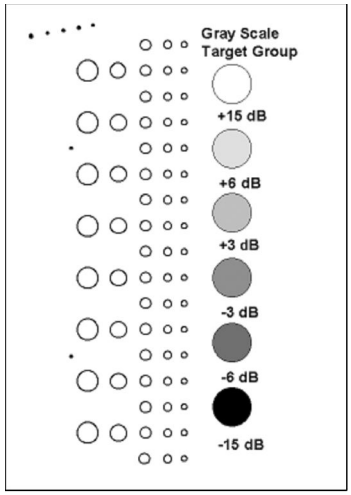

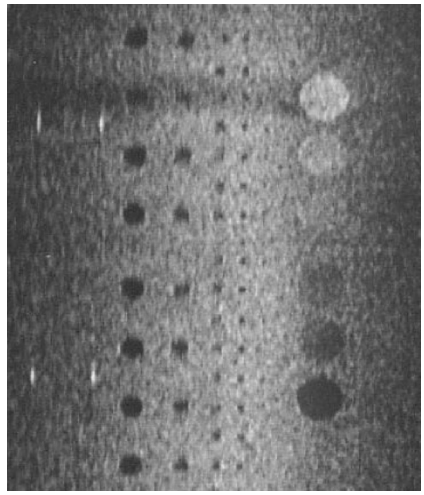

Fig. 11.8 A test object designed to assess contrast resolution. Note that there is mixture of targets with different contrast and cystic targets of different sizes.

In many cases, the same test object with the same wire filaments as described above may be suitable. Manufacturers of test objects will quote the accuracy to which the wires are positioned and hence a calliper measurement can be easily carried out as shown in Figure 11.10. However, the speed of sound in the TMM is critical here as any deviation from 1540 m s^{-1} is potentially serious. Furthermore, if a curved-face transducer is tested, there is the possibility of refraction errors caused by oblique incidence at the test object upper surface. A final problem is that since most wire arrays in test objects form rectangles, they cannot be used to check curved measurement accuracy.

For the above reasons many centres have constructed home-made open-topped test objects for the checking of measurement accuracy. One such device is shown in Figure 11.9. These are made of transparent materials such as Perspex, allowing the wire positioning to be easily checked. The tank must be filled with a liquid with the correct speed of sound such as 9.5% ethanol by volume in water at 20°C (Martin and Spinks 2001) and this may be a little inconvenient since it is difficult to transport without losing liquid.

Recent developments

The principles underpinning the test objects and techniques described above have been established for several decades and throughout that period there have been concerns about their suitability for the intended

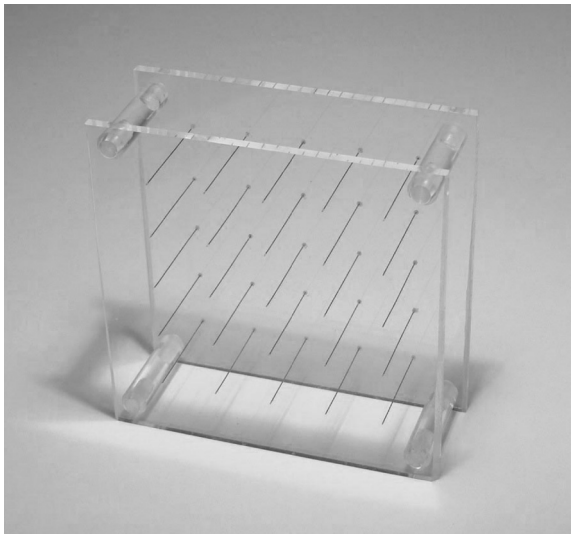

Fig. 11.9 An open-topped test object. The matrix of 0.5-mm-diameter steel pins is mounted between two Perspex plates using 25.0 mm spacing between pins.

purpose. Among the drawbacks identified is the lack of firm evidence which links any of the above parameters to clinical utility or diagnostic accuracy. This may in part be due to lack of resource to generate the necessary evidence but the problems of subjectivity are well rehearsed. Furthermore it seems very likely that a machine which is optimally set up for one clinical examination may well be sub-optimal for another. Faced with these problems, researchers have devised new methods which are aimed at providing a combination of factors rather than a complex array of supposedly independent ones. Two interesting examples are given here.

The Edinburgh pipe phantom

Pye *et al.* (2004) have devised a test based on a test object which contains a number of pipes running diagonally in a fairly conventional TMM. The pipes are created with a wide range of diameters to cover the resolution of scanners over a wide frequency range. They introduced a figure of merit which is based on a resolution integral in an attempt to express the resolution of the machine over a large depth range. There is evidence that older (and presumably poorer) machines perform less well on this test and that a variety of faults can be reliably detected. A typical image is shown in Figure 11.11. This device is commercially available (Precision Acoustics Ltd, Dorchester, UK). The synthesized approach may turn out to have much wider applicability.

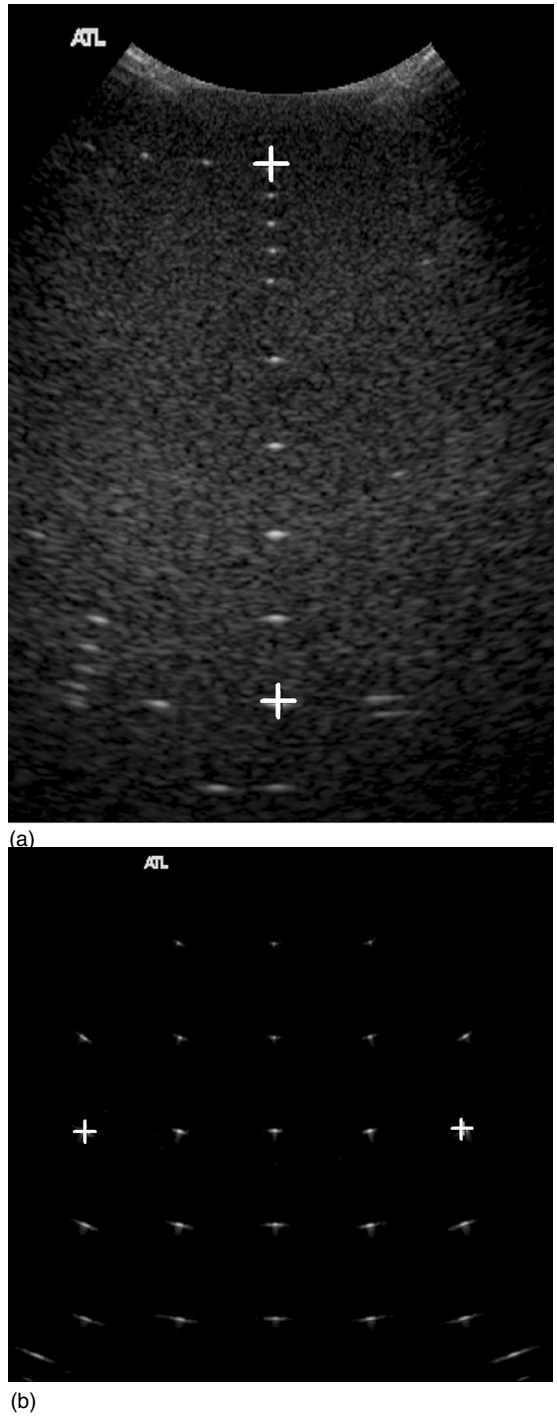

Fig. 11.10 (a) Calibration of axial distance measurements. Target spacing is measured over a large axial distance to minimize positioning errors. (b) Calibration of lateral distance measurements using an open-topped test object. Calliper markers are placed at the centres of the target images. The focus is set to the depth of the measurement to minimize target width.

The TCC system

Satrapa *et al.* (2006) have introduced a new test object which has an array of cylindrical voids which are scanned automatically in a computerized system and which captures a 3D volume containing many slices. The entire 3D volume is then analysed using dedicated software to calculate a profile of the signal-to-noise ratio achieved by the machine as a function of depth (see Figure 11.12). This is another attempt to combine the various spatial and greyscale parameters into a single value which may be better related to clinical performance than any single one of them alone.

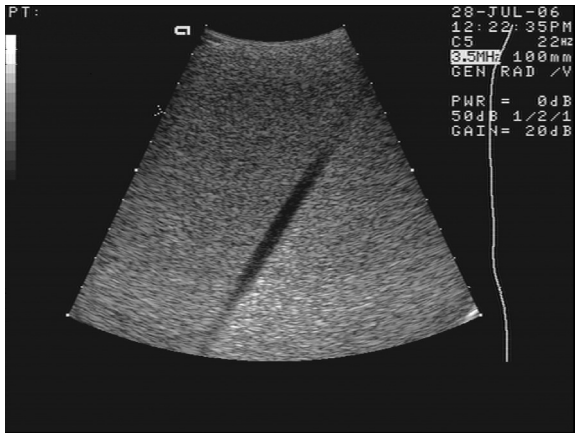

Fig. 11.11 Image obtained from the Edinburgh pipe test object.

Doppler testing

Virtually all testing of ultrasound systems performed in hospitals covers only B-mode imaging. In clinical use, Doppler ultrasound is also important, yet this aspect of machine performance is not usually tested in hospitals. This section describes relevant guidance and standards, the design of test objects for Doppler ultrasound, and some quantities which can be measured. A review of the design and application of Doppler test objects is given in Hoskins (2008).

Standards and guidance

Both the IPEM and AIUM have produced documents which describe in detail the design and use of test objects (AIUM 1993, 2002, IPEM 1994, in press). IEC standards have been produced for fetal Doppler (IEC 1995) and for CW Doppler (1993), and technical guidance has been produced on the design of a standard for PW Doppler (IEC 1999). At the time of writing, standards for fetal and CW Doppler are being revised and standards for PW Doppler and colour flow are being written.

Test objects for Doppler ultrasound

The design of test objects suitable for Doppler is more difficult than for B-mode imaging as the Doppler test object must include a moving target to simulate the moving blood. There are two types of moving-target

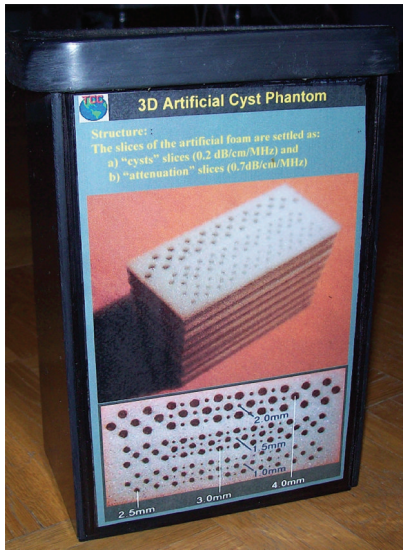

(a)

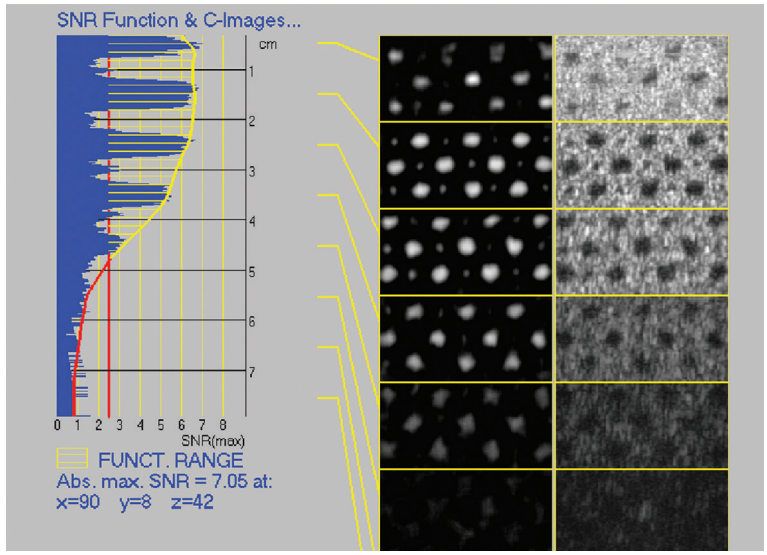

(b)

Fig. 11.12 The test object designed by Tissue Characterization Consulting (TCC) and typical output from it.

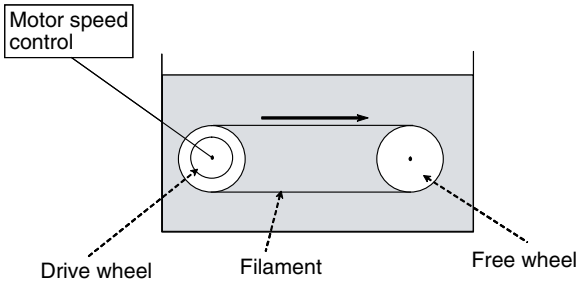

Fig. 11.13 Components of a string phantom. The string is driven in a circuit by a drive wheel. The speed of the drive wheel may be controlled using an external computer to produce waveforms with a physiological appearance.

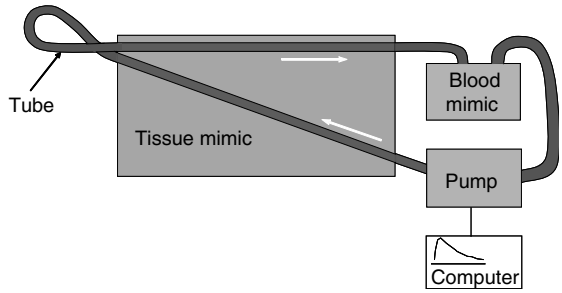

Fig. 11.14 Components of a flow phantom. These are the tissue mimic, tube and blood mimics. The pump may be controlled using a computer to obtain physiological flow waveforms.

test object which are available commercially; the string phantom and the flow phantom.

String phantom

In this device, the moving string simulates moving blood. The components of the string phantom are illustrated in Figure 11.13. Choice of the string is important as the scattering characteristics of blood need to be matched. Filaments, such as cotton and silk, are spiral-wound, with a repeat pattern at distances that are comparable with the wavelength of ultrasound. This repeat pattern gives rise to high-amplitude scattering along certain directions, which distorts the Doppler spectrum, making this type of filament unsuitable (Cathignol *et al.* 1994). The use of commercial systems based on the use of spiral-wound filaments is not advised. A suitable filament is O-ring rubber, as this scatters ultrasound in all directions in a similar manner to blood (Hoskins 1994). The most important feature of the string phantom is that the velocity can be accurately measured. The true string velocity may be calculated from the speed of rotation of the drive wheel. The device is especially suited to the checking of velocity estimates made using Doppler.

The string phantom is a relatively straightforward system to set up and use, and its size enables it to be used as a portable test object. Recent guidance (IPEM in press) on basic performance testing of Doppler systems is based on the use of a string phantom.

Flow phantom

This device simulates flow of blood within a vessel. The components of the flow phantom are illustrated in Figure 11.14. The main design criterion is that the acoustic properties of the tissue mimic, the blood mimic and the vessel must be matched to those of human tissue. The tissue mimic is usually a gel-based material, as described above. The blood mimic must have the correct viscosity, as well as correct acoustic properties. A suitable blood mimic has been described by Ramnarine *et al.* (1998), which is based on the use of nylon particles suspended in a solution of glycerol and dextran. Matching the acoustic properties of the artery is much more difficult. Rubber-based materials, such as latex, have the correct acoustic velocity, but the attenuation is high and nonlinear. This mismatch of acoustic properties results in distortions in the shape of the Doppler spectrum obtained from flow within the tube. This is mainly important when flow phantoms are used for calibration of quantities involving the mean frequency, such as volumetric flow. In this case, the mean frequency in the flow phantom is overestimated as a result of the spectral distortion. Unfortunately, all commercial-based flow test objects are based on the use of tubes of latex or similar material, and the calibration of volumetric flow using these devices is, therefore, unreliable. A 'wall-less' approach in which the tissue mimic is in direct contact with the blood mimic is the ideal arrangement. The most stable of wall-less test objects uses polyurethane as the tissue mimic; however, this approach is unreliable as the acoustic velocity is not correctly matched to tissue, as noted above. In research laboratories, flow phantoms can be designed which are correctly matched to human tissue (Hoskins 2008, Ramnarine *et al.* 2001).

The flow phantom is a complex device to assemble and use, and is generally restricted to a few specialist centres. Recent guidance (IPEM in press) on basic

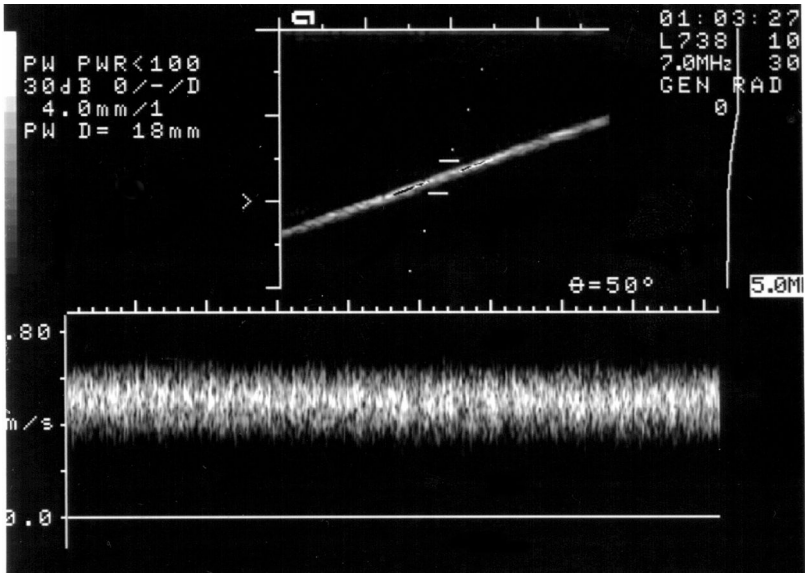

Fig. 11.15 Ultrasound imaging of a string phantom for checking of Doppler velocity estimation. The angle cursor is aligned with the string. The maximum velocity is measured using the manual cursor.

performance testing of Doppler systems does not include use of a flow phantom.

Quantities of interest

There are three main classes of quantity that are of interest: velocity, sensitivity and resolution. The use of test objects to measure these quantities is described below.

Velocity

The estimation and display of blood velocity is a key task of Doppler systems; hence, it is appropriate to test the accuracy of this quantity. Velocity measurements may be checked using a string phantom (Figure 11.15). The string is set at a constant velocity. The spectral Doppler sample volume is positioned at the level of the moving string using the B-mode image to guide placement. Spectral Doppler data are acquired, and velocity may be estimated using the mean Doppler frequency, or more commonly the maximum Doppler frequency. The string velocity is then compared to that estimated using spectral Doppler. In general, modern commercial systems overestimate maximum velocity, as explained in Chapter 9. Use of a string phantom to assess velocity measurement error is recommended in IPEM (in press).

Sensitivity

The acquisition of noise-free Doppler signals from vessels which are deep, or which are small, is a key task determining Doppler performance. This task is dependent on the strength of the Doppler signal from blood, compared to the clutter signal from the tissue and the strength of the electronic noise. The flow phantom is a suitable test object to assess penetration depth. The flow phantom design should include a vessel which is angled at 30–45° with respect to the surface. The penetration depth is the maximum depth from which spectral Doppler or colour flow signals can be obtained (Figure 11.16). Generally this measurement would not be performed in routine testing, as it requires a flow phantom which requires special local expertise to set up and use.

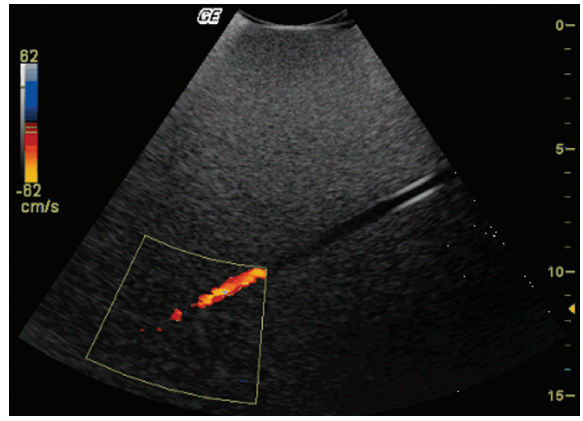

Fig. 11.16 Penetration depth measurement. The depth is measured at which the colour flow can no longer be distinguished.

Resolution

The measurement of both spatial and temporal resolution is relevant for Doppler systems. Spatial resolution

in the context of colour flow refers to the ability of the system to distinguish adjacent regions of blood moving at different velocities or in different directions. Temporal resolution refers to the ability of the system to distinguish rapidly changing flow patterns at a single location. These are important aspects of performance; however, procedures for measuring these quantities have not been adequately developed at the time of writing. Recent guidance (IPEM in press) does not include measurement of these quantities; however, a discussion of potential techniques is provided in the review article by Hoskins (2008).

Questions

1. Describe how an air test is carried out to determine transducer performance, and provide examples of what aspects of performance can be tested.
2. What typically are the desirable design characteristics of tissue-mimicking test objects?
3. What is penetration depth and how would this be measured?
4. What is spatial resolution and how would this be measured for B-mode imaging? Distinguish between lateral and axial resolution.
5. Describe the main components of a string phantom.
6. Describe what performance tests for spectral Doppler can be performed using a string phantom.

References

AIUM (1993). *Performance Criteria and Measurements for Doppler Ultrasound Devices*. Laurel, MD: American Institute of Ultrasound in Medicine.

AIUM (2002) *Performance Criteria and Measurements for Doppler Ultrasound Devices: Technical Discussion*, 2nd edn. Laurel, MD: American Institute of Ultrasound in Medicine.

Cathignol D, Dickerson K, Newhouse VL, Faure P, Chaperon JY (1994). On the spectral properties of Doppler thread phantoms. *Ultrasound in Medicine and Biology,* **20**, 601–10.

Dudley NJ, Chapman E (2002). The importance of quality management in fetal measurement. *Ultrasound in Obstetrics and Biology,* **19**, 190–6.

Gibson NM, Dudley NJ, Griffith K (2001). A computerised quality control testing system for B-mode ultrasound. *Ultrasound in Medicine and Biology*, **27**, 1697–711.

Hoskins PR (1994). Choice of moving target for a string phantom. I. Backscattered power characteristics. *Ultrasound in Medicine and Biology,* **20**, 773–80.

Hoskins PR (2008). Simulation and validation of arterial ultrasound imaging and blood flow. *Ultrasound in Medicine and Biology,* **34**, 693–717.

IEC (1993). *61206. Ultrasonics – Continuous-Wave Doppler Systems – Test Procedures.* Geneva: International Electrotechnical Commission.

IEC (1995). *61266. Ultrasonics – Hand-Held Probe Doppler Foetal Heartbeat Detectors – Performance Requirements and Methods of Measurement and Reporting.* Geneva: International Electrotechnical Commission.

IEC (1999). *61895. Ultrasonics – Pulsed Doppler diagnostic systems – Test Procedures to Determine Performance.* Geneva: International Electrotechnical Commission.

IPEM (1994). *Report 70. Testing of Doppler Ultrasound Equipment.* York: Institute of Physical Sciences in Medicine.

IPEM (1995). *Report 71. Routine Quality Assurance of Ultrasound Imaging Systems.* York: Institute of Physical Sciences in Medicine.

IPEM (in press). *Quality Control of Ultrasound Imaging Systems.* York: Institute of Physical Sciences in Medicine.

Martin K, Spinks D (2001). Measurement of the speed of sound in ethanol/water mixtures. *Ultrasound in Medicine and Biology,* **27**, 289–91.

Pye SD, Ellis W, MacGillivray T (2004). Medical ultrasound: a new metric of performance for grey-scale imaging J. Phys. Conference Series. Conference on Advanced Metrology for Ultrasound in Medicine (AMUN 2004), Date: 2004 Natl Phys Lab Teddington England. *Advanced Metrology for Ultrasound in Medicine,* **1**, 187–92.

Ramnarine KV, Nassiri DK, Hoskins PR, Lubbers J (1998). Validation of a new blood mimicking fluid for use in Doppler flow test objects. *Ultrasound in Medicine and Biology*, **24**, 451–9.

Ramnarine KV, Anderson T, Hoskins PR (2001). Construction and geometric stability of physiological flow rate wall-less stenosis phantoms. *Ultrasound in Medicine and Biology,* **32**, 245–50.

Satrapa J, Schultz HJ, Doblhoff G (2006). Automated quality control of ultrasonic B-mode scanners by applying an TMM 3D cyst phantom. *Ultraschall in der Medizin*, **27**, 262–72.

Skolnick ML (1991). Estimation of ultrasound beam width in the elevation (section thickness) plane. *Radiology*, **180**, 286–8.

Chapter 12

Safety of diagnostic ultrasound

Francis Duck and Adam Shaw

Introduction: risk and hazard

The words 'risk' and 'hazard' are emotive terms when used commonly. They are sometimes used to imply that an action should be avoided so as to ensure that there are no risks involved. Strictly, hazard describes the nature of the threat (e.g. burning, electrocution) while the associated risk takes into account the potential consequences of the hazard (e.g. death, scarring) and the probability of occurrence. Ultrasound scanning is potentially hazardous, but the real questions are: 'Is there any risk for the patient? And if so, what is the correct way to manage this risk?' The purpose of this chapter is to explain the scientific basis informing the responses to these safety questions, and to describe the ways by which the enviable safety record of diagnostic ultrasound may be maintained.

Whenever an ultrasound scan is carried out, some part of the patient is exposed to an external influence – the ultrasound beam. As it travels through the body, the ultrasound beam interacts with the tissue in ways giving a lasting biological effect, if the exposure is sustained and of sufficient strength. For instance, it is well known that elevated temperature affects normal cell function and that the risk associated with this particular hazard is dependent on the degree of elevation, the duration for which the elevation is maintained and the nature of the exposed tissue. During every scan with every transducer, some of the ultrasound energy is converted to heat and causes temperature elevation; the ultrasound is therefore a source of thermal hazard. The degree of elevation (that is, the severity of the hazard) will vary throughout the region of the scan and will depend on many properties of the ultrasound field and the exposed tissues. If the maximum temperature increase within the exposed region lies within the range normally occurring in tissue, the hazard may be considered to be small, and so may the risk to the patient. If the maximum temperature increase is outside the normal range, factors such as the duration of the elevation and the sensitivity of the tissue to damage must be borne in mind when assessing risk.

A second hazard arises from the presence of gas within soft tissues. Gas may occur naturally, for instance air in the alveoli of lungs or gas in the intestines. Alternatively gas bubbles may be introduced deliberately in the form of gas contrast agents. When such 'gas bodies' are exposed to ultrasound they can give rise to a variety of local mechanical effects which can cause damage to cells or tissue structures. The oscillation of the gas surface that causes the mechanical effects is termed 'acoustic cavitation' for a free bubble, or 'gas body activation' for the more general case. In these cases the hazard, a bubble caused to oscillate by the ultrasonic wave, gives a risk of tissue damage that will vary depending on the size of the oscillation, where the bubble is, and what cellular changes result.

The prudent sonographer, therefore, should consider the safety aspects of each examination, and only undertake it if the benefits to the patient from the expected diagnostic information outweigh the risks. This chapter aims to provide the sonographer with the information needed to assess the risks associated with ultrasound examinations. It first reviews how ultrasound output and exposure are related to hazard and risk. Thermal and mechanical processes and effects are then reviewed, leading to a discussion of the safety indices now presented on scanners to assist users in making risk/benefit judgements. A brief review of epidemiological evidence is given. The partnership between manufacturers and users in managing safety is reviewed, including an overview of standards and regulations. Finally, situations giving rise to specific safety issues are discussed.

Those wishing to gain further background knowledge, or explore the topics in greater depth are recommended to refer to other recent texts on ultrasound safety (AIUM 2008; Barnett and Kossoff 1998;

Diagnostic Ultrasound: Physics and Equipment, ed. Peter Hoskins, Kevin Martin and Abigail Thrush. Published by Cambridge University Press.

McKinlay 2007; ter Haar and Duck 2000). Succinct tutorials on a number of safety topics have also been prepared by the European Committee for Medical Ultrasound Safety (ECMUS) on behalf of the European Federation of Societies for Ultrasound in Medicine and Biology (EFSUMB), and are freely available on the EFSUMB web site (www.efsumb.org/ecmus.htm).

What does ultrasound exposure mean?

During an ultrasound scan, the imaged tissues are exposed to ultrasound beams and pulses (the ultrasound field) used to acquire the image or Doppler waveform. To measure the ultrasound exposure of the tissue, it is necessary to characterize the ultrasound field in terms of a number of standard parameters. We have seen in Chapter 2 that ultrasound is a longitudinal pressure wave and so, as the ultrasound wave passes a particular point, the pressure at that point will increase and decrease in a cyclic manner. Figure 12.1 shows a representation of the acoustic pressure variation with time for a typical pulsed Doppler ultrasound pulse near to the focus. The very rapid change from negative to positive pressure and the larger positive than negative pressure is normal for these pulses. There are many different properties that can be measured. The main parameters used to describe output and how they are measured are described in Appendix E.

From a safety perspective, we want to know what is happening inside the exposed tissue. Obviously this is not an easy thing to do, so, instead of using tissue, measurements are made in a substitute medium which is well characterized and reproducible: the medium that is currently chosen is water.

Seventy per cent of most soft tissues consists of water and, in many ways, ultrasound travels through water in a similar way to how it travels through soft tissue. The main difference is that water absorbs very little ultrasound compared to tissue and so the measured values in water are higher than would be expected in tissue. Measurements made in water are called acoustic output measurements (or, more correctly, 'free-field acoustic output measurements'). Using this term allows the concept of 'exposure measurements' and 'exposure parameters' to be reserved for what happens in tissue rather than what happens in a tank of water.

Very often this important distinction is not properly made when values are reported. Whatever names are attached to them, it is almost certain that any values for acoustic output and exposure parameters you see have come from measurements made in water. Estimates of exposure levels in tissue made from these, usually referred to as 'estimated *in-situ* values', are usually approximations derived from very simple models of tissue properties and structure.

The relationship between risk, hazard, exposure and acoustic output is outlined in Figure 12.2. It can be seen that as we move from actual measurements of acoustic output parameters in water to estimates of exposure, hazard and risk, our assessments become less and less certain. A semi-formal evaluation of hazard and risk in diagnostic ultrasound has been published elsewhere (Duck 2008).

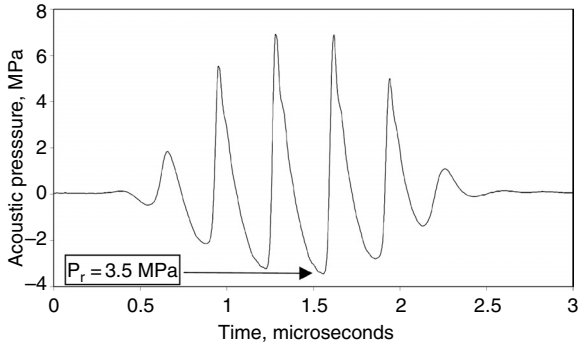

Fig. 12.1 Variation of acoustic pressure with time in a pulsed Doppler ultrasound pulse near the focus in water.

What happens to tissue exposed to ultrasound – and does it matter?

Thermal effects

When an ultrasound pulse travels through tissue, some of the energy in the pulse is absorbed by the tissue and is converted to heat, which in turn produces a temperature rise. In most soft tissues, the rate at which energy is absorbed per unit volume, q_v, depends on the amplitude absorption coefficient, α_0, of the tissue, the acoustic frequency, f, of the pulse and the intensity, I:

$$q_v = 2\,\alpha_0 f I \qquad (12.1)$$

The factor 2 arises because the intensity absorption coefficient is twice the amplitude absorption coefficient. Since the intensity varies throughout the field, the rate of energy absorption and the temperature rise also vary. To discuss the effects on tissue temperature in more detail, it is easiest to consider a fixed beam mode, such as a pulsed Doppler beam interacting with soft tissue, in which the temperature is initially uniform. When the field is first applied, energy will be absorbed at a rate

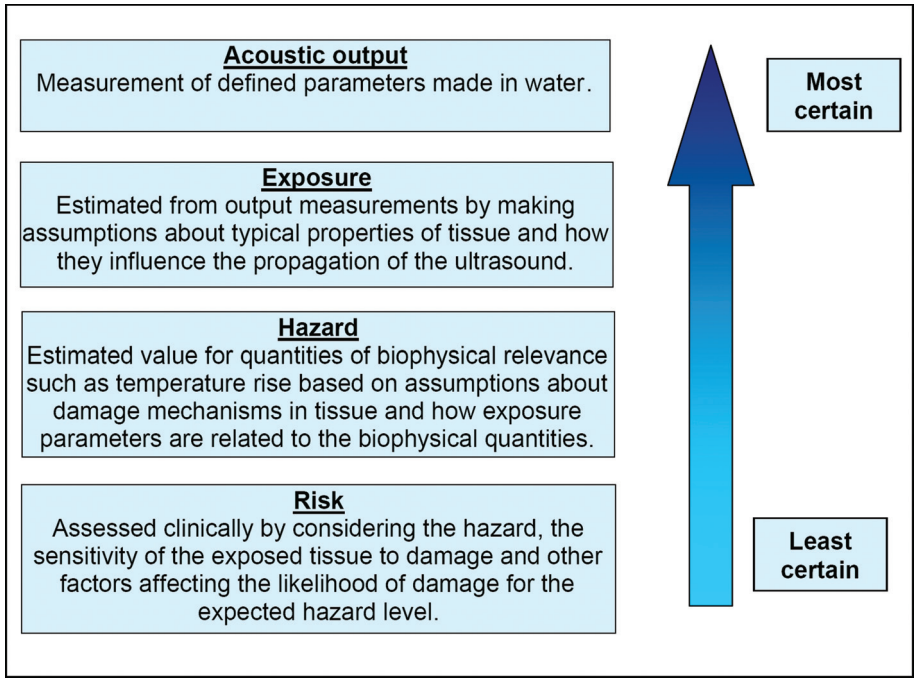

Fig. 12.2 Relationship between acoustic output, exposure, hazard and risk.

proportional to the local intensity, which means that the temperature will increase fastest at the focus. As time goes on, the temperature will continue to increase as more energy is absorbed, but the regions where the increase has been greatest (for example, at the focus) will start to lose some of their heat by conduction to neighbouring cooler regions, and so the rate of increase will begin to slow. Commonly, the rate of heat loss by conduction will nearly cancel out the rate of energy absorption after approximately 30 seconds and so the temperature in the focus approaches its equilibrium value very rapidly. In wider regions of the beam, where the initial temperature increase was more uniform, such as near the transducer, very little heat will be lost by conduction and so the temperature will continue to increase at its initial rate. A second effect also becomes significant: as it generates ultrasound, the transducer itself begins to heat up. This heat conducts into the tissue, enhancing the temperature rise near the transducer. In many cases, after several minutes exposure, the temperature near the transducer may significantly exceed the focal temperature. (In practice, transducer self-heating may even limit the development of some new technologies, for example radiation-force elastography.) Where the beam is broader, conductive losses will be smaller and perfusion becomes more important, particularly close to large blood vessels.

The presence of bone in the field will increase the temperature rise. Bone strongly absorbs ultrasound at all frequencies and so the ultrasound energy is almost completely absorbed in a very small volume and the temperature increases rapidly. Because the absorption takes place in a small region, the temperature gradients and also the conductive heat losses will become large. This means that the temperature will quickly approach its final value. The large conductive heat losses also dominate the perfusion losses so the presence of blood flow is unlikely to significantly reduce the temperature.

It is sometimes argued that you would have to hold the transducer stationary for hours to get any significant temperature rise and that, anyway, blood flow takes all the heat away. This argument is misleading. Most of the temperature increase occurs within the first minute, and it is certainly not safe to assume that blood flow will limit the temperature rise to levels which pose no risk.

Temperature predictions

In principle it is possible to predict the temperature distribution using theoretical models if enough is known about the *in situ* intensity distribution and the properties of the tissue. In practice, accurate predictions are difficult since the *in situ* intensity can only be approximated from acoustic output measurements and because of lack of knowledge about the properties of living tissue.

Values reported in the literature show large variations. This means that all estimates of temperature rise in tissue are uncertain. Consequently, alternative approaches have been developed such as the use of tissue-mimicking phantoms to make measurements of temperature rise and simplified, approximate methods of estimating the maximum temperature increase, e.g. thermal indices.

Temperature measurement

Ideally, of course, it would be possible to measure the temperature rise in the patient during the ultrasound examination. Unfortunately, with current technology, this is not yet possible. However, it is possible to measure the temperature rise in a tissue-mimicking phantom, also called a thermal test object or TTO (Shaw *et al.* 1999). Figure 12.3a shows a schematic diagram of one of these TTOs. This is a much more direct way of evaluating the heating potential of ultrasound scanners which automatically caters for most of the complexities which are ignored by other methods. TTOs are available commercially, and have provided important results (for example, Shaw *et al.* 1998, which is discussed later). An international specification for TTOs exists (IEC62306 2005) and it is likely that direct measurement of temperature rise in phantom materials will become more widespread over the next few years. This will undoubtedly allow the relationship between ultrasound exposure and biological hazard to be put on a much firmer foundation than it is currently. One area where temperature measurement has recently become mainstream is in determining the contact temperature between the transducer and the patient. IEC60601–2–37 (2007) places a limit on the temperature of the transducer face: this limit is 50°C when the transducer is radiating into air (to replicate the case where the scanner is active even though the patient is not being scanned) and 43°C when the transducer is in contact with a suitable TTO. TTOs that comply with the standard are available commercially (Figure 12.3b). Companies who claim compliance with this standard when seeking CE marking or other regulatory approval must undertake type-testing to ensure that their scanners meet this limit.

Thermal indices

Since it is impossible for the user to know how much temperature increase is occurring in the body, the idea of the thermal index (TI) was developed to provide some guidance. A TI is a rough estimate of the increase in temperature that occurs in the region of the ultrasound scan. A TI of 2.0 means that you can expect a temperature rise of about 2°C. TI values can provide extra information to help weigh up the risks and benefits to an 'average' patient as the examination progresses. They are not supposed to apply to any particular patient and other factors such as the physical state of the patient must be considered when making a risk assessment. These indices were originally introduced in the so-called 'Output Display Standard' or

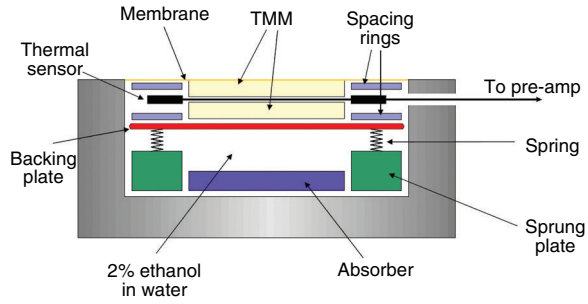

(a)

(b)

Fig. 12.3 (a) Diagram of a thermal test object. The temperature rise in the middle of the tissue-mimicking material (TMM) is measured with a small thermocouple of less than 0.5 mm in diameter. (b) Photograph of a commercial thermal test object for testing surface temperature rise against the limits specified by the IEC.

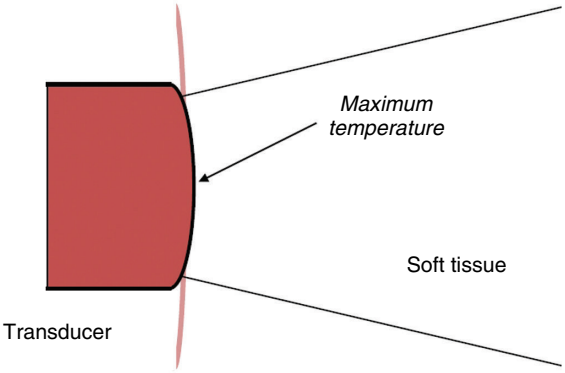

Fig. 12.4 Diagram showing conditions for the soft-tissue thermal index (TIS) for scanning. These conditions are also assumed to apply for the calculation of bone-at-focus thermal index (TIB) for scanning.

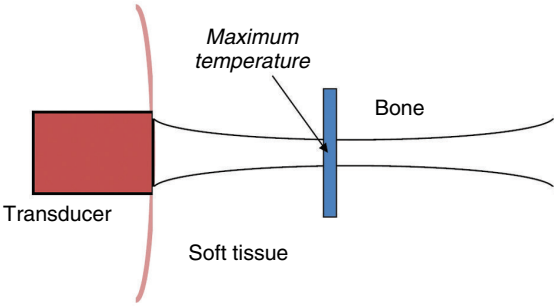

Fig. 12.5 Diagram showing the conditions for the bone-at-focus thermal index (TIB).

ODS (AIUM/NEMA 2004) and more recently incorporated into IEC Standards: first in IEC60601–2–37 (2001) and later IEC62359 (2005)

The thermal index itself has a very simple definition. It is the ratio between two powers. The first is the power exposing the tissue during use, W. The second is the power, W_{deg}, required to cause a maximum temperature increase of 1°C anywhere in the beam, with identical scanner operating conditions. This temperature is that reached with the beam held stationary under 'reasonable worst-case conditions' allowing thermal equilibrium to be achieved, and is intended to be a temperature which could be approached but never exceeded *in vivo*.

The difficulty with calculating TI lies mostly in the estimation of W_{deg}, the power giving a worst-case 1°C rise. In order to simplify the problem, three tissue models have been chosen to distinguish three applications. They give rise to three thermal indices; the soft-tissue thermal index (TIS); the bone-at-focus thermal index (TIB); and the cranial (or bone-at-surface) thermal index (TIC). Figures 12.4, 12.5 and 12.6 show these

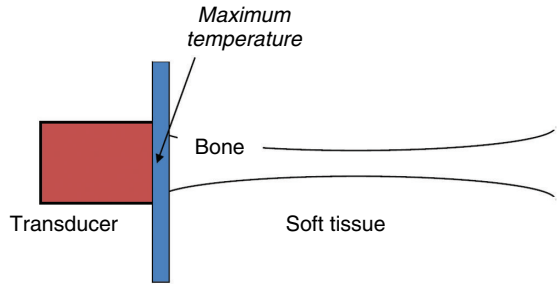

Fig. 12.6 Diagram showing the conditions for the cranial (bone-at-surface) thermal index (TIC).

three conditions. The tissue models are based on simple assumptions about the acoustic and thermal properties of tissue, including the assumption that the tissue attenuation coefficient is uniform at 0.3 dB cm^{-1} MHz^{-1}. For bone, a fixed proportion of the incident power is assumed to be absorbed in the bone layer. Clearly, from the basic definition of TI, all three thermal index values depend linearly on the acoustic power emitted by the transducer. If the machine controls are altered in such a way as to double the power output, the TI displayed will increase by a factor of 2.

In addition to the dependence on power, one of the thermal indices, soft tissue (TIS), also depends on the frequency of operation of the transducer. This is because the absorption coefficient of soft tissue depends on frequency, and hence so does the heating (see Equation (12.1)).

A practical feature of the models is the prediction of where the greatest heating occurs. For a stationary beam (such as in pulsed Doppler or M-mode) the greatest heating for bone (TIB) is at the focus (see Figure 12.5). On the other hand for scanned transducers it is predicted that the greatest heating will always be at the surface (see Figure 12.4), and the calculation is for this location and not the temperature that may be found elsewhere within the imaged organ.

Until better methods are developed, these TI values are more helpful than any other information you are likely to see and you should take note of the values when you can. However, don't be misled by the apparent precision of the value on the screen. The methods for calculating TI ignore several important complications, such as transducer self-heating and the simplicity of the models. The true temperature rise may a factor of 2 (or sometimes more) higher or lower than the number indicated.

On current-generation equipment, TI values can usually be found around the edge of the scanner

screen – often in the top right corner – indicated by the letters TIS, TIB or TIC followed by a number that changes when the scanner controls are altered. The mechanical index, MI, is displayed similarly (see Equation (12.3)). If the scanner was bought before about 1996, it will probably not display the index values (unless the firmware has been upgraded more recently). If they are not visible, it may be necessary to turn on the display of these values. Check the manual or ask your supplier how to do this. Smaller, portable or low-output equipment will often not display TI or MI. The same applies to older equipment. Again, check the manual or ask your supplier if you are not sure.

Although they do provide useful information to the user, the regulatory reason behind displaying TI (and MI) values is so that the manufacturer can comply with the regulatory requirements for selling their equipment. A practical side effect of their introduction in 1992 was that manufacturers were allowed to generate higher output levels than were allowed previously for most types of examination, including obstetric.

Does temperature rise matter?

What are the risks or benefits associated with an increased temperature? According to Miller and Ziskin (1989) the range of 'normal' core temperatures is approximately 36–38°C in man, and a temperature of 42°C is 'largely incompatible with life'. To maintain life requires the careful balance of many chemical processes. Changing cellular temperature not only changes the rate at which these reactions take place, it also affects the equilibrium position between competing reactions. A further complication is the denaturing of enzymes and other large molecules: this becomes particularly important above 45°C.

Clearly, it is undesirable to elevate the whole body above its natural temperature, but during an ultrasound examination only a small volume of tissue is exposed. Does it matter if this is affected? Generally, the human body is quite capable of recovering from such an event. There are, however, several regions that would not tolerate it so well, namely the reproductive cells, the unborn fetus and the central nervous system (brain and spinal cord). In view of the large number of obstetric examinations carried out, damage to the fetus is a particular concern.

There is growing evidence that clinical ultrasound scanners operating towards the top end of their power range are capable of producing temperature rises above the WFUMB recommendations. One study carried out at the National Physical Laboratory for the UK Department of Health (Shaw *et al*. 1998) measured, amongst other things, the temperature rise produced in tissue-mimicking phantoms by a range of clinical pulsed Doppler ultrasound systems. The front panel controls of the systems were adjusted to produce the maximum spatial-peak temporal-average intensity and the temperature rise produced in these phantoms was then measured at different positions in the ultrasound field.

From the 21 Doppler and two other fields studied, it appeared unlikely that a temperature rise of more than 1.5°C would occur in soft tissue in the absence of bone or other strongly absorbing material. The exceptions might be for exposure of the first-trimester fetus through the full bladder, when a temperature rise of up to 3°C was considered possible, or the use of intracavity probes, where prolonged exposure may result in higher temperature rises within 1 cm of the transducer face. However, when the ultrasound beam impinges on bone or other strongly absorbing material (even if that material is not the subject of the examination), the temperature rise may be much higher. Seventy-five per cent of the systems studied produced a temperature rise in a bone mimic of between 1.5°C and 4°C, with even higher temperatures considered possible if these same fields were used for examinations through the full bladder, for instance for the third-trimester fetus. Although it is important to remember that the exact study conditions are unlikely to be replicated in most examinations, under the modelled conditions 50% of the systems gave temperature rises in excess of 4°C and 15% in excess of 8°C.

Non-thermal mechanisms and effects

Ultrasound is a mechanical vibration. It follows that biological responses may arise directly from mechanical disturbances of the tissue structure, rather than indirectly from heating as described above. In past discussions, two main categories of non-thermal effects have been identified which have been referred to 'cavitation effects' and 'non-thermal, non-cavitation effects'. Whilst this general division remains valuable, it will be seen from the following that a clearer division is between those effects that are mediated by the presence of gas in the tissue, and those arising in the absence of gas. The first includes a number of effects that should not strictly be called 'cavitation', and have been referred to as 'gas-body activation'.

Cavitation and other gas-body mechanisms

Acoustic cavitation refers to the response of gas bubbles in a liquid under the influence of an acoustic

(ultrasonic) wave. It is a phenomenon of considerable complexity (Leighton 1994, 1998), and for this reason it is common to simplify its description into two categories. Stable (or non-inertial) cavitation refers to a pulsating or 'breathing' motion of a bubble whose diameter follows the pressure variation in the ultrasonic wave. During the compression in the wave, the bubble contracts in size, expanding again as the rarefaction phase in the wave passes. Over time the bubble may grow by a process of 'rectified diffusion': or it may contract and dissolve back into the liquid. Cavitation only occurs if there exist suitable cavitation nuclei to seed the cavitation process. These nuclei are typically microbubbles or solid particles in suspension, or bubbles trapped in crevices at a solid surface. For safety discussions, the most important sources of cavitation nuclei are those introduced *in vivo* in the form of contrast materials, and these are discussed below.

Bubbles have a resonant frequency, f_r, depending on their radius, R_o, which for a spherical air bubble in water is given by:

$$f_r R_o \approx 3 \text{ Hz m} \tag{12.2}$$

This expression is a reasonable approximation for bubble radii greater than 10 μm, but also suggests that typical diagnostic frequencies cause resonance in bubbles with radii of the order of 1 μm.

Of course the existence of an oscillating bubble (i.e. a hazard) does not automatically result in a risk. It is necessary to relate its behaviour with something that could be potentially damaging. When a suspension of cells is exposed to ultrasound and stable cavitation occurs, shear stresses can rupture the cell membranes. Shear is a tearing force, and many biological structures are much more easily damaged by tearing than by compression or tension. Destruction of blood cells in suspension by ultrasound may occur in this way, and this has been shown *in vitro* for erythrocytes, leucocytes and platelets. In addition, the existence of a second effect, not causing cell destruction, may occur. Gaps can open transiently in the cell membrane during ultrasound exposure, allowing the passage of larger biomolecules such as DNA, an effect known as sonoporation.

The second class of cavitation activity has been termed inertial cavitation. It is more violent and potentially more destructive than stable cavitation, occurs at higher peak acoustic pressures, and can be generated by short ultrasound pulses. The bubble undergoes very large size variations, and may violently collapse under the inertia of the surrounding liquid (hence the term 'inertial cavitation'). As with stable cavitation, local shear stresses are generated which may cause lysis of adjacent cells. Acoustic shocks are generated which can propagate stress waves outwards. In addition, enormously high, localized pressures and temperatures are predicted to occur, and the energy densities are sufficient to cause free radical ($H^{\bullet}$ and $OH^{\bullet}$) generation local to the collapsing bubble.

Whilst bubbles may undergo stable (and non-harmful) oscillations in ultrasound beams at very low pressures, the onset of inertial cavitation only occurs above a threshold for acoustic pressure. An analysis by Apfel and Holland (1991) quantified this threshold, assuming that a full range of bubble sizes were present to provide nucleation centres. This resulted in the formulation of a 'mechanical index', MI, which was intended to quantify the likelihood of onset of inertial cavitation:

$$MI = \frac{p_r}{\sqrt{f}} \tag{12.3}$$

where p_r is the peak rarefaction pressure *in situ*, and f is the ultrasound frequency. For MI < 0.7 the physical conditions probably cannot exist to support bubble growth and collapse. Exceeding this threshold does not, however, mean there will automatically be a biological effect caused by cavitation.

The destructive outcome of cavitation on cells in culture is well documented. *In vivo*, there is evidence for acoustic cavitation when using extracorporeal lithotripsy. However, there is no evidence at present that diagnostic pulses generally cause cavitation within soft tissues. There are only two specific conditions when the presence of gas *in vivo* can alter this. These are with the use of contrast materials and for the exposure of soft tissues in the presence of gas bodies, such as in the lung and in the intestine.

Contrast materials

Much of the previous discussion would appear to be of direct relevance to the use of contrast materials. When injected into the blood stream, ultrasound contrast agents introduce a plentiful supply of cavitation nuclei, which in principle could result in the generation of free radicals, cell lysis or sonoporation as described above. Extrapolation from studies carried out *in vitro* to what may happen *in vivo* is, however, notoriously difficult. For example, free-radical scavengers in blood strongly limit the lifetime of any radicals generated *in vivo*, and hence the potential for damage. Most contrast

agents break up when they are exposed to ultrasound. Nevertheless, there is good evidence that bubble fragments continue to circulate for a considerable time after the initial disintegration. For this reason it is considered unwise to use contrast materials during lithotripsy or at any time during the preceding day in order to minimize the chance of the contrast fragments acting as cavitation nuclei in the lithotripsy field. More seriously, microvascular damage may often result from exposure of gas-filled contrast agents *in vivo* to pulsed ultrasound at *in situ* rarefaction pressures of less than 1 MPa, well within the diagnostic range (Miller and Quddus 2000). International bodies have published reviews and guidelines for the safe use of contrast agents (Barnett *et al.* 2007, EFSUMB 2008).

Lung capillary haemorrhage

Exposure of the pleural surface of lungs to diagnostic levels of ultrasound has been consistently shown to cause alveolar capillary bleeding. This has been observed in experiments on a variety of small mammals. Pressure thresholds for damage in small animals are about 1 MPa, which is well within the diagnostic range. It is unclear exactly the mechanism responsible. Similar small haemorrhages (petechiae) have also been observed in the exposed intestines of small animals, and related to the presence of intestinal gas. Whatever the cause, diagnostic pulse amplitudes can cause damage when fragile tissue structures are exposed to pulsed ultrasound whilst being adjacent to gas bodies.

Lung and intestinal haemorrhage from ultrasound exposure has never been observed in humans. It has been suggested that the lungs of smaller animals are more susceptible to this form of damage than those of larger mammals, where the pleural layers and perhaps the alveolar membranes are thicker and stronger. If so, the relevance of these animal studies to clinical scanning may be restricted to studies in neonates, particularly cardiac examinations. Even so such alveolar haemorrhages would generally be almost without clinical importance, provided they were limited in extent.

Epidemiological evidence for hazard

Epidemiology is concerned with the patterns of occurrence of disease in human populations and of the factors influencing these patterns. Epidemiological methods have also been used to search for risks associated with any external agents, such as diagnostic ultrasound, and to look for associations between exposure and unwanted outcome. There have been a number of studies to investigate the possible association between exposure to ultrasound *in utero* and childhood maldevelopment.

This section summarizes briefly the outcome of the more important epidemiological studies into ultrasound exposure *in utero*. Fuller reviews may be found elsewhere (EFSUMB 1996, Salvesen 2007), in which the details of the literature may be found.

Birth weight

One review of available data on birth weight suggests that those children exposed to ultrasound imaging were on average heavier than those not exposed. Conversely a non-significant reduction in birth weight was noticed within a large randomized controlled trial using CW Doppler examinations. Subsequent studies have been unable to demonstrate an association between exposure and birth weight or subsequent growth. In view of the conflicting evidence presented by these studies, it is currently concluded that there is no evidence to suggest an association between exposure to ultrasound and birth weight.

Childhood malignancies

There have been three well-managed case-control studies into ultrasound and childhood malignancies, all of which were of sufficient size to have statistical validity. No association with childhood malignancy was found in any study.

Neurological development

A range of neurological functions have been examined and no association between ultrasound exposure *in utero* and subsequent hearing, visual acuity, cognitive function or behaviour has been found. An association with dyslexia reported earlier was not found in later larger studies. Further studies have suggested a possible association between ultrasound exposure and handedness, with a gender-biased tendency towards left-handedness. The effects were small and remain to be confirmed by others.

Speech development

Reports of altered speech development associated with ultrasound exposure are confusing, showing in one case delayed speech development and in another a lower level of referral to speech therapist in the exposed group. There is no clear evidence associating ultrasound with altered speech development.

In summary, there is no independently verified evidence to suggest that ultrasound exposure *in utero* has

Table 12.1 The upper limits of exposure specified by the Food and Drug Administration in the USA. The upper limit of 6.0 for thermal index is advisory. At least one of the quantities MI and I_{sppa} must be less than the specified limit.

	Derated I_{spta} (mW cm^{-2})	Derated I_{sppa} (W cm^{-2})	Mechanical index (MI)	Thermal index (TI)
All applications except ophthalmology	720	190	1.9	(6.0)
Ophthalmology	50	Not specified	0.23	1.0

caused an alteration in the development and growth of the fetus. All studies have either proved to be negative, or when positive findings have appeared they have not been verified, or have been shown to result from poorly designed studies. New studies will be difficult to structure, because of the difficulty of finding an unexposed control group, because of the widespread use of ultrasound during pregnancy throughout the world. It is necessary to sound a note of caution, however. Details of ultrasound exposure are missing in many of the studies, which commonly record neither exposure intensities nor dwell time. There are no studies into the outcomes following exposure to pulsed Doppler or Doppler imaging, where intensities and powers are known to be higher than in pulse–echo imaging. Whilst the results of epidemiological studies so far are comforting, they cannot be used to support an argument that it is safe to extend exposure *in utero* to include the higher levels associated with Doppler ultrasound. Further epidemiological studies focused specifically on Doppler exposure would be needed before such confidence can be claimed.

How is safety managed?

The successful management of safety for medical ultrasound involves everyone: manufacturers, users and other experts. Manufacturers must comply with standards intended to make the equipment safe. Users must make sure that they use the equipment in an appropriate and safe manner. Both groups, together with other experts such as embryologists, biochemists and physicists, must contribute to the development of national and international standards to keep ultrasound safe without unduly restricting its use and benefits.

The manufacturers' responsibility

The Medical Device Directive in Europe and the Food and Drug Administration (FDA) in the USA both make demands of manufacturers regarding safety of their scanners and provision of information to purchasers and users. The standards supporting these directives are generated by the International Electrotechnical Commission (IEC) and by the American Institute of Ultrasound in Medicine and the National Electrical Manufacturers Association (AIUM/NEMA) in the USA. AIUM/NEMA defined thermal and mechanical indices, and these were discussed earlier. They are intended to give some safety-related indication to sonographers; these indices are now available on most current ultrasound scanners. The IEC has published a number of measurement and performance standards.

US Food and Drug Administration

Any equipment sold in the USA must meet the US FDA regulations requiring that manufacturers supply information on acoustic output and ensure that certain derated acoustic parameters do not exceed allowable levels. Most commonly, manufacturers follow what is known as 'Track 3'. The exposure limits are set out in Table 12.1.

In order to comply manufacturers must also, however, provide on-screen indication of thermal and mechanical indices according to the methods set out in the Output Display Standard. Track 3 has the potential benefit of improved imaging through removing lower output restrictions that had been used previously. Removing these restrictions also means that the potential risk to the patient through exposure to ultrasound is increased and that users must be more aware of the safety issues.

European Medical Devices Directive

One of the main drivers for the development of international and European specification standards over the last few years has been the European Communities (1993) Medical Devices Directive or MDD. The MDD requires that all medical devices (except custom-made and devices intended for clinical investigation) meet essential requirements for safety and performance and carry a CE mark before they are placed on the market in the EC. The CE mark is the manufacturer's declaration

Table 12.2 Exemption levels for the declaration of output to the FDA, associated with fetal heart monitors and similar equipment.

Index	Exemption levels based on acoustic output
MI	Peak negative pressure < 1 MPa AND $f_{awf} > 1$ MHz
TI	Output beam intensity < 20 mW cm^{-2} AND Spatial-peak temporal-average intensity < 100 mW cm^{-2}. AND 10.5 MHz > $f_{awf} > 1$ MHz AND $A_{aprt} < 1.25$ cm^2

that the device conforms to these requirements. The MDD includes requirements for the visual display or warning of emission of potentially hazardous radiation, and for the indication of accuracy of equipment with a measuring function. The normal method for a manufacturer to demonstrate that they have complied with these requirements would be for them to follow procedures laid down in international standards. Standards recognized as demonstrating compliance with particular safety requirements are listed in the Official Journal of the European Communities. These are normally IEC or ISO standards where such standards exist. Since ultrasound scanners are pieces of electromedical equipment, all relevant parts of the 60601 series (Safety and Essential Performance) of IEC standards apply, but the only listed standard which is specific to diagnostic ultrasound is IEC60601–2–37.

IEC 60601–2–37, 'Medical electrical equipment, Part 2: Particular requirements for the safety of ultrasonic medical diagnostic and monitoring equipment', effectively implements the older AIUM/NEMA Output Display Standard (ODS) methods and requires calculation and display of TI and MI values. To support these displayed values, manufacturers must provide specific information relating to the acoustic output of their scanners in water under conditions which produce the maximum indices for each operational mode (B-mode, M-mode, colour flow etc.). Some of this information is tabulated in the equipment manual. Equipment which cannot generate indices of 1.0 or above, or which meets certain other low-output criteria (usually, this applies only to fetal Doppler and peripheral vascular Doppler devices only; see Table 12.2), need not provide such detailed output information. In addition, 60601–2–37 sets an upper limit of 43°C for the temperature of the transducer surface in contact with the patient: the user should be aware that this limit is only intended to be safe for contact with adult skin. Transducers that are left running in free air are allowed to reach 50°C according to the standard.

The users' responsibility

The role of the sonographer in managing safety is obviously vital. The user must ensure that they are properly trained and that they keep their knowledge up to date with changing technology and practices. They must choose and use scanners that are appropriate for the type of examination and the condition of the patient. They must follow good practice for reducing the risk to the patient. They must take part of the responsibility for ensuring that the equipment they use is properly maintained and meets necessary standards.

Proper training

It is obvious, but worth repeating, that all users need to be trained in and familiar with both the relevant anatomy and physiology for the examinations they make and the strengths and weaknesses of the equipment they use. As new equipment and techniques are developed, further training will be needed to ensure that, for instance, different imaging artefacts are understood and an accurate diagnosis is made. The greatest risk to the patient still comes from misdiagnosis and that should never be overlooked.

To complement this, users need also to appreciate the current thinking with respect to hazard posed by the ultrasound exposure itself and should seek training either through their own department, their professional body, BMUS or published literature. Various committees and professional bodies have offered guidance to the sonographer when it comes to assessing the possible risks (AIUM 1993, 2008, Barnett 1998, NCRP 2002). A summary of the various positions taken by national and international bodies has been given by Barnett *et al*. (2000). EFSUMB publish a clinical safety statement, which is kept under annual review. The current version may be found at www.efsumb.org/ecmus.

The British Medical Ultrasound Society recently published revised guidelines for safety, prepared by the BMUS Safety Group and based on the best expert judgements available. These documents are reproduced

in Appendix C, and are also from the BMUS website, available www.bmus.org.

The BMUS guidelines include recommended action levels associated with values of MI and TI under some specific conditions (see Appendix C). Nelson *et al.* (2009) have put forward further suggested guidelines to be used for setting and monitoring acoustic output during scanning. For prenatal scanning, TI = 0.5 is recommended as a general upper limit for extended use, with graded time limits for higher values, reaching a limit of 1 minute for TI > 2.5. For post-natal examinations, the equivalent limits are TI < 2 for extended scanning, time-limited to 1 minute for TI > 6. Under all conditions, MI should be limited to 0.4 if gas bodies may be present, and be increased as needed in their absence.

Appropriate equipment

If a probe is intended for a specific purpose, it should only be used for that purpose because choice of working frequency, acoustic output levels and field geometry are tailored to the intended use. A probe that is perfectly safe for adult cardiac use may not be safe for an obstetric or neonatal cephalic examination. If possible, use equipment that provides safety information to the user – this will generally be in the form of TI and MI displays – and take note of this information and your knowledge of the patient when planning and carrying out the scan.

In general, you should be less concerned about examining 'normal', non-pregnant adults. You should be more concerned when examining:

- the fetus (or the maternal abdomen near the fetus)
- neonates
- patients with fever or elevated core temperature
- patients under anaesthetic or during surgery.

In some types of examination, TI and MI are more likely to underestimate the amount of heating or cavitation. In general, you should be more cautious for:

- fetal examination through the full bladder
- the use of trans-vaginal, trans-rectal or other internal probes
- transcranial examination
- the use of injected ultrasound contrast agents.

Good safety practice

Keeping up to date with current thinking on ultrasound safety and risk minimization will allow the sonographer to make the best decisions on how to maximize the benefit to the patient whilst reducing any risks. The previous section on use of appropriate equipment, in conjunction with the list below, gives some simple guidelines.

- Only carry out an examination if there are clinical grounds to do so.
- Make sure you get the information you need to make a good diagnosis. There is more chance of causing harm by misdiagnosis than through heating or cavitation.
- Reduce the amount of time that the probe is in contact with the patient. You can do this by stopping the examination as soon as you have the information you want and by removing the probe during the examination if you need to talk to the patient or to a colleague and are not able to concentrate on the image on the scanner.
- Generally, Doppler modes (PW, colour or power Doppler) are more likely to cause heating and cavitation. So, use greyscale imaging to find the clinical site and only use Doppler modes if they are necessary and when you have found the site.
- The most cautious approach is to display TIB most of the time. Only display TIS if you are sure that there is no bone, developing bone or cartilage anywhere in the region you are scanning. Only display TIC for transcranial examinations.

Proper maintenance

The final point is that users are not stuck with the equipment they are given. They can and must play an active role in making sure that the equipment is properly maintained and repaired (normally through their medical physics department), and they can actually help develop better and safer equipment by making safety issues an important issue with manufacturers. They can do this both by questioning manufacturers directly (and, of course, a trained and knowledgeable sonographer will be able to ask more challenging questions) and by taking active part in the debates within BMUS, the professional bodies, BSI and IEC. It is these debates that, in the long run, produce better international standards with which the equipment bought by individual hospitals and departments will comply.

Is exposure increasing?

An important practical question in discussions of ultrasound safety is whether current clinical practice causes higher ultrasound exposure to the patient population than was so in the past. There are three overlapping but distinct questions.

(1) Are the acoustic pressures, intensities or powers used today higher than those used for the same applications in the past, either average or maximum values?

Table 12.3 Maximum ultrasound exposure measured in water, from B-mode and M-mode operation.

Application	Range	Median
B-mode imaging and M-mode		
Peak rarefaction pressure, p_r (MPa)	0.45–5.54	2.4
Spatial peak pulse average intensity, I_{sppa} (W cm^{-2})	14–933	230
M-mode only		
Spatial peak temporal average intensity, I_{spta} (mW cm^{-2})	11.2–430	106
Total acoustic power (mW)	1–68	9
B-mode only		
Spatial peak temporal average intensity, I_{spta} (mW cm^{-2})	0.3–991	34
Total acoustic power (mW)	0.3–285	75

Table 12.4 Maximum ultrasound exposure measured in water for pulsed Doppler and Doppler imaging modes.

	Range	Median
Spectral pulsed Doppler		
Peak rarefaction pressure, p_r (MPa)	0.67–5.32	2.1
Spatial peak pulse average intensity, I_{sppa} (W cm^{-2})	1.1–771	144
Spatial peak temporal average intensity, I_{spta} (mW cm^{-2})	173–9080	1180
Acoustic power (mW)	10–440	100
Doppler imaging		
Peak rarefaction pressure, p_r (MPa)	0.46–4.25	2.38
Spatial peak pulse average intensity, I_{sppa} (W cm^{-2})	60–670	275
Spatial peak temporal average intensity, I_{spta} (mW cm^{-2})	21–2050	290
Acoustic power (mW)	15–440	90

(2) Has the introduction of any new scanning modes (such as Doppler imaging or harmonic imaging) or transducers (such as those for trans-vaginal or trans-oesophageal scanning) been accompanied by altered exposure?
(3) Has the clinical use of ultrasound altered over the years, by the numbers of scans being carried out, and/or by the exposure dwell time used?

Increasing output from diagnostic scanners

During the 1990s, evidence was published for a continuing trend towards the potential use of higher ultrasound output. The most probable cause at that time was the relaxation of regulatory limits applied by the FDA in the USA (see above) in particular related to the allowed intensity for non-cardiovascular scanning, including obstetric scanning. As a result, manufacturers have increasingly used the higher intensities to exploit new methods of scanning, with the result that output is generally tending to move towards the limits set by the FDA. A summary of acoustic outputs during the mid1990s for M, B and Doppler modes of operation is given in Tables 12.3 and 12.4 (Barnett and Kossoff 1998, Chapter 3). These values may be taken as being broadly representative of present output, even though the surveys on which they are based are now somewhat dated.

New diagnostic modes of operation

The introduction of pulsed Doppler during the 1980s and of Doppler imaging during the 1990s were the two most important changes giving rise to increased output. Table 12.4 summarizes the exposure associated with these modes. Overall, the greatest intensities are associated with pulsed Doppler operation, although some settings for Doppler imaging can give rise to intensities commonly associated only with pulsed Doppler. These occur when Doppler imaging is used with a narrow colour box, high line density and high frame rate. All forms of Doppler imaging, whether colour-flow imaging or so-called 'power Doppler', use the same range of acoustic output.

Whilst Doppler modes are associated with the highest intensities, the highest pulse amplitudes (given by either rarefaction pressure, p_r or I_{sppa}) for Doppler applications are broadly similar to those used for imaging. On average, maximum rarefaction pressures are about 2.5 MPa, although extreme examples of pressures reaching over 8 MPa have been reported. Newer imaging applications such as harmonic imaging can be expected to use amplitudes confined to the upper range, since it is only at such pressures that harmonics are generated significantly in tissue.

Other changes in technology have also altered exposure. This is particularly true with the development of higher-frequency probes, and those for intraluminal use, such as trans-rectal, trans-oesophageal and trans-vaginal transducers. The output from such transducers is ultimately limited by FDA regulations in the USA; most manufacturers also work to these same limits in other parts of the world, although this is not generally a legal requirement. However, the FDA regulations do not set limits based on predicted temperature rise in tissue, apart for ophthalmic use (see above). Since interstitial transducers generally operate at higher ultrasound frequencies, they are capable of causing greater tissue heating, whilst still operating within the regulations, than is true for transducers operating at a lower frequency.

Increase in use of diagnostic ultrasound

In England, there were 2.41 million obstetric/gynaecological ultrasound scans reported to the Department of Health in the year April 2007–March 2008, a 27% increase over the previous decade. A much greater increase in non-obstetric scans, 63%, was reported during the same period, reaching an annual total of 4.69 million. It is clear from these and other data that exposure to ultrasound, quantified in terms of proportion of the population exposed, is growing, and may be expected to continue to grow. Within this group the majority of scan times will be short, not least because of time pressures within ultrasound clinics. Nevertheless, there are reasons why some patients may be exposed for more extended periods. This may arise because the procedure requires it (fetal breathing studies, flow studies or guided interventional procedures, for example) or because there is an increased usage of ultrasound by novice practitioners who are yet to develop mature skills and confidence in ultrasound scanning. In general it may be concluded that overall exposure of the population to ultrasound for medical diagnostic reasons is currently growing strongly, and may be expected to continue to do so for the foreseeable future.

Safety for specific uses of diagnostic ultrasound

Reviews of the safety of ultrasound often explore the exposure and the mechanisms for biological effects, but only occasionally review the safety aspects of the specific tissues being exposed (see for example Barnett *et al*. 1997). Often it is assumed that embryological and fetal exposure is the only concern. Some general recommendations are based upon a rationale specific to exposure *in utero*. This is true of the World Federation recommendations on heating (Barnett 1998), which were developed from investigations only into thermal teratology. It is helpful, therefore, to consider separately the safety concerns relating to a few particular uses of diagnostic ultrasound.

Diagnostic ultrasound during the first trimester

Probably the most critical question concerns the exposure of the embryo during the early stages of pregnancy. This is a period of rapid development and complex biochemical change, which includes organ creation and cell migration. There is widespread evidence that during this period the developing embryo is particularly sensitive to external agents, whose effect on subsequent development may range from fatal developmental malformation to minor and subtle biochemical disturbance. There are gaps in our knowledge and understanding of the way in which ultrasound may interact with embryonic tissue, and whether any adverse effect may result in developmental problems because of the particular sensitivity of the tissue at this time. Moreover, this sensitivity may be cyclic, with some tissues being sensitive only during particular time-bands of rapid cell development and differentiation. Heat is a teratogen, and any temperature increase from the absorption of ultrasound can disturb subsequent development, if of sufficient magnitude and maintained for sufficiently long. Fortunately the tissue with the greatest tendency to heat, bone, only starts to condense at the end of the first trimester. In the absence of bone, present evidence suggests that temperature rises of more than 1.5°C will not occur within embryonic tissue at present diagnostic exposures. Whilst this suggests that significant developmental changes may not occur, the kinetics of biochemical processes are known to be temperature-sensitive, and little research has investigated the

influence of small temperature changes induced locally on membranes and signal-transduction pathways. There is no evidence that cavitation occurs either, since there are no gas bubbles to act as nucleation sites within the uterus. Radiation pressure is exerted on embryonic tissue during exposure, however, and certainly amniotic fluid is caused to stream around the embryo during exposure. Acoustic streaming itself seems to present no hazard. Nevertheless the force which causes streaming is also exerted on embryological tissues. This radiation force has been suggested by Ang *et al.* (2006) to be the cause of the observed alteration in neuronal migration in mouse embryos from exposure to diagnostic ultrasound. Thus although our present understanding suggests that current practice is safe, there is sufficient uncertainty about the detailed interaction processes to advise caution.

Diagnostic ultrasound during the second and third trimesters

Bone ossification is the main developmental change during the second and third trimesters of pregnancy of significance to ultrasound safety. As bone condenses it forms local regions of high attenuation. Ultrasound energy is absorbed more by the fetal skeleton than by fetal soft tissues, preferentially causing heating. This is important in part because soft tissues alongside this bone will also be warmed by thermal conduction, reaching a higher temperature than expected from ultrasound absorption alone. Neurological tissues are known to be particularly sensitive to temperature rise, and the development of brain tissue, and of the spinal chord, could be affected if adjacent skull or vertebral bone were heated too much. Within the fetal haematopoietic system, the bone marrow is the main site of blood formation in the third trimester of pregnancy. Abnormal cell nuclei in neutrophils in guinea pigs have been reported after 6 minutes exposure at 2.5°C temperature elevation. This temperature increase in bone is within the capability of modern pulsed Doppler systems.

Cavitation is unlikely to occur during these later stages in pregnancy in diagnostic fields, as is the case during the first trimester, because of the absence of available nucleation sites. Radiation pressure effects can occur, and streaming will be caused within fluid spaces *in utero*. It seems unlikely that streaming, or other radiation pressure effects, has safety significance at this stage. The development of collagenous structures and an extracellular matrix gives increased strength to fetal tissues.

Obstetric scanning on patients with fever

It is noted in the WFUMB recommendations that 'care should be taken to avoid unnecessary additional embryonic and fetal risk from (heating due to) ultrasound examinations of febrile patients'. If a mother has a temperature, her unborn child is already at risk of mal-development as a result of the elevated temperature. This being so, it is sensible not to increase this risk unnecessarily. This does not mean withholding obstetric scanning from patients if they have a temperature. The methods of limiting exposure, including minimizing thermal index, limiting the duration of the scan and avoiding casual use of Doppler techniques, should be employed with particular vigilance in these cases.

Neonatal scanning

Two particular concerns have been raised to do with neonatal scanning: these are neonatal head scanning and cardiac scanning. The reasons for caution are different for each, so they will be dealt with separately. Often, scanning is carried out when neonates are seriously ill, and the paramount needs for diagnosis should be judged against any potential for hazard and consequent risk.

Neonatal head scanning

The exposure of the neonatal head to diagnostic ultrasound carries with it the same safety issues as for second- and third-trimester scanning. Neuronal development is known to be particularly sensitive to temperature. Temperature increases of a few degrees can occur in bone when exposed to diagnostic ultrasound. This means that there is the potential for brain tissue close to bone to experience temperature elevations by thermal conduction. The temperature increases may occur either close to the transducer or within the skull. At the surface there are two potential sources of heat. First, the ultrasound beam is absorbed by the skull bone. The cranial thermal index (TIC) provides the user with an estimate of this temperature rise. Second, transducer self-heating can further increase the surface temperature, whether or not the transducer is applied over bone or the anterior fontanelle. Transducer heating may increase the surface temperature by a few degrees when transducers are operated at the highest powers. The other place which may heat preferentially lies at the inner surface of the skull bone where it is exposed to the ultrasound beam, again giving the potential to heat adjacent neural tissues. In this case the more appropriate safety index is the bone-at-focus thermal index, TIB.

Neonatal cardiac scanning

Neonatal cardiac scanning, including Doppler blood-flow imaging, may expose surrounding pleural tissue. There is good experimental evidence for alveolar capillary damage both in adult small animals and in juvenile larger animals, although there is no evidence for lung damage in humans – even in neonates. The experimental evidence suggests that as pleural tissue matures it thickens and becomes stronger, so preventing capillary rupture. Immature (and hence structurally weak) neonatal pleura may be vulnerable to stress caused by diagnostic ultrasound pulses. The relevant safety index is the mechanical index (MI), and this should be kept to a minimum appropriate to effective diagnosis.

Ophthalmic scanning

The eye is the only tissue identified separately for regulation by the Food and Drug Administration in the USA, and the only case for which thermal index is used for regulation. The limit for derated time-averaged intensity is 50 mW cm^{-2} (in comparison with 720 mW cm^{-2} for all other applications), and 0.23 for MI (compared with 1.9) – see Table 12.1. The thermal index limit is 1.0. The reason for the regulatory caution is the particular sensitivity of parts of the eye to potential damage. The cornea, lens and vitreous body of the eye are all unperfused tissues. This means that they dissipate heat only by means of thermal conduction. Furthermore, the lack of blood perfusion limits the ability to repair any damage arising from excess exposure. The acoustic attenuation coefficient of the lens is about 8 dB cm^{-1} at 10 MHz, and since a lens has a greatest thickness of about 4 mm about one-half of the incident acoustic power may be deposited there. A further specific concern is that the lens lies very close indeed to the transducer under normal scanning conditions. Transducer self-heating becomes an important secondary source of heat under these circumstances. For all these reasons particular care is exercised in the design of systems specifically for ophthalmic use. If general-purpose scanners are used for eye studies, great care needs to be exercised to reduce to an absolute minimum any chance of lens heating.

Summary and conclusions

Ultrasound has an enviable record for safety. All the epidemiological evidence points to the conclusion that past and current practice has presented no detectable risk to the patient and can be considered safe. Nevertheless there is ample evidence that modern scanners, designed in accordance with national and international standards and regulations, can warm tissues by several degrees under some circumstances. If gas bubbles or other pockets of gas lie in the ultrasound field, the tissues may be damaged from stresses from cavitation-like oscillations. Radiation pressure, sufficient to cause acoustic streaming *in vivo*, is exerted on all exposed tissues. These are important facts underpinning the responsibilities of the manufacturers to produce safe equipment to use, and for the users of ultrasound in managing their scanning practice.

Since 1992, changes to the regulations in the USA have resulted in recent generations of scanning equipment that display safety indices giving users feedback so that more informed safety judgements can be made. These changes have also had the effect of enabling progressively higher outputs to be used in, for example, obstetric scanning. Greatest intensities and powers, and the greatest potential heating, occur when using pulsed Doppler modes. There is considerable overlap between modes, however. Particular safety concerns pertain during all obstetric scanning, during neonatal scanning, during ophthalmic scanning and when using contrast materials.

Standards and Definitions

AIUM/NEMA UD3 rev. 2 (2004). Standard for real-time display of thermal and mechanical acoustic output indices on diagnostic ultrasound equipment. UD 3–2004. American Institute for Ultrasound in Medicine / National Electrical Manufacturers Association, USA.

European Communities (1993). Council Directive 93/42/EEC of 14 June 1993 concerning medical devices. Official Journal of the European Communities, 169, 12.7.1993.

IEC 60601–2–37 Ed 1 (2001). Medical Electrical Equipment: Particular requirements for the safety of ultrasound diagnostic and monitoring equipment. Geneva: International Electrotechnical Commission.

IEC 60601–2–37 Ed 2 (2007). Medical Electrical Equipment: Particular requirements for the safety of ultrasound diagnostic and monitoring equipment. Geneva: International Electrotechnical Commission.

IEC 62306 (2005). Ultrasonics – Field characterization – Test objects for determining temperature elevation in medical diagnostic ultrasonic fields. Geneva: International Electrotechnical Commission.

IEC 62359 (2005). Ultrasonics – Field characterization – Test methods for the determination of thermal and mechanical indices related to medical diagnostic ultrasonic fields. Geneva: International Electrotechnical Commission.

Questions

1. What are the two main hazards associated with diagnostic ultrasound?

2. What is the meaning of estimated *in situ* exposure, and how is it usually calculated? (It is also called derated exposure.)
3. What are the three forms of the thermal index, and what conditions do they relate to?
4. Apart from ultrasound absorption, what is the other main source of heat during ultrasound scanning?
5. What is the formula for mechanical index?
6. What is the maximum fetal temperature elevation, recommended by WFUMB, which may be sustained without reservation on thermal grounds?
7. Under which three conditions may cavitation or gas-body effects be of a safety concern during ultrasound scanning?
8. What is the meaning of the terms inertial cavitation and non-inertial (i.e. stable) cavitation.
9. Which are the main international and national bodies that are responsible for ensuring the safe design and sale of diagnostic ultrasound equipment?
10. What are the main criteria by which a sonographer can ensure safe exposure of the patient?
11. Which modes of operation are most likely to give (a) a high TI and (b) a high MI?

References and bibliography

AIUM (1993). *Bioeffects and Safety of Diagnostic Ultrasound*. Rockville, MD: American Institute of Ultrasound in Medicine.

AIUM (2008). Bioeffects Consensus Report. *Journal of Ultrasound in Medicine,* **27**, 503–632.

Ang E, Gluncic V, Duque A, Schafer M, Rakic P (2006). Prenatal exposure to ultrasound waves impacts neuronal migration in mice. *Proceedings of the National Academy of Sciences of the U S A*, **103**, 12903–10.

Apfel RE, Holland CK (1991). Gauging the likelihood of cavitation from short-pulse, low-duty cycle diagnostic ultrasound, *Ultrasound in Medicine and Biology*, **17**, 179–85.

Barnett SB , ed. (1998). WFUMB Symposium on Safety of Ultrasound in Medicine. *Ultrasound in Medicine and Biology,* **24**(Suppl 1).

Barnett SB, Kossoff G, eds. (1998). *Safety of Diagnostic Ultrasound*. Progress in Obstetric and Gynecological Sonography Series. New York: Parthenon.

Barnett SB, Rott H-D, ter Haar GR, Ziskin MC, Maeda K (1997). The sensitivity of biological tissue to ultrasound. *Ultrasound in Medicine and Biology,* **23**, 805–12.

Barnett SB, ter Haar GR, Ziskin MC, *et al.* (2000). International recommendations and guidelines for the safe use of diagnostic ultrasound in medicine. *Ultrasound in Medicine and Biology,* **26**, 355–66.

Barnett SB, Duck F, Ziskin M (2007). WFUMB symposium on safety of ultrasound in medicine: Conclusions and recommendations on biological effects and safety of ultrasound contrast agents. *Ultrasound in Medicine and Biology*, **33**, 233–4.

Duck FA (2008). Hazards, risks and safety of diagnostic ultrasound. *Medical Engineering and Physics,* **30**, 1338–48.

EFSUMB (1996). Tutorial paper. Epidemiology of diagnostic ultrasound exposure during human pregnancy. *European Journal of Ultrasound*, **4**, 69–73.

EFSUMB study group (2008). Guidelines and good clinical practice recommendations for contrast enhanced ultrasound (CEUS) – update 2008. *Ultraschall in Medizin*, **29**, 28–44.

Leighton TG (1994). *The Acoustic Bubble*. London: Academic Press.

Leighton TG (1998). An introduction to acoustic cavitation In FA Duck, AC Baker, HC Starritt, eds., *Ultrasound in Medicine.* Bristol: Institute of Physics Publishing, pp. 199–223.

McKinlay A (guest editor) (2007). Effects of ultrasound and infrasound relevant to human health. *Progress in Biophysics and Molecular Biology*, **93**, 1–420.

Miller DL, Quddus J (2000). Diagnostic ultrasound activation of contrast agent gas bodies induces capillary rupture in mice. *Proceedings of the National Academy of Sciences of the U S A,* **97**, 10179–84.

Miller MW, Ziskin MC (1989). Biological consequences of hyperthermia. *Ultrasound in Medicine and Biology,* **15**, 707–22.

NCRP (2002). *Report 140. Exposure Criteria for Medical Diagnostic Ultrasound: II. Criteria Based on all Known Mechanisms*. Bethesda, MD: National Council for Radiation Protection and Measurements.

Nelson TR, Fowlkes JB, Abramowicz JS, Church CC (2009). Ultrasound biosafety considerations for the practicing sonographer and sonologist. *Journal of Ultrasound in Medicine*, **28**, 139–50.

Salvesen KA (2007). Epidemiological prenatal ultrasound studies. *Progress in Biophysics and Molecular Biology*, **93**, 295–300.

Shaw A, Bond AD, Pay NM, Preston RC (1999). A proposed standard thermal test object for medical ultrasound. *Ultrasound in Medicine and Biology,* **25**, 121–32.

Shaw A, Pay NM, Preston RC (1998). Assessment of the likely thermal index values for pulsed Doppler ultrasonic equipment – Stages II and III: experimental assessment of scanner/transducer combinations. *NPL Report CMAM 12*. Teddington, UK: National Physical Laboratory.

ter Haar G. Duck FA, eds. (2000). *The Safe Use of Ultrasound in Medical Diagnosis*. London: BMUS/BIR.

Chapter 13

3D ultrasound

Peter Hoskins and Tom MacGillivray

Introduction

3D imaging techniques such as CT, MRI and PET, will be familiar to the modern imaging specialist. The strength of ultrasound imaging lies in its real-time ability and, as this book has discussed to this point, this has been based on 2D imaging. The operator moves the 2D transducer around and, where necessary, builds up a 3D map in his or her own head of the 3D structures in the body. Many modern ultrasound systems now come with a 3D scanning option which is available for the operator to use. Clinical uses for these systems are becoming established, mainly in obstetrics and cardiology as discussed below. The purpose of this chapter is to describe the technology of 3D ultrasound, including examples of clinically useful applications and measurements. Further reading, on the history and technology of 3D ultrasound, may be found in review articles by Fenster *et al*. (2001) and Prager *et al*. (2009).

Terminology

The terms '1D', '2D', '3D' and '4D' are used. The 'D' in every case refers to 'dimension'. '1D' is one spatial dimension, in other words a line; for example a 1D transducer consists of a line of elements. '2D' is two spatial dimensions, which is an area. A 2D transducer consists of a matrix of elements. '3D' is three spatial dimensions, in other words a volume. 3D scanning refers to the collection of 3D volume data. '4D' is three spatial dimensions and one time dimension. 4D scanning refers to the collection of several 3D volumes over a period of time. Examples include the visualization of the heart during the cardiac cycle, or of the fetus during fetal movement. Table 13.1 summarizes this terminology.

In addition to the spatial and time dimensions, there is the issue of velocity measurement through Doppler ultrasound. Blood flow is complex and the velocity of blood at any particular point in the vessel generally requires knowledge of all three components of velocity (along x, y and z). Conventional clinical ultrasound systems provide only one component of velocity, in the direction of motion of the transducer, as discussed in Chapters 7, 9 and 10. This limitation is also true for 3D ultrasound in that it too only obtains one component of velocity, in the direction of the ultrasound beam.

Table 13.1 Dimension terminology.

Term	Description
1D	Line
2D	Area
3D	Volume
4D	Dataset consisting of several volumes collected over a period.

3D/4D ultrasound systems

These systems can be divided into two types which depend on the ultrasound transducer used.

- *2D-array transducers*: the operator positions the transducer and the ultrasound beam is electronically swept through a 3D volume.
- *Conventional ultrasound transducers*: these steer the beam within a 2D plane, hence collection of 3D data is achieved by movement of the transducer. The 3D volume is then built up of many 2D scan planes. A common requirement for these systems is that there must be knowledge of where the data are collected from, in order that the 2D slices are put in the correct location within the 3D volume. There are several solutions to this problem depending on the system used.

The sections below describe the systems which are commonly used for collection of 3D/4D data.

Freehand systems

In freehand 3D scanning a conventional ultrasound transducer is swept across the patient's skin

Diagnostic Ultrasound: Physics and Equipment, ed. Peter Hoskins, Kevin Martin and Abigail Thrush. Published by Cambridge University Press.

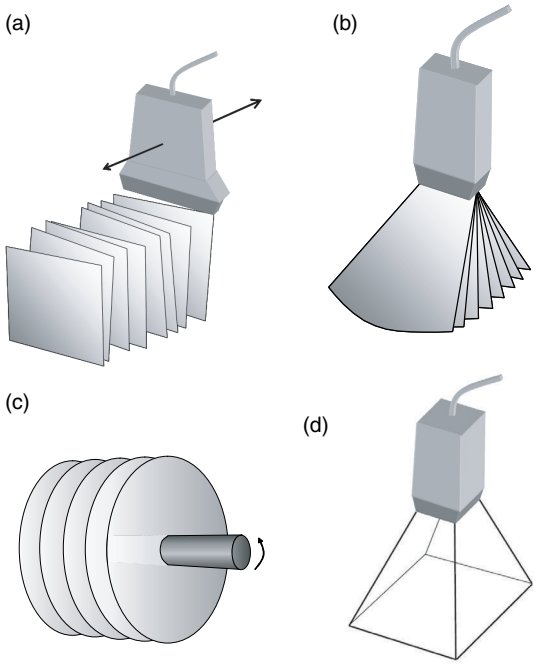

Fig. 13.1 Different 3D scanning modes. (a) Freehand 3D scanning where the transducer is swept over the skin by the operator and the 3D volume is built up as a series of 2D scan planes. (b) Mechanically steered array real-time 3D, where the 2D scan planes are swept back and forth through a mechanical motion of the linear array within its housing to produce a series of 3D volumes. (c) Endoprobe 3D ultrasound, where retraction of the ultrasound transducer builds up the 3D dataset as a series of 2D scan planes which are assumed to be parallel to each other. (d) Matrix array 3D ultrasound where the 3D volume is built up by electronic steering of the beam throughout the 3D volume to produce a pyramid-shaped dataset.

(Figure 13.1a). In this system knowledge of the transducer position in space is obtained using a tracking device. The result is a 3D dataset consisting of 2D scan planes whose position is correctly allocated in the 3D space (Figure 13.2).

The basic components of the tracking system are a target attached to the transducer, and a remote sensor or receiver several feet away which is able to track the position and orientation of the target in space. Note that it is insufficient just to track the position. At a single location in space the transducer may be pointed in many different directions so that knowledge of the transducer orientation is also needed. Two commonly used tracking systems are optical and electromagnetic.

- *Electromagnetic systems*: a small transmit device placed near the patient generates a magnetic field. A sensor coil is attached to the ultrasound transducer, and is connected to a receiver. Movement of the coil through the magnetic field induces voltage in the coil from which the receiver estimates the position and orientation in space. These systems do not require line of sight (i.e. a clear uninterrupted path between coil and receiver); however, they may suffer distortions due to the presence of other hospital equipment.
- *Optical systems*: typically several infrared sources such as LEDs (light-emitting diodes) are attached to the ultrasound transducer (Figure 13.3), and the positions of the LEDs are recorded using two cameras. A processing unit combines the images of the LEDs from the two cameras and provides information on the position and orientation of the LEDs. These systems require clear lines of sight between the transducer and the tracking device. Optical tracking is more widely used for freehand scanning than electromagnetic tracking due to the effect of hospital equipment on electromagnetic systems, as noted above.

For freehand systems it is the position and orientation of the target (LEDs or coil) which are tracked, not the transducer. As the target and the transducer are rigidly connected, the computer system used in freehand scanning is able to estimate the position and orientation of the 2D scan plane from that of the target. In order to do this the tracking system must be calibrated; i.e. the computer system must be provided with sufficient information to convert target position and orientation coordinates into scan-plane position and orientation coordinates. The simplest calibration method consists of scanning a steel plate, moving the transducer through a series of translations and rotations. More complex calibration methods require dedicated phantoms (Fenster *et al.* 2001, Mercier *et al*. 2005).

Freehand systems allow virtually any ultrasound system to be converted at a later stage into a 3D system. There is no restriction on the type of transducer which may be used, so that systems based on linear arrays, phased arrays and mechanically driven transducers are all suitable for conversion into 3D ultrasound systems using the freehand approach.

The time for acquisition of a 3D volume is typically a few seconds. If the operator moves the transducer too quickly then the distance between adjacent 2D slices may be too great and parts of the 3D image will not

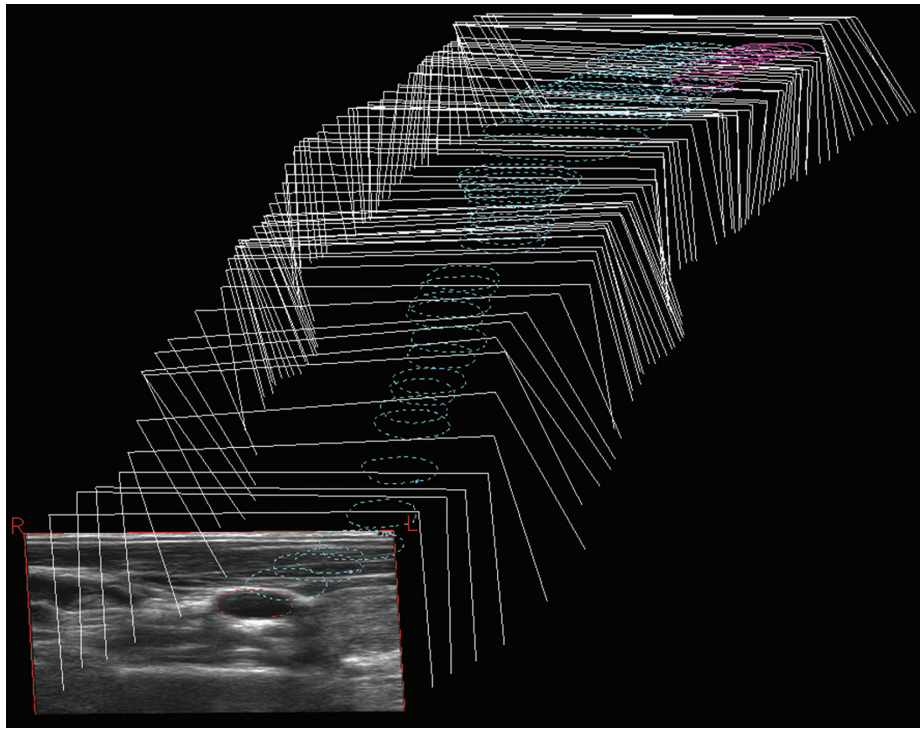

Fig. 13.2 A series of 2D images are shown after positioning using an optical tracking system. Also shown are the lumen boundaries of the artery which were obtained by the operator.

be visualized. The use of colour flow slows down the frame rate, requiring slower scanning speeds. In arterial applications the vessel wall moves during the cardiac cycle and it may be necessary to cardiac-gate the received data, so that only one 2D frame is acquired every cardiac cycle. This requires very slow scanning speeds of 0.5–1 mm per second, with total scan times of typically 1–2 minutes.

The requirements for the setting up of a tracking system, transferring image data to an external computer and 3D acquisition and analysis mean that medical physics support is needed. The support needed may be lessened by the availability of freely downloadable software for acquisition and processing, such as that provided by Cambridge University in the UK (Prager *et al*. 2002).

Mechanically steered array systems

In these systems a linear array is contained within a fluid-filled housing. The transducer is held against the patient, and the linear array is swept back and forth within its housing in a controlled manner using a mechanical driver. The 2D scan plane is swept through the tissues, producing a pyramid-shaped 3D volume (Figure 13.1b). There is still the requirement that the system knows the location of the 2D scan planes within the 3D volume, and this is looked after by the machine itself with no need for the operator to get involved in calibration. Each time the transducer sweeps back and forth a new volume is produced. This is useful in applications where there is movement, such as in obstetrics. Movement of fetal limbs and facial movements, such as mouth opening, can be observed in real time. Typically 5–10 volumes per second can be obtained provided that the 2D sector angle and the 3D sweep angle are reduced. Larger sector angle and sweep angle will result in a larger 3D volume being interrogated, but at the expense of a reduction in the number of volumes which can be obtained per second. These systems are commonly used in obstetrics and general radiology.

Endoprobe 3D ultrasound

3D imaging may be achieved by controlled retraction of the transducer by the operator or using a mechanical pull-back system. This is typically used in transrectal scanning and in intravascular ultrasound. In the 3D reconstruction it is assumed that the 2D slices are aligned parallel with each other (Figure 13.1c). Though this is a reasonable assumption in, for example, transrectal imaging, it is unlikely to be true in intravascular

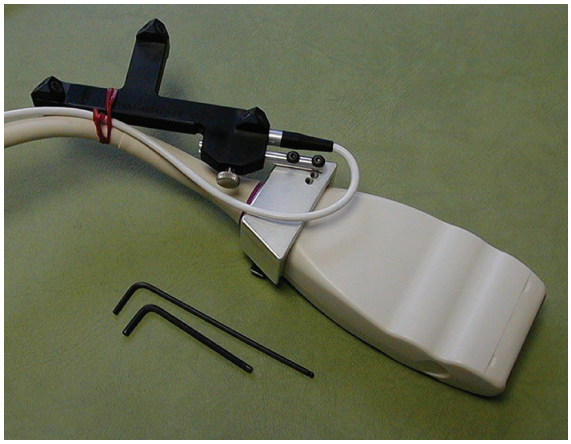

(a)

(b)

Fig. 13.3 (a) A linear array is shown to which is attached a tool with a series of infrared light sources. The light sources are detected by the two cameras of the tracking unit. (b) Close-up of the tool with LEDs attached.

ultrasound (IVUS) where vessels are curved, and where the operator has no control over the orientation of the catheter and transducer within the vessel. Typically a 3D volume can be acquired in 5–10 seconds.

2D phased array probes

These matrix transducers are designed to electronically steer the beam within a 3D volume (Figure 13.1d). The operator positions the transducer on the patients skin, and a series of 3D volumes are automatically collected. The small footprint of the transducer makes it ideally suited for cardiac applications. Typically 10–20 volumes per second are collected for adult applications, and 20–40 for paediatric applications.

Visualization

A problem with all types of 3D datasets, whether they are produced by MRI, CT or ultrasound, is visualization. The possible types of visualization which have been developed for MRI and CT are also applicable to ultrasound, and are described below.

2D display

Display of all the 3D raw data at the same time would be very confusing. 3D datasets are actually most commonly viewed as a series of 2D slices. Figure 13.4 shows a 3D fetal study in which three 2D orthogonal (at 90° with respect to each other) views are provided simultaneously, along with a shaded surface view (see below) of the 3D structures. Figure 13.5 shows a 3D rectal study in which three 2D orthogonal views are shown, along with a composite image of the orthogonal planes. The position of each of the 2D slices within the 3D volume can be controlled by the operator.

Other variants of this display method allow the operator to choose the position and orientation of the 2D plane. One advantage of the 3D technique is that 2D planes can be visualized which would be impossible to obtain using conventional 2D imaging.

Shaded surface display

In this method the surface of an object is highlighted and displayed. One common example is highlighting of the fetal face and body, to look at facial features and real-time actions such as mouth opening (Figure 13.6). The boundary or surface of the structure of interest is ideally identified using fully automated image-processing methods as these are rapid and require no user intervention. Automated boundary identification is possible when the boundary is sufficiently clear. When automated surface identification fails then a semi-automated method involving some user input of key surface points may be tried, or even a fully manual method involving specification of many points on each 2D slice of the 3D image. Boundaries are clearest when the structure of interest is adjacent to fluid; for example the fetus, which is surrounded by liquor, and the heart chambers, which contain blood. The intensity of the echoes received from the tissues of the fetus or heart is much higher than the intensity of echoes received from the liquor or blood, making the boundary of the heart or fetus easy to identify. For other features of interest

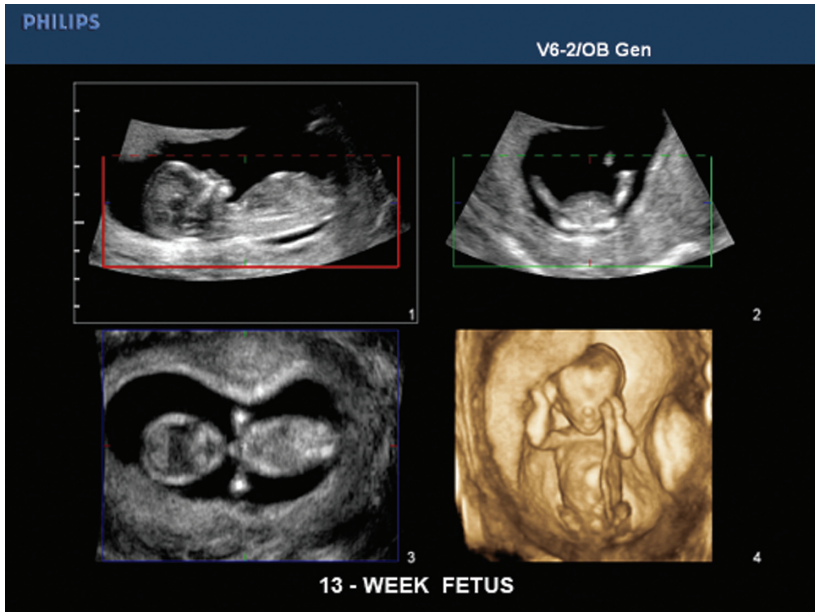

Fig. 13.4 Display of the 3D dataset using three orthogonal 2D slices of a 13-week fetus. The 4th image shows a surface shaded view of the fetus.

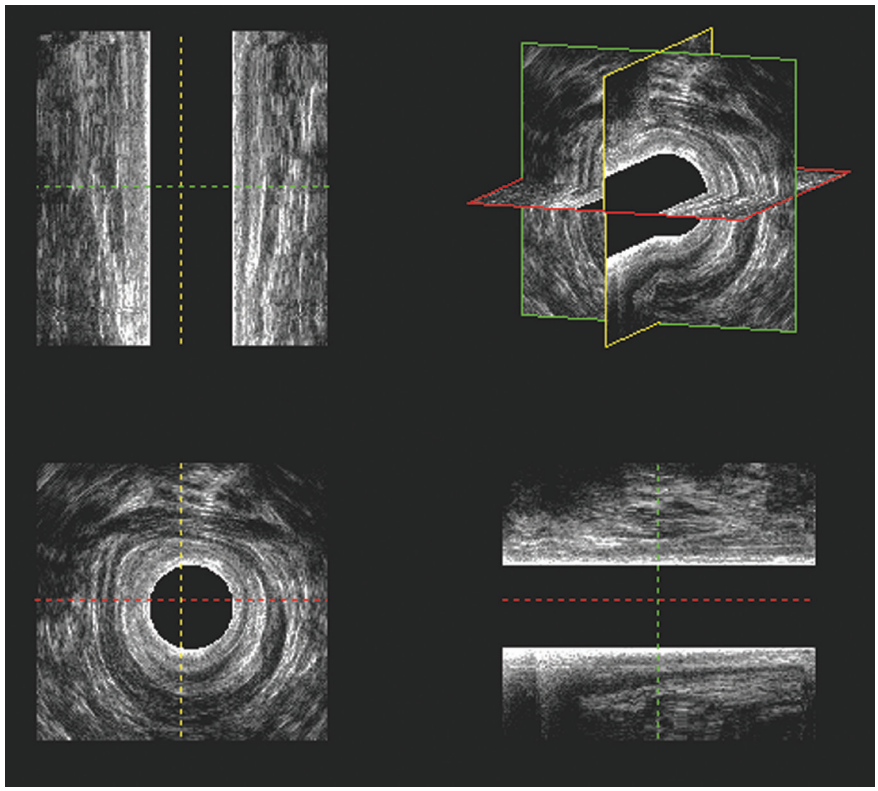

Fig. 13.5 Display of the 3D dataset using three orthogonal 2D views in a rectal study. The upper right image is a composite showing all three 2D images. Images courtesy of BK Medical (Herlev, Denmark).

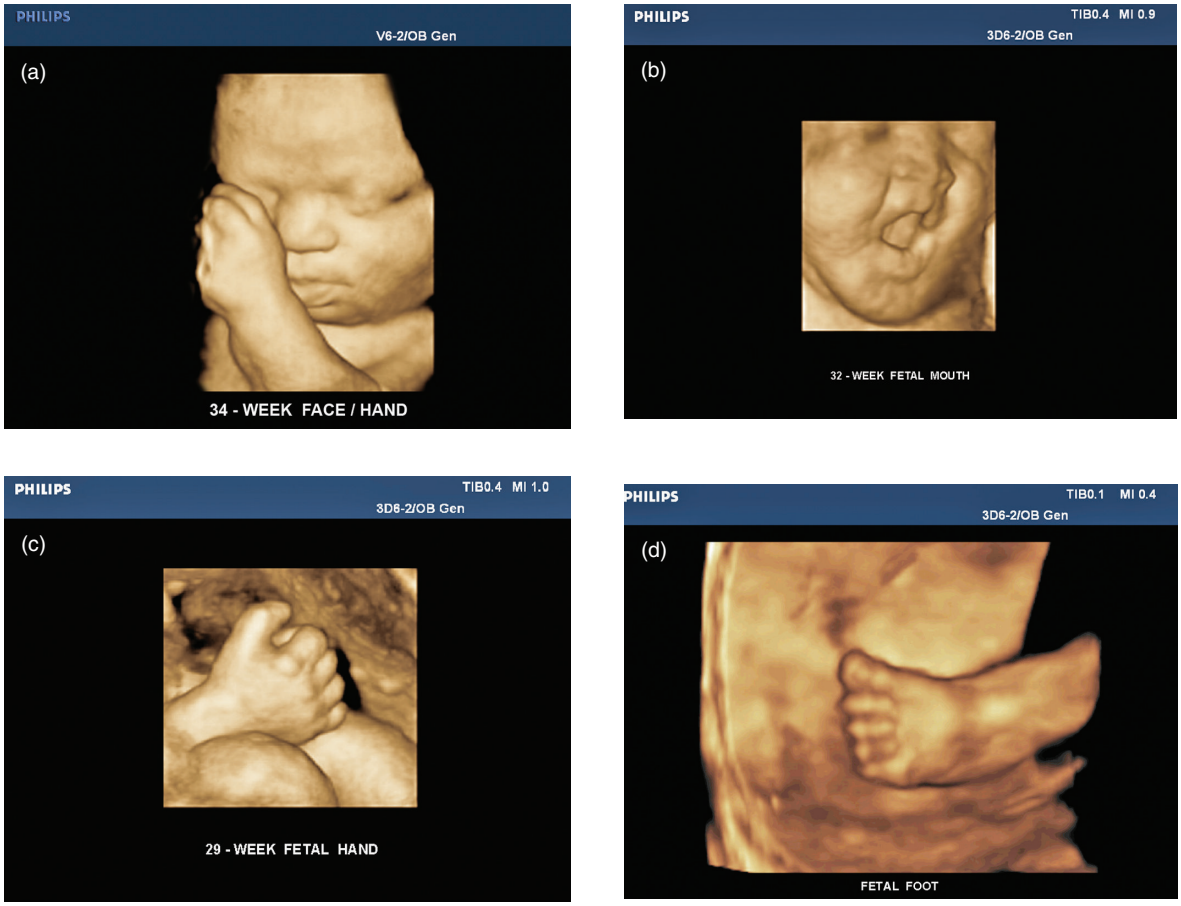

Fig. 13.6 Surface shaded view of a fetus. (a) Face and hands at 34 weeks, (b) face at 32 weeks with open mouth, (c) hand at 29 weeks, (d) foot.

such as tumours, the echo brightness may be similar to the surrounding tissue, making it more difficult for automated methods to identify the tumour boundary. For these reasons most 3D ultrasound applications of surface shading involve the heart and fetus.

Once the surface is identified the displayed grey level for each pixel of the surface is adjusted to make the displayed object look realistic. One regime might be that the grey level depends on the orientation of the surface; this is a simple technique that does not need operator intervention. Other more complex techniques involve illumination from a virtual light source. This technique may require operator intervention to position the virtual light source. For viewing it is common practice to rotate the shaded surface, though static images are used for recording in patients' notes or reports.

Surface shading is an excellent method for allowing the operator to visualize the 3D shape of a structure. The method is intuitive as, in our everyday lives, we all perceive objects as solid structures which we can walk around to gain an impression of their shape. The surface shading method is replicating this process within the computer.

The mathematical details of the surface shading method may be complex, and are the subject of considerable research. Interested readers could start with the text by Udapa and Herman (2000). The key step is boundary identification. Where the contrast between different tissue types is high and noise is low automated methods have reasonably high success in identifying the correct structures. In other 3D imaging techniques, especially CT, these methods are now routinely used to provide shaded images showing different organs. In ultrasound scanning, as noted above, the surface shading method is most easily suited to fetal and cardiac applications.

Stereoscopic viewing

The display methods described above involve projecting a 3D object onto a 2D plane and so are often

best suited to relatively simple structures. Most anatomy has some curvature and contains complex structures that overlap or partially obscure each other (Fronheiser *et al*. 2007). It can be difficult to appreciate all of this detail with conventional display methods and so this presents a greater challenge. Stereoscopic viewing offers an alternative method of visualizing objects in a 3D ultrasound scan by creating the sensation of depth. This can enhance perception of a scan and also complement other display methods.

Stereoscopic viewing takes advantage of the human visual system. Human eyes are separated by a small horizontal distance and so the left and right eyes receive slightly different perspectives of the same scenery. The brain processes these differences to create a stereo image enabling the perception of depth. So by providing each eye with an image that views an object in an ultrasound scan from a slightly different perspective it is possible to improve viewing.

There are various means of producing and displaying stereographic images. These include the use of polarizing filters to view separate right and left image pairs, complementary colour image pairs viewed through red/green glasses (similar to those used in the entertainment industry for viewing 3D films), liquid crystal light glasses that display right and left image pairs to each eye (similar to those used for virtual reality) and modern computer screens such as lenticular displays and liquid crystal displays.

For stereoscopic viewing to work with ultrasound there must be sufficient contrast between the objects of interest and surrounding tissue. Some anatomical structures such as cysts, ventricles and abscesses as well as lesions surrounded by low echogenic tissue, i.e. some tumours and haematomas, provide good contrast in ultrasound images and are therefore well suited. Breast tumours and cardiac structures such as the mitral valve are also suitable for stereo display. In obstetrics stereoscopic viewing improves visibility of primary features such as fetal skull and spine (Nelson *et al.* 2008). Augmented stereoscopic vision has applications in surgery as it allows the combination of radiographic data from different sources (e.g. ultrasound, CT and MR imaging) with the surgeon's vision (Gronningsaeter *et al.* 2000).

Applications

Fetal

Pictures of the baby's face generated by surface shading are now widely used to help parental bonding with the baby (Figure 13.6). 3D also aids in the systematic examination of organ structure and the detection of abnormalities, commonly refereed to as sonoembryology (Benoit *et al*. 2002).

Examination of the fetal heart in real time in 3D is difficult due to the high heart rate (2–3 beats per second). However, a technique has been developed

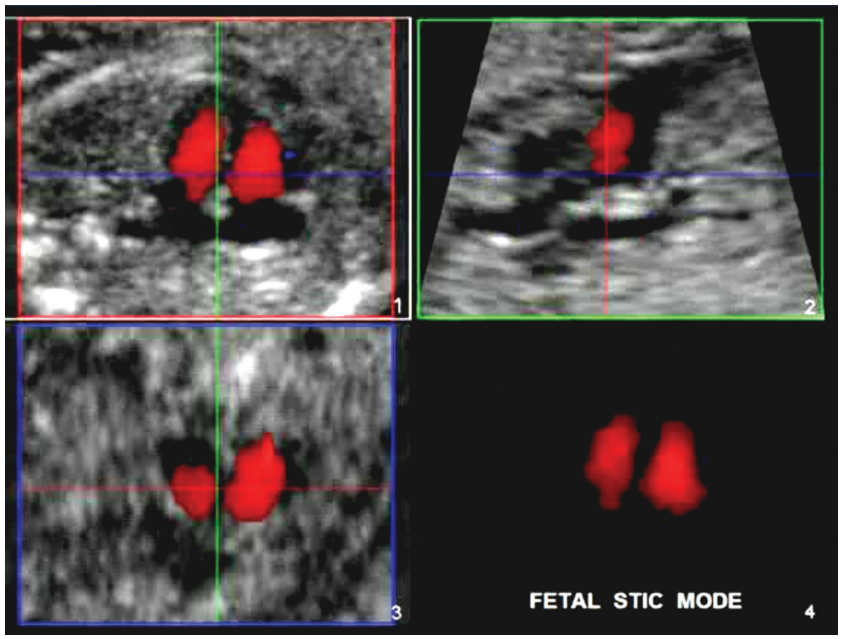

Fig. 13.7 Fetal cardiac images taken using the STIC technique. Colour flow images of three orthogonal planes are shown.

which involves reconstruction of the 3D volume in the computer (Yagel *et al.* 2007). Typically a slow sweep through the fetal heart is used in which 2D frames are collected for 10–30 seconds. Image processing is used to detect those frames corresponding to the systolic peak, and this then allows the timing of each frame within its cardiac cycle to be estimated. A series of 3D volumes are then generated from the 2D slices, each volume corresponding to a different time point in the cardiac cycle. This technique is referred to as STIC (spatio-temporal image correlation). Both 3D B-mode and 3D colour flow data can be acquired using this approach (Figure 13.7). Clinical applications of 3D fetal heart ultrasound concern the identification of congenital abnormalities.

Cardiac applications in adults

3D cardiac ultrasound systems have been used for three decades (Salustri and Roelandt 1995). Commercial systems have been based on acquisition of 2D data using both transcutaneous and transoesophageal approaches. Clinical applications of 3D cardiac ultrasound have only become routinely used since the introduction of 2D matrix transducers. The difference in echo brightness between cardiac tissues and blood allows the generation of surface shaded images which are useful for real-time visualization of the 3D structures of the heart. Figure 13.8 shows an apical four-chamber view. Common clinical uses of 3D ultrasound involve the measurement of chamber volumes, the assessment of congenital abnormalities and valvular motion and flow dynamics (Lang *et al.* 2006).

Trans-rectal

The use of 2D ultrasound is well established for examination of rectal tissues, for applications such as tumour diagnosis and staging and detection of rectal tears and fistulae. The use of rotating 3D transducers may have advantages over 2D due to the ability to make 3D measurements of volume, and to examine 3D structures and anatomy (Figure 13.9).

Intra-vascular ultrasound

Three-D IVUS scanning has been mainly used in research labs, where measurements of plaque volume and structure are of interest over time, or following intervention (Cervinka *et al.* 2006, Kawasaki *et al.* 2005).

Other applications

Three-D ultrasound techniques have been used in many other applications, but mainly on a research basis. Examples include abdominal (liver, spleen, kidney), oesophageal, arterial and muscular.

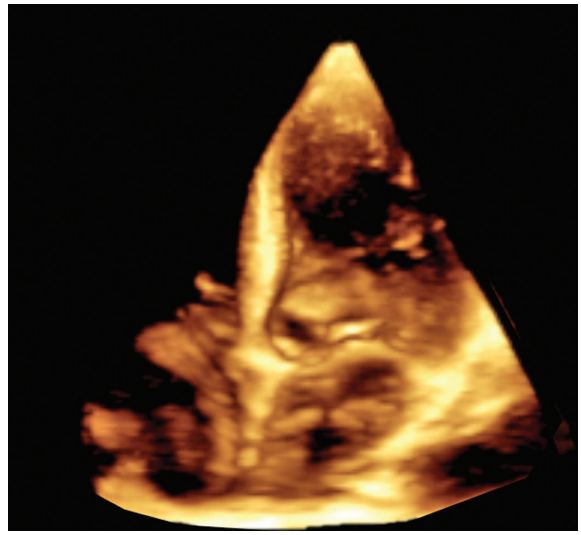

Fig. 13.8 Surface shaded apical four-chamber view of an adult heart.

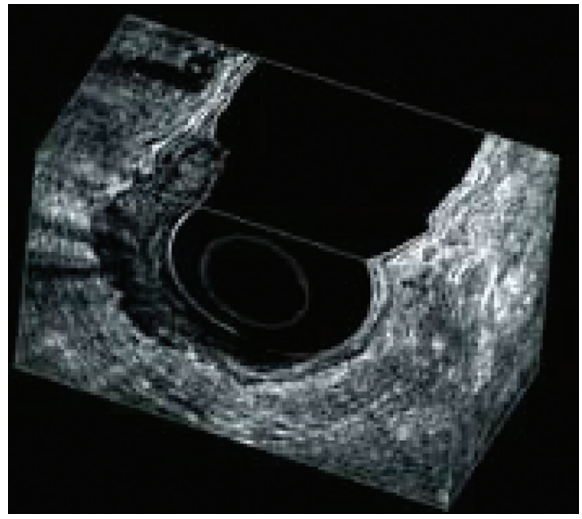

Fig. 13.9 Box display for a 3D rectal study showing a rectal tumour. Image courtesy of BK Medical (Herlev, Denmark).

Measurements

It is often desirable to extract measurements from medical images in order to reveal and diagnose disease, examine a patient's response to treatment or in obstetrics to monitor the progression of pregnancy. In 3D

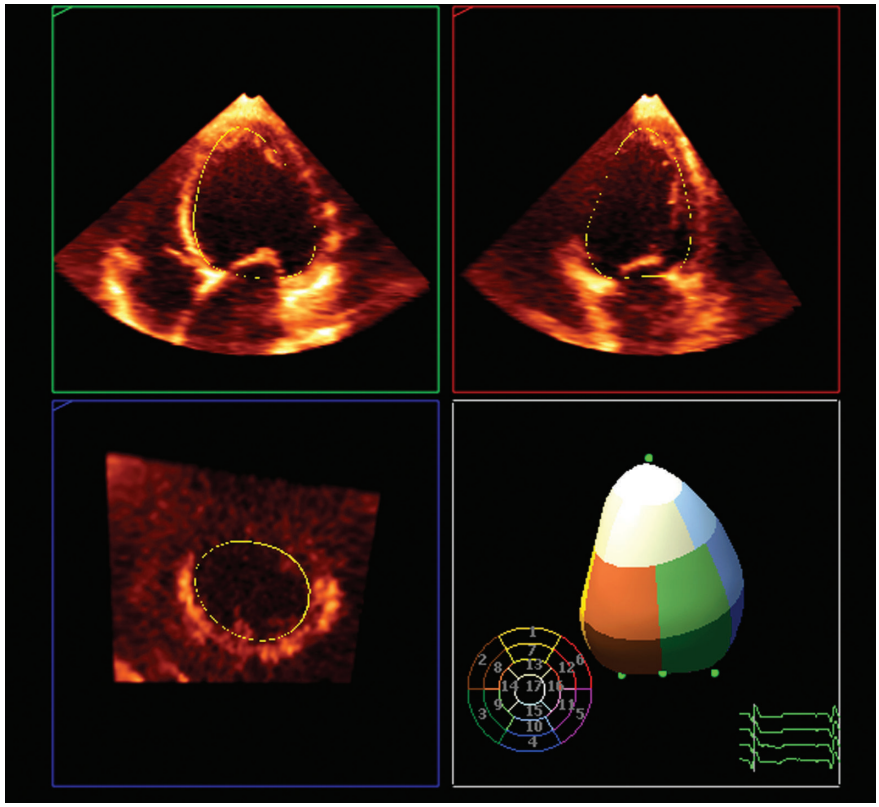

Fig. 13.10 3D left ventricular volume quantification. The inner surface of the left ventricle is obtained using a semi-automated method allowing the LV volume to be obtained at each time point in the cardiac cycle.

ultrasound a wider range of measurement possibilities exist compared to conventional 2D ultrasound, similar to CT and MR imaging.

Distances

As a volume of data is collected with 3D ultrasound it is possible to measure distances through any direction within the scan. Measurements are not just restricted to straight lines but can take the form of any path through the scan volume. This involves operator interaction to define the measurement path by selecting points by hand on a series of 2D slices. Examples of such measurements include tumour length and fetal body measurements which reflect the gestational age of the fetus.

2D shapes

As previously mentioned with 3D ultrasound it is possible for the operator to choose the position and orientation of a 2D plane through the scan volume revealing images of anatomy which would be impossible to obtain using conventional 2D imaging. This allows the quantification of shapes and areas of structures or lesions. In IVUS or endoscopic ultrasound the scan is often viewed lengthwise so that the operator can identify areas of plaque along a vessel or tumour shapes down the oesophagus that are sometimes missed by conventional 2D viewing of such data.

3D volumes

One of the greatest strengths of 3D ultrasound is the capacity for measuring volume. 3D ultrasound does not require assumptions of any specific geometry as is the case with conventional 2D ultrasound. The operator can identify the boundary of an object of interest in a series of slices through the scan and then obtain its volume. This process is very common in IVUS where the vessel wall is segmented by hand in order to calculate regions of plaque volume (Ainsworth *et al.* 2005). Freehand scanning can be employed to measure the volume of large organs such as the liver (Treece *et al.* 2001). Further details of 3D volume measurement are provided in Chapter 6.

4D measurements

Using a mechanically steered array or a 2D array it is possible to record a sequence of 3D images over time.

In cardiology measurements of volume at different points throughout the cardiac cycle provide valuable information (Figure 13.10). Left ventricular volume is determined by semi-automatic segmentation, i.e. the operator marks points on the object boundary while computational processing performs a more detailed search to complete the segmentation (Krenning *et al.* 2003). Repeating this process at regular time intervals not only returns a series of volume measurements but also enables the analysis of additional parameters such as ejection fraction (i.e. the fraction of blood pumped out of a ventricle with each heart beat), wall thickening and global and regional left ventricular rotation.

Questions

1. What do 3D and 4D mean?
2. What are two means by which the transducer may be tracked in space in freehand 3D scanning?
3. Describe two means by which 3D data may be acquired using a 1D phased array.
4. Describe two ways in which 3D data may be visualized.
5. Describe one way by which the 3D volume of an organ may be measured.

References

Ainsworth CD, Blake CC, Tamayo A, *et al.* (2005). 3D Ultrasound measurement of change in carotid plaque volume: a tool for rapid evaluation of new therapies. *Stroke*, **26**, 1904–9.

Benoit B, Hafner T, Kurjak A, *et al.* (2002). Three-dimensional sonoembryology. *Journal of Perinatal Medicine,* **30**, 63–73.

Cervinka P, Costa MA, Angiolillo DJ, *et al.* (2006). Head-to-head comparison between sirolimus-eluting and paclitaxel-eluting stents in patients with complex coronary artery disease: an intravascular ultrasound study. *Catheterization and Cardiovascular Interventions,* **67**, 846–51.

Fenster A, Downey DB, Cardinal HN (2001). Three-dimensional ultrasound imaging. *Physics in Medicine and Biology,* **46**, R67–R99.

Fronheiser PMP, Noble JR, Light E, Smith SW (2007). Real time stereo 3D Ultrasound. *IEEE Ultrasonics Symposium*, 2239–42.

Gronningsaeter A, Lie T, Kleven, *et al.* (2000). Initial experience with stereoscopic visualization of three-dimensional ultrasound data in surgery. *Surgical Endoscopy*, **14**, 1074–8.

Kawasaki M, Sano K, Okubo M, *et al.* (2005). Volumetric quantitative analysis of tissue characteristics of coronary plaques after statin therapy using three-dimensional integrated backscatter intravascular ultrasound. *Journal of the American College of Cardiology,* **45**, 1946–53.

Krenning BJ, Voormolen MM, Roelandt JRTC (2003). Assessment of left ventricular function by three-dimensional echocardiography. *Cardiovascular Ultrasound,* **1**, 12–19.

Lang RM, Mor-Avi V, Sugeng L, Nieman PS, Sahn DJ (2006). Three-dimensional echocardiography. the benefits of the additional dimension. *Journal of the American College of Cardiology,* **48**, 2053–69.

Mercier L, Lango T, Lindseth F, Collins DL (2005). A review of calibration techniques for freehand 3-D ultrasound systems. *Ultrasound in Medicine and Biology,* **31**, 449–71.

Nelson TR, Ji EK, Lee JH, Bailey MJ, Pretorius DH (2008). Stereoscopic evaluation of fetal bony structures. *Journal of Ultrasound in Medicine*, **27**, 15–24.

Prager RW, Ijaz UZ, Gee AH, Treece GM (2009). Three-dimensional ultrasound imaging. *Journal of Engineering Medicine*, DOI. 10.1243/09544119JEIM586.

Prager R, Gee A, Treece G, Berman L (2002). Freehand 3D ultrasound without voxels: volume measurement and visualisation using the Stradx system. *Ultrasonics*, **40**, 109–15.

Salustri A, Roelandt JRTC (1995). Ultrasonic 3-dimensional reconstruction of the heart. *Ultrasound in Medicine and Biology,* **21**, 281–93.

Treece G, Prager R, Gee A, Berman L (2001). 3D ultrasound measurement of large organ volume. *Medical Image Analysis,* **5**, 41–54.

Udapa JK, Herman GT (2000). *3D Imaging in Medicine*. Boca Raton: CRC Press.

Yagel S, Cohen SM, Shapiro I, Valsky DV (2007). 3D and 4D ultrasound in fetal cardiac scanning: a new look at the fetal heart. *Ultrasound in Obstetrics and Gynecology*, **29**, 81–95.

Chapter 14

Contrast agents

Carmel Moran and Mairéad Butler

Introduction

Contrast agents are used in all imaging modalities to increase the sensitivity of the imaging technique by altering the image contrast between different structures. Ultrasonic contrast agents are composed of a solution of gas-filled microbubbles. It is the dramatic increase in scattering which can be achieved with these microbubbles which has made them useful both in difficult-to-image patients and in areas for which the ultrasound signal is reduced. Injection of the contrast microbubbles and observation of their real-time passage in an ultrasound image can significantly improve the sensitivity and diagnostic power of ultrasonic imaging.

Ultrasonic contrast agents were initially used by a cardiologist in the 1960s, who used physiological saline as an intra-cardiac ultrasound contrast medium in the anatomic identification of mitral valve echoes. Microbubbles, formed in the saline after shaking, increased the contrast in the images. Intravenously injected agitated saline is still used today in cardiac studies in the assessment of patent foramen ovale. However, it was not until the mid-1980s that clinical interest resulted in development of a wide range of potential ultrasound contrast agents, some of which were the early precursors of current commercially available contrast agents. A history of the early development of ultrasonic contrast agents can be found in Ophir and Parker (1989).

Contrast microbubbles

Commercially available ultrasonic contrast agents are microbubbles filled with a gas and surrounded by a thin outer layer or shell (Figure 14.1). Gas-filled microbubbles scatter ultrasound, and hence increase the magnitude of the received echo, much more effectively than a liquid or solid-filled microbubble of comparable size.

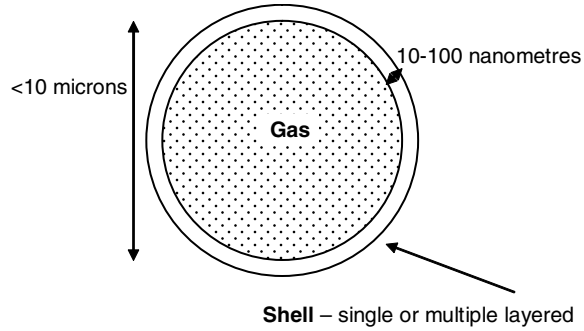

Fig. 14.1 Schematic diagram of a contrast microbubble illustrating the gaseous interior surrounded by a thin outer shell.

Free gas microbubbles, that is microbubbles with no shell, dissolve rapidly in blood. The addition of a shell ensures that the microbubbles survive passage through the lungs and to the organ of interest. In commercial preparations of microbubbles, the shells of the microbubbles must be biocompatible and tend to be either fat (lipid) or protein (albumin) based (Figure 14.2, Table 14.1). Different shell compositions can create microbubbles with different properties, e.g. lifetime and response to ultrasound.

Early contrast microbubbles, such as Levovist and Albunex, are often referred to as first-generation agents. These agents tended to be air-filled but proved to be relatively unstable in comparison to more recent microbubble preparations in which air has been replaced by high-molecular-weight gases such as fluorocarbons (or SF_6). Such gases dissolve less readily in blood.

The average size of commercially produced ultrasonic contrast microbubbles lies in the range of 2–6 μm, comparable in size to red blood cells. Prior to the commercial manufacture of ultrasonic contrast agents, agitated saline or dyes were used for some clinical applications. However, microbubbles formed in this

Diagnostic Ultrasound: Physics and Equipment, ed. Peter Hoskins, Kevin Martin and Abigail Thrush. Published by Cambridge University Press.

Table 14.1 Examples of ultrasonic contrast agents for clinical use.

Contrast agent	Manufacturer	Outer material	Gas	Diameter	Charge	Licensing and use	Supplied and reconstitution	Dose
Imagify™ (AI 700)	Acusphere Inc	Poly-L-lactide-co-glycolide	Decafluorobutane	Mean 2 µm	Negative	Awaiting approval in USA	In 20 ml vial, reconstituted with sterile water	Not available
Definity ®(USA/Canada) Luminity™ (EU)	Lantheus Medical Imaging Inc.	Lipids: DPPA, DPPC, MPEG5000, DPPE	Octafluoropropane	98% < 10 µm	Negative	EU and USA approved for suboptimal echocardiograms for opacification of the left ventricle and to improve delineation of the endocardial border	Single vial containing lipid solution with gas in the vial headspace is rapidly shaken for 45 s using a Vialmix™	Bolus: 10 µl kg^{-1} with saline flush Infusion: 1.3 ml in 50 ml saline, initial rate 4 ml min^{-1} Max: 2 bolus or 1 infusion dose
Imagent®	Imcor Pharmaceuticals Inc	Lipid: DMPC	Perfluorohexane/Nitrogen	99.8% < 10 µm	Neutral	USA approved, LVO, EBD	Reconstituted with 10 ml sterile water	Not available
Sonazoid™/ NC100100	GE Healthcare	Lipid: HEPS	Perfluorobutane	Median 2.6 µm 99.9% < 7 µm	Negative	Japan approved Focal liver lesions	Reconstituted with sterile water	Not available
SonoVue™ (BR1)	Bracco Diagnostics Inc	Lipids: Macrogol 4000, DSPC, DPPG, Palmitic Acid	SF_6	99% < 11 µm	Negative	EU approved imaging chambers in the heart and large blood vessels	Supplied in vial of 25 mg dry powder and glass syringe of 5 ml saline. The saline is added to the powder and the mixture hand shaken for 20 s	2–2.4 ml
Optison™/ FS069	GE Healthcare	Albumin	Octafluoropropane	93% < 10 µm	Slight negative	USA and EU approved To opacify the left ventricle and to improve the delineation of the left ventricular endocardial borders	Supplied as a single vial of clear solution with a white layer; the gas is in the vial headspace. To re-suspend the microbubbles the vial is inverted and gently rotated.	0.5 ml at no greater than 1 ml s^{-1} Max. 5 ml in 10 min, 8.7 ml per patient study
Echovist®	Bayer Schering Pharma Inc	Galactose	Air	Median 2 µm 99.9% <= 12 µm	Neutral	EU and USA approved To enhance gynaecological ultrasound images and assess tubal patency	Supplied as a vial containing 3 g galactose microparticles and a 1 ml aqueous solution containing galactose. The solution is vial of microparticles and the mixture shaken vigorously for 5 s, suspending the particles	2–5 ml for uterine cavity Additional 1–2 ml for tubal patency, max dose 30 ml

HEPS, hydrogenated egg phosphatidylserine; DPPA, dipalmitoyl glycerophosphate; DSPC, distearoyl glycerophosphocholine; DPPC, dipalmitoyl glycerophosphocholine; DPPE, dipalmitoyl glycerophosphoethanolamine; DPPG, dipalmitoyl glycerophosphoglycerol; DMPC, dimyristoyl phosphatidylcholine; MPEG, methoxypoly(ethylene glycol).

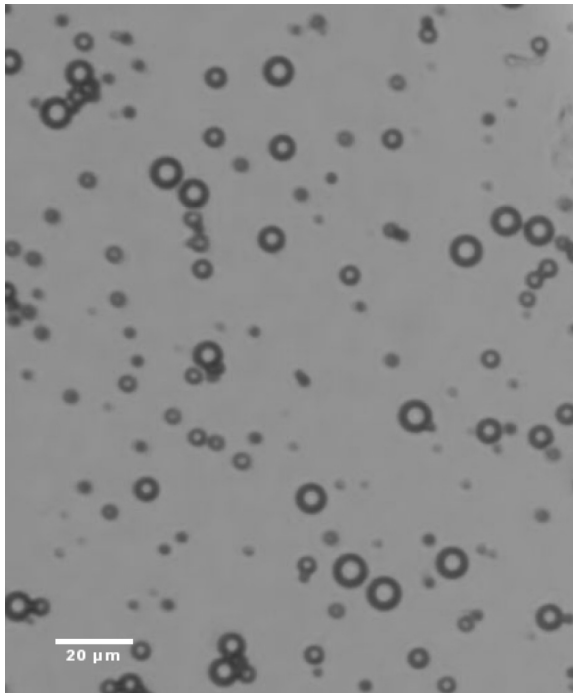

Fig. 14.2 Optical microscopic image of contrast microbubbles (Definity®/Luminity ™).

manner tended to be large (>10 µm) so were unable to pass through the lung capillary bed.

In Table 14.1, a selection of some of the contrast agents which are more widely commercially available is presented. This is not an exhaustive list but demonstrates the range of compositions, size of microbubbles and recommended clinical applications and dosages of the agents.

The behaviour of the microbubble within the ultrasound beam is complex and depends on several factors including shell composition, transmit frequency and transmit power. This behaviour leads to a number of possibilities for imaging over and above simple increase in received echo strength. These issues are covered in more detail below.

Commercially available ultrasound contrast agents

Ultrasound contrast microbubbles have a finite lifetime as microbubbles, and as such require activation (agitation or injection of saline followed by agitation) prior to clinical usage. There are many ultrasound contrast agents in developmental stages, the ones described in Table 14.1 are those which are currently available for clinical use, although some agents may only be licensed

Fig. 14.3 SonoVue™ vial in preparation kit. Once the mini-spike is inserted into the vial, the saline is injected and the solution is gently agitated.

Fig. 14.4 Vialmix with vial of Luminity™. Vial is rapidly agitated for 45 s in mixer prior to withdrawal from the vial. The rapid shaking forces the head gas into the lipid solution.

for specific clinical applications in different countries. Figures 14.3, 14.4 and 14.5 show three of the contrast agents currently available and the kit required for activation of the agents.

Fig. 14.5 Vial of Optison. Optison is activated by gentle inversion and rotation of the vial to resuspend the microbubbles, yielding a milky-white solution.

Interaction of microbubbles and ultrasound

When the ultrasound pulse insonates a microbubble the compressibility of the gas within the microbubble and the difference in acoustic impedance between the gas-filled microbubble and the surrounding tissue will cause the ultrasound to be strongly scattered.

Microbubble oscillations

When the ultrasound pulse insonates a gaseous microbubble it forces the microbubble to undergo oscillation – contracting during the compression (positive) part of the cycle and expanding during the rarefaction (negative) part of the cycle (Figure 14.6).

Microbubble resonant frequency

The degree of scattering (and oscillation) is maximum if the ultrasonic wave is at the resonant frequency of the microbubbles. The resonant frequency is the frequency at which the microbubbles oscillate most easily. This is similar to a wine glass 'singing' at a specific frequency on rubbing the rim. The frequency at which a microbubble resonates depends on the size of the microbubble. The resonant frequency of a microbubble, of a similar size to a red blood cell, is such that it lies within the clinical diagnostic frequency range of ultrasound. It must be remembered that although average diameters are often

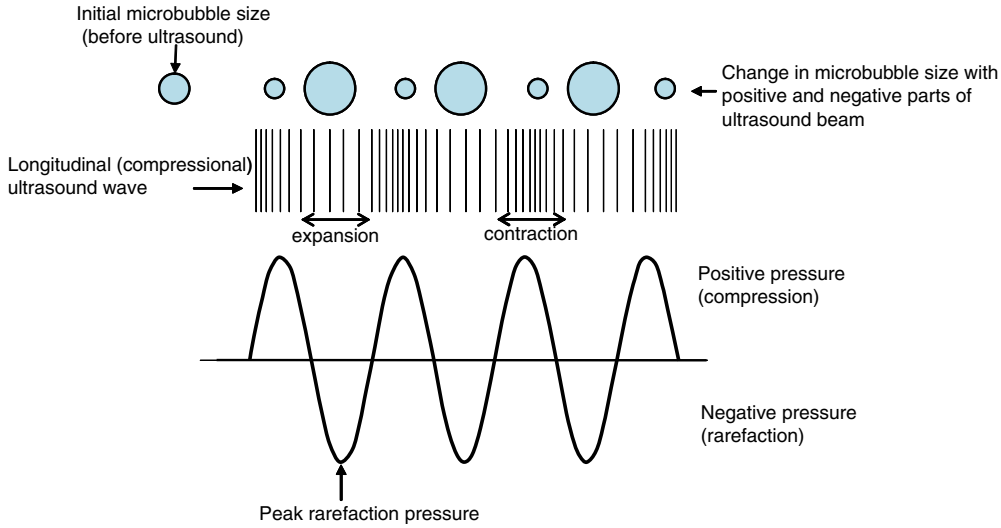

Fig. 14.6 Schematic diagram showing a microbubble contracting during the positive part of the ultrasound wave and expanding during the negative part of the wave.

quoted by commercial contrast agent manufacturers the range in size may vary from sub-micron up to 10 μm diameter; thus there is likely to be a broad range of diagnostic frequencies over which resonant behaviour may be observed. Additionally the resonant frequencies will depend on the type of shell.

Microbubble and acoustic pressure

The reaction of the contrast microbubbles with varying acoustic pressure is also of importance when imaging contrast agents *in vivo*. On most ultrasound scanners the acoustic pressure is not directly displayed but both the thermal and mechanical safety indices are displayed. The mechanical index (MI) is defined as:

$$\mathrm{MI} = \frac{p_r}{\sqrt{f}} \qquad (14.1)$$

where p_r is the peak rarefaction pressure of the ultrasound wave *in situ* (also known as the peak negative pressure) and f the frequency. It describes the likelihood of onset of mechanical damage in a homogeneous tissue. This topic is addressed more fully in Chapter 12. At low acoustic pressure ($p_r < 0.1$ MPa), and low MI the majority of microbubbles oscillate symmetrically in the ultrasound beam, expanding during the negative part of the cycle and contracting during the positive part of the cycle. The scattered ultrasound signal from the microbubble will therefore be of the same frequency as the incident wave. This is known as linear behaviour (Figure 14.7).

As the acoustic pressure is increased ($p_r > 0.1$ MPa) the bubble cannot contract as much as it can expand; this is due to the presence of the gas within the microbubbles. As a result the bubble begins to oscillate asymmetrically or unevenly, with the microbubble expanding more than it contracts. This is referred to as non-linear behaviour. Because of the asymmetric oscillations, the backscattered signal will be different in both magnitude and frequency content to the scattered wave from linear oscillations which are obtained at lower acoustic pressures. The non-linear scattered wave will contain the frequency of the incident beam as well as frequencies known as harmonics. The second harmonic is twice the incident frequency. This is seen in music: for the bugle, the lowest note is the first (fundamental) frequency (equivalent to the incident ultrasound beam). On changing lip shape while blowing, the note played is changed, and the next note heard is twice the frequency of the first (second harmonic). The next highest note is three times the fundamental frequency (third harmonic). Usually for microbubbles it is the second-harmonic signal which is detected from non-linear (asymmetric) oscillations produced from higher-pressure incident ultrasound beams.

At even higher acoustic pressures ($p_r > 1.4$ MPa, MI > 0.7 for a 4 MHz pulse), the shell of the microbubbles can be forced to crack or rupture, releasing the gas from the microbubble. The resulting free gas bubbles will strongly scatter ultrasound. However, they will dissolve rapidly into the bloodstream and therefore can only be visualized in one or two frames of ultrasound.

This violent interaction between the microbubbles and the high-pressure ultrasound pulse will result in a scattered wave which has a wide range of frequency components.

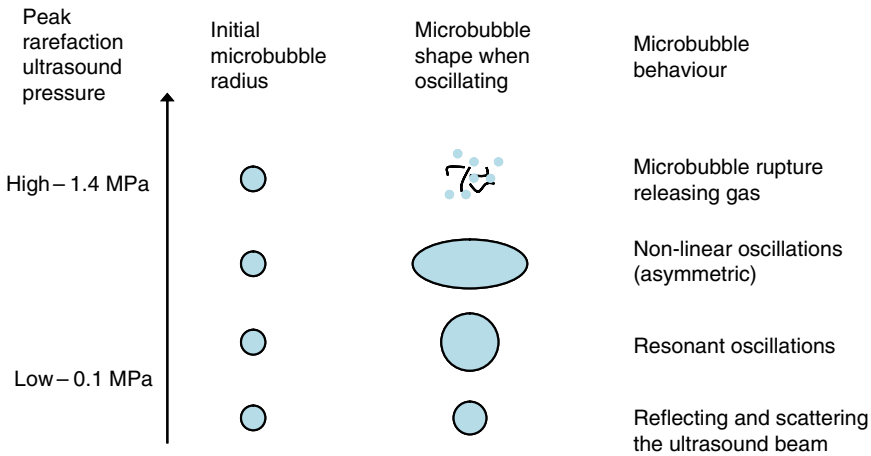

Fig. 14.7 Schematic diagram showing interaction of microbubbles with increasing acoustic pressure. As the acoustic pressure increases, the microbubbles oscillate non-linearly and eventually collapse, releasing free gas bubbles.

The specific acoustic pressure at which each of these phenomena takes place has been shown to be dependent upon many parameters, including the composition of the encapsulating shell, the size of the microbubbles and the proximity of the microbubbles to other structures such as cell and vessel walls. It must also be emphasized that although an indication of the maximum acoustic pressure generated in the scan plane is given by the displayed MI value on the screen, there is a wide variation of the acoustic pressure both laterally across the scan plane and at depth which is likely to cause a range of different interactions within each scan plane. By modifying the acoustic output of the scanner the predominant acoustic interaction can be changed but that is not to say that the other interactions do not occur.

This short section summarizes a vast range of research literature which is now available on the interaction between microbubble and ultrasound waves (Kollman 2007).

Contrast-specific imaging techniques

As previously described, the scattered ultrasound beam from the microbubbles can contain different frequencies to the incident ultrasound beam. Although the scattered signal from tissue can also contain different frequencies, these are generated by other mechanisms and are more likely to occur at depth and at higher pressures (see Chapter 2). Current techniques for imaging contrast microbubbles rely predominantly on separating the different frequency components from tissue and microbubbles.

For simplicity, contrast-specific techniques can be viewed as either low-MI imaging techniques where the acoustic pressure is such that the majority of the contrast microbubbles are not disrupted by the ultrasound wave or high-MI techniques where the acoustic pressure is such that microbubble destruction is maximized in the scan plane. Before reviewing these imaging techniques it is worthwhile reflecting upon both fundamental and second-harmonic imaging which were initially used to image contrast agents clinically.

Fundamental imaging

Prior to the development of contrast-specific imaging techniques, contrast microbubbles were imaged in a manner similar to that used for routine B-mode imaging such that the bandwidth over which the scattered ultrasound wave was received matched that of the transmitted ultrasound wave. In addition, doses of contrast agents tended to be of the order of several ml compared to doses now, which tend to be smaller. Use of injections of several ml resulted in significant, and in some instances long-lasting, attenuation distal to, or in some instances within, the vessel or organ of interest. This was particularly true for cardiac studies. However, the use of contrast agents proved to be of great importance in colour Doppler studies specifically in small vessels, such as capillaries, where without contrast the blood signal level was too low to be detected. In such vessels, injection of contrast agents could enhance the strength of the backscatter signal from the blood, thus raising the signal above the level of the clutter signal and increasing the diagnostic potential of the study (Figure 14.8).

Second-harmonic imaging

As discussed previously, at relatively modest acoustic output pressures (0.1 – 0.3 MPa) and at diagnostic ultrasound frequencies, the wave that is scattered from contrast microbubbles is non-linear and incorporates harmonics of the incident fundamental frequency (including sub-harmonics, which are harmonics generated at fractions of the fundamental frequency). Second-harmonic imaging isolates the received ultrasound wave centred at twice the transmit frequency, and uses this to form the B-mode image. By using this technique at modest acoustic pressures the ratio of the backscatter signal from contrast agent compared to tissue, known as the contrast-to-tissue signal ratio, can be increased significantly. However, the technique has limitations, because even at these acoustic pressures non-linear propagation of ultrasound through soft tissue results in generation of tissue harmonics (see Chapter 2). Non-linearity is more pronounced at depth and becomes increasingly important as the acoustic pressure is increased. Secondly, second-harmonic imaging necessitates the use of broad-bandwidth transducers to ensure that the received second harmonic signal can be separated from the fundamental frequency. Consequently, the transmit frequency bandwidth is narrowed to reduce overlap with the receive bandwidth (Figure 14.9). This limitation in transmit and receive bandwidths can result in a reduction in spatial resolution.

Low-MI techniques

Low-MI techniques have two distinct characteristics. First, using these techniques the contrast microbubbles are not destroyed and yet generate a significant non-linear, harmonic component and, second, at low

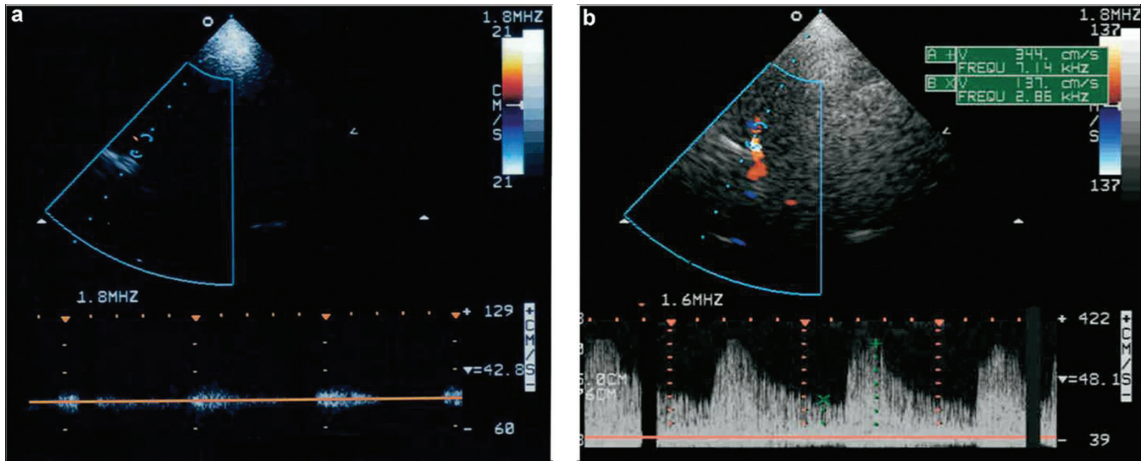

Fig. 14.8 (a) Suspected middle cerebral artery (MCA) stenosis on unenhanced transcranial colour-coded duplex sonography. In the Doppler frequency spectrum only suspicious low-frequency bidirectional signals can be obtained. In colour mode the MCA is barely visible. (b) Improvement of the Doppler frequency spectrum and the colour mode depiction of the MCA after application of an ultrasound contrast agent. Flow velocities > 300 cm s^{-1} indicate the presence of a high-grade MCA stenosis. Reprinted from Stolz EP and Kaps M, Ultrasound contrast agents and imaging of cerebrovascular disease. *Seminars in Cerebrovascular Diseases and Stroke*, vol. 5, 111–31. Copyright (2005) with permission from Elsevier.

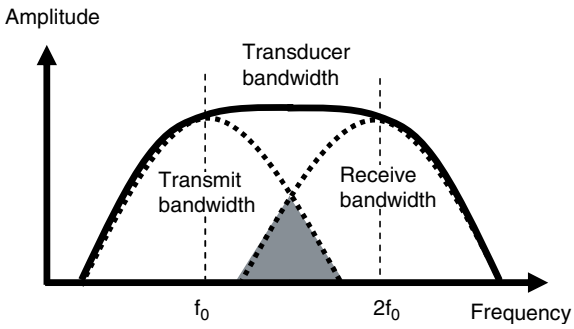

Fig. 14.9 Schematic diagram illustrating the overlap (shaded region) in the transmitted and receive bandwidths in second harmonic imaging.

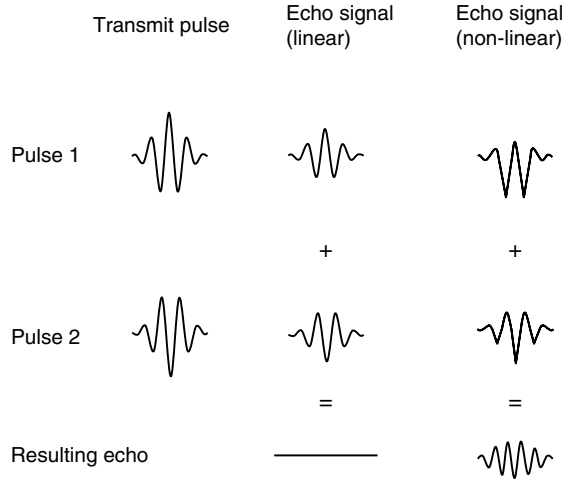

Fig. 14.10 Schematic illustration of pulse-inversion imaging. The incident pulse sequence is composed of two pulses: the second pulse the inverse of the first. On receive, the scattered signals are summed, resulting in linearly scattered signals cancelling and non-linear signals not cancelling.

MI tissue harmonics are not generated to the same level as microbubble harmonics, resulting in improved contrast-to-tissue signal ratio, i.e. there is more signal detected from contrast microbubbles than from the tissue. Low-MI techniques rely upon the processing of the scattered signal from multiple (two or more) transmitted pulses. These pulses can vary in amplitude or phase or in both amplitude and phase. Because of the requirement for multiple transmitted pulses these low-MI techniques have been shown to work best in vessels in which the microbubbles are moving slowly and thus have minimal movement of the bubbles between consecutive insonations. Moreover there is a reduction in frame rate due to the multiple transmitted pulses. However, because this is a low-MI technique (MI 0.05–0.1) the majority of the contrast

microbubbles are not destroyed between consecutive insonations. These low-MI techniques are routinely used in abdominal contrast imaging and for cardiac stress–echo studies. Individual imaging techniques are addressed below.

Low MI – pulse inversion (harmonic imaging)/phase inversion

The bandwidth limitations of second-harmonic imaging are overcome using pulse-inversion/phase-inversion techniques where rather than removing the fundamental signal from the scattered signal, it is subtracted. In these techniques, two consecutive ultrasound pulses are transmitted – the second pulse being inverted with respect to the first (180° out of phase). Upon reception, when the two received signals are added together the linear signals summate to zero (cancel); that is, they respond equally to positive and negative pressures. Pulse inversion imaging was introduced in Chapter 4. As discussed earlier, microbubbles respond differently to positive and negative pressures, hence the received signals do not summate to zero and, since contrast microbubbles are the principal source of non-linearity, these images will have a high contrast-to-tissue ratio (Figure 14.10).

Low MI – amplitude modulation (AM)/power modulation (PM)

In a similar manner to that employed in pulse-inversion imaging, in amplitude or power modulation the amplitude of the pulse is changed rather than the phase of the signal. Two, or in some instances three, consecutive pulses of varying amplitude (often in a half amplitude, full amplitude, half amplitude sequence) are emitted from the transducer in succession. Low-amplitude pulses generate less harmonics than higher-amplitude pulses and subtracting the low-amplitude response from the high-amplitude response removes the linear contribution to the scattered signal, with the remaining signal being from the non-linear scatterers (Figure 14.11).

Low MI – pulse-inversion amplitude modulation (PIAM)

This technique comprises a combination of the previous two techniques with consecutive insonating pulses varying in both amplitude and phase. Although requiring more processing to form an image, this method of detecting signals from microbubbles has been found to be very sensitive.

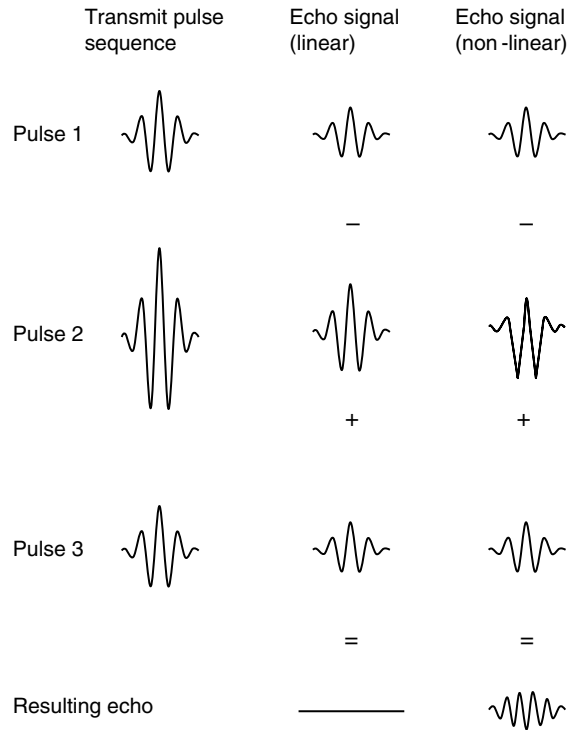

Fig. 14.11 Schematic illustration of pulse amplitude/power modulation. The incident pulse sequence is composed of three pulses – one half-amplitude pulse followed by a full pulse followed by a second half-amplitude pulse. When received, the scattered responses of the half-amplitude pulses are subtracted from the scattered responses of the full-amplitude pulse. When the pulses are scattered from a linear target, the signals will cancel out; when the scattered signal contains a harmonic (non-linear) component the signals will not cancel out.

High-MI techniques

Stimulated acoustic emission, flash imaging, intermittent imaging

In the majority of abdominal imaging clinical cases, low-MI techniques are used to observe the wash-in dynamics and patterns of blood within vessels and potential lesions. In these instances the contrast microbubbles are not destroyed and can remain in the vasculature for extended periods. Higher-MI techniques are known to destroy the contrast microbubbles but

are a more sensitive indicator of the presence of bubbles. By following a strict protocol, high-MI techniques can be used to give an indication of the perfusion of different organs, and this has been used to most effect within the myocardium. During a cardiac study and initially using a low-MI imaging technique, contrast microbubbles can be observed entering the left ventricle and subsequently into the myocardium. By emitting one, or several, high-MI pulses (flash pulse), the contrast microbubbles are forced to collapse, releasing free gas which gives a much enhanced backscattered signal (stimulated acoustic emission) for a short time, destroying the microbubbles in the scan field. By observing and quantifying the subsequent re-filling dynamics of the myocardium at low MI values, an indication of myocardial perfusion can be measured. The high-pressure MI pulse may be triggered directly from the ECG or from a pre-defined time sequence in the contrast set-up, thus generating the name – intermittent imaging (Figure 14.12).

Performing a contrast scan

A baseline scan is performed using non-contrast software initially to determine whether the patient requires contrast to aid diagnosis. If a contrast study is necessary, the ultrasound scanner is set up in a contrast protocol and, assuming no contra-indications, the contrast is prepared/activated and the patient set up for an IV injection into the femoral vein. Usually a three-way tap is used so that a saline flush can be injected immediately after the contrast. The bolus is drawn from the vial and injected at a rate of no more than 1 ml s^{-1} over a period of 5–10 s and is followed immediately by a saline flush at the same speed of injection. The time of the injection is noted and the patient is scanned throughout. When a low-MI study is being undertaken, the output power of the scanner is kept very low (MI < 0.1) to ensure that the contrast microbubbles do not collapse during the scanning session. In the majority of instances, switching to a low-MI contrast-specific imaging mode will result in the image becoming very dark and in some instances very little anatomical information may be visualized on the screen. These images are formed from the non-linear signals and hence, without contrast present, there is limited generation of non-linearities from tissue at these low output powers. As a result the technique is reliant on the expertise of the sonographer to maintain the position and orientation of the ultrasound beam when scanning. In some high-end commercial scanners, when contrast mode is selected the image on the screen sub-divides into two – one showing the normal

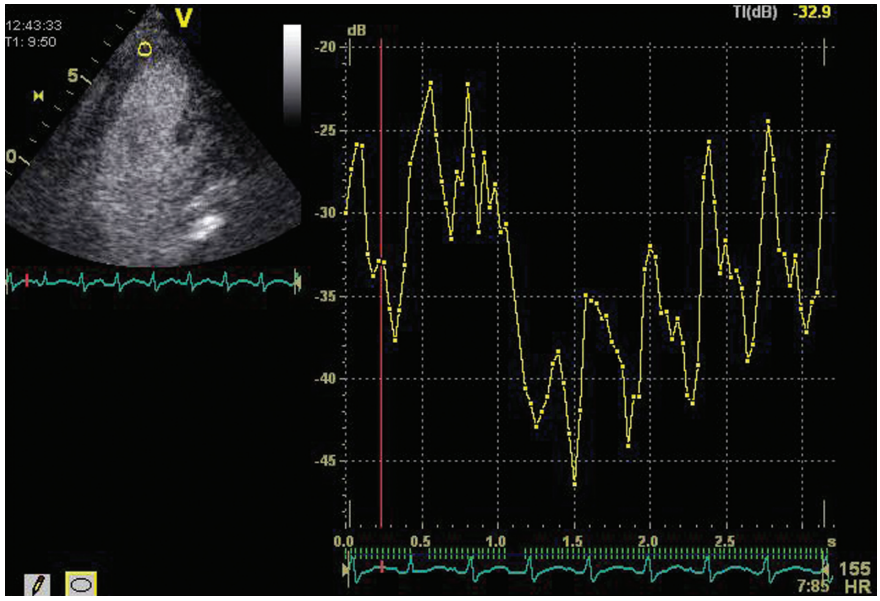

Fig. 14.12 Clinical example of a contrast perfusion study in an apical two-chamber view of the left ventricle during infusion of SonoVue™ with graphical display illustrating variation in backscatter signal in selected ROI within the myocardium. A pulse-inversion imaging technique is used to image reperfusion of the myocardium following application of a high-MI pulse. Image courtesy of Dr Stephen Glen, Stirling Royal Infirmary, Scotland.

B-mode image formed over the whole bandwidth of the transducer, at low MI values, and on the other the image formed from the non-linear signals. The ability to be able to simultaneously visualize the structural information whilst observing the filling dynamics of vessels is of great benefit and ensures that the correct scanning position is maintained throughout a scanning session.

Once the contrast has been injected, it is generally visualized initially in a feeding vessel to the organ of interest. Initial strong attenuation of the ultrasonic beam may occur causing shadowing of distal structures. As the bolus of contrast distributes throughout the organ, the more distal structures may then become visible again. Study of the filling dynamics and distribution of the agent around lesions, specifically in the liver, has been shown to have high diagnostic power (see EFSUMB guidelines). Acquisition of images and cine loops during contrast enables a review of the acquired images. Dependent on the quantity of agent used and the manufacturer's recommendations a second and possibly third dose of contrast agent may be given to provide further diagnostic information.

Infusion injections are often used in cardiac perfusion studies to maintain a steady flow of contrast. The contrast agent is diluted with saline and placed in an infusion pump and run continuously throughout the study. Infusion studies generally take longer than bolus studies but have the potential to provide quantifiable results. In many instances the contrast has to be gently agitated within the infusion pump to ensure that the bubbles are evenly distributed in the syringe.

Machine settings

During ultrasound contrast studies, it is important that none of the settings of the scanner are adjusted while the study is being undertaken. When the contrast-specific imaging mode is selected, the gain is set at a relatively low level to ensure that enhancement is visualized as the contrast arrives in the scan plane. This gain setting as in normal B-mode imaging will not affect the beam transmitted from the probe but only the image that is displayed on the screen. The majority of high-end ultrasound scanners have contrast-specific imaging protocols offering either a pulse-inversion or amplitude-modulation imaging technique. Once selected these packages switch to a low MI value (low power output), which should not be adjusted by the operator throughout the scan. Varying the power output will affect the amplitude of the transmitted beam and, as discussed previously, can determine the microbubble response to the beam. For the assessment of cardiac perfusion, the large-amplitude pulse can be triggered from the ECG or directly by selecting a scanner option enabling rapid destruction of the contrast microbubbles. In addition, as with B-mode scanning, higher frequencies will increase resolution and lower frequencies will increase penetration.

Quantification

Quantification of microbubble enhancement is challenging due to the difficulty in controlling the number of bubbles in a region of interest, therefore comparisons between different scans or administrations of contrast agent are difficult even when machine settings are kept the same. However, since microbubble contrast agents are blood-pool agents they can be useful as indicators of physiological parameters such as vascular flow volume, blood flow velocity and perfusion rate, although accuracy is an issue because of the reasons described above. A method of looking at contrast agent enhancement in a region of interest is the time–intensity curve, where backscattered intensity from microbubbles is plotted against time. This curve shows how the concentration of microbubbles in a region of interest changes as the blood flows through it. These curves can be used to assess the change of echo intensity with time, with their shape depending on the organ of interest and whether the contrast is administered as a bolus or infusion. A bolus will provide enhancement for up to 2 minutes as the microbubbles wash in and wash out of the region of interest as they circulate, while an infusion can provide enhancement for longer periods as the microbubbles are administered at a steady pace over time (see Table 14.1 for rates of infusion and bolus administration methods). Figure 14.13 shows a typical time–intensity curve after a bolus injection of contrast. The data can be collected from regions-of-interest within an organ or vessel. The intensity of the backscatter signal is measured during and after a bolus injection of contrast. From this curve, parameters such as peak intensity, mean transit time and time to peak can be measured.

Clinical applications of contrast agents

Ultrasonic contrast agents are becoming increasingly accepted in diagnostic clinics when used in combination with contrast-specific imaging techniques described above. A comprehensive review of the clinical applications in which the use of contrast agents is considered to improve diagnostic potential has been

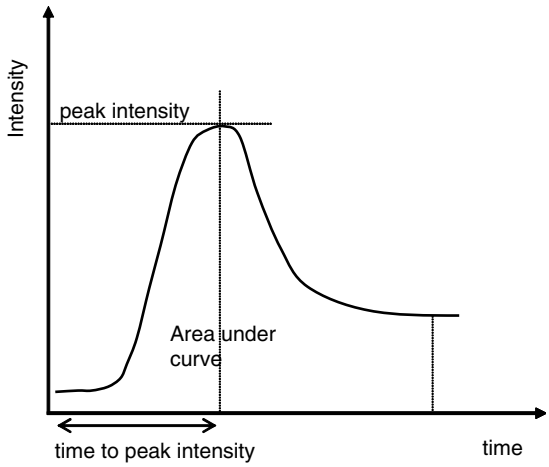

Fig. 14.13 Typical time–intensity curve after a bolus injection of contrast.

published by the European Federation of Societies for Ultrasound in Medicine and Biology (EFSUMB), in which guidelines and recommendations for good practice are outlined. Although commercially available contrast agents are licensed principally for use in the liver, breast or for cardiac endocardial border definition, guidelines are also provided for assisting in studies which are not currently licensed (off-licence) including renal, spleen and pancreatic, transcranial, urological and cardiac perfusion studies. Low-MI techniques are recommended for all organs except for cardiac perfusion applications, for which high-MI techniques in combination with low-MI techniques are useful in identifying perfusion defects.

Liver

The use of contrast agents to aid in the detection and diagnosis of focal liver lesions is now well established (EFSUMB study group 2008) and outwith cardiac applications the liver is the organ most widely studied using contrast. After a bolus contrast injection there are three distinct phases of enhancement within the liver. These are the arterial, portal-venous and late phase, occurring 10–20 s, 30–45 s and more than 120 s after injection respectively. By studying the enhancement patterns of focal liver lesions during these three phases, detection and classification of the lesions are possible (Figure 14.14).

Kidney

Although some contrast agents are licensed for imaging large vessels (SonoVue™) there is no agent which is licensed for imaging the kidney; therefore this represents an off-licence application. After a bolus injection, enhancement is visualized first in the cortex, 10–15 s after bolus injection. Medullary enhancement then follows. Shadowing can occur due to the high vascularity of the cortex attenuating the signal from medulla. Currently differentiation between malignant and benign renal lesions within the kidney is not possible (Figure 14.15).

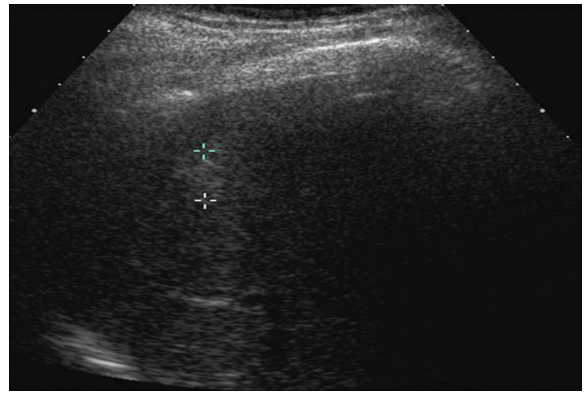

(a)

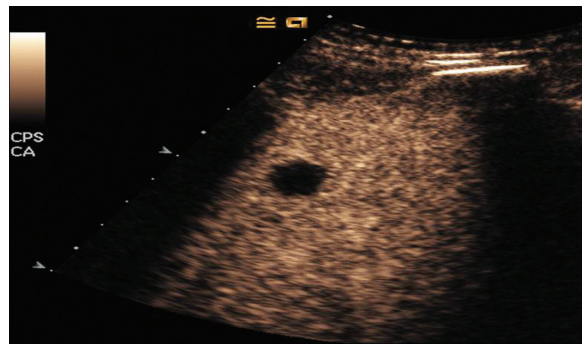

(b)

Fig. 14.14 (a) Image with an echogenic liver metastasis (between callipers) acquired in fundamental imaging. (b) Image acquired 1 min 24 s after bolus injection of SonoVue™ (portal-venous stage). Low reflective area in the contrast-enhanced image is indicative of malignancy. Reproduced with permission from Dr Paul Sidhu, King's College Hospital, London.

Spleen and pancreas

Use of contrast agents to study the pancreas is relatively new and is currently not licensed. Contrast can be used to improve delineation and sizing of pancreatic lesions or for studying blunt trauma injury (Figure 14.16).

Transcranial

SonoVue™ is licensed for use in transcranial studies. Colour Doppler or duplex sonography can be used,

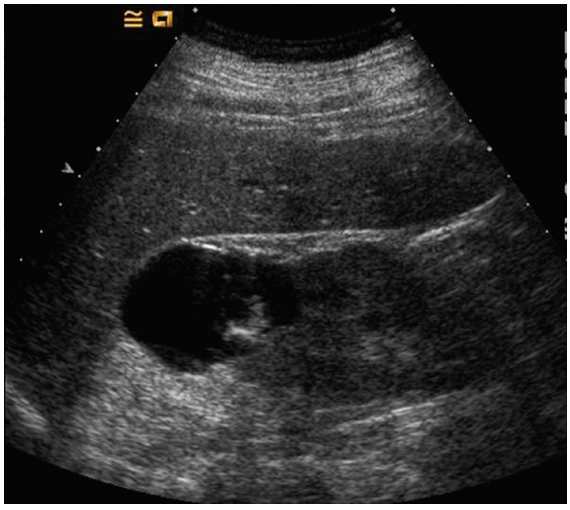

(a)

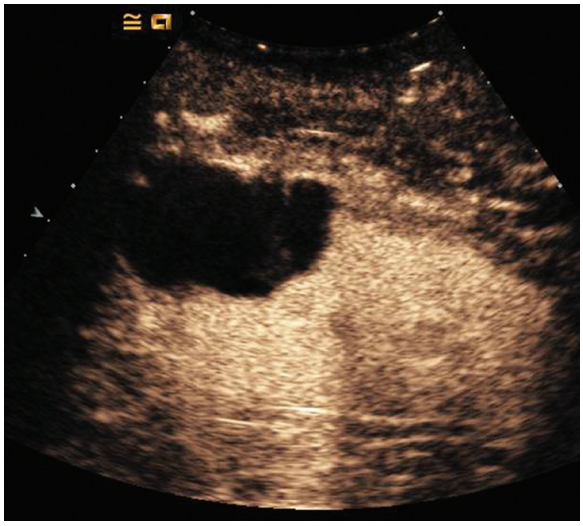

(b)

Fig. 14.15 (a) Image suggests a complex renal cyst in fundamental imaging. (b) Acquired after a bolus injection of SonoVue™ using a low-MI imaging technique. No septation enhancement evident, therefore lesion unlikely to be malignant. Reproduced with permission from Dr Paul Sidhu, King's College Hospital, London.

after a bolus injection, to aid differentiation of transcranial vessels which are occluded or which have low flow. It is specifically useful in those patients who have a poor signal-to-noise ratio in unenhanced ultrasound cerebral studies as it enhances simultaneously in several vessels, showing brain anatomy and areas of blood flow (Figure 14.8).

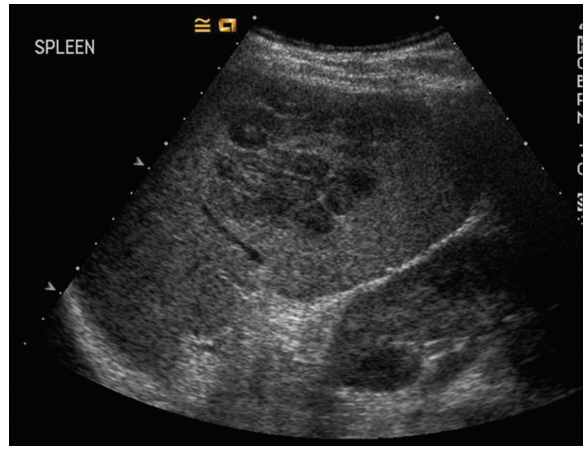

(a)

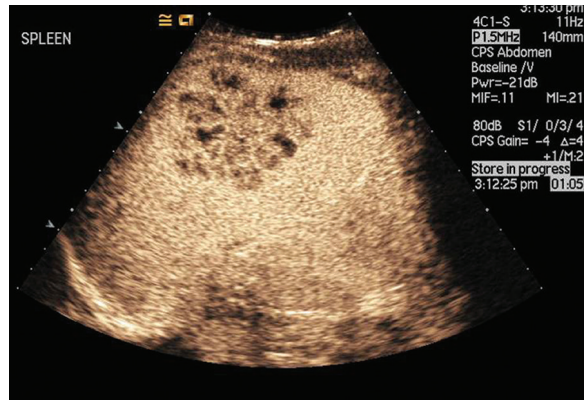

(b)

Fig. 14.16 (a) Image suggests a possible splenic cyst in fundamental imaging. (b) Acquired after a bolus injection of SonoVue™ and using a low-MI technique to image the spleen. Honeycomb pattern suggestive of a spleen abscess. Reproduced with permission from Dr Paul Sidhu, King's College Hospital, London.

Cardiac applications

Almost all ultrasonic contrast agents have been licensed for specific cardiac applications such as endocardial border definition and left ventricular opacification. Identification and enhancement of cardiac chamber borders is of specific benefit during stress–echo studies where the patient is either physically (by exercise) or pharmacologically stressed. During such studies the heart is ultrasonically scanned at specific time-points, generally at rest, low stress, peak stress and at recovery, and the movements of individual cardiac chamber walls are continuously assessed using ultrasound. In difficult-to-image patients, sections of the heart walls may be indistinct. Injection of contrast

enhances these borders, enabling a global assessment of cardiac wall movement. Such cardiac studies are performed in real time, using low-MI contrast-specific imaging techniques. Contrast can be injected as a bolus but if a cardiac perfusion study (see below) is also to take place on the same patient, an infusion may be used.

No contrast agent is licensed for the assessment of myocardial blood flow and consequently cardiac perfusion. However, by using a combination of high- and low-MI imaging techniques it is possible to get an indication of relative blood flow within different segments of the myocardium. When microbubbles are administered via an infusion, after a period dependent on heart-rate and blood flow dynamics a consistent level of contrast enhancement may be observed within the myocardium. This can be visualized using a low-MI contrast-specific imaging technique. If the pressure output of the scanner is increased to a high MI value for a single or several frames, the microbubbles in the scan plane are forced to collapse, releasing free gas which, as discussed previously, only lasts a short period in the blood. By rapidly returning to low-MI imaging, it is possible to visualize and quantify by increasing brightness the return of contrast to each of the segments in the myocardium. By mapping each of the segments it is possible to build up knowledge of the myocardial blood flow within different myocardial segments (Figure 14.12).

Safety of contrast agents

The main risks associated with the use of ultrasound contrast agents are embolic risk, allergic reaction, toxicity and biological effects due to acoustic cavitation. The safety of two commercially available contrast agents (Definity®/Luminity™ and Optison) was recently addressed retrospectively in a large multi-centre study which indicated that the incidence of severe adverse reactions was less than that associated with contrast agents used for other imaging modalities. However, it is the likelihood of acoustic cavitation occurring under routine clinical application which is of most concern. Gas bodies do not exist under normal conditions within the blood or soft tissue. When contrast microbubbles are injected into the body, they provide a potential source of cavitation nuclei. Cavitation has previously been shown to result in high speed fluid jets, localised high temperatures (>1000°C) and sonochemical reactions. Whether intact microbubbles are capable of causing cavitation effects is still under investigation. The potential bioeffects from these processes have been reviewed by The World Federation of Ultrasound in Medicine and Biology (WFUMB) in a series of articles. Current recommendations for the safe use of ultrasonic contrast agents included: (1) scanning at low MI; (2) scanning at higher frequencies; (3) reducing total acoustic exposure time; (4) reducing contrast dose; (5) adjusting the timing of cardiac triggering during cardiac contrast studies. The safety of contrast agents is more fully addressed in Chapter 12.

Artefacts in contrast imaging

In Chapter 5, the source of the most commonly observed artefacts in clinical ultrasound imaging were discussed. In this section, we address those artefacts which are particularly relevant to contrast-enhanced clinical scanning.

Propagation artefacts

In ultrasound imaging, it is assumed that attenuation within soft tissue is constant and this is corrected on the ultrasound image by the use of time-gain compensation sliders. Of particular diagnostic interest is localized regions of increased attenuation which create a shadow (reduced brightness) beyond the region of increased attenuation. A common example of the diagnostic potential of this is shadowing due to calcified plaque in vessels. Ultrasound contrast agents, although strong scatterers of ultrasound, are also strong attenuators. As the contrast agent arrives in an organ via a feeding vessel, it is usual that the distal part of the organ temporarily disappears from the screen due to the high attenuation of the microbubbles. After a period dependent upon contrast agent dose, rate of injection, scanner set-up and organ dynamics, the contrast will begin to clear from the organ and the distal part of the image will begin to reappear. This is particularly evident in bolus injections where a large number of scatterers are injected over a period of 1–2 s. Although shadow artefacts are useful in diagnosis in clinical scanning, due to their transient nature in contrast-enhanced studies they are currently not considered useful (Figure 14.17).

Multiple scattering

Within an imaging system, it is assumed that the transmitted ultrasound pulse travels only to targets on the

beam axis and back to the transducer. When contrast agents are injected into this path, a range of different phenomena can occur. First, due to the number of scatterers present, multiple scattering is likely to occur, resulting in a delay in the return path of the ultrasound beam, and hence echoes from beyond the contrast-enhanced region will be displayed at greater depth than the true position of the source.

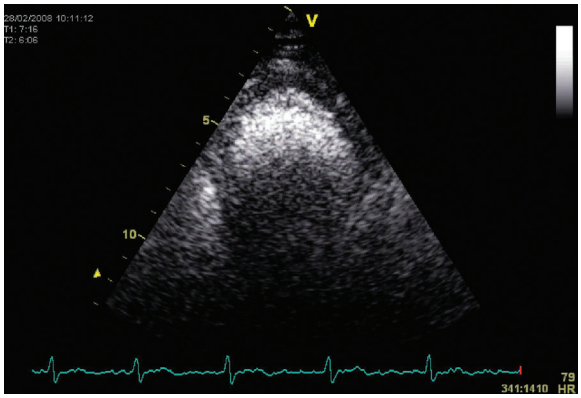

Fig 14.17 Shadowing caused by bolus injection of contrast (SonoVue™). In this two-chamber view of the heart, as the contrast bolus enters the left ventricle, it strongly attenuates the ultrasound beam and distal regions of the heart are difficult to visualize. After several cardiac cycles, the contrast will begin to clear and the whole ventricle will be visualized. Image courtesy of Dr Stephen Glen, Stirling Royal Infirmary, Scotland.

Colour blooming

In colour Doppler imaging, after the injection of contrast an artefact known as colour blooming may occur. As contrast enters a vessel the magnitude of the backscattered signal increases, giving a corresponding large increase in Doppler signal. This increase in signal can expand outwith the width of the vessel, causing 'blooming', and can be corrected by reducing the Doppler gain (Figure 14.18).

Summary

Contrast agents for use with ultrasound are in the form of microbubbles – gas bubbles encapsulated in a thin outer layer. Microbubbles expand and contract in the ultrasound beam, generating linear and non-linear signals. Ultrasound contrast agents can be used clinically for scanning vascular organs. There are contrast-specific scanning modes available on ultrasound scanners which make use of the non-linear scattering from contrast microbubbles, allowing the signals from microbubbles to be distinguished from tissue. Used appropriately ultrasound contrast agents offer ways to improve the diagnostic ability of ultrasound scans.

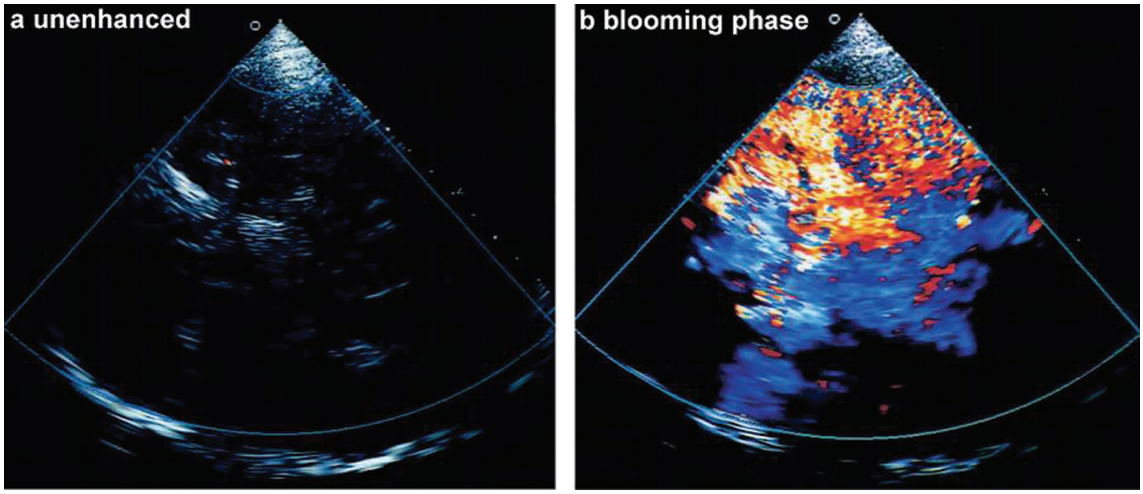

Fig. 14.18 Blooming effect during ultrasound contrast application in a patient with inadequate acoustic cranial bone window: (a) unenhanced examination; (b) blooming phase after ultrasound contrast bolus injection. Reprinted from Stolz EP and Kaps M, Ultrasound contrast agents and imaging of cerebrovascular disease. *Seminars in Cerebrovascular Diseases and Stroke*, vol. 5, 111–31. Copyright (2005) with permission from Elsevier.

Questions

1. How does the resonant frequency of a microbubble change with microbubble size?
2. How does the response of a microbubble to ultrasound change with acoustic pressure?
3. How does harmonic imaging work?
4. What is the second harmonic?
5. Why does harmonic imaging work well with contrast agents?
6. What are the main risks and hazards associated with ultrasound contrast agents?
7. Summarize some clinical areas where contrast agents can be used.
8. What ultrasound artefacts can be associated with contrast imaging and what are their effects?

Acknowledgement

The authors would like to acknowledge that grant funding from the British Heart Foundation supported the posts of Carmel Moran and Mairéad Butler.

References

EFSUMB study group (2008). Guidelines and good clinical practice recommendations for contrast enhanced ultrasound (CEUS) – update 2008. *Ultraschall in Medizin*, **29**, 28–44.

Gramiak R, Shah P, Kramer D (1969). Ultrasound cardiography: contrast study in anatomy and function. *Radiology*, **92**, 939–48.

Klibanov AL (2007). Ultrasound molecular imaging with targeted microbubble contrast agents. *Journal of Nuclear Cardiology,* **14**, 876–84.

Kollmann C (2007). New sonographic techniques for harmonic imaging – underlying physical principles. *European Journal of Radiology,* **64**, 164–72.

Main ML, Goldman JH, Grayburn PA (2007). Thinking outside the 'box' – the ultrasound contrast controversy. *Journal of the American College of Cardiology,* **50**, 2434–7.

Ophir J, Parker KJ (1989). Contrast agents in diagnostic ultrasound. *Ultrasound in Medicine and Biology,* **15**, 319–33.

Chapter 15

Elastography

Peter Hoskins

Introduction

The term 'elastography' is used to describe techniques which provide information related to the stiffness of tissues. It has long been known that diseased tissues such as tumours are stiffer than the surrounding normal tissue. Indeed one of the oldest diagnostic methods is the assessment of the stiffness of tissues by palpation; if a stiff lump is found then the lump may well be diseased. Ultrasound techniques generally work by replicating this process; the tissue is squeezed and the response to squeezing is measured using the ultrasound system.

Ultrasound elastographic techniques in this chapter are classified in two ways based on the underlying measurement principle:

- *Strain techniques*: these rely on the compression of the tissues, and the measurement of the resulting tissue deformation and strain using ultrasound. These may be referred to as 'static' methods.
- *Shear-wave techniques*: these rely on the generation of shear waves, and the measurement of shear-wave velocity within the tissues using ultrasound, from which elastic modulus may be estimated. These may be referred to as 'dynamic' methods.

The first of these techniques provides information mainly on strain; the estimation of elastic modulus is challenging and not much performed outside research labs. The second technique does provide information on elastic modulus, but is more technically challenging, especially for 2D image formation.

This chapter concentrates on elastography methods which have been adopted commercially, in order to offer understanding to sonographers and other users of the techniques available in routine clinical practice. Other elastographic techniques have been described which, though promising, have yet to find their way into commercial systems. Details of these can be found in review articles such as those by Ophir *et al.* (1999) and Greenleaf *et al.* (2003).

Elasticity

When a material is subject to a force it is stretched or compressed. The general terminology and principles used to describe this process can be illustrated using a simple material such as a rubber band or a wire (Figure 15.1). If a weight is attached to a strip of the material, the strip stretches. If the weight is increased the strip stretches further. Eventually the strip will break when the weight becomes too much.

In Figure 15.1 a weight W is attached to a strip of material. The stretch from the original length is d. For a simple material, such as rubber, the stretch is proportional to the added weight. A simple equation describing this behaviour is:

$$stress/strain = constant \qquad (15.1)$$

For Figure 15.1 the stress is the force W divided by the cross-sectional area A. This has units of N m^{-2}, the same units as pressure.

$$stress = force/area \qquad (15.2)$$

For the example of Figure 15.1 this gives:

$$stress = F/A$$

The strain is the change in length d divided by the original (non-distended) length D. This has no units.

$$strain = \frac{length\ (after) - length\ (before)}{length\ (before)} \qquad (15.3)$$

For the example of Figure 15.1 this gives:

$$strain = d/D$$

Diagnostic Ultrasound: Physics and Equipment, ed. Peter Hoskins, Kevin Martin and Abigail Thrush. Published by Cambridge University Press.

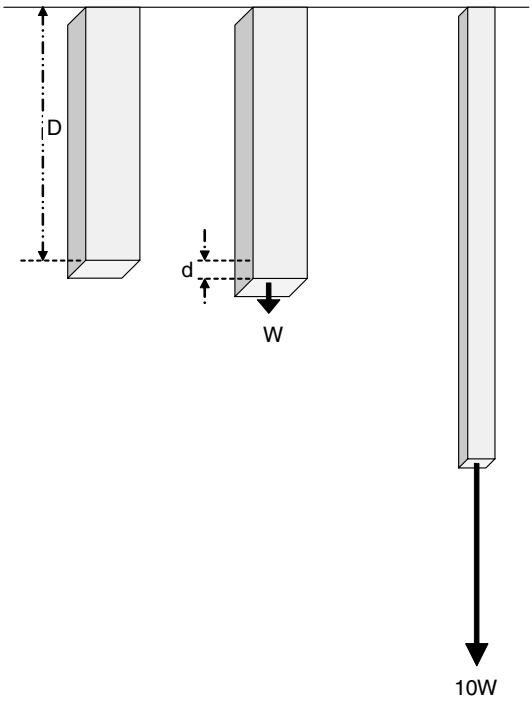

Fig. 15.1 Stretching of a simple elastic material by a force *W*. The unstretched material has a length *D*. A weight *W* stretches the material by an amount *d*. In the case of soft tissue the material is incompressible (density does not change) so that the stretch will result in reduction of the cross-sectional area. This is small for small stretches, but when a large force is applied the material will stretch by a large amount and there is a clear reduction in cross-sectional area.

The constant in Equation (15.1) is commonly referred to as Young's modulus, *E*. Equation (15.1) then becomes:

$$E = stress/strain \tag{15.4}$$

For many materials, including human soft-tissues, the density of the material is virtually unchanged by stretching or compression. In Figure 15.1 a large stretch will therefore result in reduction of the cross-sectional area of the strip; in other words, extension in one direction is compensated by contraction in the other directions.

Typical values of Young's modulus are given for hard materials in Table 15.1 and soft materials including soft tissues in Table 15.2. Note that there is a factor of a million between the values in the two tables. A compilation of published work on the Young's modulus of biological tissues can be found in Duck (1990) and Sarvazyan (2001). The Young's modulus of tissue mimics, as used in ultrasound phantoms, is described in Dineley *et al.* (2006) and Madsen *et al.* (2005).

Table 15.1 Young's modulus values for harder materials.

Material	*E* (GPa)
Non-human materials	
Diamond	1220
Steel	200
Wood (oak)	11
Nylon	1–7
Vulcanized rubber	0.010–0.100
Human tissues	
Tooth enamel	20–84
Femur	11–20

Table 15.2 Young's modulus values for softer materials.

Material	*E* (kPa)
Non-human materials	
Silicone rubber	500–5000
PVA cryogel tissue mimic	35–500
Agar/gelatine tissue mimic	10–70
Human tissues	
Artery	700–3000
Cartilage	790
Tendon	800
Healthy soft tissues [a]	0.5–70
Cancer in soft tissues [a]	20–560

[a] Breast, kidney, liver, prostate.

General principles of strain elastography

The steps needed for estimation of the elastic modulus using lab-based or imaging-based methods are illustrated in Figure 15.2.

- *Apply known force*: the force or stress compressing or stretching the tissues must be known.
- *Measure change in dimensions*: the change in dimensions of the tissues is measured, and the strain calculated from Equation (15.3).
- *Estimate Young's modulus*: Young's modulus is estimated from Equation (15.4).

This apparently simple set of steps is difficult to achieve except for the most simple of circumstances, such as the isolated thin strip of Figure 15.1. In the body there are a number of complexities in the estimation of Young's modulus which are explored in more detail later in this chapter. The main problem which is discussed at this stage is the lack of knowledge of the force or stress to which the tissue is subject. Difficulty in estimating the true tissue stress means that strain elastography concentrates on the estimation of tissue strain, not on the estimation of Young's modulus.

Strain and strain-ratio

Figure 15.3 shows an idealized uniform tissue in which are embedded two lesions, one stiff and one soft. The block of tissue is subject to a uniform force which causes compression of the block in the vertical direction, and also expansion of the block in the horizontal direction. For materials such as soft tissue whose density does not change when they are compressed this is the usual result – compression in one direction leads to stretching in another direction. In the compressed block, the soft lesion is compressed more than the surrounding tissue, which in turn is compressed more than the hard lesion. The change in dimensions which arise as a result of compression is the strain (Equation (15.3)). The strain in the direction of the applied force (vertically in the case of Figure 15.3) is shown, as this is the measurement usually made using ultrasound. As stiff lesions are resistant to compression they are usually associated with low strain values. A strain value of zero would imply that the lesion was very hard. Figure 15.4 shows the two lesions and the reference region from Figure 15.3, pre- and post-compression. The reference region is usually a part of the image which is known or

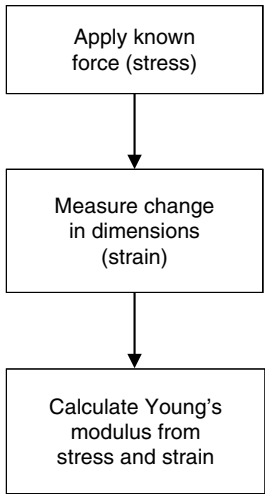

Fig. 15.2 Steps required for estimation of elastic modulus.

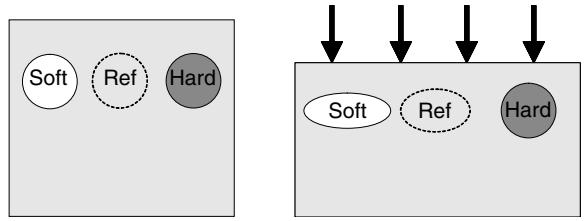

Fig. 15.3 Effect of compression on a block of material in which are embedded two lesions, one soft and one hard. Application of a uniform force compresses the tissue. As the tissue is incompressible (no change in density) the block of tissue expands in the direction perpendicular to the stretch. There is little change in the dimensions of the hard lesion, but the soft lesion alters significantly.

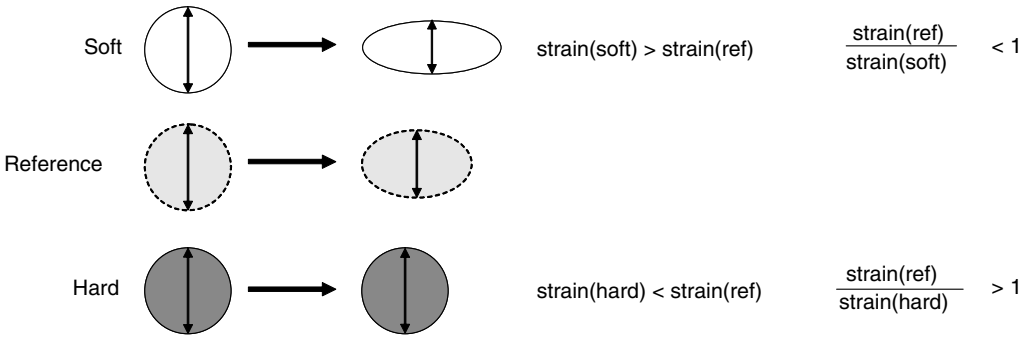

Fig. 15.4 Illustration of the dependence of strain on stiffness for the two lesions and the reference region of Figure 15.3.

assumed to be normal, to which the lesion can be compared. The strain-ratio is:

$$strain\text{-}ratio = \frac{strain\ (reference\ region)}{strain\ (lesion)} \qquad (15.5)$$

In clinical practice the strain-ratio is sometimes used as a surrogate index for stiffness in the absence of a true index of stiffness such as Young's modulus.

Clinical and research strain elastography systems

In the research literature there are several methods for elastography based on measuring the change in tissue dimensions (the strain) arising from an applied force. An external compression device may be used, in order to control the rate and frequency at which the tissues are compressed (reviewed in Greenleaf *et al.* 2003, Ophir *et al.* 1999). Commercial systems rely on the use of the transducer or the acoustic radiation force to compress the tissue. These methods have the advantage of being clinically acceptable as the operator can both image and compress the tissues with one hand, without the involvement of separate compression devices which would require a second person to operate. The strain-based methods described below are based on the technology available on current commercial systems.

Strain elastography using an externally applied force

Commercial ultrasound systems generally use the transducer itself to compress the tissues. The operator presses the transducer in and out of the tissues while the ultrasound system records images. In the case of endoluminal elastography controlled movement of the transducer is difficult, and compression is achieved by the inflation of a plastic sheath, by the injection of water into the sheath using a syringe which the operator controls.

There are two main methods for estimation of tissue movement, one using the amplitude of the received echoes extracted from the RF data, and one using the Doppler (DTI) data.

Strain estimation from A-lines

Figure 15.5 shows a uniform tissue in which there is a stiff lesion. A-scan lines are shown passing through the centre of the lesion pre- and post-compression. The received echoes as a function of depth are shown in Figure 15.6b. The ultrasound system estimates the amount by which the tissue has moved at each point

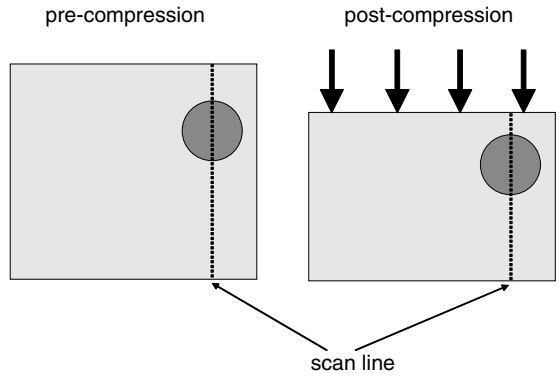

Fig. 15.5 Location of an A-scan line pre- and post-compression (see Figure 15.6).

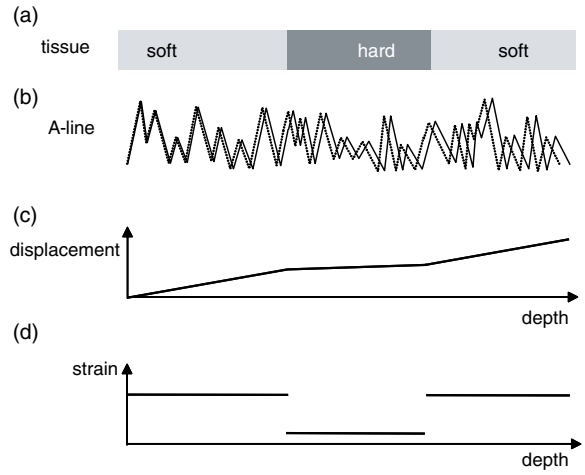

Fig. 15.6 Steps in the estimation of strain from A-scan lines pre- and post-compression. (a) Idealized tissue consisting of a hard lesion surrounded by softer tissue; (b) A-lines from Figure 15.5 are shown with the post-compression line (dotted) displaced; (c) displacement estimated from (b); (d) strain estimated from (c).

as a result of the compression (Figure 15.6c), and from this estimates the strain (Figure 15.6d).

This method for estimation of tissue displacement relies on the use of signal-processing methods which compare the A-line pre- and post-compression. Essentially, these are search algorithms which identify any change in position or stretching of image features. In its most simple form the method assumes that the tissue only moves in the direction of the A-line. However, it was noted above that tissue spreads sideways when compressed. To account for this, some systems incorporate search features which explore up and down an individual A-line (axially), and also between adjacent

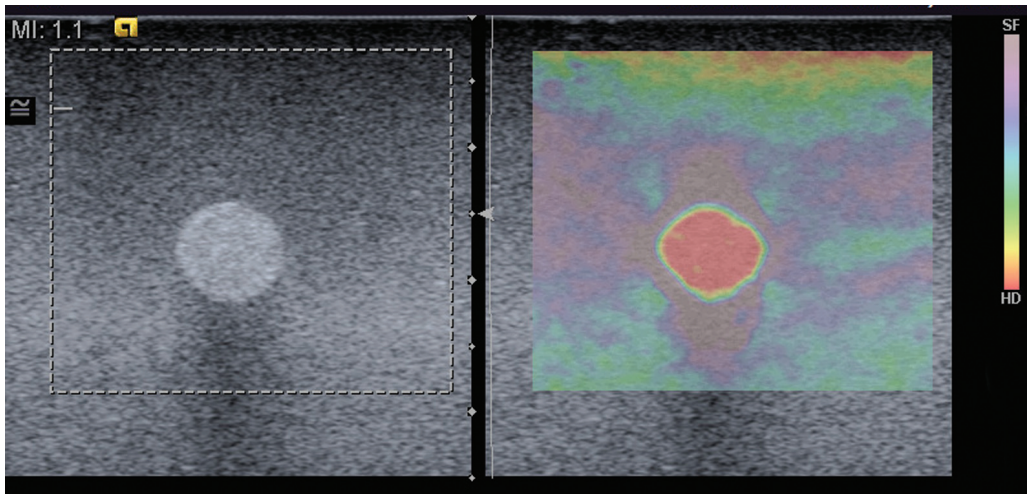

(a)

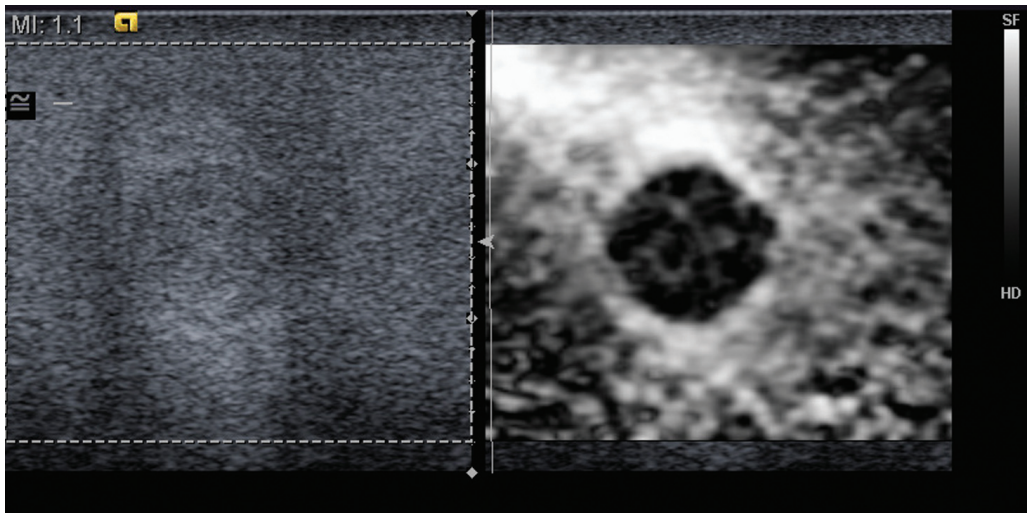

(b)

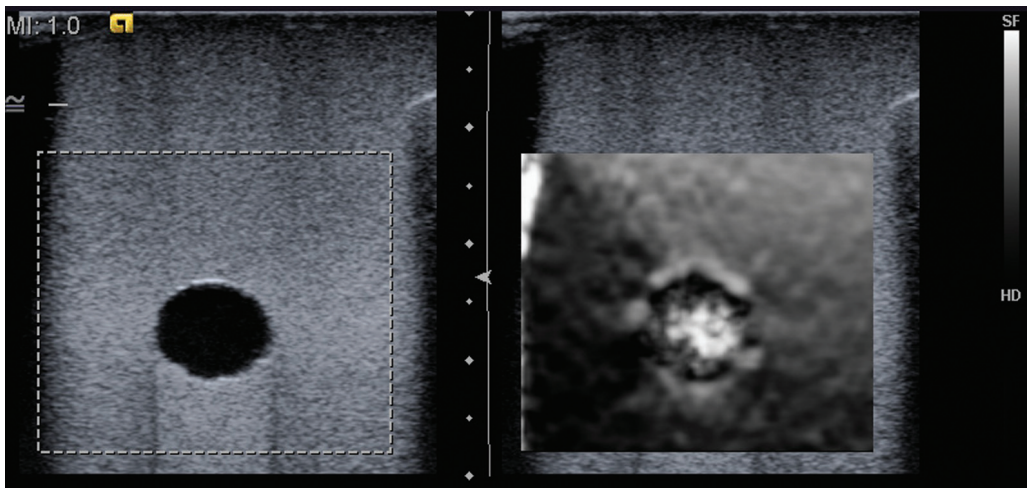

(c)

Fig. 15.7 Strain images for lesions in breast phantoms. Each figure shows the B-mode image on the left and the strain image on the right. (a) stiff echogenic lesion on B-mode, with low strain (red); (b) stiff lesion in which the lesion has the same echogenicity as the surrounding tissue, with low strain (black); (c) fluid-filled structure shown as an echo-free region on the B-mode, with high strain (white).

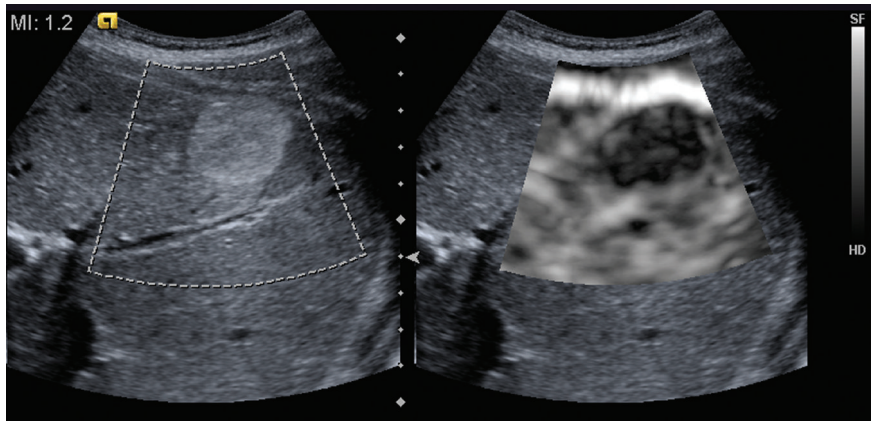

(a)

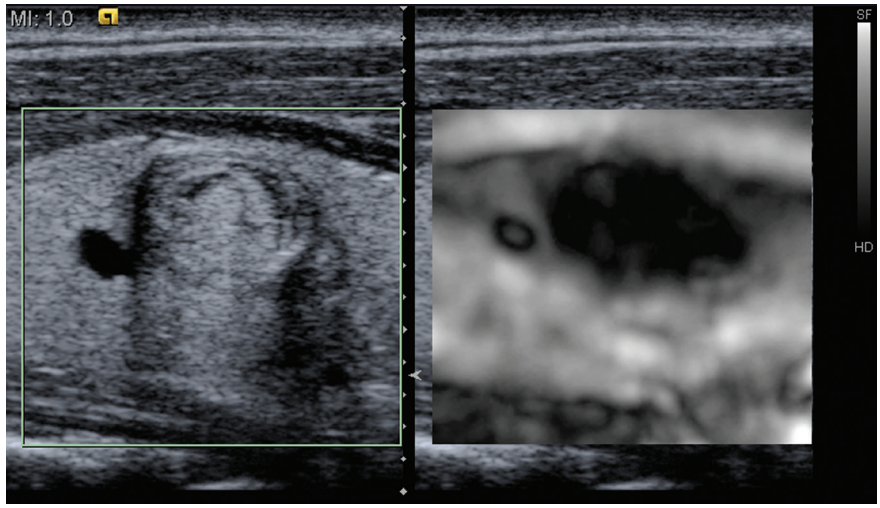

(b)

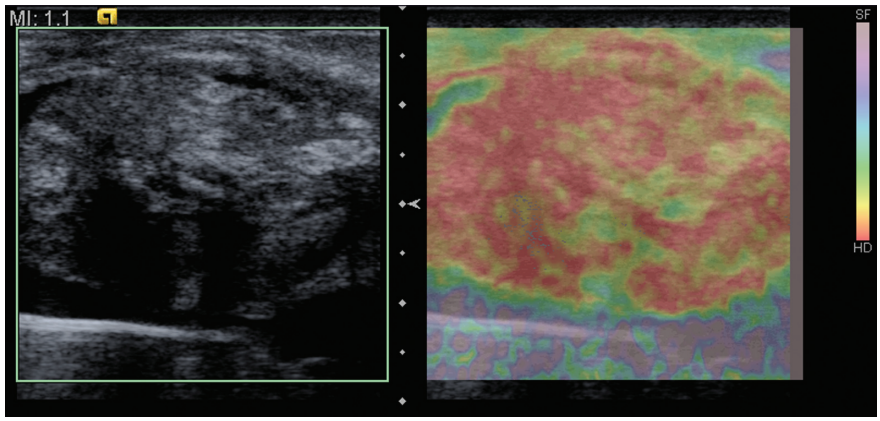

(c)

Fig. 15.8 Strain images of lesions in patients. Each figure shows the B-mode image on the left and the strain image on the right. (a) Liver haemangioma with decreased strain compared to the surrounding tissue; (b) thyroid mass with decreased strain; (c) muscle mass with decreased strain.

A-lines (transversely). This helps improve the estimation of strain and the appearance of the strain image. Further details of correlation-based search algorithms used for strain estimation are provided by Yamakawa and Shiina (2001) and Shiina *et al.* (2002).

Figure 15.7 shows typical images of strain in hard and soft lesions in phantoms. Figure 15.8 shows examples of clinical images. The displayed strain may be presented in colour or in greyscale. Strain elastography based on A-line methods is especially suitable for real-time use, and has the advantage over off-line methods of immediate visualization of strain. A further advantage is that the degree of compression tends to be less than that required for DTI methods (below), which reduces artefacts associated with lesions moving out of the beam during compression.

Strain estimation from Doppler tissue imaging

Methods for estimation of strain were described in Chapter 10, in the context of cardiac imaging using Doppler tissue imaging (DTI). The same methods may be used to estimate strain in elastography. The steps of the process are given below. Figure 15.9 shows each step for imaging of a hard lesion in a breast phantom. In the example, the lesion is clearly visible on the B-mode image (Figure 15.9a), though the lesion in clinical studies may not be so clearly visible.

- *Estimate tissue velocities*: the estimation of tissue velocity by the ultrasound system is performed with respect to the position of the transducer. As the transducer is pushed into the tissues, the tissues are compressed, and in the ultrasound image this appears as a movement of the tissues towards the transducer. Similarly, when the transducer is withdrawn, the appearance in the ultrasound image is of the tissue moving away from the transducer. These movements give rise to a DTI image of velocity (Figure 15.9b). A sequence of DTI images is recorded as the transducer is pressed in and out of the tissue.
- *Estimate velocity gradient:* the change in velocity with distance along each image line is estimated from the DTI data (Figure 15.9c).
- *Estimate strain:* the strain is estimated from the velocity gradient image (Figure 15.9d). The strain values within the hard inclusion are much reduced compared to the adjacent tissue. Note also the red halo at the top and bottom of the inclusion on the strain image. This is a commonly seen artefact associated with the strain estimation process.

In order to generate a sufficiently large velocity, the tissue must be pressed in several mm, more than is required for A-line based methods. This approach results in two potential artefacts: one is the displacement of lesions out of the imaging plane, and the other is the halo artifact as shown in Figure 15.9d.

Quantification of elasticity from strain images

As noted above the estimation of Young's modulus requires knowledge of the true stress applied to the tissue. In general this is difficult to obtain, and the strain-ratio may be used instead as an index of elastic modulus. The estimation of strain-ratio involves comparison of the strain in the lesion with the strain in an adjacent 'reference' region (Equation (15.5)). In Figure 15.10 regions of interest are shown placed in the hard lesion of an elastography phantom, and an adjacent 'reference' region at the same depth. The strain values as a function of time during the compression of the tissues are also shown for both regions. The strain reaches a maximum at the point of maximum compression, and the strain-ratio measurement may be taken from this time-point. In the example of Figure 15.10 the strain-ratio has a value of 10, indicating that the lesion is some 10-times as stiff as the surrounding tissue. Figure 15.11 shows the strain-ratio calculated in a strain image from a diseased prostate; in this case the strain-ratio has a value of 28, indicating that the lesion is very stiff.

Change in strain with depth

When the tissue is compressed externally with the transducer, the force of compression is not uniform throughout the image. The force of compression decreases with depth. This means that a lesion, of similar hardness and size, will compress more the nearer it is to the transducer (Figure 15.12). The decrease in strain with depth within the tissue of an elastography phantom can also be seen in Figure 15.9d. This has two important consequences. The first consequence is that elastography by compression using the transducer is most effective for lesions near the surface, in practice less than about 5 cm depth. The second consequence is that, when estimating the strain-ratio, the reference region should be placed at the same depth as the lesion. The use of a reference region at a different depth will lead to a different strain-ratio.

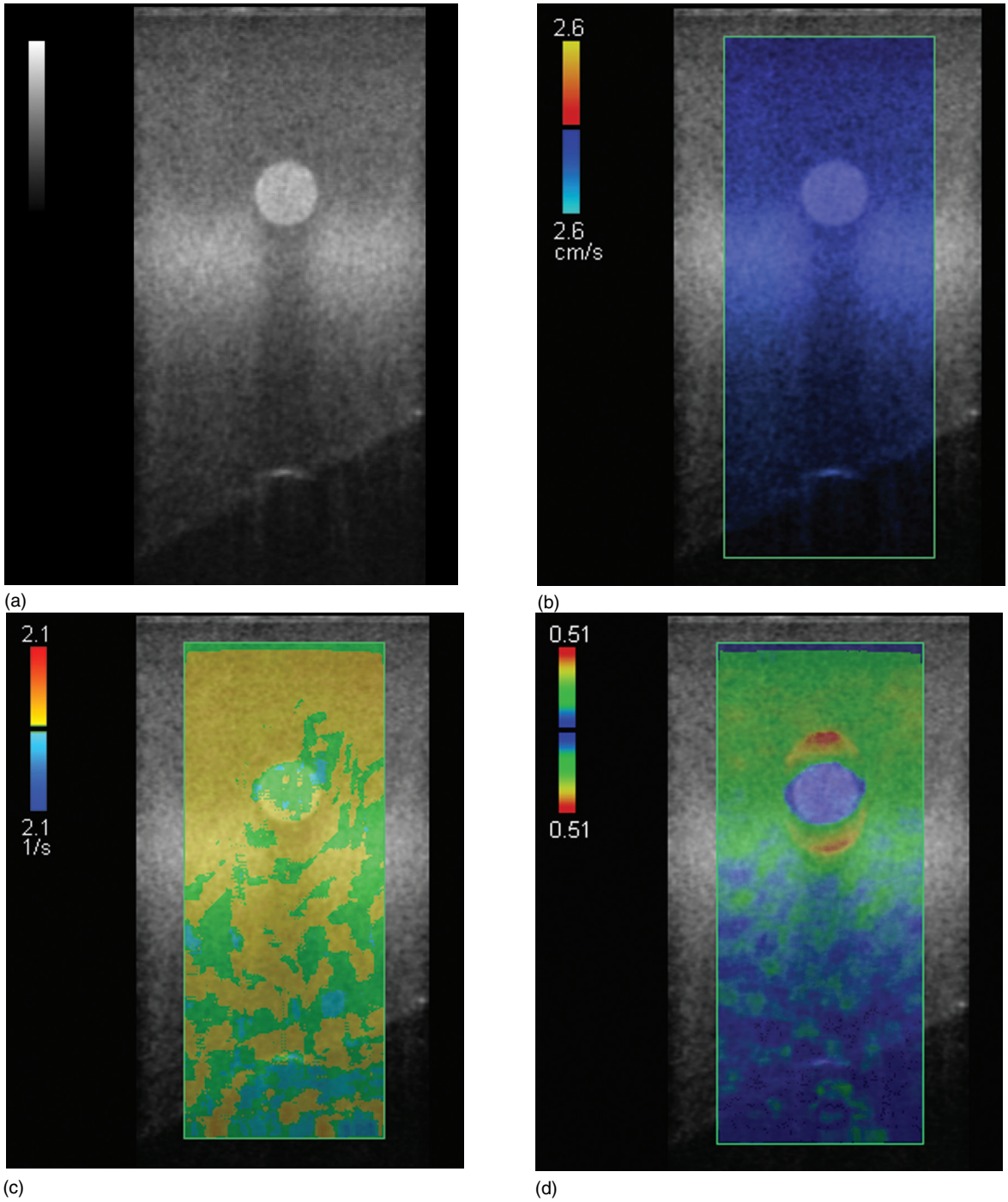

Fig. 15.9 DTI estimation of the strain. (a) B-mode image of a stiff lesion in a breast phantom; (b) DTI velocity image; (c) velocity gradient image; (d) strain image showing reduced strain in the lesion, and also regions of increased stiffness above and below the lesion which are artefacts.

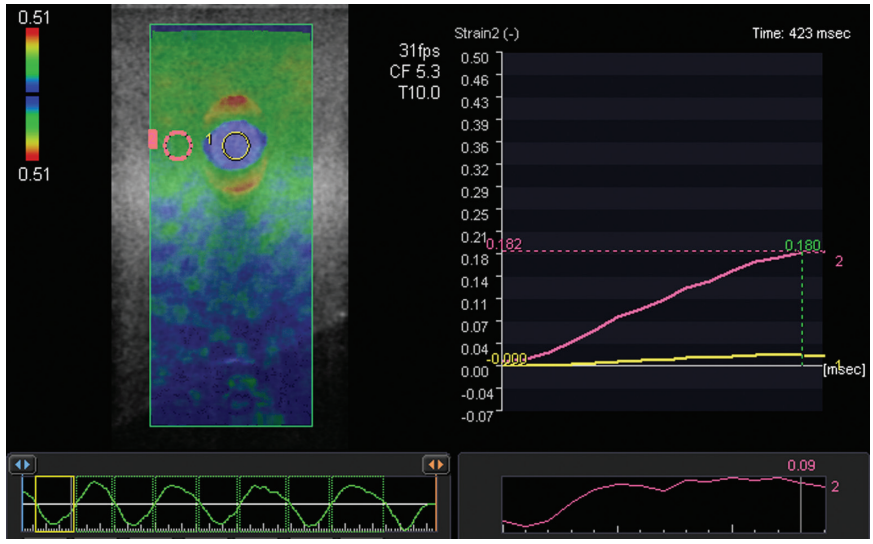

Fig. 15.10 Estimation of the strain-ratio for a stiff lesion. Areas of interest are placed within the lesion and in an adjacent region at the same depth. A graph of strain versus time is shown during the compression phase. The maximum compression values are 0.180 and 0.018, giving a strain-ratio value of 10.

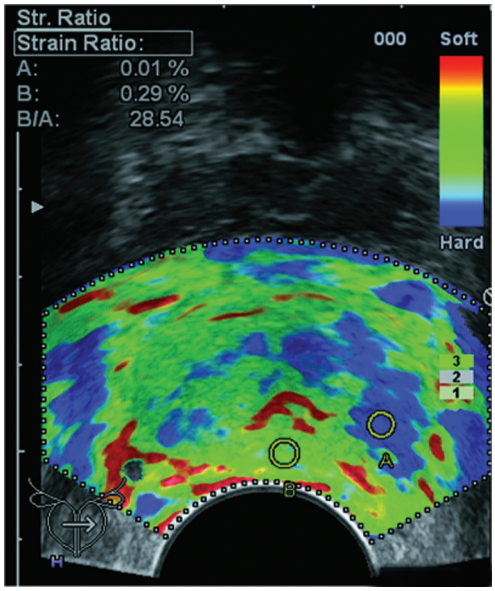

Fig. 15.11 Estimation of strain-ratio in a prostate lesion. Areas of interest are placed within the lesion and in an adjacent region. The strain-ratio has a value of 28.

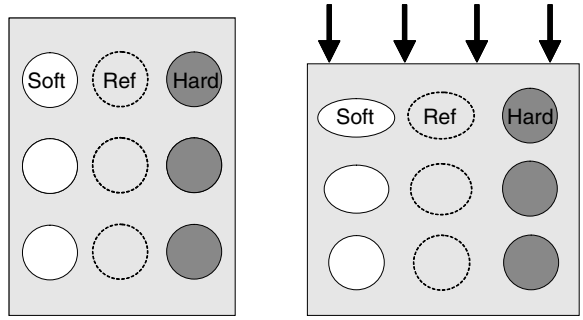

Fig. 15.12 Effect of depth on strain. For a uniform force applied to the block of tissue, the degree of compression reduces with depth.

Strain elastography using acoustic radiation force

An ultrasound beam generates a radiation force which is directed in the direction of wave propagation. The magnitude of the force is highest in the focal zone, and increases with overall output power. Acoustic radiation force imaging (ARFI) involves the use of a high-output beam to displace a region of tissue, and imaging beams to monitor the displacement (Nightingale *et al.* 2001, 2002, 2006). The minimum sequence of beams used in ARFI is illustrated in Figure 15.13. The ARFI technique sends a high-output ultrasound pulse to produce displacement of the tissue in the focal region. This is usually called the 'pushing beam' or 'pushing pulse' as its job is to produce a small movement of the tissues. The displacement produced is typically 1–20 μm, sufficient to be detected using an ultrasound system. The displacement reaches a peak after 1 ms and the tissue restores to its normal position within 5 ms. The pushing pulse is

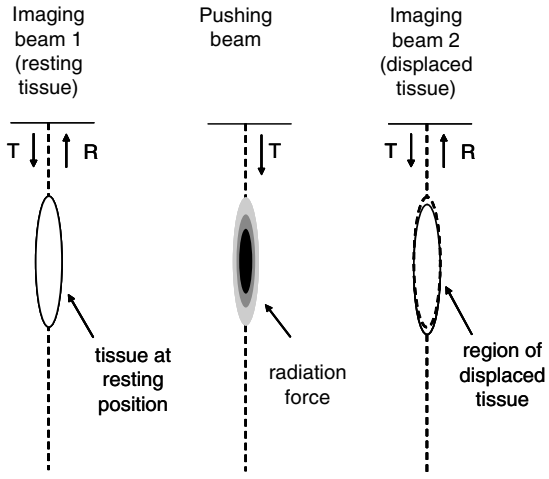

Fig. 15.13 Sequence of ultrasound beams used for ARFI elastography. (left) An imaging beam records the position of the tissue in its resting position; (middle) a pushing beam produces a radiation force which displaces tissue in the focal region; (right) a second imaging beam sent immediately after the pushing beam records the position of the displaced tissue.

not used for imaging purposes; this requires separate imaging pulses. At least two ultrasound pulses are used in a conventional transmit/receive imaging manner, one sent before the pushing pulse to monitor the position of tissue prior to displacement, and a second immediately after the pushing pulse to monitor the position of the tissue while it is displaced. In practice more complicated sequences may be used involving several pushing pulses interleaved with imaging pulses, followed by a series of imaging pulses to monitor the return of the tissue to its undisturbed position (Nightingale *et al.* 2002). Comparison between the received A-lines for each imaging pulse is performed to estimate the movement of the tissues. Each line of the ARFI image therefore requires a minimum of three ultrasound pulses; a pushing-pulse and at least two imaging-pulses. Figure 15.14 shows an image of a lesion in the liver obtained using the ARFI technique. It was noted above that compression of the tissues using an external force may be ineffective for deeper tissues. In these situations ARFI may be used to overcome this limitation.

Estimation of elastic modulus using strain elastography

The estimation of elastic modulus using strain elastography relies on methods for estimation of the applied

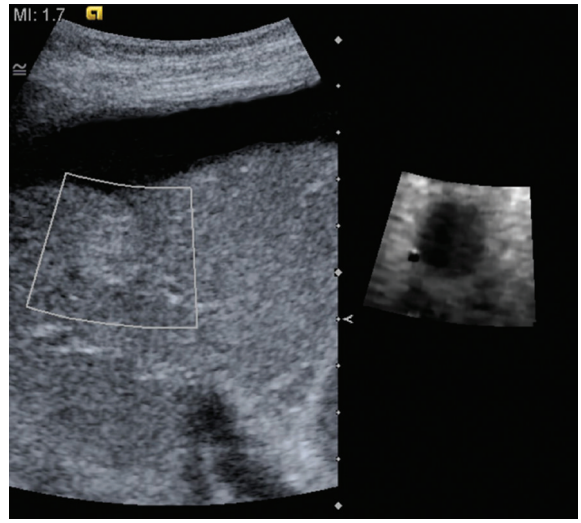

Fig. 15.14 ARFI elastography in the liver. The B-mode image shows an indistinct lesion. The strain image shows that the lesion has increased hardness with much improved image contrast.

stress at each point within the tissue. A method is needed to estimate the force applied to the tissue from the ultrasound transducer or the radiation force, and then a method to determine how that force is distributed through the tissue. Measurement of the applied force could be achieved using a force transducer attached to the ultrasound transducer, or through calculation of the radiation force from the pushing pulse. The force distribution in tissue is not uniform; this is shown in Figure 15.9d and Figure 15.12 where the resulting strain decreases with depth. In general the force distribution in patients is affected by the shape of the transducer, the shape and mechanical properties of the underlying tissues and the size and duration of the applied force. Current commercial ultrasound systems do not include the technology to estimate the stresses within the tissues, and hence do not provide a means for estimating elastic modulus from strain elastography.

Elastic moduli and wave generation

This section discusses elastic moduli and wave generation, in order to understand how shear waves can be used to estimate stiffness (as discussed in the next section). In general for waves such as those used in medical ultrasound systems, the speed of the wave as it travels through the tissue is determined by the density of the tissue and the appropriate elastic modulus.

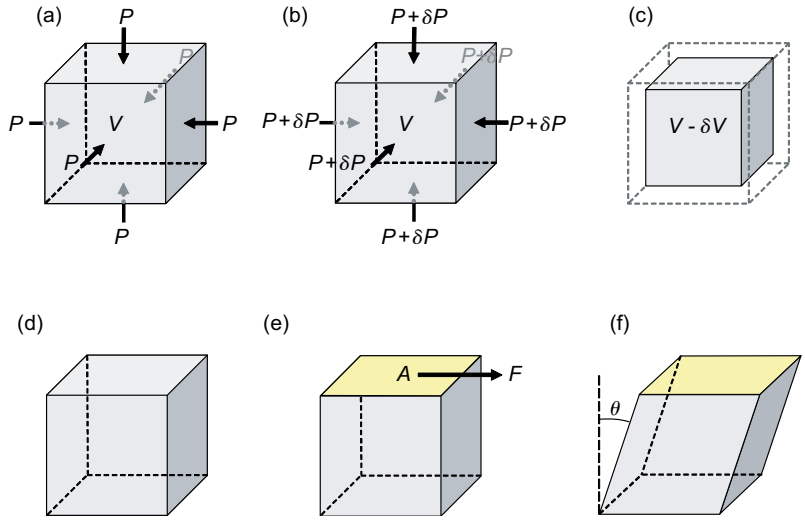

Fig. 15.15 Effect of tissue compression and shear. Compression: (a) a cube of tissue of volume *V* is shown subject to pressure *P* on all sides; (b) an increase in pre ssure to *P*+δ*P* results in (c) compression of the cube by an amount δ*V*. Shear: (d) a cube of material is shown; (e) this is subject to a force acting parallel to one of the sides resulting in (f) the cube being pulled over to one side, by an amount shown by the angle *θ*.

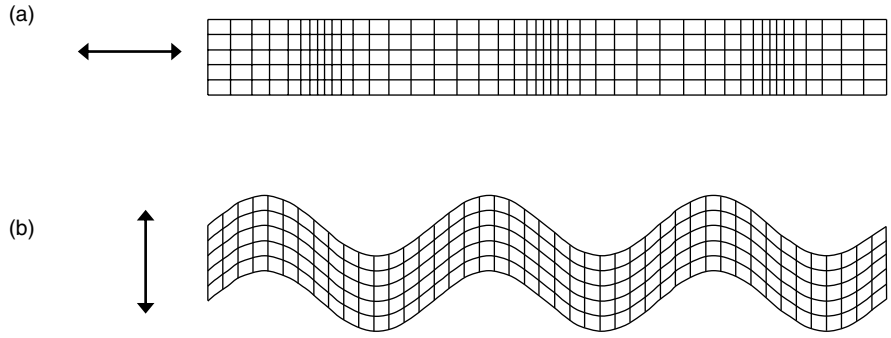

Fig. 15.16 Propagation of waves. (a) In compressional waves the tissue moves to and fro in the same direction as the wave motion; (b) in shear waves the tissue moves transverse to the wave motion.

Bulk modulus B and pressure waves

When a material is subject to increased pressure the material will be compressed. The bulk modulus describes the change in volume of a material occurring as a result of compression. Figure 15.15a–c shows a cube of material of volume *V* subject to a pressure *P* on all sides. As a result of a change in pressure to *P*+δ*P* the cube compresses, causing a reduction in volume by an amount δ*V*. The bulk modulus *B* expresses these changes as an equation. The minus sign indicates that an increase in pressure results in a decrease in volume:

$$B = \frac{-\ change\ in\ pressure}{fractional\ change\ in\ volume} = \frac{-\delta P}{\delta V / V} \quad (15.6)$$

When a tissue is subject to a change in pressure, for example by being struck or compressed, pressure waves will be generated which propagate through the tissue. The waves generated by a diagnostic ultrasound transducer are called either compressional waves or longitudinal waves. The speed of propagation of the pressure wave is controlled by the bulk modulus, as shown in Equation (15.7):

$$c_l = \sqrt{\frac{B}{\rho}} \quad (15.7)$$

where c_l is the speed of the wave, *B* is the bulk modulus, and *ρ* is the average density.

Figure 15.16a illustrates the propagation of compressional waves. At any one point the material

Table 15.3 Features of shear and compressional waves.

	Shear waves	Compressional waves
Changes in local density	No	Yes
Elastic modulus	G (shear modulus)	B (bulk modulus)
Speed of waves in soft tissue	1–10 m s^{-1}	1400–1600 m s^{-1}
Can wave travel through fluid?	No (at low frequencies)	Yes

oscillates to and fro in the direction of motion of the wave. There are changes in density as the wave propagates, illustrated in Figure 15.16a, since changes occur in the area of each element at different locations.

Shear modulus G and shear waves

When an object is subject to a force parallel to one surface, that surface will be dragged in the direction of the force. This force is called a shear force. This is illustrated in Figure 15.15d–f, where the shear force drags one surface of a cube in the direction of the force. The shear force is transmitted through the rest of the cube, causing the cube to be distorted, or sheared, in the direction of the force. The shear modulus describes the ability of the material to withstand a shear force F. The amount of shear is represented by the angle θ. The shear modulus expresses these changes as an equation:

$$G = \frac{shear\ stress}{shear\ strain} = \frac{F/A}{\tan(\theta)} \qquad (15.8)$$

When a shear force is applied to a material, shear waves are generated which travel through the material. The propagation of the shear waves is controlled by the shear modulus as shown in Equation (15.9).

$$c_s = \sqrt{\frac{G}{\rho}} \qquad (15.9)$$

where c_s is the speed of the wave, G is the shear modulus, and ρ is the density.

Figure 15.16b illustrates the propagation of shear waves. At any one point the material oscillates to and fro perpendicular to the direction of motion of the wave. For shear-wave propagation there is no change in density with time. This is illustrated in Figure 15.16b by the area of each element remaining the same at different locations. The passage of shear waves relies on the ability of adjacent elements of the tissue to remain connected while a shear force is applied. Though solids and soft tissues support shear waves, application of a shear force in a fluid results in gross motion of the fluid, resulting in disconnection of adjacent elements, and therefore fluids do not support shear waves. Table 15.3 briefly summarizes the characteristics of shear waves and compressional waves.

Provided that the tissue can be assumed to be incompressible (no change in density) and uniformly elastic the shear modulus G is related to Young's modulus E by the following equation:

$$E = 3G \qquad (15.10)$$

Combining Equations (15.9) and (15.10) gives:

$$E = 3\rho c_s^2 \qquad (15.11)$$

Equation (15.11) provides a means for determining tissue stiffness from the measured shear-wave velocity.

Values of elastic moduli in body tissues

Figure 15.17 illustrates the values for bulk modulus B, shear modulus G and Young's modulus E for different body tissues. The range of G and E is very large, by a factor of 10^7, or 10 million.

Shear-wave elastography

The steps for estimating tissue stiffness from shear wave velocity are described below and illustrated in Figure 15.18.

- *Induce shear waves in the tissue:* if the tissue is vibrated then shear waves will be produced which will travel in all directions. These travel at a speed which is dependent on the local density and the local elastic modulus, according to Equation (15.9). Typical frequencies for which shear waves are generated are in the range 10–500 Hz. The speed of propagation of shear waves is typically 1–10 m s^{-1}. For 50 Hz shear waves in healthy liver the speed is about 1 m s^{-1} and the corresponding wavelength is 20 mm.
- *Measure the speed of propagation through the tissue of interest:* for the region of tissue which is

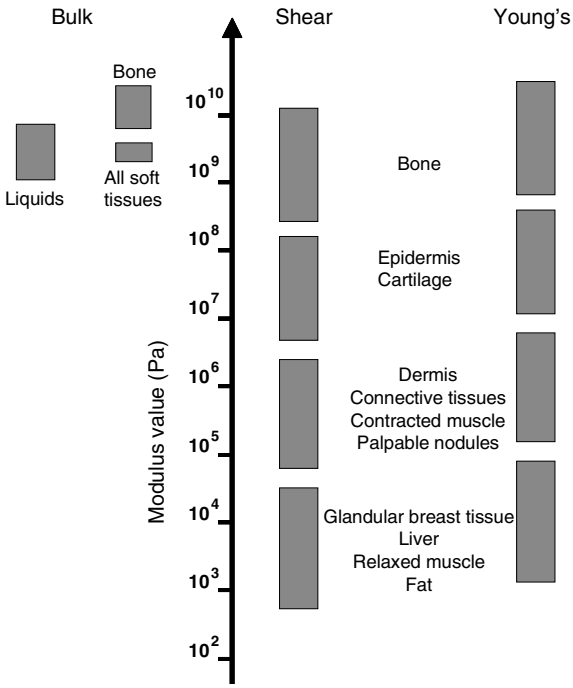

Fig. 15.17 Values of bulk modulus *B*, shear modulus *G* and Young's modulus *E* for different tissues. The values for *B* in soft tissues occupy a narrow range which is similar to that for fluids. The values for *G* and *E* occupy over 7 orders of magnitude (a factor > 10 000 000). (Reprinted with permission from Sarvazyan *et al.* (1998). Shear wave elasticity imaging: a new ultrasonic technology of medical diagnostics. *Ultrasound in Medicine and Biology*, 24, 1419–35.)

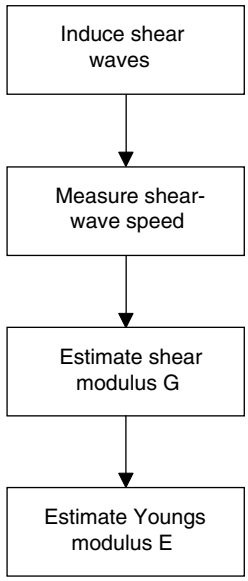

Fig. 15.18 Steps in the estimation of elastic modulus using shear waves.

Table 15.4 Density of soft tissues. Values are taken from Duck (1990). Values are reported as mean (range), or mean, or range.

Tissue	Density (kg m^{-3}) mean (range)
Fat	928 (917–939)
Muscle – skeletal	1041 (1036–1056)
Liver	1050 (1050–1070)
Kidney	1050
Pancreas	1040–1050
Spleen	1054
Prostate	1045
Thyroid	1050 (1036–1066)
Testes	1040
Ovary	1048
Tendon (ox)	1165
Average soft tissues,[a] mean (S.D.)	1047 (5)

[a] Excluding fat and tendon.

of interest the speed of propagation of the shear waves is measured using the ultrasound system.

- *Estimate the stiffness:* use of Equation (15.11) provides a value for the stiffness, calculated from the measured shear-wave velocity and the density of the tissue of interest. As density cannot be measured *in vivo* non-invasively, this requires an assumption to be made on the density of tissues. Manufacturers give little detail of this. Values for the density of various tissues are provided in Table 15.4 (from Duck 1990). The average density for a range of soft tissues (breast, prostate, liver, kidney) is 1047 ± 5 kg m^{-3}.

The generation of shear waves relies on a method to induce motion within the tissues. Commercial methods use a hand-held transducer to both generate and detect the shear waves. Methods may be divided into those that generate shear waves by the use of an external vibrator applied to the skin, and those which generate shear waves internally within the tissue by acoustic radiation force.

Elastic modulus estimation using shear waves generated from an external actuator

Methods described in the literature include external vibrators separate from the ultrasound transducer (reviewed in Greenleaf *et al.* 2003; Ophir *et al.* 1999). This section concentrates on methods adopted

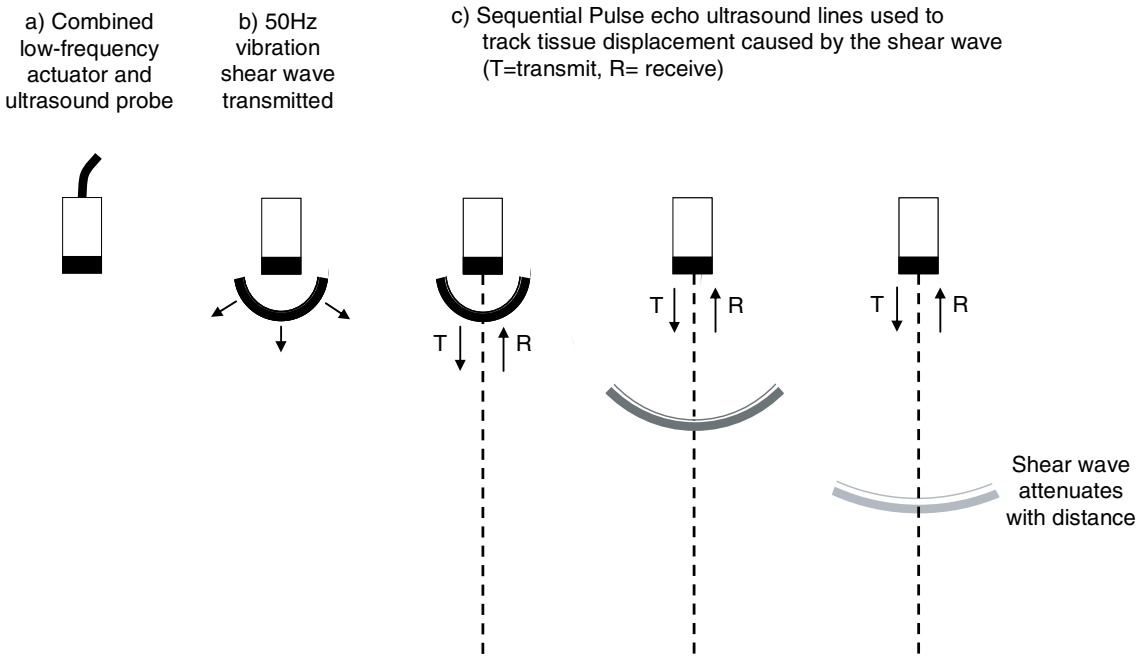

Fig. 15.19 Production of shear waves and acquisition of ultrasound beams using a combined actuator–ultrasound system. (a) Schematic diagram of the combined transducer; (b) shear waves are produced by the actuator; (c) sequential A-line data are captured.

clinically in which the ultrasound transducer is used to both produce and detect the shear waves (Sandrin *et al.* 2002, 2003). This is referred to as 'transient elastography' as it produces a shear wave which is of short duration, as opposed to the continuous vibration produced in MRI-based dynamic elastography techniques (discussed in Greenleaf *et al.* 2003). The method described by Sandrin *et al.* is not based on the use of an imaging device, instead the operator must manually place the probe on the patient's skin in a region where the operator knows that the liver will be insonated. This method produces a single value of Young's modulus from one location.

The system described by Sandrin *et al.*, and adopted commercially, uses a combined vibrator and ultrasound transducer (Figure 15.19a). The vibrator is a piston source which indents the tissue to produce shear waves and the ultrasound transducer measures the shear-wave velocity. This is an A-line-based technique; in other words a single line of ultrasound is acquired, and a single measurement is made, of the velocity of shear waves. No image is acquired. The steps involved are illustrated in Figure 15.19 and described below.

- *Production of shear waves*: the piston vibrator is pressed against the patients skin by the operator, usually to insonate the liver. Activation of the vibrator indents the tissue at a low frequency of 50 Hz for 20 ms. The shear waves which are produced travel through the tissues (Figure 15.19b).
- *Ultrasound acquisition*: the ultrasound system is operated in pulse–echo mode (Figure 15.19c), acquiring ultrasound data along a single beam direction. The shear waves cause the tissue to be displaced in the direction of the beam, so that in each consecutive A-line the position of the shear wave appears slightly deeper.
- *Ultrasound processing:* the A-line data are processed using cross-correlation algorithms to estimate the displacement of the tissue between consecutive A-lines, from which the resulting strain is calculated. The shear wave velocity is then calculated from the change in strain with time (Figure 15.20).
- *Estimation of elastic modulus:* Young's modulus may be estimated from the shear-wave velocity using Equation (15.11). An assumed value for the tissue density is required.

Unlike pulse–echo techniques, the transmission and reception phases of the shear-wave system described

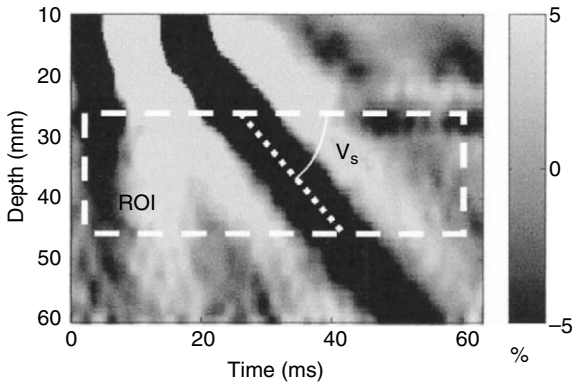

Fig. 15.20 Strain values for sequential A-lines are displayed for a period of 60 ms following initiation of the shear wave. The wave velocity is the slope of the wave pattern. (Reprinted with permission from Sandrin *et al.* (2003). Transient elastography: a new noninvasive method for assessment of hepatic fibrosis. *Ultrasound in Medicine and Biology*, 29, 1705–13.)

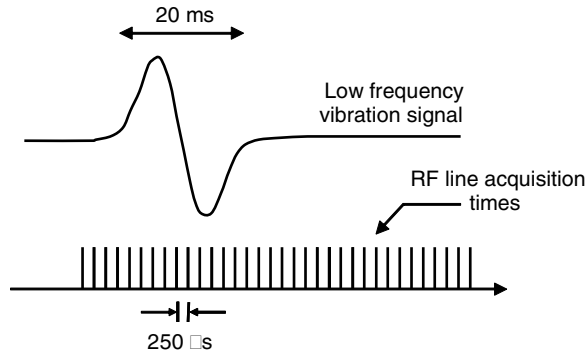

Fig. 15.21 Diagram demonstrating that the 50 Hz vibration and ultrasound pulse–echo signals overlap. (Reprinted with permission from Sandrin *et al.* (2003). Transient elastography: a new noninvasive method for assessment of hepatic fibrosis. *Ultrasound in Medicine and Biology*, 29, 1705–13.)

here overlap (Figure 15.21). The effect of vibrator movement on the received A-lines must therefore be removed before shear-wave velocity can be correctly estimated. Sandrin *et al.* (2002) assume that the shear waves attenuate quickly, so that the vibrator movement is deduced from the displacement estimated from deep echoes.

In order to measure the shear-wave velocity, a sufficient number of A-lines must be acquired while the shear wave passes from the vibrator to the bottom of the ultrasound field of view. The ultrasound system measures to a depth of about 6 cm. For a shear wave whose velocity is 3 m s^{-1}, the wave will travel 6 cm in 20 ms. For at least 20 A-lines to be acquired while the shear wave travels 6 cm requires a time between ultrasound pulses of at least 1 ms, or a PRF of 1000 Hz. This is easily achievable for a single beam; however, to produce a 2D image involving many image lines requires high-frame-rate techniques, as discussed below.

Elastic modulus estimation from shear waves produced using radiation force

Single-region methods

The use of radiation-force methods to produce distension of the tissue within the ultrasound beam focal region is described above. The basic radiation-force method produces a single region, within the tissue, of high acoustic output. The resulting tissue distension within the region causes the production of shear waves which propagate through the tissue in 3D. The ultrasound system may be used to monitor the propagation of the waves through the tissue (Figure 15.22). This technique, proposed by Sarvazyan *et al.* (1998), has been used in published studies on phantoms and in excised tissues (Nightingale *et al.* 2003), and *in vivo* in the liver of volunteers (Palmeri *et al.* 2008).

Commercial implementations of this method provide a single value of shear-wave velocity corresponding to a local region of tissue, usually the liver (Castera *et al.* 2005, Foucher *et al.* 2006). The location of the region, highlighted on the B-mode image, is controlled by the operator (Figure 15.23). Once the region is positioned, the operator actuates the high-output pulse which produces shear waves. These are generated just to one side of the region of interest. The shear waves travel from the high-output focal area through the region of interest. The progression of the shear wave through the region of interest is monitored using imaging beams, enabling estimation of the time of travel of the shear wave from its origin at the high-output focus to the region being sampled. The shear-wave velocity is displayed, from which the operator can estimate elastic modulus using Equation (15.11).

Multi-region (supersonic) methods

A recognized problem with shear waves generated from radiation force is that the shear waves have low amplitude. This limits the distance over which the shear waves can be tracked using ultrasound imaging. Higher-amplitude shear waves may be generated by increasing the ultrasound output power; however, this has patient-

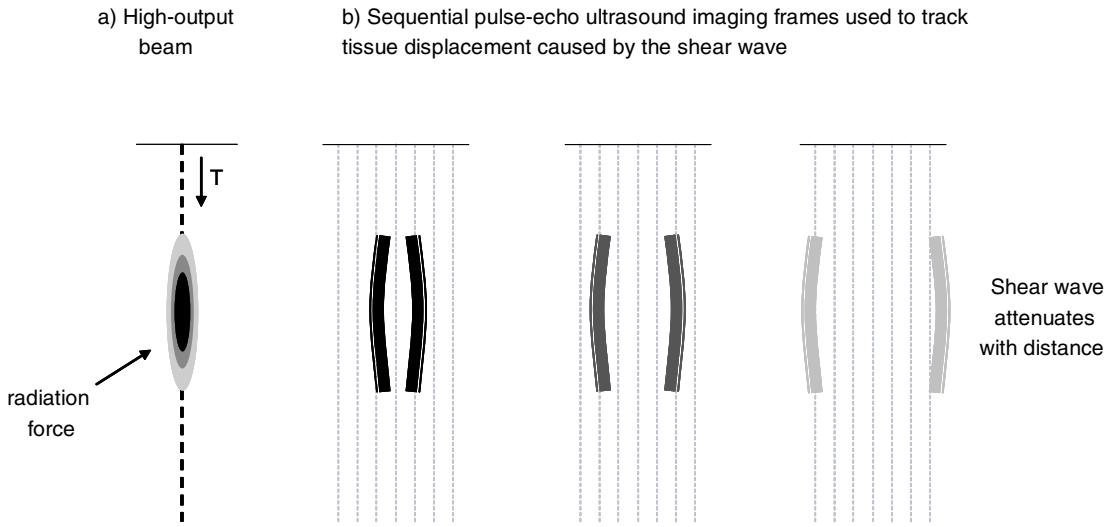

Fig. 15.22 Shear-wave imaging using ARFI. (a) A high-output ultrasound beam produces a radiation force which displaces tissue in the focal region producing shear waves which propagate in 3D. (b) High-frame-rate imaging techniques are used to track the tissue displacement caused by the shear wave.

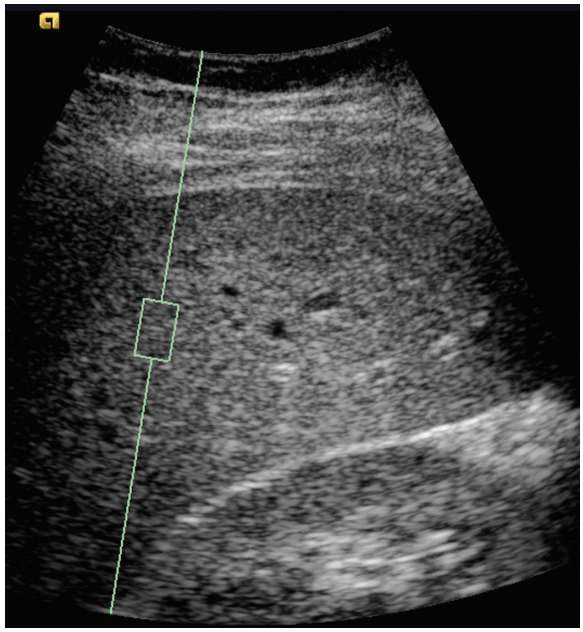

Fig. 15.23 ARFI based estimation of shear-wave velocity from a single region. The operator places the region (green box) at the desired location within the tissue, in this example the liver. The ARFI pulse is activated by the operator and the machine displays the shear-wave velocity, in this case 0.9 m s^{-1}.

safety and transducer-heating implications. The shear-wave amplitude may be increased by the use of multiple regions (Bercoff *et al.* 2004). In this technique high-output-source regions are generated at increasing depths, one after the other (Figure 15.24a). This is equivalent to a high-output source moving rapidly through the tissues, where the speed of the source is greater than the speed of the shear waves which are generated. The shear waves from each source summate to produce a cone (referred to as a 'Mach cone') which travels through the tissue (Figure 15.24b). In general, when the source of waves moves faster than the wave speed, the source is said to be moving at 'supersonic' speed. This effect most commonly occurs when an aircraft travels faster than the speed of sound in air. The supersonic technique produces shear waves of increased amplitude, which therefore are easier to detect using ultrasound imaging. Tracking of the shear waves requires high-frame-rate imaging. The methods for production of a high frame rate, up to 20 000 frames s^{-1}, are described in Chapter 3. From the detected ultrasound images, the tissue displacement and strain and the shear-wave velocity are estimated. Local tissue stiffness may then be calculated from Equation (15.11). Clinical examples are shown in Figure 15.25.

Further considerations for shear-wave elastography

The explanations so far in this chapter represent the usual way of explaining the difference between compressional waves and shear waves; in one the oscillation is in the direction of wave motion, in the other it is transverse to the direction of wave motion. However,

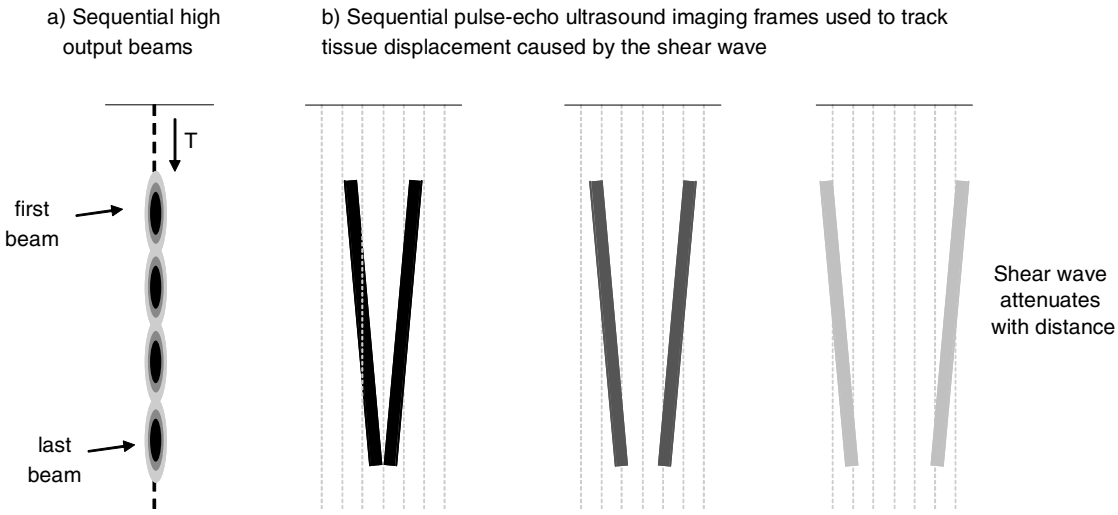

Fig. 15.24 Shear-wave imaging using supersonic ARFI techniques. (a) Sequential high-output beams are generated with focal regions of increasing depth along the same line. (b) A shear wave cone is formed, and high-frame-rate imaging techniques are used to track the tissue displacement caused by the shear wave.

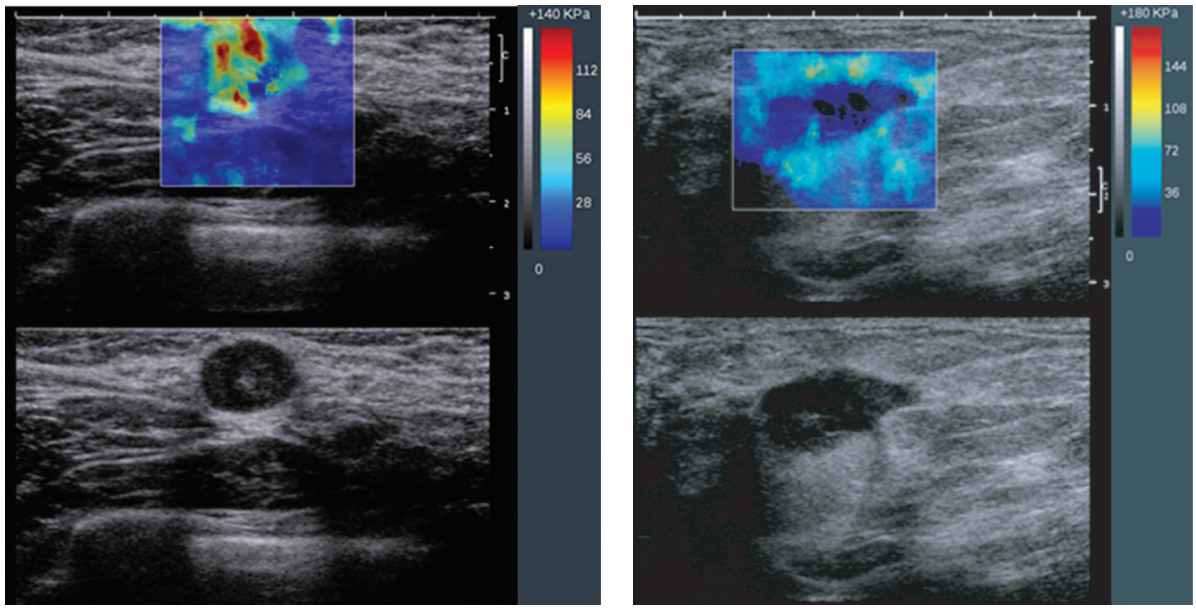

(a) (b)

Fig. 15.25 Clinical examples using supersonic shear-wave imaging in the breast. (a) Echolucent region on the B-mode image has high stiffness, confirmed as a metastatic lymph node by pathology. (b) Echolucent region on the B-mode image has low stiffness, confirmed as an abscess by pathology.

the examples in Figure 15.16 apply to plane waves; that is, waves generated by a very large source. In shear-wave elastography the source cannot be assumed to be very large. In some cases it is more appropriate to consider a point source, and in this case the propagation of waves is more complicated. Several papers discuss this

in detail (Carstensen *et al*. 2008, Catheline *et al*. 1999a, 1999b, Giannoula and Cobbold 2008, Sandrin *et al*. 2004). There are three waves produced; a classic compressional wave which exhibits longitudinal motion, a classic shear wave which exhibits transverse motion, and a third wave arising from the 'coupling term'. The paper by Sandrin *et al.* (2004) is especially enlightening, revealing that the third wave has the same velocity as that of the shear wave, yet has a longitudinal component. This is especially important in the technique described above based on the work of Sandrin *et al.* (2002, 2003), which measures longitudinal displacement in order to measure shear wave velocity.

Further developments

The approach taken in this chapter has been to introduce the essential components of tissue elastic behaviour by assuming that the tissue is uniform, incompressible and fully elastic in that once the stress is removed the tissue returns fully and immediately to its unstressed state. In practice real soft tissues are more complex than this. Different organs and components of organs are 3D, and their elastic properties may differ when examined from different directions. The material may not be fully elastic in that there may be a time delay before the tissue is restored to its unstressed state; in these circumstances the tissue is said to be 'viscoelastic'. For the idealized tissues considered in this chapter, a uniform, elastic, incompressible material needs only one constant to describe its behaviour when subject to stress, Young's modulus. One has seen the difficulty involved in obtaining just one constant, Young's modulus, from ultrasound imaging. More accurate descriptions of the mechanical behaviour of tissues require the estimation of a greater number of physical constants and in order to achieve this the complexity of the imaging procedures must increase. Further reading on more advanced measurements can be found in journal papers; e.g., Han *et al*. (2003), Sridhar *et al*. (2007).

Questions

1. Describe what happens when an elastic material is stretched, and explain what Young's modulus is.
2. Describe briefly the two types of elastography systems available commercially.
3. What is the measurement termed the strain-ratio, and how should it be performed?
4. Describe briefly how Young's modulus may be estimated from shear-wave velocity.
5. Describe the principles of strain elastography based on the use of A-line data.
6. Describe the minimum sequence of beams used in acoustic radiation-force imaging (ARFI).
7. Describe two methods by which radiation-force techniques may be used to obtain elastography images.
8. Describe what a shear wave is and two methods by which they can be generated.
9. State the steps required for estimation of elastic modulus using shear-wave elastography.

References

Bercoff J, Tanter M, Fink M (2004). Supersonic shear imaging: a new technique for soft tissue elasticity mapping. *IEEE Transactions on Ultrasonics, Ferroelectrics and Frequency Control*, **51**, 396–409.

Carstensen EL, Parker KJ, Lerner RM (2008). Elastography in the management of liver disease. *Ultrasound in Medicine and Biology,* **34**, 1535–46.

Castera L, Vergniol J, Foucher J, *et al.* (2005). Prospective comparison of transient elastography, fibrotest, APRI, and liver biopsy for the assessment of fibrosis in chronic hepatitis C. *Gastroenterology,* **128**, 343–50.

Catheline S, Wu F, Fink M (1999a). A solution to diffraction biases in sonoelasticity: the acoustic impulse technique. *Journal of the Acoustical Society of America,* **105**, 2941–50.

Catheline S, Thomas JL, Wu F, Fink MA (1999b). Diffraction field of a low frequency vibrator in soft tissues using transient elastography. *IEEE Transactions on Ultrasonics, Ferroelectrics and Frequency Control,* **46**, 1013–19.

Dineley J, Meagher S, Poepping TL, McDicken WN, Hoskins PR (2006). Design and characterisation of a wall motion phantom. *Ultrasound in Medicine and Biology,* **32**, 1349–57.

Duck FA (1990). *Physical Properties of Tissue.* London: Academic Press.

Foucher J, Chanteloup E, Vergniol J, *et al.* (2006). Diagnosis of cirrhosis by transient elastography (FibroScan): a prospective study. *Gut*, **55**, 403–8.

Giannoula A, Cobbold RSC (2008). Narrowband shear wave generation by a finite-amplitude radiation force: the fundamental component. *IEEE Transactions on Ultrasonics, Ferroelectrics and Frequency Control,* **55**, 343–58.

Greenleaf JF, Fatemi M, Insana M (2003). Selected methods for imaging elastic properties of biological tissues. *Annual Review of Biomedical Engineering*, **5**, 57–78.

Han LH, Noble JA, Burcher M (2003). A novel ultrasound indentation system for measuring biomechanical properties of in vivo soft tissue. *Ultrasound in Medicine and Biology,* **29**, 813–23.

Madsen EL, Hobson MA, Shi HR, Varghese T, Frank GR (2005). Tissue-mimicking agar/gelatin materials for use in heterogeneous elastography phantoms. *Physics in Medicine and Biology*, **50**, 5597–618.

Nightingale KR, Palmeri ML, Nightingale RW, Trahey GE (2001). On the feasibility of remote palpation using acoustic radiation force. *Journal of the Acoustical Society of America,* **110**, 625–34.

Nightingale K, Soo MS, Nightingale R, Trahey G (2002). Acoustic radiation force impulse imaging: in vivo demonstration of clinical feasibility. *Ultrasound in Medicine and Biology,* **28**, 227–35.

Nightingale K, McAleavey S, Trahey G (2003). Shear-wave generation using acoustic radiation force: in vivo and ex vivo results. *Ultrasound in Medicine and Biology,* **29**, 1715–23.

Nightingale K, Palmeri M, Trahey G (2006). Analysis of contrast in images generated with transient acoustic radiation force. *Ultrasound in Medicine and Biology,* **32**, 61–72.

Ophir J, Alam SK, Garra B, *et al.* (1999). Elastography: ultrasonic estimation and imaging of the elastic properties of tissues. *Journal of Engineering in Medicine*, **213**, 203–33.

Palmeri ML, Wang MH, Dahl JJ, Frinkley KD, Nightingale KR (2008). Quantifying hepatic shear modulus in vivo using acoustic radiation force. *Ultrasound in Medicine and Biology,* **34**, 546–58.

Sandrin L, Tanter M, Gennisson JL, Catheline S, Fink M (2002). Shear elasticity probe for soft tissues with 1-D transient elastography. *IEEE Transactions on Ultrasonics, Ferroelectrics and Frequency Control,* **49**, 436–46.

Sandrin L, Fourquet B, Hasquenoph JM, *et al.* (2003). Transient elastography: a new noninvasive method for assessment of hepatic fibrosis. *Ultrasound in Medicine and Biology,* **29**, 1705–13.

Sandrin L, Cassereau D, Fink M (2004). The role of the coupling term in transient elastography. *Journal of the Acoustical Society of America*, **115**, 73–83.

Sarvazyan A, Skovoroda A, Emelianov S, *et al.* (1995). Biophysical bases of elasticity imaging. *Acoustical Imaging*, **21**, 223–40.

Sarvazyan AP, Rudenko OV, Swanson SD, Fowlkes JB, Emelianov SY (1998). Shear wave elasticity imaging: a new ultrasonic technology of medical diagnostics. *Ultrasound in Medicine and Biology,* **24**, 1419–35.

Sarvazyan AP (2001). Elastic properties of soft tissue. In M Levy, HE Bass, R Stern, eds., *Handbook of Elastic Properties of Solids, Liquids and Gases, vol. 3. Elastic Properties of Solids: Biological and Organic Materials, Earth and Marine Sciences*. New York: Academic Press, pp. 107–27.

Shiina T, Nitta N, Ueno E, Bamber JC (2002). Real time tissue elasticity imaging using the combined autocorrelation method. *Journal of Medical Ultrasound*, **29**, 119–28.

Sridhar M, Liu J, Insana MF (2007). Viscoelasticity imaging using ultrasound: parameters and error analysis. *Physics in Medicine and Biology*, **52**, 2425–43.

Yamakawa M, Shiina T (2001). Strain estimation using the extended combined autocorrelation method. *Japanese Journal of Applied Physics*, **40**, 3872–6.

Appendix A

The decibel (dB)

The dB is the unit which is normally used to describe the relative amplitude of echoes in ultrasound systems. In practice, the absolute amplitude of an echo signal (expressed in volts) is rarely of interest. It is more useful to know how echoes compare with one another. The ratio of the two amplitudes can be expressed in decibels (dB). As the dB is used only for ratios, there are no other units involved (e.g. mW, MPa). The dB is a logarithmic scale, so, in very simple terms, if the ratio is 1000:1 or 1 000 000:1, rather than writing out lots of zeros, the dB scale effectively counts the zeros, rather like expressing these numbers as 10^3 or 10^6. The Bel is simply $\log_{10} R$, where R is the ratio. Hence a ratio of 1000:1 is 3 Bel, and a ratio of 1 000 000:1 is 6 Bel. In practice, the unit of 1 Bel (ratio of 10) is often too large and it is more useful to use the decibel, which is one-tenth of a Bel. Hence, the ratio R in dB is given by $R\,(\text{dB}) = 10\log_{10} R$ dB. The dB, as defined above, is used to express only ratios of power or intensity. For example, as an ultrasound pulse propagates through tissue and is attenuated, the ratio of the intensities within the pulse at two different depths can be expressed in dB. The ratio of the intensities

$$\frac{I_2}{I_1}(\text{dB}) = 10\log_{10}\left[\frac{I_2}{I_1}\right]\text{dB} \qquad \text{(A.1)}$$

As described in Chapter 2, the intensity of a pulse is proportional to the square of the acoustic pressure, i.e. $I \propto p^2$. So the ratio of two intensities

$$\frac{I_2}{I_1} = \frac{p_2^2}{p_1^2} = \left[\frac{p_2}{p_1}\right]^2$$

That is, the intensity ratio is equal to the pressure ratio squared. The intensity ratio in dB can be expressed in terms of the pressure ratio:

$$\frac{I_2}{I_1}(\text{dB}) = 10\log_{10}\left[\frac{p_2}{p_1}\right]^2$$

This equation can be rewritten as

$$\frac{I_2}{I_1}(\text{dB}) = 20\log_{10}\left[\frac{p_2}{p_1}\right]\text{dB} \qquad \text{(A.2)}$$

Equation (A.2) is used whenever two amplitudes (pressure, voltage) are compared, whereas Equation (A.1) is used to compare power or intensity levels. An intensity ratio of 10 equates to 10 dB and a ratio of 2 to 3 dB. For pressure or voltage ratios of 10 and 2, the corresponding numbers are 20 and 6 dB, respectively.

A further important advantage of the dB scale is that it simplifies the combination of ratios. As the dB is a logarithmic unit, instead of multiplying the two ratios together, the corresponding values in dB are simply added. For example, an intensity ratio of 20 (2×10) equates to 13 dB (3 dB + 10 dB). A pressure ratio of 40 ($2 \times 2 \times 10$) equates to 32 dB (6 dB + 6 dB + 20 dB).

Diagnostic Ultrasound: Physics and Equipment, ed. Peter Hoskins, Kevin Martin and Abigail Thrush. Published by Cambridge University Press.

Appendix

B The binary system

A number in the decimal system consists of several digits, each representing a quantity of units, 10s or 100s, etc. For example, the decimal number 6473 represents 6 thousands plus 4 hundreds plus 7 tens plus 3 units. The value of 1 count in each column is a power of 10, i.e. $1 \times 100 = 10^2$, $1 \times 1000 = 10^3$. The maximum count of a 4-digit number is 9999. When counting from zero, the digit in the right-hand column (units) is increased until it reaches 9, and on the next count it returns to 0, while the digit in the 10s column is increased by 1. Each column carries over into the next to the left after a count of 9. The binary system operates in an identical fashion but the value of one count in each column is a power of 2, e.g. 2^3, 2^2, 2^1, 2^0. In decimal terms, the values of the digits are 8, 4, 2 and 1, and the maximum count in each column is 1. So the maximum value for a 4-digit number is 1111, which is 15 in decimal. Counting from 0, the digit on the right (2^0 column) changes from 0 to 1. On the next count, it goes back to 0 and the digit to the left (2^1 column) goes from 0 to 1. In the binary system, a digit is referred to as a bit (short for binary digit). So 1111 is a 4-bit number.

Appendix C

The British Medical Ultrasound Society. Guidelines for the safe use of diagnostic ultrasound equipment

Prepared by the Safety Group of the British Medical Ultrasound Society.[1]

Reproduced by kind permission of the British Medical Ultrasound Society.

Part I: Basic Guidelines

The following Basic Guidelines should be read in conjunction with *Detailed guidelines for the safe use of diagnostic ultrasound equipment* which follow below.

Key principles for the safe use of ultrasound

- Medical ultrasound imaging should only be used for medical diagnosis.
- Ultrasound equipment should only be used by people who are fully trained in its safe and proper operation. This requires:
  - an appreciation of the potential thermal and mechanical bioeffects of ultrasound,
  - a full awareness of equipment settings,
  - an understanding of the effect of machine settings on power levels.
- Examination times should be kept as short as is necessary to produce a useful diagnostic result.
- Output levels should be kept as low as is reasonably achievable whilst producing a useful diagnostic result.
- The operator should aim to stay within the BMUS recommended scan times (especially for obstetric examinations).
- Scans in pregnancy should not be carried out for the sole purpose of producing souvenir videos or photographs.

[1] In this Appendix, Part I and Part II of the BMUS Guidelines are published together. As a result, the duplicate Figure C.1a has been removed, and all figures are placed together.

Background

Diagnostic ultrasound is an imaging modality that is useful in a wide range of clinical applications and, in particular, prenatal diagnosis. There is, to date, no evidence that diagnostic ultrasound has produced any harm to humans (including the developing fetus).

Despite its apparent excellent safety record, ultrasound imaging involves the deposition of energy in the body, and should only be used for medical diagnosis, with the equipment only being used by people who are fully trained in its safe and proper operation. It is the scan operator who is responsible for controlling the output of the ultrasound equipment. This requires a good knowledge of scanner settings, and an understanding of their effect on potential thermal and mechanical bioeffects.

A fundamental approach to the safe use of diagnostic ultrasound is to use the lowest output power and the shortest scan time consistent with acquiring the required diagnostic information. This is the ALARA principle (i.e. as low as reasonably achievable). It is acknowledged that in some situations it is reasonable to use higher output or longer examination times than in others: for example, the risks of missing a fetal anomaly must be weighed against the risk of harm from potential bioeffects. Consequently, it is essential for operators of ultrasound scanners to be properly trained and fully informed when making decisions of this nature.

The thermal index (TI) and mechanical index (MI) were introduced to provide the operator with an indication of the potential for ultrasound-induced bioeffects. TI provides an on-screen indication of the relative potential for a tissue temperature rise. MI provides an on-screen indication of the relative potential for ultrasound to induce an adverse bioeffect by a non-thermal

Diagnostic Ultrasound: Physics and Equipment, ed. Peter Hoskins, Kevin Martin and Abigail Thrush. Published by Cambridge University Press.

mechanism such as cavitation. Three forms of the TI may be displayed:

1. *The thermal index for soft tissue (TIS).* This is used when ultrasound only insonates soft tissue, as for example, during obstetric scanning up to 10 weeks after last menstrual period (LMP).
2. *The thermal index for bone (TIB).* This is used when the ultrasound beam impinges on bone at or near its focal region, as for example, in any fetal scan more than 10 weeks after LMP.
3. *The thermal index for cranial bone (TIC).* This is used when the ultrasound transducer is very close to bone, as for example, during transcranial scanning of the neonatal skull.

Obstetric examinations

Any potential bioeffects are likely to be of greatest significance in the embryo or fetus. Thus when undertaking obstetric scans, the restrictions to scanning times detailed in Figure C.1a are recommended. These have been formulated on the basis of potential thermal effects arising from the scan, and are therefore based on the thermal index (TI) displayed.

MI values should be kept as low as reasonably achievable, consistent with the need to obtain diagnostically satisfactory images.

More detail can be found in the Detailed Guidelines.

Non-obstetric examinations

Most other types of examination are of less concern than are obstetric scans. Specific guidance on a range of non-obstetric examinations (including gynaecological, neonatal, ophthalmic, general abdominal, cardiac etc.) can be found in the Detailed Guidelines.

Part II: Detailed Guidelines

1. Scope and purpose
2. Guidelines for probe and system use
3. Hazard and risk factors
4. Application-specific guidelines
5. References

1. Scope and purpose

These Detailed Guidelines are intended to assist all those who use diagnostic ultrasound equipment for any purpose in order that they may be able to make informed judgements about ultrasound safety, and in order to protect patients from excessive exposure. These BMUS Detailed Guidelines are based on the best scientific information available at the time of writing, using advice and evidence from international experts. They must be read and understood in conjunction with the BMUS Safety Statement (http://www.bmus.org) and the BMUS Basic Guidelines. Further background information on the safe use of ultrasound may be found in more extensive texts, including ter Haar and Duck (2000).

2. Guidelines for probe and system use

Initial power setting. Scanners should be set up so that the default (switch-on) setting of the acoustic output power control is low. If a low default setting cannot be achieved, a low setting should be selected after switching on. A low setting should be selected for each new patient. The output should only be increased during the investigation if this is necessary to produce a satisfactory result.

Exposure time. The overall examination times should be kept as short as is necessary to produce a useful diagnostic result.

Stationary probe. The probe should not be held in a fixed position for any longer than is necessary, and should be removed from the patient whenever there is no need for a real-time image or spectral Doppler acquisition. For example, using the freeze-frame or cine-loop facilities allows images to be reviewed and discussed without continuing the exposure.

Probe self-heating. Endo-cavitary probes (e.g. vaginal, rectal or oesophageal probe) should not be used if there is noticeable self-heating of the probe when operating in air. This applies to any probe, but particular care should be taken if trans-vaginal probes are to be used to investigate a pregnancy during the first 10 weeks after LMP.

The raised tissue temperature due to probe self-heating is likely to be greater for endo-probes than for surface probes. This is because the adjacent tissue is at an initial temperature of 37°C, or higher in the case of a febrile patient, rather than closer to room temperature as in the case of surface-applied probes. Also, there is no opportunity for heat removal by air-convection or radiation, as is the case for probes applied to the patient's skin. International Standards (IEC 2007) are intended to limit the maximum temperature of the probe in contact with the patient to 43°C, either internally or externally, or to 50°C when running in air.

Doppler modes. The use of spectral pulsed Doppler, or colour Doppler mode with a narrow write-zoom

box selected, is not recommended for the investigation of any of the sensitive tissues identified in section 3, unless the user monitors the TI (if available), and performs a risk–benefit analysis (see section 4). If the TI is not available, the user should find an alternative method of estimating the maximum likely temperature rise.

Pulsed Doppler techniques generally involve greater temporal average intensities and powers than B- or M-mode, and hence greater heating potential, due to the high pulse repetition frequencies and consequent high duty factors that are often used. In the case of spectral pulsed Doppler, the fact that the beam is held in a fixed position during an observation leads to a further increase in temporal average intensity. Colour flow mapping and Doppler power mapping involve some beam scanning, and so generally have a heating potential that is intermediate between that of B- or M-mode and that of spectral pulsed Doppler.

3. Hazard and risk factors

Awareness of scanner factors influencing hazard. Operators should understand the likely influence of the scanner controls, the operating mode (e.g. B-mode, colour Doppler imaging or spectral Doppler) and probe frequency on the thermal and cavitation hazards.

There are no universal rules for predicting the effect of scanner controls (other than the output power control) on output since, in an effort to limit outputs, manufacturers often arrange for more than one parameter to change when a particular control is adjusted. However, the following may be helpful as a general guide. In scanning modes, greater heating potential is often associated with multiple or deep transmission focus settings, and the use of write zoom (particularly with a long, narrow or deep zoom box). In spectral pulsed Doppler mode, greater heating potential is usually associated with a high pulse repetition frequency (e.g. a high limit on the frequency scale) and a shallow range gate. The likelihood of cavitation is greater for large output settings and lower frequencies. In Doppler modes, the likelihood is increased by selecting short range gates or by selecting a high Doppler frequency scale.

Sensitive tissues. Particular care should be taken to reduce the risk of thermal hazard when exposing the following to diagnostic ultrasound:

- an embryo less than 8 weeks after conception;
- the head, brain or spine of any fetus or neonate;
- an eye (in a subject of any age).

Up to 8 weeks after conception, organogenesis is taking place in the embryo. This is a period when cell damage might lead to fetal anomalies or subtle developmental changes. The brain and spinal chord continue to develop through to the neonatal period.

The presence of bone within the beam greatly increases the likely temperature rise, due to both direct absorption in the bone itself and conduction of heat from bone to adjacent tissues. Table C.1 identifies the important relevant landmarks in early pregnancy.

The eye is particularly vulnerable to thermal hazard since the lens and the aqueous and vitreous humours have no cooling blood supply. This applies to an eye of a subject of any age (e.g. child or adult) as well as a fetus, although a fetal eye is better cooled, due to its liquid environment.

Pre-existing temperature elevation. Particular care should be taken to reduce output and minimize exposure time of an embryo or fetus when the temperature of the mother is already elevated.

Thermal and mechanical indices. For scanners which display on-screen thermal index (TI) and mechanical index (MI) values, operators should continually monitor their values and use control settings that keep them as small as is consistent with achieving diagnostically useful results. There should be independent checks that the displayed TI and MI values are accurate. These should be made soon after installation and after hardware or software changes.

- The MI is an on-screen indicator of the relative potential for ultrasound to induce an adverse bioeffect by a non-thermal mechanism, including cavitation.

The mechanical index (MI) is intended to offer a rough guide to the likelihood of the occurrence of cavitation. Its value is constantly updated by the scanner, according to the control settings, using the formula $MI = p_{-0.3} / \sqrt{f}$ *where f is the pulse centre frequency and* $p_{-0.3}$ *is the maximum value of peak negative pressure anywhere in the ultrasound field, measured in water but reduced by an attenuation factor equal to that which would be produced by a medium having an attenuation coefficient of 0.3 dB cm*$^{-1}$ *MHz*$^{-1}$.

- The TI is an on-screen indicator of the relative potential for a tissue temperature rise.

Table C.1 Landmarks in early pregnancy.

Gestation from LMP	Gestation from conception/fertilization	Title of conceptus	Major relevant events
0–14 days	Nil	-	-
14–28 days	0–14 days	Zygote	Rapid cell multiplications
29–70 days	15–56 days	Embryo	Organogenesis
4.1–10 weeks	2.1–8 weeks		
10–11 weeks	8–9 weeks	Fetus	Ossification of spine starts
13–14 weeks	11–12 weeks	Fetus	Ossification of skull and long bone starts

The thermal index (TI) is intended to give a rough guide to the likely maximum temperature rise that might be produced after long exposure. Three forms of TI may be displayed, according to the application. TIS assumes that only soft tissue is insonated. TIB assumes bone is present at the depth where temporal average intensity is greatest. TIC assumes bone is very close to the front face of the probe. However, note that errors in calculating TI values, and the limitations of the simple models on which they are based, mean that TI values can underestimate the temperature elevation by a factor of up to two.

4. Application-specific guidelines

For scanners which display thermal index (TI) and mechanical index (MI) values on-screen, operators should continually monitor their values and use control settings that keep them as small as is consistent with achieving diagnostically useful results.

Where on-screen mechanical or thermal index can be displayed, the recommended exposure times and upper levels for the indices depend on the clinical application. These recommended levels are given in Table C.2 for obstetric (including gynaecological examinations when pregnancy is possible) and neonatal ultrasound, and in Table C.3 for other applications. Many scanners allow MI and one of the TI values to be displayed simultaneously: the appropriate TI value depends on the clinical application and the recommended indices to monitor are also given in Tables C.2 and C.3.

Where an on-screen thermal index (TI) or mechanical index (MI) is not displayed, try to obtain worst case estimates (considering all possible combinations of control settings) of temperature elevation (ΔT_{max}) and mechanical index (MI_{max}) for the particular probe and mode in use. If these can be obtained, assume that the MI value is equal to MI_{max} and the TI value is equal to 0.5 ΔT_{max} and refer to Table C.2 or C.3 as appropriate.

A medical physics department may be able to make these estimates, using either a thermal test object or measurements of acoustic power and intensity. For abdominal and obstetric applications, the worst-case estimate of temperature elevation should use a model similar to TIB in which soft tissue overlies bone, with the interface lying at the depth where the derated temporal average intensity is a maximum. For other applications (e.g. the eye or superficial bone), the model used should be appropriate to the particular tissues involved.

The operator should aim to stay within BMUS recommended scan times. If there is a clinical need to exceed these recommended times, the ALARA principle should still be followed. When overall times longer than those recommended here are essential, the probe should be removed from the patient whenever possible, to minimize exposure.

Thermal index values and maximum exposure time recommendations for fetal and neonatal tissues

TI values are intended to give a rough indication of the likely equilibrium temperature rise that might be produced. However, theoretical (Jago et al. 1999) and experimental (Shaw et al. 1998) studies have shown that, in some circumstances, TI can underestimate the temperature elevation by a factor of up to two. As a safety precaution, the TI values given in Table C.2 are assumed to be half the actual worst-case temperature elevations. Thus a TI value of 1 is considered to correspond to a worst-case temperature elevation of 2°C.

Following their review of the literature on the effects of temperature elevation on animal fetuses, the WFUMB (1998) concluded that an ultrasound exposure that elevates human embryonic or fetal temperature by 4°C

Table C.2 Recommended exposure time and index values for obstetric and neonatal ultrasound.

Application	Values to monitor[a]	Thermal index value			Mechanical index value		
		0–0.7	0.7–3.0	>3.0	0–0.3	>0.3	>0.7
Obstetrics up 10 weeks after LMP (and gynaecology when pregnancy is possible)	TIS and MI	✓	*Restrict time to*[b] 0.7 < TIS ≤ 1.0 : 60 min 1.0 < TIS ≤ 1.5 : 30 min 1.5 < TIS ≤ 2.0 : 15 min 2.0 < TIS ≤ 2.5 : 4 min 2.5 < TIS ≤ 3.0 : 1 min	**Scanning of an embryo or fetus is not recommended, however briefly**	✓	✓	Risk of cavitation with contrast agents[e]
Obstetrics more than 10 weeks after LMP	TIB and MI	✓	*Restrict time to*[b] 0.7 < TIB ≤ 1.0 : 60 min 1.0 < TIB ≤ 1.5 : 30 min 1.5 < TIB ≤ 2.0 : 15 min 2.0 < TIB ≤ 2.5 : 4 min 2.5 < TIB ≤ 3.0 : 1 min	**Scanning of an embryo or fetus is not recommended, however briefly**	✓	✓	Risk of cavitation with contrast agents[e]
Neonatal – transcranial and spinal	TIC and MI	✓	*Restrict time to*[b] 0.7 < TIC ≤ 1.0 : 60 min 1.0 < TIC ≤ 1.5 : 30 min 1.5 < TIC ≤ 2.0 : 15 min 2.0 < TIC ≤ 2.5 : 4 min 2.5 < TIC ≤ 3.0 : 1 min	**Scanning of the central nervous system is not recommended, however briefly**	✓	✓	Risk of cavitation with contrast agents[e]
Neonatal – general and cardiac imaging	TIB and MI recommended	✓	*Restrict time to*[c] 1.0 < TIB ≤ 1.5 : 120 min 1.5 < TIB ≤ 2.0 : 60 min 2.0 < TIB ≤ 2.5 : 15 min 2.5 < TIB ≤ 3.0 : 4 min 3.0 < TIB ≤ 4.0 : 1 min 4.0 < TIB ≤ 5.0 : 15 s 5.0 < TIB ≤ 6.0 : 5 s TIB > 6:	**not recommended**	✓	Possibility of minor damage to lung or intestine. Minimize exposure time[d]	Risk of cavitation with contrast agents[e]
Fetal Doppler heart monitoring	TI or MI are not usually available for dedicated fetal heart monitors	The power levels used by dedicated fetal heart monitors are sufficiently low that the use of this modality is not contraindicated, on safety grounds, even when it is to be used for extended periods					

✓: There is no known reason to restrict scanning times in this region.

[a] Many scanners allow MI and one of the TI values to be displayed simultaneously: the most appropriate TI value depends on the clinical application.

[b] TI > 0.7 – the overall exposure time (including pauses) of an embryo or fetus or of the neonatal central nervous system should be restricted.

[c] TI > 1.0 – the overall exposure time (including pauses) of other parts of the neonate should be restricted.

[d] MI > 0.3 – there is a possibility of minor damage to neonatal lung or intestine. If such exposure is necessary, try to reduce the exposure time as much as possible.

[e] MI > 0.7 – there is a risk of cavitation if an ultrasound contrast agent containing gas microspheres is being used. There is a theoretical risk of cavitation without the presence of ultrasound contrast agents. The risk increases with MI values above this threshold.

Table C.3 Recommended exposure time and index values for non-obstetric and non-neonatal ultrasound.

Application	Values to monitor[a]	Thermal index value		Mechanical index value	
		0–1.0	>1.0	0–0.3	>0.7
General abdominal Peripheral vascular Unlisted applications	Usually TIB and MI (use TIC and MI if bone closer than 1 cm; TIS and MI only if bone does not come into the image)	✓	*Restrict time to*[b] 1.0 < TIB ≤ 1.5 : 120 min 1.5 < TIB ≤ 2.0 : 60 min 2.0 < TIB ≤ 2.5 :15 min 2.5 < TIB ≤ 3.0 : 4 min 3.0 < TIB ≤ 4.0 : 1 min 4.0 < TIB ≤ 5.0 : 15 s 5.0 < TIB ≤ 6.0 : 5 s TIB > 6: **not recommended**	✓	Risk of cavitation with contrast agents[c]
Eye	TIS and MI recommended	✓	**Scanning of the eye is not recommended**	✓	Risk of cavitation with contrast agents[c]
Adult transcranial (imaging and stand-alone)[d]	TIC and MI	✓	*Restrict time to*[b] 0.7 < TIC ≤ 1.0 : 60 min 1.0 < TIC ≤ 1.5 : 30 min 1.5 < TIC ≤ 2.0 :15 min 2.0 < TIC ≤ 2.5 : 4 min 2.5 < TIC ≤ 3.0 : 1 min TIC > 3: **not recommended**	✓	Risk of cavitation with contrast agents[c]
Peripheral pulse monitoring	TI or MI are not usually available for dedicated peripheral pulse monitors	The output from CW Doppler devices intended for monitoring peripheral pulses is sufficiently low that their use is not contra-indicated, on safety grounds			

✓: There is no known reason to restrict scanning times in this region.
[a] Many scanners allow MI and one of the TI values to be displayed simultaneously: the most appropriate TI value depends on the clinical application.
[b] TI > 1.0 – the overall exposure time (including pauses) should be restricted.
[c] MI > 0.7 – there is a risk of cavitation if an ultrasound contrast agent containing gas microspheres is being used. There is a theoretical risk of cavitation without the presence of ultrasound contrast agents. The risk increases with MI values above this threshold.
[d] Transcranial ultrasound investigations may require higher acoustic output or longer monitoring times than other applications. When times longer than those recommended here are required, it is recommended that monitoring is paused regularly to minimize exposure.

above normal for 5 minutes should be considered potentially hazardous. Miller and Ziskin (1989) showed that there is a logarithmic relationship between temperature elevation and the exposure time needed to produce adverse biological effects in animal fetuses. They showed that, for temperatures below 43°C, the necessary exposure time reduced by a factor of 4 for every 1°C increase in temperature elevation. Adopting a maximum safe exposure time of 4 minutes for a temperature elevation of 4°C, and applying the above logarithmic rule, results in the exposure times given in Table C.4.

In Table C.2, rounded values of these exposure times have been used for obstetric exposures up to 15 minutes. The 64 and 256 minute maximum exposure times

Table C.4 Maximum safe exposure times for fetal tissue.

Temperature elevation (°C)	Maximum exposure time (minutes)
5	1
4	4
3	16
2	64
1	256

have been reduced to 30 and 60 minutes respectively as a safety precaution to reflect the present lack of knowledge about possible subtle bioeffects associated with prolonged moderate temperature elevation. No time limit is specified for TI values of less than 0.7, in accordance with the statement in the WFUMB (1998) recommendations on thermal effects that a diagnostic exposure that produces a maximum temperature rise of no more than 1.5°C above normal physiological levels (37°C) may be used clinically without reservation on thermal grounds.

In examinations of the embryo or fetus in the first 8 weeks post conception, when there is no ossified bone, only soft tissue is exposed and so TIS should be monitored. In all other obstetric applications, TIB is recommended as the particular thermal index value to monitor. This avoids the complication of constantly switching attention between TIS and TIB according to whether or not bone is being insonated, and introduces a safety factor since TIB values are always greater than or equal to TIS values.

To protect the still rapidly developing neonatal central nervous system, the time limits recommended for fetal examinations are also applied to imaging of the brain or spine of a neonate. When imaging other parts of the neonate, the recommended time limits match those for adult tissues.

Thermal index values and maximum exposure time recommendations for non-fetal tissues

In eye-scanning applications, it is recommended that TIS is monitored as this is the thermal index used in the study by Herman and Harris (1999), which concluded that, in eye scanning, TIS values should be limited to a maximum of 1.0.

In other applications TIS, TIB or TIC may be monitored depending on the tissue being scanned: in most applications TIB is recommended. AIUM (2008) concluded that there was a maximum safe exposure time for thermal damage to non-fetal tissue which depended on temperature, as shown in Table C.5.

Table C.5 Maximum safe exposure times for non-fetal tissue.

Temperature elevation (°C)	Maximum exposure time (minutes)
10	0.07
8	0.25
6	1
5	4
4	16
3	64
2	256

Harm at a particular temperature increase had not been observed for shorter times. In formulating Table C.3, we have assumed that TI may underestimate temperature rise by a factor of 2, and we have rounded the maximum exposure times. The 256 minute maximum exposure time has been reduced to 120 minutes as a safety precaution to reflect the present lack of knowledge about possible subtle bioeffects associated with prolonged moderate temperature elevation. As a precaution for transcranial ultrasound, the recommended time limits are the same as those for neonatal brain, except that there is no specific restriction when TIC is less than or equal to 1.0.

Mechanical index threshold values

The MI value of 0.3, representing the threshold for the possibility of capillary bleeding in gas-containing organs, such as the lungs and intestines, is taken from the 1992 Statement on Non-human Mammalian in vivo Biological Effects of the American Institute of Ultrasound in Medicine (AIUM 1993).

The MI value of 0.7 is chosen as the threshold for cavitation, following the theoretical study by Apfel and Holland (1991), from which the formula for MI is derived. The model used for this study assumes the availability of microbubble nuclei of all sizes. Such microbubbles are believed to be produced when the shells of some contrast agents are destroyed by pulses with higher acoustic pressures. There is experimental evidence that cavitation damage occurs in animals when contrast agents are present (Miller and Gies 1998, Skyba et al. 1998). In tissues not containing such artificially introduced nuclei, cavitation due to diagnostic ultrasound remains a theoretical possibility only, although it is produced in tissue during lithotripsy treatment (ECURS 1994) and bubble formation has been demonstrated in agar gel exposed to diagnostic levels of ultrasound (ter Haar et al. 1989).

Fig. C.1 Graphical representation of the recommended exposure times at different index values for different applications, as listed in Tables C.2 and C.3, is presented in panels a–d. It is hoped these figures may serve as useful easy reference during scanning sessions.

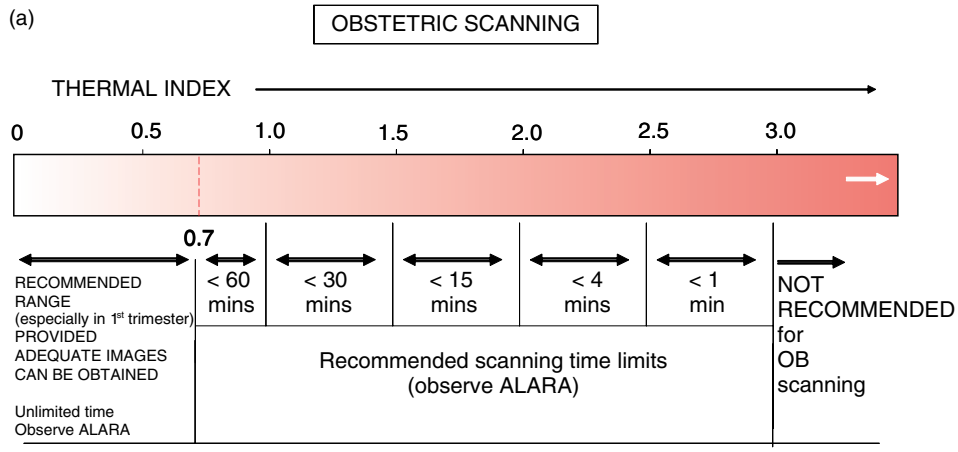

Monitor TIS up to 10 weeks post-LMP, TIB thereafter.

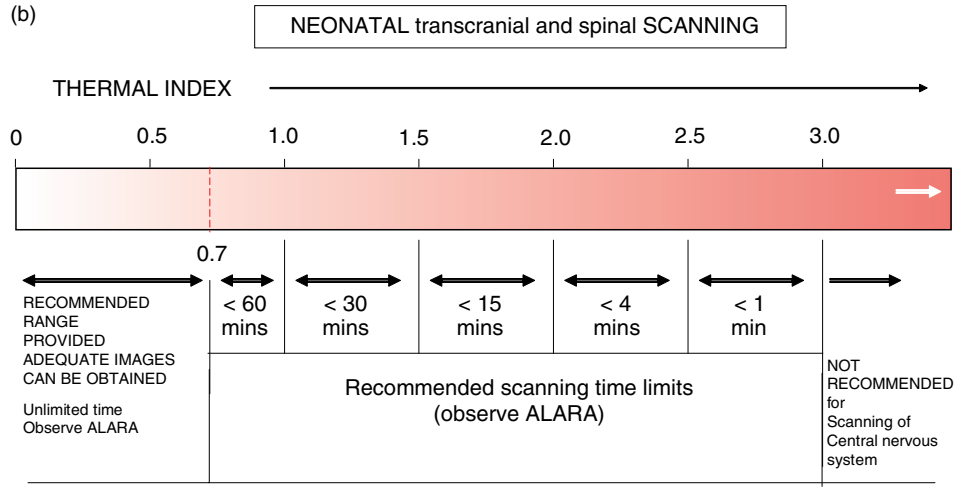

Monitor TIC. MI>0.7 should be used with caution in the presence of contrast agents

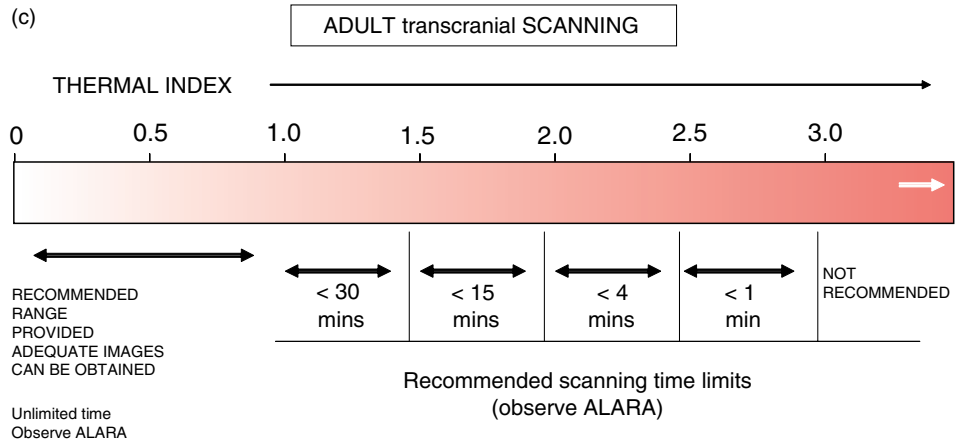

Monitor TIC. Use of TIC>3 is not recommended.
MI>0.7 should be used with caution in the presence of contrast agents

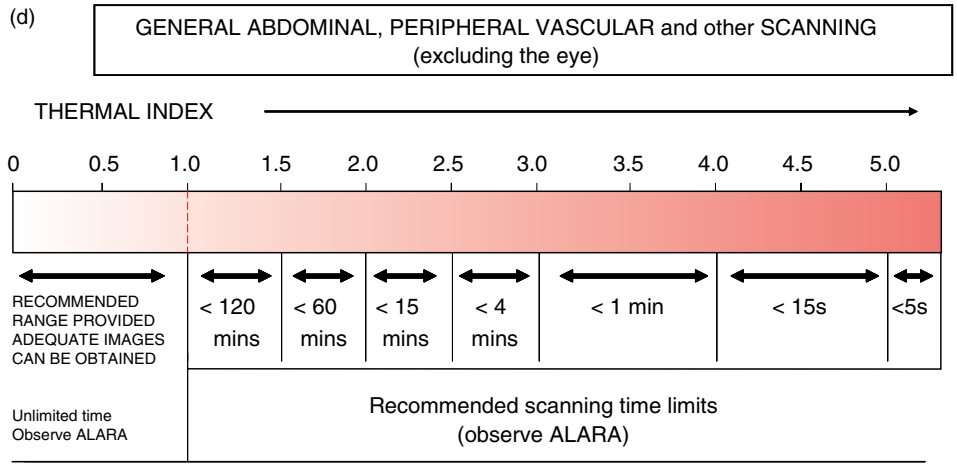

Monitor TIB, or TIC if bone closer than 1cm; TIS if no bone is in image.
Use of TI>6 is not recommended.
MI>0.7 should be used with caution in the presence of contrast agents

5. References

AIUM (1993). *Bioeffects and Safety of Diagnostic Ultrasound*. AIUM, 11200 Rockville Pike, Suite 205, Rockville, Maryland 20852–3139, USA.

AIUM (2008). American Institute of Ultrasound in Medicine Consensus Report on Potential Bioeffects of Diagnostic Ultrasound. *Journal of Ultrasound in Medicine*, **27**, 503–15.

Apfel RE, Holland KH (1991). Gauging the likelihood of cavitation from short pulse low duty cycle diagnostic ultrasound. *Ultrasound in Medicine and Biology*, **17,** 179–85.

ECURS (1994). Guidelines for the safe use of extracorporeal shock-wave lithotripsy (ESWL) devices. *European Journal of Ultrasound*, **3**, 315–16.

Herman BA, Harris GR (1999). Theoretical study of steady-state temperature rise within the eye due to ultrasound insonation. *IEEE Transactions on Ultrasonics, Ferroelectrics and Frequency Control*, **46:** 1566–74.

IEC (2007). *IEC 60601–2–37 Ed. 2.0: Medical electrical equipment – Part 2–37: Particular requirements for the basic safety and essential performance of ultrasonic medical diagnostic and monitoring equipment*. Geneva: International Electrotechnical Commission.

Jago JR, Henderson J, Whittingham TA, Mitchell G (1999). A comparison of AIUM/NEMA Thermal Indices with calculated temperature rises for a simple third trimester pregnancy tissue model. *Ultrasound in Medicine and Biology*, **25**, 623–8.

Miller DL, Gies RA (1998). Gas-body-based contrast agent enhances vascular bioeffects of 1.09 MHz ultrasound on mouse intestine. *Ultrasound in Medicine and Biology*, **24**, 1201–8.

Miller MW, Ziskin MC (1989). Biological consequences of hyperthermia. *Ultrasound in Medicine and Biology*, **15**, 707–22.

Shaw A, Pay NM, Preston RC (1998). Assessment of the likely thermal index values for pulsed Doppler ultrasonic equipment – Stages II and III: experimental assessment of scanner/transducer combinations. *NPL Report CMAM 12, April 1998.* Teddington, UK: National Physical Laboratory.

Skyba DM, Price RJ, Linka AZ, et al. (1998). Microbubble destruction by ultrasound results in capillary rupture: adverse bioeffects or a possible mechanism for in vivo drug delivery? *Journal of the American Society of Echocardiology*, **11**, 497.

ter Haar G, Duck F, Starritt H, Daniels S (1989). Biophysical characterisation of diagnostic ultrasound equipment – preliminary results. *Physics in Medicine and Biology*, **34**,1533–42.

ter Haar G, Duck FA, eds. (2000). *The Safe Use of Ultrasound in Medical Diagnosis*, London: BMUS/BIR.

WFUMB (1998). Conclusions and Recommendations on Thermal and Non-thermal Mechanisms for Biological Effects. *Ultrasound in Medicine and Biology*, **24**, Suppl 1, xv–xvi.

Appendix

D Useful contacts

BMUS Safety Group. See www.bmus.org.

The British Standards Institution (BSI) acts as the focus for the UK's input to the international standards scene. Committees within BSI mirror those within IEC and CENELEC. The particular committees are:

BSI Committee EPL/87 mirrors IEC Technical Committee 87: Ultrasonics.

BSI Committee CH/111 mirrors the diagnostic and therapeutic ultrasound aspects of IEC Technical Committees TC 62, SC 62B and SC 62D which deal with electrical equipment in medical practice.

European Federation of Societies for Ultrasound in Medicine and Biology. EFSUMB has a standing safety committee, the European Committee for Medical Ultrasound Safety (ECMUS). A Clinical Safety Statement, safety tutorials and literature reviews are available freely from the EFSUMB web site: www.efsumb.org.

Diagnostic Ultrasound: Physics and Equipment, ed. Peter Hoskins, Kevin Martin and Abigail Thrush. Published by Cambridge University Press.

Appendix E

Acoustic output parameters and their measurement

Acoustic output parameters

Many different parameters have been defined in order to try and characterize medical ultrasound fields. Due to the complexity of these fields, it is not possible to describe the parameters fully and unambiguously here. Definitions of some terms are given; the more interested reader can find further formal definitions and description in IEC 62127–1 (2007a) and AIUM/NEMA (2004). There are five which seem to be most important to safety: peak negative pressure, pulse average intensity, temporal average intensity, total power and acoustic frequency.

Peak negative acoustic pressure

The peak negative acoustic pressure (also called the peak rarefactional pressure and given the symbol p_r) is simply the most negative pressure that occurs during the pulse: in Figure 12.1, this is about 3.5 MPa. This is an important parameter because it relates to the occurrence of cavitation. Negative acoustic pressure means that the acoustic wave is trying to pull the water molecules apart; the water molecules resist this separation but if the pressure is sufficiently negative and lasts for long enough, it is possible to produce a small void, a cavitation bubble. If there are pre-existing gas bubbles or dust particles in the water, cavitation occurs more easily. A similar effect can occur in tissue.

Temporal average intensity

We can also consider the intensity of the ultrasound field at a point. Intensity is a measure of the rate at which energy is flowing through a small area around the measurement point. Intensity varies with time as the ultrasound pulse passes the point and for most practical purposes is given by:

$$i(t) = \frac{p(t)^2}{\rho c}$$

where c is the speed of sound in the medium, ρ is its density and $p(t)$ is the pressure. From this relationship, we can see that intensity is always a positive (unlike acoustic pressure, which can be positive or negative) and that intensity is highest when the pressure amplitude is highest. The time-averaged value of the intensity at a particular point is called the temporal average intensity and given the symbol I_{ta}. Imaging scanners generally produce a large number of short pulses (approximately 1 μs long) separated by relatively long gaps (perhaps 100 μs long) and these pulses are often directed along different axes so it may take several hundred milliseconds for the pattern of intensity at any point to repeat. This means that the true temporal average intensity must be averaged over the full scan repetition period or over a time which includes many scan repetition periods (see Figure E.1). Note that the time between pulses is actually much longer in relation to the pulse duration than is shown in the figure. I_{ta} is relevant because its spatial distribution is one of the main factors governing temperature rise in tissue. The maximum value of I_{ta} in the field is called the spatial peak temporal average intensity I_{spta}. This is one of the parameters on which the acoustic output is regulated in the USA by the Food and Drug Administration (FDA).

Pulse intensity integral and pulse average intensity

Instead of averaging the intensity over the whole scan repetition period, it is possible to examine only a single pulse. The pulse intensity integral (*PII* or p_i) is calculated by integrating the intensity over the duration of the pulse; p_i is greatest at the focus and this is the position where many measurements are made. Dividing p_i by the duration of the pulse gives a parameter called the pulse average intensity, I_{pa}; the maximum value in the field is the spatial peak pulse average intensity, I_{sppa}, which is also a parameter limited by FDA regulations.

Diagnostic Ultrasound: Physics and Equipment, ed. Peter Hoskins, Kevin Martin and Abigail Thrush. Published by Cambridge University Press.

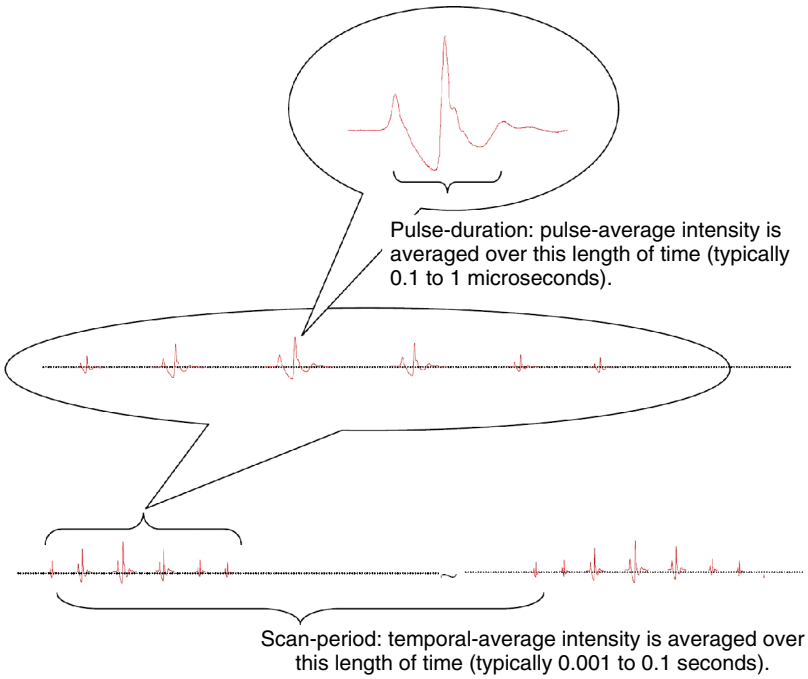

Fig. E.1 A representation of the pulse sequence in an imaging scan frame, at one point in the field. Temporal average intensity is averaged over the repeating period of the sequence, including the 'dead time' between pulses: pulse average intensity is averaged over the duration of the largest pulse.

Total power and output beam intensity

Total power is the amount of ultrasonic energy radiated by the transducer every second. This is an important parameter for safety because it is relevant to heating and is used to calculate thermal indices. It is worth noting that, for a typical imaging transducer, the total radiated power is substantially less than the total electrical power supplied to the transducer and most of the electrical energy is converted to heat in the transducer. This 'self-heating' is an important factor in determining the hazard to tissues close to the transducer. Dividing the total power by the output area of the transducer gives the output beam intensity, I_{ob}. This is the mean temporal average intensity at the transducer face.

Acoustic frequency

As the wave passes a point, the water molecules are squeezed together during the high-pressure periods and stretched apart during the low-pressure periods. The acoustic frequency is essentially the rate at which this squeezing and stretching takes place. In Figure E.1, the time between consecutive high-pressure periods is about 0.3 microseconds and so the acoustic frequency is approximately 1/(0.3 μs) = 3.3 MHz. Frequency is important to safety because the absorption coefficient of most soft tissues increases with frequency, leading to energy being absorbed in a smaller volume and producing higher temperature rises. Additionally, cavitation is more likely to occur at lower frequencies because the periods of negative pressure last for longer and cavitation nuclei have more time to grow.

Calculation of *in situ* exposure parameters

As ultrasound travels through tissue it is attenuated. That is, some of the energy is lost from the beam by absorption or scatter. This means that the *in situ* intensity (i.e. the intensity at some point in tissue) is less than the intensity measured in water at the same point in the field.

The propagation of ultrasound of the type used in medical imaging is an extremely complex phenomenon and there is no accepted way of deriving truly reliable estimates of the *in situ* exposure levels from the acoustic output measurements made in water. The most widely used method is that of 'derating', used in the US FDA regulations (see later), and the AIUM/NEMA Output Display Standard. Derating involves multiplying the value of an acoustic property measured in water by a logarithmic attenuation factor. This factor is always frequency-dependent and is often distance-dependent. The most widely used theoretical

attenuation model comes from the AIUM/NEMA Output Display Standard, and IEC 60601–2–37 (IEC 2007b), and uses a derating factor of 0.3 dB cm^{-1} MHz^{-1} to estimate exposure in tissue. The assumption is that soft tissue fills the path between the transducer and the point where the exposure level is required. The value of 0.3 dB cm^{-1} MHz^{-1} is lower than the attenuation of most soft tissues (which is typically closer to 0.44 dB cm^{-1} MHz^{-1}) to allow for the possibility of some fluid in the path (as would be the case for examination of a fetus through the bladder). The value of 0.3 dB cm^{-1} MHz^{-1} means that at 3 cm from a 3.3 MHz transducer, the derated temporal average intensity, $I_{ta.3}$, is 3 dB less than (that is, half of) the value measured in water; the derated peak negative pressure, $p_{r.3}$, is 70% of the value in water. This derating factor is used in calculating thermal and mechanical indices and, if you see the term 'derated' being used without the derating factor being specified, it is generally this AIUM/NEMA value which has been used. Other attenuation models have been proposed by the NCRP using different attenuation factors. These models are less commonly used but generally suggest higher *in situ* values than does the AIUM/NEMA derating factor.

How do you measure ultrasound?

Two types of device are used to measure the acoustic output of imaging and other medical ultrasonic equipment. The first is the hydrophone; the second is the radiation-force balance (sometimes called a power balance, a power meter or a radiation-pressure balance).

Hydrophones

Hydrophones are underwater microphones. Usually they are made of a piezoelectric material that converts the rapid pressure changes in the ultrasound pulse to an electrical signal that can be measured with an oscilloscope. If the hydrophone is calibrated, the pressure waveform can be calculated from the voltage waveform measured by the oscilloscope. In order to make measurements of real ultrasound fields, the hydrophone element must be small (1 mm) and it must be mounted in a positioning system that allows it to be moved to different positions in the field. This allows the acoustic quantities to be measured throughout the field and the spatial peak values determined. In principle, any of the acoustic properties described above can be measured with a hydrophone but this type of measurement is really only possible in a laboratory or medical physics department with substantial experience and equipment for characterizing ultrasound fields.There are two types of hydrophone in general use: the membrane hydrophone and the probe hydrophone. In general membrane hydrophones are to be preferred because they have a smoother frequency response than probes, especially at frequencies below 4 MHz, and are more stable over time. Probe hydrophones, however, are generally cheaper to buy and are available with smaller active elements.

Radiation-force balances

Radiation-force balances (RFBs) are much easier to use than hydrophones and are used to measure only one property of the ultrasound field – the total ultrasonic power radiated by the transducer. RFBs work by measuring the force exerted on a target when it absorbs or reflects an ultrasound beam. The relationship between the measured force and the incident power depends on the design of the balance and so, although this relationship can be calculated approximately, the balance should be calibrated. For most designs of balance in common use, a power of 1 mW produces a force equivalent to approximately 69 μg. Measuring power from diagnostic equipment is complicated by the fact that output powers are relatively low and the fields are focused and scanned. The resulting low forces require considerable sensitivity for the balance design. The focused and scanned nature of the fields means that the relationship between the measured force and the total power can only be determined approximately (in other words, two transducers which generate the same ultrasonic power may produce different readings on the RFB).

References

AIUM/NEMA (2004). *UD3 rev. 2. Standard for real-time display of thermal and mechanical acoustic output indices on diagnostic ultrasound equipment. UD 3–2004.* American Institute for Ultrasound in Medicine/National Electrical Manufacturers Association, USA.

IEC (2007a). *62127–1, Ultrasonics – Hydrophones – Part 1: Measurement and characterization of medical ultrasonic fields up to 40 MHz.* Geneva: International Electrotechnical Commission.

IEC (2007b). *60601–2–37 Ed 2. Medical Electrical Equipment: Particular requirements for the safety of ultrasound diagnostic and monitoring equipment.* Geneva: International Electrotechnical Commission.

Glossary of terms

1D 1-dimension; referring to a line in space.

2D 2-dimensions; referring to an area in space.

3D 3-dimensions; referring to a volume in space.

4D 4-dimensions; referring to the movement of a volume through time.

A to D conversion See 'analogue-to-digital conversion'.

A to D converter See 'analogue-to-digital converter'.

A-line Single ultrasound scan line, usually in a 2D ultrasound image consisting of many A-lines.

A-mode Display of echo amplitude with depth for a single ultrasound line.

Absorption Mechanism by which energy is transferred from the ultrasound wave to the tissue resulting in reduction in wave amplitude and heating of the tissues. See 'absorption coefficient', 'attenuation'.

Absorption coefficient The property of a medium which describes the rate at which an ultrasound energy is converted to heat. Usually the absorption coefficient is expressed in dB cm^{-1} at a particular frequency, or in dB cm^{-1} MHz^{-1}. See 'attenuation coefficient'.

Acoustic Relating to sound or ultrasound. See 'sound', 'ultrasound'.

Acoustic cavitation The mechanical response of gas cavities to a sound field. Acoustic cavitation is divided into two classes, inertial cavitation (when the cavity eventually collapses violently) and non-inertial cavitation (when the cavity grows and contracts cyclically). See 'inertial cavitation', 'non-inertial cavitation'.

Acoustic impedance Fundamental property of a medium in the context of sound wave propagation.

Acoustic intensity See 'intensity', 'I_{sppa}', 'I_{spta}'.

Acoustic lens Curved region of the face of a transducer used to focus the beam in the tissue; usually used in single-element transducers, or in array transducers to provide focusing in the elevation plane.

Acoustic pressure The amount by which the pressure exceeds the ambient pressure at any instant. In the compression part of the wave, the acoustic pressure is positive, and in the rarefactional phase, the acoustic pressure is negative. The unit of measurement is megapascal, MPa. See 'pressure'.

Acoustic radiation force imaging (ARFI) Ultrasound elastography method in which tissue displacement is produced at the focal spot by the radiation force generated from a high-output beam (the 'pushing beam'), with measurement of tissue displacement performed by several imaging lines using cross-correlation techniques. See 'elastography'.

Acoustic shock An abrupt alteration in acoustic pressure in a propagating acoustic wave. Typically a high positive peak pressure follows immediately behind a decompression.

Activation The process of reconstituting an ultrasound contrast agent prior to clinical use. See 'contrast agent'.

Active group Group of elements of the transducer which are used to produce the current ultrasound beam. See 'aperture'.

Adaptive image processing Image processing where the degree of processing, e.g. edge enhancement or noise reduction, is adjusted at each location in the image dependent on the local image content. See 'image processing', 'edge enhancement', 'noise reduction'.

ADC See 'analogue-to-digital converter'.

AIUM (American Institute of Ultrasound in Medicine) American ultrasound professional body that, amongst other things, produces standards documents and codes of practice for ultrasound.

Aliasing Incorrect estimation of Doppler frequency shift occurring in pulsed Doppler systems when the pulse repetition frequency is too low or the target velocity is too high. See 'pulse repetition frequency', 'pulsed-wave Doppler'.

Amplifier Device used to increase the size of the received ultrasound signal; the amplification for ultrasound is depth-dependent in order to boost the smaller echoes received from greater depths or area of low scatter/backscatter. See 'time-gain control'.

Amplitude Maximum excursion of a wave in either the positive or negative direction.

Amplitude demodulation Method used in B-mode imaging to extract the envelope of the received ultrasound signal, involving rectification and smoothing of the signal. See 'demodulation'.

Amplitude modulation An imaging technique for detecting ultrasound scattering from non-linear scatterers, e.g. contrast agents. Generally, three consecutive pulses are emitted in the incident pulse sequence – a half-amplitude pulse, followed by a full-amplitude pulse followed by a second half-amplitude pulse. When received, the scattered response of the half-amplitude pulses are subtracted from the scattered response of the full-amplitude pulse – responses from linear scatterers will cancel, those from non-linear scatterers will not. See 'contrast imaging'.

Analogue Relating to devices and electrical signals in which the voltage may vary continuously. See 'digital'.

Analogue-to-digital conversion Conversion of an analogue signal into a digital signal. See 'analogue', 'analogue-to-digital converter', 'digital'.

Analogue-to-digital converter Device for converting analogue (continuously varying voltage) to digital (voltage levels with only two allowed values corresponding to '0' and '1') signals. See 'analogue', 'digital'.

Angle General: a measure of the orientation or amount of rotation between two lines. In Doppler ultrasound: abbreviation for the angle between the Doppler ultrasound beam and the direction of motion of the moving blood or tissue. See 'angle cursor'.

Angle cursor Relating to spectral Doppler ultrasound: marker, such as a line, on the ultrasound B-mode image, present when pulsed-wave spectral Doppler is activated, which can be rotated in order to align it with the vessel wall. This is performed for the purpose of providing the ultrasound machine with information on the beam–vessel angle, to enable the machine to convert Doppler frequency shift to velocity using the Doppler equation. See 'beam–vessel angle', 'Doppler equation'.

Angle dependence Relating to Doppler ultrasound or colour flow; variation of the Doppler ultrasound frequency shift with the angle between the beam and direction of motion of the target, leading to a reduction in Doppler frequency shift as the angle approaches 90°. See 'cosine function', 'Doppler equation'.

Annular array Transducer consisting of several ring elements arranged concentrically.

Annular array scanner Mechanical scanner consisting of an annular array transducer. See 'annular array', 'mechanical scanner'.

Aperture Portion of the piezoelectric plate used to generate the current ultrasound beam; note the position of the aperture on the plate will change as different beams are formed; e.g. in a linear array the aperture is made up of a group of elements, with the elements forming the aperture changing in order to sweep the beam through the tissues. See 'piezoelectric plate'.

Apodization Technique used to improve beam formation and spatial resolution; by excitation of elements non-uniformly in transmission, and non-uniform amplification of received echo-signals in reception. See 'beam-former'.

Area Quantity representing the 2D size of an object or image; often measured using the calliper system for tissues imaged in cross section using an ultrasound system. See 'calliper system'.

ARFI See 'acoustic radiation force imaging'.

1D array Array consisting of a single line of elements (e.g. 128), allowing electronic focusing in the scan plane, with focusing in the elevation plane achieved through the use of an acoustic lens. See 'array'.

1.5D array Array consisting of several lines of elements arranged in a rectangular grid (e.g. 128 by 5), allowing electronic focusing in the scan plane, with some limited electronic focusing in the elevation plane in order to improve elevation resolution. See 'array'.

2D array Array consisting of a square of elements (e.g. 64 by 64), allowing electronic focusing and beam-steering in 3D. See 'array'.

Array Piezoelectric plate consisting of many elements; typically 128 for a 1D array, 192–640 for a 1.5D array and several thousand for a 2D array. See '1D array, '1.5D array, '2D array'.

Artefact Error in the displayed image or measurement, the source of the error arising from the patient, the ultrasound machine or the operator. In general artefacts arise when the assumptions used by the machine to create images or calculate quantities are not valid; e.g. 'mirror image artefact'. See 'error', 'measurements'.

Attenuation The loss of energy from an ultrasound wave as it propagates: lost energy may be absorbed and generate heat or may be scattered and generate new ultrasound waves. Attenuation is commonly given in a logarithmic scale in decibels (dB). It is the opposite of amplification. See 'absorption', 'attenuation coefficient'.

Attenuation artefact Increased or decreased brightness on the ultrasound image occurring when the attenuation in one part of the image does not match the assumed value set by the TGC control. See 'enhancement', 'TGC'.

Attenuation coefficient Quantity describing the attenuation of plane waves through tissue; unit is dB cm^{-1} MHz^{-1}; e.g. most soft tissues have values of attenuation coefficient in the range 0.3–1.0 dB cm^{-1} MHz^{-1}.

2D autocorrelation Relating to colour flow; improved autocorrelation method for estimation of mean Doppler frequency in which some account is taken of the variation in mean RF frequency of received echoes with position in the field of view. See 'autocorrelation'.

Autocorrelation Relating to colour flow; a method for estimation of mean Doppler frequency based on a small number (typically 3–20) of received echoes. See '2D autocorrelation', 'autocorrelator', 'colour flow'.

2D autocorrelator Relating to colour flow; improved autocorrelator for use in colour flow imaging, widely used in commercial scanners. See 'autocorrelator'.

Autocorrelator A device for use in colour flow systems which estimates the quantities displayed in the colour flow image; mean Doppler frequency, power, and variance. This device and modifications of the device are used as the basis for virtually all commercial colour flow systems. See ' 2D autocorrelator', 'colour flow', 'mean frequency (2)', 'power Doppler', 'variance'.

AVI (audio video interleave) File format used for digital video files.

Axial (1) Relating to the ultrasound beam; the direction along the beam axis.

Axial (2) Relating to blood flow; the direction along the vessel axis.

Axial resolution See 'spatial resolution'.

Azimuthal resolution See 'spatial resolution'.

B-flow B-mode-based method for visualization of blood flow, where the amplitude of blood flow signals is boosted by the use of coded pulse techniques. See 'colour B-flow', 'coded pulse'.

B-mode Ultrasound imaging mode in which the received echo amplitude is displayed in 2D, usually in greyscale; short for 'brightness mode'.

Backing layer A component of some ultrasound transducers, designed to damp motion of the element in order to prevent ringing, and to produce a short ultrasound pulse. See 'element', 'ringing', 'transducer'.

Backscatter The portion of a scattered or reflected ultrasound beam which travels in the direction back to the transducer; i.e. where the angle between incident waves and scattered/reflected waves is 180°.

Bandwidth The range of frequencies present within a signal, e.g. the bandwidth of a 6 MHz transducer is 4–8 MHz.

Baseline (1) Relating to Doppler spectral display or colour Doppler display where there are both positive and negative Doppler frequency shifts displayed; the line or marker indicating zero Doppler frequency shift. See 'colour Doppler', 'spectral Doppler'.

Baseline (2) Machine control enabling the operator to reallocate the displayed Doppler frequency shift range so that more or less is given to positive or negative Doppler shifts. See 'colour Doppler', 'spectral Doppler'.

Beam The region of space within the tissue which contributes to the formation of an ultrasound line; the beam is a composite of the 'transmit beam' and the 'receive beam', and may have a different shape for different modalities (B-mode, colour flow etc).

Beam axis Line from the transducer face passing through the middle of the beam at each depth.

Beam-steering Capability of an ultrasound system where the direction of the beam is able to be altered; required in e.g. phased array and mechanical transducers for collection of sector data, and linear arrays for collection of Doppler data from steered angles and for compound scanning. See 'Doppler ultrasound', 'compound scanning', 'mechanical scanner', 'phased array'.

Beam-steering angle Machine control enabling the operator to adjust the direction of the beam, in e.g. Doppler ultrasound.

Beam-steering array Transducer consisting of a phased array, in which the beam is steered through space by adjustment of delays to the elements. See 'phased array'.

Beam-stepping array Transducer consisting of a linear or curvilinear array, in which the beam is stepped along the face of the array by activation of different groups of elements. See 'curvilinear array', 'linear array'.

Beam–vessel angle Relating to spectral Doppler ultrasound; angle between the Doppler ultrasound

beam and the vessel wall; measured using the angle cursor. See 'angle cursor'.

Beam-width Dimensions of the beam in the lateral and elevation directions. See 'elevation plane', 'spatial resolution'.

Beam-former Part of the ultrasound system that deals with formation of the ultrasound beam. See 'transmit beam-former', 'receive beam-former'.

Beam-forming Formation of the ultrasound beam using the beam-former. See 'beam-former'.

Bifurcation A section of the arterial tree in which an artery has split into two sub-branches; e.g. common carotid divides into the internal carotid and external carotid.

Binary Generally: phenomena with two outcomes, '0' or '1', or 'true' or 'false'. In signal processing: relating to digital signals. See 'digital'.

Blood Fluid suspension of mainly red cells contained in the vascular system.

Blood flow Flow of blood, through the heart, arteries, veins or micro-circulation.

Blood mimic Suspension of particles in a fluid used in a flow phantom; the blood mimic may be designed to match the acoustic and viscous properties of human blood so that the spectral Doppler and colour flow signals produced are more realistic. See 'flow phantom'.

Blood-mimicking fluid (BMF) See 'blood mimic'.

Blood–tissue discriminator Component of the colour flow processor; which decides whether a pixel of the colour flow image is coded for tissue using the B-mode data or for blood flow using the colour flow data; in other words the unit attempts to put colour only in regions of true blood flow. See 'colour gain', 'colour-write priority'.

BMUS (British Medical Ultrasound Society) UK professional body which, amongst other things, issues guidance on the safe use of ultrasound. See 'BMUS guidelines'.

BMUS guidelines Set of guidelines issued by BMUS on the safe use of ultrasound.

Bolus Injection of a contrast agent in a short time. See 'infusion'.

Bone-at-focus thermal index (TIB) The thermal index calculated using a model which includes bone in the focal zone of the transducer. See 'thermal index'.

Bubble See 'microbubble'.

Bubble destruction The disruption of the microbubble shell when subject to an ultrasound beam.

Bubble population The group of microbubbles within a contrast agent solution.

Bulk modulus A measure of the ability of a material to withstand a change in pressure; equal to the change in pressure divided by the fractional change in volume; unit is pascals (Pa); e.g. the bulk modulus of most soft tissues is in the range 2–5 GPa.

C-scan Image plane parallel to the face of the transducer; may be obtained using 3D ultrasound. See '3D ultrasound'.

Calibration The act of checking or adjusting the accuracy of a machine which makes a measurement, usually performed with the use of phantoms. See 'phantom', 'quality control'.

Calliper system System of on-screen cursors for the measurement of distance, area and velocity; controlled by the operator allowing positioning of cursors or lines at specific points on the ultrasound image, with on-screen readout of the measured value.

Cathode ray tube display Image display monitor, not used in modern ultrasound systems. See 'flat-screen display'.

Cavitation A general term for the behaviour of gas cavities within a liquid when subjected to mechanical stress. The stress may be due to an acoustic wave (for example, ultrasound), the rapid movement of a surface (for example the propeller of a boat) or a decompression.

Ceramic Inorganic solid that may be manufactured with piezoelectric properties, for use in the manufacture of the piezoelectric plate of an ultrasound transducer. See 'piezoelectric plate'.

CFI Colour flow imaging. See 'colour flow'.

Charts Tables or graphs showing the variation of a quantity with time; e.g. abdominal circumference with gestational age.

Cine loop Series of ultrasound frames stored in memory, able to be replayed immediately after acquisition, and in most cases able to be stored in longer-term memory for archival purposes.

Circumference Distance around the edge of a 2D object or image; often measured using the calliper system for an object imaged in cross section using an ultrasound system.

Clutter Relating to Doppler ultrasound detection of blood flow; ultrasound signals from tissue, with an amplitude typically 30–40 dB greater than that from blood. See 'clutter filter', 'wall filter'.

Clutter breakthrough Tissue motion giving rise to Doppler frequencies above the wall filter or clutter filter, resulting in their display as an artefact on spectral Doppler or colour flow, usually with complete loss of the true blood flow Doppler signal. See 'clutter', 'clutter filter', 'wall filter'.

Clutter filter Relating to Doppler ultrasound detection of blood flow; signal-processing step which attempts to remove the clutter signal, leaving behind the Doppler ultrasound signal from the moving blood. This term is usually reserved for colour flow. See 'colour flow', 'wall filter'.

Coded excitation Method for improving the penetration depth, but without loss of spatial resolution, by the use of ultrasound pulses which are longer, and have embedded within them a short code of zeroes and ones. The received echo(es) are compared against a decoding filter. This may involve a single ultrasound pulse or pairs of pulses. See 'matched filter', 'Golay pair'.

Coded pulse techniques See 'coded excitation'.

Colour B-flow Adaptation of the B-flow technique in which two pairs of coded pulses are used to obtain a rough indication of velocity of blood which is then used to colour code the B-flow image. See 'B-flow'.

Colour blooming artefact In this artefact, the colour Doppler signal (colour) extends beyond the boundaries of the imaged vessel. This artefact is commonly seen in vessels as contrast enters the vessels. It can generally be corrected by reducing the colour gain. See 'colour flow', 'contrast imaging'.

Colour box 2D region superimposed on the B-mode image within which a colour-coded flow image is visualized. See 'colour flow'.

Colour Doppler 2D imaging of blood flow where the mean Doppler frequency shift is displayed (i.e. imaging of blood velocity). See 'power Doppler'.

Colour flow General term describing a range of techniques which are used for 2D imaging of blood flow using methods based on the Doppler equation. See 'colour Doppler', 'power Doppler', 'directional power Doppler'.

Colour flow signal processor Part of an ultrasound system which processes the ultrasound signals when the machine is used in colour flow mode. See 'colour flow'.

Colour gain Relating to colour flow; machine control enabling the operator to adjust the Doppler amplitude threshold above which colour is displayed. See 'blood–tissue discriminator'.

Colour speckle Variations in the received Doppler signal, arising as a result of changes in the number and relative orientation of red cells within the sample volume, which give rise to noise on the colour flow image. See 'speckle'.

Colour-write priority Relating to colour flow; machine control enabling the operator to adjust the B-mode echo amplitude threshold, above which colour is not displayed and below which colour data are displayed. See 'blood–tissue discriminator'.

Compound error Relating to the calculation of a quantity from two or more other quantities; where the final error is a combination of errors from the other quantities. See 'error (2)'.

Compound scanning Scanning in which images are acquired with ultrasound beams from several (e.g. 5–9) different directions, reducing speckle and improving image appearance through reduction in the directional nature of the image.

Compression (1) Regions in which the local volume of tissues decreases due to locally increased pressure; in the context of a wave, the high-pressure part of the wave.

Compression (2) Reduction in the dynamic range of received signals through the use of a non-linear amplifier (in which smaller signals are boosted in size). See 'dynamic range'.

Compressional wave A name for a sound or ultrasound wave characterized by local changes in density arising through local changes in pressure. See 'sound wave', 'ultrasound'.

Constructive interference The combination of two waves which are in phase at a specific time and location, with the crest of one wave coinciding with the crest of the other wave, resulting in doubling of the net amplitude. See 'destructive interference', 'in phase'.

Continuous-wave (CW) Doppler Referring to a Doppler ultrasound system in which ultrasound is transmitted continuously; therefore requiring separate element(s) to receive the return echoes.

Continuous-wave (CW) Doppler signal processor Part of the machine which processes the ultrasound signals when the machine is used in CW Doppler ultrasound mode.

Continuous-wave duplex system Component of an ultrasound system, consisting of a combination

of a B-mode imaging system and a continuous-wave spectral Doppler system; mainly used in cardiology for the measurement of high-velocity intra-cardiac blood-flow jets. See 'duplex system'.

Continuous-wave (CW) ultrasound An ultrasound system in which ultrasound is generated (and received) continuously by the transducer. See 'continuous-wave (CW) Doppler'.

Contrast (1) Fractional difference in image values for two image regions, e.g. organ tissue and tumour; in general detection of lesions is easier when contrast is higher, and very difficult when there is no contrast.

Contrast (2) Relating to contrast agents. See 'contrast agent'.

Contrast agent A substance which is administered, typically intravenously, to enhance differentiation between tissues and to visualize blood flow for diagnostic purposes. See 'contrast imaging', 'microbubble'.

Contrast-specific imaging Imaging techniques developed to improve the detection of ultrasound contrast agents for the purposes of improved clinical diagnosis. See 'amplitude modulation', 'flash imaging', 'harmonic imaging', 'intermittent imaging', 'non-linear imaging', 'pulse-inversion imaging', 'second-harmonic imaging'.

Contrast-to-tissue signal ratio Ratio of the backscattered signal from a contrast agent to the backscattered signal from tissue. See 'backscatter'.

Cosine function Mathematical function whose value is dependent on the angle, varying from 1 at an angle of 0°, to 0 at angle of 90°, to −1 at an angle of 180°. See 'angle dependence', 'Doppler equation', 'sine function'.

Cosine wave Same as sine wave, but shifted by half a wavelength (or by a phase of 180°). See 'sine wave'.

Cranial (orbone-at-surface) thermal index (TIC) The thermal index calculated using a model in which bone lies at the surface. See 'thermal index'.

Cross-correlation Method for estimation of displacement from ultrasound A-lines, used in strain elastography. See 'strain elastography', 'acoustic radiation force imaging'.

Curvilinear array Array transducer in which the array is curved in order to generate a diverging field of view. See 'array'.

Curvilinear format Arrangement of scan lines from a curvilinear array, in which the scan lines diverge with distance from the transducer producing a wider field of view with depth. See 'curvilinear array'.

Cut-off filter See 'wall filter'.

Cut-off frequency Value of the wall-filter in Hz. See 'wall filter'.

CW See 'continuous-wave ultrasound'.

Decibel The scale used to measure, for example, the change in ultrasound wave intensity; calculated as the logarithmic ratio of one intensity to another; e.g. the acoustic intensity decreases by 1 dB if an ultrasound beam passes through 2 cm of tissue that has an attenuation coefficient of 0.5 dB cm^{-1}.

Delay line Analogue method for delaying an electrical signal; used in analogue beam-formers, but mostly not used in modern ultrasound systems with digital beam-forming. See 'digital beam-former'.

Demodulation Part of the signal processing which is performed on the received ultrasound signal, where the underlying RF signal is removed (i.e. removal of the modulating signal). See 'amplitude demodulation', 'Doppler demodulation'.

Demodulator Part of the ultrasound system which performs demodulation. See 'demodulation'.

Density Mass of a material or tissue per unit volume, unit is kg m^{-3}; e.g. the density of most soft tissues is in the range 1040–1060 kg m^{-3}.

Depth of field Maximum depth within tissue for which ultrasound is displayed on the screen of the ultrasound system. See 'field of view'.

Derating A standard means for compensating for attenuation, used to estimate in situ exposure. A common derating model for soft tissues is a homogeneous medium having an attenuation coefficient of 0.3 dB cm^{-1} MHz^{-1}.

Destructive interference The combination of two waves which are out of phase at a specific time and location, with the crest of one wave coinciding with the trough of the other wave, resulting in zero net amplitude. See 'constructive interference', 'out of phase'.

Diameter Distance from one side to the other of a (roughly) circular structure, such as an artery in cross section.

DICOM (Digital Imaging and Communications in Medicine) Standard for storing and transmitting images, including specification of a file format. See 'picture archiving and communication system'.

Diffraction Change in the direction of a wave as it passes through an opening or around a barrier.

Diffuse reflection Similar to 'reflection', but occurs when the interface dimensions are comparable to the wavelength, resulting in strong reflections over a narrow range of angles. See 'reflection'.

Digital Description of electrical devices or electrical signals, in which the signals have two discrete voltage levels corresponding to '0' and '1'. See 'analogue'.

Digital beam-former Beam-former which processes ultrasound signals which have been digitized. See 'beam-former'.

Digital zoom Relating to ultrasound images which are stored in digital form; where the image is magnified on the screen by using a more limited part of the stored data. See 'write zoom'.

Digitization Conversion of analogue (continuously varying voltage) signals to digital (two discrete voltage levels corresponding to '0' and '1') signals, using an analogue-to-digital converter. See 'analogue', 'analogue-to-digital converter', 'digital'.

Directional power Doppler 2D imaging of blood flow where the power of the Doppler signal is displayed, colour-coded with the direction of blood flow. See 'colour Doppler', 'power Doppler'.

Display Monitor on which the ultrasound images are viewed by the operator. See 'liquid crystal display'.

Disturbed flow Relating to blood flow; where there are regions within a vessel or the heart in which there are periodic changes in the direction and magnitude of blood velocity, often appearing as local circulating flow called 'vortices', often seen immediately distal to a narrowing such as a stenosis. The vortices may be shed downstream where they die out after a few diameters. In clinical ultrasound there is generally no distinction made between disturbed flow and turbulence. It may lead to changes in the Doppler spectrum including spectral broadening and high-frequency spikes. See 'spectral broadening', 'turbulence', 'vortice'.

Doppler angle cursor See 'angle cursor'.

Doppler aperture Portion of the piezoelectric plate used to generate and receive the Doppler beam. See 'aperture'.

Doppler beam The region of space within the tissue from which the Doppler signal can arise. See 'sample volume'.

Doppler demodulation Method used in pulsed Doppler systems to remove the high-frequency RF component of the received signal, leaving behind the Doppler shift frequencies. See 'demodulation'.

Doppler equation Equation describing the relationship between the Doppler shift frequency, the target velocity and the direction of motion of the blood or tissue. See 'Doppler ultrasound (1) and (2)'.

Doppler gain Machine control enabling the operator to alter the amplification of the Doppler ultrasound signals, resulting in increase or decrease of brightness of the spectral Doppler display. See 'spectral display'.

Doppler shift Difference in ultrasound frequency between that of the transmitted ultrasound and the received ultrasound; e.g. the typical maximum Doppler shift from a healthy femoral artery is 2–4 kHz. See 'Doppler equation'.

Doppler signal processor Part of the ultrasound machine whose input is the RF signal from the Doppler beam, and whose output is the estimated Doppler signal; note that there are separate processors for spectral Doppler and for colour flow. see 'colour flow', 'spectral Doppler'.

Doppler speckle Variations in the received Doppler signal amplitude, arising as a result of changes in the number and relative orientation of red cells within the sample volume, which give rise to noise on the Doppler spectral data. See 'speckle'.

Doppler tissue imaging (DTI) Doppler-based ultrasound imaging method which provides 2D display of the velocities and other derived indices (e.g. strain) within moving tissue; mostly used in cardiac imaging.

Doppler tissue signal processor Part of the machine which processes the ultrasound signals when the machine is used in Doppler tissue imaging mode. See 'Doppler tissue imaging'.

Doppler ultrasound (1) Ultrasound which has been frequency-shifted as a result of scattering from a moving target. See 'Doppler equation'.

Doppler ultrasound (2) General term used to describe ultrasound systems whose design is based on use of the Doppler equation. see 'Doppler equation'.

Drop-out Relating to colour flow images; loss of colour due to the variable nature of the calculated mean frequency or power. Occurs when an incorrectly low value of mean Doppler frequency or power is estimated, which is below the threshold value used in the blood–tissue discriminator; is most marked at low velocities and in small vessels.

DTI See 'Doppler tissue imaging'.

Duplex system Ultrasound system, or component of an ultrasound system, consisting of a combination of a B-mode imaging system and a pulsed-wave spectral Doppler system. See 'continuous-wave duplex system'.

Dynamic elastography See 'shear-wave elastography'.

Dynamic focussing Progressive shift in the focal depth during receive mode, in order to produce best spatial resolution as a function of depth.

Dynamic range Ratio of largest to smallest signal that the ultrasound system is capable of processing; this will be less than the range of received echoes so these must be compressed. See 'compression (2)'.

Echo (1) Generally, following an initial sound, a delayed sound arriving back at the source, after reflection from an object.

Echo (2) In pulsed ultrasound; the ultrasound signal detected by the transducer consisting of reflections and scattering from tissues along the line of the beam.

Echo-ranging Method used to measure the depth of water beneath a boat, by timing a short burst of ultrasound from transmission to reception; see 'pulse–echo'.

ECMUS European Committee for Medical Ultrasound Safety.

Edge enhancement Image-processing method that accentuates the appearance of edges, usually at the expense of increase in the noise level. See 'image processing'.

Edge shadowing artefact Shadow commonly seen below the edges of cystic structure, occurring as a result of refraction.

EFSUMB European Federation for Societies of Ultrasound in Medicine and Biology.

Elastic Behaviour of a material which stretches or deforms in response to an applied force, returning immediately to its resting state when the force is removed. See 'elastic modulus', 'viscoelastic'.

Elastic modulus Property of an elastic tissue which describes its response to a deformation; a quantity describing the change in dimensions (strain) that occurs due to an applied force (stress); units are pascals (Pa). See 'bulk modulus', 'elastic', 'shear modulus', 'Young's modulus'.

Elastography Ultrasound techniques that provide information related to the stiffness of tissues. See 'shear-wave elastography', 'strain elastography'.

Electromagnetic tracking system See 'magnetic tracking system'.

Electronic beam-forming Formation of the beam by a transducer consisting of elements in which there is control of the timing and amplitude of the excitation voltage applied to each element during transmission, and of the delays and amplification of the voltages applied to each element during reception. This is used as the basis for beam-forming in modern ultrasound systems. See 'beam-forming', 'digital beam-forming'.

Electronic focusing Focusing of the beam using electronic beam-forming. See 'electronic beam-forming'.

Electronic noise Random noise produced from the ultrasound system, which is displayed when the gain is set too high, or when there is no ultrasound signal in deep tissues to which the ultrasound beam cannot penetrate. In B-mode and spectral Doppler the noise appears as a random greyscale pattern which changes rapidly with time. In colour Doppler the noise results in random estimates of mean frequency shift which appear as a mosaic of colours which change rapidly with time.

Element A part of the transducer which converts electrical energy into sound waves and vice versa; there may be one element (in a single-element transducer) or, more commonly in modern transducers, there are many elements (in phased and linear arrays). See 'piezoelectric plate', 'transducer'.

Elevation Relating to an ultrasound beam; the direction which is perpendicular to the 2D scan plane. See 'axial', 'lateral'.

Elevation plane The plane perpendicular to the scan plane for a 2D ultrasound system. See 'scan plane'.

Elevation resolution See 'spatial resolution'.

3D endoprobe Endoprobe which has the capability of collecting 3D data, e.g. by mechanical retraction of the transducer within the endoprobe housing.

Endoprobe Transducer designed for insertion into a body cavity or surgical wound.

Endoprobe 3D ultrasound system 3D ultrasound imaging system based on the use of a 3D endoprobe. See '3D endoprobe'.

Enhancement Increased brightness seen in B-mode imaging below a cystic structure. The TGC control default position assumes uniform attenuation with depth. The attenuation within the cyst is much lower

than the machine expects, resulting in a brighter area displayed below the cyst.

Epidemiology The study of the distribution and occurrence of disease, typically based on statistical analyses of large population samples.

Error (1) Generally in life and in ultrasound: a mistake, a condition of non-functioning, a situation where the expected outcome is not obtained, an artefact. See 'artefact'.

Error (2) Relating to the measurement of quantities such as distance, area, volume, velocity; the difference between the true value of the quantity and that measured. See 'measurements', 'random error', 'systematic error'.

Exposure levels A description of the ultrasound field under standard conditions, typically in water or estimated in situ, such as rarefaction pressure, acoustic intensity and acoustic power.

Extracorporeal lithotripsy A therapeutic ultrasound method which uses high-amplitude acoustic shocks to cause destruction of renal calculi.

Far-field Term applied to the acoustic field from a transducer consisting of a plane disc for distances beyond which destructive interference does not occur; old term not that useful for understanding the beams formed by modern multi-element imaging systems. See 'near-field'.

Fast Fourier transform (FFT) Computationally efficient version of the Fourier transform, especially suited for implementation in hardware or software. See 'Fourier transform'.

FDA The Food and Drug Administration; the agency in the USA with responsibility for licensing the manufacture and sale of ultrasound scanners.

Field of view Depth and width of the displayed ultrasound image. See 'depth of field'.

Filament Component of a string phantom, where the movement of the filament gives rise to the Doppler signals, simulating those produced from blood. See 'O-ring rubber', 'string phantom'.

Filter See 'wall filter'.

Filter value See 'wall filter value'.

Flash artefact Relating to colour flow systems; generation of colour within the tissue as a result of movement of the transducer or patient.

Flash filter Component of the colour flow signal processor which suppresses flash artefacts. See 'flash artefact'.

Flash imaging Contrast-imaging technique in which a low mechanical index (MI) pulse is used to image the contrast agent wash-in to a region of interest. By emitting a high-MI pulse, the microbubbles in the region collapse, releasing free gas which gives an enhanced backscattered signal. When imaging the enhanced signal from collapsing microbubbles is seen as a bright flash on the monitor, hence the term 'flash' imaging.

Flash pulse A high-MI pulse (or several pulses) which destroys the contrast microbubbles in the scan plane. See 'contrast-specific imaging'.

Flat-screen display Image display monitor, which is used as standard on modern ultrasound systems, which is very thin compared to older cathode ray tubes. See 'liquid crystal display'.

Flow Movement of a fluid such as blood.

Flow phantom Device used to test spectral Doppler and colour flow systems, in which the flow of blood in an artery is mimicked by the flow of a fluid in a vessel commonly embedded in tissue mimic. See 'blood mimic', 'tissue-mimicking material'.

Flow rate Volume of a fluid passing through a vessel or region per unit time; units are $L\ s^{-1}$, or $mL\ s^{-1}$; e.g. the average flow rate in the common carotid artery in adults is about $6\ mL\ s^{-1}$.

Flow rate (of blood in an artery) Quantity which may be measured using an ultrasound system; e.g. using a combination of mean velocity obtained from Doppler ultrasound data (usually the time-averaged maximum velocity) and the diameter obtained from the B-mode image. See 'diameter', 'time-average velocity (TAV)'.

Fluorocarbon (also known as perfluorcarbons) The gas which is generally found within commercially available contrast agents. Fluorocarbons have very low water-solubility compared to air, thus delaying bubble dissolution. See 'gas', 'microbubble'.

Focal depth (1) Distance from the transducer where the spatial resolution of a beam has its minimum value. See 'spatial resolution'.

Focal depth (2) Machine control allowing the operator to adjust the position of the beam focus.

Focus Position in an ultrasound beam where the spatial resolution has its minimum value.

Forward flow Relating to blood flow in arteries; flow in the direction away the heart, the dominant situation for flow in arteries. See 'reverse flow'.

Fourier transform Method for estimating the frequency components within a signal. See 'fast Fourier transform'.

Frame averaging A processing feature relevant to the displayed image, in which the displayed image is a weighted average of the current image and several previous images; used for the purposes of noise reduction, but also results in blurring of objects which are moving rapidly.

Frame rate Number of ultrasound image frames acquired per second.

Free gas The gas released from a contrast microbubble after the shell has been compromised. The gas which escapes is no longer surrounded by shell. See 'gas', 'microbubble'.

Free radical A chemical species that is highly reactive.

Freehand 3D ultrasound system System for acquiring 3D ultrasound data, based on acquisition of 2D images while the probe is moved by hand. See 'optical tracking system', 'magnetic tracking system', '3D endoprobe', 'mechanically steered array'.

Freehand ultrasound Movement of the ultrasound transducer by hand, as opposed to movement by a mechanical system; the basis for virtually all modern ultrasound scanning.

Freeze Machine control which results in suspension of real-time imaging with the last acquired frame displayed on the screen.

Frequency Property of a wave; the number of oscillations passing a given point per second; unit is hertz or Hz; e.g. ultrasound transducers typically have frequencies between 1 and 18 MHz.

Fundamental imaging Conventional B-mode imaging in which the ultrasound beam is transmitted and received over the same frequency bandwidth (frequency range) to form the B-mode image. See 'harmonic imaging'.

Gain Machine control enabling the operator to alter the amplification of the received ultrasound signals, resulting in increase or decrease of brightness on the display.

Gamma curve Relationship between the image value and displayed grey level; a smooth curve which is described by a specific function ($V_{out} = V_{in}\gamma$) with a single variable γ. Adjustment of γ can be used to change the grey-level appearance. See 'grey-level curve'.

Gas Material encapsulated by the shell within microbubbles; the gas can be air or a heavier gas such as fluorocarbon. See 'fluorocarbon', 'free gas', 'microbubble'.

Gas body A general term used to represent any collection of gas or vapour. Gas bodies are designed and manufactured to be the active ingredient of ultrasound contrast agents. See 'gas'.

Gas body activation The interaction of acoustic waves with gas bodies. Applied, especially, to non-inertial cavitation involving gas bodies in biological systems.

Gate Range of depths from which Doppler signals are obtained using pulsed-wave Doppler. See 'sample volume'.

Gate position Relating to Doppler spectral display; machine control enabling the operator to adjust the depth of the region from which Doppler signals are acquired. See 'gate size'.

Gate size Relating to Doppler spectral display; machine control enabling the operator to adjust the length of the region from which Doppler signals are acquired. See 'gate position'.

Geometric spectral broadening Relating to spectral Doppler, where a target with a single velocity will give rise to a range of Doppler frequency shifts due to the finite size of the Doppler aperture. Ultrasound is received from the target with a range of angles; commonly resulting in overestimation of maximum blood velocity. See 'intrinsic spectral broadening'.

Gigapascal (GPa) The unit of measurement commonly used for elastic modulus in hard tissues such as bone and tooth enamel, equivalent to 10^9 pascal. See 'elastic modulus'.

Golay pair In coded excitation, a pair of ultrasound pulses whose codes are designed to eliminate range artefacts when the received echoes are detected, filtered and combined. See 'coded excitation', 'range artefact'.

Grating lobe Weaker beams, produced by linear arrays on either side of the main lobe, giving rise to reduction in image contrast and other artefacts.

Grey-level curve Relationship between the image pixel value and the displayed grey level. See 'gamma curve'.

Harmonic Additional frequencies, usually multiples of the base frequency F_o, e.g. $2F_o$, $3F_o$, $4F_o$; in ultrasound

the received echo may contain harmonics arising from non-linear effects within the tissue, especially during imaging of contrast agents. See 'contrast agent', 'harmonic imaging'.

Harmonic imaging Mode of ultrasound imaging in which the receive beam-former is adjusted to receive harmonics of the transmit frequency, usually for the purpose of improved image contrast. See 'harmonic'.

Hazard Any actual or potential source of harm.

Hertz (Hz) Unit of frequency. See 'frequency'.

High-frame-rate imaging Ultrasound imaging in which beam-forming produces higher than usual frame rates (up to several thousand Hz), usually with sacrifice of field of view and/or image quality. See 'plane-wave imaging', 'synthetic-aperture imaging'.

High-MI techniques Contrast-specific imaging techniques which rely upon the destruction of microbubbles within the scan plane. See 'contrast-specific imaging'.

High-pass filter See 'wall filter'.

Human error Relating to the measurement of a quantity (e.g. distance, volume); where part of the error arises from variations from one time to another by the operator.

IEC (International Electrotechnical Commission) An international body with responsibility to set technical and safety standards for the manufacture of goods, including medical ultrasound equipment. See 'standards'.

Image processing Changes made to an image in order to improve its appearance and to help improve the detection of abnormalities. See 'noise reduction', 'edge enhancement', 'adaptive image processing'.

In phase Relating to two waves of the same frequency, for which wave peaks occur at the same time or distance (phase difference = 0°). See 'out of phase'.

Incompressible Material or tissue whose density does not change when compressed. See 'shear wave', 'pressure wave', 'bulk modulus', 'shear modulus', 'Young's modulus'.

Inertial cavitation The class of acoustic cavitation for which a bubble undergoes very large cyclic changes in volume, dominated by the inertia of the surrounding liquid, and associated with very high transient internal temperatures and pressures. It commonly results in bubble instability and violent collapse.

Infusion Method for injecting contrast agents at a set rate, over time, usually by means of an infusion pump. See 'bolus'.

Insonation Application of ultrasound to a region of tissue.

Intensity The power (e.g. of an ultrasound wave) flowing through unit area; unit is W cm^{-2}; e.g. the intensity (spatial peak pulse average) for B- and M-mode imaging is in the range 14–933 W cm^{-2}. See 'I_{sppa}', 'I_{spta}'.

Interference The combination of two or more waves, with the amplitude at any one position and time being the combination of the amplitudes from each of the individual waves. See 'destructive interference', 'constructive interference'.

Intermittent imaging Contrast-specific imaging technique for imaging contrast agents over a pre-defined time sequence or triggered from an ECG. See 'contrast-specific imaging'.

Intravascular ultrasound (IVUS) Imaging of arteries or the heart using a transducer which is located within the artery or heart, where the transducer is attached to a catheter which is fed into the artery via an arterial puncture, usually of the femoral artery.

Intrinsic spectral broadening Relating to spectral Doppler, where a target with a single velocity will give rise to a range of Doppler frequency shifts; due to the characteristics of the scanner rather than the blood flow. The dominant cause is geometric spectral broadening. See 'geometric spectral broadening'.

Invert Machine control enabling the operator to turn the display upside down (for spectral Doppler), and to reallocate the colour scale (for colour Doppler), e.g. red to blue.

Inverted mirror-image artefact Relating to spectral Doppler, where the true Doppler waveform appears inverted in the opposite channel, occurring when the Doppler gain is set too high.

IPEM (Institute of Physics and Engineering in Medicine) UK professional body which produces (amongst other things) guidance on quality assurance of ultrasound systems.

I_{sppa} Spatial peak pulse average intensity. See 'intensity'.

I_{spta} Spatial peak temporal average intensity. See 'intensity'.

JPEG File format used for single-image digital files.

Kilopascal (kPa) The unit of measurement commonly used for elastic modulus in soft tissues such as muscle and liver, equivalent to 10^3 pascal. See 'elastic modulus'.

Laminar flow Relating to blood flow; where at low velocities fluid elements follow well-defined paths with little mixing between adjacent layers. See 'disturbed flow', 'turbulence'.

Lateral Relating to an ultrasound beam; the direction within the 2D scan plane which is perpendicular to the beam axis. See 'axial (1)', 'elevation'.

Lateral resolution See 'spatial resolution'.

LCD See 'liquid crystal display'.

LED See 'light-emitting diode'.

Light-emitting diode A device for producing light or infra-red radiation; used in optical tracking systems for freehand 3D ultrasound. See 'optical tracking system'.

Line Portion of the ultrasound image along a single direction radiating from the transducer, corresponding to ultrasound information acquired from a single beam, also known as 'scan line'.

Line density Number of scan lines per unit distance of the transducer for a 2D ultrasound system, or number of scan lines per unit area of a 2D array transducer.

Linear array Transducer consisting of many (128–256) elements arranged in a line, enabling electronic beam-forming. There is some beam-steering capability (typically 20–30°), sufficient to enable image compounding and production of steered Doppler beams. See 'array', ' 1D array', '1.5D array'.

Linear format Relating to an ultrasound image, in which the scan lines are parallel and directed vertically down from the transducer (usually a linear array).

Liquid crystal display Widely used image-display device, which uses liquid crystal technology.

Lithotripsy See 'extracorporeal lithotripsy'.

Longitudinal wave Wave, such as ultrasound or sound, in which the direction of motion of the local particles is in the same direction as that of the wave. See 'transverse wave'.

Low-MI techniques Contrast-specific imaging techniques which rely upon the non-destruction of microbubbles. See 'contrast-specific imaging'.

M-mode Ultrasound mode in which A-line data are displayed as a function of time. Useful for accurate measurement of the change in the dimensions of moving structures, e.g. in the heart.

Mach cone Expanding shear wave produced by a supersonic source. See 'supersonic imaging'.

Magnetic tracking system Device for tracking the position and orientation in space of a transducer, e.g. using a small transmit device to generate a 3D magnetic field within which ultrasound scanning takes place, and sensor coil attached to the transducer which sends electrical signals to a receiver; used in freehand 3D ultrasound. See 'freehand 3D ultrasound'.

Main lobe Relating to the detailed distribution of ultrasound energy from the transducer which has high intensity in several specific directions, called lobes. The main lobe corresponds to the direction intended to have the highest intensity, and is another name for the ultrasound beam. See 'side lobe'.

Matched filter In coded excitation; design of the decoding filter which results in compression of the energy of the received echo into a signal with maximum signal-to-noise ratio. See 'coded excitation'.

Matching layer A component of most ultrasound transducers, designed to maximize the transmission of acoustic energy into the tissues; achieved by suitable choice of acoustic impedance.

Matrix array See '2D array'.

Maximum (Doppler) frequency Peak value of the Doppler frequency at any one time; see 'maximum frequency waveform'.

Maximum frequency envelope See 'maximum frequency waveform'.

Maximum frequency waveform Maximum Doppler shift versus time waveform derived from the Doppler spectral waveform; used in estimation of some waveform indices; usually acquired in stand-alone Doppler systems where the beam–vessel angle is unknown. See 'pulsatility index', 'resistance index'.

Maximum velocity waveform Maximum velocity versus time waveform; identical in shape to the maximum frequency envelope but has units of velocity; used in estimation of some waveform indices; acquired using duplex systems where the beam–vessel angle can be measured. See 'resistance index', 'pulsatility index', 'flow rate'.

MDD The European Medical Devices Directive, which sets conditions for the manufacture and sale of

medical equipment, including ultrasound scanners, for the European Community.

Mean Doppler frequency See 'mean frequency (1) and (2)'.

Mean frequency (1) Average value of the detected Doppler frequencies at any one time.

Mean frequency (2) One of the values which is produced from autocorrelator-based frequency estimators of colour flow systems, equal to the mean Doppler frequency. See 'variance', 'power (2)'.

Mean frequency waveform Waveform of mean Doppler frequency versus time. May be used to estimate waveform indices, but this is generally not advised as the mean Doppler frequency is prone to error. See 'maximum frequency envelope', 'maximum velocity waveform'.

Measurements Values of specific indices or quantities measured using the ultrasound system (see 'distance', 'area', 'volume', 'velocity', 'volumetric flow', 'resistance index', 'elastic modulus') or relevant to the performance of the ultrasound system (see 'spatial resolution', 'mechanical index', 'thermal index', 'intensity', 'power (1)').

Mechanical index (MI) An indicator calculated from the ratio between the peak rarefactional pressure (MPa) and the square root of acoustic frequency (MHz). MI may be used as a general indicator of the behaviour of ultrasound contrast agents when exposed to ultrasound.

Mechanical scanner Ultrasound system in which the beam is swept through the tissues by mechanical movement of the element(s).

Mechanical wave Wave that requires a medium such as tissue for propagation; examples include shear waves, sound and ultrasound. See 'shear wave', 'sound wave', 'ultrasound'.

Mechanically steered array Transducer used for 3D imaging which consists of a curvilinear or linear array located within a fluid-filled housing, where the array is swept to and fro mechanically, hence sweeping the scan plane through the tissue to collect a series of 3D volumes. See 'Mechanically steered array 3D ultrasound system'.

Mechanically steered array 3D ultrasound system System for 3D ultrasound in which 3D data are collected using a mechanically steered array transducer. See 'mechanically steered array'.

Megahertz (MHz) The unit of measurement commonly used for ultrasound frequency, equivalent to 10^6 hertz.

Megapascal (MPa) The unit of measurement commonly used for acoustic pressure and related quantities such as elastic modulus, equivalent to 10^6 pascal. See 'elastic modulus', 'pressure'.

Memory General: an area of the computer used to store information. Medical ultrasound: an area of the computer used to store ultrasound images.

MI See 'mechanical index'.

Microbubble The most common configuration of contrast agents, in which a small gaseous bubble is encapsulated by a thin shell. Usually between 2 and 10 μm in diameter and used to enhance contrast in ultrasound imaging. See 'contrast agent'.

Mirror-image artefact Appearance of a second version of a region of tissue where there is a strong reflector present; scattered echoes in front of the interface are received in the normal manner, and also via the interface, resulting in their display below the interface.

Misregistration Relating to 2D or 3D images; positioning of ultrasound data (B-mode, colour flow, etc.) at an incorrect location within the displayed image. Usually occurring as a result of speed-of-sound artefacts. See 'multiple scattering artefact', 'refraction artefact', 'range error', 'speed-of-sound artefacts'.

Mixing Relating to processing of the ultrasound signal; where one signal is combined with a second reference signal, to produce a composite signal with a low-frequency component and a high-frequency component which can be removed by high-pass filtering. See 'Doppler demodulation'.

Modulus See 'elastic modulus'.

MPEG File format used for digital video files.

Multi-path artefact See 'mirror-image artefact'.

Multiple-beam acquisition Technique to increase the frame rate by the simultaneous acquisition of several (e.g. four) receive beams for each broadened transmit beam. See 'high-frame-rate imaging'.

Multiple scattering artefact Related to contrast agents; the ultrasound beam can be scattered from many microbubbles as it travels through a region of interest. This means that it will take longer to be detected and the ultrasound scanner will place the echoes deeper than their source because of the delay in detecting. See 'misregistration'.

Multiple-zone focusing Method to improve the transmit beam formation and spatial resolution; by dividing the field of view into several depth regions (zones) each acquired sequentially using a separate ultrasound pulse, with each transmit pulse focused for each zone. A consequence of this method is a reduction in frame rate.

Near-field Term applied to the acoustic field from a plane disc, for distances up to which destructive interference does occur; old term not that useful for understanding the beams formed by modern multi-element imaging systems. See 'far-field'.

NEMA The National Electrical Manufacturers Association in the USA.

Noise Generally, any feature of the image which is unwanted which obscures the feature of interest. The dominant noise in ultrasound imaging is speckle and electronic noise, and also clutter breakthrough for Doppler and colour flow. See 'Doppler speckle', 'colour speckle', 'electronic noise', 'clutter breakthrough'.

Noise reduction Image-processing method which reduces the noise in an image, usually at the expense of some loss of spatial resolution. See 'frame averaging', 'image processing'.

Non-inertial cavitation A class of acoustic cavitation associated with low acoustic pressures, characterized by small-scale stable bubble oscillations. Collapse of the bubble or gas body does not occur.

Non-linear distance Distance of a curved structure; e.g. crown–rump length.

Non-linear imaging A method of constructing images from non-linear signals detected from non-linear scatterers. Useful for imaging at depth and contrast agents. See 'contrast-specific imaging'.

Non-linear propagation Movement of waves through a tissue characterized by changes in the ultrasound pulse shape with time due to different parts of the pulse travelling at different speeds, resulting in a steepening of the pulse with the generation of additional frequencies or harmonics.

Non-uniform insonation Relating to the insonation of blood flow in arteries; where the beam-width is less than the vessel diameter resulting in large parts of the vessel not being insonated.

NPL The National Physical Laboratory, Teddington, UK.

Nyquist limit Relating to estimation of frequency using regular sampling of the signal, where the upper limit of frequency estimation is half the sampling frequency. For Doppler ultrasound, see 'aliasing'.

O-ring rubber Filament used in a string phantom which gives Doppler signals similar to those from blood, as opposed to spiral-wound filaments such as cotton or silk which give preferential scattering at certain angles. See 'filament', 'string phantom'.

Optical tracking system Method for tracking the position and orientation in space of a transducer, e.g. using a pair of infra-red sensors to record the position of infra-red LEDS attached to the transducer; used in freehand 3D ultrasound. See 'freehand 3D ultrasound'.

Oscillation The sequence of expansion and contraction of the microbubble. See 'resonance'.

Out of phase Relating to two waves of the same frequency, where one wave is displaced by half a wavelength (phase difference = 180°). See 'in phase'.

Output Display Standard A document prepared by the AIUM and NEMA in the USA which defines the Safety Indices and their use. Now included in IEC Standard 60601–2–37.

Output power See 'power (1)'.

PACS See 'picture archiving and communication system'.

Parallel beam-forming See 'multi-beam acquisition'.

Partial volume effect Generally, change in the value or image display when the quantity being calculated does not occupy the entire pixel or voxel. In power Doppler, reduction in the displayed power near the edge of a vessel when the sample volume only partially covers the region of flowing blood.

Peak negative pressure See 'rarefaction pressure'.

Pencil probe Simple ultrasound transducer used for Doppler, with no imaging capability, usually consisting of one element (CW Doppler) or two elements (PW Doppler), about the size of a pencil.

Penetration Ability of an ultrasound system to visualize deep tissues. See 'penetration depth'.

Penetration depth Maximum depth at which ultrasound information can be obtained; may be different for each modality (B-mode, spectral Doppler, colour flow). See 'penetration'.

Perfluorcarbon See 'fluorocarbon'.

Perfusion Blood flow to organs and tissues. Perfusion is important as a means to limit temperature rise caused by the absorption of ultrasound.

Persistence See 'frame averaging'.

Petechiae Rounded spots of haemorrhage on a surface such as skin, mucous membrane, serous membrane or on a cross-sectional surface of an organ.

Phantom Construction or device for testing the properties of an ultrasound system; may attempt to mimic the acoustic properties of human tissue, and other properties, e.g. the viscous properties of blood in the case of the flow phantom. See 'tissue-mimicking', 'tissue-mimicking phantom', 'flow phantom', 'string phantom', 'thermal test object'.

Phase The position in time or distance for a single sinusoidal wavelength; mathematically expressed as an angle so that 0° is the start of the wave, 360° is the end of the wave. See 'in phase', 'out of phase'.

Phase aberration Changes in the shape of the wavefront from the transducer which occur as a result of non-uniformity of speed-of-sound values within the beam; typically occurring as the beam propagates through the subcutaneous fat layer resulting in defocusing of the beam and loss of spatial resolution.

Phase domain Relating to estimation of blood or tissue velocity, through manipulation of the phase of the detected ultrasound signals. See 'time domain'.

Phase-domain systems Relating to PW Doppler systems for measuring blood or tissue velocity, where the estimation of target velocity is undertaken using phase-domain techniques. See 'time-domain systems'.

Phase-inversion imaging See 'pulse-inversion imaging'.

Phased array Transducer consisting of many (128–256) elements arranged in a line, enabling electronic beam-forming to be performed. The elements are small, enabling considerable beam-steering and the production of sector images, mostly used in cardiology.

Picture archiving and communication system Network-based system which allows the transfer of images from several different types of medical imaging system to: workstations (for reporting, viewing and further processing), printers for hardcopy, and storage systems for data archival. See 'DICOM'.

Piezoceramic Ceramic material manufactured with piezoelectric properties, for use in the manufacture of the piezoelectric plate of an ultrasound transducer. See 'piezoelectric plate'.

Piezoelectric Property of a material, describing its ability to change its dimensions on the application of an electrical voltage, and vice versa, hence able to produce ultrasound waves when stimulated appropriately; the main physical phenomenon behind medical ultrasound imaging.

Piezoelectric plate Component of a transducer which converts the electrical voltage changes into an ultrasound signal, and vice versa; the most important component of the ultrasound system. See 'element', 'transducer'.

Pixel 'Picture element'; the smallest component of a digital image; typically rectangular, with typical ultrasound images consisting of 500 by 500 pixels.

Plane disc source Ultrasound transducer consisting of a single element, usually circular.

Plane wave Wave which propagates through space as a flat sheet. See 'spherical wave'.

Plane-wave imaging Ultrasound imaging technique in which all array elements are activated in transmission to produce a plane wave in order to insonate the whole field of view in one pulse, hence allowing very high-frame-rate imaging of several thousand frames per second; used to visualize the movement of shear waves in shear-wave elastography. See 'high-frame-rate imaging', 'shear-wave elastography'.

Plate See 'piezoelectric plate'.

PMN-PT Abbreviation for lead titanate doped with lead, magnesium and niobium; the material from which the piezoelectric plate of some (wideband) transducers is constructed. See 'piezoelectric plate'.

Point target In relation to spatial resolution measurement; target whose dimensions are much less than the spatial resolution.

Portable Able to be carried; usually a low-weight ultrasound system or phantom which can be easily carried by a typical operator.

Power (1) The amount of energy transferred per unit time; unit is watt (W) or Joules/second; e.g. typical B-mode imaging systems deliver an acoustic power of 0.3–285 mW.

Power (2) One of the values which is produced from autocorrelator-based frequency estimators of colour flow systems, related to the amplitude of the received Doppler signals. See 'variance', 'mean frequency (2)', 'power Doppler'.

Power Doppler 2D imaging of blood flow using the power of the Doppler signal. See 'power (2)', 'colour Doppler', 'directional power Doppler'.

Power modulation See 'amplitude modulation'.

Pre-amplifier Device(s) for increasing the amplitude of the electrical signal detected by the element(s)

from the received echoes in order to allow subsequent processing. See 'receiver'.

Pressure Force per unit area in a direction at 90° to the surface of an object; unit is pascal (Pa) or N m^{-2}; e.g. the peak rarefraction pressure for pulsed Doppler systems is in the range 0.6–5.3 Pa.

Pressure wave Wave, such as a sound wave or ultrasound wave, in which local pressure changes travel through a medium such as gas, liquid or solid; where the speed of propagation is controlled by the local density and the local bulk modulus. See 'compressional wave', 'longitudinal wave', 'bulk modulus'.

PRF See 'pulse repetition frequency'.

PRI See 'pulse repetition interval'.

Printer Hardcopy device connected to an ultrasound scanner, or more commonly part of a picture archiving and communication system. See 'picture archiving and communication system'.

Priority encoder See 'blood–tissue discriminator.

Propagation Movement of a wave through a medium or tissue.

Propagation artefact Transient, decreased brightness distal to contrast-filled regions due to attenuation of the contrast microbubbles within the scan plane. See 'contrast-specific imaging'.

Pulsatility index (PI) An index measured from the Doppler waveform, usually from the maximum frequency envelope, which provides information on the degree of diastolic flow. See 'resistance index'.

Pulse Ultrasound wave of short duration which, for the purposes of ultrasound imaging, is transmitted along a beam.

Pulse–echo Technique used in ultrasound imaging to provide information on the depth from which received echoes arise, involving timing the delay between transmission and reception, dividing by 2, and multiplying this by the assumed average velocity of 1540 m s^{-1}.

Pulse inversion amplitude modulation (PIAM) Relating to contrast agents. A combination of pulse inversion and amplitude modulation for imaging contrast agents. See 'amplitude modulation', 'pulse inversion'.

Pulse-inversion imaging Method for improving image quality which uses two consecutive pulse–echo lines, with the second pulse an inverse of the first. When received echoes are combined the harmonic content remains. Used in harmonic imaging and contrast imaging. See 'contrast-specific imaging', 'harmonic'.

Pulser Component of an ultrasound system which produces electrical signals at radiofrequencies (e.g. 10 MHz), where the signals are then modified by the transmit beam-former to produce the electrical pulses applied to the transducer for generation of the ultrasound beam. Note that there may be several pulsers to cover a range of ultrasound transmit frequencies.

Pulse repetition frequency (PRF) Number of ultrasound pulses transmitted per second; value will be different for each modality (B-mode, spectral Doppler, colour flow).

Pulse repetition interval (PRI) Time between consecutive transmitted pulses; the inverse of pulse repetition frequency. See 'pulse repetition frequency'.

Pulsed-wave (PW) Doppler Doppler ultrasound technique in which ultrasound pulses are used, as opposed to a continuous-wave technique. See 'spectral Doppler', 'colour flow'.

Pulsed-wave (PW) Doppler signal processor Part of the machine which processes the ultrasound signals when the machine is used in PW Doppler ultrasound mode.

Pulsed-wave (PW) ultrasound An ultrasound system in which ultrasound is generated as pulses. See 'colour flow', 'pulse echo', 'pulsed-wave Doppler'.

Pushing beam In acoustic radiation force imaging, a high-output beam which is used to produce deformation of tissue at the focal region. See 'acoustic radiation force imaging'.

PW See 'pulsed-wave ultrasound'.

PZT Abbreviation for lead zirconate titanate; the material from which the piezoelectric plate of many transducers is constructed. See 'piezoelectric plate'.

PZN-PT Abbreviation for lead titanate doped with lead, zinc and niobium; the material from which the piezoelectric plate of some (wideband) transducers is constructed. See 'piezoelectric plate'.

Quality assurance General: set of actions whose aim is to produce items or service of a specified quality. In ultrasound: assessment of equipment performance using test objects to ensure compliance with relevant standards.

Quality control General: set of activities designed to evaluate a developed product. In ultrasound: often used interchangeably with quality assurance. See 'quality assurance'.

Radial format Arrangement in which scan lines are produced 360° around a central transducer; see 'intravascular ultrasound', 'endoprobe'.

Radiation force The force exerted on a medium by an ultrasound wave. Radiation force may be exerted on a surface, on an object such as a microbubble or throughout the medium. The radiation force acts in the direction of wave propagation.

Radiofrequency (RF) Frequency of received echoes once they have been converted into electrical signals; MHz electrical signals fall within the radio portion of the electromagnetic spectrum.

Random error Relating to measurement error (e.g. of distance, volume); where the error varies over a small range, with an average value of zero for the error when the measurement is repeated many times. See 'error (2)', 'measurement', 'systematic error'.

Range ambiguity Relating to spectral Doppler and colour flow systems, detection of received echoes from the previous (not the current) echo(es), resulting in the potential display of blood flow data from deep structures rather than from the intended location.

Range artefact In coded excitation; increase (worsening) of the axial resolution which may occur after decoding. See 'coded excitation', 'Golay code'.

Range error Errors in ultrasound imaging occurring as a result of incorrect assumption of the speed of sound. Occurs when the true speed of sound is not equal to 1540 m s^{-1}. Can result in information displayed at the incorrect depth, distortion of interfaces and errors in the measured size. See 'speed-of-sound artefact'.

Rarefaction Regions in which there is increased volume (decrease in density) due to decrease in local pressure; in the context of an ultrasound wave, the low-pressure part of the wave.

Rarefaction pressure The magnitude of the negative acoustic pressure in an ultrasound wave. In pulsed beams the value of peak rarefactional pressure, that is, the greatest negative value of the acoustic pressure, is often given. See 'rarefaction'.

Read zoom See 'digital zoom'.

Real time Occurring now, as in 'real-time ultrasound', which provides information with negligible delay between acquisition and visualization; as opposed to off-line imaging such as CT where the data are acquired then visualized with a delay of a few seconds or minutes.

Receive beam The region of space within the tissue from which ultrasound signals will contribute to the beam.

Receive beam-former Component of an ultrasound system that deals with formation of the receive beam; involving adjustments of amplitude of the signal and imposition of time delays from each element before combination. Details of beam-forming are usually different for each modality (B-mode, spectral Doppler, colour flow). See 'beam-former'.

Received ultrasound Ultrasound echoes received by the transducer.

Receiver Component of the ultrasound system which amplifies the detected RF signals from each of the individual elements (or groups of elements) of the transducer, to a level where they can be further processed. The output from the receiver is a series of analogue RF signals which (in modern systems) is usually digitized then passed to the beam-former.

Reception The process of detection of ultrasound echoes arriving at the face of the transducer, following transmission.

Rectification Process applied to ultrasound signals after conversion to electrical signals, in which the negative portion of the cycle is inverted, resulting in a signal with only positive components. See 'amplitude demodulation'.

Rectified diffusion A process which can cause bubbles to expand over time in an ultrasound field, by allowing greater inward diffusion when the bubble is large (in rarefaction) than outward diffusion when the bubble is small (in compression).

Reflection General: change in direction of a wave after it has encountered an interface (dimensions >> wavelength) between two materials with different impedance, with a portion of the wave returning to the medium from which it came. In medical ultrasound: change in direction of an ultrasound beam at the interface (dimensions >> wavelength) between tissues of different acoustic impedance, with a portion of the beam returning to the medium from which it came.

Reflection coefficient For a wave which is partially reflected; ratio of the pressure of the reflected to the incident wave; values vary between 0 and 1, with 0 indicating that no reflections will occur.

Refraction General: change in direction of a wave after it has encountered an interface between two materials with different wave speed, with the portion of the wave which has entered the second medium being shifted in

direction. In medical ultrasound: change in direction of an ultrasound beam after it has encountered an interface between two tissues with different sound speed, with the portion of the ultrasound beam which has entered the second medium being shifted in direction. See 'Snell's law'.

Refraction artefact Artefact occurring in ultrasound imaging as a result of refraction, where duplicates of parts of the image may appear adjacent to the true structure. See 'refraction'.

Registration Relating to 2D or 3D images, positioning of ultrasound data (B-mode, colour flow etc.) at the correct location within the displayed image. See 'misregistration', 'speed-of-sound artefacts', 'refraction artefact', 'range error'.

Resistance Relating to blood flow, the ratio of pressure drop to flow rate; a measure of the force needed to pump blood through arteries.

Resistance index (RI) An index measured from the Doppler waveform, usually from the maximum frequency envelope, which provides information on the degree of diastolic flow. See 'maximum frequency envelope', 'pulsatility index'.

Resolution See 'spatial resolution', 'temporal resolution', 'velocity resolution'.

Resonance The vibration of a system when subject to an oscillating force at a specific frequency which is at the resonance frequency of the object. See 'resonance frequency'.

Resonance frequency The frequency at which a material or structure naturally vibrates; e.g. when struck. See 'resonance'.

Reverberation Persistence of ultrasound in a spatial region due to ultrasound waves repeatedly travelling back and forth between two interfaces where there are large changes in acoustic impedance between the materials or tissues; examples include reverberation within the PZT plate of a transducer which has no backing layer, and between the front and back walls of a cyst. The effect of ultrasound persisting may be referred to as 'ringing'.

Reverberation artefact Generation of one or more additional copies of a structure at deeper depths, occurring as a result of reverberation between two almost parallel surfaces (e.g. anterior surface of the bladder and the surface of the transducer).

Reverse flow Relating to blood flow in arteries; flow in the direction towards the heart, a normal occurrence in healthy peripheral arteries for a part of the cardiac cycle. See 'forward flow'.

RF See 'radiofrequency'.

Ringing See 'reverberation'.

Risk An assessment of the importance of a hazard, which takes account of its nature, the severity of any effect, and the probability of its occurrence. See 'hazard'.

Sample volume The region within the Doppler beam from which the Doppler ultrasound signals will be detected. See 'Doppler beam', 'gate'.

Scale Relating to Doppler spectral display or colour Doppler display; machine control enabling the operator to adjust the maximum Doppler frequency shift which is displayed; note the scale control affects the PRF and so affects aliasing.

Scan plane The region in the tissue from which the image is produced in 2D ultrasound.

Scatterer Small region of tissue which gives rise to scattering of ultrasound.

Scattering General: generation of a wave which travels in all directions, after an incident wave has encountered a small object (dimensions << wavelength), where the object has an impedance different to the surrounding material. For medical ultrasound: generation of a wave which travels in all directions, after an incident beam has encountered a small object (dimensions << wavelength), where the object has an acoustic impedance different to the surrounding tissue. See 'backscatter', 'spherical wave'.

Second-harmonic imaging An imaging mode designed to receive and construct an image from signals scattered at the second harmonic frequency. See 'contrast-specific imaging', 'harmonic', 'harmonic imaging'.

Sector format Arrangement of scan lines from a small transducer, such as a phased array, in which the scan lines diverge strongly with depth, producing a field of view which is approximately triangular in shape. See 'phased array'.

Segmentation Division of a 2D or 3D image into separate regions, demarcated by a contour or surface. In ultrasound this may be performed to identify key structures from which measurements are made, such as the fetal abdomen for circumference measurement, or the left ventricular chamber for volume measurement; ideally segmentation is

performed automatically using image-processing techniques. See 'image processing'.

Shaded surface display Display method used in 3D ultrasound, in which the boundaries of structures are displayed, with the grey-level dependent on the orientation of the surface; this gives a solid appearance to the object and provides an intuitive way for the operator to visualize the data. See 'surface shading'.

Shadowing Loss of ultrasound information below a structure which either completely absorbs or reflects the ultrasound beam, such as a gallstone, calcified arterial plaque or bowel gas, leaving no transmit beam to insonate deeper tissues.

Shear force A force applied parallel to a surface which causes the surface and the material underlying the surface to be dragged in the direction of the force. See 'shear modulus', 'shear strain'.

Shear modulus A measure of the ability of a material to withstand a shear force; defined as the shear stress divided by the shear strain; unit is pascal (Pa); e.g. the shear modulus in healthy liver is 800–1200 Pa. See 'shear force', 'shear strain'.

Shear strain A measure of the degree of distortion to a material caused by a shear force, defined as the horizontal distance a sheared face moves divided by the vertical distance. See 'shear force', 'shear modulus'.

Shear stress A sideways or tearing force; defined as the shear force divided by the area over which the force is applied. See 'shear force'.

Shear wave Wave, occurring in an elastic medium, characterized by motion of the particles with no change in local density (as opposed to pressure waves, where there is change in local density). See 'shear-wave elastography', 'transverse wave'.

Shear-wave elastography Techniques that provide information related to the elastic modulus of tissue in vivo, based on the measurement and display of shear-wave velocity. See 'strain elastography', 'transient elastography'.

Shell The surface of a microbubble which surrounds the gas. The shell is usually made from a biocompatible material. See 'gas', 'microbubble'.

Side lobe Relating to the detailed distribution in space of ultrasound energy from the transducer, where there is high intensity in several specific directions, called lobes. The side lobes are all lobes other than the main lobe. The side lobes are not useful in the formation of the ultrasound image, giving rise to loss of image contrast and other artefacts. See 'main lobe'.

Sine wave Wave with a single frequency whose amplitude as a function of time (or distance) is expressed by the mathematical sine function. See 'cosine wave'.

Single-element transducer Transducer consisting of one element which is used for both beam transmission and then reception; used in pulsed-wave ultrasound. Is now seen mainly in stand-alone pulsed-wave Doppler systems. See 'pencil probe'.

Slice thickness Width of the beam in the elevation direction. See 'spatial resolution'.

Snell's law For a wave which is refracted; a law relating the change in direction of the wave to the speed of sound in the two tissues through which the wave passes.

Soft-tissue thermal index (TIS) The thermal index calculated using a uniform soft-tissue model.

Soft tissues Tissues of the body which are not hard or fluid (e.g. not bone or blood); includes muscle, liver, kidney, brain, pancreas etc.; this is the general group for which elastographic techniques are designed. See 'elastography'.

Sonoporation The transient creation of gaps or pores in a cell membrane when exposed to ultrasound. Sonoporation is associated with stable cavitation.

Sound wave Pressure waves in a frequency range which can be heard by the human (12 Hz – 20 kHz). See 'ultrasound'.

Spatial resolution Minimum separation in space for which two separate point or line targets can be identified, or size on the image of a point object. There are three values, one for each of the principal beam directions, required for a full reporting of spatial resolution; 'axial resolution', 'lateral resolution' and 'elevation resolution'; the latter may be called 'slice width', 'slice thickness' or 'azimuthal resolution' for 2D ultrasound systems

Spatio-temporal image correlation Relating to 3D imaging of the fetal heart; where the 2D image plane is swept slowly over several seconds through the fetal heart, and the acquired 2D data are reorganized to provide a series of 3D volumes through the cardiac cycle.

Speckle Noise appearing on ultrasound images, arising from variations in the position and scattering strength of the various scatterers within the beam. See 'Doppler speckle', 'colour speckle'.

Spectral analysis See 'spectrum analysis'.

Spectral broadening Increase in the range of Doppler frequencies observed on the Doppler waveform in spectral Doppler. Has a variety of origins, some associated with disease (e.g. presence of disturbed flow and turbulence), some associated with the ultrasound system (e.g. geometric spectral broadening). See 'disturbed flow', 'geometric spectral broadening', 'intrinsic spectral broadening', 'spectral broadening index', 'turbulence'.

Spectral broadening index An index which describes the range of frequencies present in the Doppler ultrasound waveform; has been used in attempts to quantify the degree of stenosis. See 'spectral broadening'.

Spectral display 2D image of Doppler frequency shift against time showing spectral Doppler waveforms in real time, usually in a scrolling format moving from right to left with the most recent waveform data displayed on the right side of the display. See 'spectral Doppler'.

Spectral Doppler Doppler ultrasound technique which produces Doppler frequency shift versus time waveforms with full Doppler frequency shift data estimated and presented at each time point. See 'spectral display'.

Spectrum Graph of amplitude vs. frequency; showing the frequency components of a waveform, obtained using spectrum analysis.

Spectrum analyser Device for performing spectrum analysis. See 'spectrum analysis'.

Spectrum analysis Process for estimating the frequency components of a wave, usually using a variant of the Fourier transform called the fast Fourier transform (FFT). In Doppler ultrasound; the method used for estimation of the Doppler shift frequency components at each time point in the cardiac cycle. See 'fast Fourier transform', 'spectral Doppler'.

Specular reflection Enhanced brightness occurring when the interface between two regions of different acoustic impedance is perpendicular to the beam direction. See 'diffuse reflection', 'reflection'.

Speed of a wave Distance that the wave crest of a wave (or other similar point) travels per second.

Speed of sound Distance that the crest of the sound wave (or other similar point) travels per second. Values in soft tissue are 1400–1600 m s^{-1}, with an average value of about 1540 m s^{-1}.

Speed-of-sound artefacts Artefacts in ultrasound imaging occurring as a result of differences between the actual speed of sound in the tissues and that assumed by the machine (1540 m s^{-1}). See 'refraction artefact', 'range error', 'misregistration'.

Spherical wave Wave, generally from a small source, which propagates through space as an expanding sphere. See 'plane wave'.

Stable cavitation See 'non-inertial cavitation'.

Stand-alone continuous-wave Doppler system Ultrasound system used only for continuous-wave Doppler, with no imaging capability. See 'pencil probe'.

Stand-alone pulsed-wave Doppler system Ultrasound system used only for pulsed-wave Doppler, with no imaging capability. See 'pencil probe'.

Standards Widely accepted devices or methods which when adopted allow: (i) the production of equipment which is able to be connected to or integrated with equipment from a wide range of other producers; (ii) the measurements made by equipment to be defined consistently and quantified. For ultrasound the IEC is the most important source of standards, which cover all aspects of the design and testing of ultrasound systems. Other national bodies may also set their own standards, which are sometimes adopted internationally. See 'IEC, 'AIUM', 'IPEM', 'BMUS'.

Static elastography See 'strain elastography'.

Steering Process by which a beam is transmitted and received at angles other than 90° with respect to the transducer face.

Steering angle (1) The angle of the beam with respect to the transducer face. See 'steering'.

Steering angle (2) Machine control enabling the operator to adjust the steering angle; e.g. in colour flow. See 'steering angle (1)'.

Stenosis A narrowing within an artery, usually caused by atherosclerosis.

Stereoscopic viewing Relating to 3D ultrasound, where the operator visualizes 3D by the use of special glasses or other means, requiring modifications to the displayed 3D data on the screen. Similar technology to that used in 3D films in cinemas.

STIC See 'spatio-temporal image correlation'.

Stiffness Description of a material concerning its ability to withstand deformation by a force. See 'elastic', 'elastic modulus'.

Stimulated acoustic emission (SAE) Relating to contrast imaging. When imaging at high acoustic pressures (high MI) with flash pulses, the contrast

agent is forced to collapse, releasing the gas contained within. These gas bubbles with no shell give a much enhanced backscattered signal. See 'flash imaging'.

Strain Related to the distension of a tissue along a particular direction by a force or stress applied along that direction, where strain is the change in length divided by the original length of the material.

Strain elastography Techniques that provide information related to the elastic modulus of tissue in vivo, based on the measurement and display of strain. See 'strain', 'shear wave elastography'.

Strain ratio Measurement made in 2D strain elastography, where the strain in the lesion is divided by the strain in a reference region ideally placed at the same depth in order to avoid depth artefacts.

Stress For a force which is applied to a tissue; the local force divided by the area; units are pascals (Pa).

String See 'filament'.

String phantom Device for testing Doppler ultrasound systems in which the movement of blood is simulated by the movement of a filament, usually O-ring rubber. See 'filament', 'O-ring rubber'.

Sub-dicing Dividing of an element into smaller parts, for the purpose of reducing grating lobes. See 'grating lobes'.

Subharmonic A frequency which is a fraction of and less than the fundamental frequency F_o, e.g. ½ F_o. See 'harmonic'.

Supersonic Related to the production of waves by a moving source, where the velocity of the source is greater than the velocity of the waves; producing a wave with a characteristic shape called a mach cone. See 'mach cone', 'supersonic imaging'.

Supersonic imaging Ultrasound elastography technique which generates shear waves by several sequentially placed sources; equivalent to a high-output source moving through the tissues at a speed greater than that of the shear waves which are generated. The use of several sources enables shear waves of higher amplitude to be produced without increasing tissue heating. See 'supersonic'.

Surface shading Method used to allocate image grey level to each pixel of a surface of an organ or structure in 3D ultrasound, in order to make the structure look realistic. See 'shaded surface display'.

Swept array 3D transducer See 'mechanically steered array'.

Swept array 3D ultrasound system See 'mechanically steered array 3D ultrasound system'.

Swept gain See 'time gain compensation'.

Synthetic-aperture imaging Ultrasound imaging technique in which a single array element, or a very small number of array elements, produces a spherical wave in transmission in order to insonate the whole field of view in one pulse, hence allowing very high-frame-rate imaging. See 'high-frame-rate imaging'.

Systematic error Relating to the error when a measurement is made (e.g. of distance, volume). The measurement is consistently larger or smaller than the true value by a specific amount; the average value is not zero for the error when the measurement is repeated many times. See 'error', 'random error'.

Target In Doppler ultrasound, the moving blood or tissue within the sample volume.

TDI See 'Doppler tissue imaging'.

Temporal resolution Minimum separation in time for which two separate events can be identified.

Teratogen Any agent with the potential to cause developmental defects in the fetus or embryo. For example, heat.

Test object See 'phantom'.

TGC See 'time gain control'.

Thermal index (TI) A number, closely associated with temperature rise, used to indicate thermal hazard, and shown on the screen of ultrasound scanners.

Thermal test object (TTO) A device designed to measure directly the temperature rise associated with ultrasound exposure in either a soft-tissue or bone mimic material.

TI See 'thermal index'.

TIFF (tagged image file format) File format used for single-image digital files.

Time average velocity (TAV) Relating to spectral Doppler; average value of mean blood velocity over the cardiac cycle. May be obtained by averaging the mean frequency waveform, or more accurately by averaging the maximum frequency waveform and dividing by 2; used in the estimation of flow rate. See 'maximum frequency waveform', 'mean frequency waveform', 'flow rate'.

Time domain Relating to estimation of blood or tissue velocity, through manipulation of the time characteristics of the detected ultrasound signals. See 'phase domain'.

Time-domain systems Relating to PW systems for measuring blood or tissue velocity, where the estimation of velocity is undertaken using time-domain techniques. See 'phase-domain systems'.

Time-gain compensation Process by which received ultrasound signals from deeper tissues are amplified

by a greater amount in order to compensate for the decrease in received echo size with increasing depth which occurs as a result of attenuation. See 'attenuation'.

Time-gain control Ultrasound system control, whereby the operator is able to adjust the amplification of the ultrasound signal from different depths, to account for the reduction in received ultrasound signal amplitude with signals from deeper tissues, usually by the use of a set of sliders.

Time–intensity curve A curve showing how the backscattered intensity from microbubbles in a region of interest changes with time, usually as the blood flows through.

Tissue Doppler imaging See 'Doppler tissue imaging'.

Tissue-mimicking Relating to materials used in the construction of phantoms, where they have similar acoustic properties to human tissue. Typically the speed of sound, attenuation and backscatter are replicated. See 'blood mimic', 'phantom', 'tissue-mimicking phantom'.

Tissue-mimicking material (TMM) Material which has the same acoustic properties as soft tissue, generally with a speed of sound of 1540 m s^{-1} and an attenuation coefficient in the range 0.3–0.7 dB cm^{-1} MHz^{-1}.

Tissue-mimicking phantom Phantom in which the components which are insonated are tissue-mimicking. See 'tissue-mimicking'.

Transcutaneous Meaning 'through the skin or other outer body part', relating to the acquisition of ultrasound by application of the transducer to an external body part. See 'endoprobe'.

Transducer Component of the ultrasound system which generates and receives the ultrasound beam, and sweeps the beam through the tissues to produce an image.

Transducer bandwidth Frequency range (MHz) over which the transducer can transmit and receive ultrasound.

Transducer self-heating Heating, especially associated with the front face of an ultrasound transducer arising from the inefficient conversion of electrical to acoustic energy.

Transient cavitation See 'inertial cavitation'.

Transient elastography Shear-wave elastography in which an external vibrator induces a shear-wave pulse. See 'shear-wave elastography', 'vibrator'.

Transmission The process of production of ultrasound from the transducer.

Transmit beam The region of space within the tissue which the ultrasound produced by the transducer passes through; this is to some extent an idealized region in which the main energy of the ultrasound pulse is not refracted or reflected by tissues.

Transmit beam-former Component of an ultrasound system that deals with formation of the transmitted beam; involving adjustments to the amplitude and delay in time of the electrical signals applied to the transducer for the purposes of production of the ultrasound pulse. Details of beam-forming are usually different for each modality (B-mode, spectral Doppler, colour flow). See 'beam-former'.

Transmit frequency Nominal frequency of the transmitted ultrasound pulse; e.g. 6 MHz.

Transmit power Machine control enabling the operator to increase or decrease the output power; generally there is independent control for each ultrasound modality.

Transmitted ultrasound Ultrasound which has been produced by the transducer.

Transoesophageal probe Endoprobe designed for insertion down the oesophagus to allow imaging of the oesophagus and other organs such as the heart.

Transrectal probe Endoprobe designed for insertion into the rectum to allow imaging of the rectum, prostate and other organs.

Transvaginal probe Endoprobe designed for insertion into the vagina to allow imaging of the vagina, uterus, ovaries and other pelvic structures in women.

Transverse wave Wave, such as shear waves, in which the local direction of motion of the particles is at 90° to the direction of motion of the wave. See 'shear wave'.

Trapezoidal format Arrangement of scan lines from a linear array, in which the scan lines diverge with distance from the transducer, producing a wider field of view with depth. See 'linear array'.

Turbulence Relating to blood flow; where at high velocities fluid elements follow erratic paths and where there is mixing between adjacent layers. May lead to increased spectral broadening. See 'disturbed flow', 'laminar flow', 'spectral broadening'.

Ultraharmonic A frequency which is a rational (ratio of two integers) multiple of the fundamental frequency F_o, e.g. $^3/_2 F_o$, $^5/_2 F_o$. See 'harmonic'.

Ultrasonic Relating to ultrasound. See 'ultrasound'.

1D ultrasound Ultrasound system or component of an ultrasound system in which information only along a single line is used, usually in the form of an amplitude–depth plot; rarely used now.

2D ultrasound Ultrasound system or component of an ultrasound system in which information in a 2D plane is used or displayed; the most common method of operation of modern ultrasound systems.

3D ultrasound Ultrasound system or component of an ultrasound system in which information in a 3D volume is used or displayed.

4D ultrasound Ultrasound system capable of producing real-time 3D ultrasound; (i.e. three dimensions in space, one dimension in time).

Ultrasound Generally: sound waves with frequencies too high to be heard by the human ear. For medical ultrasound: sound with a frequency used for diagnosis or therapy in humans and animals (currently 0.5–60 MHz).

Ultrasound contrast agent (UCA) See 'contrast agent'.

Ultrasound system Machine using ultrasound for the purposes of diagnosis or therapy.

Variance One of the values which is produced from autocorrelator-based frequency estimators of colour flow systems, related to the variation in the amplitude of the received Doppler signal amplitude. See 'autocorrelator', 'mean frequency (2)'.

Velocity Distance an object or wave travels per second; units are m s^{-1}; e.g. the velocity of blood in arteries is 0–6 m s^{-1}, of ultrasound in soft tissue is 1400–1600 m s^{-1}, of shear waves in soft tissue is 1–10 m s^{-1}.

Velocity profile Relating to blood flow in an artery, graph of velocity against distance along the diameter of the vessel.

Velocity ratio Ratio of the blood velocity estimated within the stenosis to that in an undiseased region, such as proximal to the stenosis; used in the estimation of the degree of stenosis.

Velocity resolution The minimum difference in blood or tissue velocity which can be visualized using an ultrasound system.

Vessel axis Line passing through the centre of each cross section of a vessel.

Vibrator Device for producing low-frequency (10–500 Hz) vibrations in tissue, used in transient elastography. See 'transient elastography'.

Video clip See 'cine loop'.

Viscoelastic Behaviour of a material which stretches or deforms in response to an applied force, but when the force is applied or removed the strain is not achieved immediately, but after a brief time delay. See 'elastic'.

Volume Quantity representing the 3D size of an object or image; may be measured using advanced measurement facilities available on some 3D ultrasound systems.

Volume flow See 'flow rate'.

Volumetric flow See 'flow rate'.

Vortex Region of recirculating flow, which may be stable (contained at one location), or shed (travels downstream for a few diameters, after which it dies out). See 'disturbed flow'.

Vortex shedding Relating to blood flow; where a local region of recirculating flow, e.g. immediately distal to a stenosis, may be shed and travel downstream for a few diameters. See 'disturbed flow'.

Vortices Plural of vortex (see vortex).

Voxel Volume element; i.e. building block of a 3D dataset which is composed (usually) of several thousand voxels.

Wall filter (1) Relating to Doppler ultrasound detection of blood flow; signal-processing step which attempts to remove the clutter signal, leaving behind the Doppler ultrasound signal from the moving blood, by removing low-frequency signals; this term usually reserved for 'spectral Doppler'. See 'clutter filter'.

Wall filter (2) Relating to spectral Doppler systems; machine control enabling the operator to adjust the velocity or Doppler frequency below which the signal is removed. See 'wall filter (1)'.

Wall filter value Value of the wall filter, typically ranging from 50 Hz (obstetrics) to 300+ Hz (cardiology). See 'wall filter (2)'.

Wall thump filter See 'wall filter (1)'.

Wash-in The time required for the contrast agent to enter a region of interest .

Wash-out The time required for contrast to clear, either by dissolution or by blood flow, from the region of interest.

Wave Generally, a periodic disturbance which travels through space, with transfer of energy but not mass. See 'shear wave', 'pressure wave', 'ultrasound', 'sound'.

Waveform In general: for a quantity which varies periodically in time, the display of the value of the quantity with time for one period. In blood flow: the velocity–time or flow rate versus time data for a

single cardiac cycle. In Doppler ultrasound: the Doppler frequency shift versus time spectral display for a single cardiac cycle.

Waveform indices Relating to Doppler ultrasound; quantities which are derived from the spectral Doppler waveform which may be useful in diagnosis. See 'resistance index', 'pulsatility index', 'spectral Doppler'.

Wavelength Property of a wave; the distance between two consecutive crests or other similar points on the wave.

WFUMB World Federation for Ultrasound in Medicine and Biology.

Write zoom Magnification of a part of the displayed image, performed in real time, enabling the ultrasound field to be restricted to only that part displayed, hence allowing increase in frame rate and/or scan line density. See 'digital zoom'.

Young's modulus Property of an elastic material; defined in terms of the stretch of a thin sample of the material, resulting from a force which is applied to one end of the material (when the other end is tethered); a quantity describing the change in dimensions (strain) that occurs due to an applied force (stress). See 'elastic modulus', 'bulk modulus', 'shear modulus'.

Zoom Magnification of the displayed image. See 'digital zoom', 'write zoom'.

Index